Décryptage des modifications précoces du phosphoprotéome en réponse à BMP9 et BMP10 dans les cellules endothéliales

Mohammad Al Tarrass

THÈSE

Pour obtenir le grade de

DOCTEUR DE L'UNIVERSITÉ GRENOBLE ALPES

École doctorale : CSV- Chimie et Sciences du Vivant
Spécialité : Biologie cellulaire
Unité de recherche : Laboratoire Biologie et Biotechnologie pour la Santé (BioSanté)

Décryptage des Modifications Précoces du Phosphoprotéome en Réponse à BMP9 et BMP10 dans les Cellules Endothéliales

Deciphering Early Phosphoproteome Changes in Response to BMP9 and BMP10 in Endothelial Cells

Présentée par :

Mohammad AL TARRASS

Direction de thèse :

Sabine BAILLY — Directrice de thèse
DIRECTEUR DE RECHERCHE, INSERM U1292 (Biosanté), Université Grenoble Alpes, France

Claire BOUVARD — Co-encadrante de thèse
MAITRE DE CONFERENCES, INSERM U1292 (Biosanté), Université Grenoble Alpes, France

Rapporteurs :

Aristidis MOUSTAKAS
PROFESSEUR, Department of Medical Biochemistry and Microbiology, Uppsala University, Sweden

Franck VANDERMOERE
DIRECTEUR DE RECHERCHE, Institut de Génomique Fonctionnelle, CNRS U5203, Université de Montpellier, France

Thèse soutenue publiquement le **24 octobre 2023**, devant le jury composé de :

Sabine BAILLY DIRECTEUR DE RECHERCHE, INSERM U1292 (Biosanté), Université Grenoble Alpes, France	Directrice de thèse
Aristidis MOUSTAKAS PROFESSEUR, Department of Medical Biochemistry and Microbiology, Uppsala University, Sweden	Rapporteur
Franck VANDERMOERE DIRECTEUR DE RECHERCHE, Institut de Génomique Fonctionnelle, CNRS U5203, Université de Montpellier, France	Rapporteur et Président du jury
Philippe FRACHET MAITRE DE CONFERENCES, Institut de Biologie Structurale CNRS U5075, CEA, Université Grenoble Alpes, France	Examinateur
Anne-Clémence VION CHARGE DE RECHERCHE, l'institut du thorax IRS, Inserm U1087/CNRS U6291, Nantes Université, France	Examinatrice

Invitée

Claire BOUVARD MAITRE DE CONFERENCES, INSERM U1292 (Biosanté), Université Grenoble Alpes, France	Co-encadrante de thèse

Acknowledgements

Firstly, I would like to express my great appreciation to the honorable jury members: **Dr. Aristidis Moustakas** and **Dr. Franck Vandermoere** for evaluating my thesis manuscript, as well as **Dr. Anne-Clémence Vion** and **Dr. Philippe Frachet** for accepting to evaluate my thesis work.

I would like to thank my Comité de suivi de these (CSI) members **Dr. Delphine Pflieger**, **Dr. Corrine Albiges Rizo** and my previous M2 mentor **Dr. Maxim Balakirev** for their valuable input during our annual CSI meeting.

I would like to acknowledge the financial support of **GRAL**, a program from the Chemistry Biology Health (CBH) Graduate School of University Grenoble Alpes, which supported me financially at both personal and technical levels during the first three years. I am also grateful to the **Agence Nationale de la Recherche/Inserm** for funding my fourth year. This work was also funded by Commissariat à l'énergie atomique (**CEA**), the Fondation pour la Recherche Médicale (**FRM**), the Association Maladie de Rendu-Osler (**AMRO/HHT France**), the association **FAVA-multi**, and the H2020-msca-ITN-2018 (**V.A. Cure-84316**).

I was lucky to be a member in the BMP family in angiogenesis and lymphangiogenesis team (**BAL**) at CEA-Grenoble. I would like to express my deepest gratitude to my supervisor, **Dr. Sabine Bailly**. Not only she is a great scientific researcher whom I learned a lot from scientifically, she is a great supporter as well. Thanks for your trust, kindness, guidance, ideas, discussions, and availability whenever needed. I feel fortunate to have been your student for these four years. Thank you for believing in me and allowing me to be part of **BAL team**, no doubt one of the excellent research groups in the vascular field. I am also very grateful to my co-supervisor, **Dr. Claire Bouvard**, for her guidance on my research project, her advice, and her support throughout my PhD. You've been a kind and sweet mentor during these four years, and I was delighted to work with you, especially in the last year on the second project related to inflammation. I know that soon you will defend your HDR, and I want to wish you the best of luck for that! Sabine and Claire, it has been a pleasure working with both of you, and in French I would like to tell you: *Merci mille fois*!

Additionally, I am very grateful to **Valentin Azemard**, who joined the team in the last year of my PhD. Without your help in the last six months, I would have never had the time to finish all the experiments required for the submission of my first paper. I truly enjoyed working with you, and on a personal side, I consider you one of the kindest people I have ever met. I would like to extend my thanks to all the other members of the BAL team, past and present. In particular, I want to thank also **Dr. Agnes Castan** for providing scientific and technical instructions and for her support throughout these four years. I learned from you how to view cell signaling as a puzzle of missing pieces that requires patience to assemble together! Furthermore, I would also like to express my thanks to **Dr. Emmanuelle Tillet** and **Dr. Nicolas Ricard** for your valuable scientific insights during our team meetings. BAL team, needless to say, I enjoyed all the time we spent together in and outside the lab, and I hope we can always stay in touch. I would also like to express my gratitude to lot of my fellows who have already earned their PhDs during these four years, especially my friend since 8 years, **Tala Al Tabosh**, in addition to **Martina Rossi**. We began our PhD journeys together, and your support and companionship made this journey more enjoyable. I would also like to thank those who are on the path to earning their PhD, including my new friend and neighbor **Yasmin Rida** and my office-mate **Jean le Pennec**. I was very happy to have

the opportunity to know you guys this last year and to share with you all the moments of the last stretch of my PhD.

Moreover, I want to acknowledge **Mohamad Skayni**, who joined the lab for his Master internship to work with me and Claire on the inflammation project. With your assistance Mohamad, we continued the work I started in my third year, which yielded very interesting results that we hope to publish soon. I am very happy about your recent acceptance as a PhD student in Montpellier. I also want to congratulate **Lea Vialet**, who was also an M2 intern in the team and recently joined the team as a PhD student. I wish you all, Mohamad, Lea and Yasmin, the best for your PhD projects!

To all BCI members, thanks a lot for welcoming me for these 4 years and providing a friendly atmosphere! In particular, I would like to thank **Nadia C.**, **Nadia A.**, **Laurent G.**, **Josian D.**, **Odile F.** and **Claude C.** for their scientific insights and support during several occasions. Thanks to **Véronique Collin** for helping in flow cytometry experiments and indeed for **Isabelle Zanotti** for all the administrative help and for being very caring on multiple occasions.

I would like to thank our collaborators at the Edyp laboratory, **Yohann Coute** and **Lucid Belmudes**, for their help in performing very successful phosphoproteomic analyses, which led to exciting results during this PhD. I am also very grateful to **Dzenis Koca**, **Hequn Liu**, and **Dr. Christophe Battail** for their tremendous help in conducting all the complicated bioinformatics analyses of the phosphoproteomic data.

I would not have reached this point without my dear parents. I would like to dedicate this work to the memory of my father, **Abed Al Kader Al Tarrass**, who tragically lost his life in the Beirut explosion on August 4th, 2020. His top priority was my education, where he dedicated himself to ensure that this day would eventually arrive. Thanks Dad… Your loss during my PhD was deeply felt and had a deep impact on my psychological condition. However, I made the decision to continue this PhD as a dedication to you and as a symbol of my enduring love and gratitude. You always wanted to see me continuing my studies to earn my PhD. Although you will not be there to witness this moment, I promise to always do my best to make you proud of me from above. ***Mom*** *and* ***Dad****, everything I am and all that I will achieve, I owe it to you, and I can never fully repay you for everything you've done for me*.

Furthermore, I would like to extend my thanks to the rest of my family, especially my sisters **Faten** and **Zahraa**, aunt **Shukreya** for all your prayers and endless love, and to my mother in law **Hindiye** for all the love and support. Special thanks to my brothers in law, **Ali** and **Muhammed**, who were always supportive and were like real brothers but from another mother ;) I love you so much…

Last, but not least, in addition to my academic milestone, the most significant milestone during this PhD journey was marrying the love of my life, **Jinan**. Everything would have been harder without you. I thank you from the bottom of my heart for always being wonderful and supportive. Your faith in me, patience, and love have been a constant source of strength during all the ups and downs of this PhD adventure. I am deeply grateful for you, and I want you to know that your presence has given deeper meaning to all my accomplishments. If I want to talk about your impact in my life, I think I would write another 300+ papers ;) but I just want to tell you that you will forever hold a special place in my heart, love you to the moon and back Aşkım <3…

Table of contents

List of Figures

List of Tables

Abbreviations

ActR: Activin Receptor
ALK: Activin receptor-Like Kinase
ALK1ca: Constitutively Active ALK1
ALP: Alkaline Phosphatase
AM: Adrenomedullin
AMH: Anti-Müllerian Hormone
Ang: Angiopoietin
AP2: Adaptor Protein 2
ASK1: Apoptosis Signal-Regulating Kinase 1
ATF2: Activating Transcription Factor-2
ATP: Adenosine Triphosphate
AVMs: Arteriovenous Malformations
BAD: Bcl2 Associated Agonist of Cell Death
BAEC: Bovine Aortic Endothelial Cells
BMP: Bone Morphogenetic Protein
BMPER: Bone Morphogenetic Protein-Binding Endothelial Regulator
cAMP: Cyclic Adenosine Monophosphate
CBP: CREB Binding Protein
c-CBL: Casitas B-lineage Lymphoma
CCL2 (MCP-1): Monocyte Chemoattractant Protein-1
Cdc42: Cell Division Control Protein 42 Homolog
CDK: Cyclin Dependent Kinase
cGMP: Cyclic Guanosine Monophosphate
CID: Collision-Induced Dissociation
CIN85: Cbl-Interacting 85-Kda Protein
CIS: Cytokine Inducible SH2-containing Protein
CK2: Casein Kinase 2
cPML: Cytoplasmic Form of Promyelocytic Leukemia
CREB: cAMP-response element binding protein
CV2: Crossveinless 2
Dab2: Disabled-2
DAG: Diacylglycerol
DDA: Data-Dependent Acquisition
DIA: Data-Independent Acquisition
Dll: Delta-like ligand
DNMT3A: DNA methyl transferase 3A
ECD: Extracellular Domain
ECs: Endothelial Cells
EMT: Epithilail-to-mesynchymal Transition
ENG (CD105): Endoglin
eNOS: Endothelial Nitric Oxide Synthase
Eps15: Epidermal Growth Factor Receptor Pathway Substrate 15
Eps15R: Eps15 Homolog Receptor
ER: Endoplasmic Reticulum
ERK: Extracellular Signal-Regulated Kinase
ESI: Electrospray Ionization
ET-1: Endothelin-1
FAK: Focal Adhesion Kinase
FDR: False Discovery Rate
FGF2: Fibroblast Growth Factor 2
FOX: Forkhead Box
FSS: Fluid Shear Stress
FT-ICR: Fourier Transform Ion Cyclotron Resonance
GADD45β: Growth Arrest and DNA Damage-Inducible 45 Beta

GDF: Growth and Differentiation Factor
GEF: Guanine Nucleotide Exchange Factor
GF: Growth Factor
GPCRs: G Protein-Coupled Receptors
Grb2: Growth Factor Receptor-Bound Protein 2
GS: Glycine/Serine
GSK3β: Glycogen Synthase Kinase 3β
GTP: Guanosine Triphosphate
HAECs: Human Aortic Endothelial Cells
HMVECs: Human Dermal Microvascular Endothelial Cells
HPAECs: Human Pulmonary Artery Endothelial Cells
HUAECs: Human Umbilical Artery Endothelial Cells
HUVECs: Human Umbilical Vein Endothelial Cells
hESCs: Human Embryonic Stem Cells
HSC: Hepatic Stellate Cells
HES: Hairy and Enhancer-Of-Split
HEY: Hairy Ears, Y-Linked
HHT: Hereditary Hemorrhagic Telangiectasia
HILIC: Hydrophilic Interaction Liquid Chromatography
HPAH: Heritable PAH
HpH-RPLC: High pH Reversed Phase Liquid chromatography
HSP27: Heat Shock Protein 27
ICAM-1: Intercellular Adhesion Molecule-1
ICD: Intracellular Domain
ID: Inhibitor of Differentiation
IKK: IκB kinase
IL: Interleukin
IMAC: Immobilized Metal Affinity Chromatography
IP: Immunoprecipitation
IP3: Inositol 1,4,5-trisphosphate
IPAH: Idiopathic PAH
I-SMAD: Inhibitory SMAD
iTRAQ: Isobaric Tags for Relative and Absolute Quantitation
Jag: Jagged
KO: Knock Out
LAP: Latency-associated Peptide
LC: Liquid Chromatography
LIMK1: LIM Kinase 1
LOF: Loss of Function
LPS: Lipopolysaccharides
LSECs: Liver Sinusoidal Endothelial Cells
m/z: Mass-to-Charge
MALDI: Matrix Assisted Laser Desorption and Ionization
MAML: Mastermind-Like
MAPK: Mitogen Activated Protein Kinase
MAPKAPK2/3 (MK2/3): MAPK activated protein kinase 2/3
MAPKK (MAP2K): MAPK Kinase
MAPKKK (MAP3K): MAPK Kinase Kinase
MEK: Mitogen-Activated Protein Kinase Kinase
MSK: mitogen- and stress-activated protein kinase
MLK2/3: Mixed-Lineage Kinase 2 and 3
MC3T3-E1: Mouse Calvarial 3T3-E1
MH1: Mad Homology 1 (MH1)
mLECs: Mouse Lung Endothelial Cells
MMPs: Matrix Metalloproteinases
MOAC: Metal Oxide Affinity Chromatography
MRM: Multiple Reaction Monitoring
MS: Mass Spectrometry
MSI: Mass Spectrometry Imaging
mTOR: Mammalian Target of Rapamycin
mTORC2: mTOR Complex
NCK1: Non-Catalytic Region of Tyrosine Kinase Adaptor Protein 1
NES: Nuclear Export Signal
NET1: Neuroepithelial Cell Transforming 1
NFkB: Nuclear Factor Kappa B
NHS ester: Peptide-Reactive Group

NICD: Notch intracellular domain
NLS: Nuclear Localization Sequence
NO: Nitric Oxide
PAEC: Pulmonary Artery Endothelial Cell
PAH: Pulmonary Arterial Hypertension
PAK2: P21-Activated Kinase 2
PDE-5: Phosphodiesterase Type-5
PDGF: Platelet-Derived Growth Factor
PDK: Phosphoinositide-Dependent Protein Kinase
PECAM1: Platelet Endothelial Cell Adhesion Molecule 1
PH: Pulmonary Hypertension
PI3K: Phosphoinositide 3-Kinase
PIAS: Protein Inhibitor of Activated STAT
PIP2: Phosphatidylinositol 4,5-Bisphosphate
PK: Protein Kinase
PLCγ1: Phospholipase Cγ1
PKI: Inhibitory Peptide for PKA
PlGF: Placental Growth Factor
PO4: Phosphate Group
PP2Cα: Protein Phosphatase 2C Alpha
pProtein: Phosphorylated Protein
PS1: Presenilin 1
PSMs: Peptide Spectrum Matches
PTEN: Phosphatase and TENsin Homolog
PTMs: Posttranslational Modifications
PTMsigDB: Post-Translational Modification Signature Database
PTPs: Protein Tyrosine Phosphatases
RAB11: Ras-related Protein 11
Rac: Ras-related C3 Botulinum Toxin Substrate
Raf: Rapidly Accelerated Fibrosarcoma
RBPJk (CSL): Recombination Signal Binding Protein for Immunoglobulin Kappa J Region
RGD: Arginyl-glycyl-aspartic Acid
Rho: Ras Homolog
RING: Really Interesting New Gene
RNAi: RNA Interference
ROCK: Rho-related Protein Kinase
R-SMAD: Receptor-regulated SMAD
RUNX: Runt-related Transcription Factor
S (Ser): Serine
SARA: SMAD Anchor for Receptor Activation
SAX: Strong Anion Exchange
SBE: SMAD Binding Element
SCX: Strong Cation Exchange
sGC: Soluble Guanylate Cyclase
SGK1: Serum and Glucocorticoid Activated Kinase 1
SHB: SH2 domain-containing adaptor protein B
Shc: Src Homology 2 Domain-Containing Transforming Protein
SILAC: Stable Isotope Labeling by Amino Acids in Cell Culture
SMAD: Suppressor of Mothers Against Decapentaplegic

Smurf: SMAD Ubiquitination-related Factor
SOCS: Suppressor of Cytokine Signaling
Sos: Son of Sevenless
SRM: Selected Reaction Monitoring
STAT: Signal Transducer and Activator of Transcription
T (Thr): Threonine
TAB: TAK1-binding Protein
TAK1: TGF-β activated kinase 1
TCR: T-Cell Receptor
TFII-I: Transcription Factor-II-I
TGF-β1: Transforming Growth Factor β1
Tie2: Tunica Interna Endothelial Cell Kinase 2
TMD: Transmembrane Domain
TMT: Tandem Mass Tag
TNF-α: Tumor Necrosis Factor-α
TOF: Time of Flight

TRAF6: Tumor Necrosis Factor-Receptor Associated Factor 6
USP4: Ubiquitin-Specific Peptidase 4
VCAM-1: Vascular Cell Adhesion Molecule-1
VE-cadherin: Vascular Endothelial Cadherin
VEGF: Vascular Endothelial Growth Factor
VSMCs: Vascular Smooth Muscle Cells
WHO: World Health Organization
WT: Wild Type
XIAP: X-Linked Inhibitor of Apoptosis Protein
Y (Tyr): Tyrosine
2D-PAGE: Two-Dimensional Polyacrylamide Gel Electrophoresis

Thesis Summary

BMP9 and BMP10 are key factors in vascular homeostasis, acting via high-affinity receptors (ALK1, BMPRII, and Endoglin) on endothelial cells (ECs). Mutations in this signaling pathway are associated with two rare vascular diseases, hereditary hemorrhagic telangiectasia (HHT) and pulmonary arterial hypertension (PAH), with no currently identified cures. Molecular mechanisms driving the pathogenesis of these diseases is not yet clear. So far, only the canonical SMAD signaling pathway is well studied in response to BMPs, including BMP9 and BMP10, while the activation of alternative pathways by these ligands remains poorly understood, particularly in ECs.

The aim of this work is to address early phosphoproteomic changes in ECs in response to short-term stimulation with BMP9 and BMP10. Discovering new phosphorylated targets and pathways activated by these ligands would enhance our understanding of the molecular mechanisms governing their roles in vascular homeostasis, while identifying potential therapeutic targets for vascular diseases.

I performed mass spectrometry phosphoproteomic analysis of human umbilical vein endothelial cells (HUVECs), stimulated or not with BMP9 or BMP10 for 30 min. To identify downstream-regulated pathways, differentially regulated phosphosites were analysed using different bioinformatics tools. Treatment with BMP9 and BMP10 induced a highly similar phosphoproteomic profile, allowing the identification 289 differentially phosphorylated proteins. Among these, we identified phosphorylation of the activating residues of SMAD1, direct substrate of ALK1, thus validating our phosphoproteomic approach. Bioinformatic analyses highlighted the activation of MAPK signaling in response to BMP9 and BMP10. We identified a central role for the MAPK pathway (MEKK4/P38) leading to the phosphorylation of Eps15-S796 and HSP27-S78/82. Moreover, I showed that BMP10-induced activation of P38 plays an important role in the regulation of a subset of BMP10 target genes. BMP10-induced activation of P38 required a transcriptional step through expression of GADD45β. I also found that BMP10 regulated the phosphorylation of the endothelial transcription factor ERG. Our bioinformatic analyses also highlighted reduced CDK4/6 activity and cell cycle regulation. In line with these data, I showed that BMP10 induced a G1 cell cycle arrest in ECs, reinforcing its role as a vascular quiescence factor. Moreover, our data highlighted a crosstalk between BMP9/10 and JAK/STAT3 signaling pathways through phosphorylation of gp130, a co-receptor of IL-6 family of cytokines. I found that BMP9 and BMP10 attenuated IL-6-induced activation of JAK/STAT pathway via SMAD-induced expression of SOCS3. Preliminary data from mouse models with impaired Bmp9/10 signaling suggests a possible immunomodulatory role of this pathway.

Overall, this work shows that BMP9/10 can activate both direct and indirect (transcription-dependent) pathways in ECs. The direct pathway involves rapid activation of SMADs, essential for inducing BMP target genes. Among these, I identified GADD45β, which leads to indirect P38 activation, and SOCS3, which inhibits IL-6/JAK/STAT3 signaling. Given the important role of IL-6 in inflammation, this study provides potential therapeutic approaches in the context of HHT and PAH pathogenesis, where inflammation has been associated with both diseases.

While I was able to validate and decipher the mechanisms for several important hits and pathways, I could not study many other intriguing targets due to the lack of specific tools, such as particular phospho-specific antibodies. However, with the development of such tools, I hope that the vascular biology community will further benefit from this unique high-throughput phosphoproteomic study of BMP9/10-mediated signaling, which would aid in characterizing the roles of these ligands not only under physiological conditions but also in pathological vascular diseases, such as HHT and PAH.

Résumé de Thèse

BMP9 et BMP10 jouent un rôle central dans l'homéostasie vasculaire, en agissant sur les cellules endothéliales (CE) par l'intermédiaire de récepteurs à haute affinité (ALK1, BMPRII et Endogline). Des mutations dans cette voie de signalisation sont associées à deux maladies vasculaires rares, la télangiectasie hémorragique héréditaire (HHT) et l'hypertension artérielle pulmonaire (HTAP), pour lesquelles il n'existe pas de traitement curatif. Les mécanismes moléculaires à l'origine de la pathogenèse de ces maladies ne sont pas clairs. Jusqu'à présent, seule la voie de signalisation canonique SMAD en réponse aux BMP, a été étudiée en détails, alors que l'activation de voies alternatives reste mal comprise, en particulier dans les CE.

L'objectif de ce travail est d'étudier les modifications phosphoprotéomiques précoces dans les CE en réponse à une stimulation à court terme avec BMP9 et BMP10. La découverte de nouvelles cibles phosphorylées et de nouvelles voies activées par ces ligands améliorerait notre compréhension des mécanismes moléculaires régissant leur rôle dans l'homéostasie vasculaire, et permettrait l'identification de cibles thérapeutiques potentielles pour les maladies vasculaires.

J'ai effectué une analyse phosphoprotéomique par spectrométrie de masse des cellules endothéliales de la veine ombilicale humaine (HUVEC), stimulées ou non par BMP9 ou BMP10 pendant 30 minutes. Les phosphosites différentiellement régulés ont été analysés à l'aide de différents outils bioinformatiques afin d'identifier les voies de signalisation régulées. Le traitement par BMP9 ou BMP10 ont induit des profils phosphoprotéomiques très similaires, permettant l'identification de 289 protéines différentiellement phosphorylées. Parmi celles-ci, nous avons identifié la phosphorylation des résidus activateurs de SMAD1, substrat direct d'ALK1, validant ainsi notre approche phosphoprotéomique. De plus, nous avons identifié un rôle central de la voie MAPK (MEKK4/P38) conduisant à la phosphorylation de Eps15-S796 et HSP27-S78/82. J'ai aussi montré que l'activation de P38 induite par BMP10 joue un rôle important dans la régulation d'un sous-ensemble de gènes cibles de BMP10. L'activation de P38 induite par BMP10 nécessite une étape transcriptionnelle via l'expression de GADD45β. J'ai également découvert que BMP10 régulait la phosphorylation du facteur de transcription endothélial ERG. Nos analyses phosphoprotéomiques ont aussi mis en évidence une réduction de l'activité CDK4/6 et du cycle cellulaire. J'ai ensuite montré que BMP10 induit un arrêt du cycle cellulaire en G1 dans les CE, confirmant son rôle de facteur de quiescence vasculaire. De plus, nos données ont mis en évidence une interaction entre les voies de signalisation BMP9/10 et JAK/STAT3 par le biais de la phosphorylation de gp130, un corécepteur des cytokines de la famille IL-6. Des données préliminaires provenant de modèles murins dont la signalisation Bmp9/10 est altérée suggèrent un rôle immunomodulateur de cette voie.

Ce travail montre que BMP9 et BMP10 peuvent activer des voies de signalisation de manière directe et indirecte (par l'intermédiaire d'une étape de transcription) dans les CE. La voie directe implique une activation rapide des SMAD, essentielle pour induire les gènes cibles de la BMP. Parmi ceux-ci, j'ai identifié GADD45β, qui conduit à l'activation indirecte de P38, et SOCS3, qui inhibe la signalisation IL-6/STAT3. Étant donné le rôle crucial d'IL-6 dans l'inflammation, et le rôle potentiel de l'inflammation dans l'HHT et l'HTAP, cette étude

pourrait permettre le développement de nouvelles approches thérapeutiques pour ces maladies. D'autres cibles qui semblaient intéressantes n'ont pas pu être explorées, en raison du manque d'outils (phospho-anticorps). J'espère qu'avec le développement futur de tels outils, cette étude de phosphoprotéomique en réponse BMP9/10 sera utile à la communauté de la biologie vasculaire et fera avancer les connaissances sur ces maladies vasculaires.

Introduction

Chapter 1. The Dynamic Blood Vasculature

1.1 Components of the vascular system

The cardiovascular system or the blood vascular system comprises an extensive network of blood vessels powered by the pumping action of the heart. It serves as the body's transportation system that ensures continuous supply of oxygen and nutrients to all body organs as well as the removal of metabolic waste products. This system not only nourishes our organs but also regulates body temperature, maintains fluid balance, and supports the immune response. The blood vasculature comprises five distinct types of vessels, each with its specific function:

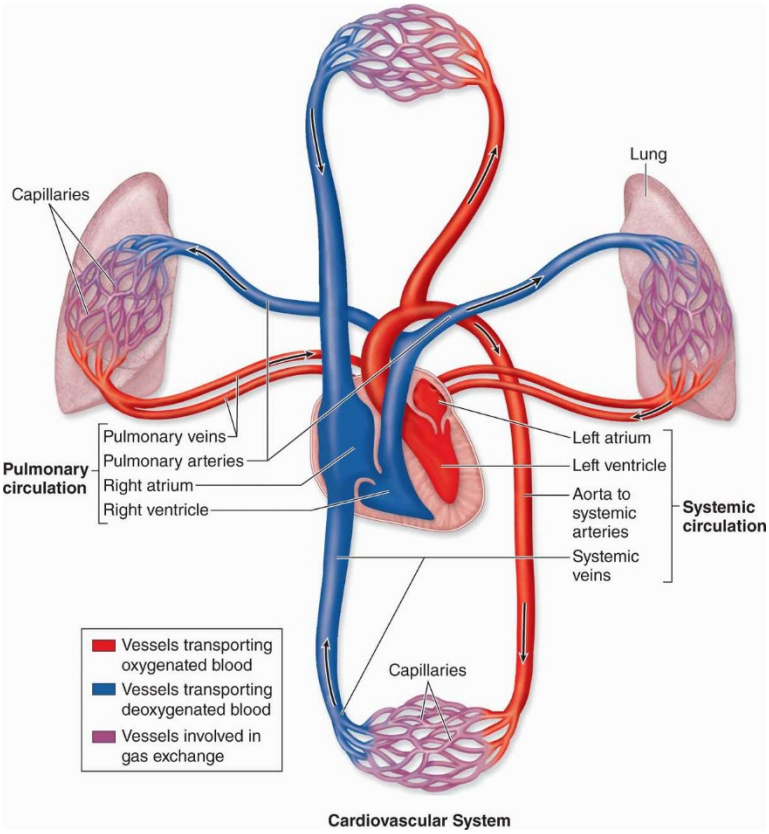

Figure 1. Systemic and Pulmonary Circulatory Systems.

The blood circulatory system consists of two circuits: the pulmonary circuit, responsible for oxygenating the blood and removing carbon dioxide (CO2) within the lungs, and the systemic circuit, which efficiently delivers the oxygen-rich, CO2-poor blood to all vascularized tissues throughout the body, facilitated by the rhythmic pumping action of the heart. Figure was taken from https://basicmedicalkey.com/the-circulatory-system-2/

1. Arteries: Vessels that carry oxygenated blood away from the heart (excluding the pulmonary and umbilical arteries).

2. Arterioles: Smaller branches of arteries that play a vital role in regulating vascular tone in response to changes in blood flow.

3. Capillaries: The smallest vessels where the exchange of gases, nutrients, and metabolic waste products takes place between the blood and tissues.

4. Venules: Post-capillary small veins that receive deoxygenated blood after the exchange of nutrients and oxygen in tissues.

5. Veins: Formed by the merging of venules, these vessels transport deoxygenated blood back to the heart (excluding pulmonary and umbilical veins).

There are two important circulation processes that occur within our body: the pulmonary circulation and the systemic

circulation. During pulmonary circulation, deoxygenated blood collected from the tissues is returned through veins to the right atrium of the heart and is subsequently transported to the lungs though the pulmonary artery. In the lungs, the blood receives oxygen and eliminates carbon dioxide. Oxygenated blood then returns through the pulmonary vein from the lungs to the left side of the heart. In the systemic circulation, the oxygenated blood that has returned to the left side of the heart is pumped out through the aorta to all body organs to provide them with oxygen and nutrients, ensuring their proper functioning. The cycle begins again when deoxygenated blood flows back to the right side of the heart (Figure 1) [1].

All blood vessel types, with the exception of the capillaries, exhibit three distinct layers: tunica intima, tunica media, and tunica adventitia, arranged in a specific order from the inner lumen outward (Figure 2) [2]. The tunica intima consists of a tightly packed monolayer of endothelial cells (ECs) that align along the direction of blood flow. Being in direct contact with the blood,

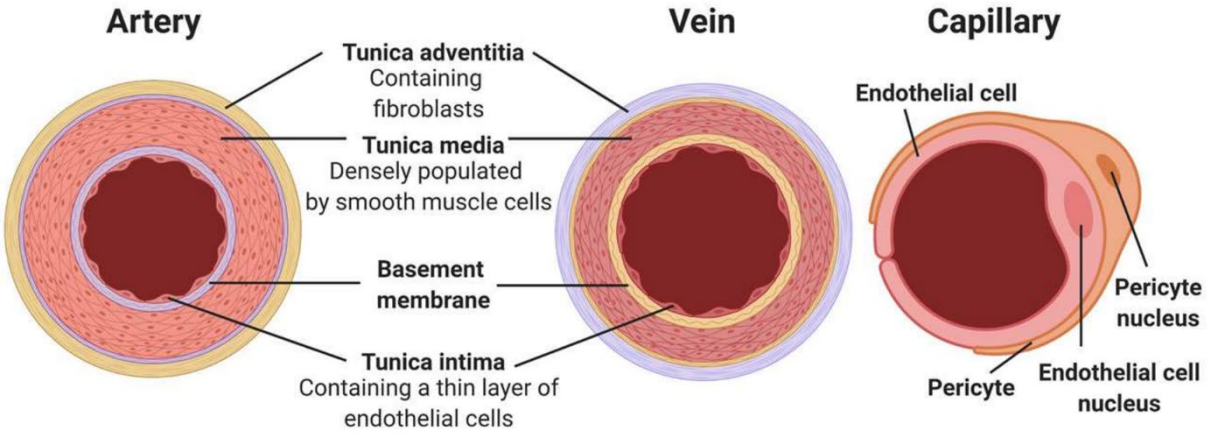

Figure 2. General Transverse view of the anatomical structure of different blood vessels.

Figure was taken from "Current Progress in Vascular Engineering and Its Clinical Applications" by Jouda H. et al, Cells 2022.

ECs possess the remarkable ability to detect and respond to changes in the blood's physicochemical and biological properties, enabling them to perform functions such as preventing blood clotting, supporting immune responses and transmitting signals to regulate cells in other layers [3]. The tunica media is composed of multiple layers of smooth muscle cells (SMCs) embedded in a three-dimensional extracellular matrix (ECM) rich in collagen type-I/III, elastin and proteoglycan. The tunica media contributes significantly to the mechanical strength and vascular reactivity of the blood vessels. Finally, the tunica adventitia contains fibroblasts responsible for depositing a loose ECM enriched in collagen, which primarily serves to anchor the vessel to surrounding tissues and ensure vascular integrity [4].

Lymphatic vessels constitute another crucial component of our body's vascular system, called the lymphatic system, which serves important functions such as maintaining fluid balance, facilitating immune cell transportation, and eliminating waste and toxins [5]. These vessels form an extensive network that parallels our blood vessels, working as a drainage system that

collects excess fluid from the surrounding tissues and returns it to the bloodstream. Lymphatic vessels merge together to form larger structures known as lymphatic ducts.

1.2 Formation of blood vessels

The complex network of the blood vessels is established through two collaborative mechanisms known as vasculogenesis and angiogenesis. Once the vascular system reaches maturity, it enters a quiescent state, a hallmark of adult endothelium [6]. However, the quiescent endothelium can be re-activated under certain physiological circumstances, such as wound healing, placentation, and endometrial regeneration after menstruation, as well as various pathological conditions like tumorigenesis [7].

1.2.1 Vasculogenesis

Vasculogenesis marks the initial phase of blood vessel development [8–10]. The first vascular structure in the embryo is formed from cells of the mesoderm. Mesoderm cells migrate to the yolk sac and differentiate into hemangioblasts. These latter then form clusters called blood islets or blood islands (Figure 3). The peripheral cells of these islets, called angioblasts, differentiate into ECs, while the cells in the center of the islets give rise to hematopoietic cells. The islets merge, forming the primitive vascular plexus. Several factors guide vasculogenesis, including vascular Endothelial Growth Factor (VEGF), Fibroblast Growth Factor 2 (FGF2) and Transforming Growth Factor β1 (TGF-β1) [11].

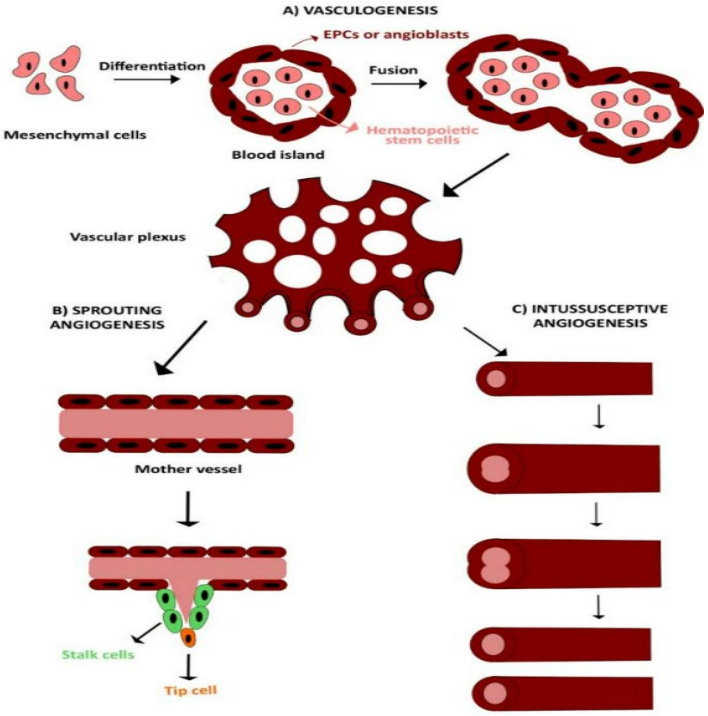

Figure 3. Vasculogenesis (A) and angiogenesis (B-C).

Vasculogenesis involves the de novo formation of blood vessels from aggregated endothelial precursor cells (EPCs or angioblasts), which assemble in structures called blood islands. The fusion of multiple blood islands leads to the formation of the early vascular plexus, from which primitive blood vessels emerge. On the other hand, angiogenesis occurs after vasculogenesis, hence involving the formation of new blood vessels from pre-existing ones. It encompasses two mechanisms: sprouting angiogenesis (B) and intussusceptive angiogenesis (C), which will be further developed below. The figure was taken from "Endothelial TRPV1 as an Emerging Molecular Target to Promote Therapeutic Angiogenesis" by Negri et al, Cells 2020.

Then a series of remodeling and maturation processes occur following the formation of the primary vascular plexus, through a process called angiogenesis (Figure 3), which will be further detailed below. Through angiogenesis, the initial homogeneous plexus differentiates into distinct types of blood vessels, including arteries, capillaries, and veins.

1.2.2 Angiogenesis

Following the establishment of primary vascular networks during embryogenesis, the vasculature undergoes an additional developmental process called angiogenesis [10, 12]. This process involves the proliferation and migration of ECs, as well as the reorganization of cells and the extracellular matrix. Unlike vasculogenesis, where vascular networks are formed from precursor cells, angiogenesis involves the generation of new microvessels from pre-existing ones through either sprouting or splitting (intussusceptive) mechanisms (Figure 3) [12]. Sprouting angiogenesis is a highly regulated process governed by various molecules and signaling pathways that orchestrate each step, starting from the induction of sprout formation (activation phase) to the establishment of arterial/venous identity in the newly formed vessels (maturation phase).

The placenta constitutes one of the principal sites of blood vessel formation which develops during pregnancy and attaches to the uterine wall [13]. It enables the exchange of essential substances like nutrients, oxygen, and waste products between the mother and the developing fetus. This exchange takes place through a specialized structure called the umbilical cord, which connects the fetus to the mother's placenta. The umbilical cord vasculature is composed of one umbilical vein and two umbilical arteries [13] (Figure 4).

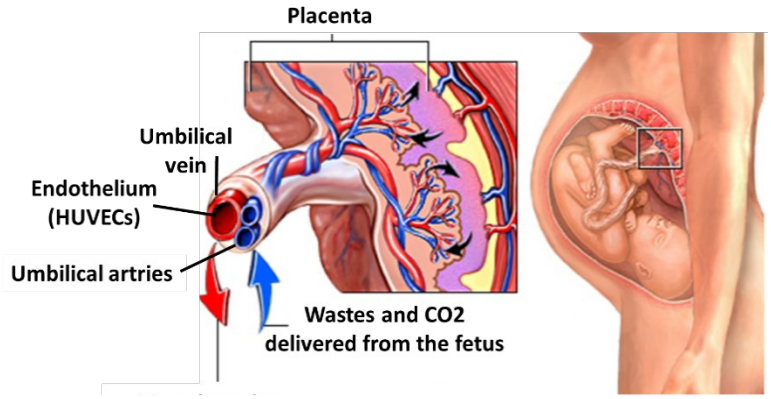

Figure 4. Vasculature of the umbilical cord of the placenta.

The umbilical cord is made up of one vein and 2 arteries. The endothelium constituting the inner lining of the umbilical vein is composed of cells called the human umbilical vein endothelial cells (HUVECs). The umbilical vein carries oxygenated (O2) and nutrient-rich blood from the placenta to the fetus, whilst the umbilical arteries carry carbon dioxide (CO2; deoxygenated blood) and waste products from the fetus back to the placenta for elimination. Figure adapted from https://socratic.org/questions/what-is-the-cord-that-connects-the-fetus-to-the-placenta

Unlike the majority of blood vessels in the body, these vessels play exceptional roles in the maternal-fetal circulation, whereby the umbilical vein carries oxygenated and nutrient-rich blood from the placenta to the fetus [14]. On the other hand, the umbilical arteries carry deoxygenated blood and waste products from the fetus back to the placenta for elimination. Nevertheless, both the umbilical vein and umbilical arteries are lined with specialized cells called human umbilical vein endothelial cells (HUVECs) and human umbilical artery endothelial cells (HUAECs), respectively [14]. HUVECs have been the predominant endothelial cell type used for *in-vitro* endothelial cell model since 1973 [14, 15]. This is primarily attributed to the ease, speed, and cost-effectiveness of their isolation process.

Lymphangiogenesis refers to the process of formation of new lymphatic vessels from pre-existing ones [16]. During lymphangiogenesis, new lymphatic vessels sprout and grow from existing lymphatic vessels or from lymphatic endothelial progenitor cells. In adults, lymphangiogenesis occurs physiologically during the development of the corpus luteum and wound healing [16]. However, lymphatic vessel growth is also associated with a number of pathological conditions, including tumor metastasis, inflammation, and transplant rejection [16, 17]. Adult lymphangiogenesis primarily occurs through the sprouting of new vessels from pre-existing ones [16].

Both angiogenesis and lymphangiogenesis are controlled by various key signaling molecules including VEGF [18], platelet-derived growth factor (PDGF) [19, 20], Angiopoietins [21, 22], bone morphogenetic protein 9 (BMP9)/BMP10 [23] among others [24, 25]. In the following section, I will introduce the key signaling pathways involved in sprouting angiogenesis, followed by focusing on how the formation of blood vessels by sprouting angiogenesis occurs.

1.2.2.1 Key Signaling pathways regulating Angiogenesis

1.2.2.1.1 Vascular endothelial growth factor (VEGF) pathway

VEGF-mediated signaling is considered the main molecular driver in vascular development, governing essential processes such as the early differentiation of angioblasts in vasculogenesis and the induction of sprouting in both normal and pathological angiogenesis. The VEGF family comprises 5 different members in mammals: VEGF-A (prototypical member of the VEGF family), placental growth factor (PlGF), VEGF-B, VEGF-C, and VEGF-D [26]. All five members exert their cellular effects by binding to specific cell membrane-bound tyrosine kinase receptors known as VEGFR1-3 [18]. These receptors exhibit partially overlapping expression patterns, with VEGFR1 predominantly found in monocytes and macrophages, VEGFR2 in vascular endothelial cells and their embryonic precursors, and VEGFR3 in lymphatic ECs [18]. VEGF-A is the predominant pro-angiogenic member of this family, and its effects on endothelial cells are primarily mediated through VEGFR2. VEGF-A can also bind to VEGFR1 with higher affinity than VEGFR2, but this receptor has low kinase activity, thus acting as a decoy receptor [27]. Alternative splicing of VEGFR1 leads to the production of a soluble form of the receptor, which is secreted by various cell types and plays an anti-angiogenic role [26]. In contrast, VEGF-A does not bind to VEGFR3. This receptor, predominantly found in lymphatic vessels, interacts with VEGF-C and VEGF-D, promoting lymphangiogenesis. Upon binding to VEGFR2 on the surface of ECs, VEGF triggers the activation of various pro-angiogenic signaling molecules, promoting EC proliferation, migration, survival, and permeability [18, 28]. Figure 5 illustrates the different signaling pathways induced by VEGF in ECs [18, 28]. The binding of VEGF dimer to VEGFR2 induces receptor dimerization and activation through trans-autophosphorylation at multiple tyrosine (Tyr; Y) sites, including Y951, Y1054, Y1059, Y1175, and Y1214 [18]. These phosphorylated tyrosine residues serve as docking sites for SH2 domain-containing proteins such as phospholipase Cγ1 (PLCγ1), phosphoinositide 3-kinase (PI3K), SH2 domain-containing adaptor prote in B (SHB), and others. PLCγ1 binding to p-Y1175

leads to its phosphorylation and activation. Activated PLCγ then hydrolyzes phosphatidylinositol 4,5-bisphosphate (PIP2), generating diacylglycerol (DAG) and inositol 1,4,5-trisphosphate (IP3). DAG activates protein kinase C (PKC), which in turn activates the mitogenic rapidly accelerated fibrosarcoma (Raf)/mitogen-activated protein kinase kinase (MEK)/extracellular signal-regulated kinase (ERK) cascade, stimulating EC proliferation [18] (Figure 5). IP3 activation results in the release of intracellular Ca2+, mainly from the endoplasmic reticulum (ER), which activates endothelial nitric oxide synthase (eNOS), leading to increased synthesis of the vasodilator nitric oxide (NO) and enhanced vascular permeability [18].

Simultaneously, PI3K activation triggers the generation of membranous PIP3, which in turn activates phosphoinositide-dependent protein kinase (PDK). PDK then recruits and

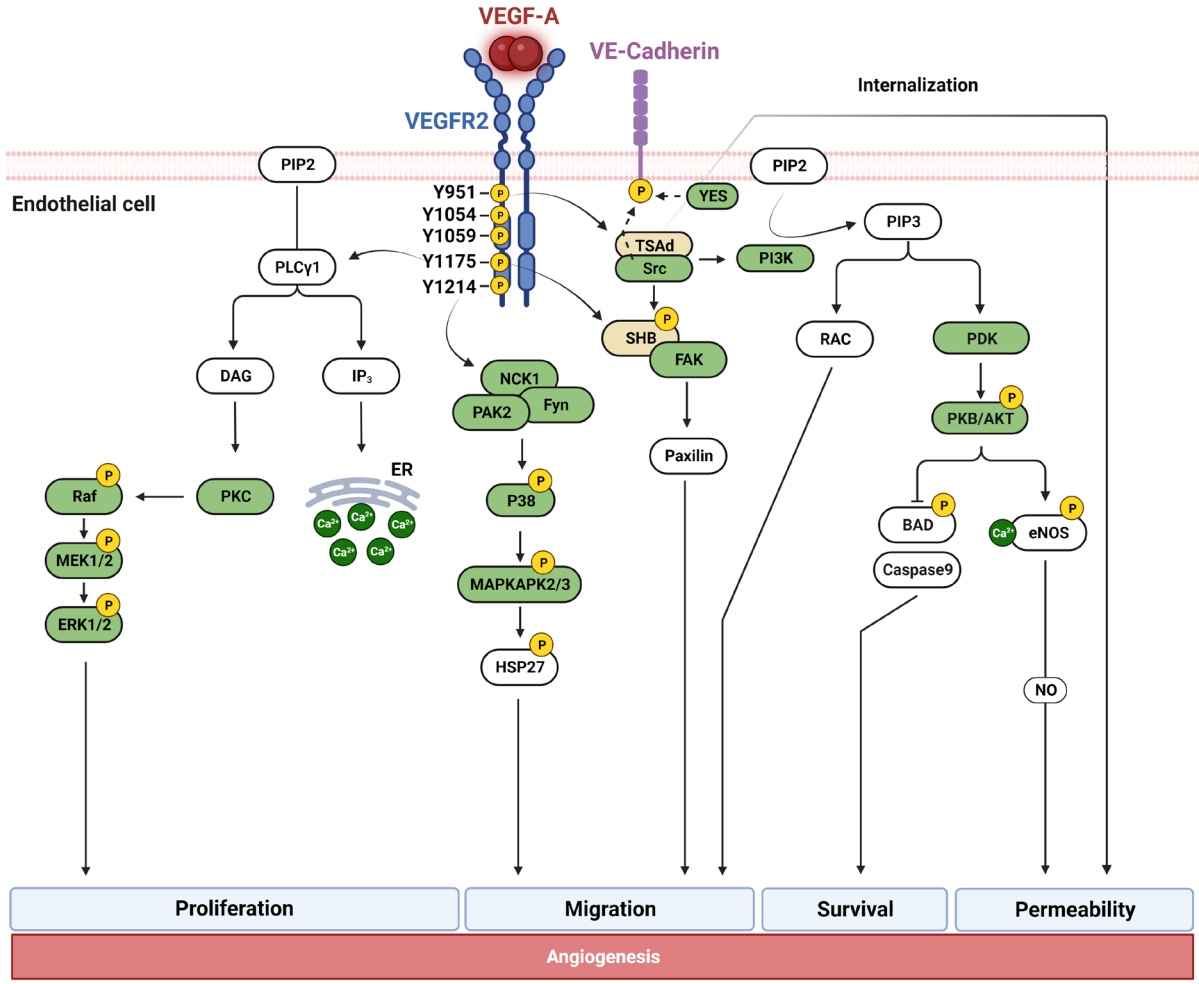

Figure 5. Key signaling pathways downstream of VEGF-A/VEGFR2.

All the pathways and abbreviations are explained in section 1.2.2.1.1. Figure created with biorender.

phosphorylates PKB, also known as AKT. Once activated, AKT phosphorylates various downstream effectors, including eNOS, which enhances vascular permeability [29] and inhibits pro-apoptotic factors such as Bcl2 associated agonist of cell death (BAD) and caspase 9, thus supporting cell survival [30]. Activation of the non-receptor tyrosine kinases Src and

YES, both belonging to the Src kinase family, has been proposed to increase vascular permeability by directly or indirectly phosphorylating vascular endothelial cadherin (VE-cadherin) and disrupting intercellular adherens junctions [31]. Src also plays a role in cell migration by phosphorylating SHB bound to p-Y1175, which interacts with phosphorylated focal adhesion kinase (FAK) and regulates cell attachment and migration [32]. Fyn, another member of the Src kinase family, is recruited to phosphorylated VEGFR2, where it binds to the adaptor molecule non-catalytic region of tyrosine kinase adaptor protein 1 (NCK1), which is bound to p-Y1214. The Fyn/NCK1/ p21-activated kinase 2 (PAK2) complex activates the p38 mitogen activated protein kinase (MAPK) pathway and subsequent activation of MAPKAPK2/3-heat shock protein 27 (HSP27) axis, promoting EC migration [33] (Figure 5).

1.2.2.1.2 Platelet-derived growth factor (PDGF)-PDGFRβ pathway

PDGF was originally discovered in platelets, but it was later found to be secreted by various types of cells [34, 35]. PDGF plays multiple roles in cell regulation, acting as a potent chemoattractant, promoting cell survival, and stimulating cell division in mesenchymal cells such as pericytes, smooth muscle cells, and fibroblasts [36, 37]. One of its crucial functions through its action on fibroblasts is its involvement in wound healing [34, 35].

PDGF exists in five different isoforms: homodimer (PDGF-AA, PDGF-BB, PDGF-CC, PDGF-DD) and heterodimer (PDGF-AB). PDGF signals through two related receptor tyrosine kinases known as PDGFRα and PDGFRβ. All PDGF isoforms share a conserved PDGF/VEGF homology domain. Similar to VEGF, PDGF binding to its receptor triggers dimerization, auto-phosphorylation, and subsequent signal transduction pathways involving molecules like ERK and PI3K/AKT, among other pathways [21].

During angiogenesis, endothelial cells secrete PDGF-BB. This isoform is responsible for attracting and stimulating the proliferation of vascular smooth muscle cells (vSMCs) and pericytes expressing PDGFRβ. These cells then cover the developing blood vessels, promoting vessel maturation [37]. Thus, PDGF plays a critical role in vessel maturation during both embryonic development and wound healing processes.

1.2.2.1.3 Angiopoietin-1-Tie2 pathway

Angiopoietins 1–4 (Ang1–4) are a family of angiogenic growth factors that primarily act through the tunica interna endothelial cell kinase 2 (Tie2) receptor, which is predominantly expressed on ECs. Ang1 functions as a Tie2 agonist, enhancing the structural integrity of blood vessels, while Ang2 predominantly acts as a Tie2 antagonist [38]. Ang1, the most extensively studied member, is secreted by mural cells and plays a crucial role in vessel stabilization by binding to Tie2 [19]. Ang1-Tie2 signaling promotes EC survival by activating the anti-apoptotic PI3K/AKT pathway [39]. It also reduces vascular permeability by strengthening intercellular endothelial junctions. This signaling pathway decreases the phosphorylation levels of junctional proteins such as VE-cadherin and platelet endothelial cell adhesion molecule 1 (PECAM1), facilitating their localization to the junctions [40]. Moreover, Ang1-Tie2 signaling

exhibits anti-inflammatory properties by inhibiting VEGF-induced expression of pro-inflammatory adhesion molecules like intercellular adhesion molecule-1 (ICAM-1) and vascular cell adhesion molecule-1 (VCAM-1) [41]. On the other hand, Ang2 acts as a natural antagonist of Tie2 in a context-dependent manner. Under hypoxic conditions, ECs secrete Ang2 from intracellular stores, antagonizing Tie2 signaling and promoting vascular destabilization [42, 43]. This feature is essential during the activation phase of sprouting angiogenesis. Subsequently, decreased Ang2 secretion shifts the Ang1/Ang2 balance in favor of Ang1, promoting vessel maturation.

1.2.2.1.4 Notch pathway

The Notch pathway serves as a key regulator of vascular sprouting and arteriovenous specification. In mammals, this signaling pathway involves four receptors, namely Notch1 to Notch4, and two families of ligands: (1) Delta-like ligands (Dll), including Dll1, Dll3, and Dll4, and (2) Jagged ligands (Jag), including Jag1 and Jag2 [44, 45]. Both Notch ligands and receptors are transmembrane proteins that primarily signal through trans-activation, where the ligand on one cell binds to its receptor on the adjacent cell, thereby activating Notch signaling in the receptor-presenting cell (Figure 6). The binding of ligands to receptors triggers sequential proteolytic cleavage events of the Notch receptor, leading to the release of the Notch intracellular domain (NICD) by γ-secretase. Subsequently, NICD translocates to the nucleus, where it forms a transcriptional complexes with recombination signal binding protein for immunoglobulin kappa J region (RBPJk or CSL) and the co-activator mastermind-like (MAML) to regulate the expression of target genes [44, 45]. Notch signaling plays a critical role in the regulation of essential processes during sprouting angiogenesis. It is involved in controlling vascular branching by regulating the balance between tip cells and stalk cells, as well as promoting arterial specification.

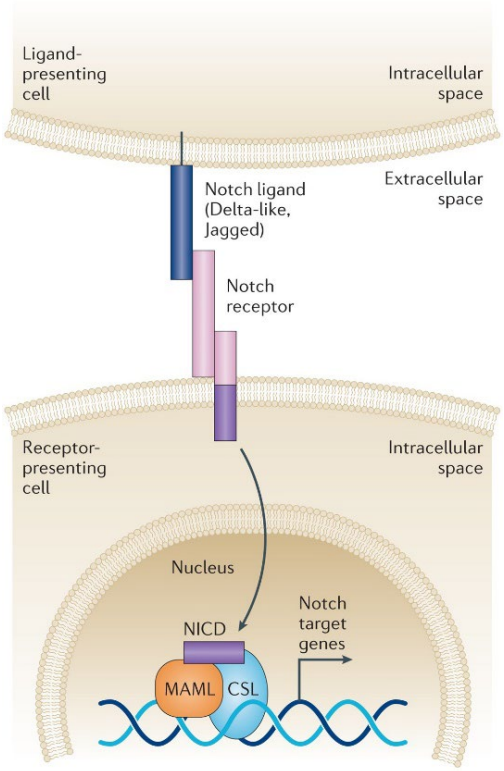

Figure 6. Notch Signaling.

Upon binding to its ligand (Delta-like or Jagged) on an adjacent cell, the Notch receptor undergoes activation. This activation triggers the cleavage of the Notch intracellular domain (NICD), which subsequently translocates to the nucleus. Inside the nucleus, NICD forms a transcriptional complex with recombination signal binding protein for immunoglobulin kappa J region (CSL or RBPJk) and mastermind-like (MAML), resulting in the regulation of Notch target genes. Image taken from "Therapeutic modulation of Notch signalling — are we there yet?" by Andersson and Lendahl, Nature Reviews Drug Discovery, 2014.

1.2.2.1.5 TGFβ/BMP Signaling Pathway

TGFβ superfamily comprises 33 different ligands including TGFβ1 ,BMP9 and BMP10, which play important roles in vascular development and maturation [46, 47]. More details about the signaling of this family will be discussed in a separate dedicated chapter.

1.2.2.2 Sprouting Angiogenesis

In case of hypoxia during physiological processes like development and wound healing, as well as in pathological conditions such as tumorigenesis, the deprived parenchymal cells secrete the master proangiogenic factor VEGF to attract an adequate blood supply by promoting the formation of new blood vessels towards the hypoxic area [12]. The spatial distribution of VEGF in the surrounding microenvironment plays a crucial role in guiding the differentiation of endothelial tip cells, which are located at the leading edge of the growing vasculature and characterized by long filopodial protrusions enriched in VEGFR2 [48] (Figure 7). Consequently, tip cells respond to the VEGF gradient by initiating directed migration towards the hypoxic region [49]. Prior to migration, ECM degradation occurs through the action of matrix metalloproteinases (MMPs). Subsequently, this clears the path for migrating ECs and facilitates their invasion into the surrounding tissue. VEGF also increases vascular permeability through NO-mediated vasodilation, allowing plasma proteins to extravasate and form a provisional scaffold that supports the migration of ECs [12]. Additionally, VEGF or hypoxia (independent of VEGF) disrupt the interaction between ECs and mural cells by enhancing the production of Ang2 from ECs, which acts as an antagonist of the Tie2 receptor. These changes

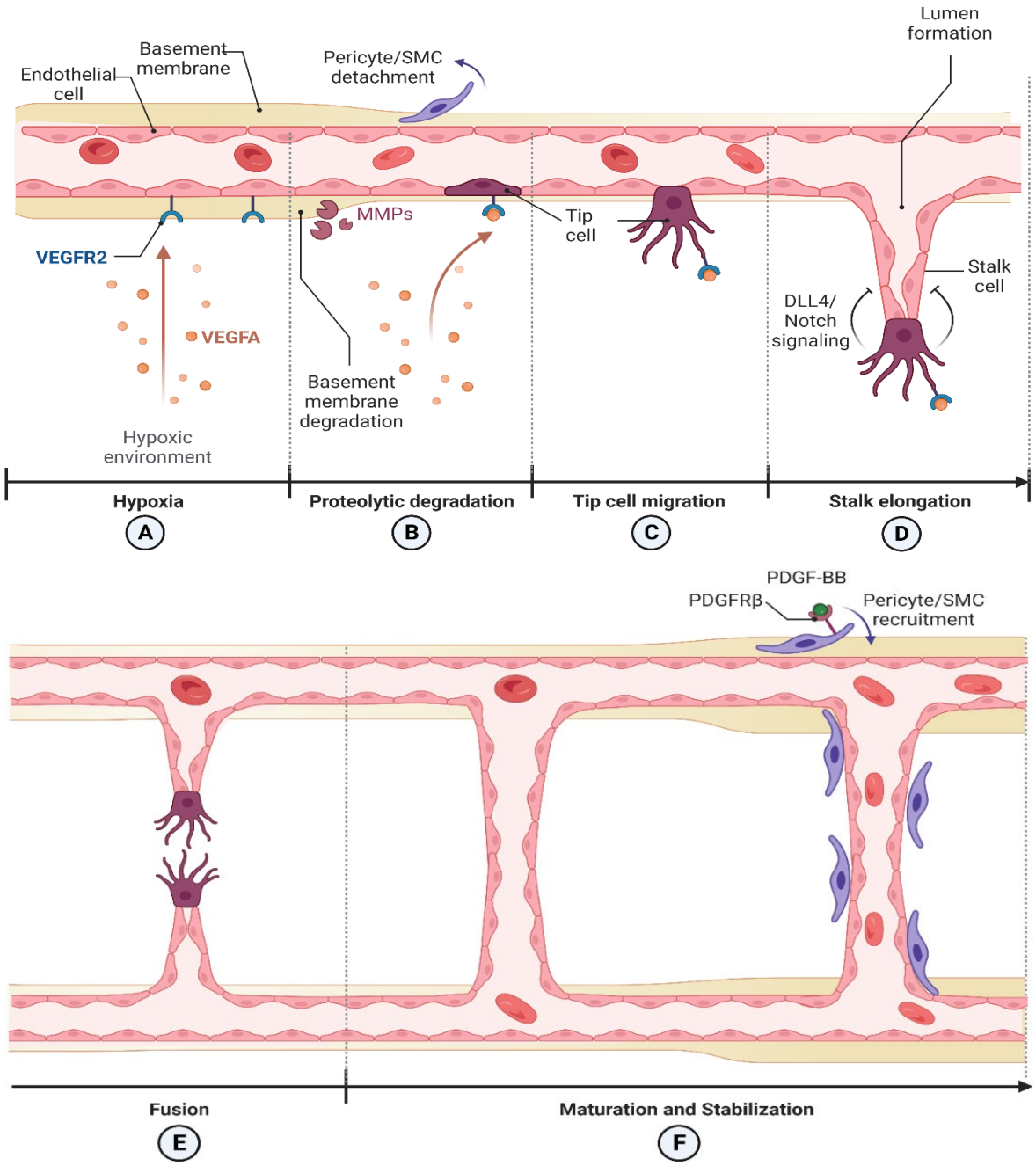

Figure 7. Sprouting angiogenesis.

(A) Under local hypoxic conditions, the hypoxic tissue releases VEGF-A, which serves as a trigger for angiogenesis. (B) This initiates the degradation of the extracellular matrix (ECM) surrounding the blood vessels through the action of matrix metalloproteases (MMPs) which enhances detachment of mural pericytes and smooth muscle cells (SMCs) accompanied with the selection of tip cells and stalk cells. (C) Tip cells, located at the leading edge of the sprout, respond to the gradient of VEGF-A through their extensive filopodia and migrate in the direction of the VEGF-A gradient. (D) On the other hand, stalk cells, positioned behind the tip cells, actively proliferate and ensure the elongation of the sprout while maintaining a connection with the existing vessel. Maintaining the appropriate balance between tip and stalk cells is regulated by Dll4-Notch signaling. (E) The sprout continues to elongate until it fuses and forms a nascent vessel with a lumen, which eventually becomes perfused, leading to improved oxygenation of the surrounding tissue. (F) Following perfusion, the nascent vessel undergoes maturation and stabilization. This is achieved through the secretion of new ECM components and the recruitment of mural cells, which provide structural support to the vessel. Figure adapted from biorender.

weaken the interactions between ECs and the extracellular matrix, facilitating EC migration [42, 50]. As the leading tip cell migrates, the sprout extends through the proliferation of trailing stalk cells stimulated by VEGF. The sprouts continue to elongate until tip cells at the front interact with each other through their filopodia, resulting in fusion and the formation of nascent vessels (Figure 7). At this stage, cell migration ceases, and lumen formation takes place through a complex process involving cell repulsion within endothelial cords, rearrangement of cell junctions, and changes in cell shape [12].

Maintaining the appropriate balance between tip and stalk cells during sprouting angiogenesis is crucial for efficient and controlled branching. Among the various factors implicated in regulating tip/stalk cell specification, the Notch signaling pathway mediated by Dll4 is the most extensively studied [44]. In response to proangiogenic signals, tip cells upregulate Dll4, acquiring an invasive and migratory phenotype. Binding of Dll4 to Notch1 receptors on neighboring cells activates Notch signaling and induces a stalk cell phenotype in these cells [51]. As a result, these cells become less responsive to pro-angiogenic signals mediated by VEGF. This effect is mediated through the upregulation of target genes of the HES (hairy and enhancer-of-split) and HEY (Hairy Ears, Y-Linked) family of transcription factors by Notch1. HES/HEY factors downregulate the expression of Dll4 and the VEGF receptors VEGFR2 and VEGFR3, while upregulating the expression of the decoy receptor VEGFR1 [51, 52]. This molecular cascade helps to maintain the balance between tip and stalk cells during sprouting angiogenesis. In addition to Dll4, another ligand called Jag1 is also involved in regulating tip/stalk cell specification. Tip cells express high levels of Dll4 and low or no Jag1, while stalk cells show the opposite pattern of ligand expression. Jag1 on stalk cells acts as an antagonist by competing with Dll4 for binding to Notch1 on tip cells [49].

1.2.2.3 Intussusceptive angiogenesis

Intussusceptive angiogenesis, a distinct mode of angiogenesis, is characterized by the splitting of pre-existing blood vessels to generate smaller vessels [53] (Figure 3). Interestingly, intussusceptive angiogenesis has also been identified in small arteries and veins, where it plays a role in vascular pruning and the alteration of branch angles in bifurcating vessels, highlighting its significance in vascular remodeling [54]. It involves the intraluminal protrusion of endothelial cells towards each other, forming an intussusceptive pillar. Subsequent formation of junctional complexes and infiltration of interstitial components, including pericytes and collagen-secreting myofibroblasts, facilitate the separation of the two channels. As this process progresses longitudinally, the pillar grows in size, eventually leading to the splitting of the entire capillary [55]. Despite its importance, the molecular mechanisms underlying intussusceptive angiogenesis remain largely unknown.

Chapter 2. The TGF-β Superfamily

2.1 Ligands of the TGF-β Superfamily

2.1.1 Diversity

The transforming growth factor beta (TGF-β) family was discovered in the early 1980s [56–58]. Back then, the term "transforming growth factor" was chosen due to the observation that these factors were first secreted by transformed fibroblasts infected with the RNA Moloney sarcoma virus, and that these factors possess different transforming properties, depending on the different cell lines used. These factors were then found to be TGF-β [59].

Nowadays, the TGF-β superfamily comprises 33 identified members in mammals encoded by TGF-β related genes that have been identified as a result of human genome sequencing project. These include TGF-β isoforms (TGF-β1, TGF-β2, and TGF-β3), bone morphogenetic proteins (BMPs), growth and differentiation factors (GDFs), activins/inhibins, nodal, and anti-Müllerian hormone (AMH) (Figure 8) [60, 61].

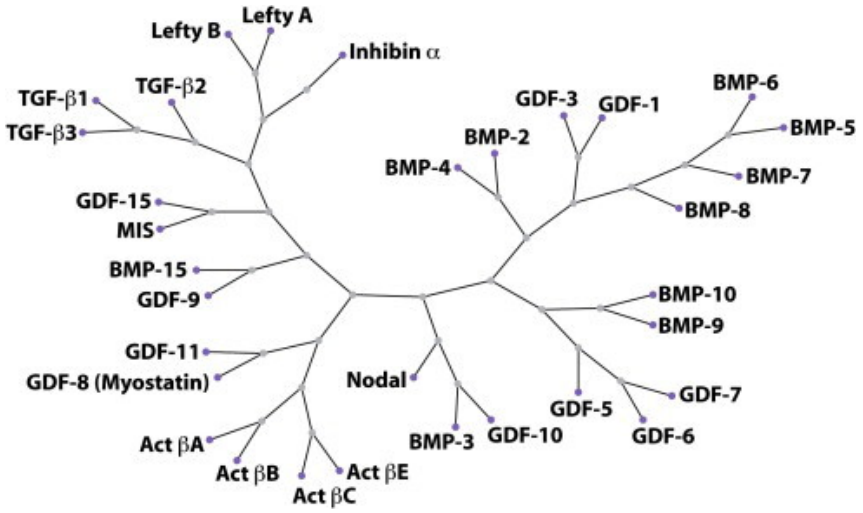

Figure 8. Phylogenetic tree of the 33 TGF-β superfamily ligands in humans.

The tree was generated through alignment of the C-terminal mature domains. Figure adapted from "Structural studies of the TGF-βs and their receptors" by Hinck, FEBS Letters, 2012.

All members of the TGF-β superfamily are structurally related proteins that share a conserved cysteine knot structure. However, they can be broadly categorized into two main subfamilies based on their sequence similarity and signaling properties: the TGF-β subfamily and the BMP subfamily. The former includes the 3 TGF-β isoforms TGF-β1, TGF-β2, and TGF-β3, along with activins (A and B), nodal, myostatin, and several GDFs. On the other hand, the BMP subfamily comprises all 10 BMPs (BMP2-10 and BMP15), AMH, and the remaining GDFs [62].

2.1.2 Synthesis, Maturation, and Structure

TGF-β family proteins are synthesized as precursor molecules (pre-pro-proteins) consisting of an N-terminal signal peptide that directs them towards the secretory pathway, a ~250-residue pro-domain that ensures proper folding, and a ~110-residue C-terminal mature polypeptide (also called the growth factor (GF) domain) that binds cognate receptors [63]. After signal peptide removal, dimerization of precursor molecules occurs through the formation of intermolecular disulfide bonds in the endoplasmic reticulum (ER), resulting in homo- and heterodimeric pro-proteins [61]. The majority of TGF-β family proteins contain 7-9 cysteine pattern, where the fourth cysteine in this pattern plays a crucial in the dimerization process [61]. However, in the exceptional cases of GDF3, GDF9, BMP15, lefty A, and lefty B, these members lack the fourth cysteine in the cysteine pattern and thus have eight or six cysteines, and are thus assumed not form dimers [61]. Homo- and heterodimeric pro-proteins are further processed by proteolytic cleavage occurring in the Golgi apparatus or in the extracellular space at basic residues by furin-like pro-protein convertases, thus separating the prodomain from the mature polypeptide, which often remains non-covalently associated to each other [63, 64]. Mature processed dimers are then secreted into the extracellular space to act via their specific receptors [64]. Notably, the association of the prodomains with the mature dimer forms a complex that is not always active. For instance, TGF-β [65], GDF8 (myostatin) [66], and GDF11 [67] are inactive when the prodomains are present. In contrast, BMP4 [68], BMP7 [69], and BMP9 [70] are active when associated with their prodomain.

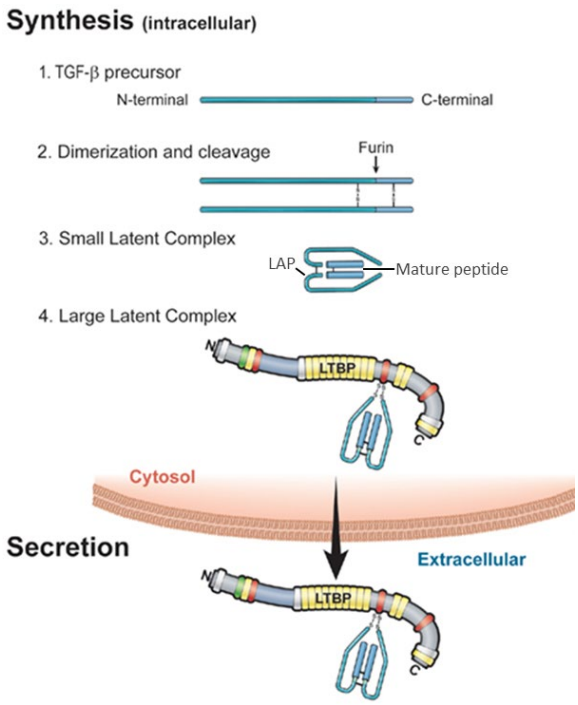

Figure 9. Schematic illustration for synthesis of TGF-ß1, secretion and activation.

(1) TGF-ß is synthesized as a pre-pro-protein precursor; (2) Two TGF-ß precursor proteins dimerize through disulfide linkages forming a TGF-ß dimer that is cleaved by furin convertases; (3) Resulting product yields a small latent TGF-ß complex with latency-associated peptide (LAP; light blue) and mature TGF-ß peptide (dark blue) that are connected by non-covalent bonds; (4) The large latent complex is formed by covalent linking between small latent complex and latent TGF-ß binding protein (LTBP), then secreted and incorporated into extracellular matrix. Figure was adapted from "Biological Significance of Local TGF-ß Activation in Liver Diseases" by Hayashi, Front Physiol., 2012.

The most studied member for its synthesis and secretion is TGF-β1 (Figure 9). The mature dimer of TGF-β1 is associated with its prodomain called LAP (latency-associated peptide), which controls TGF-β activity, bioavailability and conformation [65]. Activation of TGF-β1 can be achieved by releasing the latent complex through exposure to low or high pH, or, more physiologically, by the cleavage of LAP by certain proteases, competition by certain matrix molecules, or through Integrins [71].

Three-dimensional structures have been resolved for more than 15 members of the TGF-β family, either in complex with receptors, antagonists, prodomains, or in their unbound form [72]. Figure 10 (A and B) shows structures of TGF-β1 [73] and BMP9 [74] pro-complexes which structurally highlight TGF-β family diversity [63]. The prodomain contains an arm domain flanked by shorter, partially α-helical, amino- and carboxy-terminal straitjacket elements. TGF-β1 and BMP9 pro-complexes reveal overall crossed-arm and open-arm butterfly-like shape conformations, respectively, with markedly different orientations between arm domain monomers. In the crossed-arm conformation of pro-TGF-β1, the arm domains point toward one another and dimerize at the bowtie.

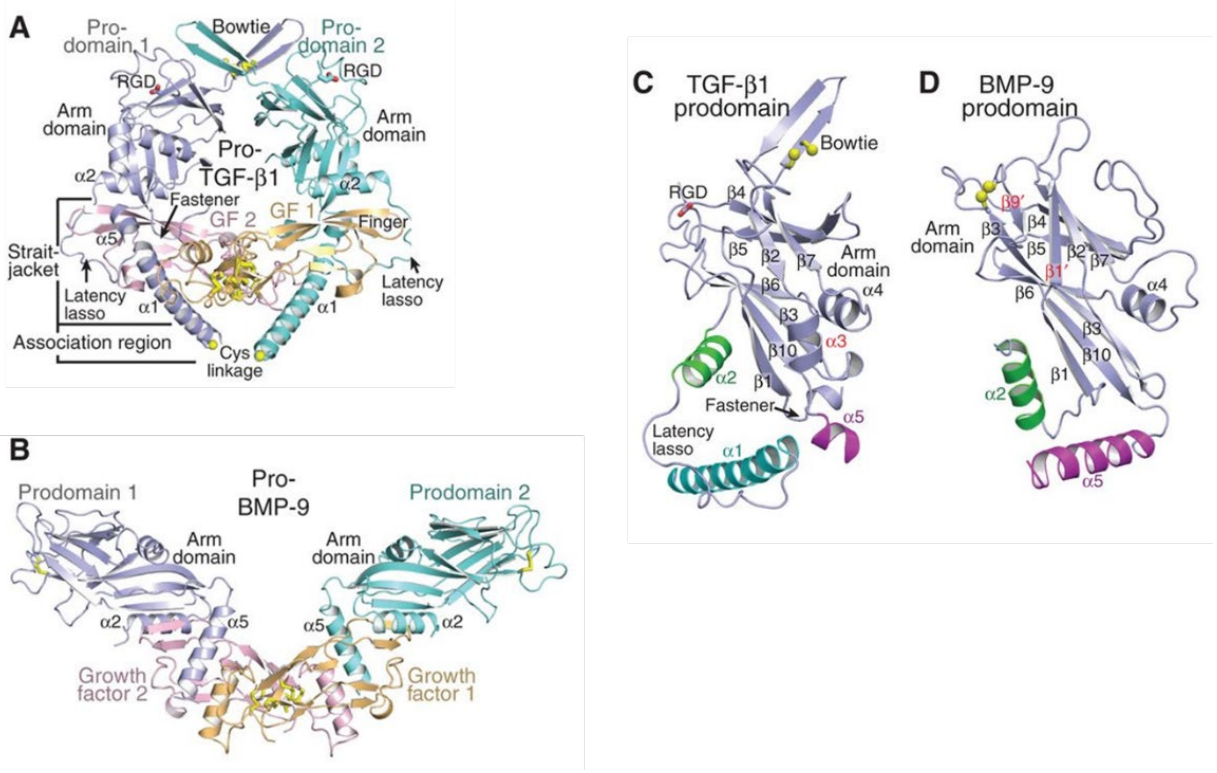

Figure 10. Crystal structures of pro-TGF-β1 and pro-BMP9.

*(**A, B**) Crystal structures in cartoon representations of pro-TGF-β1 (Shi et al. 2011) (A), and pro-BMP-9 (Mi et al. 2015) (B) in identical orientations with superimposition on GF dimers. (**C, D**) Crystal structures in cartoon representations of the prodomain structures of TGF-β1 (C) and BMP9 (D) monomers in identical orientations after superimposition on the arm domains. Arm domain secondary structural elements common or unique to TGF-β1 and BMP-9 are labeled in black and red, respectively. TGF-β1 bears a latency lasso, an extended loop that connects the α1 and α2 helices, as well as Arginyl glycyl aspartic acid (RGD) motifs which are absent in BMP9. All figures were adapted from "Structural Biology and Evolution of the TGF-β Family" by Hinck, Cold Spring Harb Perspect Biol., 2016.*

Despite the clear differences in orientation, TGF-β1 and BMP9 arm domains display two β-sheets (resembling fingers) that partially overlap in the hydrophobic core (Figure 10C, D). Long twisting loops along with an α4-helix (resembling a wrist) cover the remainder of the core. Notably, from the C-terminus of the α1-helix of TGF-β1, the prodomain wraps around the fingertips of the ligand by disulfide bonds with a structure named latency lasso (Figure 10 A, C). This latter, along with the α1-helix and the fastener region, play important roles in

inhibiting TGF-β signaling by blocking both the type-I and type-II receptor binding sites in what is referred to as the latency [73]. In contrast, BMP ligands lack this segment and the associated disulfide bond [75]. Additionally, TGF-β1 and -β3 contain arginyl-glycyl-aspartic acid (RGD) motifs defining their ability to bind and to be activated by integrins [76].

Despite these differences, all family members share a centralized cysteine knot formed by specific disulfide bonds, enhancing the stability and folding of the ligand. This cysteine knot is a characteristic feature for TGF-β family and is also found in other growth factors as well such as PDGF and VEGF [72]. While some TGF-β family proteins may freely diffuse after secretion, the majority of mature ligand complexes are often locally retained in the ECM of tissues such as basement membranes, cartilage and bone which act as reservoirs for TGF-β family proteins [64]. Specific ECM proteins, (e.g. collagens, glycoproteins, fibronectin, thrombospondin and fibrillins) associate with these ligands and selectively bind and retain them [77]. These associations regulate the deposition, activation, and release of TGF-β family proteins, influencing their signaling and cellular responses. Proteolytic degradation of ECM proteins, either during physiological remodeling or in response to injury or invasion, can lead to the release and activation of these ligands, further modulating their biological effects. Therefore, ECM proteins play a crucial role in both sequestering and facilitating the activities of TGF-β family proteins based on their interactions and secreted ligand complexes ensuring their mode of action in a highly controlled fashion, rather than by free diffusion.

2.1.3 Brief Summary on the Functional Diversity of TGF-β Superfamily

TGF-β family proteins display multiple roles in cell proliferation, differentiation, growth, migration, apoptosis and extracellular matrix production and are thus considered maintenance factors for homeostasis [61]. The biological effects of TGF-β family proteins are highly contextual, where the same cell type may show different or opposite responses to the same ligand under different biological contexts [78]. Some TGF-β family ligands are made available to cells with concentration gradients *in-vivo*, resulting in graded effects of cell differentiation and function by the responsive cells. Furthermore, different ligands activate specific groups of genes in a manner that depends on their concentration, which is crucial for determining the fate of cells during normal development. As indicated by their name, the BMP/GDF subfamily was initially identified through the study of BMP2 and BMP4, which showed the ability to induce bone formation and impact skeletal development [79, 80]. However, many other BMP/GDF proteins were named based on sequence similarities without fully understanding their precise functions. It is important to be cautious when assuming their biological roles solely based on their names, particularly for BMPs or GDFs. However, as recent studies in the past two decades discovered the diverse functions of BMPs, which go beyond bone development to include organs like the kidneys, pancreas, and cardiovascular system, these ligands were proposed to be alternatively named “body” morphogenetic proteins [81]. In later sections of this chapter, I will further discuss the diverse roles and functions of various

TGF-β family proteins from a signaling perspective in different contexts, with a particular focus in chapter 3 on the roles of BMP9 and BMP10 in endothelium.

2.3 Receptors of TGF-β Superfamily

TGF-β superfamily ligands elicit a classical membrane-to-nucleus signal through transmembrane receptor complexes composed of two type-I and two type-II Serine/Threonine kinase receptors, in addition to a type-III co-receptor that lacks any enzymatic activity. In humans, TGF-β superfamily receptors comprise 7 type-I receptors, called activin receptor-like kinase (ALK) 1-7 and 5 type-II receptors (ActRIIA, ActRIIB, BMPRII, AMHRII and TGFBRII). Figure 11 illustrates the key domains of these receptors [82]. The extracellular domain, which is on the N-terminal side of the peptide sequence, is N-glycosylated and contains at least ten cysteines that determine the structure of this domain [83]. Three of these cysteines form a characteristic region of receptors of this family called "cysteine box" and are located near the transmembrane domain [83]. These receptors have a single transmembrane region.

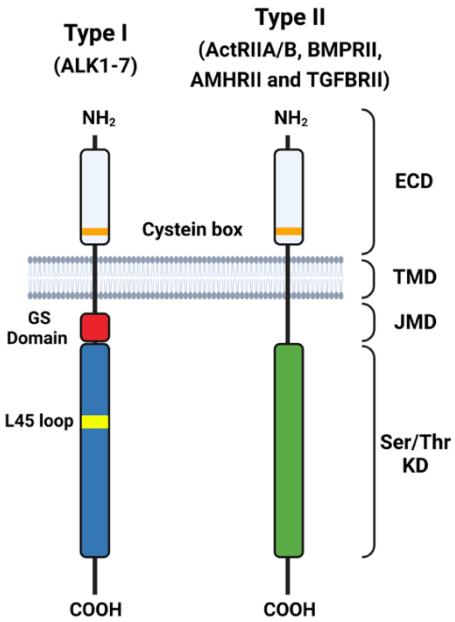

Figure 11. Schematic diagram for the key features of type-I and type-II TGF-β superfamily receptors.

Both receptor types are transmembrane proteins with an amino-terminal signal peptide, a small extracellular domain (ECD), a single hydrophobic transmembrane domain (TMD), and an intracellular region composed of a juxtamembrane domain (JMD) and a serine/threonine kinase domain (Ser/Thr KD). A cysteine box is found in the extracellular domain of both receptor types. Type-I receptors differ from the Type-II receptors mainly by the presence of a GS box (required for activation) and L45 loop that defines specificity for kinase substrates. Figure created with Biorender.

For the type-I receptors, the intracellular domain can be divided into 3 subdomains: the Glycine/Serine (GS) box, the kinase domain and the cytoplasmic tail (Figure 11). The GS box is a highly conserved domain of 30 amino acids and is considered a characteristic of type-I receptors, located just before the kinase domain. This region takes its name from the characteristic sequence it contains (SGSGSG). Moreover, this region contains the sites of phosphorylation of the type-I receptor by the type-II receptor [84]. The kinase domain has a canonical sequence of serine/threonine kinases [85]. Structural analysis of the kinase domains of these receptors have revealed the presence of a β3-sheet involved in binding to ATP [86, 87] and an L45 loop specific for type-I receptors that allows interaction with substrates [88].

In addition to the type-I and type-II receptors, TGF-β superfamily receptors comprises two high molecular weight glycoprotein co-receptors, betaglycan and endoglin (ENG or CD105) [89]. Both co-receptors comprise a long extracellular domain, a transmembrane domain and a short cytoplasmic domain without kinase activity. Despite the absence of this latter, both

co-receptors play a role in potentiating the responses to selected ligands. This is the case for the 3 TGF-β isoforms by betaglycan and BMP9 and BMP10 by ENG [89]. A key difference between both co-receptors is that betaglycan exists as a monomer and forms 1:1 complexes with growth factors, whereas ENG exists as a dimer and forms 2:1 complexes with the growth factors [90]. In the absence of a ligand, type-I and type-II receptors can be found as monomers, homo- or hetero-dimers. For instance, in the absence of TGF-β, TβR2 can form homodimers [91]. This homodimer formation has also been shown for the TGF-β type 1 receptor (ALK5) [92], but also for BMP receptors (ALK3, ALK6 and BMPR2) [93]. It has been shown that heterocomplexes between the two receptor types are detected to a low degree in the absence of ligand and significantly enhanced upon ligand binding [94]. Importantly, even though these receptors show a certain level of preformed complexes, their signaling is inhibited in the absence of ligands due to interactions with other proteins [95, 96].

2.3 SMAD Proteins as Signaling Effectors

Suppressor of Mothers Against Decapentaplegic (SMADs) are a family of transcription factors that are critical for transmitting signals to the nucleus from the TGF-β superfamily in response to activated TGF-β family receptors [97]. Functional studies have demonstrated that this family of transcription factors comprises 3 classes of proteins in humans, which range from about 400 to 500 amino acids in length, with structural and functional differences: (1) receptor-regulated SMADs (R-SMADs) comprising SMAD1, SMAD2, SMAD3, SMAD5 and SMAD8, (2) the common mediator (co-SMAD) SMAD4 and (3) inhibitory SMADs (I-SMADs) SMAD6 and SMAD7 [98].

R-SMADs and SMAD4 possess a structure characterized by two conserved globular domains referred to as Mad homology 1 (MH1) and MH2. These domains, located at the N-terminal and C-terminal ends, respectively, are joined together by a distinct linker region. The MH1 domain primarily governs the binding to DNA and contains the NLS (nuclear localization sequence), whereas the MH2 domain facilitates interactions with different proteins, including type-I receptors (in the case of R-SMADs), other SMADs, and nuclear transcriptional partners (Figure 12). The linker region consists of a proline-rich flexible segment and phosphorylation sites recognized various types of protein kinases including MAPKs, cyclin dependent kinases (CDKs), among others [99]. Moreover, the linker region of R-SMADs contains binding sites for SMAD ubiquitination-related factor (Smurf) ubiquitin ligases for polyubiquinitation, and in SMAD4, a nuclear export signal (NES) important for the regulation of intracellular dynamics of SMAD4 [97]. The SMAD MH2 domain is highly conserved in all SMADs and is one of the most versatile protein-interacting modules in signal transduction [97]. In R-SMADs, MH2 domains possess a characteristic Ser-Ser-X-Ser (SSXS) motif in their C-terminal extremities that is phosphorylated by activated type-I TGF-β family receptors, leading to activation of R-SMADs (Figure 12). On the other hand, I-SMADs are structurally distinct from R-SMADs and SMAD4. The MH1 domain and the C-terminal type-I receptor phosphorylation site are missing in SMAD6 and SMAD7, while the rest of the MH2 domain is conserved. This allows SMAD6 and SMAD7 to compete with R-SMADs for receptor and SMAD4 binding, but without being

phosphorylated themselves [97, 100–102]. In the basal state, SMAD4 is dispersed throughout the cell and undergoes a continuous shuttling between the cytoplasm and the nucleus [103]. However, R-SMADs are predominantly concentrated in the cytoplasm which is thought to result from the action of cytoplasmic SMAD-binding factors [97, 103, 104].

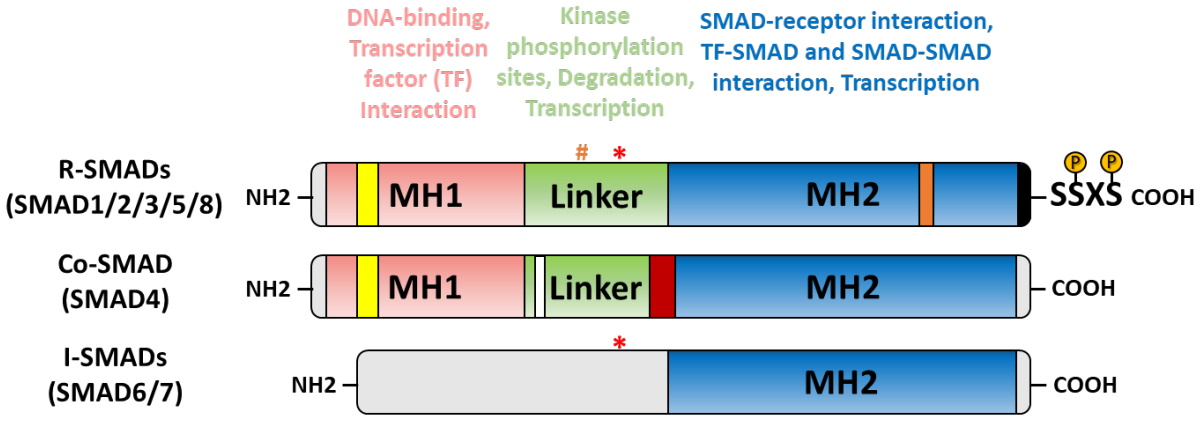

Figure 12. Main functional domains of different human SMAD isoforms.

Yellow rectangle in MH1 domain represents the nuclear localization sequence (NLS). C-terminal SSXS motif bearing type-I receptor phosphorylation sites is highlighted in black within R-SMADs. Orange rectangle within R-SMADs MH2 domain represents the L3 loop. White rectangle in the linker region represents the nuclear export signal (NES). * *represents Proline-Tyrosine rich motif (PPXY).* # *represents phosphorylation sites for MAPK, CDKs and other kinases. All text abbreviations are explained in the main text. Figure was generated using Microsoft PowerPoint, and the details presented in the figure were adapted from the references mentioned in the main text of this paragraph.* Ⓟ *= phosphorylation. Figure created in PowerPoint.*

2.4 Signaling by TGF-β Superfamily

2.4.1 Canonical SMAD Signaling

2.4.1.1 Ligand Binding and Formation of Tetrameric Receptor Complexes

Ligand binding promotes the formation and stabilization of the heterotetrameric receptor complexes composed of two type-I receptors and two type-II receptors, with the dimeric ligand interfacing with the four receptor extracellular domains [64]. Ligand-induced complex formation rapidly leads to phosphorylation of GS domain residues of the type-I receptor by the type-II receptor, which was first demonstrated for TGF-β [105]. The authors showed that TGF-β binding induces the phosphorylation of ALK5 at serine and threonine residues of the GS box (Thr185, Thr186, Ser187, Ser189, and Ser191). The phosphorylation of the type-I receptor by the type-II receptor leads to conformational changes opening the L45 loop which makes the catalytic site accessible to substrates and adenosine triphosphate (ATP) [106]. Notably, point mutations in the GS box, e.g., T204D for ALK5, results in the appearance of a negative charge (aspartic acid) in place of a neutral amino acid (threonine). This negative charge mimics the phosphorylation of the type-I receptor on its GS box and results in a constitutively active

receptor, i.e. whose activity does not depend on the presence of the ligand or on the kinase activity of the type-II receptor [84]. After activation of type-I receptors by phosphorylation of their GS box by type-II receptors, signal transduction is initiated.

2.4.1.2 Activation of R-SMADs by Phosphorylation and Oligomerization

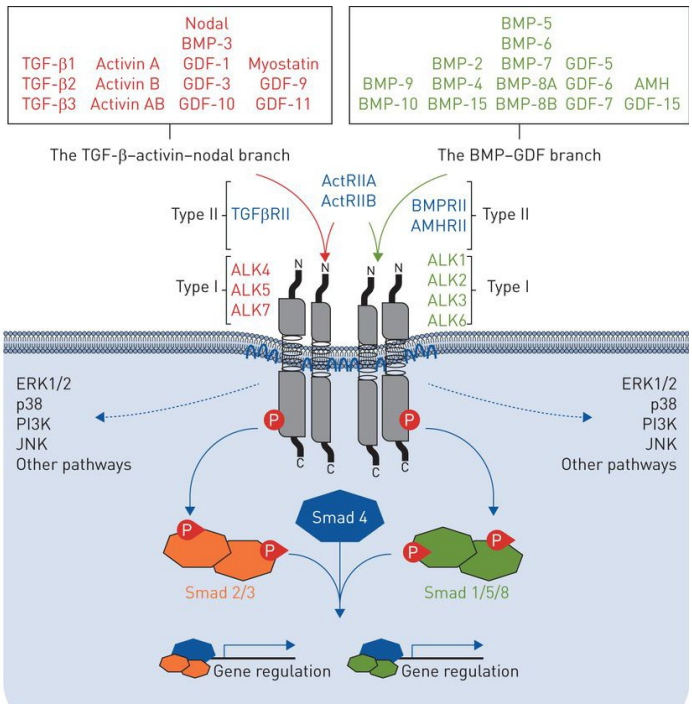

Figure 13. General signaling pathways induced by TGF-β superfamily ligands.

The TGF-β-activin-nodal branch signals through TGF-β receptors and activates SMAD2/3 mediators, while the BMP-GDF branch signals through BMP receptors to activate SMAD1/5/8 pathway. Specific type-I and type-II receptors participating in each signaling branch, along with additional non-canonical pathways (will be further demonstrated in section 2.4.2) are specified in the figure. Figure was taken from "Targeting transforming growth factor-β receptors in pulmonary hypertension" by Guignabert and Humbert, Eur Respir J., 2021.

The epitope in the type-I receptor family that is responsible for the selectivity in R-SMAD phosphorylation is the L45 loop of the kinase domain (Figure 11), which binds to the L3 loop and the adjacent α-helix 1 in the carboxy-terminal MH2 domains of R-SMADs [88, 107]. The binding is stabilized by interactions between the phosphorylated GS domain of the type-I receptor and SMADs. Upon binding to the dimeric ligands and formation of heterotetrameric receptor complexes, the type-I receptor kinases phosphorylate the Serine residues in the SSXS (X=any amino acid) motif at the carboxy-terminal end of the R-SMADs [108]. SMAD1, and its close homologs SMAD5 and SMAD8, are phosphorylated by BMP receptors to mediate BMP responses, whilst SMAD2 and its close homolog SMAD3 are phosphorylated by TGF-β receptors to mediate TGF-β and activin responses [107] (Figure 13). However, the specificity in R-SMAD phosphorylation is not absolute. For instance, TGF-β has been also shown to phosphorylate SMAD1 and SMAD5 via ALK5 [109], or ALK2 and ALK3 [110]. Moreover, BMP2 and BMP9 were shown to induce phosphorylation of SMAD2/3 via ALK3 and ALK1, respectively [111, 112].

Receptor-mediated phosphorylation at the C-terminal region of R-SMADs creates a binding site for SMAD4 [113]. Subsequently, R-SMADs dissociate from the type-I receptor to form trimeric complexes with SMAD4. For TGF-β and activin-specific SMADs, such complexes can consist of one molecule of SMAD4 together with two SMAD2, two SMAD3, or one each of SMAD2 and SMAD3. The same scenario also applies to the BMP-specific SMADs [114]**.** SMAD

complexes are then translocated to the nucleus by specific mechanisms, where they regulate the transcription of their target genes, in cooperation with other co-factors (co-repressors or co-activators) [115].

2.4.1.3 Integration of the Signal by Endocytosis of the Receptors

An important step in signal transduction is the endocytosis of receptors. Receptors of the TGF-β superfamily ligands undergo endocytosis after ligand binding and formation of heterotetrameric complexes. This internalization can occur in two ways: endocytosis by clathrin-coated pits [116] or endocytosis by caveolae [116–118]. Clathrin is a cytoplasmic protein recruited to the inner surface of the cytoplasmic membrane where it induces the formation of internalization pits, in partnership with dynamin. The Adaptor Protein 2 (AP2) binds clathrin and participates in endocytosis. The internalized vesicles then lose their clathrin envelope and become early endosomes [119]. Internalization via clathrin-coated pits into early endosomes has shown to be necessary for SMAD activation [120]. TGF-β receptor endocytosis is the most comprehensively studied [114, 121] (Figure 14). Clathrin-mediated internalization of TGF-β receptors directs them into early endosomes. Within these endosomes, they interact with various mediators, including Disabled-2 (Dab2), cytoplasmic form of promyelocytic leukemia (cPML), and SMAD anchor for receptor activation (SARA), which facilitates the presentation of SMAD2, and to some extent SMAD3, to ALK5, leading to the promotion of their phosphorylation enhancing SMAD-dependent signaling [122–124] (Figure 14A). In an analogous manner, endofin acts as an anchor for SMAD1 in signaling via BMP receptors [125].

Moreover, TGF-β receptors which are internalized into early endosomes have the capability to be sorted into recycling endosomes, allowing them to return to the cell surface for another round of ligand stimulation (Figure 14C). This recycling mechanism has been observed in various cell types and involves several key proteins, including the small GTPase Ras-related protein (RAB11), the adaptor Cbl-interacting 85-kDa protein (CIN85), the ubiquitin ligase Casitas B-lineage lymphoma (c-CBL), and the retromer complex [121].

The second type of endocytosis is by lipid rafts, and more precisely by caveolae, which represent invaginations existing in the plasma membrane. These invaginations contain sphingolipids, cholesterol, and caveolins (mainly caveolin-1). The group of Petra Knaus discovered a co-localization and a direct interaction between caveolin-1 and BMP2 receptors, as well as between epidermal growth factor receptor pathway substrate 15 homolog receptor (Eps15R), a protein present in clathrin pits, and BMP2 receptors [126, 127]. This type of endocytosis has been described to target the activated receptors for degradation, but this has been shown to be dependent on the receptor understudied. For instance, endocytosis of TGF-β receptors by lipid rafts promotes their interaction with the SMAD7/Smurf2 ubiquitylation complex and targets them for degradation in proteasomes and lysosomes [116] (Figure 14B). Conversely, association of lipid rafts with BMP receptors is important for BMP-induced

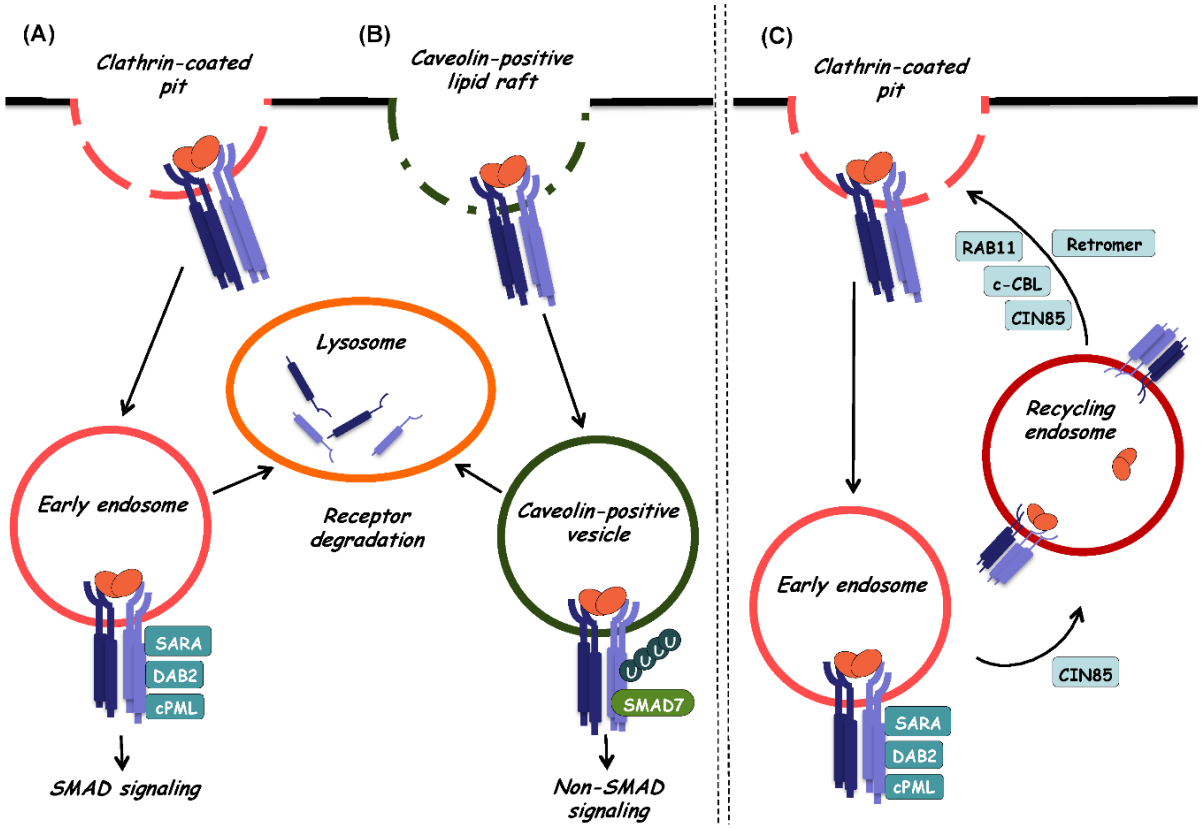

Figure 14. Internalization and sorting of TGF-β receptors.

*(**A**) TGF-β induced SMAD-dependent signaling is initiated at the cell surface in clathrin-coated pits. Following this, TGF-β receptors undergo endocytosis via clathrin-coated pits forming early endosomes. During early stages of endocytosis, the association of TGF-β receptors with SARA, cPML, and Dab-2 adaptor proteins enhances TGF-β-induced SMAD activation, leading to the propagation of SMAD-dependent signaling. However, TGF-β receptors in early endosomes can be also sorted for degradation via entering to late endosomes (not shown) and finally reaching lysosomes for degradation. (**B**) Internalization of TGF-β receptors can also occur at caveolin-positive lipid raft compartments on the cell membrane, leading to their entry into caveolin-positive vesicles. In these latter, the TGF-β type I receptor preferentially associates with SMAD7, which can control receptor turnover through the recruitment of ubiquitin ligases and de-ubiquitinating enzymes, thus regulating subsequent lysosomal degradation of receptors. Nevertheless, lipid raft/caveolar-mediated endocytosis of TGF-β receptors can also promote non-SMAD TGF-β signaling, as SMAD7 competes with SMAD2/3 for interaction with the TGF-β type I receptor. (**C**) TGF-β receptors which are internalized via clathrin-coated pits into early endosomes can be also sorted to recycling endosomes, enabling them to return to the cell surface, where they can respond again to ligand stimulation. This mechanism has been shown in different cell types and involves several proteins including the small GTPase RAB11, the adaptor protein CIN85, the ubiquitin ligase c-CBL, and the retromer complex. Figure was taken from "TGF-β Signaling" by Tzavlaki and Moustakas, Biomolecules 2021.*

SMAD1/5/8 phosphorylation [128]. These studies demonstrate that the mode of receptor endocytosis and the specific type of receptor involved has a significant impact on the signaling pathway, either by enhancement of the signal or the degradation of these receptors.

2.4.1.4 Transcriptional Regulation by SMADs

As illustrated above, TGF-β superfamily encompasses a wide range of ligands, as well as a considerable variety in receptors with varying affinities for different ligands. As these ligands signal mainly via phosphorylated SMAD2/3 (pSMAD2/3) or pSMAD1/5/8 transcription factors,

it is complicated to explain how this simple two-way activation system controls the expression of a somewhat unique set of target genes by each ligand. Consequently, one would ask: what mechanisms can explain the precise matching of ligands with their corresponding sets of target genes established and hence illustrate the functional diversity of these ligands? As stated above, activating type-I and type-II receptors induces the formation of SMAD complexes which act directly on DNA as transcription factors via the β-loop of the MH1 domain. All R-SMADs, with the exception of most frequent expression isoform of SMAD2, bind DNA directly, as does SMAD4 [129]. The sequence recognized by MH1 domain of SMAD3 and SMAD4 is GTCT, or its reverse complement AGAC, which was first identified in 1998 by Zawel et al. [130]. This sequence is generally referred to as the SMAD-binding element (SBE). In contrast, pSMAD1/5–SMAD4 complexes bind distinct sites, defined as G(R)CG(N)C-$(N)_5$-GTCT or GGCGCC-A$(N)_4$-GNC(R') (N is any base, R=A or G, and R'=A, C, or G [115]. SMAD1/5 MH1 domain binds The GRCGNC sequence, while the GTCT or GNCR' binds the SMAD4 MH1 domain.

However, since the affinity of SMADs to DNA is too low [131], their transcriptional regulation requires interaction with other co-factors (co-activators co-repressors) [115]. These include members of transcription factor families such as Runt-related transcription factor (RUNX), E2F, Forkhead box (FOX), cAMP-response element binding protein (CREB) and many others [132, 133]. Indeed, pR-SMADs/SMAD4/co-factor complexes require specific DNA-binding sequences with the correct distance and orientation on the target promoters. Thus, of the hundreds of promoters that contain SMAD-responsive elements, only a few will have the necessary sequences for binding these complexes. For this, one explanation of response specificity is the selectivity of interaction between co-factors and either pSMAD2/3 or pSMAD1/5/8.

Another reason of response specificity can be explained by cell type, which plays a very important role for determining ligand-induced transcriptional responses. Depending on the differential expression of receptors and co-factors in each cell type, responses to the same ligand may vary. Furthermore, studies have demonstrated that differences in chromatin accessibility across different cell types, which can be attributed to unique histone methylation patterns for example, play a significant role in modulating the transcriptional regulation mediated by SMADs [134]. Therefore, TGF-β superfamily signals are believed to play a crucial role in facilitating the accumulation of appropriate SMAD complexes within the nucleus. Subsequently, the cell assesses how this accumulation aligns with its existing nuclear SMAD-binding partners to control the regulation of specific genes residing in accessible chromatin regions.

Another level of response specificity is the affinity of the ligand-receptor interactions as well as the affinity of transcriptional complexes induced by the ligands, which defines different potencies in the transduced signal. Morikawa et al nicely illustrated the differences in transcriptional regulation in HUVECs by two different BMPs, BMP9 (1ng/mL) and BMP6 (50ng/mL), using ChIP-seq of SMAD1/5. Despite the fact that these 2 stimulations resulted in

equivalent p-SMAD1/5 levels, several BMP9-specific binding sites such as HEY1 and JAG1 loci were detected. However, increasing the concentration of BMP6 up to 200ng/mL enhanced SMAD1/5 binding to these BMP9-specific binding sites in a BMP6 dose-dependent manner. On the other hand, common SMAD1/5 binding sites for both BMP9 and BMP6, such as the *ID1* locus which exhibits strong SMAD1/5-binding affinity, were already strongly upregulated at 20ng/mL BMP6. Therefore, differences in ligand affinity and potency, which are interestingly not necessarily reflected by the level of phosphorylated SMADs measured by traditional methods, can define another level of response specificity.

2.4.1.5 Termination of SMAD Signaling: Several Control Points

Mechanisms terminating the signals transmitted to the cells constitutes an important control system for signal duration and consequently a tight control of the resulting cellular functions. In 2002, Inman and his colleagues demonstrated that the phosphorylation of R-SMADs is unstable and that they must undergo repeated cycles of phosphorylation by the activated receptors to maintain their activity [135]. Since then, many studies have demonstrated different control points for both the activated receptors and SMADs which enhanced our knowledge on terminating and controlling SMAD signaling (Figure 15).

Numerous proteins have been reported to interact with the activated receptors, many of them acting as negative regulators [108]. These interactions generally lead to either promoting their de-phosphorylation by phosphatases [136, 137] or targeting them for degradation [138, 139]. For instance, protein phosphatase 1 (PP1) α de-phosphorylates ALK1 resulting in its in-activation [140]. Similarly, PP1 can also interact and in-activate ALK5 leading to the Inhibition of TGF-β signaling [136]. Receptors can be targeted for degradation through different mechanisms that involves other kind of post translation modifications, most frequently being polyubiquitylation (addition of ubiquitin chains for proteins). The best characterized mechanisms for this latter are those described for ALK5 which are mediated by different E3-ubiquitin ligases such as Smurf1/2, WWP1, and NEDD4-2 in association with I-SMADs, which were reviewed by Hata and Chen in 2016 [108]. An additional mechanism of regulating ligand-receptor signaling is through cleavage of the extracellular domain of TGF-β family receptors. For example, the extracellular domain of ALK5 can be cleaved by the ADAM-17 metalloprotease, resulting in reduced TGF-β signaling due to a decrease in receptor numbers on the cell membrane [141]. Furthermore, various proteins present in the ECM act as ligand traps, such as decorin, follistatin, noggin, chordin, Cerberus and others have been identified to bind and sequester specific members of the TGF-β family, thereby preventing or terminating their downstream signaling [142–144].

Similarly, pR-SMADs have also shown to be regulated by dephosphorylation and degradation. For instance, protein phosphatase 2C alpha (PP2Cα) reduces the level of p-SMAD2/3 [145]. The same phosphatase was shown to be also active on p-SMAD1/5/8 [146]. Later on, other R-SMAD phosphatases have been identified [147–149]. R-SMADs, as well as the co-SMAD4, can

also undergo proteosomal degradation by the E3-ubiquitin ligase system, thus restricting their availability for the signaling and consequently shutting down the pathway [97, 150].

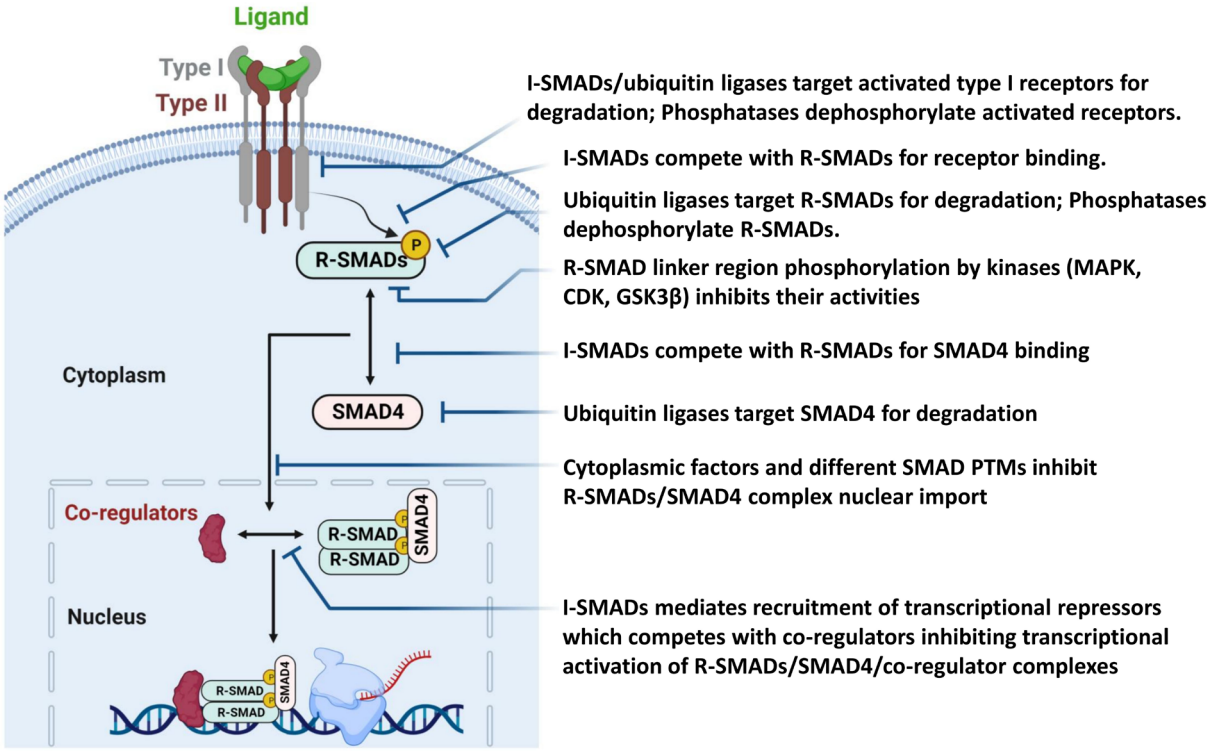

Figure 15. Mechanisms Controlling Termination of SMAD Signaling.

Each mechanism was briefly explained in section 2.4.1.5 including references from which this figure was created. All abbreviations were previously mentioned. Figure created with Biorender.

Another way for regulating signal duration is by manipulating the linker region of R-SMADs. In addition to the SSXS phosphorylation motif of the MH2 domain of SMADs by type 1 receptors, SMADs can be phosphorylated at other sites in the linker region by different endogenous kinases, including MAPKs and CDKs [151], which was shown to impair their nuclear accumulation and corresponding signaling activity [97]. Phosphorylation of SMADs can also impair their stability. For instance, Glycogen Synthase Kinase 3β (GSK3β) phosphorylates SMAD1 and SMAD3, which induces their complexation with Smurf1 and their degradation [152, 153]. I-SMADs are strong negative regulators of SMAD signaling. They can inhibit TGF-β family signaling through various mechanisms including down-regulation of cell surface type-I receptors in cooperation with ubiquitin ligases, interfering with the interactions between R-SMADs and type-I receptors or SMAD4, and transcriptional regulation in the nucleus [154] (Figure 15). SMAD6 preferentially targets the BMP pathway (SMAD1/5/8) [155], whereas SMAD7 acts on both BMP and TGF-β pathways [156]. Notably, SMAD7 expression is induced by TGF-β, activin and BMPs [157] and that of SMAD6 by BMPs [158], highlighting the negative feedback mechanism by I-SMADs in the regulation and termination of SMAD signaling. The MH2 domains of SMAD6 and SMAD7 can associate directly with the activated receptors, or even to SMAD4, and thus act by competing with R-SMADs. I-SMADs are predominantly localized in the nucleus of most cell types [154] and have been described to act by interfering

with the formation of SMAD–DNA complex [159]. Moreover, I-SMADs can act as transcriptional repressors through the recruitment of negative transcriptional regulators such as histone deacetylases [160, 161].

2.4.2 Non Canonical Signaling Pathways

In addition to the canonical SMAD signaling pathways, activated receptors of TGF-β superfamily ligands have shown during the past two decades that they can activate a diverse array of non-canonical signaling pathways to regulate a variety of cellular responses [64, 162, 163]. When discussing non-canonical signaling pathways by the TGF-β superfamily, it is very important to emphasize the concept of "context-dependency". The activation of these non-canonical signaling pathways is strongly influenced by the specific context in which it occurs, especially that these pathways can occur in SMAD-dependent and SMAD-independent manners (will be further discussed in the upcoming subsections). Non canonical signaling pathways induced by TGF-β superfamily include MAPK (encompassing ERK, Jun N-terminal kinase (JNK), and P38), PI3K-AKT, Rho-like GTPases, Protien kinase A (PKA) and Signal transducer and activator of transcription (STAT) signaling pathways [64, 162, 163]. Mechanistically, there is still much to uncover regarding the relationship between the activated receptor complexes and downstream non-canonical effectors in response to TGF-β, activin, or BMP receptors. In the following subsections, I will highlight the activation of different non-canonical pathways by various members of the TGF-β superfamily such as TGF-β (most extensively studied member), BMP2, BMP6, among others. While focusing on TGF-β as the most extensively studied member, it is crucial to note that the signaling illustrations to be presented are not exhaustive and unique for TGF-β family signaling, but are important signaling mediators of many other growth factors and cytokines as well. The activity of these pathways in response to TGF-β family members can vary depending on different factors such as the ligand studied, ligand concentration, cell type, culture conditions, and many other variables, all of which define the term ''context-dependency'' for the activation or inhibition of these non-canonical pathways by TGF-β superfamily.

2.4.2.1 MAPK (P38, JNK, ERK) and IKK/NF-kB Signaling

MAPK signaling cascades consist of at least three sequential kinase components: a MAPKKK (MAP3K), a MAPKK (MAP2K), and a MAPK. MAP3Ks phosphorylate and activate MAP2Ks, which, in turn, phosphorylate and activate MAPKs (P38, JNK, and ERK). These latter facilitates the transmission of signals to downstream effectors, including other kinases and transcription factors, to regulate a wide range of biological processes, including cell growth, differentiation, and survival [164, 165]. TGF-β activates different non-canonical MAPK signaling pathways. Among these, the P38 and the JNK signaling pathways are the best characterized in the context of TGF-β signaling. TGF-β activates P38 via MKK3/6 [166–169] and JNK via MKK4 [170, 171] in different cell lines (Figure 16). Multiple experimental approaches including expression of dominant negative SMAD3, utilization of SMAD3 $^{-/-}$ and SMAD4 $^{-/-}$ cells, and modification of type-I receptor L45 loop to impair SMAD binding and activation, demonstrated that the

activation of P38 and JNK pathways by TGF-β occurs in a SMAD independent manner [167, 170, 172]. However, P38 and JNK activation by BMPs or TGF-β can be either rapid or delayed. It was suggested that direct and rapid activation of these pathways does not depend on SMADs [170, 171], whilst prolonged and delayed activation of these pathways likely depends on SMAD-mediated transcriptional events (Figure 16). For instance, Takekawa et al demonstrated that activation of P38 is dependent on SMAD-mediated upregulation of growth arrest and DNA damage-inducible 45 beta (GADD45β), a MEKK4 activator [173], as spotted in human dermal fibroblasts, human keratinocytes and pancreatic carcinoma cells [174]. This mechanism was further supported by other studies [175, 176] (Figure 16).

As previously mentioned, MAPKKKs serve as the upstream kinases of MAPKKs, and in the case of MKK4 and MKK3/6, the best studied upstream MAPKKK for TGF-β is TGF-β activated kinase 1 (TAK1). TAK1 is a TGF-β1 stimulated serine/threonine kinase and has been initially spotted as a TGF-β pathway kinase by rescue and complementation of a MAPKK mutant in saccharomyces cerevisiae [177]. TAK1 activation is mediated by a range of other stimuli like pro-inflammatory cytokines, such as tumor necrosis factor-α (TNF-α) [178], interleukin (IL)-1 [179] and environnemental stresses [180], hence serving as a converging point between different signaling pathways activated by different stimuli. TAK1 is associated in the activation of the diverse array of cellular kinases including P38, JNK and inhibitor of nuclear factor kappa B (IKK) [179, 181]. TAK1 regulates a variety of crucial cellular processes encompassing cell survival, cell differentiation, apoptosis and inflammation [182]. Moreover, TAK1 has shown to play important roles in vascular development. Embryonic deficiency of TAK1 results in a phenotype resembling that obtained from null mutations in the type III receptor ENG and type I receptor ALK1 encoding genes [183].

Mechanistically, TGF-β induced activation of TAK1 is remarkably distinct from that of SMAD2/3, where this latter requires phosphorylation by ALK5 to relay the signal onwards. The activation of TAK1 relies on the tumor necrosis factor-receptor associated factor 6 (TRAF6), a ubiquitin ligase that belongs to the really interesting new gene (RING) family of ubiquitin ligases (Figure 16). Following ligand induced formation of heteromeric complexes of ALK5 and TβRII, TRAF6 interacts with the activated receptors via the TRAF domain. Following this interaction, the RING domain of TRAF6 E3 ubiquitin ligase activity is activated, leading to the formation of polyubiquitin chains on TRAF6 at lysine 63. These chains then act as scaffolds for the recruitment and activation of protein kinases. Consequently, TRAF6 binds TAK1 and mediates its subsequent polyubiquitination and activation, which further facilitates the recruitment and activation of protein kinases. Consequently, TRAF6 binds TAK1 and mediates its subsequent polyubiquitination and activation, which further facilitates the activation of downstream kinases like P38 and JNK [184–186]. Moreover, few studies have shown that TRAF6 induces the proteolytic cleavage of ALK5 in a process dependent on presenilin 1 (PS1) ubiquitin ligase. This cleavage gives rise to an intracellular domain (ICD) of ALK5, which translocates to the nucleus to promote invasion of specific types of cancer cells [187, 188]. Some studies have shown that TRAF4 also interacts with ALK5, leading to Lys63

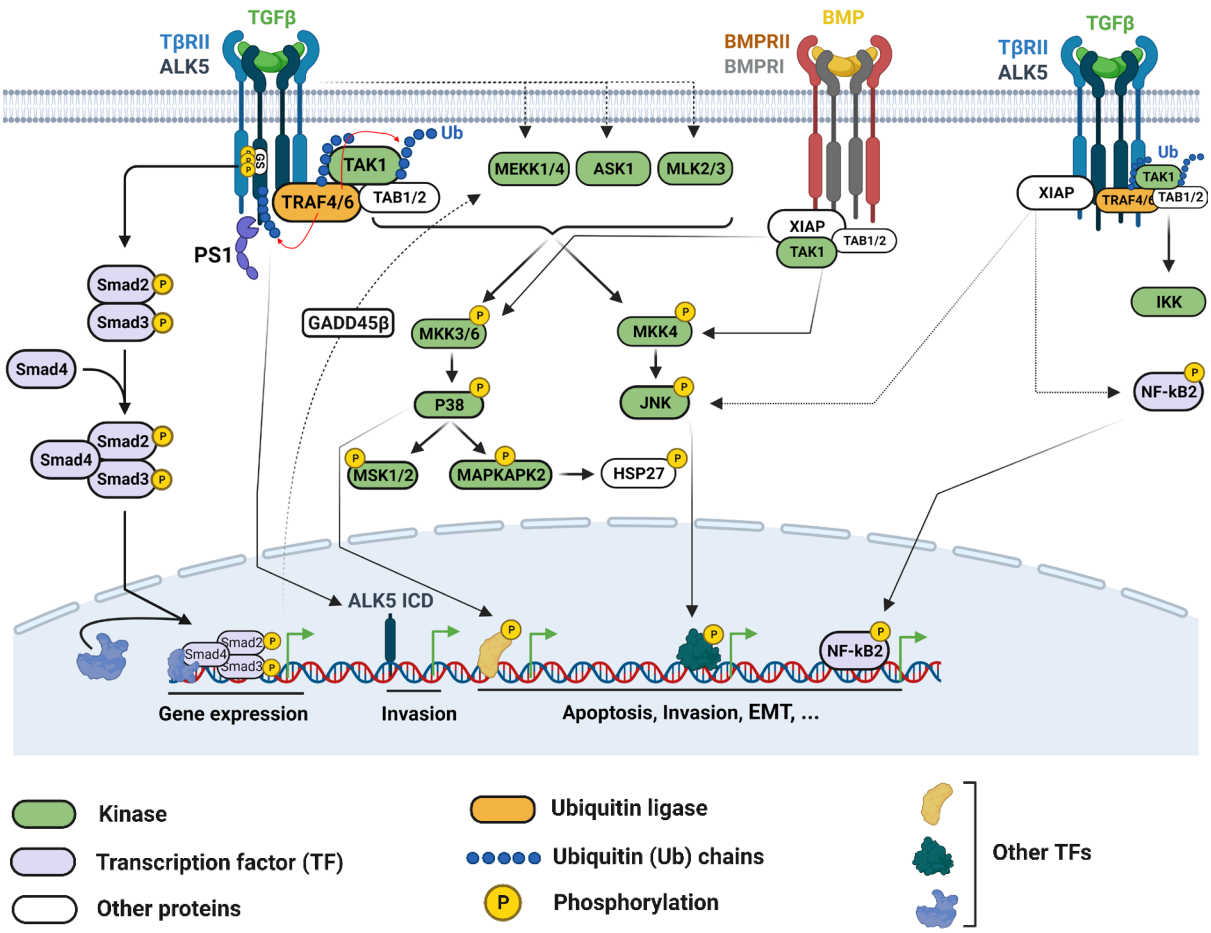

Figure 16. TGFβ and BMP-induced activation of canonical SMAD and non-canonical P38, JNK and IKK pathways.

Ligand-bound TGFβ receptors activates canonical signaling through pSMAD2/3/SMAD4 complexes that regulate expression of TGFβ SMAD dependent target genes. On the other hand, activated TGFβ receptors can directly activate non canonical signaling pathways which are independent from SMADs. Activated receptors interact with TRAF4/6 ubiquitin ligases leading to their activation through Lys63-linked polyubiquitylation, which then recruits and activates the MAP3K TAK1 which form complexes with TAB1/2. This leads to activation of downstream MAPK2 kinases MKK3/6 and MKK4, which activates P38 and JNK MAPK, respectively. TRAF6 can also induce proteolytic cleavage of ALK5 through Lys63 polyubiquitylation and recruitment of presenilin 1 (PS1), generating the intracellular domain (ICD) of ALK5, which translocates into the nucleus to play a role in regulating cell invasion. TAK1-TAB1/2 complexes also activate IKK and NF-kB2 pathway. A second link between TGFβ and BMP receptors to intracellular kinases involves XIAP, which functions as an E3 ubiquitin ligase. BMP receptors can form complexes with TAK1 and TAB1, and this complex was suggested to promote BMP-induced activation of downstream MAPK signaling. Moreover, XIAP has been also shown to mediate TGFβ-induced activation of JNK and NF-kB pathways. On the other hand, Other MAP3K (MEKK1/4, ASK1, MLK2/3) have been shown to mediate TGFβ-induced activation of P38 and JNK pathways, independent of TAK1. Nevertheless, activated P38 and JNK kinases phosphorylate and activate various downstream target kinases (such as MAPKAPK2 and MSK downstream of P38) and transcription factors. These activated kinases and/or transcription factors, working or not in conjunction with other cofactors and activated SMADs, cooperate altogether to regulate various TGFβ-induced cellular processes including invasion, apoptosis and EMT. Notably, TGFβ can also activate non-canonical MAPK signaling through a delayed SMAD-dependent regulation of certain genes (e.g., GADD45β that activates MEKK4). Remaining abbreviations in the figure are described in the main text. Figure created with Biorender.

polyubiquitylation of TRAF4 and subsequent activation of TAK1 [189]. Moreover, TAK1 forms complexes with TAK1-binding protein 1 (TAB1) and TAB2, which participates in the activation

of P38 and JNK pathways, as well as NF-κB pathway [190] (Figure 16). Apart from TAK1, many other kinases belonging to the MAP3K family including mixed-lineage kinase 2 and 3 (MLK2/3), MEKK1/4 and apoptosis signal-regulating kinase 1 (ASK1) have been also reported in TGF-β-mediated P38 and JNK activation via MKK3/MKK6 and MKK4 respectively [191–194] (Figure 16). Some of these studies have showed that TAK1 doesn't mediate the TGF-β-induced activation of P38 pathway in certain contexts [193]**.** However, the mechanisms by which these kinases are recruited to the activated TGF-β receptors are not so clear. A second link between TGF-β superfamily receptors to intracellular kinases involves the X-linked inhibitor of apoptosis protein (XIAP), which functions as an E3 ubiquitin ligase [162, 195–197]. Through overexpression and Co-IP experiments performed in HEK293 cells, Reffey et al demonstrated that XIAP interacts with several members of the TGF-β receptor superfamily, notably ALK1, ALK4, and ALK5 [196]. In this context, XIAP mediated TGF-β-induced activation of both JNK and nuclear factor kappa B (NF-κB) pathways, leading to the regulation of TGF-β responsive genes but not apoptosis. Notably, these responses occurred in a SMAD4-dependent TAK1-independent manner, supporting the notion that TAK1 does not always mediate TGF-β-induced non-canonical MAPK signaling pathways.

In addition to TGF-β, BMPs have been also shown to activate P38 and JNK pathways [177, 198–201] (Figure 16). BMP receptors can form complexes with TAK1 and TAB1, and this complex was suggested to promote BMP signaling during Xenopus embryogenesis [197]. In Schwann cells, BMP7 activated P38 pathway in a SMAD4 independent manner [202]. In mouse pro-osteoblasts and primary cultured osteoblasts, BMP2 activated both P38 and JNK pathways in a time dependent manner, but the onset of this activation was delayed compared with activation of SMADs, suggesting an indirect mechanism [200]. Besides directly phosphorylating various transcription factors, the activation of P38 also triggers the downstream activation of several kinases including mitogen- and stress-activated protein kinase 1/2 (MSK1/2), and MAPK activated protein kinase 2/3 (MK2/3) and consequent phosphorylation of various downstream targets. For instance, P38-mediated activation of MK2, first identified substrate for P38 [203], leads to the phosphorylation of different cellular substrates, with the multifunctional protein HSP27 being one of the first identified and most extensively studied substrates of MK2 [204]. BMP2- and BMP6-induced activation of P38 MAPK resulted in phosphorylation of HSP27, which was inhibited using a pharmacological inhibitor for P38 [201]. Moreover, *in-vitro* kinase assays using immunoprecipitated MK2 from BMP2 treated Mouse calvarial 3T3-E1 (MC3T3-E1) cells demonstrated P38-MK2 activation through phosphorylation of recombinant HSP27 [200]. Few studies have also shown that TGF-β can also activate P38-MK2-HSP27 [205–207] or P38/MSK1 [208] pathways (Figure 16). One of the crucial consequences of JNK or P38 MAPK activation is apoptosis, which has been recognized as a developmental activity of BMPs and as a mechanism of tumor suppression by TGF-β [184, 185, 199, 209, 210]. TGF-β-induced JNK and/or P38 signaling also contribute to TGF-β-induced epithilail-to-mesynchymal transition (EMT), another well described role for TGF-β signaling [211, 212]. Furthermore, the activation of these pathways by TGF-β is involved

in the endothelial-mesenchymal transition (EndMT), which has been reported to occur through both SMAD-dependent and SMAD-independent pathways [213].

Despite the fact that ALK5 and TβRII have been described as serine-threonine kinases, they can be phosphorylated at tyrosine (Tyr) residues or function as tyrosine kinases themselves [214–216] (Figure 17). Galliher and Schiemann demonstrated that Src-induced Tyr284 phosphorylation of TβRII triggered the recruitment of Src homology 2 domain-containing transforming protein (Shc) and growth factor receptor-bound protein 2 (Grb2) to the receptor complex and activation of P38 MAPK signaling pathway [217]. Similar to TβRII, ALK5 can be also phosphorylated on Tyr residues upon TGF-β stimulation, which triggers Tyr phosphorylation of Shc. This leads to the formation of a Shc/Grb2/ Son of Sevenless (Sos) complex, ultimately leading to the activation of the Ras-Raf-MEK-ERK1/2 MAPK signaling pathway [215]. Very recent work by Yakymovych et al shows that, before TGF-β stimulation, inactive Src was complexed with TβRII. Upon TGF-β-induced formation of the ALK5-TβRII receptor complexes, TβRII phosphorylates ALK5 on Tyr182. This triggers the interaction of Src's SH2 domain with phosphorylated tyrosine residues in ALK5 and its subsequent phosphorylation on several tyrosine residues (Tyr428/429) [218] (Figure 17). Notably, ERK1/2 activation induced by TGF-β superfamily is also context dependent (cell type, culture conditions, etc.), and as described above, it can also occur in a rapid or delayed manner. For instance, rapid activation of Ras and/or ERK1/2 has been observed in response to BMPs in osteoblasts, myoblasts, endothelial cells, and cancer cell lines [219–221]. On the other hand, Simeone et al demonstrated that TGF-β-induced activation of ERK occurred with a maximal phosphorylation obtained after hours rather than minutes, and showed that the mechanism is dependent on SMAD4 and de-novo protein synthesis [222]. Activation of ERK signaling by TGF-β and BMPs has been implicated in different functions, depending on the ligand and cell type studied. Zhou et al demonstrated that BMP4 treatment of HUVECs leads to the activation of the MEK-ERK 1/2 pathway in a dose- and time-dependent manner, which can be blocked by MEK inhibitors. Furthermore, the authors show that the capillary sprouting induced by BMP4 is dependent on ERK signaling but is not affected by inhibiting the SMAD pathway, suggesting a SMAD-independent mechanism. ERK activation has also been shown to be essential in TGF-β-induced EMT and required for adherens junction disassembly and cell motility [223]. Target genes that mediate the role of ERK in TGF-β-induced EMT have been identified [224] and their functions include integrin-based remodeling of cell-matrix interactions, endocytosis and cell motility. Similar to TGF-β, BMP7 induced EMT, cell migration and invasion in certain cancer cells via both ERK and PI3K pathways [225].

2.4.2.2 PI3K/AKT Signaling

The PI3K/AKT pathway, also known as the PI3K/AKT/mammalian target of rapamycin (mTOR) pathway, is a critical signaling pathway involved in regulating various cellular processes, including cell growth, survival, proliferation, metabolism, and apoptosis [226, 227]. TGF-β and BMPs have been shown to activate the serine/threonine kinase PKB/AKT, through PI3K. Similarly to the aforementioned pathways, this has shown to be mediated by SMAD

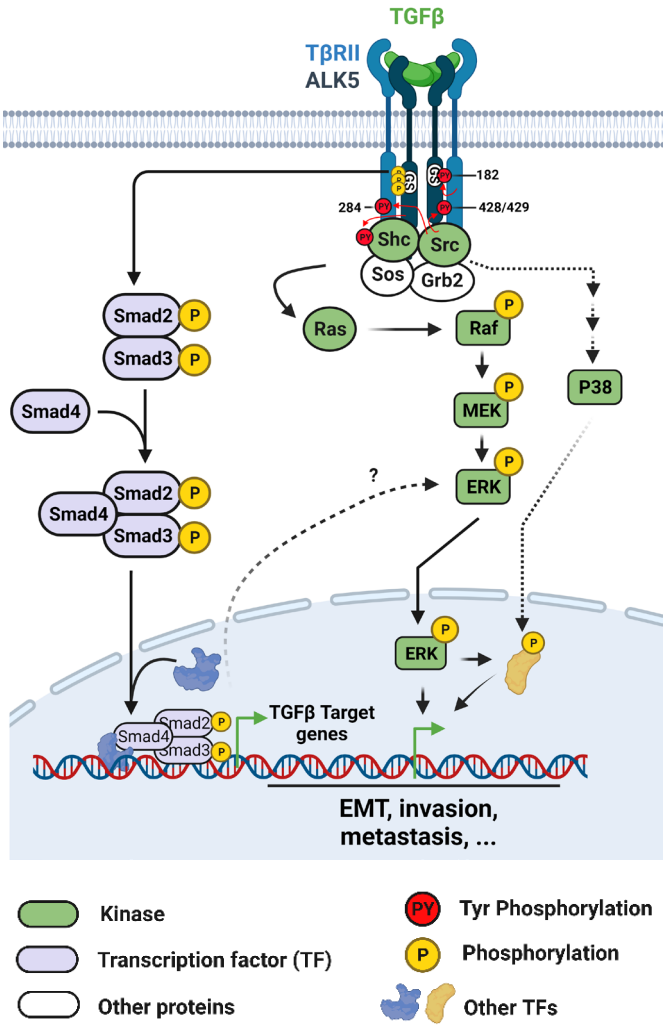

Figure 17. TGFβ-Induced activation of ERK signaling through tyrosine kinase activities.

Upon TGFβ binding, TGFβ receptors become activated and undergo phosphorylation at different tyrosine (Tyr; Y) residues. ALK5 is Tyr phosphorylated by both TβRII and Src kinases at different residues (Y284, Y428/429, Y182…). This leads to the recruitment and subsequent Tyr phosphorylation of Shc, followed by the formation of Shc/Sos/Grb2 complexes. These complexes play a crucial role in transmitting signals that activate the Ras/Raf/MEK/ERK signaling pathway. Additionally, this complex has also been implicated in activating P38 MAPK signaling. TGFβ can also activate ERK signaling through a delayed SMAD-dependent mechanism dependent on de novo protein synthesis. Activated ERK signaling leads to the phosphorylation of specific transcription factors. Consequently, these phosphorylated transcription factors regulate the transcription of genes associated with different functions including EMT, invasion, and metastasis, either independently or in cooperation with activated SMAD complexes. All other abbreviations are described in the main text. Figure created with Biorender.

independent or SMAD-dependent mechanisms [228–231]. Direct activation of the pathway has been suggested to occur through the interaction of the regulatory subunit of PI3K, p85, with ALK5 [232], and together they relay the activation of TGF-β-induced activation of AKT [228, 233] (Figure 18). Additionally, TGF-β-induced PI3K and AKT signaling is activated by receptor-mediated Lys63 ubiquitination of TRAF6, thereby activating not only TAK1, but also ubiquitination, membrane recruitment and activation of AKT [234]. In addition to these direct SMAD-independent mechanisms, TGF-β can in-directly activate PI3K/AKT through expression of miR-216a/217 microRNA cluster which suppresses the expression of SMAD7 and the AKT inhibitor PTEN (phosphatase and tensin homologue) [235]. Additionally, TGF-β also triggers the activation of the mTOR complex 2 (mTORC2), which phosphorylates and further activates AKT (Figure 18). TGF-β-induced activation of the PI3K/AKT/mTOR pathway plays an important role in regulating various cellular functions. In mammary epithelial cells and keratinocytes, TGF-β triggers rapid a ctivation of the mTORC1/S6K/S6 pathway, leading to increased protein synthesis, cell size, motility, and invasion [233]. Furthermore, AKT activation in response to TGF-β also has notable effects on EMT processes [236]. AKT directly phosphorylates Twist and stabilizes NF-κB and the EMT transcription factor Snail by phosphorylating GSK3β. This modulation

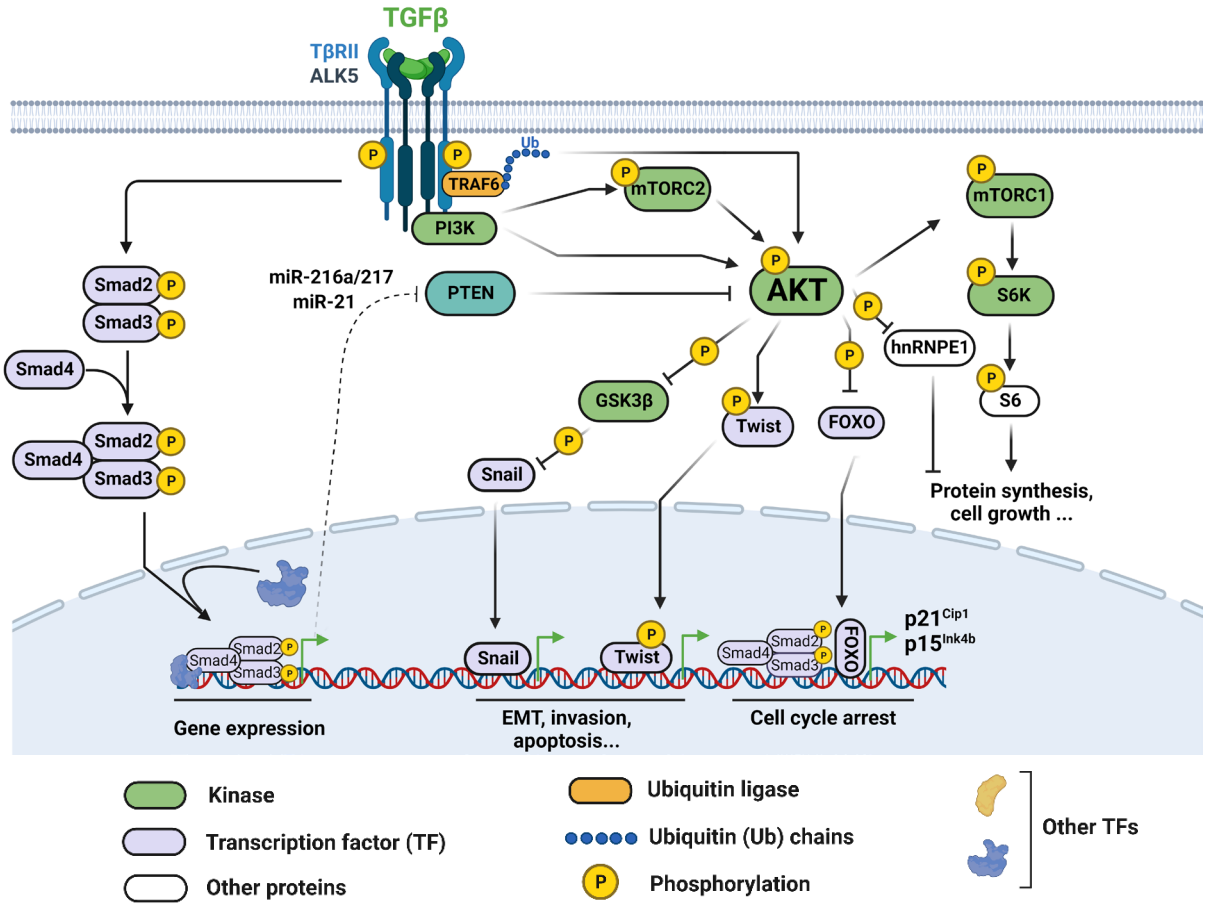

Figure 18. TGF-β-induced activation of PI3K/AKT Pathway.

TGFβ induces the activation of PI3K through the interaction of the p85 subunit of PI3K with the TGFβ receptors. PI3K then activates AKT/PKB, which controls numerous downstream targets and functions. AKT promotes protein synthesis through different mechanisms such as (1) activation of mTORC1/S6K/S6 and (2) direct phosphorylation and inhibition of the translational inhibitor hnRNPE1. Furthermore, AKT triggers the phosphorylation of the Twist transcription factor and GSK3β. This latter leads to the inhibition of GSK3β, resulting in the stabilization of Snail. These two events play crucial roles in regulating many genes implicated in EMT and apoptosis. In certain cell types, TGFβ can also enhance AKT signaling through inhibition of PTEN phosphatase through increased expression miR-216a/217 and miR-21. Nevertheless, activation of the PI3K/AKT pathway by TGFβ can counteract the SMAD/FoXO-mediated transcriptional responses during growth arrest or apoptosis in certain contexts. This occurs through the phosphorylation of FOXO proteins, which hinders their nuclear translocation and thereby inhibits their ability to carry out their transcriptional functions. Additionally, TGFβ also triggers the activation of mTORC2 leading to enhanced AKT activation forming a supporting feedback loop in PI3K-AKT activation. Remaining abbreviations are detailed in the main text. Figure created with Biorender.

enhances the transcriptional regulation of multiple genes involved in EMT [237, 238]. Despite its growth-inhibitory effects and cell cycle arrest, TGF-β-induced activation of AKT promotes the phosphorylation of the forkhead transcription factor (FOXO). This phosphorylation attenuates nuclear translocation and transcriptional activities of FOXO in various SMAD-mediated responses crucial for growth arrest, such as the induction of p15 and p21 expressions [239, 240] (Figure 18). Moreover, TGF-β-induced activation of mTORC2 promotes cytoskeletal reorganization, Ras homolog A (RhoA) activation, and cell migration, thus playing a crucial role in cellular motility [241]. Overall, the TGF-β-induced activation of the

PI3K/AKT/mTOR pathway orchestrates diverse downstream cellular functions, impacting processes such as protein synthesis, cell size, migration, invasion, EMT, and proliferation.

2.4.2.3 Rho-Like GTPases

RhoA/B, Ras-related C3 botulinum toxin substrate (Rac), and cell division control protein 42 homolog (Cdc42) are members of the Rho family of small GTPases. These proteins act as molecular switches, cycling between an active guanosine triphosphate (GTP)-bound state and an inactive guanosine diphosphate (GDP)-bound state, to control a wide range of cellular functions, including cytoskeletal dynamics, cell adhesion, cell migration and cell division [242]. TGF-β and BMPs can activate Rho-like GTPases in a cell-context dependent manner (Figure 19). For example, in epithelial cells and primary keratinocytes, TGF-β activates RhoA within 5 minutes, followed by rapid attenuation by 15 minutes [243, 244]. In mesenchymal stem cells, BMP2 induces rapid activation of RhoA and Rho-related protein kinase (ROCK) after cell spreading [245]. Rapid onset of the pathway and the utilization of SMAD3 or SMAD4 dominant-negative mutant cells suggested that RhoA activation by TGF-β or BMPs is likely independent of SMAD signaling [243, 246]. On the other hand, a delayed activation of RhoA and Cdc42 by TGF-β was shown in several cell types to be dependent on SMAD activities for the expression of neuroepithelial cell transforming 1 (NET1), a guanine nucleotide exchange factor (GEF), which is an activator of RhoA [247–249] (Figure 19). Paradoxically, TGF-β has been shown to downregulate RhoA protein levels through Par6 scaffolding protein [250]. Upon TGF-β stimulation, receptor complexes accumulate at tight junctions, leading to the phosphorylation of Par6 by TβRII. This event recruits the E3 ubiquitin ligase, Smurf1, to the activated receptor complex. Subsequently, the Par6-Smurf1 complex facilitates localized ubiquitylation and degradation of RhoA in a protein kinase Cζ (PKCζ)-dependent manner [250, 251]. This unique regulatory mechanism enables TGF-β to induce the dissolution of tight junctions, a critical step in EMT. Hence, these findings suggest that TGF-β can regulate RhoA activity in two distinct phases and within different cellular compartments. Rapid activation of RhoA in the early phase of signaling might be complemented by the localized down-regulation of RhoA levels at tight junctions in a later stage. Both steps of this regulation of RhoA in response to TGF-β appear to be important for TGF-β-induced EMT [250, 252]. Apart from activating RhoA, TGF-β also triggers the activation of another GTPase called Cdc42, inducing the activation of several downstream effectors including P21-activated kinase (PAK). Like RhoA, the activation of Cdc42 and PAK by TGF-β has been shown to occur independently of the canonical SMAD signaling pathway [253]. Furthermore, LIM kinase 1 (LIMK1), an effector of PAK network downstream from Rac and Cdc42, binds to BMPRII (Figure 19) [254, 255]. This interaction acts synergistically with Cdc42 to activate LIMK1, which promotes phosphorylation and inactivation of cofilin, an actin depolymerizing factor, inducing changes in the actin cytoskeleton dynamics in response to BMP4 and BMP7.

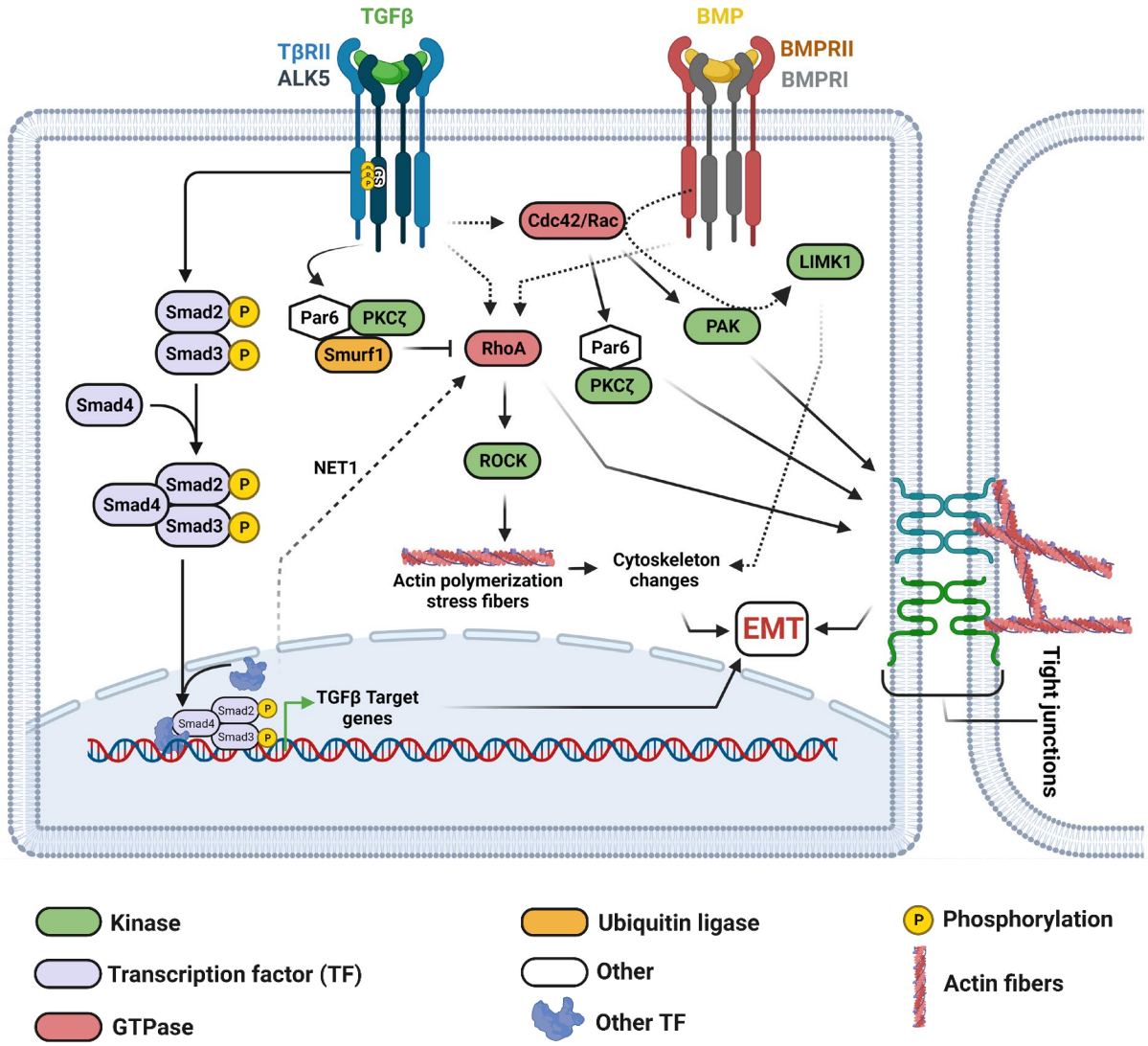

Figure 19. TGF-β-induced activation of Rho family of small GTPases.

TGFβ can activate RhoA and Rho-associated protein kinase (ROCK) through both direct SMAD-independent and indirect SMAD-dependent mechanisms, leading to actin polymerization and stress fiber formation. Additionally, activated TGFβ and BMP receptors facilitates the recruitment of Cdc42 and/or Rac1, which in turn activate several downstream effectors including PAK, Par6/PKC complex, and LIMK1. These effectors play crucial roles in the regulation of tight junctions and actin polymerization. On the other hand, TβRII mediated phosphorylation of Par6 can mediate the recruitment of Smurf1, leading to the degradation of RhoA and subsequent dissociation of tight junctions. Collectively, these mechanisms promote the regulation of actin polymerization and tight junctions which are essential in TGFβ-mediated control of cell migration and other cellular processes involved in EMT. Figure created with biorender.

2.4.2.4 JAK/STAT Signaling

The JAK/STAT Family members

The JAK/STAT signaling pathway comprises ligand-receptor complexes, JAKs (Janus kinases), and the STAT transcription factors. A recent comprehensive review by Xiaoyi Hu et al provides an excellent overview of this pathway [256]. The JAK family consists of four members: JAK1, JAK2, JAK3, and TYK2, whilst the STAT family consists of seven members: STAT1-4, STAT5a,

STAT5b, and STAT6. JAKs are non-receptor protein tyrosine kinases involved in transmitting regulatory signals from activated cytokine receptors to STATs. Numerous cytokines utilize JAK kinases to relay their signaling through their specific receptors [256].

JAK/STAT signaling pathway and regulation

The JAK/STAT signaling pathway involves a series of molecular events that lead to the activation of specific cellular responses. To simplify the high complexity of the JAK/STAT pathway mediated by a large variety of cytokines, I will be focusing on the well-known pro-inflammatory cytokine IL-6 as an example. Initially, the ligand interacts with its specific receptor, promoting sequential formation of a hexameric receptor complex: The IL-6 ligand binds to an IL-6 receptor (IL-6R), and the resulting dimer then attaches to the gp130 (also known as CD130 or IL6R-β) transmembrane receptor common for many cytokines, forming a trimer. Subsequently, the trimer homodimerizes to generate the hexameric (IL-6·IL-6R·gp130)2 signaling complex [257]. The binding between the ligand and the receptor triggers the trans-phosphorylation of JAKs, which are constitutively associated with the receptors [258]. Activated JAKs then induce tyrosine phosphorylation of the bound receptors, creating a docking site for STATs. In the case of IL-6, JAK phosphorylates primarily STAT3 at Tyr705, leading to the dissociation of STAT3 from the receptor. STAT3 subsequently forms homodimers or heterodimers through SH2-domain–phosphotyrosine interactions. These dimers translocate to target gene promoters, regulating the transcription of specific target genes [256, 258, 259] (Figure 20). Additionally, IL-6 has been found to activate the MAPK and the PI3K signaling cascade. However, the underlying molecular mechanisms for the activation of these pathways are still not fully understood [260].

Several negative regulators are responsible for maintaining the balance and steady state of the JAK/STAT signal transduction pathway. The regulation of this pathway involves three primary types of negative regulators: protein inhibitor of activated STAT (PIAS), members of the suppressor of cytokine signaling (SOCS) / cytokine inducible SH2-containing protein (CIS) family, and protein tyrosine phosphatases (PTPs) [256] (Figure 20). PIAS is a protein that mainly interact with STAT dimers to inhibit STAT binding to DNA, thereby blocking JAK/STAT signal transduction. PTPs dephosphorylate STATs resulting in their in-activation. The SOCS family members have been extensively studied and characterized in various cellular and physiological contexts and includes CIS and SOCS1-7 [261, 262]. Interestingly, SOCS family of cytokines are among the genes which are induced by the activated STATs in the nucleus, thus demonstrating a negative feedback mechanism for the regulation of JAK/STAT signaling [261, 262]. SOCS3 is considered among the most potent inhibitors within the SOCS family due to its ability to exert its effects at multiple levels of the JAK-STAT signaling pathway [262]. SOCS3 mediates inhibition of downstream signaling by 3 different mechanisms: (1) competition via SH2-domain-mediated binding to cytokine receptors at intracellular domain, (2) inhibition of the catalytic activity of JAKs through binding the KIR region and (3) degradation of receptors or downstream associated proteins via the proteasomal pathway [263]. SOCS3 mainly targets the IL-6 family cytokine-receptor complex containing the signaling receptor gp130 [262, 263].

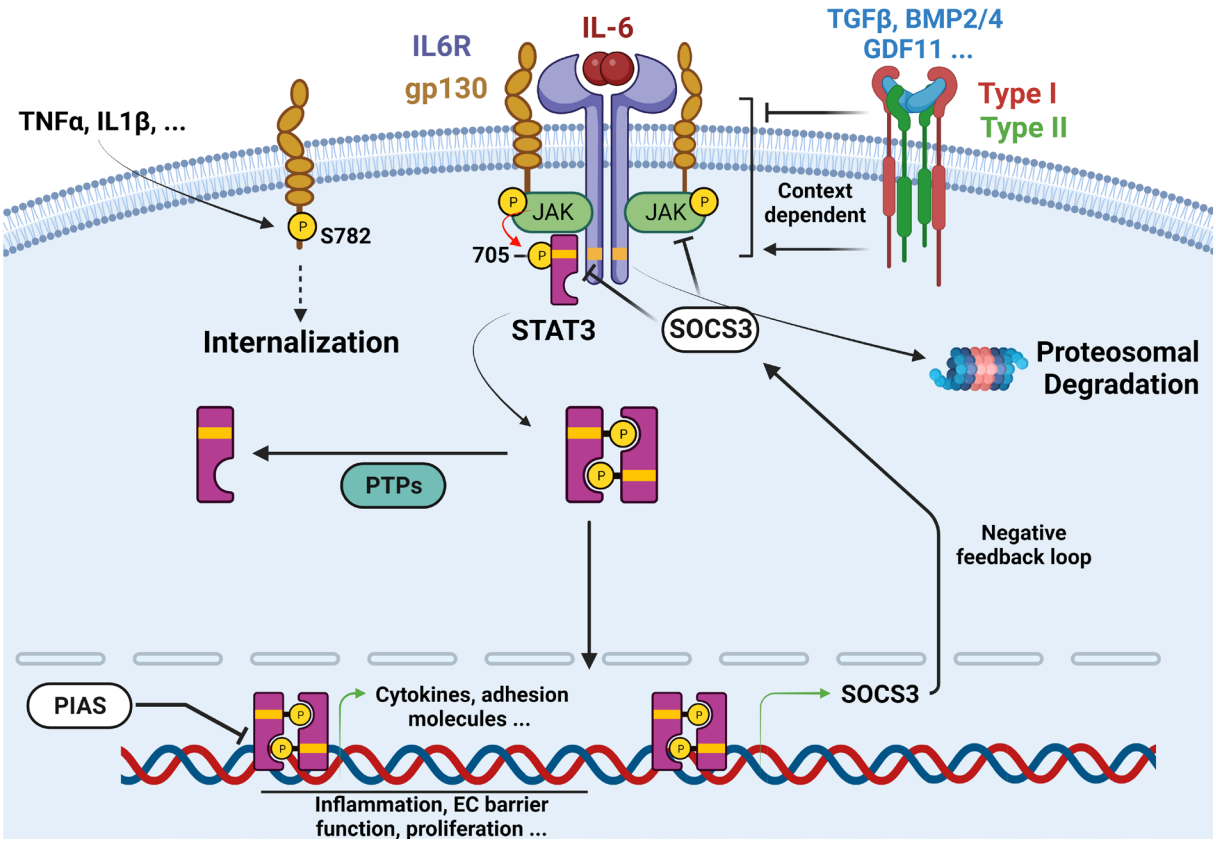

Figure 20. Schematic diagram of BMP9 and BMP10 synthesis and processing.

BMP9 is mainly produced by the hepatic stellate cells (HSCs), while BMP10 is mainly produced in the heart. HSCs can also produce small amounts of BMP10 which can give rise to heterodimers of BMP9/BMP10. The initial steps during synthesis involve the dimerization of inactive precursors, followed by their subsequent cleavage by convertases. This process generates two forms: the non-covalently prodomain-bound BMP (pd-BMP) and the mature BMP, both of which are active in case of BMP9 and BMP10. Active BMPs are then released into the blood circulation to act via their specific receptors on ECs. Figure was created using Biorender.

In addition, the aforementioned mechanisms, the phosphorylation of gp130 at Ser782 by several cytokines, such as TNFα, IL1β, and IFNγ, has been also shown to play a significant role the negative regulation of this pathway. This phosphorylation event leads to a decrease in the cell surface availability of gp130, thereby contributing to the downregulation of the signaling pathways mediated by gp130, including IL-6/JAK STAT3 signaling [264, 265] (Figure 20).

Regulation JAK/STAT signaling pathway by TGF-β Superfamily

Regulation of JAK/STAT signaling has also been reported in response to different TGF-β superfamily ligands in several cell types. TGF-β activates JAK1-STAT3 signaling in hepatic stellate cells, as well as JAK2 in fibroblasts, which play roles in TGF-β-induced fibrosis [266, 267]. Recently, GDF11 has shown to induce a dose-dependent phosphorylation and activation of STAT3 in C2C12 differentiated myotubes that promotes muscle atrophy [268]. Moreover, BMP10 overexpression in mouse transgenic hearts induced pSTAT3 [269].On the other hand, conflicting reports have shown that TGF-β superfamily ligands can also attenuate the activation of JAK/STAT signaling. For instance, Qu et al showed that BMP10 and BMP4 exhibited opposite regulation of pSTAT3 in P19 embryonic carcinoma cells [269]. Moreover,

TGF-β inhibited IL-6-induced STAT3 activation in acute myeloid leukemia blast cells, as well as IL-12-induced JAK-STAT signaling in T lymphocytes [270, 271]. However, the mechanism of this inhibition was poorly understood and was highly context dependent. Bright and Sriram showed that attenuation of IL-6 induced pSTAT3 occurs after a delayed treatment of the cells with TGF-β (20h), and this was attributed to decreased expression of JAK1/2 and Tyk2 [270]. On the other hand, Wierenga et al showed that co-stimulation of T-lymphocytes with IL-12 and TGF-β for only 15 mins resulted in strong attenuation in IL-12 induced pSTAT3, pSTAT4, pJAK2 and pTyk2, without affecting their protein expression [271]. Short term stimulations with BMP4 and BMP2 rapidly attenuated IL6-induced STAT3 activation in multiple myeloma cells, which consequently resulted in inhibition of proliferation and induction of apoptosis of these cells [272, 273]. In the mammary gland, TGF-β-induced activation of SMAD2/3/4 complex inhibits the transcription activity of STAT5, leading to inhibition of mammary gland differentiation and lactation [274]. Few studies have also shown that TGFβ can regulate SOCS3 expression, however the outcomes of this regulation were context dependent as well. For instance, TGFβ stimulation attenuated IL-6 induced SOCS3 expression in Th17-cells [275]. More recently, Dees et al showed that TGF-β induced the expression of DNA methyl transferase 3A (DNMT3A) and DNMT1 in fibroblasts in a SMAD-dependent manner to silence the expression of SOCS3 by promoter hypermethylation [276]. On the other hand, TGF-β induced the expression of SOCS3 in B lymphocytes, macrophages and osteoclasts [277–279]. BMPs have never been shown to regulate SOCS3 expression.

Altogether, different studies have highlighted positive and negative regulation of JAK/STAT signaling by TGF-β superfamily ligands. However, the specific mechanisms governing this regulation remain poorly understood and context dependent.

2.4.2.5 PKA signaling

Among the extensively studied pathways for signal transduction is the cyclic Adenosine 3',5'-cyclic monophosphate (cAMP)-signaling. In this pathway, ligands bind to G protein-coupled receptors (GPCRs) and trigger a series of events involving activation of G proteins and adenylyl cyclase (AC). As a result, intracellular levels of the second messenger cAMP are elevated. This increase in cAMP levels subsequently activates several effector molecules, including the cAMP-dependent PKA [280]. PKA represents one of the first identified kinases which was identified since 1968 by two chemists, Edmond H. Fischer and Edwin G. Krebs. Inactive PKA is composed of four subunits, forming a tetrameric structure. It consists of two regulatory (R) subunits and two catalytic (C) subunits which are inhibited due to their interaction with R subunits. Elevation of cAMP levels in response to different stimuli allows cAMP to bind to the PKA-R subunits, which leads to conformational changes and dissociation of the tetrameric complex releasing the PKA-C subunits. Consequently, catalytically active subunits phosphorylate downstream PKA target proteins in the cytoplasm and the nucleus and initiate a wide array of cellular responses [280].

The first study shedding light that TGF-β ligands can activate PKA was back in 1998 [281]. The authors showed that TGF-β1 within 15 mins induced PKA activation in mesangial cells, which was completely blocked by an inhibitory peptide for PKA (PKI). Despite the fact that the authors in this study showed that TGF-β induced activation of PKA is cAMP-independent, the exact molecular mechanism behind this activation remained unknown. Few years later, Zhang et al showed that TGF-β stimulation of Mv1Lu cells induced the formation of a complex between activated R-SMADs, SMAD4 and the regulatory subunits of PKA. Consequently, this results in the release of the catalytic subunit from the PKA holoenzyme and downstream activation of CREB, a well-known downstream substrate of PKA [282]. This mechanism was further supported by other studies in other cell lines including neuroblasts and pancreatic acinar cells [283–285].

BMPs were also shown to induce the activation of PKA signaling in different cell types. Treatment of PAEC (pulmonary arterial endothelial cells) with H89, a potent PKA inhibitor, inhibited BMP2- and BMP4-induced eNOS phosphorylation and activation, suggesting that the mechanism is dependent on PKA [286]. BMP4 also promoted the differentiation of neural crest-derived cells into noradrenergic neurons in a PKA-dependent manner [287]. Interestingly, the authors in this study showed that effect of BMP4 on this differentiation process is cAMP-independent. Through Co-immunoprecipitation experiments, Ohta et al revealed the formation of a transcriptional complex comprising pSMAD1/5/8, pCREB, and CREB binding protein (CBP) [288]. Additionally, they reported that the promoter of inhibitor of differentiation 1 (*ID1*), an early response gene activated by BMPs, contains a binding site for CRE (cAMP response element), which, when stimulated with a cAMP analog, enhances the response of BMP4-induced BRE (BMP Response Element) luciferase activity. Importantly, they observed that pretreating the cells with H89 significantly reduced this effect, thus highlighting a role of PKA-CREB signaling in potentiating BMP4-induced transcriptional response.

In summary, various studies have shed light on the activation and significance of PKA signaling in the context of TGF-β and BMP signaling. However, the specific mechanism underlying this regulation is not yet fully understood. While one proposed mechanism suggests the formation of SMAD complexes with PKA-R subunits for TGF-β signaling, this interaction has never been demonstrated for BMPs. Further investigations are required to comprehensively unravel PKA signaling activation by TGF-β and BMPs.

2.4.3 Crosstalk between SMAD and Non-SMAD signaling pathways

As demonstrated in the previous sections, many studies have shown that TGF-β exert its cellular responses by activating both SMAD and non-SMAD pathways. Several crosstalk mechanisms have been reported between SMAD and non-SMAD pathways, resulting in both positive and negative interactions [289].

TAK1 was shown to stimulate SMAD7 expression to regulate SMAD signaling pathways induced by TGF-β [290]. Moreover, TAK1 also binds to the SMAD MH2 domain, thus inhibiting R-SMAD transactivation [291]. A crosstalk among the downstream effectors of TAK1 like P38

MAPK, activating transcription factor-2 (ATF2) and SMADs has been also reported to fine-tune TGF-β1-induced target gene expression [168, 169, 208]. On the other hand, TAK1-mediated P38 and JNK activation via TGF-β receptors is also governed by SMAD6 and SMAD7 in a context dependent manner. For instance, Both I-SMADs downregulated BMP-induced activation of P38 and TAK1 probably by interacting with TAK1 or TAB1 [199, 292]. Moreover, SMAD6 also mediates the recruitment of A20, a deubiquitylase to TRAF6, thus inhibiting polyubiquitination of TRAF6 and hence TGF-β-induced activation of TAK1, P38 and JNK [293]. In contrast to SMAD6, SMAD7 enhanced TGF-β mediated stimulation of P38 MAPK and JNK [210, 294]. ERK signaling can downregulate TGF-β signaling by inducing cleavage of cell-surface ALK5 [141]. This shedding of ectodomain of ALK5 is mediated by ADAM17, which is activated by ERK. In addition, ERK can directly phosphorylate the linker region of various SMAD proteins to alter their subcellular localization and inhibit their nuclear translocation and transcriptional activity [295, 296]. On the other hand, TGF-β/BMP signaling can also regulate MAPK signaling. For instance, BMP4 can attenuate ERK activation by upregulating the expression of an ERK phosphatase, Dusp9, thereby maintaining a properly balanced ERK activity to ensure self-renewal of mouse embryonic stem cells [297].

AKT also directly affects SMAD activities in response to TGF-β and, thus, SMAD-mediated transcription responses. As demonstrated in section 2.4.2.2, AKT can negatively regulate SMAD-mediated transcription by phosphorylating the FOXOs, which are required in several SMAD-mediated responses important in growth arrest [239, 240]. Phosphorylation of FOXO proteins by AKT hampers their nuclear localization, and prevents their participation in SMAD-mediated transcription regulation. On the other hand, AKT activation was shown to enhance ALK5 stability by phosphorylation and promoting membrane localization of a deubiquitylating enzyme, USP4 (ubiquitin-specific peptidase 4), which deubiquitylates and thus stabilizes ALK5 and promotes non-SMAD pathways [298]. Additionally, the PI3K-AKT pathway could also induce phosphorylation of SMAD3 at residues preceding the carboxy-terminal region, leading to increased transcription activity of SMAD3, thereby enhancing TGF-β signaling [299]. Moreover, GSK3β has been also identified as a significant regulator of SMAD proteins. GSK3β phosphorylates SMAD1 and SMAD3 in their linker region, serving as a crucial step in the sequential control of SMAD activation and subsequent degradation in response to signals from BMP, TGF-β, and Wnt pathways [300, 301]. Mechanistically, it has been demonstrated that SMAD proteins are activated by BMP or TGF-β signaling through phosphorylation at two serine residues located at the carboxy-terminal end. Following this activation, additional phosphorylation events occur at the linker region of SMADs which are mediated by ERK or P38, as well as CDK8 or CDK9. These phosphorylation events prime SMADs for interaction with and further phosphorylation by GSK3β, regulating their transcriptional potential [300, 301].

Several studies have shown that TGF-β superfamily ligands can crosstalk with JAK-STAT signaling either in a positive or negative manner, depending on the cell type. STAT3 was shown to interact with SMAD3 to antagonize TGF-β signaling [302]. A direct cross talk between STAT3 and SMAD1 is required for BMP-2- and LIF-induced differentiation of primary fetal neural

progenitor cells into astrocytes [303]. The JAK-STAT pathway can also indirectly regulate SMAD3 activity by enhancing the expression of the inhibitory SMAD7. Interferon-γ, acting through JAK1 and STAT1, induces expression of SMAD7, which then inhibits phosphorylation and activation of SMAD3 [304].

In addition to all these previously reported crosstalks, TGF-β superfamily ligands can further crosstalk with many other signaling pathways including Wnt, Notch, Hippo, Hedgehog, and NF-κB pathways, all of which were nicely reviewed in an excellent review by Luo et al [289]. To conclude this chapter, many reports have shown that TGF-β superfamily ligands can activate both SMAD signaling and non-SMAD signaling pathways to regulate downstream functions. Activation of these non-canonical pathways has been much more studied for TGF-β compared to BMPs, and was rarely reported in ECs. Furthermore, activation of non-SMAD pathways can occur either in SMAD-dependent or SMAD-independent manner, and both SMAD and non-SMAD pathways affect each other through mutual activation or inhibition dependent on the cellular context and biological processes involved.

Chapter 3. BMP9/BMP10-ALK1 Signaling

In this chapter, my focus is directed towards BMP9 and BMP10, the two ligands that have been used in my PhD project. Since 2002, our research team focuses on uncovering a novel signaling pathway in the vascular system, facilitated by the transmembrane receptor ALK1. During the period 2005-2007, several groups including our research group identified BMP9 and BMP10 as the high-affinity ligands for ALK1 [70, 305, 306]. Mutations in the signaling pathway of BMP9 and BMP10 have been linked to two rare vascular disorders: hereditary hemorrhagic telangiectasia (HHT) and pulmonary arterial hypertension (PAH) [47], which will be further developed in the last two sections of this chapter. During the last 20 years, our team, among others, has been focusing on studying the roles of BMP9, BMP10, and ALK1 in the endothelium to propose new therapeutic approaches in vascular diseases, particularly HHT and PAH.

3.1 Synthesis, Expression and Regulation of BMP9 and BMP10

BMP9 and BMP10 are two closely related ligands within the TGF-β superfamily. They exhibit a high degree of sequence similarity (65% identity at the protein level of the mature form) and follow a typical cysteine knot structure shared by other BMPs of the family. BMP9 is mainly produced by the hepatic stellate cells (HSCs) in the liver, while BMP10 is mainly produced by cardiomyocytes in the right atrium of the heart in adults. HSCs can also produce small amounts of BMP10 which can give rise to heterodimers of BMP9/BMP10 [307] (Figure 21). Similar to other members of the family, these ligands are synthesized as pre-proproteins, which consist of three main parts: an N-terminal signal peptide, a prodomain, and a C-terminal mature growth factor domain. To form functional dimers, the pre-proproteins undergo dimerization through the formation of a single disulfide bond, which connects two mature regions, resulting in pro-BMPs. After dimerization, proBMP9 and proBMP10 undergo proteolytic cleavage mediated by subtilisin-related pro-protein convertases (e.g. Furin) [308, 309]. This cleavage gives rise to two distinct forms of the ligands: A complexed form with the prodomain remaining non-covalently bound to the mature growth factor domain (pd-BMP9 and pd-BMP10; around 100 KDa), and another form consisting of the mature growth factor domain alone, without the prodomain (BMP9 and BMP10; around 25 KDa) [307]. As mentioned previously, prodomains are known to confer latency to TGF-β and some other members of this family. Interestingly, this latency mechanism does not apply to the binding of pd-BMP9 and pd-BMP10 to their high-affinity receptor ALK1 on endothelial cells (ECs) [309, 310]. However, in C2C12, which do not express ALK1, only BMP10 was able to induce expression of ID3, but not pd-BMP10 [311]. This suggests that the prodomain of BMP10 might have the ability to modulate its activity depending on the specific type I receptor involved.

BMP9 and BMP10 display distinct expression patterns in various tissues at different developmental stages. In mice, BMP10 is mostly expressed in the heart in a spatio-temporal manner. BMP10 synthesis begins in the right atrium at embryonic day 8.5 (E8.5), becomes

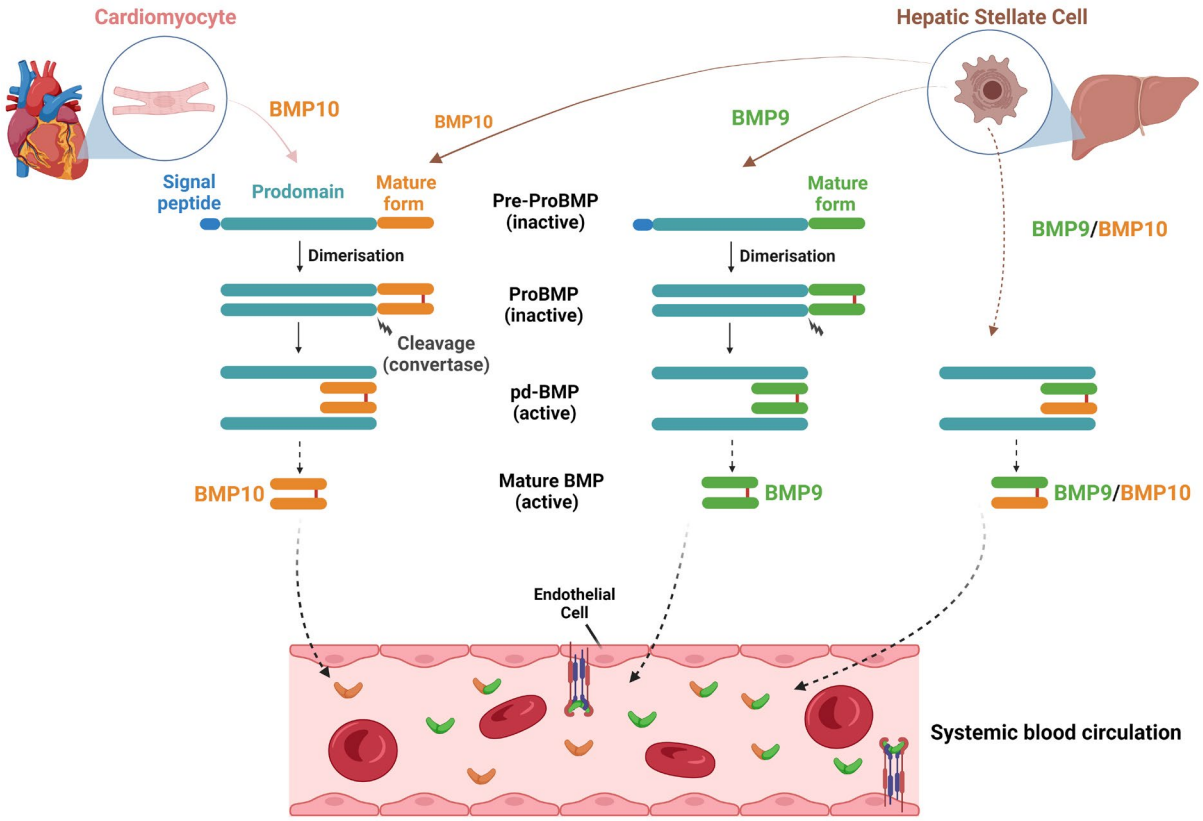

Figure 21. Schematic diagram of BMP9 and BMP10 synthesis and processing.

BMP9 is mainly produced by the hepatic stellate cells (HSCs), while BMP10 is mainly produced in the heart. HSCs can also produce small amounts of BMP10 which can give rise to heterodimers of BMP9/BMP10. The initial steps during synthesis involve the dimerization of inactive precursors, followed by their subsequent cleavage by convertases. This process generates two forms: the non-covalently prodomain-bound BMP (pd-BMP) and the mature BMP, both of which are active in case of BMP9 and BMP10. Active BMPs are then released into the blood circulation to act via their specific receptors on ECs. Figure was created using Biorender.

enriched in ventricles and right atrium at E14.5 which persists until postnatal day 7 (P7), and then becomes restricted in the right atrium in adult mice [47, 312]. BMP10 cardiac expression has also been shown in humans [313]. On the other hand, BMP9 is mainly produced by hepatic stellate cells which begins around E9.75-E10 in mice [314]. Our group has demonstrated that hepatic stellate cells are also capable of synthesizing BMP10, but at much lower quantities in comparison to those produced by the heart [314]. Few studies have also suggested that the brain septum and the lungs may also secrete low levels of BMP9 from yet unidentified cell sources [315, 316]. Heterodimerization of BMPs, such as BMP2-BMP7 and BMP4-BMP7, is a well-known phenomenon that expands the functional diversity of this ligand family and often enhances the potency of the formed dimers [317–319]. Notably, our group has identified biologically active BMP9-BMP10 heterodimers in mouse and human plasma, proposing hepatic stellate cells as their likely physiological source [314]. However, the physiological role of BMP9-BMP10 heterodimers still requires further investigation. Different forms of BMP9 and BMP10 can be detected in the systemic blood circulation. However, given the existing knowledge and available tools, determining the ratios of active to in-active forms, as well as

the ratios of homodimeric to heterodimeric BMP9 and BMP10, presents a significant challenge in this field [47].

Very little is known regarding the regulation of BMP9 and BMP10 local expression and activity. Interestingly, the structure of pd-BMP9 reveals that it can exist in two different conformations: a cross-armed conformation and an open-armed conformation [74]. In addition to being blood circulatory factors, BMP9 and BMP10 could be also be trapped in the ECM. For instance, cross-armed conformation of pd-BMP9 was suggested to occur *in-vivo* by binding to the extracellular matrix, thus locally controlling BMP9 activity [74]. In the case of BMP10, but not BMP9, it has been demonstrated that the prodomain can form stable complexes with extracellular matrix proteins fibrillin-1 and fibrillin-2. These interactions suggest that fibrillin-1 and fibrillin-2 could potentially serve as effective candidates to sequester and regulate the activity of BMP10 [320]. The regulation of BMP10 activity was further highlighted by our group through the observation of increased immunoreactivity and activity in plasma following purification steps using an anti-BMP10 column [314]. This suggests that such treatment releases a fraction of BMP10 that was not initially detected in the crude plasma. Similar increases in BMP activity upon purification from tissues have been reported long time ago for other BMPs [321], indicating the potential release of inhibitors that maintain BMPs in an inactive state. Notably, BMP9 and BMP10 do not bind to the natural BMP antagonist noggin, which may contribute to the potent effect of BMP9 compared to other BMPs in bone formation [322]. Another modulator, named crossveinless 2 (CV2) or BMPER (Bone Morphogenetic Protein-binding Endothelial Regulator), has been shown to bind to BMP9 and BMP10 and was proposed to inhibit the SMAD pathway [323, 324]. However, the role of CV2 as an inhibitor of BMP9 signaling remains a debate topic, as a more recent study suggested that CV2 does not inhibit BMP9 signaling [325]. Therefore, there is currently no definitive evidence regarding a potential *in-vivo* antagonist that could contribute to a "reservoir" of BMP9 or BMP10.

3.2 Receptors of BMP9 and BMP10

In 1996, Panchenko et al discovered that the type I receptor ALK1 is highly expressed in endothelial cells [326]. Using in situ hybridization, the authors demonstrated the expression of ALK1 in different blood vessels of adult rat tissues (lungs, aorta, vena cava and other organs), and more specifically in endothelial cells. In the same year, it was shown that mutations in the *ACVRL1* gene encoding ALK1 were recognized as being responsible for the development of the Rendu-Osler disease type, a rare vascular disease which is also known as hereditary hemorrhagic telangiectasia (HHT) [327]. In adult endothelium, ALK1 expression is predominantly arterial and is higher in the pulmonary compared to the hepatic vasculature [328, 329]. Besides ECs, ALK1 expression was recently reported in hepatic resident macrophages called Kupffer cells [330]. Endoglin (ENG), also known as CD105, constitutes a co-receptor for ALK1. Embryonic mice predominantly expressed endoglin in ECs exhibiting high expression levels in the endocardium and capillaries, moderate expression in arteries and relatively weaker expression in veins [331]. While Eng shares similar expression patterns to

Alk1 during early embryogenesis [331], its expression in adult mice is stronger on the venous side and is low in the lungs, skin, brain and intestine but high in the liver [332]. Besides ECs, endoglin is also expressed in mesenchymal stem cells, some hematopoietic progenitors and immune cells such as monocytes, macrophages and mast cells, suggesting additional roles outside of the endothelium [333]. The expression patterns of ALK1 and ENG are dynamically regulated, being upregulated in actively angiogenic endothelium and downregulated in quiescent adult endothelium [328, 331]. Both receptors are also found to varying extents in capillaries [328, 332]. Being predominantly expressed on ECs, both ALK1 and ENG play crucial roles in the formation and development of the vascular system. As previously reviewed, global deletion of *Acvrl1* or *Eng* (gene encoding endoglin) is embryonic lethal due to severe vascular defects [334].

ALK1 was initially suggested to be a TGF-β receptor based on early studies that observed activation of chimeric receptors containing the extracellular domain of ALK1 and the cytoplasmic domain of the TGF-β receptor ALK5 by TGF-β1 and TGF-β3 [335]. However, this hypothesis was then debated because Alk1 and Alk5 were found to have different expression patterns *in-vivo* [336], and mice lacking Alk5 did not develop the same vascular defects seen in mice lacking Alk1 [337]. In the work that proposed TGF-β1 and TGF-β3 as ligands for ALK1 [335], the authors also described the existence of another unidentified ligand for ALK1 in the serum which remained mysterious for several years. During the period 2005-2007, several groups, including our research group, identified BMP9 and BMP10 as the high-affinity ligands for ALK1 [70, 305, 306]. These two ligands were shown to bind to ALK1 with a very higher affinity (EC_{50} of approximately 50pg/mL) which was much higher compared to other BMPs that bind to their respective receptors ALK2, ALK3, and ALK6 (EC_{50} of around 50ng/mL) [47]. BMP9 and BMP10 also have the ability to bind to other BMP type-I receptors, albeit with lower affinities compared to ALK1. Precisely, BMP9 was found to bind to ALK2, while BMP10 was proposed to bind to ALK3 and ALK6 [47]. Moreover, both BMP9 and BMP10 can directly bind to the homodimeric co-receptor ENG [338]. ENG has been described as a co-receptor for various ligands including BMP2, BMP7, and activin A. However, unlike BMP9 and BMP10, the binding of BMP2, BMP7, and activin A to ENG is indirect and requires the co-expression of a type-I or type-II receptor [339, 340]. Therefore, ENG is suggested to capture circulating BMP9 and BMP10 and present them to the type-I and type-II receptors. This mechanism helps to increase the local supply of BMP9 and BMP10, especially that these ligands lack the heparin-binding region present in other BMPs, which allows them to interact with certain components of the extracellular matrix and regulate their bioavailability [341]. In addition to its high affinity for BMP9 and BMP10, ENG may play an additional role in displacing the prodomain of BMP9, which in turn promotes signaling through ALK1 [342].

Regarding the type-II receptors, BMP9 and BMP10 can bind to the 3 type-II receptors ActRIIB, BMPRII, and ActRIIA in decreasing order of affinity for BMP9, but with similar affinities for BMP10 [343]. However, there are significant differences in the expression levels of these three

receptors in ECs with BMPRII found to be much more highly expressed in compared to ActRIIA and ActRIIB [47].

3.3 Canonical Signaling of BMP9 and BMP10 in ECs through activation of SMADs

The binding of BMP9 and BMP10 to their receptors involves a sequential receptor complex formation. As mentioned previously, these ligands bind to receptor complexes consisting of ALK1 and either BMPRII, ActRIIA, or ActRIIB, with the assistance of the co-receptor endoglin. In contrast to TGF-β and activin proteins, which primarily bind to their respective high affinity type-II receptors, BMP9 and BMP10 bind with high affinity to ALK1 or type-II receptors as well as their co-receptor endoglin. It has been proposed the formation of a temporary complex involving the ligand BMP9 or BMP10, endoglin, and ALK1. Subsequently, endoglin is released, enabling the ligand-ALK1 complex to interact with the type-II receptor, initiating downstream signaling [338]. It is important to note that BMP9 and BMP10 can bind directly to both ALK1 and the type-II receptors, even in the absence of endoglin [343]. Supporting this notion, *in-vivo* studies have shown that overexpression of Alk1 can restore impaired signaling caused by the deletion of endoglin [344]. Following the formation of heteromeric complex, the type-II receptor phosphorylates ALK1 at the level of serine residues within GS domain (Figure 22A and B). This leads to the activation of the Ser/Thr (S/T) kinase domain of ALK1, which in turn phosphorylates C-terminal serine residues in the SXSS motif of the R-SMADs (SMAD1/5/8) [334, 345] (Figure 22B). The phosphorylation of SMAD1/5/8 occurs within a short timeframe of approximately 5 minutes. Importantly, duration of SMAD1/5/8 phosphorylation varies depending on the concentration of BMP9 or BMP10. Lower doses (0.1 ng/mL) result in a shorter duration, typically lasting a few hours, while higher doses (10 ng/mL) can extend the phosphorylation period up to 24 hours [305, 346]. Following phosphorylation, the ligand-receptor complexes are rapidly internalized through endocytosis, where they can be either recycled back to the cell membrane or undergo degradation through proteolysis [347]. Phosphorylated SMAD1/5/8 (pSMAD1/5/8) then forms a trimeric complex with SMAD4, which translocate to the nucleus and associates with other transcriptional regulators to modulate the expression of their specific target genes. The outcome of BMP9 and BMP10 signaling in ECs is believed to ensure vascular quiescence, a hallmark of mature endothelium [6, 348] (Figure 22B). Strong target genes for BMP9 and BMP10 include *ID1*, *ID2* and the I-SMADs (*SMAD6* and *SMAD7*), the latter forming a negative feedback loop to regulate the signaling [305]. Notably, a recent study by Salmon et al demonstrated that pd-BMP9 and pd-BMP10 exhibited comparable potency to their respective growth factor domains, as assessed by *ID1* gene induction. Furthermore, microarray experiments revealed that pd-BMP9 and pd-BMP10 induced highly similar transcriptional regulation, suggesting that they act as functionally equivalent ALK1 ligands *in-vitro* on endothelial cells [325]. Interestingly, recent unpublished data from our lab further supports this notion (work under review).

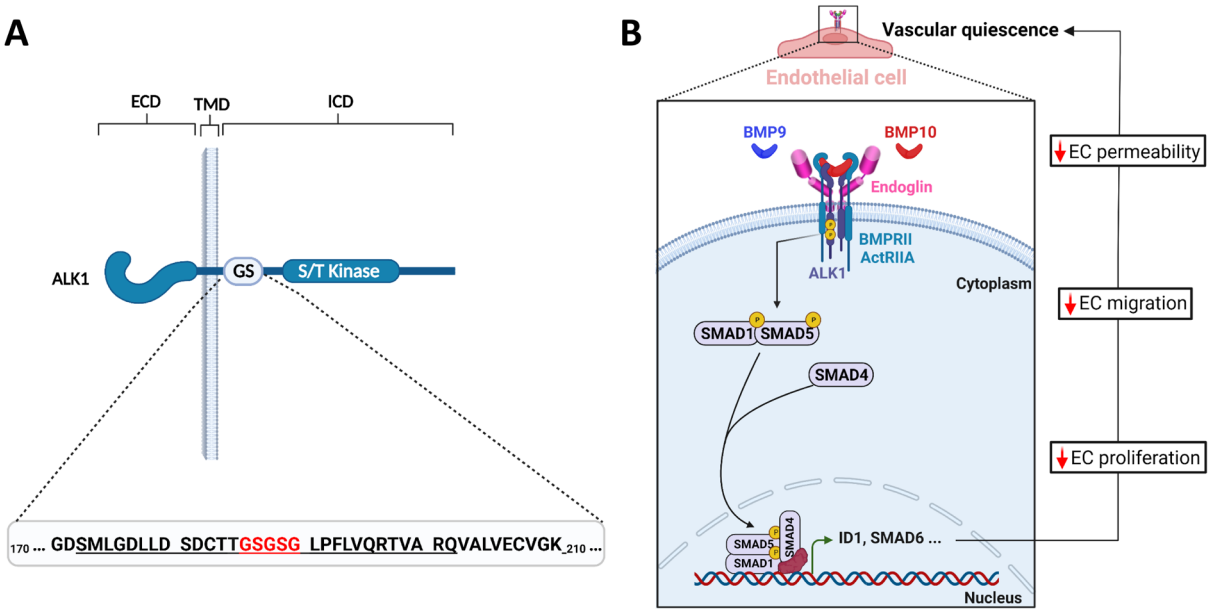

Figure 22. BMP9 and BMP10 Signaling Pathway.

*(**A**) Schematic illustration of different domains of type-I receptor ALK1. ALK1 is composed of an extracellular domain (ECD) for BMP9 and BMP10 binding, a transmembrane domain (TMD) and an intracellular domain (ICD) comprising the GS box and the S/T kinase domain. Sequence highlighted represents the 170-210 amino acid region around the GS box (underlined). The SGSGSG characteristic core sequence of this domain is labeled in red. (**B**) BMP9 and BMP10 homo- or hetero-dimers bind with high affinity to a receptor complex consisting of ALK1, endoglin, and either BMPRII, ActRIIA, or ActRIIB on the surface of ECs. Upon ligand binding, ALK1 is phosphorylated by the type II receptor, leading to its activation. Activated ALK1 then phosphorylates R-SMADs 1/5/8, which forms a complex with SMAD4 and translocate to the nucleus. In the nucleus, the SMAD complex interacts with other transcriptional cofactors (co-activators or co-repressors) to modulate the expression of many target genes. The general outcome of this pathway results in decreased EC proliferation, permeability and migration, promoting vascular quiescence. Both figures were created using Biorender.*

As mentioned in the previous chapter, TGFβ superfamily ligands exhibit a highly context-dependent mode of activation of downstream signaling pathways. In ECs, in addition to the phosphorylation of SMAD1/5/8, BMP9 was also shown to mediate the phosphorylation of SMAD2, albeit at much weaker intensities in comparison to pSMAD1/5/8. For instance, BMP9-induced pSMAD2 occurs in an ALK1 dependent ALK5 independent manner and was only detectable at BMP9 concentrations ≥ 1ng/mL, whilst the phosphorylation of SMAD1/5/8 can be detected at concentrations as low as 0.1ng/mL BMP9 in pulmonary arterial ECs [112, 349]. Moreover, the activation of SMAD2 by BMP9 through ALK1 was found to be dependent on the presence of the ActRII receptor and the EC type [112]. On the other hand, the responses involving SMAD1/5/8 and induction of ID proteins relied on the presence of both BMPRII and ActRII receptors [112]. Hence, it is suggested that different type-II receptors play a role in regulating the activation of the dominant SMAD1/5/8 pathway compared to the weaker SMAD2 branch in response to BMP9-ALK1 signaling [112, 349].

The BMP9/10-ALK1 SMAD signaling pathway has been demonstrated to be a mechanosensitive pathway responsive to the force exerted by flowing blood on the endothelial cells (also known as hemodynamic shear stress). HUVECs exposed to varying levels

of fluid shear stress (FSS) exhibited a peak activation of SMAD1/5/8 phosphorylation when subjected to physiological FSS levels ranging from 10 to 20 dyn/cm2 [350]. Furthermore, several studies have shown that flow potentiates the SMAD1/5/8 response to soluble BMP9 [351–354]. *In-vivo* studies conducted in mice and zebrafish revealed that ALK1 expression was more prominent in regions experiencing higher blood flow, indicating its regulation by hemodynamic forces [328, 329, 331].

Apart from the activation of the canonical SMAD signaling pathway, BMP9 also regulates and/or crosstalks with other non-canonical signaling pathways in both endothelial and non-endothelial cells. However, the specific mechanisms governing the modulation of these pathways remain poorly understood and context dependent. In the following section, I will emphasize the roles of BMP9 and BMP10 signaling in the regulation of these pathways and highlight the consequential physiological outcomes of such modulation, with a particular focus on endothelial cells.

3.4 Physiological Roles of BMP9 and BMP10 Signaling

3.4.1 Roles in the Endothelium

As mentioned previously, BMP9 and, to a lesser extent, BMP10, have been characterized as inhibitors of various endothelial cell functions such as proliferation, migration, tube formation, and angiogenesis [23, 355]. In the following subsections, I will provide an overview of the different physiological roles of BMP9 and BMP10 in the endothelium.

3.4.1.1 Effects on Proliferation and Migration

The coordination of EC proliferation and migration is crucial for the formation of mature blood vessels during angiogenesis. Before the identification of ALK1's ligand, our group found that overexpression of constitutively active ALK1 (ALK1ca) inhibited both proliferation and migration of human microvascular ECs (HMVECs) from the dermis, as well as migration of pulmonary HMVECs and HUVECs [356, 357]. Accordingly, ALK1ca overexpression inhibited EC proliferation, but had no impact on tube formation in HUVECs [358]. Both BMP9 and BMP10 were shown to suppress proliferation and migration of HMVECs from the dermis [305], which was confirmed by Scharpfenecker et al [306], who showed similar effects of BMP9 on fibroblast growth factor 2 (FGF2)-stimulated bovine aortic endothelial cells (BAEC). Additionally, BMP9 was shown to inhibit proliferation [112, 359] and migration [360] of human pulmonary artery ECs (HPAECs). Still, few opposing results have been reported for the roles of BMP9 and BMP10 in the endothelium. For instance, overexpression of ALK1ca enhanced migration in microvascular ECs [361]. BMP9 and BMP10 have also demonstrated pro-angiogenic and proliferative functions in certain endothelial cells derived from embryonic stem cells, both *in-vitro* and *in-vivo* [362–365]. However, the current consensual working model is that BMP9 and BMP10 are circulating vascular quiescent factors [6].

3.4.1.2 Roles in Vascular Permeability and Inflammation

Endothelial cells play also a critical role in managing the integrity of the vascular barrier. This barrier is responsible for controlling the movement of plasma proteins and circulating cells across the endothelial layer, which is tightly controlled by a number of extracellular stimuli and mediators to maintain tissue homeostasis. During inflammation, vascular permeability is disrupted to aid migration of immune cells from the blood to injury or infection sites. However, impaired regulation of endothelial permeability is associated with several pathological conditions including chronic inflammation, edema, and tumor angiogenesis.

BMP9 and BMP10 have shown to be implicated in regulating vascular permeability and inflammation. *In-vitro* studies using HPAECs indicate that BMP9 can protect against EC excessive permeability induced by factors such as tumor necrosis factor alpha (TNFα), lipopolysaccharides (LPS), or thrombin [366, 367]. Moreover, it was observed that BMP9 and BMP10 inhibit the release of CCL2 (MCP-1), a key chemoattractant molecule involved in inflammation, by HPAECs [368]. Moreover, the group of Bruno Larrivée showed that BMP9 administration decreased vascular permeability *in-vitro* in hyperglycemic ECs [369]. Mechanistically, they suggested that BMP9 counteracts hyperglycemia-induced permeability by limiting VEGFR2 signaling, inhibiting VE-cadherin internalization, and inducing the expression of the tight junction component occludin [369] (Figure 23).

Altogether, these findings suggest that BMP9 and BMP10 act as EC protective factors against inflammation either directly or by limiting vessel permeability and/or injury. However, the exact mechanisms underlying these effects remains poorly understood.

3.4.1.3 Consequences of BMP9 and BMP10 Loss: Further Insights from Mouse Models

In-vivo, BMP9 and BMP10 exhibit both similar and specific functions, which are influenced by factors such as their expression site, expression kinetics, localization, and the presence of specific combinations of receptors on target cells. To better understand the overall physiological roles of BMP9 and BMP10, studies have utilized different mouse models deficient in *Bmp9* and/or *Bmp10*, or their signaling pathways, which were recently reviewed [47, 370].

In particular, *Bmp9*-knockout (KO) mice in a C57BL/6 genetic background were found to be viable, fertile and did not display any obvious blood vascular defects [371–373]. Nevertheless, these *Bmp9*-KO mice exhibited some subtle defects in their lymphatic vasculature characterized by enlarged collecting vessels, reduction in the number of lymphatic valves and impaired lymphatic drainage [374, 375]. Interestingly, our group showed that when *Bmp9* was deleted in a different mouse strain, the 129/Ola, a more severe phenotype was observed which was characterized by a significant reduction in fenestrations of liver sinusoidal endothelial cells (LSECs), accompanied by inflammation and liver fibrosis [376]. Subacute neutralization of endogenous BMP9 results in lung vascular injury, characterized by increased

endothelial permeability and the extravasation of neutrophils, which was reversed by re-administration of BMP9 to these mice [14].

On the other hand, *Bmp10*-KO mice experience embryonic lethality between embryonic days E9.5 and E10.5 due to the failure of cardiac trabeculation [377]. As previously mentioned, the expression of Bmp10 in mice is observed around E8.5. Notably, this expression precedes the expression of Bmp9 in the liver, which is detected around E9.75-E10. Thus, the absence of Bmp9 before E9.75 was initially suspected to contribute to this cardiac phenotype. However, attempts to mitigate this phenotype by knocking in the Bmp9 gene into the Bmp10 locus were unsuccessful, confirming a specific role of Bmp10 in cardiac development that may be independent of signaling through ALK1 [372]. To overcome embryonic lethality and investigate the impact of Bmp10 loss on the adult mouse vasculature, strategies such as inducible knockdown or the administration of neutralizing Bmp10 antibodies were employed to delete Bmp10 postnatally. However, in all cases, the deficiency of *Bmp10* alone in these postnatal mice did not result in any defects in blood vasculature [371–373]. However, very recent work conducted by Paul Oh's group has proposed a specific role for BMP10. They found that inducible Bmp10-KO mice, but not Bmp9-KO mice, exhibited arteriovenous malformations (AVMs) in developing retinas, postnatal brain, and adult wounded skin [312]. Surprisingly, administration of BMP10 in these mice, but not BMP9, was able to prevent retinal AVMs in mice with simultaneous loss of *Bmp9* and *Bmp10* [312]. The underlying mechanism remain to be characterized. It is worth mentioning that the latter study was conducted using a hybrid mice background consisting of 129 Ola and C57BL/6 strains. To better understand the contribution of BMP10 in lymphatic function, further investigations are needed to determine if the observed lymphatic phenotype in *Bmp9*-KO mice is solely attributed to the reduction in overall ALK1 signaling caused by the absence of one ligand or if it represents a specific function of BMP9. Similarly, the impact of Bmp10 deletion on liver vasculature has not been explored.

Importantly, only the loss of both *Bmp9* and *Bmp10*, either through genetic means or through the use of antibodies or ligand traps, resulted in overt vascular phenotypes. These mice were characterized by defects in retinal vascularization, including increased vascular density and arteriovenous shunting (direct connections between arteries and veins), as well as impaired closure of the ductus arteriosus [371–373, 378–380]. These observations suggested that BMP9 and BMP10 may have redundant roles during postnatal angiogenesis. These models will be further developed below when used as preclinical models for HHT.

Altogether, these findings highlight the complex and dynamic roles of BMP9 and BMP10 in vascular development and angiogenesis, suggesting both redundant and distinct functions depending on the specific context (e.g., tissue examined, genetic background, age, among other possible factors).

3.4.2 Signaling Mechanisms Governing the Regulation of EC Functions through BMP9/BMP10/ALK1 signaling

As highlighted in figure 5, VEGF stands out as one of the most powerful pro-angiogenic factors. It transmits signals through several signaling pathways, primarily involving P38, MEK/ERK, and PI3K/AKT, to regulate various EC functions critical to angiogenesis. These include EC migration, proliferation, arteriovenous specification, survival, and permeability (Figure 5). Only few studies attempted to decipher the mechanisms by which BMP9/BMP10/ALK1 signaling regulates these functions in ECs through studying their effect, either solely, or in combination with other factors such as VEGF. In the following subsection, I will explain how BMP9 and BMP10 signals can either block or crosstalk with other pathways in the endothelium to carry out these functions which defines them as endothelial quiescent factors [6, 348].

3.4.2.1 Regulation of PI3K/AKT Signaling

The PI3K/AKT signaling pathway plays a central role in regulating various biological processes within the endothelium, including EC survival, growth, proliferation and vascular permeability [381, 382]. This pathway can be activated by key endothelial factors (e.g. VEGF, ANG1; section 1.2.2.1), but also by blood flow-driven shear stress [383, 384]. Several studies have shown that BMP9 negatively regulates PI3K/AKT signaling [385–387]. Mechanistically, this mechanism has been shown to be dependent on BMP9-induced activation of PTEN, a well-known phosphatase that downregulates PI3K/AKT signaling [388]. Treatment of HUVECs and mouse lung ECs (mLECs) with BMP9 for 2 hours strongly attenuated AKT phosphorylation, and this was shown to occur via BMP9 through decreased phosphorylation, which activated the phosphatase activity of PTEN, and stabilization of PTEN [386]. These results were further supported by Alsina-Sanchís et al, who showed that 2h pretreatment of HUVECs with BMP9 activated PTEN and strongly attenuated AKT phosphorylation, both in the presence or absence of VEGF [385]. Interestingly, the authors from the two aforementioned studies showed that this effect is observed only after a minimum of 2 hours pre-incubation with BMP9, suggesting an indirect mechanism requiring de-novo protein synthesis. Supporting this notion, Ola et al showed that BMP9 mediates transcriptional repression of CK2 kinase via SMAD4 [387]. Since CK2 has been shown to mediate inactivation of PTEN through inhibitory phosphorylation [389], they showed that repression of CK2 resulted in decreased PTEN phosphorylation, consequently activating PTEN.

Activated AKT phosphorylates multiple downstream effectors, including mTOR. However, It was shown that BMP9 rapidly induces the expression of serum and glucocorticoid activated kinase 1 (SGK1) via activation of SMAD1/5/8 [390]. Consequently, BMP9-induced upregulation of SGK1 in ECs leads to the activation of the mTORC1/S6 Kinase/S6 pathway, resulting in increased protein synthesis [391]. The elevated expression of SGK1 plays a crucial role in proper vessel development [392, 393]. Traditionally, cell growth and division were considered parallel processes. However, it has been observed that SGK1 can be partially activated when AKT is inhibited, with SGK1 still activating similar downstream effectors as AKT [394–396].

Consequently, SGK1 enables the inhibition of cell proliferation while maintaining an active metabolic state. Therefore, this suggests a mechanism by how BMP9 exhibits both promotion of cell growth and anti-proliferative effects [397].

3.4.2.2 Regulation of ERK Signaling

The Raf/MEK/ERK signaling cascade plays a key role in EC proliferation, but has also shown to be implicated in other EC functions including migration [398, 399], EC integrity and cell fate [400]. BMP9 has been also shown to attenuate ERK phosphorylation in ECs. For instance, the study by Alsina-Sanchís et al showed that BMP9 dampens VEGF-induced activation of not only AKT but also ERK signaling [385]. As mentioned in the above section, the authors in this study showed that the effect of BMP9 on ERK was delayed, supporting an indirect pathway. Accordingly, Medina-Jover et al suggested that BMP9-induced expression of SGK1 downregulates the activation of ERK, resulting in decreased EC proliferation [391]. However,

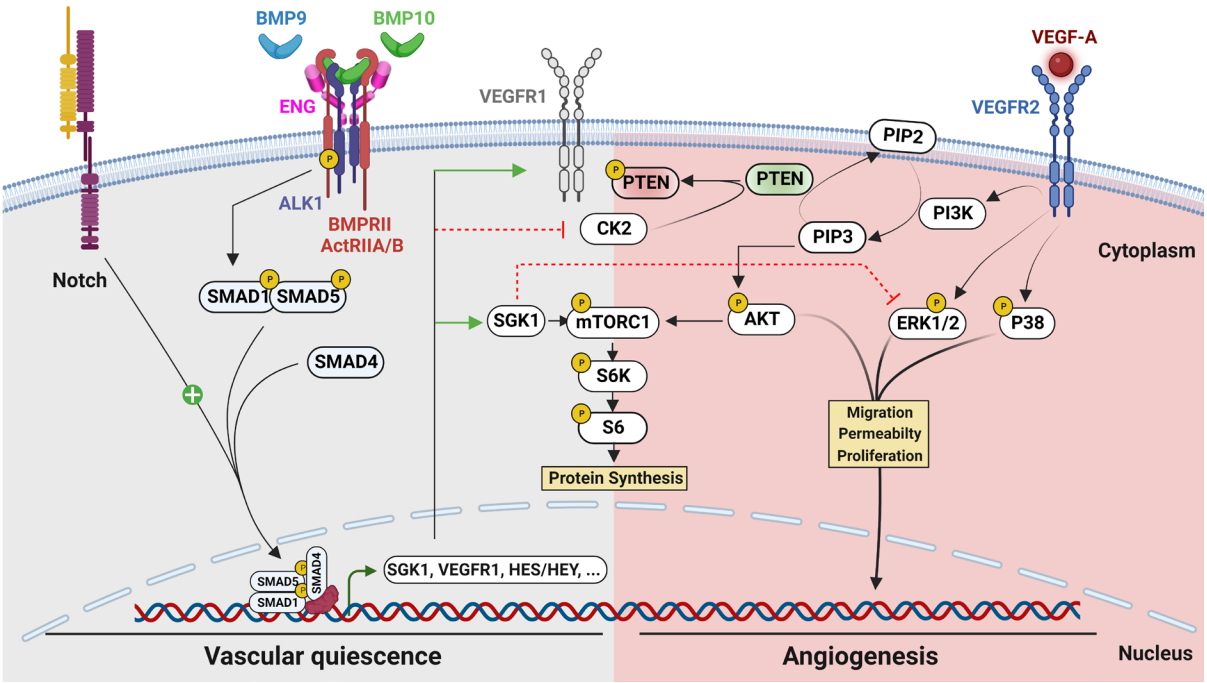

Figure 23. Schematic illustration of the negative crosstalk by BMP9/10-ALK1 pathway on VEGF/VEGFR2 signaling in endothelial cells (ECs).

Upon binding to their receptors, BMP9 and BMP10 activate the SMAD1/5 pathway, leading to the transcriptional regulation of many target genes involved in vascular maturation and homeostasis, in collaboration with other signaling pathways like Notch. BMP9/10-ALK1 signaling has been shown to strongly attenuate VEGF signaling through few described mechanisms. For instance, BMP9/10-ALK1 has shown to stronlgly attenuate PI3K/AKT pathway through increased PTEN phosphatase activation, possibly due to decreased expression of its negative regulator CK2 kinase, a negative regulator of PTEN. Moreover, BMP9 induces the expression of VEGFR1, a decoy receptor for VEGF, thus restricting VEGF downstream signaling. BMP9/10 also induces the expression of SGK1 kinase, which activates the mTORC1/S6K/S6 pathway, thus regulating protein synthesis. Through an unknown mechanism, SGK1 induction by BMP9/10 also inhibits VEGF-induced activation of the ERK pathway, resulting in decreased EC proliferation. Dashed lines represent unknown mechanisms; +, positive cooperation; Ⓟ Phosphorylation; yellow rectangles represent functions. Green and red lines represent activation and repression, respectively. Figure was created using biorender

the exact mechanism of how SGK1 regulates ERK signaling remains yet uncharacterized. In addition, our group suggested that overexpression of constitutively active ALK1 inhibited EC migration in a SMAD-independent manner via inhibiting JNK and ERK MAPK pathways. On the other hand, at least one study reported opposing results regarding this negative regulation of ERK signaling by BMP9/ALK1 in ECs. The group of B Larrivée et al showed that BMP9 can activate ERK phosphorylation within a short time frame of 10-15mins in an ALK1 dependent manner [378].

3.4.2.3 Regulation of P38 MAPK

P38 MAPK signaling mediates regulation of several biological processes involving cytoskeletal dynamics, inflammatory reactions, and stress responses, which affects several EC functions including migration, permeability and apoptosis [33]. Very little is known about regulation of P38 signaling by BMP9 and its implication in BMP9-regulated EC functions. Two studies have showed that BMP9 induces the expression of the vasoconstrictor endothelin-1 (ET-1) in both HPAECs and HMVECs [349, 360]. These studies highlighted that BMP9 induces slight phosphorylation of P38. Through the use of pharmacological inhibitors, Park et al showed that ET-1 induction by BMP9 was P38 dependent and plays a role in the attenuation of EC migration [360]. Surprisingly, through the use of siRNA, they showed that the expression of ET-1 by BMP9 was dependent on SMAD1/5, but not on SMAD4, and only partially dependent on ALK1 and BMPR2 receptors. Moreover, Alsina-Sanchís et al have also showed that BMP9 induced phosphorylation of P38. Interestingly, the authors demonstrated that, while BMP9 dampens VEGF-induced activation of ERK and AKT pathways, a synergistic effect was observed when both ligands were employed on ECs [385]. Activation of P38 signaling by pro-angiogenic factors (e.g., VEGF) is associated with promoting EC migration. Given that, it remains unclear how to explain the role of P38 in BMP9-mediated attenuation of EC migration [360] and how BMP9 augments P38 activation by VEGF [385]. Therfore, it is crucial to approach the above findings with caution to draw out clear conclusions, where further investigations are necessary to unravel the specific mechanisms regarding the regulation of P38 signaling and their roles by BMP9/BMP10/ALK1 signaling in ECs.

3.4.2.4 Crosstalk with Notch signaling

As emphasized in section 1.2.2.1.4, the Notch signaling pathway plays pivotal roles in angiogenesis by regulating crucial EC functions such as cell fate determination, migration, differentiation, and proliferation [52, 359, 401–404]. Several studies have emphasized the collaborative interplay between BMP9/BMP10 signaling and Notch signaling in ECs to counteract VEGF signaling effects, promoting vascular quiescence maturation and arterialization. B Larrivée et al showed that BMP9/BMP10/ALK1/SMAD signaling synergizes with Notch signaling resulting in the simultaneous upregulation of Notch target genes HEY1 and HEY2. This coordinated activation suppresses VEGF signaling and inhibits tip cells formation [378]. Notably, the authors also demonstrated that BMP9 and BMP10-induced HEY1 and HEY2 occurs independently of the canonical Notch activation. Furthermore, DLL4

and BMP9 cooperatively induced the expression of HEY1/2 genes and effectively suppressed proliferation in human aortic endothelial cells (HAECs) [359]. The authors demonstrated that this inhibitory impact on HAEC proliferation resulted from the modulation of various cell cycle-related proteins, highlighting a crucial role of the cyclin dependent kinase (CDK) 4/6 inhibitor P27KIP1 as a central mediator of endothelial quiescence. Mosaic bead-sprouting assays using ECs with knockdown of ALK1, SMAD4, or HEY2 demonstrated their enrichment at the tip cell position, consistent with previous experiments utilizing ECs with knockdown of SMAD1 and SMAD5 [405]. Together, these studies demontsarte that Notch and BMP9/BMP10/ALK1 signaling pathways display cooperative signal transduction in order to maintain vascular homeostasis.

3.4.3 Roles in Non-Endothelial Cells

In addition to their established roles in the endothelium, BMP9 and, to a much lesser extent, BMP10 have been demonstrated to play significant roles in various tissues, regulating diverse functions such as osteogenesis, metabolism, neurogenesis, inflammation, tumorigenesis, adipogenesis, heart development, liver and lung homeostasis, among others. [324, 373, 377, 406]. In MC3T3-E1 pro-osteoblasts, kinetic stimulation by BMP9 leads to rapid activation of multiple signaling pathways, including PI3K/AKT, ERK, and JNK [407]. The activation of the PI3K pathway was evident through the phosphorylation of AKT and its downstream kinase GSK3β. Through the use of kinase inhibitors, they demonstrated that AKT/GSK3β is essential for the expression of ALP (alkaline phosphatase) and Runx2 genes, which were critical for BMP9-induced differentiation of osteoblasts. A more recent study conducted by the same group has found that the activation of the PI3K pathway, rather than the ERK and JNK pathways, plays a major role in upregulating the expression of HIF1α [408]. Upregulation of HIF1α mediated the expression of PDK1 which played an important role in BMP9-mediated osteoblast differentiation. BMP9 has been found to enhance the proliferation of the hepatic cell line HepG2 [409]. Kinetic stimulation by BMP9 revealed the activation of PI3K pathway, whilst ERK and JNK pathways were not significantly affected. Using kinase inhibitors and RNA interference (RNAi), the authors demonstrated that the proliferative effects of BMP9 in HepG2 cells were primarily mediated by the PI3K pathway. Importantly, these effects were found to be independent of SMAD4. Addante et al showed that BMP9 induced apoptosis of hepatic progenitor cells (oval cells) [410]. In these cells, the apoptotic effect of BMP9 was attributed to the activation of the p38 MAPK pathway, involving ALK2 and TAK1 as crucial components for this activation. On the other hand, BMP10 was shown to play a role in trophoblast differentiation through activation of p38 MAPK pathway in human embryonic stem cells (hESCs) [411].

Hence, the activation of distinct non-canonical signaling pathways by BMP9 and BMP10 has been reported in various non-endothelial cell types, revealing their diverse roles in different tissues. However, the underlying mechanisms responsible for the activation these pathways remain unclear with signaling pathway that seem highly cell-context dependent.

3.5 General overview of the Pathologies Associated with impaired BMP9 and BMP10 signaling

Our initial understanding of the roles played by BMP9 and BMP10 in endothelial functions originated from human data. In 1990's, mutations in two orphan receptor genes, *ACVRL1* (encoding ALK1) and *ENG* (encoding endoglin), were found to be associated with the rare vascular disease HHT [327, 412]. Few years later, in 2000, mutations in *BMPR2* (encoding the type-II BMP receptor BMPRII) were identified in another rare vascular disease called PAH (Pulmonary Arterial Hypertension) [413]. Although both diseases involve the same signaling complex expressed in endothelial cells, they exhibit distinct characteristics, setting them apart from each other.

3.5.1 Hereditary hemorrhagic telangiectasia (HHT)

3.5.1.1 Brief Overview of the Disease

HHT is an autosomal dominant genetic disorder that affects approximately 1 in 5000 to 8000 individuals worldwide [414]. It is characterized by various vascular abnormalities, including the presence of small vascular malformations known as telangiectasia, which appear as red spots on the skin or mucous membranes [415–419]. Telangiectasia in the nose can lead to recurrent epistaxis [420], most common symptom for HHT, while intestinal telangiectasia can cause gastrointestinal bleeding [417]. These bleeding events can result in anemia [421]. Additionally, HHT is associated with the formation of arteriovenous malformations (AVMs) in specific organs (lungs, liver, and brain) which are abnormal networks of blood vessels that directly connect arteries to veins, bypassing the normal capillary network [422] (Figure 24). The presence of AVMs in internal organs can be asymptomatic, but could also lead to different complications depending on their location and severity. Around 70% of HHT patients have hepatic AVMs, which have been reported to increase cardiac output. Pulmonary AVMs are found in 15%-45% of patients and can increase the risk of stroke. Cerebral AVMs, although less common (10%-23% of patients), can have severe consequences such as brain hemorrhage and seizures [414]. Mutations in *ENG* and *ACVRL1* genes are responsible for approximately 90% of HHT cases and give rise to two forms of the disease, HHT1 and HHT2, respectively [307]. In addition to *ACVRL1* and *ENG*, a small proportion of cases (<2%) are attributed to mutations in the *SMAD4*, resulting in a combined syndrome of HHT and juvenile polyposis [423]. More recently, mutations in *GDF2* (gene encoding BMP9) have been identified in a few patients with HHT-like symptoms [424–426]. However, the involvement of BMP9 mutations in HHT is still under debate, as only a limited number of cases have been described. Despite that HHT is caused by germline loss of function (LOF) mutations in *ENG* or *ACVRL1* that are expressed by all vascular beds in the body, vascular malformations appear focally and strictly in characteristic locations [427]. In addition, related patients carrying the same mutation can display different manifestations of the disease, which might be due to modifier genes or other causes [428]. However, it sems clear that HHT heterozygosity cannot fully explain the localized and diverse nature of vascular lesions, leading to the hypothesis of a "second-hit" event that

triggers these lesions [429]. Ongoing research has identified a range of potential triggers that could work in conjunction with HHT gene heterozygosity to induce the development of vascular lesions. These postulated secondary factors include inflammation, angiogenic stimuli, shear stress, modifier genes, and even somatic mutations occurring in the WT HHT gene allele [429].

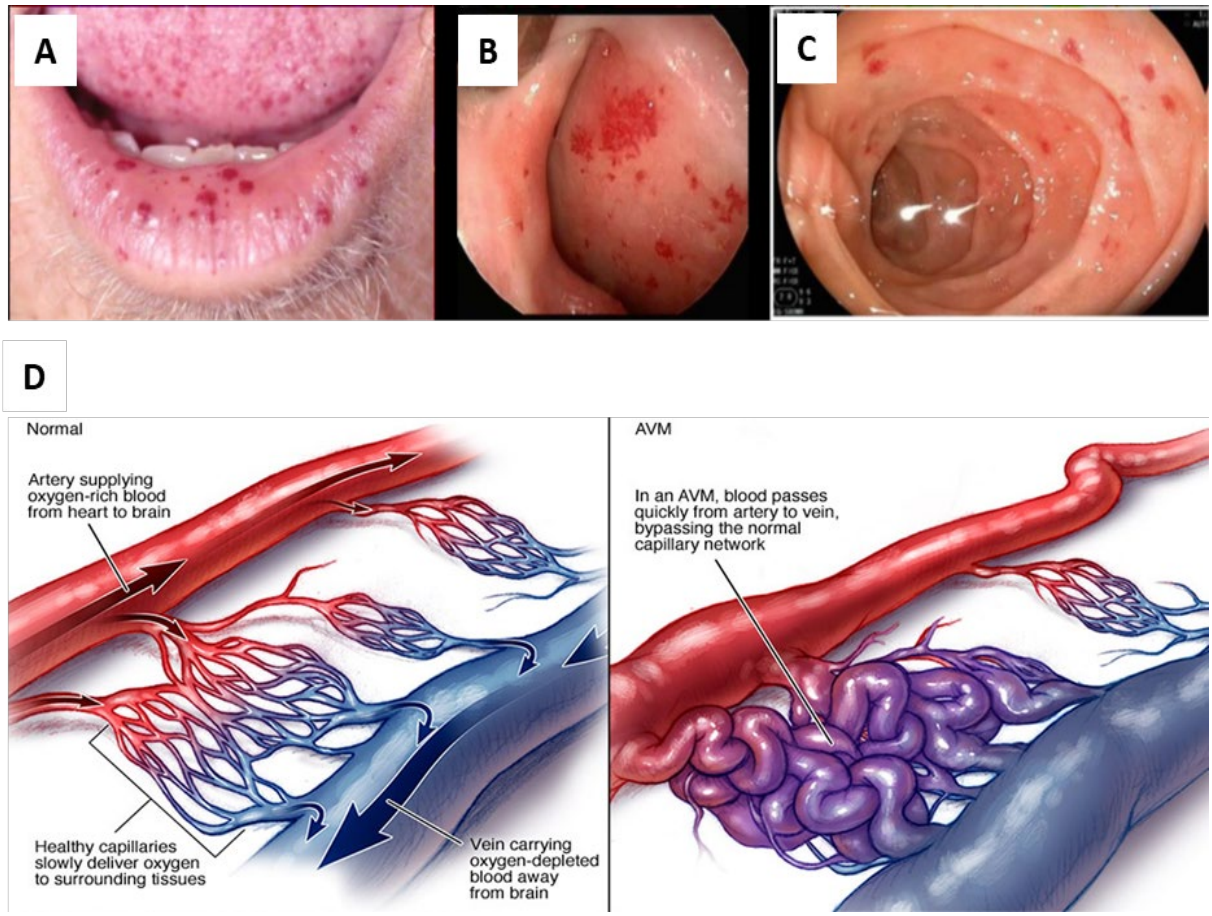

Figure 24. HHT Telangiectasia and AVMs.

A-C, Typical telangiectasia of HHT patients. A, *Telangiectasia on the lip and tongue of an HHT patient.* ***B*** *and* ***C,*** *Endoscopic views of telangiectases in the nasal septum (B) and small intestine (C) of HHT patients.* ***D*** *Normal Capillary network vs Arteriovenous Malformations (AVMs). Images were taken from " The pulmonary vascular complications of hereditary haemorrhagic telangiectasia" by Faughnan et al, European Respiratory Journal, 2009 (**A**), "Manifestations of hereditary hemorrhagic telangiectasia in children and adolescents" by Folz et al, Eur Arch Otorhinolaryngol, 2006 (**B**), "Diagnosis and treatment of patients with hereditary hemorrhagic telangiectasia (Rendu-Osler-Weber syndrome) at a university hospital in Colombia" by Mosquera-Klinger et al, Revista colombiana de Gastroenterología, 2019 (**C**), and https://nchmd.org/health-library/articles/con-20155121/ (**D**).*

To date, the detailed molecular mechanism leading to HHT pathogenesis remains poorly understood. Nevertheless, treatment options for HHT were recently reviewed [414, 430] and include surgery for certain AVMs and anti-VEGF therapy, which has shown success in reducing epistaxis, the most common manifestation in HHT, and cardiac output in patients with severe liver involvement.

3.5.1.2 Current Treatments

Current treatments for HHT focus on reducing the risk and severity of bleedings while managing resulting anemia [422]. Medical measures are employed to control HHT-related epistaxis, with treatment plans that are usually stepwise and tailored to the severity of bleeding in individual patients [422]. Moisturizing topical therapy is recommended as the first-line treatment for HHT-associated epistaxis. Second-line options include the antifibrinolytic agents such as tranexamic acid, which can be taken orally to slow down clot breakdown and prevent or manage HHT-related epistaxis [422]. The effectiveness of tranexamic acid in reducing epistaxis severity has been confirmed through two randomized control trials, with minimal adverse events reported [431, 432]. For patients who show no improvement with the aforementioned measures to control epistaxis, antiangiogenic agents or ablative therapies such as laser photocoagulation, radiofrequency ablation and injection sclerotherapy may be used to seal or collapse the abnormal hemorrhagic nasal vessels. However, these approaches typically offer only temporary improvement and do not cure the disease [422, 433]. Epistaxis and gastrointestinal bleeding, separately or combined, often lead to iron-deficiency anemia, which is treated with iron supplementation or red blood cell transfusions [422]. For pulmonary AVMs and some accessible brain AVMs, surgical resection or embolization is performed to halt blood flow into the lesions and reduce the occurrence or risk of bleeding [422, 434, 435]. Patients with severe hepatic involvement are referred for orthotopic liver transplantation [422].

3.5.1.3 Future Treatments

Individual case reports of HHT patients have indicated that the use of bevacizumab, an anti-VEGF antibody dedicated for cancer treatment and as an immunosuppressor with anti-angiogenic properties following organ transplantation, has significantly improved HHT symptoms [436–438]. Following these reports, since 2012, anti-VEGF treatment using bevacizumab was tested on HHT patients in several clinical trials [414]. Below, I will summarize various studies that highlight data obtained from animal models and clinical trials, showing the promising progress in HHT therapy development [370].

3.5.1.3.1 Preclinical models

Recent studies have increased their efforts to identify potential therapeutic targets for HHT using different animal models [370]. These studies have highlighted various approaches for the treatment of HHT evaluating the effectiveness of inhibiting ANG2 [439] , PI3K [385, 386, 440], mTOR [441, 414], tyrosine kinase receptors [440, 442], integrin-YAP (yes-associated protein)/TAZ [443], and VEGF signaling [444], while activating ALK1 signaling [344, 441].

As highlighted in section 3.4.1.1, the PI3K-AKT signaling pathway plays a crucial role in several EC functions, mainly EC survival and permeability, through signals transmitted by VEGF/VEGFR2, but also others mediators such as Ang1/Tie2 signaling. Several studies

highlighted that BMP9/BMP10/ALK1 signaling attenuate PI3K/AKT signaling both *in-vitro* (elaborated in section 3.4.2.1) and *in-vivo*, through activation of PTEN phosphatase. Accordingly, in the context of defective BMP9/BMP10/ALK1 signaling, over-activation of the PI3K-AKT pathway has been observed in vascular lesions from several HHT mouse models [385–387]. Interestingly, inhibiting PI3K-AKT signaling genetically or pharmacologically in these mice not only prevented but also reversed vascular dysplasia associated with HHT [385–387]. Activated AKT phosphorylates multiple downstream effectors, including mTOR (Figure 23). Notably, over-activation of mTOR signaling downstream of AKT was also observed in BMP9/BMP10-immunoblocked mice, and blocking it reduced vascular defects in these mice [442]. Interestingly, alpelisib, a more specific PI3K inhibitor, has shown promising results in mouse models of venous malformations, as it effectively reduced venous malformation volume and induced regression of cutaneous lesions [445], thus serving as another therapeutic candidate that can be tested in the context of HHT.

During a screen of FDA-approved drugs, two potent activators of BMP signaling were identified: Sirolimus (also known as rapamycin, an immunosuppressor and mTOR inhibitor) and Tacrolimus (FK506) [441, 446]. Tacrolimus was found to activate SMAD1/5/8 signaling in both ALK1-mutated endothelial cells and BMP9/10-immunoblocked mice, while blocking VEGF-induced AKT activation, resulting in a reduction in vascular dysplasia [441]. Combining Sirolimus with Nintedanib, which targets the receptors of PDGF, FGF and VEGF, has demonstrated a synergistic effect in preventing and reversing vascular malformations, bleeding, and anemia in HHT mouse models [442].

Zhu et al. demonstrated that by utilizing adeno-associated virus-mediated expression of soluble VEGFR1, which acts as a VEGF ligand trap, reduces brain AVM severity through the inhibition of VEGF-dependent downstream signaling [447]

In addition to VEGF signaling, Ang1/Tie2 (TEK) has been also observed to be dysregulated in HHT preclinical models [439, 448, 449]. Crist et al demonstrated effective alleviation and prevention of AVM formation in Smad4-deficient mice by utilizing monoclonal antibodies targeting angiopoietin-2, inhibiting angiopoietin-Tie2 signaling pathway [439]. Using Bmp9/10 immunoblocking mouse model of HHT, elevated Ang2 (Tie2 antagonist) mRNA levels was observed in retinal ECs, and increased Ang2 protein levels were found in the lungs of Alk1+/− mutant mice [379, 450]. Recent RNA-seq studies from ECs isolated from 3 different HHT mouse models demonstrated decrease in Tek expression and increase Ang2 [449].

Another very recent work by Banerjee et al demonstrated that SMAD4 plays a crucial role in restricting flow-induced KLF4-TIE2-AKT activation [451] thus linking the TIE2 and AKT pathways. The authors showed that the loss of EC Smad4 in pups leads to excessive activation of KLF4-TIE2-AKT signaling in response to pathological shear stress, resulting in cell cycle progression-mediated loss of arterial identity and the formation AVMs. Interestingly, they showed that the use of Palbociclib (CDK4/6 inhibitor) strongly inhibited AVM formation and effectively rescued the excessive vascular front density in these mice.

Zhu et al demonstrated that treating Alk1-deficient mice with thalidomide and its safer derivative, lenalidomide (which has similar efficacy), resulted in a reduction of inflammation and hemorrhage in established brain AVMs. The authors suggested that this treatment inhibited AVM formation through the upregulation of PDGFB and its receptor PDGFR-β, enhancing vascular homeostasis [452].

3.5.1.3.2 Clinical trials

Individual case reports from HHT patients have shown that, so far, intravenous bevacizumab constitutes one of the most prominent therapies for HHT [436–438]. This has led to many clinical trials using bevacizumab [414].

Many other anti-angiogenic agents such as Trametinib (MEK inhibitor) [453], Sorafenib (Raf kinase inhibitor) [454], Pazopanib (VEGFR2 and Tie2 RTK inhibitor) [455, 456], doxycycline [457, 458] and thalidomide [459, 460] have also been tested, with case reports and ongoing clinical trials evaluating their efficacy in reducing epistaxis severity, GI bleeding, and other HHT-related symptoms [414, 461].

Clinical trials evaluating the effect of Tacrolimus on bleeding in HHT patients have also shown positive impacts on epistaxis, GI bleeding, hemoglobin levels, and transfusion needs when administered orally or as a nasal ointment [462, 463]. Sirolimus has also shown significant reduction in nosebleeds and anemia in several case reports of HHT patients [414].

Moreover, recent reports showed that Beta-blockers such as propranolol and timolol can reduce epistaxis in HHT patients [464, 465].

Adrenomedullin (AM) has been suggested as a potential biomarker involved in patients with HHT [466]. Hence, various pharmacological modulators of AM could be also considered for intervention in these patients. Among these modulators, adrecizumab demonstrated that it can effectively restore the impaired vascular barrier function, which is responsible for hemodynamic instability in sepsis [467].

Despite being the second most prevalent bleeding disorder globally, HHT currently lacks any FDA-approved drugs. All the available therapeutic approaches primarily focus on minimizing the risk and severity of bleeding episodes while effectively managing the resulting anemia [414]. It is important to mention that drug repurposing, which involves exploring existing medications for new therapeutic uses, can hold promising potentials for addressing rare diseases such as HHT.

3.5.2 Pulmonary arterial hypertension (PAH)

Pulmonary hypertension (PH) is an incurable condition associated with a high mortality rate around 2.8 years when left untreated [468]. It is characterized by a resting mean pulmonary arterial pressure exceeding 20 mmHg, along with normal pulmonary arterial wedge pressure (≤ 15 mmHg) and elevated pulmonary vascular resistance (> 3 Wood units), as measured

through right heart catheterization [469]. The World Health Organization (WHO) has classified PH into five groups, encompassing over 30 different types [469]. Among these, pulmonary arterial hypertension (PAH) is a rare vascular disorder with and estimated prevalence ranging from 10 to 52 cases per million [470]. Germline mutations in *BMPR2* are major predisposing factors for idiopathic (15-40%) and heritable (60-80%) PAH (IPAH and HPAH, respectively) [471]. Moreover, less frequent mutations have been identified in other gene components of the BMP signaling pathway, including *ACVRL1*, *ENG*, *SMAD9*, *GDF2*, and *BMP10* [471, 472]. Notably, mutations in the genes encoding the ligands BMP9 and BMP10 are more frequently reported in PAH in comparison to HHT. PAH is characterized by pulmonary vascular remodeling, including media hypertrophy, adventitial fibrosis, thrombotic lesions, and perivascular infiltration of inflammatory cells [473]. Although the exact pathogenic mechanisms remain elusive, thrombosis, vasoconstriction, proliferation and inflammation in the lung microcirculation are believed to contribute to disease progression [474, 475]. The resultant increase in pulmonary vascular resistance places excessive strain on the right ventricle, eventually leading to right heart failure and mortality.

Unfortunately, despite ongoing research efforts, no definitive cures for PAH have been discovered so far, with the exception of lung transplantation for eligible individuals. Currently approved therapies for PAH aim to slow down clinical manifestations by targeting three central pathways involved in regulating pulmonary vascular tone: the endothelin-1 (ET-1), nitric oxide (NO), and prostacyclin pathways (Figure 25) [476]. These pathways control the release of vasoconstrictors or vasodilators from endothelial cells (ECs) that act on neighboring vascular smooth muscle cells (vSMCs) via paracrine signaling to regulate their contractility. Endothelin-1, produced primarily by ECs, is one of the most potent vasoconstrictors and promotes vSMC proliferation [477] (Figure 25). It binds to two types of G-protein coupled receptors, ETA and ETB. ETA is primarily expressed on vSMCs mediating ET-1-induced vasoconstriction. ETB is expressed by both ECs and vSMCs and exerts opposing effects for ET-1, where its binding to ETB on ECs promotes vasodilation and antiproliferative effects by reducing ET-1 bioavailability and promoting synthesis of vasodilators such as NO and prostacyclin by ECs [477]. Notably, both ET-1 and its receptors were found to be elevated in PAH patients [478–480]. Consequently, approved treatments for PAH include the selective ETA inhibitor ambrisentan, dual ETA/ETB inhibitors such as bosentan and its derivative macitentan, which improved hemodynamics and exercise capacity in patients [476] (Figure 25).

Nitric oxide (NO), an endogenous vasodilator, is produced by ECs through endothelial NO synthase (eNOS) [476]. Gaseous NO released by the endothelium diffuses to the underlying medial layer, where it binds to and activates soluble guanylyl cyclase (sGC) in vascular smooth muscle cells vSMCs. Consequently, sGC converts guanosine triphosphate (GTP) to cyclic guanosine monophosphate (cGMP), promoting vSMC relaxation (Figure 25). Reduced NO bioavailability is observed in PAH patients due to downregulation of eNOS expression or reduced activity [474]. As such, drugs targeting the NO-sGC-cGMP pathway have shown

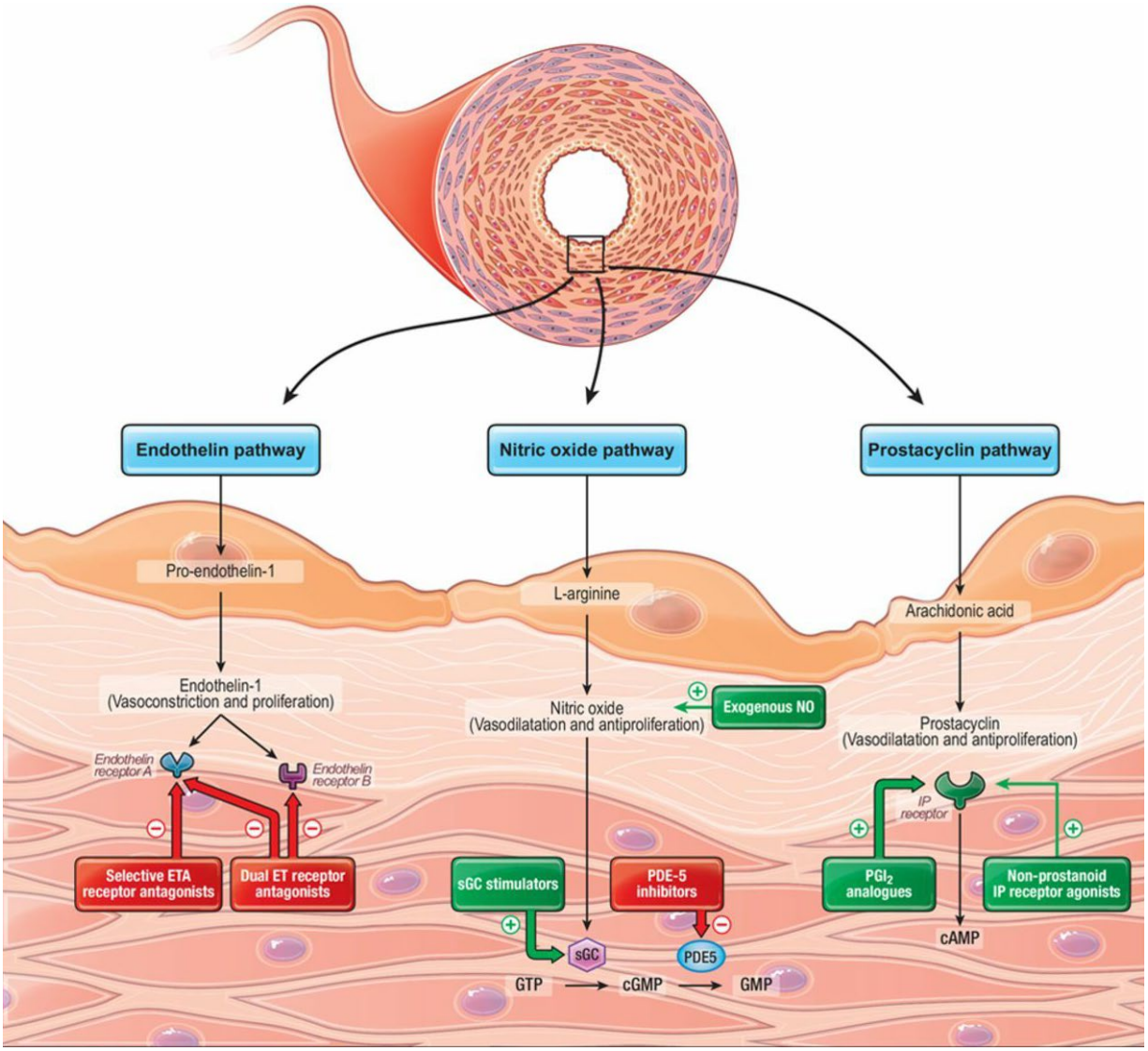

Figure 25. Schematic diagram of the three key vasomotor pathways targeted by current PAH therapies.

In PAH, endothelial dysfunction leads to a decrease in the production of endogenous vasodilators nitric oxide (NO) and prostacyclin, and an increase in the vasoconstrictor endothelin-1 (ET) which also promotes smooth muscle cell proliferation. Consequently, the three key vasomotor pathways targeted by existing PAH therapies are as follows: (1) Endothelin Pathway: This pathway can be inhibited using selective and nonselective endothelin receptor antagonists, which help counteract the effects of endothelin and reduce vasoconstriction. (2) Nitric Oxide (NO) Pathway: Therapeutic interventions focus on enhancing the NO pathway. This can be achieved through direct administration of exogenous NO, inhibiting phosphodiesterase type-5 (PDE-5) to prevent NO degradation, or stimulating soluble guanylate cyclase (sGC) to promote NO-induced vasodilation. (3) Prostacyclin Pathway: Activation of the prostacyclin pathway can be accomplished by administering prostanoid analogues or nonprostanoid IP (I-prostanoid) receptor agonists, which help increase vasodilation and counteract the effects of endothelin. This figure was taken from "Advances in Therapeutic Interventions for Patients with Pulmonary Arterial Hypertension" by Humbert et al, Circulation, 2014.

beneficial outcomes and are approved for PAH patients [476]. These include the sGC stimulator riociguat, which enhances cGMP synthesis by sensitizing sGC to NO and directly stimulating sGC, as well as PDE5 inhibitors like sildenafil and tadalafil that prevent cGMP degradation [476].

Prostacyclin is a potent vasodilator and inhibitor of vSMC proliferation and is mainly produced by ECs [474] (Figure 25). Reduced expression of prostacyclin synthase and prostacyclin receptor is observed in PAH patient, and deletion of the prostacyclin receptor I-prostanoid (IP) in mice exacerbated chronic hypoxia-induced Pulmonary hypertension [481, 482]. Intravenous administration of synthetic prostacyclin (epoprostenol) was the first approved treatment for PAH and is associated with improved survival in severe cases [476]. Other approved prostacyclin analogues for PAH include iloprost and treprostinil, which can be administered through various routes [476]. Selexipag, a nonprostanoid IP receptor agonist, is highly selective for the IP receptor and has a longer half-life, showing efficacy in improving pulmonary vascular resistance, exercise capacity, and survival in PAH patients [483, 484].

Deficiency of BMPRII in the pulmonary endothelium disrupts the equilibrium between growth-inhibitory SMAD1/5/8 signaling and growth-promoting SMAD2/3 signaling due to the binding of activins to ActRIIA [485]. Therefore, a novel therapeutic approach is currently being investigated to restore this balance and normalize cellular proliferation in patients with PAH [486–488] . This approach involves the use of sotatercept, a first-in-class fusion protein comprising the extracellular domain of ActRIIA fused to the human IgG1 Fc domain. Sotatercept acts as a ligand trap for members of the TGF-β superfamily, specifically activins and growth differentiation factors, but also BMP9 and BMP10. By sequestering free activins, sotatercept has been shown to rebalance these two signaling axes and reduce proliferation of ECs and vascular smooth muscle cells (vSMCs) in-*vitro*. Recently, a phase 3 trial using sotatercept in PAH patients resulted in a greater improvement in exercise capacity (as assessed by the 6-minute walk test) than placebo [486–488].

While current therapies provide beneficial effects in terms of cardiopulmonary hemodynamics, exercise capacity, and disease progression rate, the disease still progresses and mortality rates remain high [476] . The limited long-term effectiveness of these treatments underscores the need for exploring new therapeutic approaches that can effectively block or preferably reverse disease progression.

Chapter 4. Mass-Spectrometry (MS) Phosphoproteomics

4.1 Protein Phosphorylation

Protein posttranslational modifications (PTMs) involve the modification of amino acid side chains within proteins. These modifications encompass a wide range of around 400 types, including phosphorylation, acetylation, methylation, ubiquitination, and many others [489]. PTMs play a significant role in regulating various aspects of protein functions, regulating their activity, stability, localization and interactions with other molecules, enabling proteins to carry out diverse roles in biological systems [489]. Protein phosphorylation constitutes one of the most extensively studied PTM and plays a crucial role in diverse cellular processes across various organisms [490]. This reversible process involves the activity of protein kinases, which attach phosphate groups (PO_4) to substrates, using adenosine triphosphate (ATP) as a donor

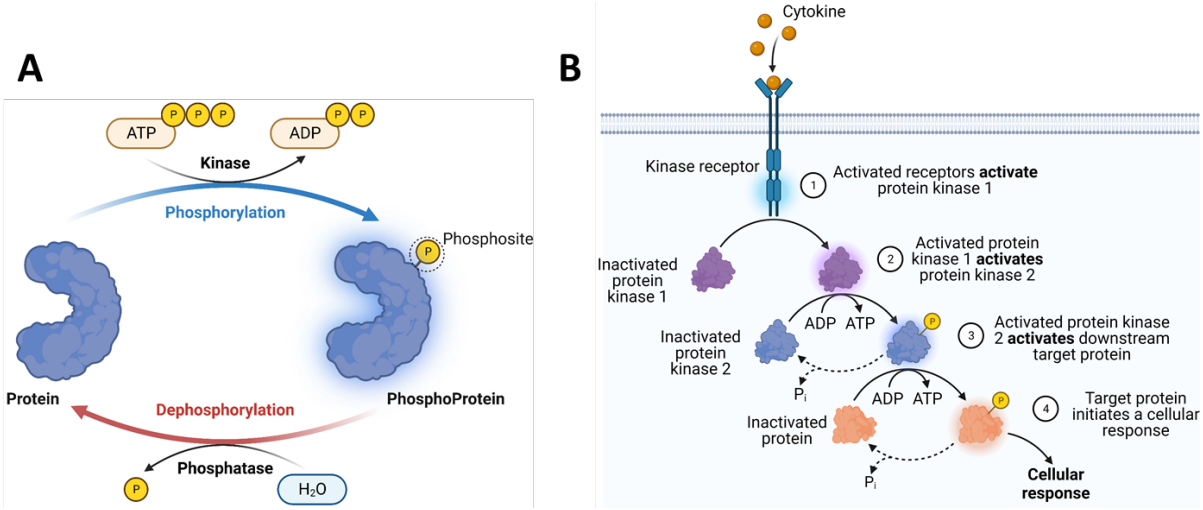

Figure 26. Protein phosphorylation and dephosphorylation.

*(**A**) Phosphorylation is the mechanism that involves the addition of a phosphate group to a protein through adenosine triphosphate (ATP) hydrolysis through the enzymatic activity of kinases. Importantly, phosphorylation is a reversible process that can be reversed by the action of phosphatases. (P) represents phosphate group. (**B**) Cytokine-induced activation of kinase receptors triggers the activation of phosphorylation-based signaling cascade to regulate different cellular processes. Both images were taken from biorender.*

for phosphate (Figure 26A). These phosphorylation events can be subsequently removed by protein phosphatases [491]. The human genome encodes around 568 protein kinases and 156 protein phosphatases [491, 492]. These two types of enzymes collaborate to regulate cellular signal transduction and cellular processes [493] (Figure 26B). In eukaryotic cells, phosphorylation primarily takes place on serine (Ser), threonine (Thr), and tyrosine (Tyr) residues. Phosphoserine (pSer) constitutes approximately 86% of the phosphorylated residues, while pThr and pTyr comprise approximately 12% and 2%, respectively [494]. These phosphorylated residues play crucial roles in cellular signal transduction, allowing signal propagation and modulation through phosphorylation-controlled signaling cascades and

networks [495] (Figure 26B). The Cell Signaling Technology PhosphoSitePlus (www.phosphosite.org) and the Kinexus PhosphoNET (www.phosphonet.ca) websites provide extensive protein phosphorylation databases, collectively listing over 200,000 known human phosphosites [491]. It has been observed that phosphorylation affects more than two-thirds of the proteins encoded by the human genome, and it is highly probable that over 90% of these proteins are subjected to this type of PTM.

4.2 Mass spectrometry (MS)-based phosphoproteomic analysis

Before the development of mass spectrometry-based techniques, the study of phosphorylation (defined as phosphoproteomic analysis) primarily relied on two-dimensional polyacrylamide gel electrophoresis (2D-PAGE), ^{32}P labeling, or Edman sequencing [496]. Edman sequencing is primarily suitable for studying individual proteins, while the other methods involve handling radioactive isotopes and are time-consuming and low-throughput. However, the introduction of mass spectrometry has revolutionized the field of proteomics, including phosphoproteomic analysis, allowing confident identification of thousands of phosphopeptides and phosphosites in a short period of time [496]. Advancements in mass spectrometry instrumentation and data processing, such as increased sensitivity, higher mass accuracy and resolution, along with phosphopeptide fractionation and enrichment methods, have further transformed phosphoproteomic analysis into a high-throughput application. Typically, mass spectrometry instruments are coupled with liquid chromatography (LC), where the complex phosphopeptide mixture is separated on a reversed-phase C18 column before entering the mass spectrometry instruments [497]. Below, I will summarize the general workflow and techniques used for phosphoproteomic analyses [498], which is also illustrated briefly in Figure 27.

4.2.1 Sample Collection and Preparation

Samples can be derived from various sources such as biological fluids, cells, and tissues. Isolated proteins are then reduced and alkylated to break disulfide bonds, stabilize cysteine residues, protect proteins from degradation and ensure efficient digestion and accurate identification of phosphorylation sites [499]. Proteins are then digested using the endoproteinase trypsin, which cleaves C-terminal of lysine and arginine residues, except when followed by a proline residue [500]. The resulting peptides generated by trypsin digestion are of suitable length for analysis by LC-MS. Besides trypsin, other endoproteinases such as Arg-C, Asp-N, chymotrypsin, Glu-C, Lys-C, and Lys-N can be used for protein digestion [501]. These endoproteinases cleave after different

amino acid residues and can be combined with trypsin to improve sequence coverage and enhance identification rates. For instance, pre-digestion or co-digestion with Lys-C has shown improved reproducibility and increased detection of phosphopeptides [502].

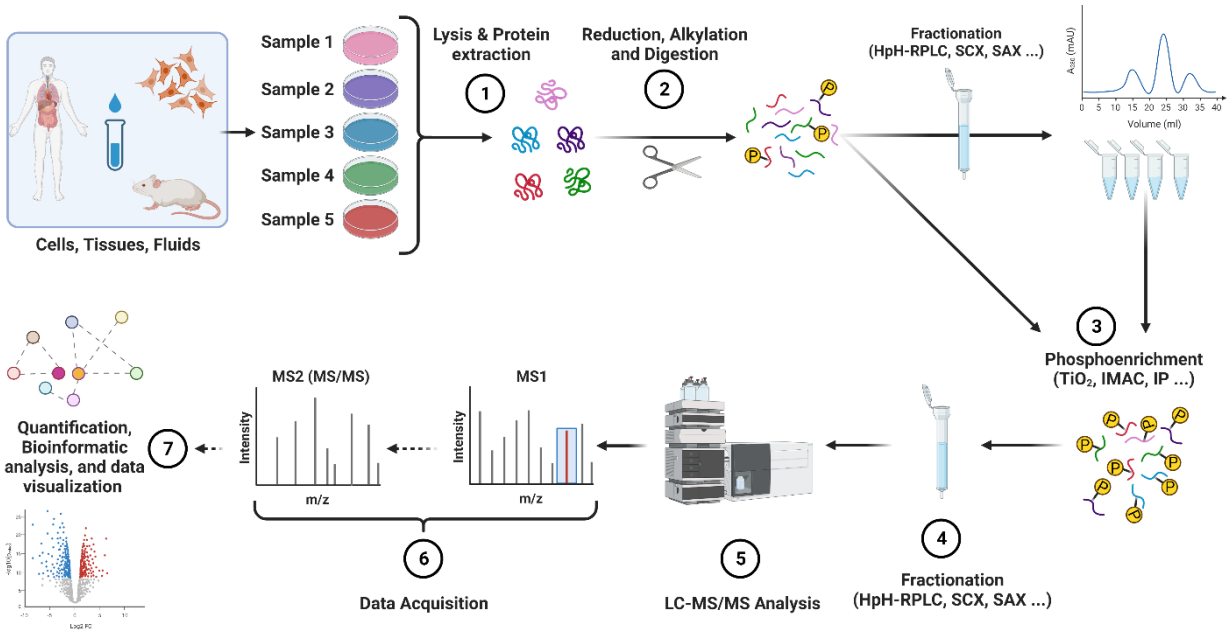

Figure 27. Schematic representation of the main workflow for mass spectrometry-based phosphoproteomic analysis.

Protein samples derived from different sources are extracted using specific buffers. The extracted proteins undergo downstream steps including reduction, alkylation, and digestion, resulting in a mixture of phosphorylated and non-phosphorylated peptides. This complex peptide mixture can either be pre-fractionated to reduce its complexity or directly subjected to phosphoenrichment to enrich phosphorylated peptides. Enriched phosphopeptides are then further fractionated and analyzed using liquid chromatography coupled to mass spectrometry (LC-MS/MS). Acquired data are presented in the form of MS1 and MS2 spectra, which are used for the identification and quantification of differentially phosphorylated proteins. Phosphoproteomic data are further analyzed utilizing various bioinformatics tools and databases providing visualization plots to facilitate the interpretation of the data and identification of potential signaling pathways and their functional implications. Figure created with biorender.

4.2.2 Phosphopeptide enrichment

Phosphorylated proteins are generally present in significantly lower amounts compared to their nonphosphorylated counterparts [503]. Furthermore, phosphorylated peptides exhibit lower ionization efficiency in positive mode, which is the mode commonly used for classical MS-based discovery proteomics, compared to their non-phosphorylated counterparts. This reduced ionization efficiency is attributed to the negative charges of the phosphate group. Consequently, enrichment techniques are crucial for the study of phosphorylated proteins. Phosphopeptide-level enrichment is commonly performed using methods such as immobilized metal affinity chromatography (IMAC), metal oxide affinity chromatography (MOAC), immunoprecipitation (IP), among others [504].

For instance, MOAC is based on the interaction between metal oxides and phosphate groups [504]. Among different metal oxides, TiO2 beads have been widely utilized for phosphoproteomic analysis studies [505]. TiO2 enrichment offers a simple and stable affinity binding between the metal oxide surface and phosphate groups. TiO2 beads also exhibit higher affinity towards monophosphorylated peptides. Notably, a small number of acidic or

nonphosphorylated peptides may still be observed in the enriched fractions, which is a common issue in both MOAC and IMAC enrichment [506]. Furthermore, to improve the resolution and sensitivity of subsequent analyses, chromatographic methods can be further employed for the fractionation of phosphopeptides prior to the analysis by LC-MS. These include high pH reversed phase LC (HpH-RPLC), hydrophilic interaction liquid chromatography (HILIC), strong anion exchange (SAX) and strong cation exchange (SCX) [507].

4.2.3 MS analysis, Protein identification and Phosphosite localization

A mass spectrometer comprises an ion source for molecule ionization, a mass analyzer for separating ions based on their m/z value, and a detector for ion measurement (Figure 28). The two major techniques used in proteomics for volatizing and ionizing molecules are matrix assisted laser desorption and ionization (MALDI) [508] and electrospray ionization (ESI) [509]. MALDI is particularly suitable for spatial mass spectrometry imaging (MSI) applications as it ionizes samples in a dry state [510]. In contrast, ESI can ionize molecules in a liquid state, making it preferred for the analysis of complex mixtures as it can be connected with liquid chromatography (LC) systems [496]. The mass analyzer is crucial for the performance of a mass

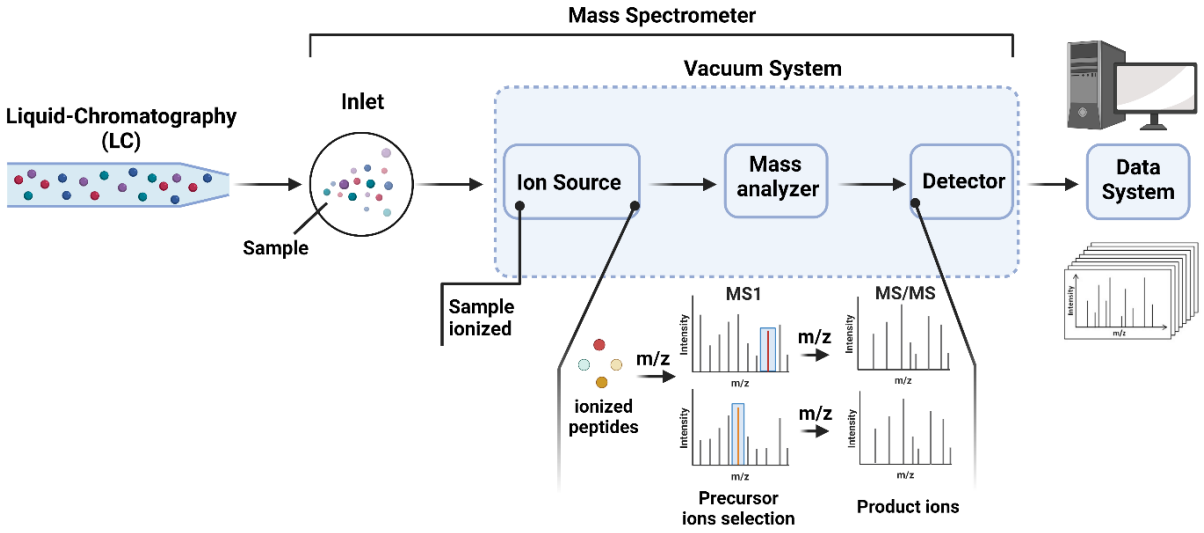

Figure 28. General Schematic Representation of The Components of a Mass Spectrometer.

A standard mass spectrometer consists of several components, including an inlet, an ion source, a mass analyzer, and a detector. Samples from liquid chromatography (LC) system are ionized through the ion source generating peptide precursor ions, which are separated by the mass analyzer according to their mass-to-charge (m/z) ratio generating MS1 spectra. Subsequently, specific peptide precursor ions are chosen for further fragmentation, resulting in the generation of product ions which gives rise to MS2 spectra. The information obtained from MS1 and MS2 spectra are processed using a data system. Figure generated with biorender.

spectrometer. Key performance mass analyzer parameters in proteomics applications include mass resolution, sensitivity, speed, dynamic range, and tandem mass spectrometry (MS/MS or MSn) capability [511]. There are five main types of mass analyzers: Quadrupole, Time of Flight (TOF), Ion Trap, Fourier Transform Ion Cyclotron Resonance (FT-ICR), and Orbitrap. For data acquisition, two methods are commonly used: data-dependent acquisition (DDA) and

data-independent acquisition (DIA) [512]. DDA selectively chooses certain peptides from the first MS cycle for fragmentation in the second cycle, while DIA allows for the fragmentation of all peptides generated in the first MS cycle. When it comes to data analysis, database search is classically used and protein identification can be done either using a MS/MS spectral library (real MS/MS spectra) or directly using a protein database.

Importantly, molecules need to be in the gas phase and charged to be detected in a mass spectrometer. Samples arriving from the liquid chromatography (LC) system are ionized in the ion source, generating peptide precursor ions (Figure 28). These precursor ions are then separated by the mass analyzer based on their mass-to-charge (m/z) ratio, resulting in the generation of MS1 spectra. Subsequently, specific peptide precursor ions can be selected for further fragmentation. This fragmentation process generates product ions, which give rise to MS2 spectra. The acquired information from both MS1 and MS2 spectra are processed using a data system for analysis and interpretation.

Low abundance of phosphopeptides, neutral loss of phosphoric acid (H_3PO_4) during fragmentation, and low intensity MS2 spectra are common factors that can limit identification of phosphopeptides and reliable determination of phosphorylation sites [513, 514]. The identification of phosphopeptides relies on software tools typically using database search engines. Individual MS2 spectra yield multiple candidate peptide spectrum matches (PSMs), which are ranked by a score. To ensure correct identifications, the MS2 spectrum must be matched with a certain level of significance. The false discovery rate (FDR) is commonly used to compute the statistical significance of these identifications, employing a target-decoy strategy where the MS2 data are searched against a sequence database and a decoy version [515, 516]. Protein inference, which involves matching peptide sequences to multiple proteins, presents a challenge when integrating scores and determining statistical significance. However, the unambiguous localization of phosphorylation sites is more challenging than identification, especially when potential sites are in close proximity within the peptide sequence and have few discriminatory fragment ions. Moreover, pinpointing the correct phosphorylation site can pose challenges when dealing with directly adjacent phosphosites or multiphosphorylated peptides. After peptide identification, specialized algorithms and computational approaches are employed to determine the exact location of the phosphorylation site within the peptide sequence. These algorithms consider various factors such as the presence of phosphorylation-specific fragment ions and neutral loss of phosphoric acid during fragmentation. At the end of the analysis, a probability score will be assigned to each of the localized phosphosites.

4.2.4 Quantitative phosphoproteomic analysis

There are two main methods for MS-based quantification: Absolute and Relative. The former method determines the absolute abundance of target analytes using internal or reference standards and calibration curves. Multiple reaction monitoring (MRM) or selected reaction monitoring (SRM) techniques are commonly used for this kind of analysis [517]. On the other

hand, relative quantification compares the abundance of target analytes between different samples or conditions. It can be achieved through label-free or stable isotopic/isobaric labeling methods. Isobaric tags for relative and absolute quantitation (iTRAQ), TMT (Tandem Mass Tagging) and SILAC (Stable Isotope Labeling by Amino Acids in Cell Culture) are examples of widely used MS-based stable isotopic labeling quantitative techniques, but they differ in their labeling strategies and applications (Figure 29). Both TMT and iTRAQ involves chemical

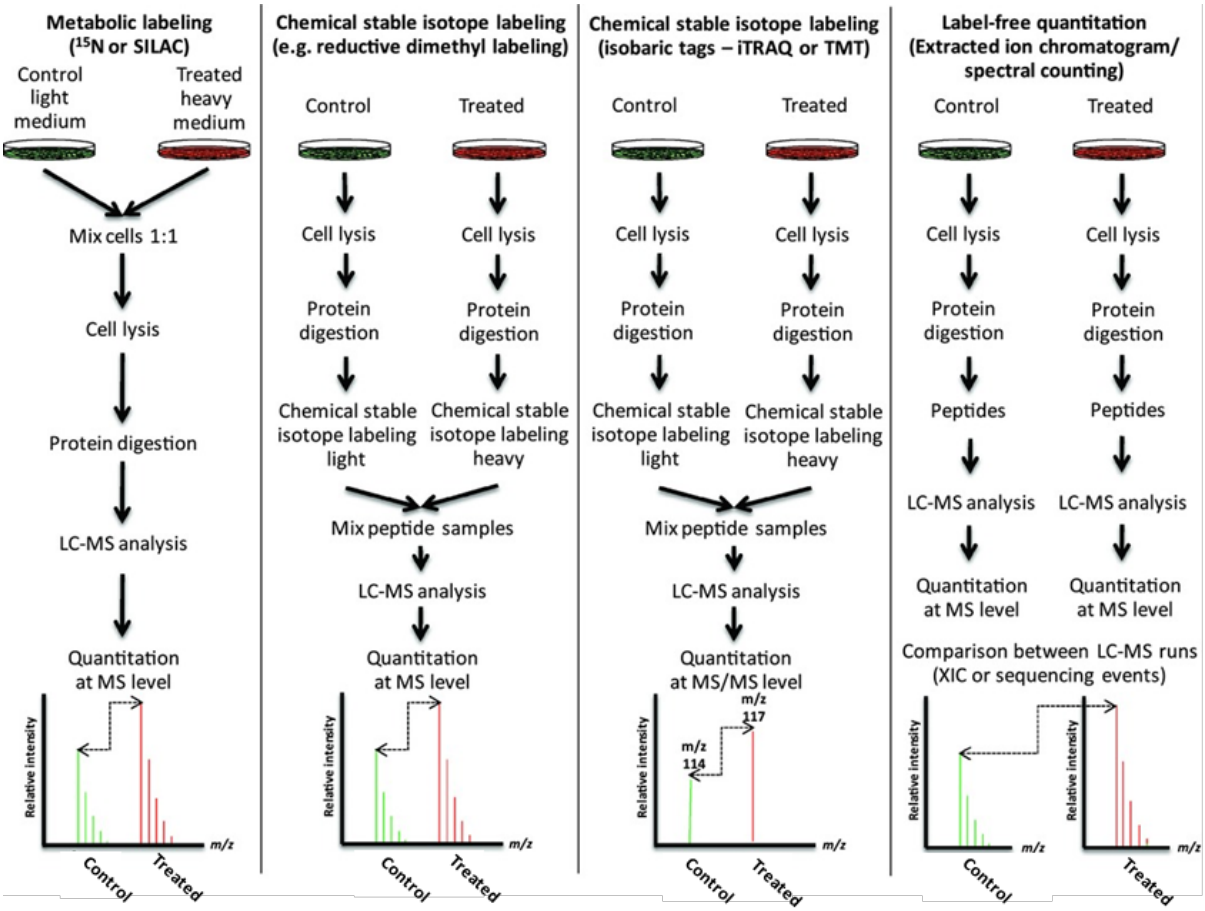

Figure 29. Comparison between Label vs Label-Free Approaches.

Figure was adapted from "Technologies and challenges in large-scale phosphoproteomic analysis" by Keller K. and Larsen M., Proteomics 2013.

labeling of peptides or proteins with isobaric tags containing distinct mass reporter ions (Figure 30), enabling multiplexing of multiple samples that are combined for downstream analysis, with quantification achieved by measuring the released reporter ions during fragmentation in the mass spectrometer [518, 519]. On the other hand, SILAC involves metabolic labeling of proteins in living cells using stable isotopes, typically by substituting regular amino acids with their isotopically labeled counterparts [520]. Other methods include ICAT and dimethyl labeling [521, 522] (Figure 29). Using this kind of techniques allows different isotopic and isobaric forms to generate distinct mass shifts, enabling quantification of phosphopeptide abundance between different samples. Table 1 summarizes the main differences between all the previously mentioned methods [521–524].

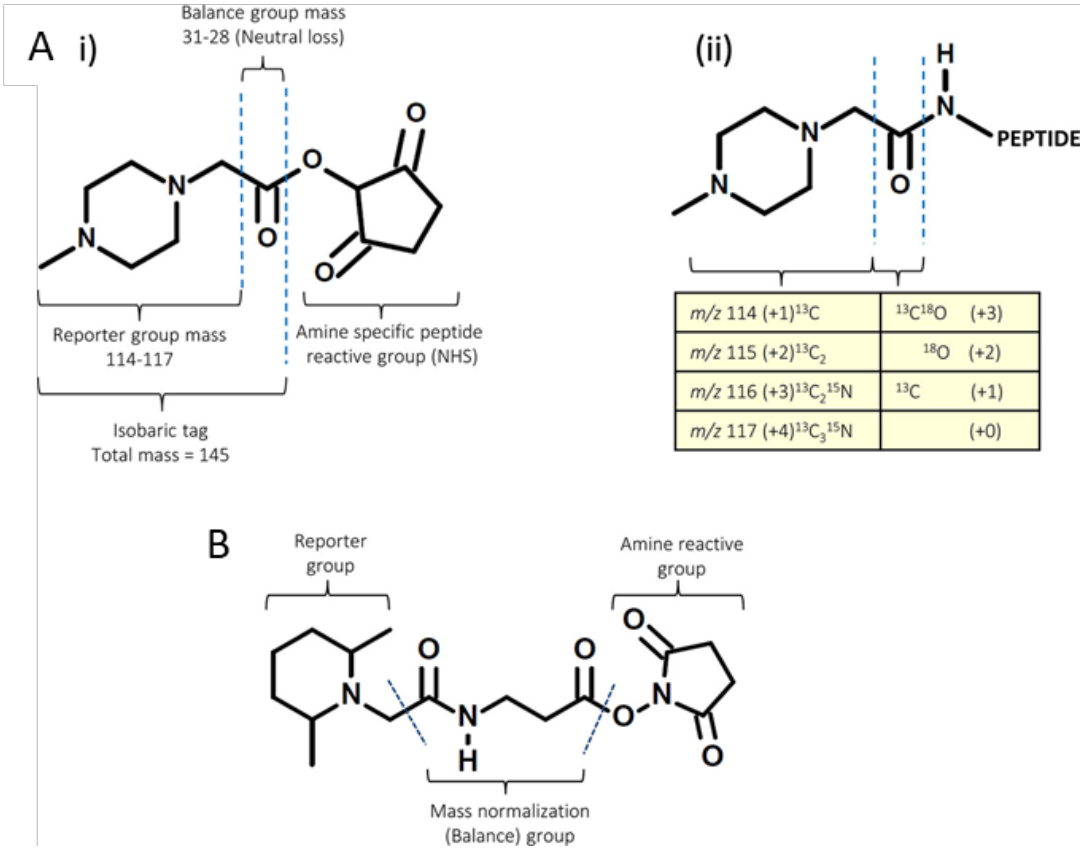

Figure 30. iTRAQ and TMT labeling strategies.

*(**A**) **(i)** iTRAQ 4-plex reagent chemical structure. The molecule comprises a reporter group, a mass balance group, and a peptide-reactive group (NHS ester). The reporter group has a mass range of m/z 114-117. The mass balance group contains a carbonyl moiety and whose mass ranges from 28 to 31 Da. Isotopic enrichment with 13C, 15N, and 18O atoms is used to maintain a constant overall mass of 145 Da for the combined reporter and balance group components in each of the four reagents of the iTRAQ 4-plex set. **(ii)** The iTRAQ tag forms an amide linkage with the peptide N-terminus or the ε-amino group of lysine. Upon fragmentation by CID (collision-induced dissociation), the tag amide bond undergoes fragmentation similar to that of backbone peptide bonds. During fragmentation, the balance moiety is lost as a neutral loss, while the charge is retained by the reporter group. The number within parentheses in the table indicates number of enriched centers in each section of the molecule. (**B**) Generic TMT reagent chemical structure. As described for the iTRAQ, the TMT molecule comprises three functional groups: (1) an amine reactive group that allows the labeling of the N-terminus and ε-amine group of lysine in peptides, (2) a mass normalization (balance) group that ensures the overall mass of the reagents remains the same, compensating for mass differences among individual reporter ions, and (3) a reporter group that provides information about the abundance of a peptide during MS/MS analysis when the samples are mixed. The structure also includes blue dashed lines that represent a cleavable linker, enabling the release of the reporter ion from the entire tag during MS/MS. Both images A and B are taken from "Isobaric labeling-based* relative quantification in shotgun proteomics" by Navin Rauniyar and John R Yates, J Proteome Res. 2014.

Table 1. Comparison of commonly used labeling methods in quantitative MS-based proteomics.

Method	Labeling Strategy	In-vivo or in-vitro?	Multiplexing	Protein Coverage	Throughput	Accuracy	Disadvantages
SILAC	Metabolic labeling through Incorporation of isotopically labeled amino acids (typically lysine and arginine) into proteins	In-vivo (living cells)	Up to 3 Samples	+++	++	+++	Expensive Time-consuming
ICAT	Chemical labeling of cysteine residues in proteins	In-vitro	Pairwise comparisons	+	+	++	Low multiplexing Only applicable to cysteine-containing proteins
TMT	Chemical labeling with isobaric tags	In-vitro	Multiplexing (up to 18 samples)	+++	+++	++/+++ (Depends on MS acquisition mode)	Expensive Low signal recovery (Signal Compression)
iTRAQ	Chemical labeling with isobaric tags	In-vitro	Multiplexing (up to 8 samples)	+++	+++	++	Expensive Low signal recovery (Signal Compression)
Dimethyl labeling	Chemical labeling of peptide N-termini and primary amines using stable isotopic versions of formaldehyde and sodium cyanoborohydride	In-vitro	Pairwise comparisons	++	++	++	Low multiplexing Labeling affects LC separation
Label free	-	-	-	+++	+++	+	Requires more demanding analytical measurements

4.3 Challenges in Phosphoproteomic Analysis by LC-MS and Data Validation

The field of phosphoproteomic analysis has greatly advanced due to improvements in liquid chromatography and mass spectrometry instrumentation, development of phosphopeptide fractionation and enrichment methods, as well as data processing techniques [497, 525].

Despite these advancements, several challenges still exist in phosphoproteomic analysis studies [503, 507], which are summarized below.

Sample preparation and complexity

Sample complexity is considered a major limitation in phosphoproteomic analysis which prevents the comprehensive characterization of the complete phosphoproteome in higher organisms [526]. Although current MS instruments have the capability to sequence a larger portion of peptides, sensitivity poses a significant challenge where many peptides require long ion injection times to generate spectra of sufficient quality.

Incomplete coverage after tryptic digestion

Another challenge is the inefficient proteolysis caused by the sequence context, which can hinder the identification of phosphorylation sites. While trypsin is considered the best proteolytic enzyme for phosphoproteomic analysis, it does not offer a complete coverage of the phosphoproteome [507]. Certain proteolytic products generated during tryptic digestion of complex protein samples, falling beneath the standard m/z window of MS spectrum acquisition, are unsuitable for LC-MS/MS analysis. Moreover, peptide sequences containing lysine or arginine in close proximity to aspartic acid, glutamic acid, phosphoserine, or phosphothreonine residues can inhibit cleavage at these sites due to intramolecular ionic interactions between positively charged lysine and arginine residues and the negatively charged phosphate group [527, 528]. To overcome this issue, the use of different endoproteinases in addition to trypsin has been proposed to improve phosphorylation site mapping [529]. Nevertheless, peptides which lack lysine or arginine residues remains poorly ionized [530, 531].

Low phosphoprotein abundance

A significant challenge in phosphoproteomic analysis is the sub-stoichiometric distribution of phosphorylated proteins compared to their unmodified counterparts [503]. This often leads to higher ion intensities for unmodified peptides that are more abundant, masking the lower abundant phosphopeptides[503]. Therefore, selective phosphopeptide enrichment methods are crucial to remove highly abundant unmodified peptides as much as possible from complex peptide mixtures in phosphoproteome analyses. Notably, quantifying both the phosphorylated and nonphosphorylated forms of a protein is essential to assess the phosphorylation degree accurately and draw conclusions regarding phosphorylation-dependent quantitative changes. However, it is common for the corresponding nonphosphorylated protein to be missing in phosphoproteomic analysis studies.

Phosphopeptide enrichment

The wide range of parameters involved in enrichment methods often leads to diverse identifications of phosphopeptides. These parameters include the choice of beads for

enrichment, protein-to-beads ratio, incubation time, loading, washing, and elution buffers [504]. Therefore, careful optimization of the enrichment approach is necessary to achieve successful isolation of phosphorylated peptides using these resin-based techniques. Another challenge is the bias in identifying monophosphorylated peptides compared to multiphosphorylated peptides. Multiphosphorylated peptides may adsorb on surfaces and metal ions during enrichment and LC-MS analysis, leading to their reduced detection [532, 533]. Strategies such as the addition of citrate or phosphoric acid can enhance the detection of multiphosphorylated peptides by LC [534, 535].

Imperfect repeatability in data dependent acquisition

One of the drawbacks is the lack of repeatability in peptide identification, which arises from the random probability distribution nature of peptide sampling through DDA and variations in chromatography. When replicating the analysis of the same sample, typically only 60-70% of the identified phosphopeptides overlap, indicating limited consistency in results [536–538]. For instance, to investigate the influence of technical replicates on the sample peptide coverage, Ham et al used quality control samples from a standard Shewanella (gram-negative bacteria) extract [538]. The authors demonstrated that the same sample had to be analyzed up to six times to achieve the best identification of the peptides present in the sample. For more complex samples, it may be necessary to have a higher number of technical replicates to ensure optimal peptide coverage.

Peptide identification and phosphosite localization

Large-scale proteomics and phosphoproteomic analysis studies face challenges in determining the quality of peptide identifications due to variations in signal intensity and unpredictable peptide fragmentation. To address this, a false discovery rate (FDR) is calculated for all identified peptide-spectrum matches (PSMs) using a decoy version of the target database. The FDR calculation helps determine the proportion of false positive identifications among the total identifications in the dataset. Another challenge in phosphopeptide characterization, which was described above, is determining the precise location of the phosphorylation site when the peptide contains multiple serine, threonine, or tyrosine residues. Although site localization can be accomplished by analyzing site-specific fragment ions, providing precise information about the modification's exact position [539, 540], MS2 spectra may not always contain specific signatures of the phosphosite position.

Validation and Interpretation of Phosphoproteomic data

MS phosphoproteomic analysis has indeed provided a high-throughput strategy for describing changes in protein phosphorylation in different experimental contexts. However, validation of these phosphosites is a pre-requisite to assess the accuracy and reliability of the identified phosphosites and to gain deeper insights into their biological significance. One commonly used approach for validation is the use of antibody-based methods, such as western blotting or immunoprecipitation. These techniques involve the use of specific antibodies that

recognize the site-specific phosphorylation of a protein [541, 542]. However, there are several limitations to antibody-based validation. First, there is only a very limited number of commercially available phosphosite specific antibodies restricting the scope of validation for majority of differentially regulated phosphosites. Secondly, antibody specificity also play an important role, whereby antibody cross-reactivity or nonspecific binding can lead to false-positive or false-negative results [543]. Moreover, even if the antibody is highly specific, the performance of this antibody can vary across different experimental conditions and samples [544, 545]. Factors such as antibody concentration, incubation time, and detection methods can affect the reliability and reproducibility of validation results.

Phosphoproteomic studies aim to gain deeper insights into the biological significance of identified phosphorylation sites. Different phosphoproteomic studies have employed gene-centric approaches using pathway databases such as KEGG, Reactome, or MSigDB to analyze the obtained data and unravel the biological significance of the identified phosphorylation events [546–549]. However, these traditional gene-centric approaches often overlook the individual phosphorylation sites and instead collapse multiple sites into a single measurement represented by the mean or median of corresponding sites [550]. This approach sacrifices valuable information and dilutes the signal within the phosphoproteome data, especially when multiple phosphosites on the same protein are differentially abundant. Moreover, the correlation between protein activity and phosphorylation is complex, as phosphorylation can either activate or inhibit a protein depending on the specific site regulated. To address these limitations, recent advancements in bioinformatics analysis tools and databases, such as post-translational modification database (PTMsigDB)[550], Kinase-swing (Kinswing) [551] among many others [552], have significantly improved phosphosite-centric analysis of phosphoproteomic data. These tools allow for a better phosphoproteomic data analysis, enabling a more comprehensive exploration of the signaling pathways regulated, the kinases involved and functional implications of the obtained phosphorylation events.

4.4 Phosphoproteomic profiling studies of TGFβ superfamily ligands

In order to gain a better understanding of the phosphoproteomic signaling activated by TGFβ superfamily ligands, several phosphoproteomic studies have been carried out over the past two decades. These studies have focused on various cell types, including different types of epithelial cells, immune cells, myoblasts and fibroblasts, among others. Table 2 provides an overviw of these phosphoproteomic studies, highlighting the study approach, ligand stimulation conditions, cell types utilized, validation of phosphoproteomic data and whether functional conclusions were derived from these studies or not.

These phosphoproteomic studies predominantly focused on the TGFβ ligand (15/19 studies), with only a limited number of investigations exploring the phosphoproteomic responses downstream of other family members including BMP2 and BMP4. Among these studies, approximately half of them were able to link the ligand-induced phosphoproteome changes to effects on protein functions, drawing out insightful functional conclusions. Stasyk et al.

conducted one of the first phosphoproteome profiling studies for TGFβ. In their study, they investigated the effects of TGFβ on MCF-7 breast cancer cells, and showed that TGFβ stimulation induced the phosphorylation of Transcription Factor-II-I (TFII-I) at Ser371 and Ser743. The authors demonstrated that these phosphorylation events were found to modulate TGFβ transcriptional responses, as assessed through microarray analysis and luciferase assays [553]. In 2013, Zakharchenko et al performed a time-resolved analysis of phosphoproteomic changes of normal human breast epithelial cells in response to TGFβ, highlighting phosphorylation 14-3-3σ at Ser69 and Ser74. They demonstrated that this phosphorylation constitutes a key process that coordinates the functional interaction between TGFβ/Smad3 and p53 pathway in the maintenance of cancer stem cells, presenting a promising therapeutic approach in breast cancer [554]. Moreover, a recent time-resolved analysis of phosphoproteomic changes of human small airway epithelial cells in response to TGFβ identified a mechanistic insight of the role of TGFbeta in EMT through the crosstalk between IκB kinase with spliced X-box binding protein 1 [555]. Another recent study conducted by Prado et al nicely illustrated early signaling mechanisms through which CD4+ T cells combine signals from T-cell receptor (TCR), TGF-β and IL-6 to form alternative SMAD3 complexes [556]. The authors demonstrated that these complexes play a crucial role in shaping early signaling networks for the determination of Treg or Th17 cell fate. In addition to providing functional roles, Okayama et al shows that analyzing tyrosine phosphoproteome changes in response to TGFβ in A549 cells identified certain protein phosphorylation profiles as possible prognostic markers for lung adenocarcinoma [557].

To the best of my knowledge, no phosphoproteomic profiling study has been published on endothelial cells in response to any member of the TGFβ family. Additionally, there are no studies assessing BMP9 and BMP10 phosphoproteomic responses in any cell type.

Table 2. Summary of MS-based Phosphoproteomic studies of TGFβ superfamily ligands from 2005-2022

Year	Stimulation Conditions	Cell Type	Validation	Functional Conclusions from Phosphoproteomic Analysis	Phosphoproteomic Approach	Reference
2005	TGFβ (5ng/ml) for 0, 1, 4, and 24 hr	MCF-7	Yes	Yes	2D Gel followed by label free MS	[553]
2009	BMP2 (300 ng/mL) or TGFβ (5 ng/mL) for 30 min	C2C12	No	Yes	SILAC followed by In gel digestion and MS	[558]
2009	BMP4 (50ng/mL) for 30, 60, and 240 min	HUES-7	No	Yes	SILAC MS	[559]
2010	TGFβ (10 ng/mL) for 48hr	HK-2	Yes	No	iTRAQ MS	[560]
2011	TGFβ (5 ng/mL) for 30 min	SW480	No	No	SILAC MS	[561]
2011	BMP4 (50ng/mL) for 30, 60, and 240 min	HUES-7	No	No	SILAC MS	[562]
2012	TGFβ (5 ng/ml) for 1, 5, 30 or 60 min	Epimastigotes	No	No	2D Gel followed by label free MS	[563]
2012	BMP9 (1ng/mL) for 8hr	ECFCs from WT and BMPR2 mutants of PAH patients	-	-	-	Conference Abstract [§]
2013	TGFβ for 1 hr	Four Breast cancer cell lines	No	No	label free MS	[564]
2013	TGFβ (5ng/ml) for 0, 5, 30, 60 and 120 min	MCF10A	Yes	Yes	2D Gel followed by label free MS	[554]
2014	TGFβ (5 ng/ml) for 5, 10, 20 min	HaCaT	Yes	No	SILAC MS	[565]
2015	TGFβ (5 ng/mL) for 48hrs	A549	Yes	Yes	label free MS	[557]
2018	TGFβ (2 ng/mL) for 30 min	RPE1	Yes	Yes	SILAC MS	[566]
2019	TGFβ (5 ng/ml) from 5 mins, 1hr, 1d, 2d	NMuMG	No	Yes	SILAC MS	[567]
2020	BMP4 1hr	H1	No	No	SILAC MS	[568]
2020	TGFβ (5 ng/mL) 24h	SMCs	No	No	DiLeucine MS	[569]
2021	TGFβ (10ng/ml) for 0,1,3d	HSAECs	Yes	Yes	label free MS	[555]
2021	TGFβ (200 ng) for 10 min	CD4+ T cells	Yes	Yes	label free MS	[556]
2022	TGFβ (2 ng/mL) for 30 min	BJ-5ta	No	No	TMT MS	BioRxiv [*]

The studies are arranged in chronological order based on the year. **§**: unpublished work presented at a conference https://www.atsjournals.org/doi/abs/10.1164/ajrccm-conference.2012.185.1_MeetingAbstracts.A6518. *****: unpublished work from BioRxiv https://doi.org/10.1101/2022.11.04.514246. **MCF-7**: Breast cancer cells, **C2C12**: Mouse myoblasts, **HUES7**: Human embryonic stem cells, **HK-2**: Human renal proximal tubule cells, **SW480**: Human colon adenocarcinoma cells, **ECFCs**: Endothelial colony forming cells, **HaCat**: Human keratinocytes, **A549**: Adenocarcinoma human alveolar basal epithelial cell, **RPE1**: Retinal pigment epithelial cells, **NMuMG**: Nontransformed mouse mammary epithelial cells, **H1**: Human

RPE1: Retinal pigment epithelial cells, **NMuMG**: Nontransformed mouse mammary epithelial cells, **H1**: Human embryonic stem cells, **SMCs**: Smooth muscle cells, **HSAECs** Human small airway epithelial cells, **MCF10A**: Normal human breast epithelial cells, **BJ-5ta**: human immortalized fibroblasts.

Main Aims of the Project

BMP9 and BMP10 are two key regulatory ligands that play crucial roles in vascular development and homeostasis by acting on their high affinity receptors (ALK1, BMPR2, Endoglin), which are highly expressed on the surface of endothelial cells. Mutations in the BMP9/BMP10 signaling pathway are associated with the development of two distinct rare vascular diseases, HHT and PAH, with unfortunately no currently identified cures. HHT is caused by heterozygous LOF mutations mainly in the genes coding for the type I receptor ALK1 or the co-receptor endoglin. In contrast, mutations in the gene coding for the type II receptor BMPR2 are found in the majority of heritable PAH (HPAH) cases. Mutations in the genes coding for ALK1 or endoglin can also lead to HPAH, albeit at a very low frequency. Importantly, mutations in BMP9 have been described in HHT and HPAH as well as in BMP10 in HPAH.
Current treatments available for HHT and PAH focus on managing the symptoms rather than addressing the underlying cause of vascular abnormalities. This is primarily due to our limited understanding of the molecular mechanisms connecting these mutations to the development of the observed abnormalities. Additionally, it remains unclear how mutations within the same signaling complex can result in the development of two distinct rare vascular diseases. Over the past two decades, various experimental findings, as discussed in chapter 2, have indicated that ligands belonging to the TGFβ family can activate non-canonical signaling pathways in addition to the well-studied canonical Smad signaling pathway. Regarding BMP9 and BMP10, the focus has largely been on the Smad signaling pathway, while our understanding of the activation of alternative pathways by these ligands in endothelial cells remains very limited. To tackle this question, the main aim of my project is to decipher the non-canonical pathways induced by BMP9 and BMP10 ligands in endothelial cells in order to enhance our understanding of the molecular mechanisms governing their role in vascular development and homeostasis. Moreover, such investigations may shed light on the molecular mechanisms driving the pathogenesis of HHT and PAH, thereby suggesting novel therapeutic approaches. Accordingly, given the fact that the binding of BMP9/10 to their receptor complex triggers the activation of the kinase activity of their high affinity receptor ALK1, the focus of this project is to explore the initial changes in phosphoproteome within endothelial cells (ECs) shortly after being stimulated with BMP9 and BMP10 utilizing Mass spectrometry phosphoproteomic analysis. With this, we aimed to tackle these main questions:

1. What proteins or signaling pathways, apart from Smads, can undergo phosphorylation and activation downstream of BMP9 and BMP10 signaling in endothelial cells (ECs)?
2. Do BMP9 and BMP10 stimulations lead to a similar phosphoproteome changes or do they possess specific signaling?
3. What are the underlying mechanisms responsible for the regulation of the newly identified targets/pathways? Are these pathways dependent on Smad signaling? Are these regulations direct or do they involve indirect mechanisms?

4. What are the functional implications of the newly identified pathways downstream of BMP9 and BMP10 in terms of their impact on endothelial cell functions and their potential crosstalk with other signaling pathways?

Chapter 5. Project 1: Deciphering Early Phosphoproteome Changes in Response to BMP9 and BMP10 in Endothelial Cells

5.1 General Context and Main Objective of the Project

BMP9 and BMP10 are two key regulators of vascular homeostasis. These two ligands bind with very high affinity to the endothelial type I receptor ALK1, and either one of the three BMP type II receptors (BMPRII, ActRIIA or ActRIIB). Mutations in this signalling pathway have been identified in two rare vascular diseases, HHT and PAH, with unfortunately no currently identified cures. So far, only the canonical SMAD signalling pathway has been well studied in response to BMPs in endothelial cells, but several studies have reported that TGFβ and BMPs can also signal via other signalling pathways (MAPK, PKA, PI3K…), which are less characterized and might be more context-dependent. As outlined in the aim section of this project, the general objective of this work was to decipher early phosphoproteomic signaling (within 30 min) initiated in response to BMP9 and BMP10 in ECs, which has never been performed before. Understanding the signaling downstream of these ligands would enhance our understanding of their role in vascular homeostasis, while also proposing novel therapeutic approaches for HHT and PAH.

5.2 Clarifying the Choice of the Methodology

To analyze the phosphoproteome, we performed a MS-quantitative phosphoproteomic analysis of HUVECs, stimulated or not with BMP9 or BMP10 for 30 mins. The first year was mainly dedicated for optimizing experimental conditions to be used for the project (stimulation duration, BMP dose, lysis buffer, etc…), which will be later empathised in the discussion part of the thesis manuscript. Then, we performed two independent label free quantification (LFQ) MS phosphoproteomic analyses using BMP10 (first year) and BMP9 (beginning of the 2nd year). From both analyses, we obtained around 2000-3000 identified and quantified phosphosites, out of which we got 89 which were differentially phosphorylated by BMP10 vs 81 by BMP9. However, we were surprised that only few (< 10%) were common to both BMP9 and BMP10. This was rather unexpected, given that both ligands were suggested to exert equivalent effects at least at the transcriptomic level on ECs *in-vitro* [325]. We considered that this could likely be because the two experiments and MS analysis were performed independently. Nevertheless, after several experiments conducted during the first and the second year in an attempt to validate our data, we were not able to find a clear story/function that can be studied from both LFQ MS analyses. Therefore, given the surprising low overlap obtained between BMP9 and BMP10 differentially phosphorylated sites (likely because the two experiments and MS analysis were performed independently), in addition

our limited findings from these analyses, we decided at the end of the 2nd year to perform TMT labeling approach using both BMP9 and BMP10. While keeping the main aim of the project, the technical aims were to: (1) have a deeper coverage of the phosphoproteome, (2) perform analysis using both BMP9 and BMP10 from the same experiment, and (3) multiplexing to reduce technical variability originating from the experimental workflow.

5.3 Results (Manuscript 1)

Below, I will present the main findings obtained from the TMT phosphoproteomic study and the associated materials and methods, which are provided in the form of an article that is nearly ready for submission.

Deciphering Early Phosphoproteome Changes in Response to BMP9 and BMP10 in Endothelial Cells

Al Tarrass M.[1], Belmudes L.[2], Koca D.[1], Liu H.[1], Al Tabosh T.[1], Azemard V[1], Ciais D[1,3], Desroches-Castan A.[1], Battail C.[1,2], Couté Y.[2], Bouvard C.[1*], and Bailly S.[1*]

[1] Biosanté unit U1292, Grenoble Alpes University, CEA, F-38000 Grenoble, France; [2] Grenoble Alpes University, CEA, INSERM, UA13 BGE, CNRS, CEA, FR2048, Grenoble, France; [3]Université Côte d'Azur, CNRS, INSERM, iBV, Nice, France

Corresponding author Email: sabine.bailly@cea.fr

Using a phosphoproteomic approach, we identified and validated, in addition to the SMAD canonical pathway, an indirect SMAD-dependent activation of GADD45β/P38 MAPK pathway, phosphorylation of ERG transcription factor, and negative regulation of cell cycle CDK4/6 pathway by BMP9 and BMP10 in endothelial cells.

Abstract

BMP9 and BMP10 are two key regulators of vascular homeostasis. These two ligands bind with high affinity to the endothelial type I receptor ALK1 together with a type II receptor. Mutations in this signaling pathway have been identified in two rare cardiovascular diseases, hereditary hemorrhagic telangiectasia and pulmonary arterial hypertension. So far, only the canonical SMAD signaling pathway has been extensively studied in response to BMPs. The aim of this work was to address early phosphoproteomic changes in endothelial cells in response to short-term stimulation (30 min) with BMP9 or BMP10 in order to identify new phosphorylated targets and signaling pathways.

We found that BMP9 and BMP10 treatment induced a very similar phosphoproteomic profile, which allowed the identification of 289 differentially phosphorylated proteins. We confirmed the activation of the canonical SMAD pathway, but also identified a central role for the MAPK pathway (MEKK4/P38), leading to HSP27-$S^{78/82}$ and Eps15-S^{796} phosphorylation. The activation of this pathway required the transcriptional upregulation of GADD45β, which, in turn, activated the P38 pathway. We also found that BMP9 and BMP10 regulated the phosphorylation of the endothelial transcription factor ERG. In accordance with our bioinformatic analyses that highlighted a repression of the CDK4/6 pathway, we found that BMP10 induced a G1 cell cycle arrest. Together, our data identified many new differentially phosphorylated proteins in response to BMP9 and BMP10 in endothelial cells, highlighting rapid direct SMAD signaling and delayed SMAD-dependent MAPK signaling. This enhances our understanding of the role of these ligands in vascular homeostasis and diseases.

Introduction

BMPs belong to the TGF-β superfamily, which comprises 33 cytokines in mammals, together with GDFs, activins, inhibins and nodal. These cytokines are involved in the regulation of many biological processes, including differentiation, morphogenesis, proliferation and tissue homeostasis [1]. Among BMPs, BMP9 and BMP10 have been shown to play a key specific role in vascular homeostasis by binding to their high affinity receptor ALK1, which is mainly expressed on endothelial cells (ECs) [2]. BMP9 and BMP10 bind to a signaling complex composed of two type I (ALK1) and two type II (BMPRII, ActRIIA or ActRIIB) serine/threonine kinase transmembrane receptors, with BMPRII being much more expressed on ECs compared to the two other type

II receptors. Following ligand binding, the type II receptor phosphorylates the GS (glycine/serine) domain of ALK1 [2]. Consequently, activated ALK1 phosphorylates the C-terminus of SMAD1 and SMAD5, allowing the recruitment of the regulatory co-SMAD, SMAD4. This trimeric SMAD complex subsequently translocates to the nucleus, where it binds to the promoters of many target genes with the assistance of other transcriptional regulators, thereby regulating their expression levels. This pathway is known as the canonical SMAD signaling pathway [3].

HHT is caused by heterozygous loss-of-function mutations mainly in the genes coding for the type I receptor ALK1 (*ACVRL1*), the co-receptor endoglin and less frequently in the transcription factor SMAD4. On the other hand, in HPAH, the majority of cases involve mutations in the gene coding for the type II receptor, *BMPR2*, with only very rare cases caused by *ACVRL1* mutations [4]. Interestingly, more recently, mutations in the genes encoding the two ligands BMP9 (*GDF2*) and *BMP10* have been described in HPAH [2]. Similarly, mutations in *GDF2* have also been described in very few cases of HHT [2]. Although several treatments are available to manage the symptoms of HHT and PAH, there is no curative treatment [5,6]. This is primarily due to our limited understanding of the molecular mechanisms connecting these mutations to the development of the observed abnormalities. Additionally, it remains unclear how mutations within the same signaling complex can result in the development of two distinct rare vascular diseases. Over the past two decades, various experimental findings have indicated that ligands belonging to the TGF-β family can activate, in addition to the well-studied canonical SMAD signaling pathway, non-canonical signaling pathways [7–9]. These include the mitogen activated protein kinase (MAPK) cascades, involving P38, c-Jun N-terminal kinases (JNK), or extracellular signal-regulated kinases 1 (ERK1) and ERK2, but also the PI3K-AKT pathway and Rho-like GTPases. Much less is known concerning the non-canonical signaling pathways regulated by BMPs. Interestingly, these pathways seem to be more cell context-dependent than the canonical SMAD pathway and have not been extensively studied in ECs in response to BMPs.

The aim of this work was to use high-resolution mass spectrometry (MS) phosphoproteomics to investigate early phosphorylation changes in response to BMP9 or BMP10 in ECs. This would enhance our understanding of the molecular mechanisms underlying their functions in vascular homeostasis and their potential contributions to HHT and HPAH pathogenesis, possibly uncovering novel therapeutic targets. Our extensive phosphoproteomic analysis identified many new phosphoproteins, allowing us to propose new signaling pathways downstream of BMP9 and BMP10 and endothelial cellular functions. In particular, we identified a new indirect pathway that involved a transcriptional step via the expression of the protein GADD45β to activate the MAPK pathway (MEKK4, P38). We demonstrated that this pathway is implicated in the phosphorylation of HSP27 and Eps15, but also in the regulation of a particular set of genes (*SELE*, *PTGS2*, and *HAS2*, encoding E-selectin, Cyclooxygenase-2 (Cox2), and hyaluronan synthase 2, respectively). We also identified many transcription factors regulated in response to BMP9 and BMP10, among which we could validate the phosphorylation of the endothelial specific transcription factor ERG (ETS related gene). Additionally, this analysis also suggested a down-regulation of progression through the cell cycle of ECs in response to BMP10, which we were able to validate.

Results

Phosphoproteome profiling of endothelial cells (ECs) stimulated by BMP9 and BMP10

To analyze in a comprehensive manner the early phosphorylation events regulated by BMP9 and BMP10, we stimulated human umbilical vein endothelial cells (HUVECs) with 10 ng/mL of BMP9 or BMP10 for 30 min. Our dataset consisted of five biological replicates under three conditions: non-stimulated, BMP9-stimulated, or BMP10-stimulated samples (Fig. 1A). The stimulations were validated by western blot analysis to confirm SMAD1/5 phosphorylation and the expression of ID1, a well-known target downstream of BMP9 and BMP10 signaling [10] (Fig. 1B). Subsequently, we processed the samples for phosphoproteomic analysis. To profile the phosphoproteome, we employed an isobaric labelling-based approach, relying on tandem mass tags (TMT) [518] to simultaneously quantify phosphorylated peptides in the BMP9 and BMP10 stimulated samples relative to non-stimulated cells (Fig. 1A). In parallel, with the same samples, we performed a proteomic analysis to investigate potential changes in the total proteome. Phosphopeptides were enriched from cell lysates using titanium dioxide (TiO2) beads, followed by offline high pH reversed-phase chromatography fractionation, and analysis using low pH reversed phase nanoliquid chromatography coupled to tandem mass spectrometry (nLC-MS/MS). Phosphopeptide enrichment was performed twice, generating 2 technical replicates that allowed the identification of a higher number of unique phosphopeptides [12]. We observed a very good quantitative reproducibility between the two replicates (Pearson's r = 0.65; Fig.S1A), allowing their combination for downstream statistical analysis. We considered only high-confidence phosphopeptides, defined as those with a probability score ≥ 0.75 for phosphorylation site localization (referred to as class I phosphosites) (detailed in Materials and Methods section). Analysis of the phosphorylated amino acid distribution showed that 88% of the identified phosphosites were on serine, 10.2% on threonine, and 1.8% on tyrosine, consistent with the expected abundance of these phosphorylated residues in eukaryotic cells [13] (Fig. 1C). The majority of these phosphosites were singly phosphorylated (67% singly, 24.8% doubly, and 8.2% triply) (Fig. 1C). Among the detected phosphosites, we identified 550 that were not previously documented in the phosphositeplus database from human data.

Quality control analysis on the quantitative data identified one sample as outlier from the BMP9-stimulated group (Fig. S1B) that was subsequently excluded from downstream analysis. Unsupervised principal component analysis (PCA) of all phosphosite abundances clearly distinguished non-stimulated (NS) samples from those stimulated with BMP9 or BMP10, but could not distinguish BMP9 from BMP10 stimulated samples (Fig. 1D).

Our analysis quantified 12,779 phosphosites mapped to 3283 proteins in the UniprotKB database (Fig. 1E, Table S1). By performing differential phosphorylation analysis on these 12,779 phosphosites ($|Log_2FC$ Stimulated_vs_Non Stimulated $| \geq 0.1$ and adj.p-value < 0.05), we identified a total of 419 differentially phosphorylated sites (DPSs) when combining data from both BMP9-*vs*-NS and BMP10-*vs*-NS stimulation, corresponding to 289 phosphoproteins annotated in the UniprotKB database (Fig. 1E, Table S1). Differential expression analysis of the total proteome, prior to phosphopeptide enrichment, quantified 6544 proteins (Fig. 1E, Table S1). Among these, only one protein, the transcription factor ID1, was differentially regulated by BMP9 and BMP10 compared to control group, which was already validated by WB analysis (Fig. 1B). Thus, none of the differentially regulated phosphosites were located on proteins exhibiting changes in their abundance upon BMP9 or BMP10 stimulation, supporting that the observed alterations in protein phosphorylation are not influenced by changes in the respective protein expression levels (Table S1).

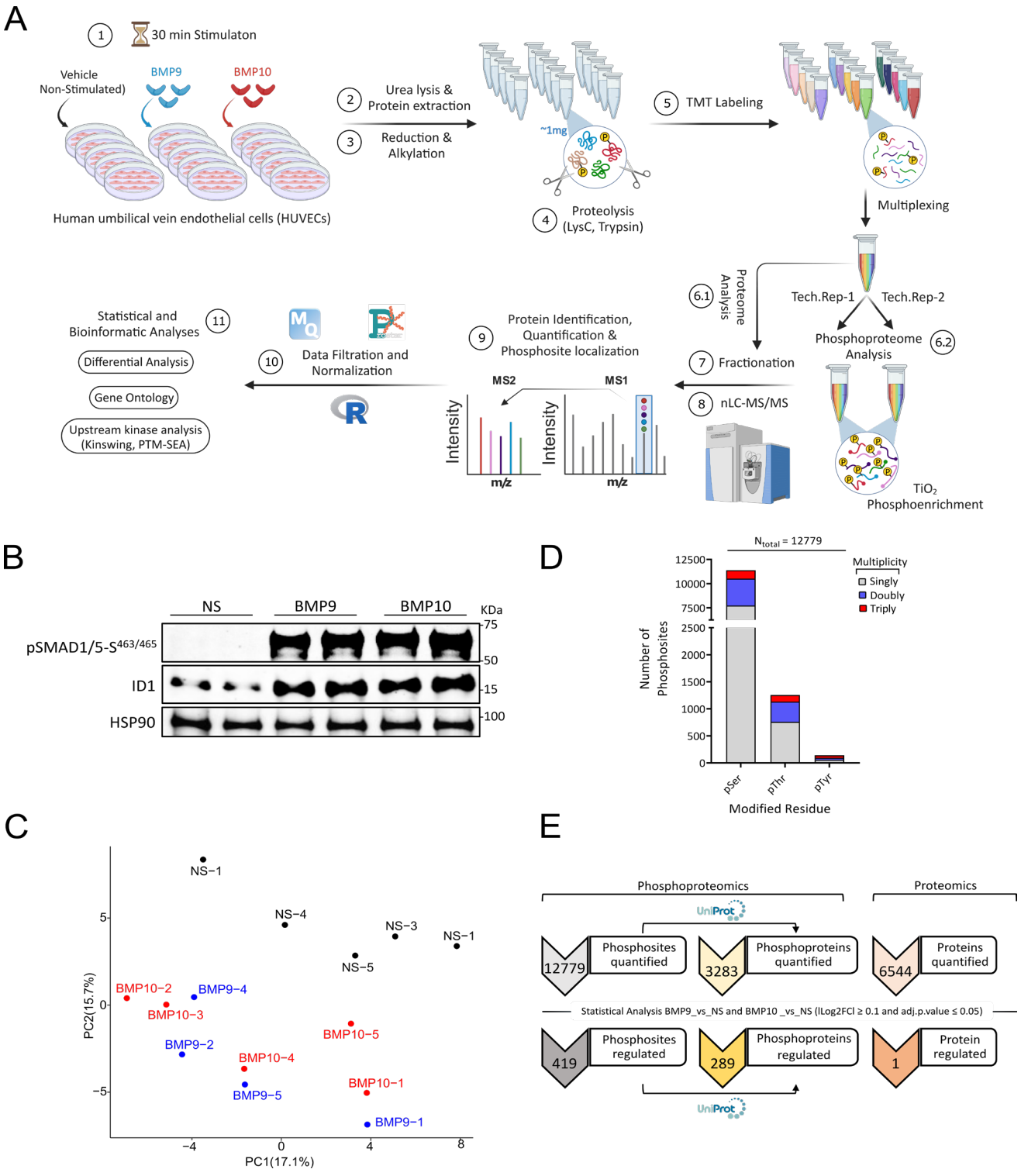

Fig. 1. Phosphoproteome protocol and profiling of BMP9 and BMP10 stimulation in human umbilical vein endothelial cells (HUVECs).
(**A**) Graphical representation of the experimental workflow for phosphoproteomic analysis. (1) Six-hours serum-starved HUVECs were stimulated or not with 10 ng/mL of BMP9 or BMP10 for 30 minutes. (2) Lysates from five biological replicates per condition were prepared and (3) subjected to reduction and alkylation, followed by (4) digestion using a combination of LysC and trypsin. (5) The resulting peptides from each sample were labeled with TMTpro16-plex reagents and pooled for subsequent analysis (6.1). A small portion of the pooled samples was reserved for proteomic analysis, while the rest was subjected to (6.2) phosphoenrichment using TiO2 beads for phosphoproteomic analysis. (7-8) The proteome and phosphoproteome samples were fractionated and analyzed using LC-MS/MS. Phosphoproteomic analysis was performed twice on two separate fractions generating two technical replicates. (9-11) Data analysis was then performed using different bioinformatics tools in R. **(B)** Western blotting analysis of two biological replicates for each condition (NS, BMP9 or BMP10) used for phosphoproteomic analyses showing the levels of SMAD1/5 phosphorylation and ID1 expression. **(C)** Distribution of the 12779 quantified

phosphosites across all samples according to their phosphorylation residue and multiplicity. **(D)** Principal component analysis (PCA) of phosphoproteomic data. **(E)** Upper numbers represent count of unique identified and quantified phosphosites and their corresponding phosphoproteins annotated in UniProtKB database (phosphoproteomic analysis), as well as that of proteins (proteomic analysis) across all samples. Bottom numbers represent total count of differentially regulated phosphosites (phosphoproteomic analysis) and proteins (proteomic analysis) by both BMP9 and BMP10.

Differential analysis identified 271 and 249 up-regulated phosphosites, versus 79 and 82 down-regulated phosphosites, in response to BMP9 and BMP10, respectively (Fig. 2A and B). The top DPSs common to both BMP9 and BMP10, including those which were further studied in this work, are highlighted on the volcano plots (Fig. 2A and B). Interestingly, BMP9 and BMP10 stimulations induced similar cell response at the prohosphoproteome level, as evidenced by the high Pearson's correlation coefficient (r) = 0.963 when comparing phosphosite abundances in BMP9- or BMP10-stimulated cells versus NS (Fig. 2C). Importantly, as a positive control, we identified phosphorylation of the activating residues on the C-terminus of SMAD1 ($S^{462/463/465}$), a direct substrate of ALK1 [14], thus validating our phosphoproteomic approach (Fig. 2D).

Interestingly, we identified both up-regulated DPSs, as expected from the BMP9/BMP10-induced activation of the ALK1 kinase, but also down-regulated DPSs (Fig. 2A and B). Accordingly, our analysis revealed differential phosphorylation of two phosphatases: ILKAP-S^{28} (Integrin-Linked Kinase-Associated Phosphatase) and CTDSPL2-S^{13} (potential phosphatase) upon BMP9 and BMP10 stimulation (Table S2). However, the functional significance of these phosphosites has not been previously described (Table S2). Furthermore, we also identified fourteen differentially phosphorylated kinases in response to BMP9 and/or BMP10 (Table S2), including ALK1, which was phosphorylated by both BMP9 and BMP10 at two distinct sites ($S^{155/161}$) (Fig. 2A and B). These sites were located within the juxtamembrane region of ALK1 (Fig. 2E), which do not correspond to the known phosphorylation sites within the GS domain of type I receptors [15]. Notably, tryptic digestion of these proteins is predicted to generate a large hydrophobic peptide containing the GS domain that is difficult to detect using MS analysis [16]. Thus, this might explain our inability to detect GS domain phosphopeptides, and why these latetr were never identified in any previous large-scale MS analyses [16]. To evaluate the functional significance of the two identified juxtamembrane phosphosites, we generated mutants that can no longer be phosphorylated at these sites by substituting serine with alanine residues (S155A, S161A, and S155A-161A). As BMP9 and BMP10 treatments induced similar responses at the phosphoproteomic level (Fig. 2C), the validation experiments performed in the rest of the manuscript were studied in response to BMP10 stimulation only, except when indicated. These mutants were tested in response to BMP10 using the ID1 promoter-derived BMP response element (BRE)-luciferase assay as previously described by our group [17]. We found that both ALK1 single and double alanine mutants exhibited a similar response as that of wild type (WT) ALK1, suggesting that these sites are dispensable for BRE activity (Fig. 2F). Additionally, we conducted the reverse experiment by substituting serine to aspartic acid, thereby introducing a negative charge mimicking receptor phosphorylation. As a positive control, we included the constitutively active mutation ALK1-Q201D [18]. Assessing BRE activity of the mutants revealed that, while ALK1-Q201D displayed constitutive activation in the absence of BMP10, ALK1-S155D, ALK1-S161D, and S155D-161D displayed responses similar to that of WT ALK1 (Fig. 2G). Together, these data support that these two ALK1 phosphosites ($S^{155/161}$) are not implicated in the canonical SMAD1/5 response. Among the other kinases identified, six corresponded to functionally characterized phosphosites (P38α-Y^{182}, ATR-S^{435}, MSK2-T^{687}, P70S6K-S^{447}, LIMK-S^{310} and SLK-S^{189}) (Table S2), but only three had commercially available phospho-antibodies. Notably, three kinases belonged to the MAPK pathway (MEKK4, P38α and MSK2), suggesting that BMP9 and BMP10 could signal through this pathway. The P70S6K belonged to the mTOR pathway, where its downstream target S6 has been previously identified to be differentially phosphorylated in HHT patient telangiectasia (Alsina-Sanchis, ATVB, 2018).

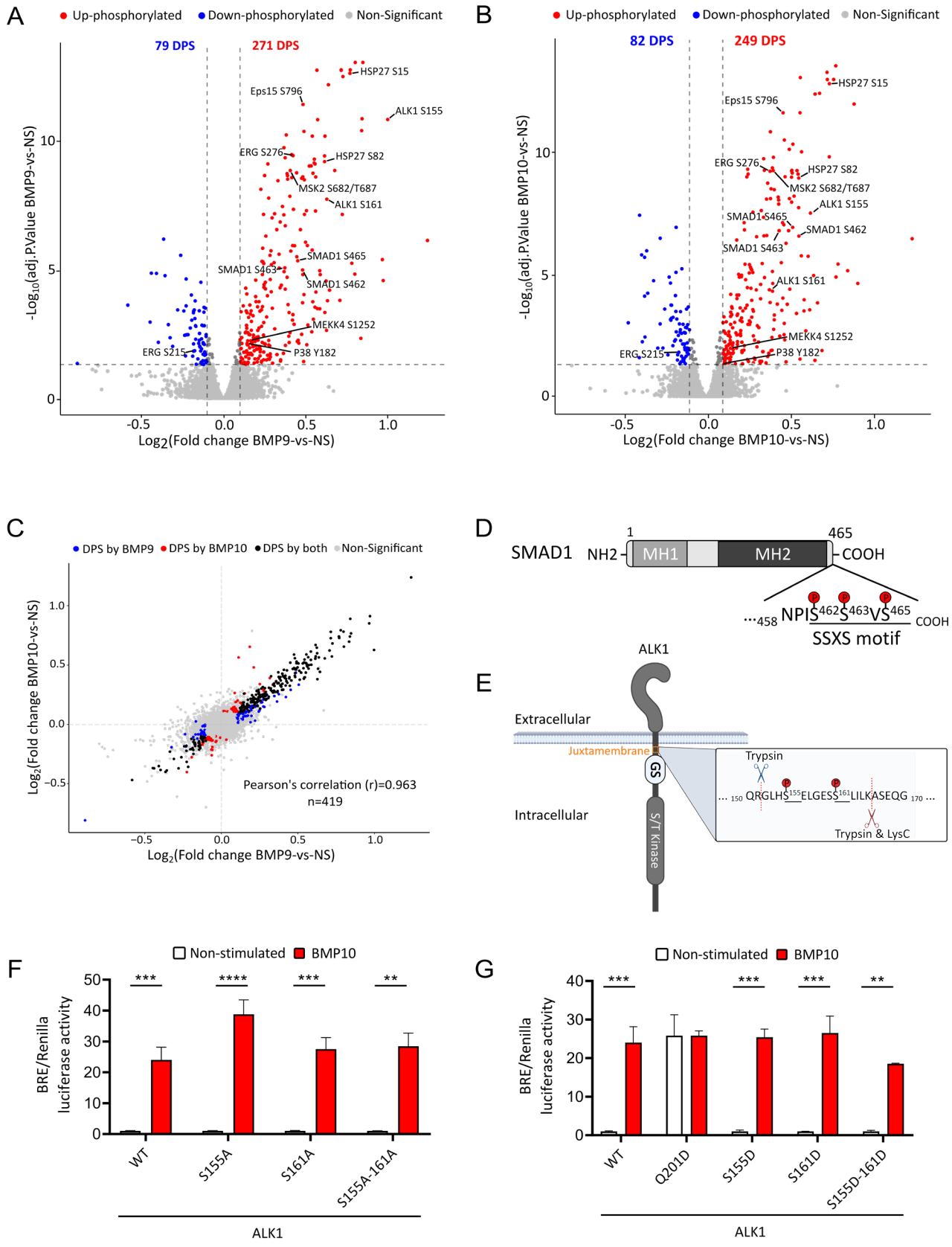

Fig. 2. Analysis of phosphoproteomic changes in response to BMP9 and BMP10 in HUVECs

(A-B) Volcano plots representing the log2 fold change in the abundance of phosphopeptides plotted against the $-\log_{10}$ adj. P.value, showing differentially phosphorylated sites (DPSs) which are down-regulated (blue) or up-regulated (red) in response to BMP9 (A) or BMP10 (B)

stimulation. DPSs from the canonical ALK1/SMAD1 signaling pathway as well as those which will be further studied in the work are annotated.
stimulation. DPSs from the canonical ALK1/SMAD1 signaling pathway as well as those which will be further studied in the work are annotated.
(**C**) Scatter plot comparing log2 fold change values of DPSs regulated by BMP9 and BMP10. Pearson correlation (r) is reported. (**D**) SMAD1 linear structure showing the MH1 and MH2 domain, along with the C-terminal SSXS motif. (**E**) Structural overview of the extracellular and intracellular domains of the type I receptor ALK1. The intracellular domain comprises two main regions, the GS domain and the Ser/Thr kinase domain. The juxtamembrane region (highlighted in red) located directly upstream of the GS domain bears the phosphopeptide obtained by phosphoproteomic analysis after digestion. Within this peptide, S^{155} and S^{161} phosphorylations were found differentially up-regulated by BMP9 and BMP10 (highlighted in A and B, respectively). (**F and G**) Relative BRE (BMP Response Element) luciferase activity measured in NIH-3T3 cells overexpressing wild-type (WT) or indicated ALK1 mutants. Serine residues were mutated to either alanine (S>A; phosphodead) (panel F) or aspartic acid (S>D ; phosphomimetic) (panel G). ALK1Q201D represents a positive control for constitutively active ALK1. BRE firefly luciferase activities were normalized to renilla luciferase activity. The data shown represent the mean ± SEM of three independent experiments. Two-way Anova followed by Sidak's multiple comparisons post test were used for statistical analysis. **P<0.01, ***P<0.001.

In order to obtain a comprehensive assessment of the underlying regulated processes, we next performed gene ontology enrichment analysis of biological processes (GO-BP) of the 289 differentially phosphorylated proteins regulated by BMP9 and/or BMP10 (Fig. 3A). Functional annotation clustering of the enriched terms produced 13 clusters for BMP9 and 14 for BMP10, with 10 clusters found to be common between both stimulations (Fig. 3A and Table S3). Interestingly, the first cluster presented contained several terms related to cell cycle regulation. Moreover, we identified several clusters with terms related to regulation of transcription, chromatin organization, and mRNA processing, supporting an important role for BMP9 and BMP10 at different levels of gene expression (Fig. 3A and Table S3). Interestingly, Wikipathway analysis highlighted only one pathway which was the VEGF-VEGFR2 pathway (Table S3).

To identify the potential upstream kinases responsible for the significant changes observed in the phosphoproteome upon BMP9 and BMP10 stimulation, we first utilized the computational algorithm KinswingR, which integrates sequence windows of phosphosites with kinase-substrate motifs [19]. This analysis identified 10 kinases predicted to have modified activities in response to both BMP9 and BMP10 (Fig. 3B). In accordance with our GO-BP analysis that highlighted the cell cycle cluster including the G1/S transition term (Table S3), Kinswing analysis revealed a significant under-activation of CDK4/6 and CDC7, key regulatory kinases involved in the G1/S transition of the cell cycle (Fig. 3B, Table S3). We also identified protein kinase R (encoded by *EIF2AK2*), which is involved in the inhibition of protein synthesis [20], and ERK5 (encoded by *MAPK7*) that belongs to the MAPK family (Fig. 3B, Table S3). On the other hand, we observed positive enrichment of CAMK2A (calcium/calmodulin-dependent protein kinase II alpha), MAPKAPK2/MK2 (a downstream kinase of P38α-MAP kinase pathway), PRKD1 (Protein Kinase D1), and PKG1 (cGMP-dependent protein kinase). PRKD1 plays a role in DAG/PKC signaling [21], while PKG1 is involved in eNOS/cGMP signaling and has been linked to aortic aneurism and arterial hypertension [22].

Next, we performed a post-translational modification signature enrichment analysis (PTM-SEA) using PTMsigDB to further define the correlation between the regulation of each phosphosite and molecular signatures of perturbations, kinase activities, and pathways obtained from curated published datasets [23]. As expected, this analysis predicted the activation of BMP type I receptor kinase (BMPRIB) due to the shared SMAD1 phosphorylation sites between different BMP type I receptors. Additionally, this analysis highlighted two top kinases, MK2 (already identified using the KinSwing analysis) and PKA (Fig. 3C, Table S3). Interestingly, in addition to the canonical SMAD1 pathway, our analysis highlighted the MEKK4/P38α/MK2 signaling pathway (Fig. 3D) with at least three P38α downstream targets among the top DPSs (Fig. 2A and B): MSK2, HSP27, a member of the small heat shock proteins which functions as a chaperone for correct protein folding, and Eps15 (epidermal growth factor receptor pathway substrate) which has been suggested to be involved in the endocytosis of cell surface receptors, including EGFR [24]. MSK2, HSP27, a member of the small heat shock proteins which functions as a chaperone for correct protein folding, and Eps15 (epidermal growth factor

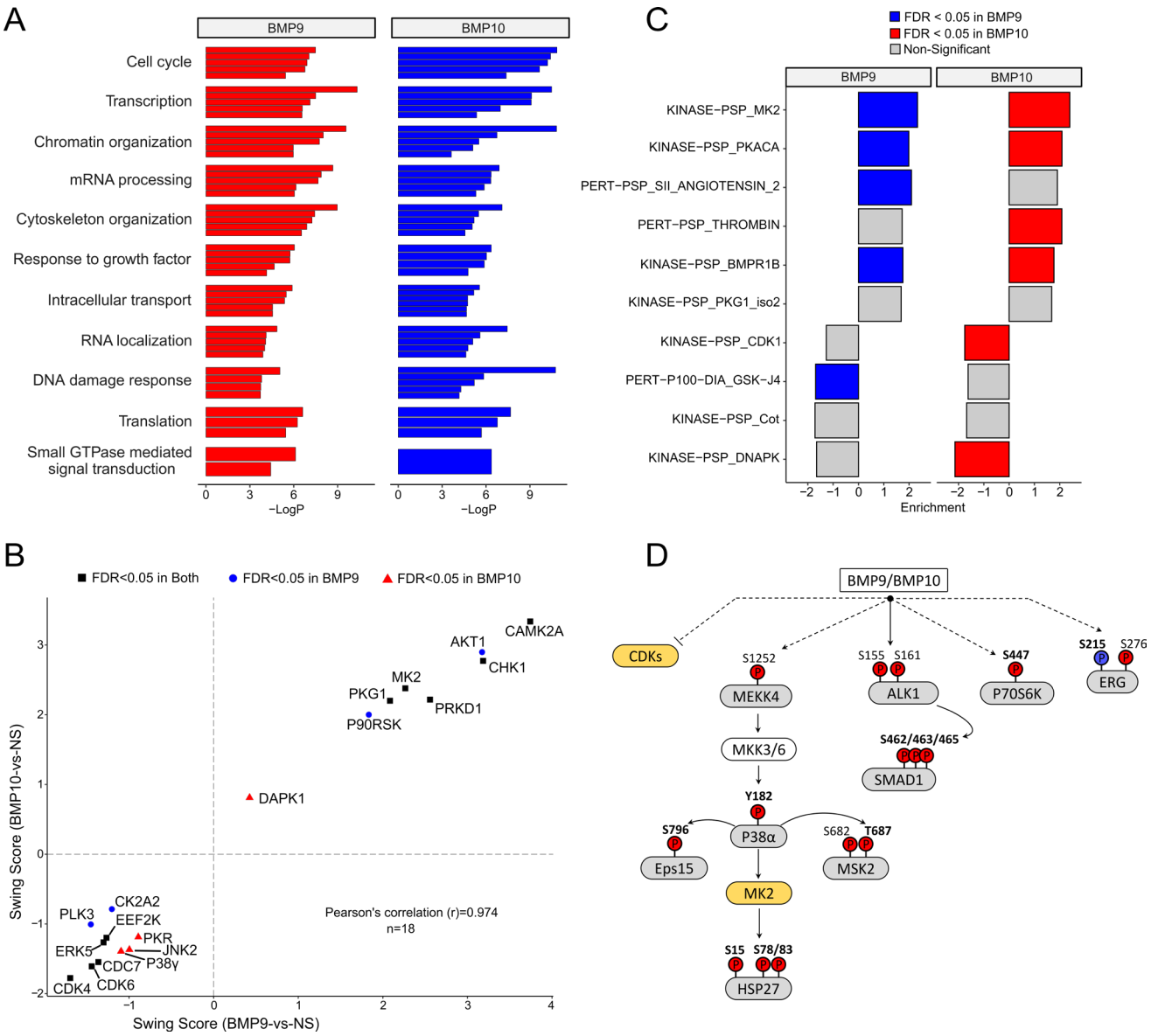

Fig. 3. Bioinformatic analysis of the phosphoproteomic changes in response to BMP9 and BMP10 in HUVECs

(A) Gene ontology (GO) analysis was conducted on biological processes (≥1.5 fold enrichment, P ≤ 0.05) using metascape, based on DPS's gene lists for BMP9 and BMP10. This analysis resulted in the generation of 13 clusters for BMP9 and 14 clusters for BMP10, corresponding to 105 and 116 GO annotations, respectively. Only the common clusters between BMP9 and BMP10 are presented. The top 5 terms from each cluster are plotted, while all other terms of each cluster are outlined in Table S3. **(B)** Scatter Plot of Kinswing S scores of kinases whose activities were predicted to be significantly changed in response to BMP9 and/or BMP10. **(C)** Post translational modification signature enrichment analysis (PTM-SEA) performed using PTMsigDB. The bar plot represents the top signatures enriched in BMP9 and/or BMP10 stimulated HUVECs compared to NS cells, ordered in terms of average FDR from both comparisons. Each bar represents a signature (kinase or perturbation). PERT; Perturbation **(D)** Hypothetical signaling framework in response to BMP9 and BMP10 based on phosphoproteomic analysis and literature-based data. Phosphorylated residues with increased abundance in response to BMP9 and BMP10 are marked in red, while those displaying decreased abundance are marked in blue. Grey rectangles represent proteins with DPSs obtained with BMP9 and BMP10, white rectangles are based on literature data. Orange rectangles represent kinases predicted by bioinformatics analysis (Kinswing and PTM-SEA). Dashed lines represent unknown mechanism.

pathway substrate) which has been suggested to be involved in the endocytosis of cell surface receptors, including EGFR [24]. In addition to the predicted under-activation of CDKs (Fig. 2A-B), we also observed the phosphorylation of P70S6K and the endothelial transcription factor ERG. Taking into account the different targets identified in the phosphoproteomic analysis and the utilized bioinformatic tools, we formulated a hypothetical signaling framework in response to BMP9 and BMP10 shown in Fig. 3D.

BMP10 signaling in HUVECs drives the activation of the P38-MK2 axis

Our phosphoproteomic analysis identified an increase in phosphorylation of P38α-Y^{182}, MSK2-S^{682}/T^{687}, HSP27-$S^{15/82/83}$, and Eps15-S^{796} in response to BMP9 and BMP10 stimulations (Fig. 2A and B). As shown in Fig. 4A, we successfully confirmed the phosphorylation P38α-Y^{182} and HSP27-$S^{78/82}$ following a 30 min stimulation with BMP10. We were unable to obtain quantifiable signals using commercially available antibodies against HSP27-S^{15} and MSK2-T^{687}, even with a positive control (data not shown). We also validated Eps15-S^{796} phosphorylation using a homemade phospho-antibody kindly provided by Dr Sakurai [25] (Fig. 4A). These phosphorylation events were also validated in response to BMP9 stimulation (Fig. S2). To assess the potential involvement of ALK1 in these phosphorylation events, we employed LDN193189, an inhibitor known to affect ALK1 kinase activity along with ALK2, 3, and 6 [26]. We found that P38α-T^{180}/Y^{182}, HSP27-$S^{78/82}$ and Eps15-S^{796} phosphorylations were all inhibited by LDN193189 (Fig. 4B). HSP27 has been shown to be phosphorylated by MK2 through P38/MK2 signaling axis [27], which was one of the top enriched kinases revealed by our bioinformatic analysis (Fig. 3B and C). Moreover, Eps15-S^{796} has been previously shown to be phosphorylated in response to TNF-α via the P38 MAPK pathway [25]. We thus tested whether these phosphorylations were dependent on P38 and MK2 kinases using specific inhibitors [25,27]. As expected, SMAD1/5 phosphorylation was not affected neither by the P38 inhibitor (SB203580) nor the MK2 inhibitor (PF3622204) (Fig. 4C). On the other hand, we found that HSP27-$S^{78/82}$ phosphorylation was inhibited by both inhibitors, while Eps15-S^{796} phosphorylation was only inhibited by the P38 inhibitor (Fig. 4C).

Notably, P38 (*MAPK14*) has been enriched in several GO-BP terms associated with transcriptional regulation (Table S3). Therefore, we tested whether P38 and MK2 kinases play a role in BMP10-induced gene regulation. To this end, HUVECs were stimulated by BMP10 for 4 hours with or without pretreatment with inhibitors targeting P38 and MK2 kinases. We found that inhibition of P38 and MK2 did not affect *ID1* nor *SMAD6* mRNA expression, two canonical targets of BMP9 and BMP10 in ECs (Fig. 4D). On the other hand, we found that the mRNA expression of *SELE* (E-selectin), *PTGS2* (Cox2), and *HAS2* were found to be dependent on P38, but not on MK2 (Fig. 4D). Collectively, these results validate several identified phosphoproteomic targets and reveal that BMP10 activates P38 MAPK signaling, resulting in the phosphorylation of HSP27-$S^{78/82}$ by P38/MK2 and Eps15-S^{796} by P38. Moreover, theand regulation of a subset of BMP10 target genes. Moreover, P38 activation mediates the regulation of a subset of BMP10 target genes independent of MK2.

BMP10 signaling in HUVECs induces a delayed activation of the P38 MAPK pathway via GADD45β expression

To further characterize the mechanisms responsible for P38-T^{180}/Y^{182}, HSP27-$S^{78/82}$ and Eps15-S^{796} phosphorylations, we performed a kinetic analysis in response to BMP10. As previously shown, we found that pSMAD1/5 was detectable after 5 min of BMP10 stimulation, reaching a plateau from 30 min until 240 min (Fig. 5A). On the other hand, P38-T^{180}/Y^{182}, HSP27-$S^{78/82}$ and Eps15-S^{796} phosphorylations started to be detected 30 min post BMP10 stimulation, peaked at 1h, and reached basal levels after 4 hours (Fig. 5A). We also stimulated the cells with different concentrations of BMP10 and found similar dose-response effects for SMAD1/5, P38-T^{180}/Y^{182}, HSP27-$S^{78/82}$ and Eps15-S^{796} phosphorylations, which started to be detectable from 0.1 ng/mL and reached a plateau at 1 ng/mL (Fig. S3).

Considering the time delay between SMAD1/5 activation and the phosphorylation of P38-T^{180}/Y^{182}, HSP27-$S^{78/82}$ and Eps15-S^{796}, we tested whether these delayed phosphorylation events were SMAD-dependent using siRNA

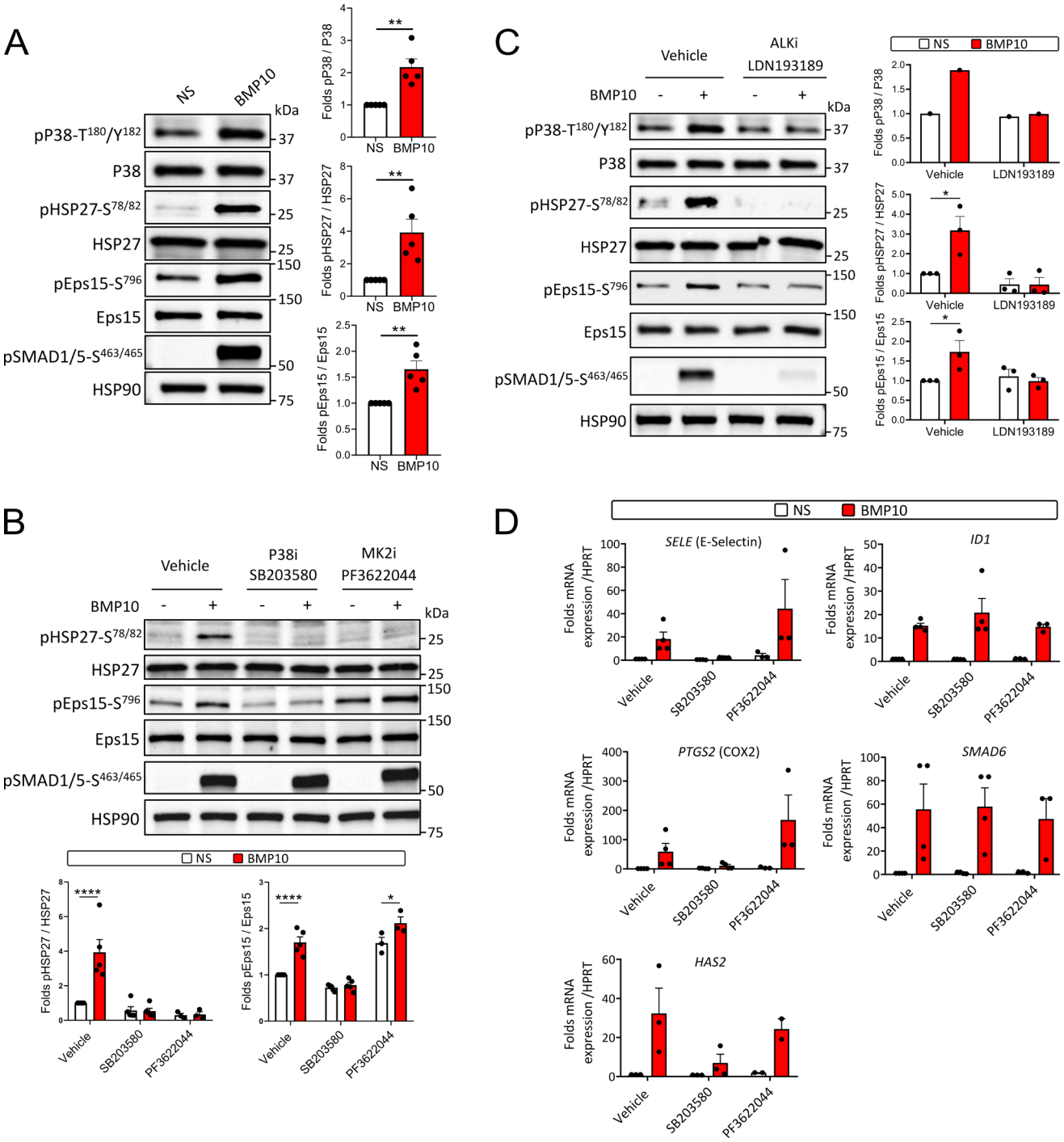

Fig. 4. BMP10 signaling in HUVECs drives the activation of the P38-MK2 axis

(A) HUVECs were stimulated with 10 ng/mL BMP10 for 30 min. Cell extracts were subjected to western blotting (WB) analysis using antibodies against phosphorylated (p) P38T^{180}/Y^{182}, P38, pHSP27-S$^{78/82}$, HSP27, pEps15-S^{796}, Eps15, pSMAD1/5-S$^{463/465}$ and HSP90 (loading control). Quantification of phosphorylation for P38, HSP27 and Eps15 reflects the normalized signal for the phosphorylated protein to total protein content, presented as mean fold change (BMP10-vs-NS) ± SEM of n=5 independent experiments. **P < 0.01 using Kolmogorov-Smirnov (KS) test. (**B** and **C**) HUVECs were pretreated with selective ALK1/2/3/6 inhibitor LDN193189 (5 µM) (Panel B), P38 inhibitor SB203580 (10 µM) or MK2 inhibitor PF3622044 (5 µM) (Panel C), or left untreated (vehicle) for 30 min. Subsequently, cells were stimulated with 10 ng/mL BMP10 for an additional 30 min. Cell lysates were then analyzed by WB using the indicated antibodies and quantification was performed as explained in (A). Data shown represent mean folds ± SEM of n=3 independent experiments. **(D)** HUVECs were pretreated with p38 inhibitor SB203580 (10 µM) or MK2 inhibitor PF3622044 (5 µM), or left untreated (vehicle) for 30 min. Cells were then stimulated with 10 ng/mL BMP10 for 4h. Real-time quantitative polymerase chain reaction (RT-qPCR) analysis was then performed to determine mRNA expression of *ID1*, *SMAD6*, *PTGS2* (Cox2), *HAS2* and *SELE* (E-Selectin). Target gene expression was normalized to HPRT mRNA level using $2^{-\Delta\Delta Ct}$ method and presented as fold induction (BMP10-vs-vehicle) ± SEM of n=3 independent experiments. Statistical analyses for panels B, C and D were performed using two-way ANOVA followed by Sidak's multiple comparisons post-test. For all panels: *P < 0.05; **P < 0.01; ***P < 0.001; ****P < 0.0001.

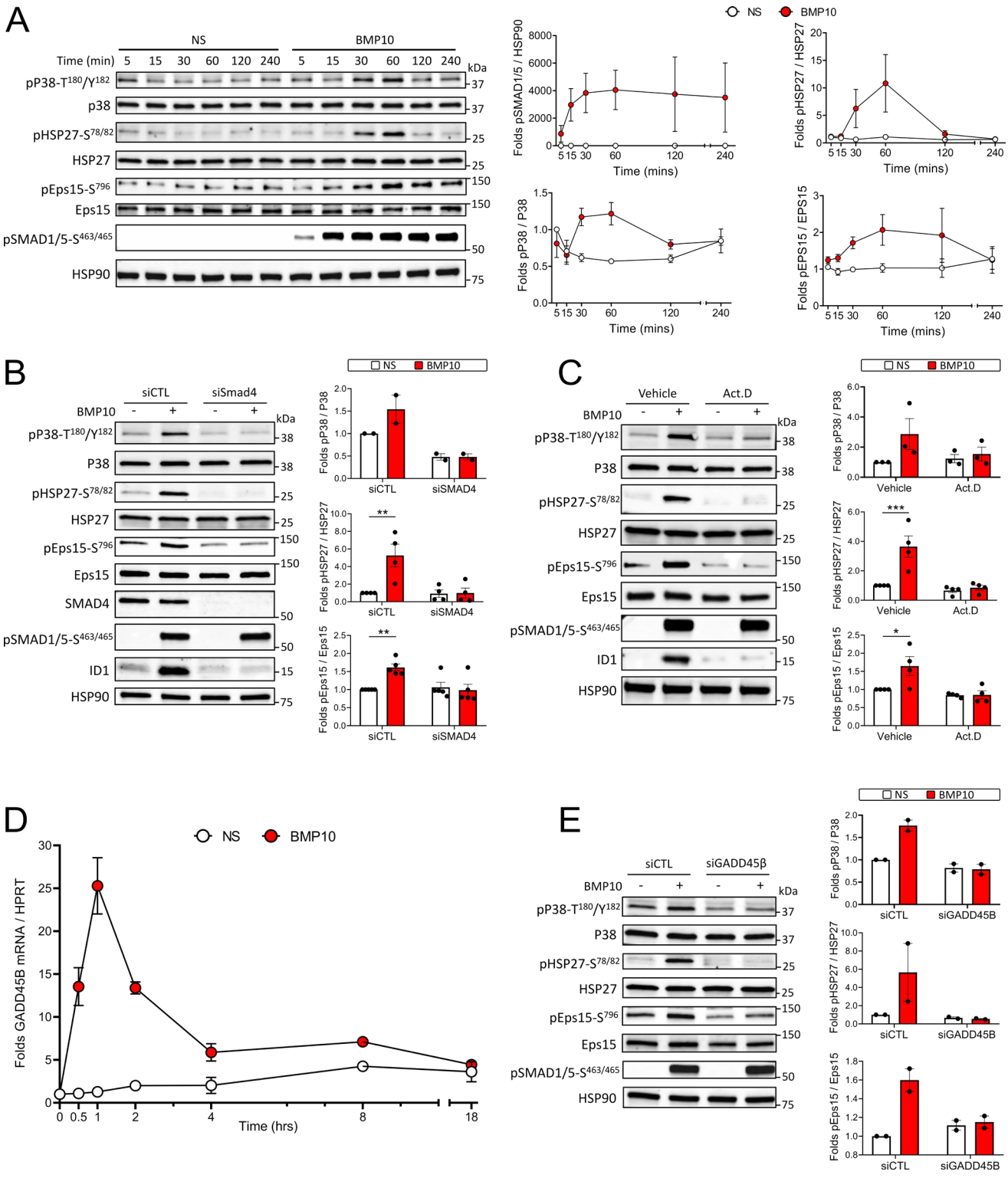

Fig. 5. BMP10 signaling in HUVECs induces a delayed activation of the P38 MAPK pathway via GADD45β expression

(A) Cells were stimulated with 10ng/mL BMP10 or vehicle for the indicated time points. Cell extracts were subjected to WB analysis using antibodies against phosphorylated (p) P38T^{180}/Y^{182}, P38, pHSP27-S$^{78/82}$, HSP27, pEps15-S^{796}, Eps15, pSMAD1/5-S$^{463/465}$ and HSP90 (loading control). Quantification of phosphorylation for P38, HSP27 and Eps15 was normalized to their respective total protein content, except for pSMAD1/5, which was normalized to HSP90. Data are presented as fold change of each sample ± SEM relative to NS 5 min. Blots are representative of n=3 independent experiments. **(B)** HUVECs were treated either with scrambled siRNA (siCTL) or siRNA against SMAD4 (siSMAD4) and then stimulated with 10ng/mL BMP10 for 30 min. Cell extracts were analyzed by WB using the indicated antibodies and quantification was performed as explained in panel A (n=3 independent experiments). **(C)** HUVECs were pre-treated either with vehicle or the transcription inhibitor actinomycin D (5 µM) for 30 minutes, then stimulated with 10ng/mL BMP10 for another 30 min. Cell extracts were analyzed by WB using the indicated antibodies and quantification of phosphorylation was normalized to total protein content. Data are

presented as mean folds (BMP10-vs-NS) ± SEM of n=3-4 independent experiments. **(D)** HUVECs were stimulated with BMP10 or vehicle for the indicated time points, and GADD45β mRNA expression was then assessed by RT-qPCR. The level of GADD45β mRNA expression was normalized to HPRT and represented as fold induction of each NS and BMP10 stimulated sample relative NS 0 min ± SEM of n=2 independent experiments. **(E)** HUVECs were treated either with siCTL or siGADD45β and then stimulated with 10ng/mL BMP10 for 30 min. Cell extracts were analyzed by WB using the indicated antibodies and quantification of phosphorylation was normalized to total protein content. Data are presented as mean folds (BMP10-vs-NS) ± SEM of n=2 independent experiments. Statistical analyses for panels A and D were performed using Kruskal Wallis with Sidak's post-test. Statistical analyses for panels B, C and E were performed using two-way ANOVA followed by Sidak's multiple comparisons post-test. For all panels: *P < 0.05; **P < 0.01; ***P < 0.001.

directed against SMAD4, the central mediator of SMAD is signaling. We confirmed the effectiveness of siSMAD4 by observing a reduction in SMAD4 expression (Fig. 5B). As expected, SMAD4 deletion did not impact SMAD1/5 phosphorylation triggered by BMP10, but completely inhibited ID1 expression (Fig. 5B). We found that P38-T^{180}/Y^{182}, HSP27-$S^{78/82}$ and Eps15-S^{796} phosphorylations were also inhibited by SMAD4 silencing (Fig. 5B), supporting that their phosphorylation was dependent on SMAD signaling. We thus tested whether the delay in BMP10-induced P38-T^{180}/Y^{182}, HSP27-$S^{78/82}$ and Eps15-S^{796} phosphorylations was due to a transcriptional step. To this end, HUVECs were pretreated with the transcription inhibitor actinomycin D 30 min prior to BMP10 addition. As expected, we found that SMAD1/5 phosphorylation induced by BMP10 was not affected by actinomycin D pretreatment, while it inhibited ID1 expression (Fig. 5D). Interestingly, we found that P38-T^{180}/Y^{182}, HSP27$^{S78/82}$ and Eps15-S^{796} phosphorylations were also inhibited by actinomycin D pretreatment (Fig. 5B). These results were further confirmed using DRB (5,6-Dichlorobenzimidazole 1-β-D-ribofuranoside), another transcription inhibitor (Fig. S4). Collectively, these data strongly suggest that BMP10 triggers the activation of the P38 pathway through a SMAD-dependent transcriptional step in HUVECs, subsequently leading to the phosphorylation of HSP27-$S^{78/82}$ by P38/MK2 and Eps15-S^{796} by P38.

It has been demonstrated that delayed activation of P38 MAPK through TGF-β stimulation is dependent on SMAD-mediated expression of GADD45β (growth arrest and DNA damage inducible beta), which activates MEKK4, an upstream MAPKKK of P38 [28,29]. Interestingly, our phoshoproteomic analysis identified MEKK4 as a differentially phosphorylated target in response to BMP9 and BMP10 stimulation in HUVECs (Fig2A and B). To explore whether GADD45β plays a role in BMP10-induced P38 activation, we assessed whether BMP10 regulates *GADD45β* mRNA expression. We found that BMP10 rapidly induced *GADD45β* mRNA expression within 30 min, peaking at 1h, and returning back near basal levels after 4h (Fig. 5C). This regulation was detectable at concentrations as low as 0.1 ng/mL, and it reached a plateau at 1 ng/mL (Fig. S5A). We next tested the effect of siRNA against GADD45β (Fig. S5B) on BMP10-induced P38-T^{180}/Y^{182}, HSP27-$S^{78/82}$ and Eps15-S^{796} phosphorylations. Interestingly, we found that these phosphorylation events were all dependent on GADD45β expression, while pSMAD1/5 was not (Fig. 5E). Together, these results strongly supports that BMP10 activates the P38 MAPK pathway via SMAD-dependent induction of GADD45β expression.

ERG is differentially phosphorylated by BMP10

Very interestingly, the phosphoproteomic analysis identified differential phosphorylation of the endothelial ETS transcription factor ERG at S^{215} (down-regulated) and S^{276} (up-regulated) by both BMP9 and BMP10 (Fig. 2A and B). Recently, ERG has emerged as a key regulator of endothelial function, playing vital roles in angiogenesis and vascular stability, transcriptional regulation of genes involved in essential endothelial functions, as well as the differentiation and maintenance of the endothelial lineage. To validate ERG phosphorylation, we performed immunoprecipitation of ERG and found that BMP10 stimulation increased ERG total serine phosphorylation (Fig. 6A). However, we did not have any specific phospho-antibody allowing to test if this phosphorylation corresponded to ERG-S^{276}. Interestingly, using a homemade

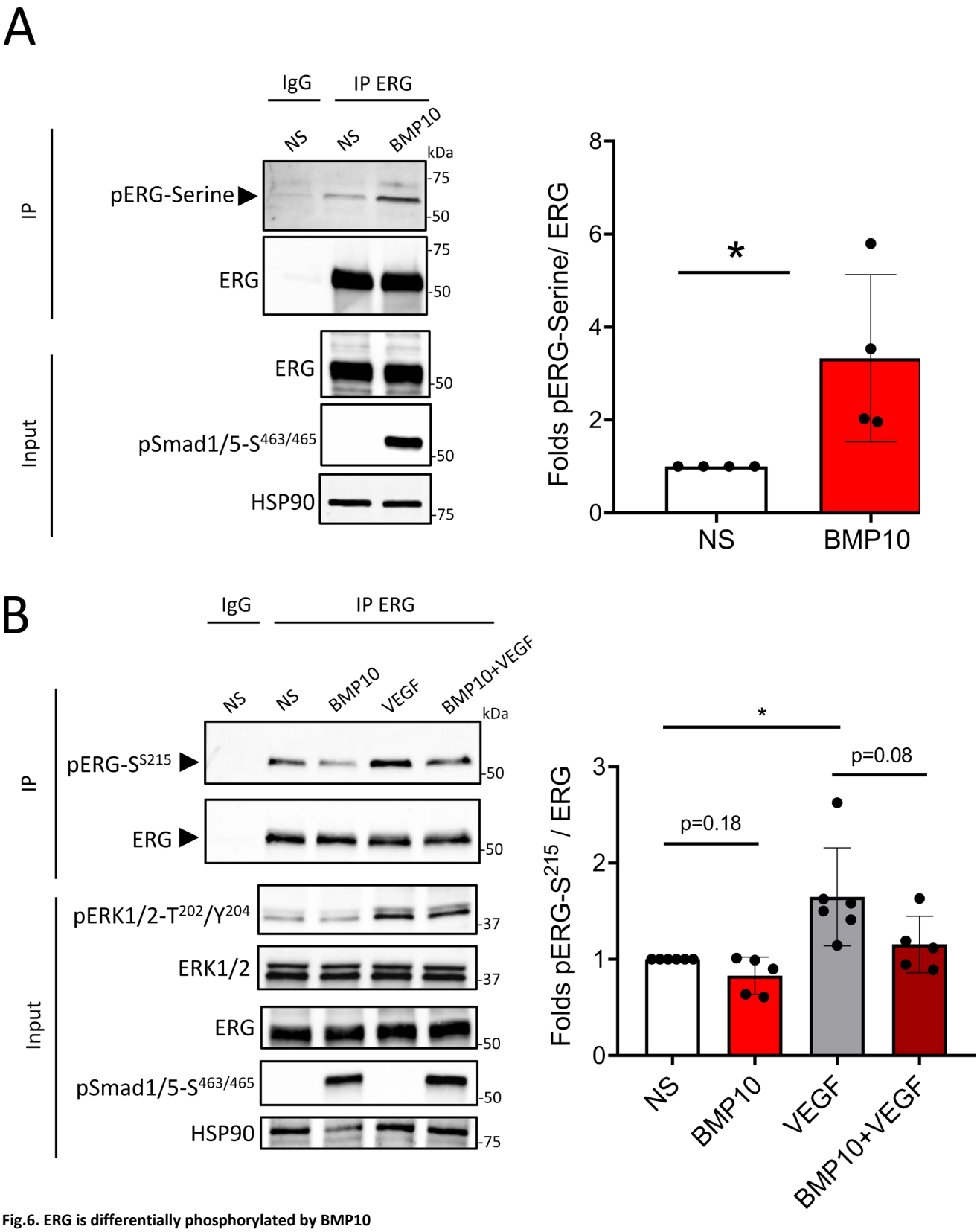

Fig.6. ERG is differentially phosphorylated by BMP10

(A) HUVECs were stimulated with 10 ng/mL BMP10 or not (NS) for 30 min. Cell extracts were subjected to immunoprecipitation (IP) using ERG antibody, followed by WB using pan phosphoserine (pSer) and ERG antibodies. Total serine phosphorylation of ERG was quantified and normalized to total ERG levels. IgG represents lysates subjected to IP using isotype control antibody. Whole cell extracts (input) were subjected to WB analysis using antibodies against pSMAD1/5, total ERG and HSP90. Data are presented as mean folds (BMP10-vs-NS) ± SEM of n=4 independent experiments. *P<0.05 using Kolmogorov-Smirnov (KS) test. **(B)** HUVECs were stimulated with 10 ng/mL BMP10, VEGF (40ng/mL), or BMP10+VEGF (10 and 40ng/mL, respectively) for 30 min. Cell extracts were subjected to immunoprecipitation (IP) using ERG antibody, followed by WB using antibodies against ERG-S^{215} and total ERG. Quantification of ERG phosphorylation reflects the normalized signal for the

pERG-S^{215} to total ERG from each sample. IgG represents lysates subjected to IP using isotype control antibody. Whole cell extracts (input) were subjected to WB analysis using antibodies against pSMAD1/5, ERG and HSP90. Statistical analyses were performed using two-way ANOVA followed by Sidak's multiple comparisons post-test. *P < 0.05.

pERG-S215 antibody generously provided by Dr. P. Hollenhorst [30], we were able to confirm the down-regulated phosphorylation of ERG-S^{215} by BMP10 (Fig. 6B). We also validated the previously reported VEGF-induced phosphorylation of ERG-S^{215} [31] and observed that the addition of BMP10 led to a reduction in this phosphorylation (Fig. 6B).

BMP10 inhibits the G1/S cell cycle transition in HUVEC

The GO-BP term analysis clearly showed that BMP9 and BMP10 affected cell cycle and G1/S transition (Fig. 3A and Table S3), which was further confirmed by the Kinswing analysis which revealed an attenuation of CDK4/6 and CDC7 activities (Fig. 3A and B). Through the examination of the substrates of these kinases, we did not find any previously reported targets for further validation (Table S2). CDK4/6 and CDC7 are pivotal regulatory kinases involved in governing the G1/S transition during the cell cycle [32,33]. We thus tested the impact of BMP10 on endothelial cell cycle. To this end, HUVECs were synchronized at the G0/G1 phase via serum starvation, followed by induction of cell cycle progression through serum replenishment in the presence or absence of BMP10 overnight stimulation. Analysis of cell cycle progression using EdU and PI staining, followed by flow cytometry analysis, revealed that BMP10 treatment reduced the proportion of cells in the S phase, both under low (0.5%) and high (5%) serum conditions (5.2 to 1,1% and 13.1 to 2.8 %, respectively, Fig. 7A). To gain further insights into the role of BMP10 in the G1/S transition, we examined downstream target genes of CDK4/6. Notably, we observed that BMP10 decreased the mRNA expression of *E2F2*, a downstream transcription factor for CDK4/6, as early as 2 hours post-stimulation (Fig. 7B). Furthermore, *CCND1* (cyclinD1, a key regulatory for CDK4/6) and *CCNA1* (cyclinA1, a key regulator of CDK2) mRNA levels were also down-regulated by BMP10 (Fig. 7B). By Western blot analysis, we further confirmed a decrease in cyclinD1 protein levels, and an increase in the CDK4/6 inhibitor P27^{KIP} in response to BMP10 (Fig. 7C). Taken together, these results indicate that BMP10 negatively regulates endothelial cell cycle, specifically by inhibiting the G1/S transition and regulation of several key regulators in this pathway.

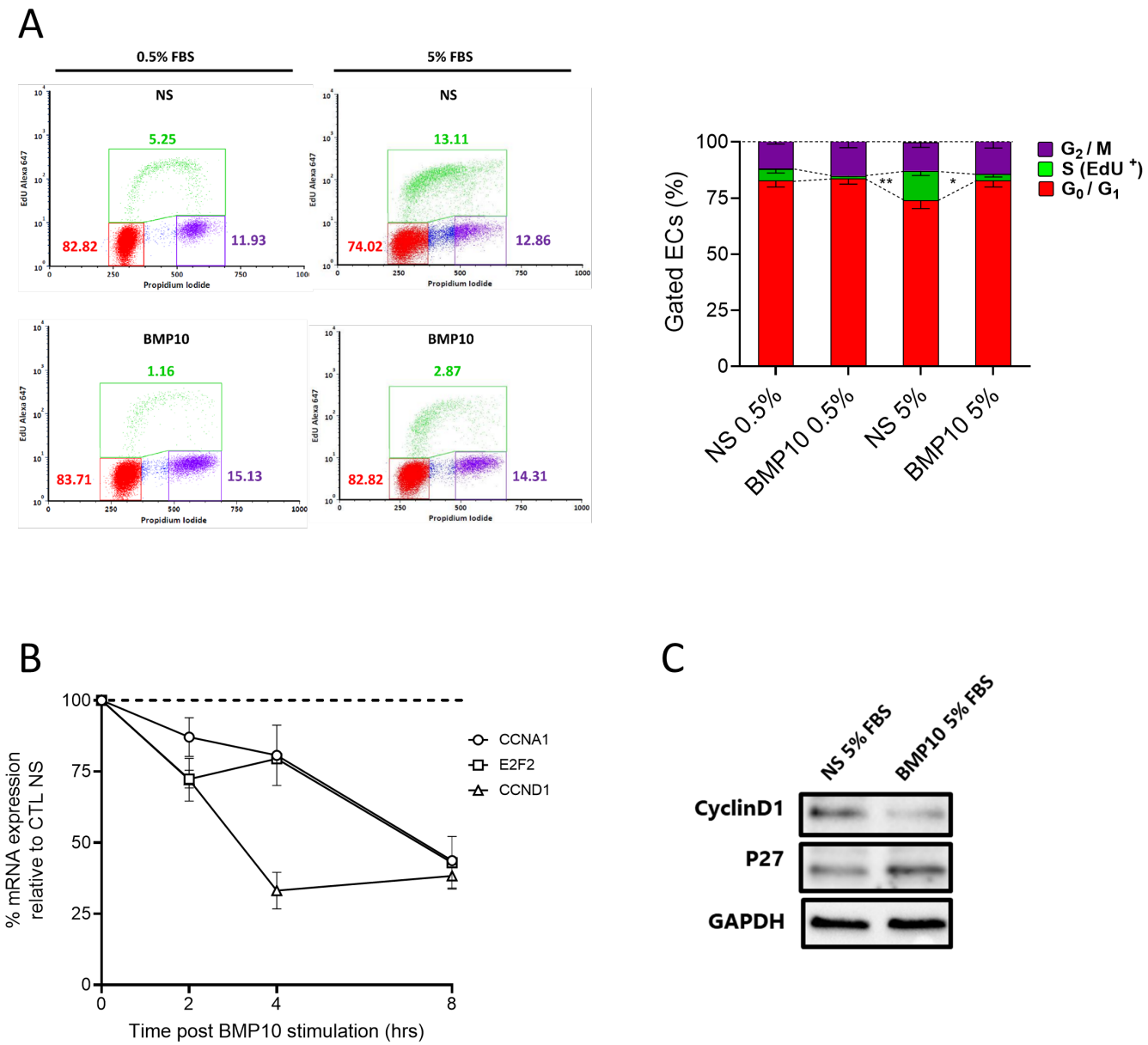

Fig. 7. BMP10 inhibits the G1/S cell cycle transition in HUVECs

(A) Cells were synchronized at the G1 phase by serum starvation for 48 hours. Subsequently, cells were then either replenished with 5% serum to progress through the cell cycle or were left under low serum conditions in the presence or absence of 10 ng/mL BMP10 overnight (16h). Cells were then treated with EdU, trypsinized, and labeled for EdU (labels S phase) and propidium iodide (PI) (total DNA content). Left panel: flow cytometry analysis assessing the distribution of different stages of the cell cycle (G1, S, G2/M) in HUVECs. Right panel: Quantification of different cell cycle stages in HUVECs from different conditions described in the left panel. Data are represented as mean % of each stage ± SEM of n=3 independent experiments and analyzed using two-way ANOVA with Sidak's multiple comparison post-test. **(B)** HUVECs were stimulated or not with 10 ng/mL BMP10 for 2h, 4h, or 8h. RT-qPCR analysis was then performed to determine mRNA expression of E2F2, CCND1 and CCNA1. Target gene expression was normalized to HPRT mRNA level using 2-ΔΔCt method and presented as relative expression (%) (BMP10-vs-vehicle) ± SEM at each time point of n=3 independent experiments. **(C)** Western blot analysis of cyclinD1 and p27 levels in HUVECs following an overnight stimulation with 10ng/mL BMP10.

Discussion

To our knowledge, this is the first study assessing BMP9 and BMP10 phosphoproteomic responses in ECs. In this work, we first identified SMAD1-$S^{462/463/465}$ phosphorylation upon BMP9 and BMP10 stimulation, which validated our technical approach. In addition to the canonical SMAD pathway, we identified many new phosphorylated proteins in response to these ligands (289), which allowed the identification of a newly activated signaling pathway in response to BMP9 and BMP10, involving MEKK4/P38 axis. This pathway was responsible for the phosphorylation of HSP27 and Eps15, but also regulation of *SELE*, *PTGS2* and *HAS2* mRNA expression. The activation of this pathway required a SMAD-dependent transcriptional step to induce GADD45β expression, consequently leading to the delayed activation of P38. We also found that the transcription factor ERG was differentially phosphorylated in response to BMP9 and BMP10. Our phosphoproteomic analysis also supported an inhibitory role for BMP9 and BMP10 on endothelial cell cycle, which was confirmed functionally through BMP10-mediated inhibition of G1/S transition.

In this study, we wanted to test both BMP9 and BMP10 signaling, as, despite sharing the same affinity to their type I receptor ALK1, they exhibit different binding affinities to the type-II receptors (BMPRII, ActRIIA and ActrIIB). However, our data clearly showed highly similar phosphoproteomic responses to BMP9 and BMP10, in accordance with a previous study that analysed their transcriptomic responses [34], supporting that at least in HUVECs, they activate very similar signaling pathways. Interestingly, our phosphoproteomic analysis showed that BMP9 and BMP10 induced differential phosphorylation of ALK1 on 2 sites,$S^{155/161}$, both located in the juxtamembrane domain, directly upstream to the GS domain, bearing sites which are phosphorylated by the type II receptor (Miyazono, Kamiya, and Morikawa 2010). However, ALK1 phosphorylation within the GS domain has never been identified in any previous large scale MS phosphoproteomic approach, while the ALK1-$S^{155/161}$ has already been described in high-throughput publications, but was never studied (Phosphositeplus, Hornbeck et al. 2012). Interestingly, phosphorylation within the juxtamembrane domain of ALK5-$S^{165/172}$ and -T^{176}, positioned similarly to the ones identified here for ALK1, have been previously described [38,39]. Accordingly to what has been previously shown for ALK5-S^{165} [38], our data support that ALK1-$S^{155/161}$ sites are dispensable for BMP10-iduced BRE luciferase activity (Fig. 2F,G). Nonetheless, these ALK5 juxtamembrane sites were shown to be important for TGF-β1-mediated functions , such as proliferation [38,39]. Of note, ALK1-$S^{155/160}$ have been shown to be phosphorylated by thrombin in ECs [40]. Together, our results support that these ALK1 juxtamembrane sites do not alter the canonical SMAD pathway, but might contribute to other BMP9 and BMP10 functional outcomes that could be interesting to further study in the future. Very interestingly, our phosphoproteomic approach revealed an important role for the P38 MAPK pathway in response to BMP10 in ECs. We could show that this activation peaked one hour after BMP10 addition, indicating an indirect mechanism. Unlike the rapid direct activation of P38 signaling within 5-10 minutes in response to growth factors like TNFα and VEGF [25,41], our findings suggest that SMAD-mediated GADD45β expression is required for this delayed activation. To our knowledge, GADD45β has been mainly studied in response to TGF-β which rapidly increases *GADD45β* mRNA expression [28,42], although it was also shown that BMP2 could also induce *GADD45β* mRNA expression in chondrocytes [43]. The mechanism of action described for MEKK4 activation via GADD45β occurs by binding of GADD45β to the MEKK4 N-terminal site, which will lead to MEKK4 dimerization, allowing the trans-autophosphorylation of MEKK4 at $T^{1493/4}$ in the kinase activation loop, leading to its activation [29]. Of note, our phosphoproteomic analysis identified MEKK4 to be differentially phosphorylated by BMP9 and BMP10 at S^{1252} which will be worth to further study in the future.

A transcriptional step for downstream signaling in response to BMP9 in ECs has been previously described [44]. It was shown that BMP9 and BMP10 induce a rapid (within 1 h) expression of *SGK1* (Serum/glucocorticoid-regulated kinase 1) mRNA in HUAEC [45]. Subsequently, another group showed that SGK1 synthesis is needed for BMP9-mediated regulation of the mTORC1/P70S6K/S6 axis [44]. Our phosphoproteomic study identified P70S6K-S^{447} phosphorylation in response to BMP9 and BMP10 (Tables S2), but we were not able to validate this site by Western Blot. Notably, this pathway has been shown to be activated in telangiectasias of HHT patients [46].

Together, our observations indicate the following scenario for BMP10 signaling (Fig. 8). BMP10 activates its receptor ALK1, which phosphorylates SMAD1, resulting in the formation of an active SMAD1/SMAD4 complex that translocates to the nucleus. This will regulate the expression of many immediate early genes including GADD45β. Subsequently, GADD45β activates MEKK4, which phosphorylates MKK3/6, leading to the activation of P38 MAPK. Activated P38 will then induce the activation of MK2, which subsequently phosphorylates HSP27-$S^{78/82}$. Activated P38 will also phosphorylate Eps15-S^{796}, independently of MK2. Our data also show that P38 is implicated in the regulation of several genes downstream of BMP10 (*E-selectin*, *HAS2*, and *PTGS2*), supporting at least two groups of genes regulated by BMP10: those that are SMAD-dependent and those that are SMAD- and P38-codependent. Notably, TGFβ-induced P38-MSK1 activation has been shown to be GADD45β-dependent [47]. We have also identified BMP9- and BMP10-induced phosphorylation of MSK2, though we couldn't validate it by western blot.

We found that BMP9 and BMP10 stimulations induce the phosphorylation of Eps15-S^{796}. This site has been previously described to be phosphorylated in response to TNFα, EGF, IL-1β [25]. However, the effect of this phosphorylation remains unknown. It has been shown that Eps15, along with its homologous protein Eps15R, act as scaffold proteins with multiple domains. These include EF-H and protein-binding modules that interact with endocytic proteins, Grb2/AP2 binding sites involved in endocytosis of many receptors including EGFR [24,48], and ubiquitin-binding domains (UIMs) [49(p. 1)]. Interestingly, S^{796} is located between Grb2/AP2 binding domains and the C-terminal UIM domain, suggesting a role in clathrin-mediated endocytosis. A direct interaction between Eps15R and BMPRII has been also previously described [50]. Eps15R interaction with SMAD1 was found to be required for BMP signalling in xenopus animal caps [51]. Together, these results support functional links between Eps15R and the BMP pathway. Due to the similarity between the functional domains of Eps15 and Eps15R, these studies suggest that Eps15 might also interact with BMP receptors and contribute to their endocytosis and/or downstream signaling in ECs.

Our phosphoproteomic analysis revealed that both BMP9 and BMP10 induced the phosphorylation of HSP27. HSP27 phosphorylation has been shown to be implicated in many biological processes including apoptosis, proliferation, migration, differentiation, transcriptional regulation and cytoskeletal organization [52–54]. HSP27 phosphorylation causes the disassembly of large oligomers and the release of actin, which promotes actin polymerization in many cell types [55,56]. An important role of HSP27 in ECs is the regulation of actin filament remodelling and EC barrier function [57–60]. Interestingly, it was recently shown that in ECs, BMP2- and BMP6-induced HSP27 phosphorylation via P38 promoted endothelial cell migration [61]. Although HSP27 phosphorylation site was not mentioned in this study, the time of stimulation used (45 min) is in accordance to the kinetic phosphorylation of P38 and HSP27 observed in response to BMP10 in our work, thus suggesting that other BMPs could activate this P38/HSP27 pathway in a similar manner. Our study also identified LIMK1-S^{310} phosphorylation to be down-regulated in response to BMP9 and BMP10 (Tables S2). LIMK1 regulates actin

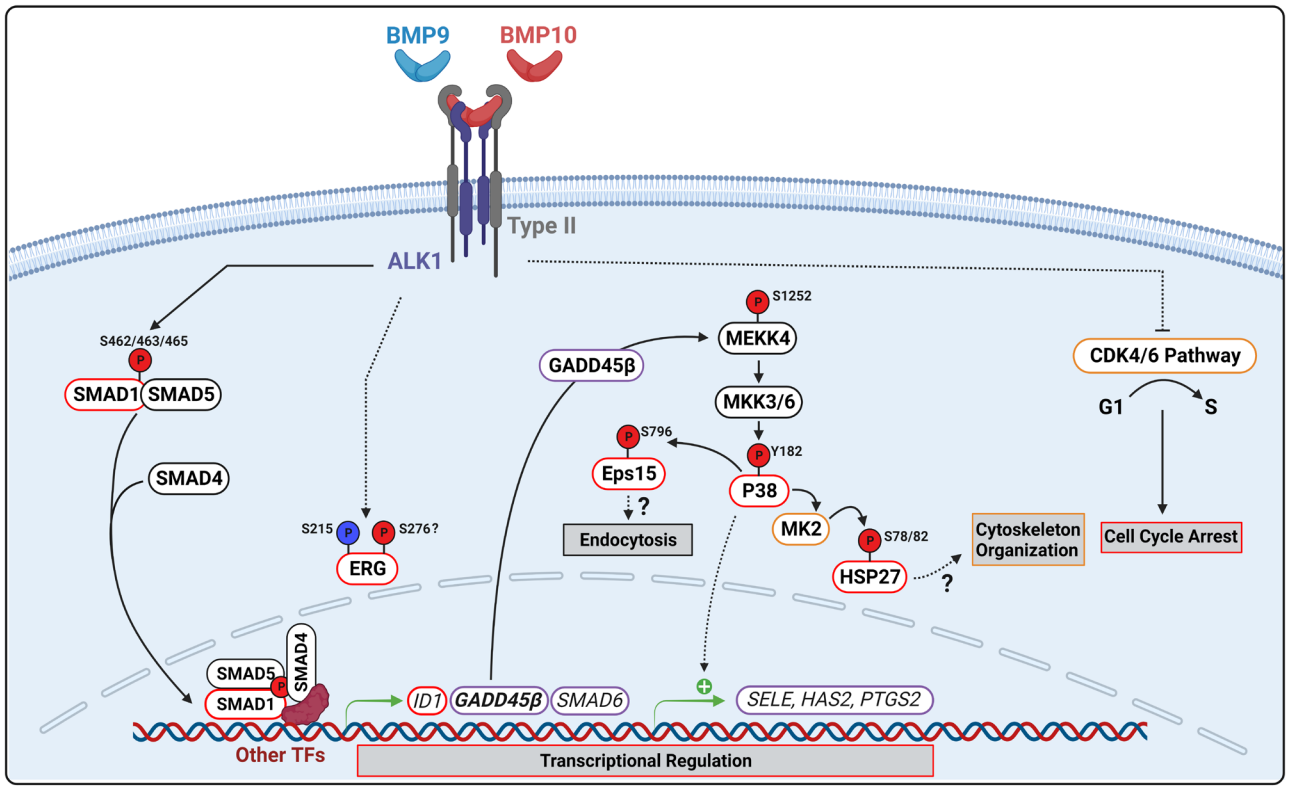

Fig. 8. BMP9/BMP10/ALK1 Signaling drives the regulation of direct and indirect pathways in ECs

Binding of BMP9 and BMP10 (BMP9/10) to ALK1 along with a type II receptor on ECs mediates the activation of ALK1, leading to the initiation of direct and indirect pathways. The direct pathway involves the SMAD cascade, where activated ALK1 phosphorylates the C-terminus of SMAD1 and SMAD5, allowing the recruitment of SMAD4, forming a trimeric SMAD complex. This trimeric SMAD complex subsequently translocates to the nucleus, where it binds to the promoters of target genes with the assistance of other transcription factors (TFs), thereby regulating their expression levels. Among these, BMP9/10 induce the expression of GADD45β, an activator of MEKK4, which mediates indirect activation of P38/MK2 signaling axis by these ligands. In this cascade, P38 phosphorylates Eps15-S^{796}, while MK2 phosphorylates HSP27-$S^{78/82}$, where these proteins been described to play important roles in endocytosis and cytoskeleton organization, respectively. Additionally, P38 activation regulates a subset of BMP9/10-induced genes, including *SELE*, *HAS2*, and *PTGS2*. On the other hand, BMP9/10 downregulates the CDK4/6 pathway leading to inhibition of G1/S transition and cell cycle arrest. Curved rectangles represent proteins and genes, while grey filled rectangles represent pathways. Proteins identified by phosphoproteomics and that were validated are highlighted in red, except for ID1, which was identified through total proteome analysis. Phosphorylated residues with increased abundance in response to BMP9 and BMP10 are marked in red, while those displaying decreased abundance are marked in blue.Orange rectangles represent kinases/pathways/processes revealed through bioinformatics analyses. Violet rectangles represent other identified targets in this study, while black rectangles represents proteins/processes described in literature. Dashed lines represent unknown mechanism.

dynamics by phosphorylating cofilin, which leads to actin depolymerization. LIMK1 has been shown to interact with BMPRII, and the interaction between LIMK1 and BMPRII inhibited LIMK1's ability to phosphorylate cofilin, which could then be alleviated by the addition of BMP4 [62(p. 1)]. While it was also shown that VEGF induces LIMK1 phosphorylation at $S^{310/323}$ via MKK4/P38/MK2 axis in HUVECS, only LIMK1-S^{323} was involved in VEGF-induced actin remodelling and cell migration [63]. LIMK1 phosphorylation might thus be an interesting hit to be further studied, given the role of actin turnover in cell migration and the involvement of cell migration in the development of HHT arteriovenous malformations (AVMs) [64].

Our work also revealed that BMP9 and BMP10 treatment induce the differential phosphorylation of the key endothelial transcription factor ERG (Fig. 6). We could validate that BMP9 and BMP10 induce ERG-Serine phosphorylation and decreased ERG-S^{215} phosphorylation. It was previously demonstrated that ERK2 phosphorylates ERG at $S^{96/215/276}$, but that only S^{215} was required for ERG activity in prostate cancer cells [30]. On the other hand, the role of ERG-S^{276} phosphorylation remains uncharacterized. It has been previously shown

that VEGF induced ERG-S^{215} phosphorylation within 15-30 min in ECs and that this phosphorylation was important to regulate Dll4 expression [31]. Interestingly, we found that BMP10 stimulation inhibited VEGF-induced ERG-S^{215} phosphorylation (Fig. 6). Of note, it was shown that ERG silencing caused a reduction in ALK1 signaling in HUVECs [65]. We were not able to go further into the mechanism of ERG phosphorylation induced by BMP10, nor the functions of these phosphorylated sites. Nevertheless, given its critical roles in ECs, ERG is certainly a target that would be worth studying in the future, to better understand the role of BMP9 and BMP10 in this context.

Our study highlighted a role played by BMP9 and BMP10 in the inhibition of endothelial cell cycle (Fig. 7), in accordance with the known role of BMP9 and BMP10 in vascular quiescence [2]. However, the molecular mechanism leading to inhibition of EC proliferation by BMP9 or BMP10 remains poorly understood. Our phosphoproteomic study was able to highlight a BMP9- and BMP10-initiated anti-proliferative signal within a 30 min stimulation. However, by looking carefully at the downstream-matched substrate phosphosites of the kinases identified by the Kinswing analysis, we could not find any phosphoprotein that had been previously described and that we could try to validate (Table S2). It has been demonstrated that BMP9 suppresses proliferation of HAECs by modulation of various cell cycle-related proteins (P21^{CIP}, P27^{KIP}, cyclin D1) (Rostama et al. 2015). This inhibition was shown to be SMAD1/5-dependent and required the expression of the CDK4/6 inhibitor P27^{KIP1}. We found that BMP10 stimulation rapidly reduces the mRNA expression of three cell cycle regulatory genes (*CCND1*, *CCNA1*, and *E2F2*) within just 2 hours, and confirms the induction of P27^{KIP1} protein after 18 hours. Accordingly, it was recently shown that cell cycle progression-mediated the loss of arterial identity and the formation of AVMs in *Smad4*$^{i\Delta EC}$ pups. Interestingly, Palbociclib (CDK4/6 inhibitor) inhibited reduced AVM formation and rescued the excessive vascular front density in these mice [67].

All in all, our study revealed 419 differentially regulated phosphosites after a 30 min stimulation by BMP9 and BMP10 in HUVECs. Although we could validate and decipher the mechanisms for several important hits and pathways, we could not study all of them due to the lack of specific tools, such as particular phospho-specific antibodies. However, with the development of such tools, we hope that the vascular biology community would benefit from this unique high-throughput phospho-proteomic study of BMP9 and BMP10-mediated signaling to further characterize the roles of these 2 ligands, both under physiological conditions but also in pathological vascular diseases, such as HHT and PAH.

Materials and Methods

Cell Culture

Human umbilical vein endothelial cells (HUVECs) were purchased from Lonza and cultured in endothelial basal medium-2 (EBM-2) supplemented with EGM-2MV SingleQuot additives (fetal bovine serum (FBS), hEGF, hydrocortisone, VEGF, hFGF-B, R3-IGF-1, ascorbic acid, GA-1000, and heparin; Lonza)). Murine NIH-3T3 fibroblasts were maintained in high glucose, sodium pyruvate and GlutaMAX-supplemented Dulbecco's modified Eagle medium (DMEM; Gibco) with 10% FBS (Biosera) and 1% Penicillin/Streptomycin (Gibco). Cells were incubated at 37 ℃ in a humidified atmosphere containing 5% CO2.

Reagents

Recombinant human BMP9 and BMP10 were purchased from R&D systems (Catalog # 3209-BP and 3956-BP, respectively). LDN193189 was purchased from Sigma (Catalog # SML0559). SB203580 (Catalog # 1202) and PF-3644022 (Catalog # 4279) were purchased from Tocris Bioscience. Actinomycin D and DRB were purchased from Sigma (Catalog # 50-76-0).

Workflow for Phosphoproteome Sample Preparation

Stimulation and Cell lysis

HUVECs were starved for 6h in EBM-2, after which they were stimulated or not for 30 min with 10ng/ml of BMP9 or BMP10. Stimulations were repeated two times with 3 biological replicates/condition in the first time and 2 biological replicates/condition in the second time generating 5 biological replicates/condition. Cells were then lysed on ice with urea lysis buffer (8M Urea, 50mM Tris-HCl pH 8, 75Mm NaCl, 1mM EDTA) supplemented with protease inhibitor cocktail (P8340) and phosphatase inhibitor cocktails 2 (P5726) and 3 (P0044) purchased from Sigma. Lysates were prepared as described in Western blotting section, and protein concentrations were determined using a µ-BCA assay kit (Thermo Scientific).

Sample preparation

1mg proteins from each sample was used to prepare samples for nLC-MS/MS analyses. Extracted proteins were reduced using 20mM of dithiothreitol for 1h at 37°C before alkylation with 55mM of iodoacetamide for 1h at 37°C in the dark. Samples were then diluted to ½ using ammonium bicarbonate and digested with LysC (Promega) at a ratio of 1:200 for 4 hours at 37 °C. Then they were diluted again to ¼ and digested overnight at 37 °C with sequencing grade-modified trypsin (Promega) at a ratio of 1:50. Resulting peptides were purified by C18 reverse phase chromatography (Sep-Pak C18, Waters) before drying down.

Peptides were then labelled using 16plex TMTpro isobaric Label Reagent kit (ThermoFisher Scientific) before mixing equivalent amounts and desalting using C18 reverse phase chromatography (Sep-Pak C18, Waters). Labelled peptides were split into three different aliquots: ~60µg for proteome wide analysis, and 2 aliquots of ~7mg for generating 2 technical replicates of phosphopeptide enrichment. Phosphopeptide enrichment was performed using titanium dioxide beads (TitanSphere, GL Sciences, Inc.) as previously described [68] before purification using C18 reverse phase chromatography (Marco SpinColumns, Harvard Apparatus).

Isobaric-labelled peptides from total proteome and phosphoproteome were fractionated into eight fractions using the Pierce High pH Reversed-Phase Peptide Fractionation Kit (ThermoFisher Scientific)following the manufacturer's instructions.

nLC-MS/MS analyses

Each fraction was analyzed by nLC-MS/MS (Ultimate 3000 RSLCnano and Q-Exactive HF, Thermo Fisher Scientific) using a 240 minutes gradient. For this purpose, the peptides were sampled on a precolumn (300 µm x 5 mm PepMap C18, Thermo Scientific) and separated in a 200 cm µPAC column (PharmaFluidics). The MS and MS/MS data were acquired by Xcalibur version 2.9 (Thermo Fisher Scientific).

Data analysis

Peptides and proteins were identified and quantified using MaxQuant version 1.6.17.0 [69], the UniProt database (*Homo sapiens* taxonomy, 20211014 download) and the database of frequently observed contaminants embedded in MaxQuant. Trypsin/P was chosen as the enzyme and 2 missed cleavages were allowed. Peptide modifications allowed during the search were: Carbamidomethyl (C, fixed), Acetyl (Protein N-term, variable), Oxidation (M, variable), and Phospho (STY, variable). Minimum peptide length and minimum number of razor+unique peptides were respectively set to seven amino acids and one. Maximum false discovery rates - calculated by employing a reverse database strategy - were set to 0.01 at peptide-spectrum match, protein and site levels. Peptides and proteins identified in the reverse and contaminant databases, and proteins only identified by site were discarded. Only class I phosphosites (localization probability ≥ 0.75) and phosphosites and proteins quantified in all replicates of at least one condition were further processed. After

log2 transformation, extracted corrected reporter abundance values were normalized by Variance Stabilizing Normalization (vsn) method in Prostar [70].

Phosphoproteomic data quality control (QC)

Output of Prostar was loaded into R software (version 4.2.1) (https://www.R-project.org/). Initial quality control was performed using PCA, unsupervised clustering (hierarchical clustering and k-means clustering), and sample cross-correlation. Function 'removeBatchEffects' of 'limma' package (version 3.54.2) [71] was used to correct for batch effects between treatments that were performed on two different days, and batch effects were denoted using design matrix in the downstream analysis. As sample BMP9-3 came as possible outlier during QC, 'lof' function of 'dbscan' package (version 1.1-11) [72] was used to measure local outlier factor (LOF). In addition to LOF, distance from the median in PCA space was used to determine that BMP9-3 is indeed the outlier (Fig. S1B). Same process was repeated for both technical replicates and for the proteomic data. QC was repeated to confirm that batch effects and outliers were successfully treated.

Differential phosphorylation analysis (DPA)

DPA was performed using 'limma' package [71]. Phosphoproteomic data consisted of two technical replicates, with 7565 phosphosites quantified in both technical replicates ("overlapping phosphosites" in further text) and 2326 (resp. 2888) phosphosites were quantified only in dataset from technical replicate 1 (resp. technical replicate 2). DPA was performed on each technical replicate individually, as well as on overlapping phosphosites ("combined analysis" in further text). Design matrix was used to denote batch effects, and in case of overlapping phosphosites, technical replicates. All P.values were corrected for multiple testing using Benjamini-Hochberg procedure, to obtain adjusted P.values (FDR). Log fold change values and P-adjusted values to be used in downstream analyses were selected such that:

1. For overlapping phosphosites, values were retrieved from the combined analysis;
2. For other phosphosites, values were retrieved from the analysis corresponding to dataset in which phisphosite was quantified.

Phosphosite is considered differentially expressed if FDR value was lower than 0.05, and absolute log fold change value was higher than 0.1. Threshold of 0.1 is selected such that 90% of the phosphosites, that have FDR value of 0.05, fall above this threshold.

For the proteomic data, differential expression analysis was performed using "limma" package [71]. Since batch effects were detected in proteomic data as well, design matrix was used to denote batch effects.

Gene Ontology (GO) overrepresentation analysis

GO over-representation analysis was performed using list of genes that encode for proteins that were differentially phosphorylated. Analysis was performed using the Metascape online tool (https://metascape.org/), accessed on 24th of August, 2023 [73], while using the Biological Processes part of GO. Using the online tool incorporated in Metascape, significantly enriched GO's were clustered based on semantic similarity. Additionally, clustering was manually annotated to improve understandability.

KinSwing analysis

KinSwing analysis was performed using the 'KinSwingR' package (version 1.16.0) [19]. As an input, KinSwing takes results of DPA (Fold change and P.value) as well as Position Weigh Matrices (PWM). PWM was built based on kinase-substrate interaction data, based on PhosphoSitePlus which is included in KinSwingR package, using the "buildPWM' function. Redundancies in data, caused my multiplicity, were removed by retaining ones that have higher Fold change and higher $-\log_{10}$(p.value). KinSwing analysis was performed on flanking sequence (SITE_+/-7_AA).

Gene set enrichment analysis (GSEA) based on PTMsigDB

GSEA was performed using the ClusterProfiler(version 4.6.2) [74] R package. PTMsigDB [23] was obtained from WebGestalt using the "WebGestaltR" (version 0.4.6, accessed on 24/08/2023) R package. GSEA sorting vector was built using the flanking sequence (SITE_+/-7_AA), and sorted based on log fold change obtained from DPA. Redundancies due to multiplicity were dealt with in same way as for KinSwing analysis (see above). GSEA exponent (weights) parameters was set to 0.75 (1 default) in order to flatten the log fold change values distribution.

Site-directed mutagenesis

Plasmids encoding ALK1 mutations were generated using PCR-based site-directed mutagenesis, whereby a pcDNA3-1(+) plasmid encoding the wild-type (WT) N-terminal HA-tagged ALK1 was modified using the QuikChange Lightning kit (Agilent) following the manufacturer's instructions. The mutated plasmids were subsequently subjected to full sequencing (Eurofins) to verify the presence and location of the mutations. Primer sequences utilized for mutagenesis are listed in supplementary table x.

Western Blotting

Following stimulations with BMP10, cells were washed twice with ice-cold phosphate-buffered saline (PBS) and lysed in a Tris-based lysis buffer supplemented with protease inhibitor cocktail (P8340) and phosphatase inhibitor cocktails 2 and 3. Equal protein quantities (10-20µg) were then resolved by SDS-polyacrylamide gel electrophoresis (SDS-PAGE) on 4–20% Precast Protein Gels (Bio-rad) and transferred onto a nitrocellulose membrane using Mini Trans-Blot system (Bio-rad). Membranes were blocked with instant block buffer (Sigma) and subsequently probed with indicated primary antibodies (table S4). Membranes were incubated with enhanced chemiluminescence substrates (ECL; Bio-rad) or SuperSignal™ West Femto Maximum Sensitivity Substrate (Thermo Scientific™ Catalog number: 34094) and images were developed using ChemiDoc™ Imaging System (Bio-Rad). Chemiluminescent signal intensity was quantified with the Image lab software V6.1 (Bio-Rad). All measurements were performed within the linear range and were normalized to the non-phosphorylated total protein or HSP90 loading control.

RNA extraction and RT-qPCR

Total RNA was extracted using the NucleoSpin RNA kit (Macherey-Nagel) following the manufacturer's instructions. 500ng of RNA was then reverse-transcribed into cDNA using the iScript cDNA Synthesis Kit (Bio-Rad). Reverse transcription quantitative PCR (RT-qPCR) was then performed using SsoAdvanced Universal SYBR Green Supermix (Bio-Rad) in a CFX96 Real-Time System (Bio-Rad). Data analysis was conducted utilizing the CFX Manager Software V3.1 (Bio-rad), then gene expression levels were calculated utilizing Livak's $2^{-\Delta\Delta Ct}$ method using HPRT as housekeeping gene, and results were presented as fold change relative to control unstimulated samples. All primer sequences used for RT-qPCR were pre-designed using primer blast tool and purchased from sigma. Table X summarizes all the genes assessed by RTqPCR with their respective primer mixes.

RNA interference

HUVECs were transfected with either a scrambled Silencer Negative Control #1 siRNA (siScr; AM4611, Ambion), pre-designed siRNA (Thermofisher) directed against human SMAD4 (siSMAD4; assay ID s8405) or human GADD45B (siGADD45B; assay ID s) at a final concentration of 10nM in 1ml of Opti-MEM (Gibco)

using 2.5µL/well Lipofectamine RNAiMAX Transfection Reagent (Invitrogen). 48h post-transfection, cells were serum starved in EBM2 for 6h and were then stimulated or not with 10ng/mL BMP10 for 30 mins.

Cell cycle analysis by Flow cytometry

HUVECs were synchronized by a 48h starvation in EBM2 containing 0.5% FBS. Next, cells were stimulated or not with BMP10 (10ng/ml) overnight in EBM2 supplemented with 0.5% or 5% FBS. For the analysis of cell cycle progression, actively proliferating cells were detected using Click-iT™ Plus EdU Alexa Fluor™ 647 (Invitrogen) according to the manufacturer's instructions with minor modifications. Thirty thousand cells were analyzed on the FACS Calibr () and data were analyzed using FCS Express Flow Cytometry Software version x.

BRE Luciferase assay

NIH-3T3 cells were transfected in Opti-MEM (Invitrogen) using lipofectamine 2000 (Invitrogen) with 75ng pGL3(BRE)2-luc, 30ng pRL-TKluc and 5ng of plasmids encoding either HA-tagged WT or generated mutants for ALK1. Five hours post transfection, cells were stimulated with or without recombinant human BMP10 (100 pg/mL) for 18 hours. Firefly and renilla luciferase activities were sequentially measured with twinlite Firefly and Renilla Luciferase Reporter Gene Assay System (Perkin Elmer) using the TECAN SPARK multimode microplate reader (Thermofisher). Final luciferase activities were reported as folds of firefly luciferase activities normalized to renilla luciferase activities.

Data and materials availability:

MS data have been deposited to the ProteomeXchange Consortium via the PRIDE partner repository [75] with the dataset identifier PXD044952.

Acknowledgments

The authors are indebted to Dr Hiroaki Sakurai (University of Toyama, Japan) and Dr Peter Hollenhorst (Indiana University School of Medicine, USA) for providing us with the phospho-EpS15-S^{796} and phospho-pERG-S^{215} antibody, respectively. We would also like to thank Dr C Cochet and Dr N Cherradi (U1292, Grenoble) as well as the group of Dr A Randi (Imperial College, London, UK) for their help in the discussion of this work. The authors would also like to thank Véronique Collin-Faure for her help in cytometry experiment and analysis. **The proteomic experiments were partially supported by Agence Nationale de la Recherche under projects ProFI (Proteomics French Infrastructure, ANR-10-INBS-08), and GRAL, a program from the Chemistry Biology Health (CBH) Graduate School of University Grenoble Alpes (ANR-17-EURE-0003) that also supported M Al Tarrass.** The flow cytometry facility was also supported by GRAL (ANR-10-LABX-49-01). This work was funded by the National Institute for Health and Medical Research (INSERM), the University of Grenoble-Alpes, by the CEA (commissariat à l'énergie atomique et aux énergies alternatives DRF/IRIG/DS), the Fondation pour la Recherche Médicale (EQU202003010188), the Association Maladie de Rendu-Osler (AMRO/HHT France), the association FAVA-multi, the H2020-msca-ITN-2018 (V.A. Cure-84316).

References

1. Katagiri, T., & Watabe, T. (2016). Bone Morphogenetic Proteins. *Cold Spring Harbor Perspectives in Biology*, *8*(6), a021899. https://doi.org/10.1101/cshperspect.a021899

2. Desroches-Castan, A., Tillet, E., Bouvard, C., & Bailly, S. (2022). BMP9 and BMP10: Two close vascular quiescence partners that stand out. *Developmental Dynamics*, *251*(1), 158–177. https://doi.org/10.1002/dvdy.395

3. Vorselaars, V. M. M., Hosman, A. E., Westermann, C. J. J., Snijder, R. J., Mager, J. J., Goumans, M.-J., & Post, M. C. (2018). Pulmonary Arterial Hypertension and Hereditary Haemorrhagic Telangiectasia. *International Journal of Molecular Sciences*, *19*(10), 10. https://doi.org/10.3390/ijms19103203

4. Tillet, E., & Bailly, S. (2014). Emerging roles of BMP9 and BMP10 in hereditary hemorrhagic telangiectasia. *Frontiers in Genetics*, *5*, 456. https://doi.org/10.3389/fgene.2014.00456

5. Robert, F., Desroches-Castan, A., Bailly, S., Dupuis-Girod, S., & Feige, J.-J. (2020). Future treatments for hereditary hemorrhagic telangiectasia. *Orphanet Journal of Rare Diseases*, *15*, 4. https://doi.org/10.1186/s13023-019-1281-4

6. Humbert, M., Sitbon, O., Guignabert, C., Savale, L., Boucly, A., Gallant-Dewavrin, M., McLaughlin, V., Hoeper, M. M., & Weatherald, J. (2023). Treatment of pulmonary arterial hypertension: Recent progress and a look to the future. *The Lancet. Respiratory Medicine*, S2213-2600(23)00264-3. https://doi.org/10.1016/S2213-2600(23)00264-3

7. Moustakas, A., & Heldin, C.-H. (2005). Non-Smad TGF-beta signals. *Journal of Cell Science*, *118*(Pt 16), 3573–3584. https://doi.org/10.1242/jcs.02554

8. Zhang, Y. E. (2017). Non-Smad Signaling Pathways of the TGF-β Family. *Cold Spring Harbor Perspectives in Biology*, *9*(2), a022129. https://doi.org/10.1101/cshperspect.a022129

9. Derynck, R., & Budi, E. H. (2019). Specificity, versatility, and control of TGF-β family signaling. *Science Signaling*, *12*(570), eaav5183. https://doi.org/10.1126/scisignal.aav5183

10. David, L., Mallet, C., Mazerbourg, S., Feige, J.-J., & Bailly, S. (2007). Identification of BMP9 and BMP10 as functional activators of the orphan activin receptor-like kinase 1 (ALK1) in endothelial cells. *Blood*, *109*(5), 1953–1961. https://doi.org/10.1182/blood-2006-07-034124

11. Thompson, A., Schäfer, J., Kuhn, K., Kienle, S., Schwarz, J., Schmidt, G., Neumann, T., Johnstone, R., Mohammed, A. K. A., & Hamon, C. (2003). Tandem mass tags: A novel quantification strategy for comparative analysis of complex protein mixtures by MS/MS. *Analytical Chemistry*, *75*(8), 1895–1904. https://doi.org/10.1021/ac0262560

12. Ham, B. M., Yang, F., Jayachandran, H., Jaitly, N., Monroe, M. E., Gritsenko, M. A., Livesay, E. A., Zhao, R., Purvine, S. O., Orton, D., Adkins, J., Camp, D. G., Rossie, S., & Smith, R. D. (2008). The

Influence of Sample Preparation and Replicate Analyses on HeLa Cell Phosphoproteome Coverage. *Journal of Proteome Research*, *7*(6), 2215–2221. https://doi.org/10.1021/pr700575m

13. Sharma, K., D'Souza, R. C. J., Tyanova, S., Schaab, C., Wiśniewski, J. R., Cox, J., & Mann, M. (2014). Ultradeep human phosphoproteome reveals a distinct regulatory nature of Tyr and Ser/Thr-based signaling. *Cell Reports*, *8*(5), 1583–1594. https://doi.org/10.1016/j.celrep.2014.07.036

14. Chen, Y. G., & Massagué, J. (1999). Smad1 recognition and activation by the ALK1 group of transforming growth factor-beta family receptors. *The Journal of Biological Chemistry*, *274*(6), 3672–3677. https://doi.org/10.1074/jbc.274.6.3672

15. Wrana, J. L., Attisano, L., Wieser, R., Ventura, F., & Massagué, J. (1994). Mechanism of activation of the TGF-β receptor. *Nature*, *370*(6488), 6488. https://doi.org/10.1038/370341a0

16. D'Souza, R. C. J., Knittle, A. M., Nagaraj, N., van Dinther, M., Choudhary, C., ten Dijke, P., Mann, M., & Sharma, K. (2014). Time-resolved dissection of early phosphoproteome and ensuing proteome changes in response to TGF-β. *Science Signaling*, *7*(335), rs5. https://doi.org/10.1126/scisignal.2004856

17. Ricard, N., Bidart, M., Mallet, C., Lesca, G., Giraud, S., Prudent, R., Feige, J.-J., & Bailly, S. (2010). Functional analysis of the BMP9 response of ALK1 mutants from HHT2 patients: A diagnostic tool for novel ACVRL1 mutations. *Blood*, *116*(9), 1604–1612. https://doi.org/10.1182/blood-2010-03-276881

18. Lamouille, S., Mallet, C., Feige, J.-J., & Bailly, S. (2002). Activin receptor–like kinase 1 is implicated in the maturation phase of angiogenesis. *Blood*, *100*(13), 4495–4501. https://doi.org/10.1182/blood.V100.13.4495

19. Engholm-Keller, K., Waardenberg, A. J., Müller, J. A., Wark, J. R., Fernando, R. N., Arthur, J. W., Robinson, P. J., Dietrich, D., Schoch, S., & Graham, M. E. (2019). The temporal profile of activity-dependent presynaptic phospho-signalling reveals long-lasting patterns of poststimulus regulation. *PLoS Biology*, *17*(3), e3000170. https://doi.org/10.1371/journal.pbio.3000170

20. García, M. A., Gil, J., Ventoso, I., Guerra, S., Domingo, E., Rivas, C., & Esteban, M. (2006). Impact of Protein Kinase PKR in Cell Biology: From Antiviral to Antiproliferative Action. *Microbiology and Molecular Biology Reviews*, *70*(4), 1032–1060. https://doi.org/10.1128/mmbr.00027-06

21. Fu, Y., & Rubin, C. S. (2011). Protein kinase D: Coupling extracellular stimuli to the regulation of cell physiology. *EMBO Reports*, *12*(8), 785–796. https://doi.org/10.1038/embor.2011.139

22. Chen, J., Wang, D., Wang, F., Shi, S., Chen, Y., Yang, B., Tang, Y., & Huang, C. (2017). Exendin-4 inhibits structural remodeling and improves Ca2+ homeostasis in rats with heart failure via the GLP-1 receptor through the eNOS/cGMP/PKG pathway. *Peptides*, *90*, 69–77. https://doi.org/10.1016/j.peptides.2017.02.008

23. Krug, K., Mertins, P., Zhang, B., Hornbeck, P., Raju, R., Ahmad, R., Szucs, M., Mundt, F., Forestier, D., Jane-Valbuena, J., Keshishian, H., Gillette, M. A., Tamayo, P., Mesirov, J. P., Jaffe, J. D., Carr,

S. A., & Mani, D. R. (2019). A Curated Resource for Phosphosite-specific Signature Analysis. *Molecular & Cellular Proteomics: MCP*, *18*(3), 576–593. https://doi.org/10.1074/mcp.TIR118.000943

24. van Bergen en Henegouwen, P. M. (2009). Eps15: A multifunctional adaptor protein regulating intracellular trafficking. *Cell Communication and Signaling*, *7*(1), 24. https://doi.org/10.1186/1478-811X-7-24

25. Zhou, Y., Tanaka, T., Sugiyama, N., Yokoyama, S., Kawasaki, Y., Sakuma, T., Ishihama, Y., Saiki, I., & Sakurai, H. (2014). p38-Mediated phosphorylation of Eps15 endocytic adaptor protein. *FEBS Letters*, *588*(1), 131–137. https://doi.org/10.1016/j.febslet.2013.11.020

26. Sanvitale, C. E., Kerr, G., Chaikuad, A., Ramel, M.-C., Mohedas, A. H., Reichert, S., Wang, Y., Triffitt, J. T., Cuny, G. D., Yu, P. B., Hill, C. S., & Bullock, A. N. (2013). A new class of small molecule inhibitor of BMP signaling. *PloS One*, *8*(4), e62721. https://doi.org/10.1371/journal.pone.0062721

27. Stokoe, D., Engel, K., Campbell, D. G., Cohen, P., & Gaestel, M. (1992). Identification of MAPKAP kinase 2 as a major enzyme responsible for the phosphorylation of the small mammalian heat shock proteins. *FEBS Letters*, *313*(3), 307–313. https://doi.org/10.1016/0014-5793(92)81216-9

28. Takekawa, M., Tatebayashi, K., Itoh, F., Adachi, M., Imai, K., & Saito, H. (2002). Smad-dependent GADD45beta expression mediates delayed activation of p38 MAP kinase by TGF-beta. *The EMBO Journal*, *21*(23), 6473–6482. https://doi.org/10.1093/emboj/cdf643

29. Miyake, Z., Takekawa, M., Ge, Q., & Saito, H. (2007). Activation of MTK1/MEKK4 by GADD45 through induced N-C dissociation and dimerization-mediated trans autophosphorylation of the MTK1 kinase domain. *Molecular and Cellular Biology*, *27*(7), 2765–2776. https://doi.org/10.1128/MCB.01435-06

30. Selvaraj, N., Kedage, V., & Hollenhorst, P. C. (2015). Comparison of MAPK specificity across the ETS transcription factor family identifies a high-affinity ERK interaction required for ERG function in prostate cells. *Cell Communication and Signaling: CCS*, *13*, 12. https://doi.org/10.1186/s12964-015-0089-7

31. Fish, J. E., Cantu Gutierrez, M., Dang, L. T., Khyzha, N., Chen, Z., Veitch, S., Cheng, H. S., Khor, M., Antounians, L., Njock, M.-S., Boudreau, E., Herman, A. M., Rhyner, A. M., Ruiz, O. E., Eisenhoffer, G. T., Medina-Rivera, A., Wilson, M. D., & Wythe, J. D. (2017). Dynamic regulation of VEGF-inducible genes by an ERK/ERG/p300 transcriptional network. *Development (Cambridge, England)*, *144*(13), 2428–2444. https://doi.org/10.1242/dev.146050

32. Rubin, S. M., Sage, J., & Skotheim, J. M. (2020). Integrating Old and New Paradigms of G1/S Control. *Molecular Cell*, *80*(2), 183–192. https://doi.org/10.1016/j.molcel.2020.08.020

33. Chuang, L.-C., Teixeira, L. K., Wohlschlegel, J. A., Henze, M., Yates, J. R., Méndez, J., & Reed, S. I. (2009). Phosphorylation of Mcm2 by Cdc7 promotes pre-replication complex assembly during

cell-cycle re-entry. *Molecular Cell*, *35*(2), 206–216. https://doi.org/10.1016/j.molcel.2009.06.014

34. Salmon, R. M., Guo, J., Wood, J. H., Tong, Z., Beech, J. S., Lawera, A., Yu, M., Grainger, D. J., Reckless, J., Morrell, N. W., & Li, W. (2020). Molecular basis of ALK1-mediated signalling by BMP9/BMP10 and their prodomain-bound forms. *Nature Communications*, *11*(1), 1621. https://doi.org/10.1038/s41467-020-15425-3

35. Miyazono, K., Kamiya, Y., & Morikawa, M. (2010). Bone morphogenetic protein receptors and signal transduction. *The Journal of Biochemistry*, *147*(1), 35–51. https://doi.org/10.1093/jb/mvp148

36. Roman, B. L., & Hinck, A. P. (2017). ALK1 signaling in development and disease: New paradigms. *Cellular and Molecular Life Sciences: CMLS*, *74*(24), 4539–4560. https://doi.org/10.1007/s00018-017-2636-4

37. Hornbeck, P. V., Kornhauser, J. M., Tkachev, S., Zhang, B., Skrzypek, E., Murray, B., Latham, V., & Sullivan, M. (2012). PhosphoSitePlus: A comprehensive resource for investigating the structure and function of experimentally determined post-translational modifications in man and mouse. *Nucleic Acids Research*, *40*(Database issue), D261–D270. https://doi.org/10.1093/nar/gkr1122

38. Souchelnytskyi, S., ten Dijke, P., Miyazono, K., & Heldin, C. H. (1996). Phosphorylation of Ser165 in TGF-beta type I receptor modulates TGF-beta1-induced cellular responses. *The EMBO Journal*, *15*(22), 6231–6240.

39. Saitoh, M., Nishitoh, H., Amagasa, T., Miyazono, K., Takagi, M., & Ichijo, H. (1996). Identification of important regions in the cytoplasmic juxtamembrane domain of type I receptor that separate signaling pathways of transforming growth factor-beta. *The Journal of Biological Chemistry*, *271*(5), 2769–2775. https://doi.org/10.1074/jbc.271.5.2769

40. van den Biggelaar, M., Hernández-Fernaud, J. R., van den Eshof, B. L., Neilson, L. J., Meijer, A. B., Mertens, K., & Zanivan, S. (2014). Quantitative phosphoproteomics unveils temporal dynamics of thrombin signaling in human endothelial cells. *Blood*, *123*(12), e22–e36. https://doi.org/10.1182/blood-2013-12-546036

41. Meta, E., Imhof, B. A., Ropraz, P., Fish, R. J., Brullo, C., Bruno, O., & Sidibé, A. (2017). The pyrazolyl-urea GeGe3 inhibits tumor angiogenesis and reveals dystrophia myotonica protein kinase (DMPK)1 as a novel angiogenesis target. *Oncotarget*, *8*(64), 108195–108212. https://doi.org/10.18632/oncotarget.22598

42. Yoo, J., Ghiassi, M., Jirmanova, L., Balliet, A. G., Hoffman, B., Fornace, A. J., Liebermann, D. A., Bottinger, E. P., & Roberts, A. B. (2003). Transforming growth factor-beta-induced apoptosis is mediated by Smad-dependent expression of GADD45b through p38 activation. *The Journal of Biological Chemistry*, *278*(44), 43001–43007. https://doi.org/10.1074/jbc.M307869200

43. Ijiri, K., Zerbini, L. F., Peng, H., Correa, R. G., Lu, B., Walsh, N., Zhao, Y., Taniguchi, N., Huang, X.-L., Otu, H., Wang, H., Wang, J. F., Komiya, S., Ducy, P., Rahman, M. U., Flavell, R. A., Gravallese, E. M., Oettgen, P., Libermann, T. A., & Goldring, M. B. (2005). A Novel Role for GADD45β as a

Mediator of MMP-13 Gene Expression during Chondrocyte Terminal Differentiation*. *Journal of Biological Chemistry*, *280*(46), 38544–38555. https://doi.org/10.1074/jbc.M504202200

44. Medina-Jover, F., Gendrau-Sanclemente, N., & Viñals, F. (2020). SGK1 is a signalling hub that controls protein synthesis and proliferation in endothelial cells. *FEBS Letters*, *594*(19), 3200–3215. https://doi.org/10.1002/1873-3468.13901

45. Araki, M., Hisamitsu, T., Kinugasa-Katayama, Y., Tanaka, T., Harada, Y., Nakao, S., Hanada, S., Ishii, S., Fujita, M., Kawamura, T., Saito, Y., Nishiyama, K., Watanabe, Y., & Nakagawa, O. (2018). Serum/glucocorticoid-regulated kinase 1 as a novel transcriptional target of bone morphogenetic protein-ALK1 receptor signaling in vascular endothelial cells. *Angiogenesis*, *21*(2), 415–423. https://doi.org/10.1007/s10456-018-9605-x

46. Alsina-Sanchís, E., García-Ibáñez, Y., Figueiredo, A. M., Riera-Domingo, C., Figueras, A., Matias-Guiu, X., Casanovas, O., Botella, L. M., Pujana, M. A., Riera-Mestre, A., Graupera, M., & Viñals, F. (2018). ALK1 Loss Results in Vascular Hyperplasia in Mice and Humans Through PI3K Activation. *Arteriosclerosis, Thrombosis, and Vascular Biology*, *38*(5), 1216–1229. https://doi.org/10.1161/ATVBAHA.118.310760

47. Heide, L. P. van der, Dinther, M. van, Moustakas, A., & Dijke, P. ten. (2011). TGFβ Activates Mitogen- and Stress-activated Protein Kinase-1 (MSK1) to Attenuate Cell Death *. *Journal of Biological Chemistry*, *286*(7), 5003–5011. https://doi.org/10.1074/jbc.M110.167379

48. Enshoji, M., Miyano, Y., Yoshida, N., Nagano, M., Watanabe, M., Kunihiro, M., Siekhaus, D. E., Toshima, J. Y., & Toshima, J. (2022). Eps15/Pan1p is a master regulator of the late stages of the endocytic pathway. *Journal of Cell Biology*, *221*(10), e202112138. https://doi.org/10.1083/jcb.202112138

49. Milesi, C., Alberici, P., Pozzi, B., Oldani, A., Beznoussenko, G. V., Raimondi, A., Soppo, B. E., Amodio, S., Caldieri, G., Malabarba, M. G., Bertalot, G., Confalonieri, S., Parazzoli, D., Mironov, A. A., Tacchetti, C., Di Fiore, P. P., Sigismund, S., & Offenhäuser, N. (2019). Redundant and nonredundant organismal functions of EPS15 and EPS15L1. *Life Science Alliance*, *2*(1), e201800273. https://doi.org/10.26508/lsa.201800273

50. Hartung, A., Bitton-Worms, K., Rechtman, M. M., Wenzel, V., Boergermann, J. H., Hassel, S., Henis, Y. I., & Knaus, P. (2006). Different Routes of Bone Morphogenic Protein (BMP) Receptor Endocytosis Influence BMP Signaling. *Molecular and Cellular Biology*, *26*(20), 7791–7805. https://doi.org/10.1128/MCB.00022-06

51. Callery, E. M., Park, C. Y., Xu, X., Zhu, H., Smith, J. C., & Thomsen, G. H. (2012). Eps15R is required for bone morphogenetic protein signalling and differentially compartmentalizes with Smad proteins. *Open Biology*, *2*(4), 120060. https://doi.org/10.1098/rsob.120060

52. Kostenko, S., & Moens, U. (2009). Heat shock protein 27 phosphorylation: Kinases, phosphatases, functions and pathology. *Cellular and Molecular Life Sciences*, *66*(20), 3289–3307. https://doi.org/10.1007/s00018-009-0086-3

53. Arrigo, A.-P. (2017). Mammalian HspB1 (Hsp27) is a molecular sensor linked to the physiology and environment of the cell. *Cell Stress and Chaperones*, *22*(4), 517–529. https://doi.org/10.1007/s12192-017-0765-1

54. Choi, S.-K., Kam, H., Kim, K.-Y., Park, S. I., & Lee, Y.-S. (2019). Targeting Heat Shock Protein 27 in Cancer: A Druggable Target for Cancer Treatment? *Cancers*, *11*(8), 1195. https://doi.org/10.3390/cancers11081195

55. Rogalla, T., Ehrnsperger, M., Preville, X., Kotlyarov, A., Lutsch, G., Ducasse, C., Paul, C., Wieske, M., Arrigo, A. P., Buchner, J., & Gaestel, M. (1999). Regulation of Hsp27 oligomerization, chaperone function, and protective activity against oxidative stress/tumor necrosis factor alpha by phosphorylation. *The Journal of Biological Chemistry*, *274*(27), 18947–18956. https://doi.org/10.1074/jbc.274.27.18947

56. Salinthone, S., Tyagi, M., & Gerthoffer, W. T. (2008). Small heat shock proteins in smooth muscle. *Pharmacology & Therapeutics*, *119*(1), 44–54. https://doi.org/10.1016/j.pharmthera.2008.04.005

57. Hirano, S., Rees, R. S., Yancy, S. L., Welsh, M. J., Remick, D. G., Yamada, T., Hata, J., & Gilmont, R. R. (2004). Endothelial barrier dysfunction caused by LPS correlates with phosphorylation of HSP27in vivo. *Cell Biology and Toxicology*, *20*(1), 1–14. https://doi.org/10.1023/B:CBTO.0000021019.50889.aa

58. Chang, E., Heo, K.-S., Woo, C.-H., Lee, H., Le, N.-T., Thomas, T. N., Fujiwara, K., & Abe, J. (2011). MK2 SUMOylation regulates actin filament remodeling and subsequent migration in endothelial cells by inhibiting MK2 kinase and HSP27 phosphorylation. *Blood*, *117*(8), 2527–2537. https://doi.org/10.1182/blood-2010-08-302281

59. Shi, Y., Jiang, X., Zhang, L., Pu, H., Hu, X., Zhang, W., Cai, W., Gao, Y., Leak, R. K., Keep, R. F., Bennett, M. V. L., & Chen, J. (2017). Endothelium-targeted overexpression of heat shock protein 27 ameliorates blood-brain barrier disruption after ischemic brain injury. *Proceedings of the National Academy of Sciences of the United States of America*, *114*(7), E1243–E1252. https://doi.org/10.1073/pnas.1621174114

60. Rada, C. C., Mejia-Pena, H., Grimsey, N. J., Canto Cordova, I., Olson, J., Wozniak, J. M., Gonzalez, D. J., Nizet, V., & Trejo, J. (2021). Heat shock protein 27 activity is linked to endothelial barrier recovery after proinflammatory GPCR-induced disruption. *Science Signaling*, *14*(698), eabc1044. https://doi.org/10.1126/scisignal.abc1044

61. Benn, A., Hiepen, C., Osterland, M., Schütte, C., Zwijsen, A., & Knaus, P. (2017). Role of bone morphogenetic proteins in sprouting angiogenesis: Differential BMP receptor-dependent signaling pathways balance stalk vs. tip cell competence. *FASEB Journal: Official Publication of the Federation of American Societies for Experimental Biology*, *31*(11), 4720–4733. https://doi.org/10.1096/fj.201700193RR

62. Foletta, V. C., Lim, M. A., Soosairajah, J., Kelly, A. P., Stanley, E. G., Shannon, M., He, W., Das, S., Massagué, J., & Bernard, O. (2003). Direct signaling by the BMP type II receptor via the

cytoskeletal regulator LIMK1. *Journal of Cell Biology*, *162*(6), 1089–1098. https://doi.org/10.1083/jcb.200212060

63. Kobayashi, M., Nishita, M., Mishima, T., Ohashi, K., & Mizuno, K. (2006). MAPKAPK-2-mediated LIM-kinase activation is critical for VEGF-induced actin remodeling and cell migration. *The EMBO Journal*, *25*(4), 713–726. https://doi.org/10.1038/sj.emboj.7600973

64. Park, H., Furtado, J., Poulet, M., Chung, M., Yun, S., Lee, S., Sessa, W. C., Franco, C. A., Schwartz, M. A., & Eichmann, A. (2021). Defective Flow-Migration Coupling Causes Arteriovenous Malformations in Hereditary Hemorrhagic Telangiectasia. *Circulation*, *144*(10), 805–822. https://doi.org/10.1161/CIRCULATIONAHA.120.053047

65. Dufton, N. P., Peghaire, C. R., Osuna-Almagro, L., Raimondi, C., Kalna, V., Chauhan, A., Webb, G., Yang, Y., Birdsey, G. M., Lalor, P., Mason, J. C., Adams, D. H., & Randi, A. M. (2017). Dynamic regulation of canonical TGFβ signalling by endothelial transcription factor ERG protects from liver fibrogenesis. *Nature Communications*, *8*(1), 1. https://doi.org/10.1038/s41467-017-01169-0

66. Rostama, B., Turner, J. E., Seavey, G. T., Norton, C. R., Gridley, T., Vary, C. P. H., & Liaw, L. (2015). DLL4/Notch1 and BMP9 interdependent signaling induces human endothelial cell quiescence via P27KIP1 and thrombospondin-1. *Arteriosclerosis, Thrombosis, and Vascular Biology*, *35*(12), 2626–2637. https://doi.org/10.1161/ATVBAHA.115.306541

67. Banerjee, K., Lin, Y., Gahn, J., Cordero, J., Gupta, P., Mohamed, I., Graupera, M., Dobreva, G., Schwartz, M. A., & Ola, R. (2023). SMAD4 maintains the fluid shear stress set point to protect against arterial-venous malformations. *The Journal of Clinical Investigation*, e168352. https://doi.org/10.1172/JCI168352

68. Sonntag, E., Milbradt, J., Svrlanska, A., Strojan, H., Häge, S., Kraut, A., Hesse, A.-M., Amin, B., Sonnewald, U., Couté, Y., & Marschall, M. (2017). Protein kinases responsible for the phosphorylation of the nuclear egress core complex of human cytomegalovirus. *The Journal of General Virology*, *98*(10), 2569–2581. https://doi.org/10.1099/jgv.0.000931

69. Tyanova, S., Temu, T., & Cox, J. (2016). The MaxQuant computational platform for mass spectrometry-based shotgun proteomics. *Nature Protocols*, *11*(12), 2301–2319. https://doi.org/10.1038/nprot.2016.136

70. Wieczorek, S., Combes, F., Lazar, C., Giai Gianetto, Q., Gatto, L., Dorffer, A., Hesse, A.-M., Couté, Y., Ferro, M., Bruley, C., & Burger, T. (2017). DAPAR & ProStaR: Software to perform statistical analyses in quantitative discovery proteomics. *Bioinformatics (Oxford, England)*, *33*(1), 135–136. https://doi.org/10.1093/bioinformatics/btw580

71. Ritchie, M. E., Phipson, B., Wu, D., Hu, Y., Law, C. W., Shi, W., & Smyth, G. K. (2015). limma powers differential expression analyses for RNA-sequencing and microarray studies. *Nucleic Acids Research*, *43*(7), e47. https://doi.org/10.1093/nar/gkv007

72. Hahsler, M., Piekenbrock, M., & Doran, D. (2019). dbscan: Fast Density-Based Clustering with R. *Journal of Statistical Software*, *91*, 1–30. https://doi.org/10.18637/jss.v091.i01

73. Zhou, Y., Zhou, B., Pache, L., Chang, M., Khodabakhshi, A. H., Tanaseichuk, O., Benner, C., & Chanda, S. K. (2019). Metascape provides a biologist-oriented resource for the analysis of systems-level datasets. *Nature Communications*, *10*(1), 1523. https://doi.org/10.1038/s41467-019-09234-6

74. Wu, T., Hu, E., Xu, S., Chen, M., Guo, P., Dai, Z., Feng, T., Zhou, L., Tang, W., Zhan, L., Fu, X., Liu, S., Bo, X., & Yu, G. (2021). clusterProfiler 4.0: A universal enrichment tool for interpreting omics data. *Innovation (Cambridge (Mass.))*, *2*(3), 100141. https://doi.org/10.1016/j.xinn.2021.100141

75. Perez-Riverol, Y., Bai, J., Bandla, C., García-Seisdedos, D., Hewapathirana, S., Kamatchinathan, S., Kundu, D. J., Prakash, A., Frericks-Zipper, A., Eisenacher, M., Walzer, M., Wang, S., Brazma, A., & Vizcaíno, J. A. (2022). The PRIDE database resources in 2022: A hub for mass spectrometry-based proteomics evidences. *Nucleic Acids Research*, *50*(D1), D543–D552. https://doi.org/10.1093/nar/gkab1038

Supplementary Table 4. Primary antibodies.

List of primary antibodies used for western blotting and immunoprecipitation

Antibody	Supplier|Reference	Dilution	Incubation conditions
pSMAD1/5 $^{S463/465}$	Cell Signaling|9516	1/1000	O.N at 4°C
pP38$^{T180/Y182}$	Cell Signaling|4511	1/1000	O.N at 4°C
P38	Cell Signaling|9212	1/1000	O.N at 4°C
pEps15 ^{S796}	Dr. Hiroaki Sakurai [25]	1/1000	O.N at 4°C
Eps15	Santa Cruz|sc-390259	1/500	O.N at 4°C
pHSP27 S78/82	R&D Systems|AF2314	1/1000	O.N at 4°C
HSP27	Cell Signaling|95357	1/1000	O.N at 4°C
ID1	Santa Cruz|sc-133104	1/500	O.N at 4°C
HSP90	Cell Signaling|4877	1/1000	1h RT
SMAD4	Cell Signaling|9515	1/1000	O.N at 4°C
ERG	Cell Signaling|97249	WB: 1/1000 IP: 0.2µg/750µg lysate in 500µl	O.N at 4°C
pERG ^{S215}	Dr. Peter Hollenhorst [30]	1/1000	O.N at 4°C
Phosphoserine (pSer)	Sigma|P5747	1/500	O.N at 4°C

Supplementary Table 5. RT-qPCR primers.

List of forward and reverse primers used for quantitative RT-qPCR designed using Primer-Blast on GenBank sequences. All listed primer pairs are separated by at least one intron on the corresponding genomic DNA or span an exon-exon junction.

Target Gene	GenBank sequence accession number	Forward (5'-3')	Reverse (5'-3')
ID1	NM_181353.3	CTGCTCTACGACATGAACGGC	TGACGTGCTGGAGAATCTCCA
SMAD6	NM_005585.5	CCTACTCTCGGCTGTCTCCT	GAATTCACCCGGAGCAGTGA
PTGS2	NM_000963.4	TAGGAATGTTCCACCCGCAGTACAG	CAGCATCGATGTCACCATAGAGTGC
HAS2	NM_005328.3	TGTGGATTATGTACAGGTTTGGTGA	GACATCTCCCCCAACACCTC
SELE	NM_000450.2	CCTGCAGTGGCCACGGTGAAT	CCAGGCTTCCATGCTCAGGGG
GADD45β	NM_015675.4	GACATCAACATCGTGCGGGT	GTCCGTGTGAGGGTTCGTG
CCND1	NM_053056.3	CCAAAATGCCAGAGGCGGA	AGGGCGGATTGGAAATGAAC
CCNA1	NM_001413923.1	CAGATTTCGTCTTCCAGCAGCAG	ACTCCACTCTTGGGGTTGCT
E2F2	NM_004091.4	CGCATCTATGACATCACCAACG	AAACATTCCCCTGCCTACCCAC

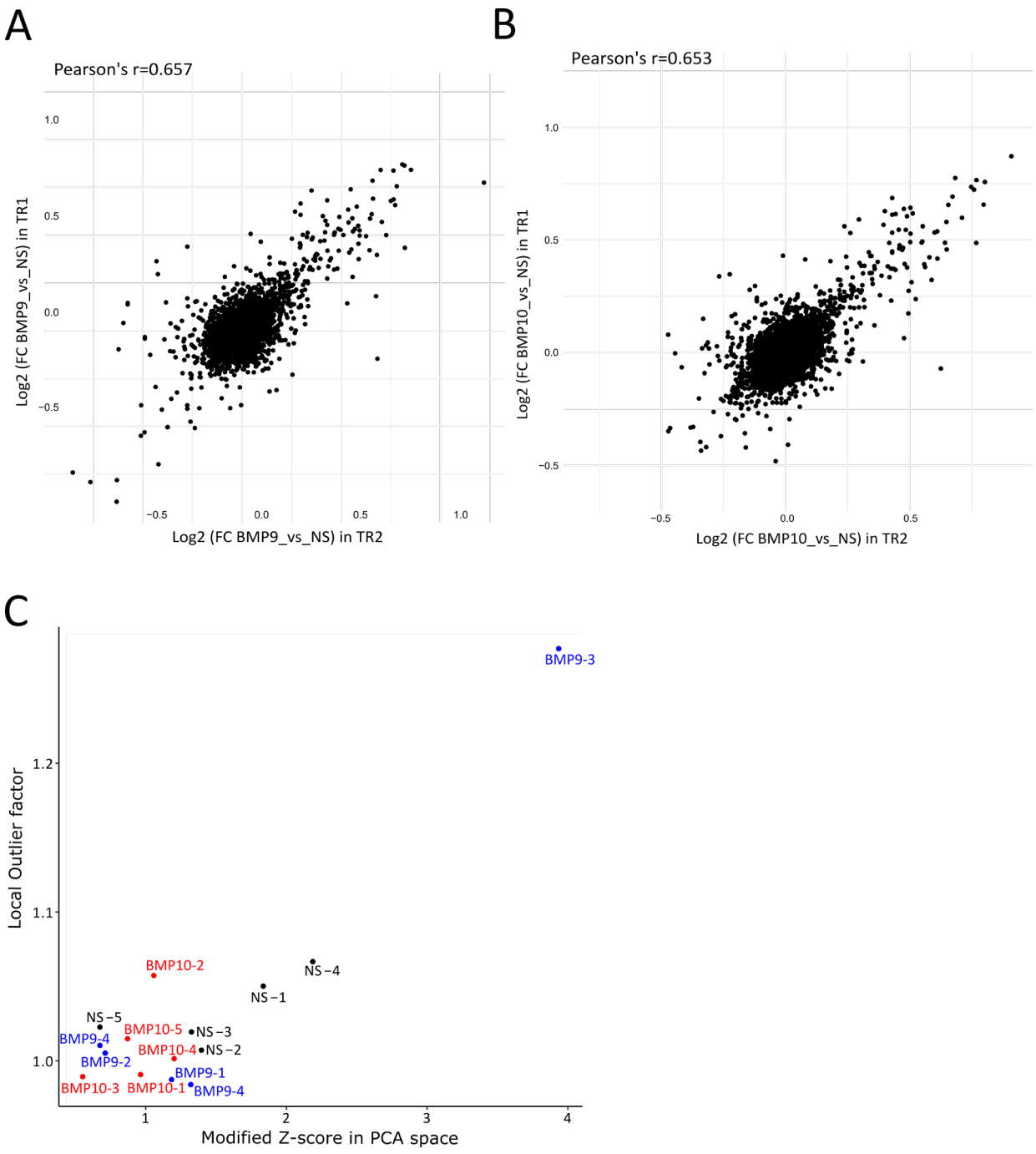

Fig. S1. Combining Technical Replicates 1 and 2 and Identifying BMP9-3 as an Outlier:
Scatter plot comparing log2 fold change values of phosphosites between Technical replicate 1 (y-axis) and technical replicate 2 (x-axis), for samples treated by by **(A)** BMP9 and **(B)** BMP10. Pearson's correlation coefficient (r) is reported. **(C)** Identification of sample BMP9-3 as an outlier by measuring local outlier factor (LOF) (y-axis) and modified Z-score (x-axis).

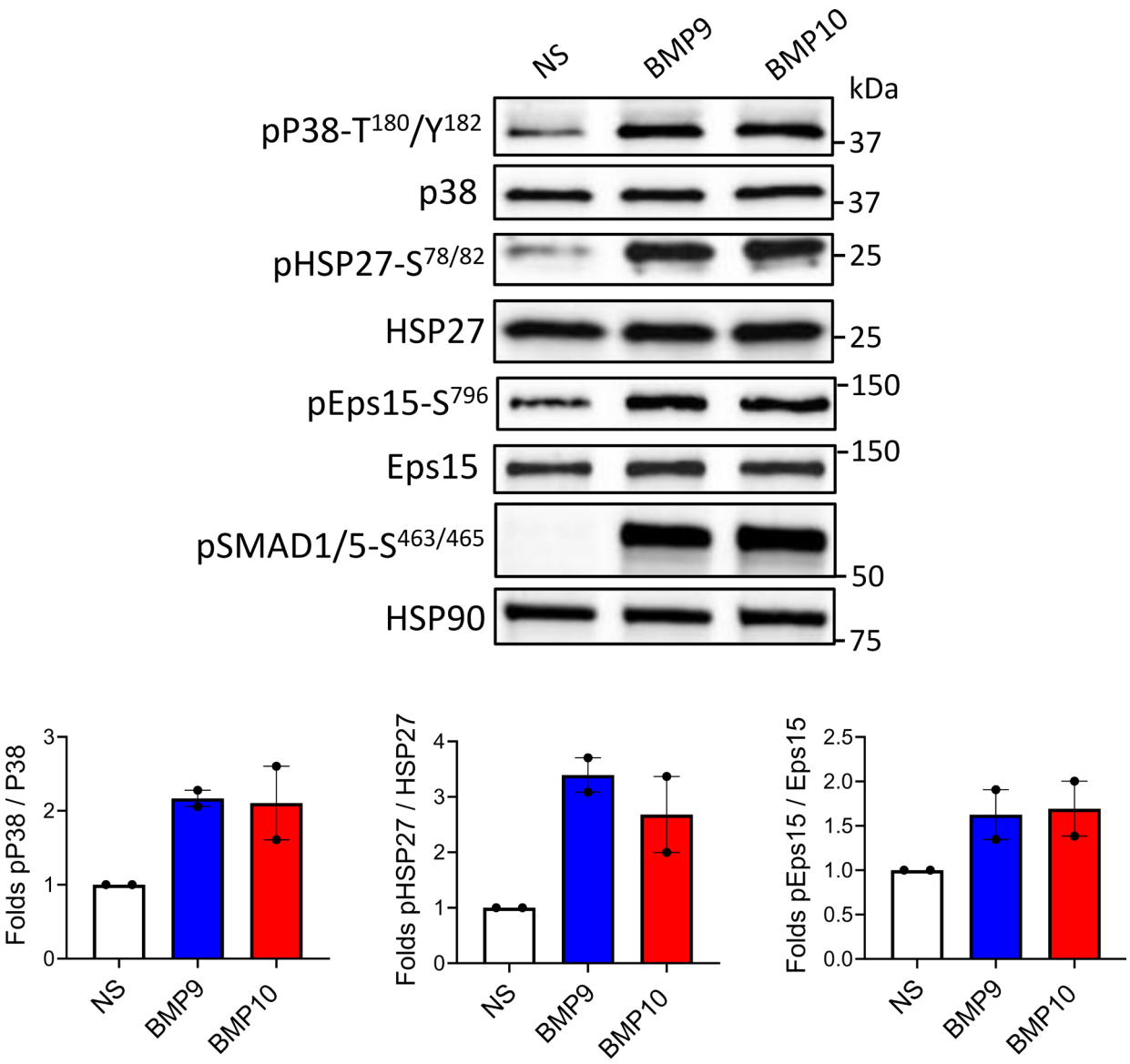

Fig. S2. BMP9 and BMP10 induce P38, HSP27 and Eps15 phosphorylations in HUVECs

HUVECs were stimulated with 10 ng/mL BMP9 or BMP10 for 30 min. Cell extracts were subjected to western blotting (WB) analysis using antibodies against phosphorylated (p) P38-T^{180}/Y^{182}, P38, pHSP27-$S^{78/82}$, HSP27, pEps15-S^{796}, Eps15, pSMAD1/5-$S^{463/465}$ and HSP90 (loading control). Quantification of phosphorylation for P38, HSP27 and Eps15 was normalized to their respective total protein content. Data are presented as mean fold change (BMP9-vs-NS or BMP10-vs-NS) ± SEM of n=2 independent experiments.

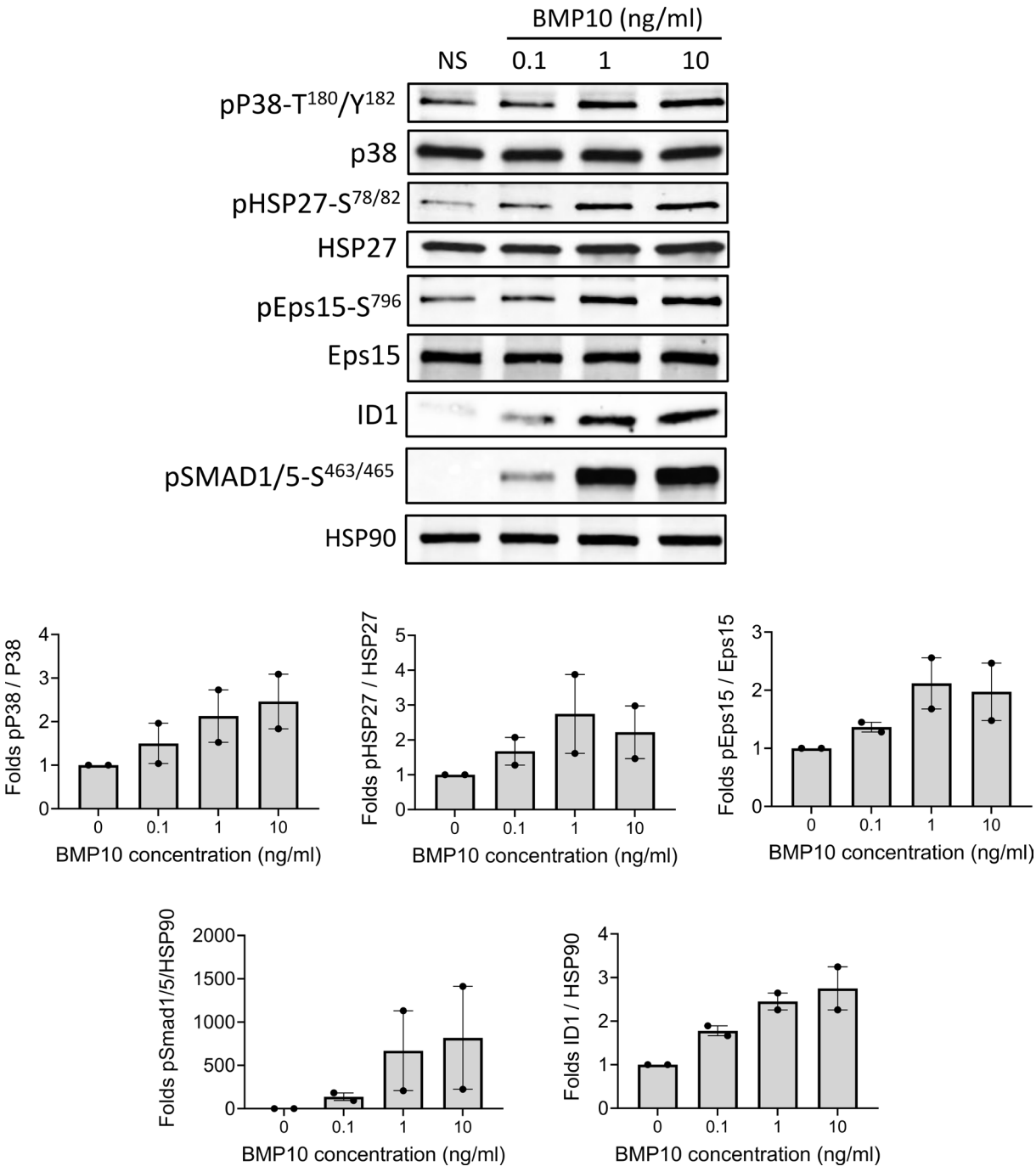

Fig. S3. BMP10 induces P38, HSP27 and Eps15 phosphorylations in a dose-dependent manner in HUVECs

HUVECs were stimulated with different doses of BMP10 (0.1, 1 or 10 ng/mL) for 30 min. Cell extracts were subjected to western blotting (WB) analysis using antibodies against phosphorylated (p) P38T^{180}/Y^{182}, P38, pHSP27-S$^{78/82}$, HSP27, pEps15-S^{796}, Eps15, pSMAD1/5-S$^{463/465}$, ID1 and HSP90 (loading control). Quantification of phosphorylation for P38, HSP27 and Eps15 was normalized to their respective total protein content, except for pSMAD1/5 and ID1, which were normalized to HSP90. Data are presented as mean fold change (BMP10-vs-NS) ± SEM of n=2 independent experiments.

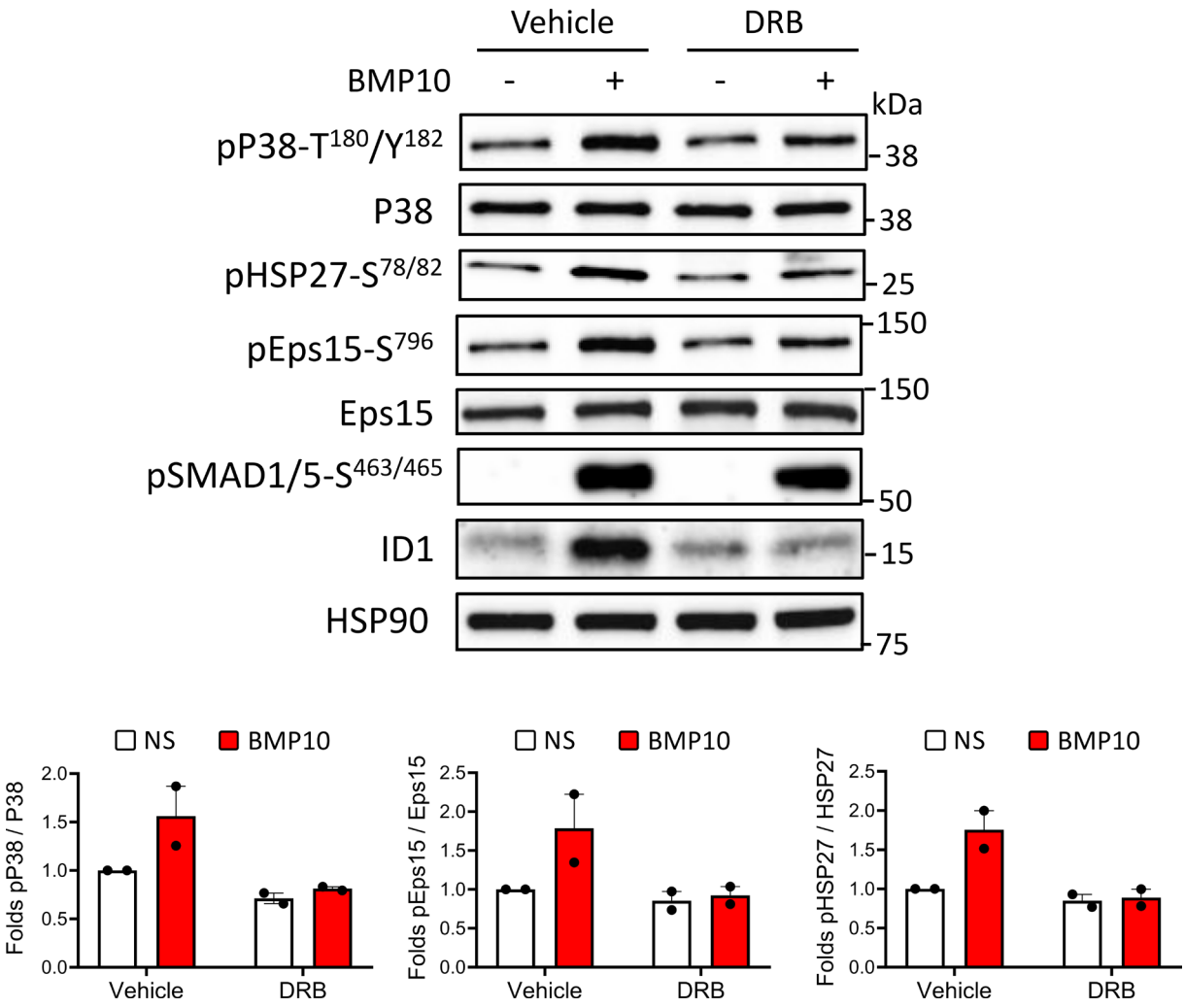

Fig. S4. BMP10 induced P38, HSP27 and Eps15 phosphorylations are inhibited by DRB transcription inhibitor

HUVECs were pre-treated either with vehicle or the transcription inhibitor DRB (5,6-Dichlorobenzimidazole 1-β-D-ribofuranoside) (100 µM) for 30 min, then stimulated with 10ng/mL BMP10 for another 30 min. Cell extracts were subjected to western blotting (WB) analysis using antibodies against phosphorylated (p) P38T^{180}/Y^{182}, P38, pHSP27-S$^{78/82}$, HSP27, pEps15-S^{796}, Eps15, pSMAD1/5-S$^{463/465}$, ID1 and HSP90 (loading control). Quantification of phosphorylation for P38, HSP27 and Eps15 was normalized to their respective total protein content. Data are presented as mean fold change (BMP10-vs-NS) ± SEM of n=2 independent experiments.

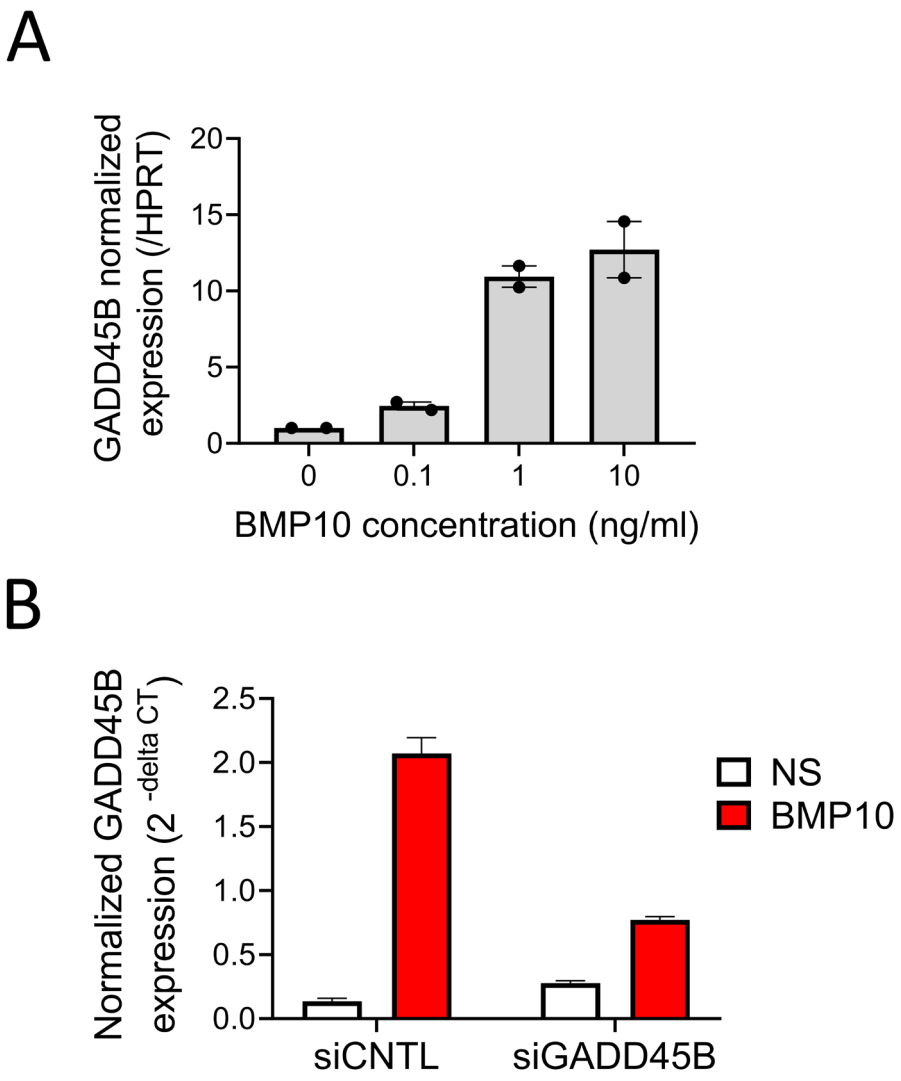

Fig. S5. BMP10 induces GADD45ß mRNA expression in HUVECs that is inhibited by siGADD45β

(**A**) HUVECs were stimulated with different doses of BMP10 (0.1, 1 or 10 ng/mL) for 30 min. RT-qPCR analysis was then performed to determine mRNA expression of GADD45β. Target gene expression was normalized to *HPRT* mRNA level using $2^{-\Delta\Delta Ct}$ method and presented as fold induction (BMP10-vs-vehicle) ± SEM of n=2 independent experiments. (**B**) HUVECs were treated either with scrambled siRNA (siCTL) or siRNA against *GADD45B* (si*GADD45B*) for 48 h, followed by stimulation with 10ng/mL BMP10 for 30 min. RT-qPCR analysis was then performed to determine mRNA expression of GADD45β. Target gene expression was normalized to *HPRT* mRNA level using $2^{-\Delta\Delta Ct}$.

5.4 Discussion of the Main Findings of the Phosphoproteomic Study

5.4.1 BMP9 *vs* BMP10 phosphoproteomic profiles

Our MS Phosphoproteomic analyses revealed highly similar phosphoproteomic profiles for BMP9 and BMP10. Despite not exhibiting a complete overlap in DPSs, we observed that the LFCs associated with DPSs regulated by each ligand were highly correlated, with Pearson's correlation coefficient of 0.96 (manuscript 1, Fig. 2C). This correlation analysis highlighted few DPSs which looked different between the two ligands. These were RNA-binding protein 12 (RBM12)-S^{413}, scaffold attachment factor B1 (SAFB1)-S^{589}, and Cyclin dependent kinase inhibitor 2A interacting Protein CDKN2AIP-S^{268}. However, none of these sites were previously described or had any antibodies so that we could validate. Nevertheless, this shows that the distinct DPSs identified for each ligand share similar regulatory patterns by both ligands, but they failed to reach the LFC or statistical threshold with one of the two ligands. These results strongly suggests that both BMP9 and BMP10 act as equivalent ligands of ALK1 *in-vitro* in ECs. This is in accordance with conclusions derived from transcriptomic studies that revealed highly similar responses of ECs to both ligands [325], as well as with recent unpublished work conducted in our team (Al Tabosh et al., under revision-Annex 1).

5.4.2 Differential Phosphorylation of ALK1 by BMP9 and BMP10

Binding of BMP9 and BMP10 to their high-affinity receptor ALK1 is thought to trigger the phosphorylation of its GS domain by the type-II receptor and subsequent initiation of signal transduction [334, 345]. However, in reference to phosphositeplus database [570], the precise phosphorylation sites within the GS domain of ALK1 in response to these ligands have never been characterized. Our MS analysis showed that both BMP9 and BMP10 induced differential phosphorylation of ALK1 at 2 sites, S155 and S161. These sites are located in the juxtamembrane domain, directly upstream to the GS domain. We did not detect any phosphorylation sites within the GS domain itself. However, this observation aligns with phosphositplus database [570] as well as a previous phosphoproteomic profiling study of TGFβ, where phosphosites within the GS domain of ALK5 have never been identified using any large-scale MS analysis [565]. The challenge in this latter has been attributed to the prediction that tryptic digestion of type-I receptors results in a large hydrophobic peptide (bearing the GS domain) that is difficult to detect by MS [565]. Phosphosites within the GS domain of ALK5, a well-studied member of type-I receptor family, were characterized back in 1994-1995 [84, 105]. Back then, the authors highlighted the crucial serine and threonine sites within the GS domain, which, upon phosphorylation by the type-II receptor, results in the activation of ALK5. Moreover, they showed that mutation of two or more of these residues impairs TGFβ/ALK5 downstream signaling. In 1996, two studies identified phosphorylation of S165, S172 and T176, within the juxtamembrane domain of ALK5, positioned directly upstream the GS domain [571, 572]. Mutations in S165 led to enhanced TGF-β1-mediated growth inhibition and extracellular matrix formation, while decreased TGF-β1-induced apoptosis, without affecting

transcriptional luciferase activity [571]. Saitoh et al demonstrated that S172A and T176V mutations in ALK5 exhibited impaired capacity of TGF-β1-mediated growth inhibition but not extracellular matrix protein production [572]. These are the only two studies which highlighted that ALK5 phosphorylation in the juxtamembrane region upstream of the GS domain plays an important role in some TGFβ-triggered functional outcomes. While both studies suggest that these sites seem to play distinct role from activating the canonical signaling by TGFβ, their conclusions on their functional roles on proliferation were contradictory. Interestingly, our study highlighted a parallel pattern with ALK1 where BMP9/BMP10 induced phosphorylation of S155 and S161. Mutation of these sites were dispensable for BMP10-iduced BRE luciferase activity, as previously demonstrated for ALK5 [571]. These results supports that these sites do not alter the canonical SMAD pathway, but might contribute to other BMP9 and BMP10 functional outcomes, as previously described for TGFβ/ALK5 [571, 572]. However, exact functions of juxtamembrane domain phosphosites in response to TGFβ or BMPs remains poorly understood.

5.4.3 BMP9/10-induced phosphorylation of P38, Eps15 and HSP27 and their Potential Roles of in ECs

As previously mentioned, our analysis highlighted strong activation of P38 MAPK signaling by BMP9 and BMP10 through phosphorylation of several proteins which have been well described in this pathway. These include P38, Eps15, MSK2, MEKK4, and HSP27. Moreover, bioinformatics analysis highlighted strong enrichment of MK2, downstream kinase of P38. Among these, we validated the phosphorylation of P38-Y^{182}, Eps15-S^{796}, and HSP27-$S^{78/82}$. Eps15-S^{796} has been shown to be phosphorylated by P38 [573], while HSP27 has shown to be a well characterized substrate downstream of MK2 [204].

5.4.3.1 P38 MAPK Pathway Activation

Our findings using different experimental approaches suggests the following model for BMP10 (and likely BMP9)-induced activation of P38 MAPK signaling in ECs (manuscript 1, Fig. 8). BMP10 initiates it's signaling by activating ALK1 receptor, which leads to the phosphorylation of SMAD1 and subsequent formation of an active SMAD1/SMAD4 complex. This complex then translocates into the nucleus to regulate the expression of downstream target genes, including the newly identified target GADD45β, an activator of MEKK4. Subsequently, GADD45β activates MEKK4, which further results in the activation of MKK3/6, eventually leading to the activation of P38 MAPK. P38 phosphorylates several downstream targets including Eps15 and MK2, where MK2 in turn phosphorylates HSP27. Noteworthy, this mechanism has been previously demonstrated for TGFβ in non-ECs about two decades ago [174]. To our knowledge, GADD45β has been mainly studied in response to TGFβ, but it was also described once that BMP2 rapidly induced by GADD45β expression in chondrocytes [574].

The initial discovery of MEKK4 activation by GADD45β was established by Saito et al [173, 575]. They illustrated that the binding of GADD45β to the N-terminus of MEKK4 leads to

structural modifications, facilitating its interaction with and phosphorylation of downstream MAPK components, including MKK6 [173]. Further mechanistic investigations revealed that GADD45β binding of MEKK4 stimulates its dimerization, followed by MEKK4-T^{1494} (=T^{1483} in mouse) auto-phosphorylation within the kinase activation loop and subsequent activation [576, 577]. We demonstrated that BMP10 increased the expression of GADD45β. Moreover, phosphoproteomic analysis identified differential phosphorylation of MEKK4-S^{1252} by BMP9 and BMP10. Despite the fact that the role of this site has never been characterized, it will be interesting to examine whether this phosphorylation is GADD45β-dependent, and whether it plays a role in MEKK4 activation and downstream signaling.

Moreover, our results also highlighted differential phosphorylation of MSK2-T^{687}, another kinase downstream of P38, but we were not able to validate this phosphorylation due to the poor quality of the antibody (data not shown). Notably, it has been shown that TGFβ-induced P38-MSK1 activation was GADD45β dependent [578], suggesting that GADD45β may also play a role in BMP9/10-induced MSK2 phosphorylation.

Two previous studies have highlighted a role of P38 and TAK1 in BMP9-induced expression of endothelin-1 (ET-1) in HPAECs [360] and HMVECs [349]. They demonstrated that this ET-1 induction takes place following 16 h of BMP9 stimulation (HPAECs) or 8 hours (HMVECs), with BMP9 concentrations used ranging from 1 to 2.5 ng/mL. However, they did not explain the underlying mechanism of this regulation. In our study, we have demonstrated several key mechanistic steps for the activation of P38 signaling by BMP10 in ECs. We also showed that BMP10-induced activation P38 plays important roles in the regulation of a subset of BMP10 target genes (*SELE*, *PTGS2*, and *HAS2*), further supporting a role of P38 in the transcriptional events downstream of BMP10 signaling. Therefore, it would be interesting to study the transcriptional and subsequent functional roles of BMP10-induced activation of P38 MAPK signaling in ECs.

5.4.3.2 Epidermal growth factor receptor substrate 15 (Eps15)

Eps15-S^{796} has been shown to be phosphorylated in response to various stimuli including TNFα, EGF, IL-1β, and was shown to be mediated through TAK1 and P38 kinases [573], which was further confirmed for BMP10 in our study. Interestingly, this site has never been described for any member of TGF-β superfamily and in ECs. However, the effect of Eps15-S^{796} phosphorylation remains yet unidentified. It has been suggested that Eps15, along with its homologous protein Eps15R (encoded by *EPS15L1*), act as endocytic adaptors and play a role in controlling membrane morphology and endocytosis of several cell surface receptors, including EGFR (epidermal growth factor receptor) [579, 580]. Eps15 and Eps15R share about 41% identical and 61% similar sequences [581]. These proteins act as scaffold proteins with multiple domains, including EH protein-binding modules that interact with endocytic proteins, sites binding to AP2 involved in endocytosis, and ubiquitin-binding domains (UIMs) [573, 581]. It has been reported that Eps15 interacts with AP2 through amino acids 666–737 and Grb2

around Pro-768 [582, 583]. Interestingly, Ser-796 is located between Grb2-/AP2 - binding domains and the C-terminal UIM (ubiquitin-interacting motifs) domain, suggesting a role in clathrin-mediated endocytosis. Interestingly, the group of Petra Knaus discovered a co-localization and a direct interaction between Eps15R and BMP2R [127]. Another study showed that Eps15R interacts with SMAD1 and is required for BMP signalling in animal caps, providing an interesting first functional link between Eps15R and the BMP pathway [584]. Due to the similarity between the functional domains of Eps15 and Eps15R, these studies suggest that Eps15 might also interact with BMP receptors and contribute to their endocytosis and/or downstream signaling in ECs. Interestingly, unpublished work has shown that both Eps15 and Eps15R play important roles in regulation of Notch signaling exclusively in the signal-sending cell (https://air.unimi.it/handle/2434/263596).

5.4.3.3 Heat shock protein 27 (HSP27)

Heat shock protein 27 (HSP27) is a small molecular chaperone which forms large oligomers that bind to monomeric actin and prevent actin polymerization [585, 586]. HSP27 is one of the best characterized substrates for MK2 [204], a downstream kinase that can be activated mainly by P38 [587] but also by ERK MAPK [588]. Phosphorylation of HSP27 causes the disassembly of large oligomers and the release of actin, which promotes actin polymerization [585, 589]. In reference to the phosphositplus database, many studies have demonstrated that HSP27 can be phosphorylated at several key residues including S15/78/82, which subsequently mediated several effects on HSP27 including its activity, nuclear translocation, and stability. Consequently, HSP27 phosphorylation has shown to be implicated in many biological processes including apoptosis, proliferation, differentiation, transcriptional regulation and cytoskeletal organization in different cell types [590–592].

Our phosphoproteomic analysis highlighted that both BMP9 and BMP10 induced phosphorylation of HSP27-$S^{15/82/83}$, which was further validated for BMP10 in our study to be dependent on GADD45β/P38/MK2 as well as TAK1 in HUVECs. An important role of HSP27 in ECs is the regulation of actin filament remodelling and EC barrier function [593–596]. Recent work by Rada et al demonstrated the mechanism that may explain the role of HSP27 in regulating EC barrier integrity. The authors demonstrated that thrombin-induced activation of P38/MK2/MK3 axis resulted in HSP27 phosphorylation and its subsequent disassembly, which was then followed by decreased phosphorylation and reassembly of HSP27 back into large oligomers. This latter dynamics was suggested to play a critical role in regulating EC barrier function, both *in-vitro* and *in-vivo*, through re-establishment of EC barrier integrity after its disruption following pro-inflammatory GPCR signaling [596]. An interesting finding in this work was that HSP27 phosphorylation was shown to be differentially regulated by MK2 and MK3, such that MK2 mediated S15 and S78 phosphorylation, whereas both MK2 and MK3 were required for S82 phosphorylation. Our MS analysis highlighted that both BMP9 and BMP10 are responsible for inducing phosphorylation at HSP27-$S^{15/82/83}$, while the peptide bearing

HSP27-S^{78} phosphosite was not detected in any condition. The phospho-antibody used in our study selectively detects HSP27 when phosphorylated at both S78 and S82. Taking this into consideration, along with results demonstrating that the MK2 inhibitor (PF3622204) effectively inhibits S15 and S78 phosphorylation but not S82 [596], this strongly suggests that BMP10 is likely responsible for phosphorylating S78 of HSP27 as well. Moreover, this suggests that, not only MK2, but also MK3 could be implicated in this phosphorylation. We could not confirm HSP27-S^{15} phosphorylation under our experimental conditions using a commercially available antibody tested, which did not give a positive signal even using anisomycin as a positive control (data not shown).

Other roles for HSP27 in ECs have been also shown, including regulation of EC proliferation [597], migration [201] and apoptosis [598]. The group of Petra Knaus has demonstrated that both BMP2 and BMP6 induced the activation of P38/HSP27 axis in different types of ECs [201]. They showed that this phosphorylation occurred within 45 minutes, which is in accordance with our kinetics, and thus could support that several BMPs can phosphorylate P38 and HSP27 in ECs. However, the authors in this study didn't study neither the mechanism behind this phosphorylation nor specified the site phosphorylated on HSP27. Nevertheless, they showed that BMP2 and BMP6 promoted EC migration via the p38-HSP27 signaling axis and highlighted HSP27 as an important regulator of endothelial outgrowth. Altogether, HSP27 phosphorylation seems to play key roles in several EC functions. Therefore, it is necessary to understand the physiological role of BMP9/10-induced phosphorylation of HSP27 in ECs.

5.4.4 Cell cycle regulation

Upstream kinase analysis using Kinswing predicted negative regulation of three key regulatory kinases involved in the G1/S transition of cell cycle: CDK4, CDK6 and CDC7. However, by looking carefully at the downstream-matched substrate phosphosites of these kinases, we found none that have been previously described that we could validate. As described in section 3.4.1.1, BMP9 and BMP10 have been generally described as quiescent factors and negative regulators of several EC functions, including proliferation. However, the mechanism of this regulation remains poorly understood. One study carrier out by Rostama et al demonstrated that BMP9, and the Notch ligand Dll4, cooperate together to suppress the proliferation of HAECs [359]. Interestingly, the authors demonstrated that this inhibitory impact resulted from the modulation of various cell cycle-related proteins. Amongst, they highlighted a crucial role of the CDK4/6 inhibitor $P27^{KIP1}$ as a central mediator of endothelial quiescence, which matches our predictions from Kinswing about the decreased activity of CDK4/6 by BMP9/10 and increased protein expression of $P27^{KIP1}$ in HUVECs after overnight exposure. Using siP27, we could not confirm the role of P27 in the inhibitory role of BMP10 on HUVEC cell cycle (n=1 experiment, data not shown). However, our findings indicate that BMP9 and BMP10 already initiate anti-proliferative signals within 30 minutes (as highlighted by Kinswing analysis). Subsequently, within a few hours, we observed a decline in essential regulatory genes for the cell cycle, such as cyclinD1 (a key cyclin for CDK4/6) and E2F2 (a

downstream transcription factor of CDK4/6). Consequently, these anti-proliferative signals were further confirmed by illustrating the role of BMP10 in inhibiting G1/S-phase transition in serum replenished HUVECs.

Very recent work by Banerjee et al demonstrated that loss of EC Smad4 in pups leads to excessive activation of AKT signaling in response to pathological shear stress [451]. This results in cell cycle progression-mediated loss of arterial identity and the formation of arteriovenous malformations (AVMs). Importantly, the authors showed that the use of Palbociclib (CDK4/6 inhibitor) strongly inhibited AVM formation and effectively rescued the excessive vascular front density in these mice. Furthermore, another interesting data was recently presented by Gael Genet at the VAC2023 international conference on vascular anomalies in Brussels. Using Bulk RNA sequencing on isolated primary retinal endothelial cells, the authors demonstrated that the cell cycle state of ECs and associated gene expression become dysregulated during the progression of vascular malformations in HHT. Interestingly, they showed that inhibiting CDK4/6 using Palbociclib successfully prevented the formation of retinal, brain, lung, and intestinal AVMs in two HHT mouse models. Therefore, both recent aforementioned studies highlight the importance of how dysregulation of EC cell cycle due to BMP9/10 signaling deficiency contributes to AVM development. Moreover, both studies suggested that restoring proper cell cycle control by blocking CDK4/6 in ECs could offer a potential therapeutic approach for treating AVMs associated with HHT, which nicely aligns with our *in-vitro* data on the regulation of EC G1/S transition by BMP10 signaling.

5.5 Other Interesting Identified Targets/Pathways

5.5.1 ETS-related gene (ERG)

Our phosphoproteomic analysis highlighted several other interesting targets that were not extensively studied in this work. Notably, one of the identified targets is the EC specific transcription factor ERG. ERG exhibited distinct phosphorylation patterns at two distinct sites, S215 (down-phosphorylated) and S276 (up-phosphorylated), in response to both BMP9 and BMP10. Earlier research by Hollenhorst et al uncovered that ERK2 mediates the phosphorylation of ERG at S96, S215, and S276 in cancer cells [599–602]. ERG-S^{276} (=S^{283} in leukemia cells) has been also described to be phosphorylated by ERK2 in in acute myeloid leukemia (AML) and T-acute lymphoblastic leukemia (T-ALL) cells, and plays a role in DNA-binding to specific hematopoietic stem and progenitor cells (HSPCs) enhancers in these cells. Recently, ERG has emerged as a major regulator of endothelial function playing crucial roles in angiogenesis and vascular stability, transcriptional regulation of genes involved in EC functions, as well as differentiation and maintenance of the endothelial lineage [603]. Interestingly, Fish et al showed that ERG can be also phosphorylated in ECs via VEGF/ERK signaling at S96, S215 and S276. The authors highlighted that phosphorylation of ERG at these three residues is essential for achieving maximum ERG activity. Furthermore, they showed that, in collaboration with P300, ERG orchestrates the regulation of a subset of VEGF target

genes including Dll4 [604]. Interestingly, our study is the first to show simultaneous and opposing changes in ERG phosphorylation at both S215 and S276 sites. Because of the absence of commercially ERG-S^{276} antibody, we confirmed ERG phosphorylation using a pan-pSer antibody following ERG immunoprecipitation. Similarly, there is no ERG-S^{215} commercial antibody, but P Hollenhorst kindly provided us with a home-made antibody for this site [599]. This allowed us to validate that BMP10 attenuates ERG-S^{215} basal levels, as well as VEGF-induced ERG-S^{215} phosphorylation, with a more significant attenuation observed on this latter. This observation would be in accordance with previous studies highlighting the antagonistic relationship between BMP9/10-ALK1 and VEGF signaling (Figure 25).

The group of Anna Randi demonstrated that ERG can be also phosphorylated by Ang1/Tie2/PI3K/AKT signaling, resulting in the accumulation of ERG at the Dll4 promoter and multiple enhancers that regulate Notch signaling and vascular stability [605]. However, using proximity ligation assay (PLA) and a pan-pSerine antibody, they demonstrated global ERG serine phosphorylation without specifying the exact phosphorylation sites resulting from PI3K/AKT signaling. Another study from the same group unveiled an interesting crosstalk between ERG and TGFβ/BMP signaling [606]. They showed that suppressing ERG expression in HUVECs led to a decrease in the expression of several crucial mediators associated with TGFβ and BMP signaling pathways, including *ACVRL1*, *BMPR2*, *ID1*, *SMAD1/2/3* and *TGFBR1*, among others. Moreover, they showed that ERG enhances SMAD1 signaling while inhibiting SMAD2/3 signaling in ECs. Using Co-IP and PLA, they demonstrated that ERG does not physically interact with SMAD1 but can bind with SMAD2/3, acting as a co-repressor for the latter. This interaction plays a pivotal role in diminishing EndoMT and liver fibrosis [606].

Collectively, several studies demonstrated that ERG is a major regulator of EC functions. However, the exact roles of ERG phosphorylation and its consequent effects on EC functions remains limited, with only few recent papers showing this phosphorylation in ECs [604, 605]. Our data demonstrates that BMP10 induced differential phosphorylation of ERG at S215 (decrease) and S276 (increase). While the functional significance of S276 phosphorylation remains uncharacterized, the importance of S215 phosphorylation is evident from its involvement in the VEGF-mediated transcriptional regulation. This suggests that BMP10 might play a role in attenuating the expression of a subset of VEGF-induced genes by reducing ERG phosphorylation at S215. Hence, it will be interesting to better understand the dual regulatory role of BMP10 in the phosphorylation of ERG at both S215 and S276 in ECs. We have recently tried to set up a functional luciferase test for ERG phosphorylation sites using different mutants generated by site-directed mutagenesis, which didn't work yet, but optimization of the experimental conditions is still ongoing.

5.5.2 Potential roles of MAPKAPK2 (MK2) in the context of BMP9 and BMP10 signaling in ECs

Bioinformatics analysis highlighted MK2 among the top kinases activated by both BMP9 and BMP10 using both predictive (Kinswing) and curated databsae (PTMsigDB) approaches. This was further evident from the phosphorylation of several proteins known to be phosphorylated by MK2. These include HSP27, PARN, CEP131, ZFP36L1/2 (BRF1/2), BAG2, NELFE, GIGYF1/2, and gp130. However, our attempts to validate direct MK2 activation encountered technical challenges. We were not able to detect MK2-$T^{222/334}$ phosphorylation by WB, which reflect MK2 activation, even when using a positive control treatment such as anisomycin (data not shown). Furthermore, we also tried to verify MK2 activity through immunoprecipitation followed by *in-vitro* kinase assay using recombinant HSP27 and ^{32}P labeling, but this was also unsuccessful. Nevertheless, we validated the phosphorylation of HSP27-$S^{78/82}$, a downstream substrate of MK2, through the use of the MK2 inhibitor PF3644022.

Several studies have revealed that MK2 plays a role in controlling the activation and inactivation of RNA-binding proteins (RBPs) [607]. These RBPs have an impact on the gene expression of various important factors like proto-oncogenes, cytokines, chemokines, and pro-inflammatory molecules regulating various processes such as cell-cycle progression, proliferation, angiogenesis, metastasis, and cell death [607–609]. Interestingly, BRF1- S^{54} and PARN-S^{557} , two RBPs, were both differentially phosphorylated by BMP9 and BMP10, and these phosphorylation sites were shown to be MK2 dependent and play a role in regulating mRNA stability [610, 611]. Another key feature is that phosphorylated serine and threonine residues of MK2 substrates often coincide with 14-3-3 binding motifs, allowing these latter to act as direct readers for P38/MK2 activation in response to various stimuli [610, 612–616]. Very interestingly, many phosphorylated sites identified in our study have been described to be MK2-dependent and to interact with 14-3-3 proteins. These include NELFE-S^{115} [614], GIGYF1-$S^{157/638}$ [616], CEP131-S^{47} [615] and BRF1-S^{54} [610], all of which were differentially phosphorylated by BMP9 and BMP10. For instance, phosphorylation of NELFE-S^{115} by MK2 promotes the recruitment of 14-3-3 and rapid dissociation of the NELF complex from chromatin, which is accompanied by RNA polymerase II elongation [614]. GIGYF proteins utilize their GYF domain to link proteins containing poly-proline containing and RNA-binding proteins, such as zinc finger protein 598 (ZNF598) and Tristetraprolin (TTP), to the non-productive mRNA cap-binding protein 4EHP. This latter promotes the translational inhibition of specific transcripts [617, 618]. A pool of GIGYF1 protein is present in p-bodies, which are cytoplasmic regions where ribonucleoprotein (RNP) granules form [616]. P-bodies are primarily composed of translationally repressed mRNAs and proteins which are related to mRNA decay [619]. Interestingly, phosphorylation of GIGYF1-$S^{157/638}$ by MK2 promotes binding of 14-3-3 to GIGYF1, which negatively affects GYF domain-dependent protein interactions, and results in GIGYF1 exclusion from p-bodies [616]. Notably, these studies align with our GO analysis of biological processes, which highlighted mRNA stability, transcriptional regulation,

and RNA transport among top enriched processes in response to BMP9 and BMP10. Another study demonstrated that the p38-MK2-14-3-3 signaling pathway also plays a role in cytoplasmic sequestration of phosphorylated CEP131-S$^{47/78}$. This process blocks the formation of centriolar satellites, which are little grain-like structures that cluster near centrosomes to control the abundance of centrosomal proteins [615, 620]. Taken together, these studies highlight the importance of MK2 activation in different processes including mRNA stability, transcriptional control, and the localization of proteins associated with diverse functions. Consequently, there is still a lot of work to do for understanding the role BMP9/10-ALK1 signaling in MK2 activation, which could uncover several novel functional outcomes for this pathway in ECs.

5.6 Other preliminary data

5.6.1 Role of TAK1 in BMP10-induced activation of P38 MAPK pathway

TNF-α-induced Eps15-S^{796} and HSP27-S$^{78/82}$phosphorylation have been described to be dependent on TAK1, another MAP3K upstream of P38 [181, 573, 621]. Interestingly, we found that pretreatment with the TAK1 inhibitor (5Z-7-oxozeanol) inhibited P38-Y^{182}, HSP27-S$^{78/82}$ and Eps15-S^{796} phosphorylations (Figure 31). Thus, our data showed complete inhibition of P38, Eps15, and HSP27 phosphorylation by BMP10 upon either the utilization of a TAK1 inhibitor but also by silencing of GADD45β (manuscript 1, Fig. 5E). Despite that both mechanisms has been described to play important roles in P38 activation, GADD45β does not appear to activate TAK1 according to previous studies [174]. Thus, because both inhibition of TAK1 or GADD45β completely inhibited P38 activation, the mechanism by which BMP10 triggers TAK1 activation remains uncertain, unless both mechanisms act dependently, a scenario that has not been previously demonstrated and falls outside the scope of this study.

5.6.2 Potential activation of PKA and CREB signaling by BMP10

During the first year of my PhD, I also performed phosphokinase proteome profiling arrays (R&D systems) in order to identify new BMP9 and BMP10 phosphoproteins. I found that BMP10 induced significant phosphorylation of CREB-S^{133} (Figure 32A). CREB is transcription factor and is recognized as a substrate for various kinases, including PKA, MK2, and MSK1/2 [622–625]. Interestingly, bioinformatics analysis of upstream kinases using PTMSigDB have highlighted MK2 but also PKA among the top kinases that seem to be activated in response to BMP9 and BMP10. Upon identifying CREB as being significantly phosphorylated by BMP10 through the kinase array, I have first tried to validate this result by WB. Initially, using the classical RIPA lysis buffer commonly used for preparation of protein lysates for WB, I encountered difficulty observing the prominent increase in CREB as observed in the kinase array. However, upon using the specialized buffer provided by the kit, called lysis buffer 6 (L6), along with the urea lysis buffer utilized for MS sample preparation, I successfully validated CREB phosphorylation by both BMP9 and BMP10 (data not shown). Using WB analysis with

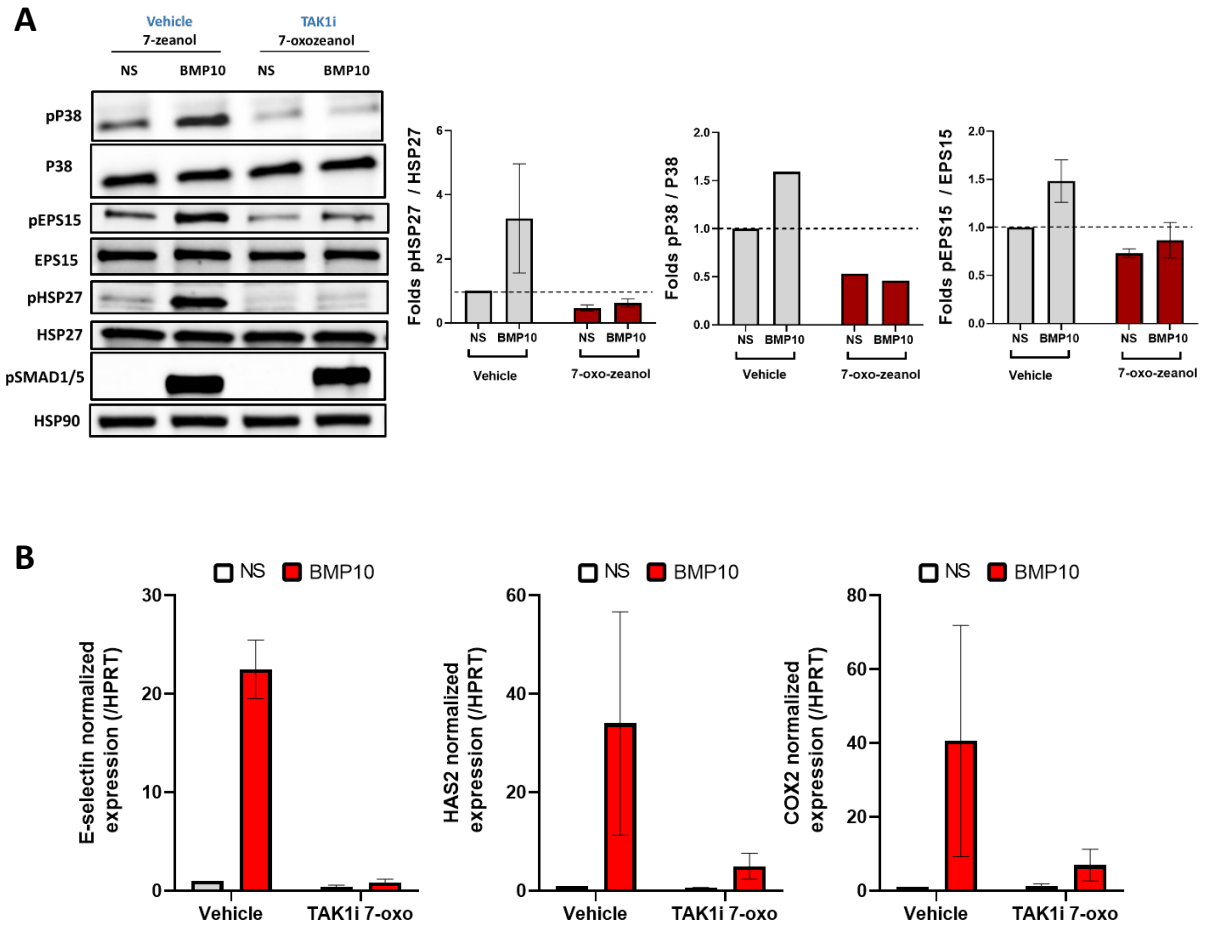

Figure 31. BMP10-induced activation of P38 MAPK also depends on TAK1 in HUVECs

(A) *HUVECs were stimulated with 10 ng/mL BMP10 for 30 min. Cell extracts were subjected to western blotting (WB) analysis using the indicated antibodies with HSP90 as loading control. Quantification of phosphorylation for P38, HSP27 and Eps15 reflects the normalized signal for the phosphorylated protein to total protein content, presented as mean fold change (BMP10-vs-NS) ± SEM of n=3 independent experiments.* ***(B)*** *HUVECs were pretreated with p38 inhibitor SB203580 (10 µM) or MK2 inhibitor PF3622044 (5 µM), or left untreated (vehicle) for 30 min. Cells were then stimulated with 10 ng/mL BMP10 for 4h. Real-time quantitative polymerase chain reaction (RT-qPCR) analysis was then performed to determine mRNA expression of ID1, SMAD6, PTGS2 (Cox2), HAS2 and SELE (E-Selectin). Target gene expression was normalized to HPRT mRNA level using $2^{-\Delta\Delta Ct}$ method and presented as fold induction (BMP10-vs-vehicle) ± SEM of n=3 independent experiments.*

phospho-PKA substrates antibody against RRXpS/T motif, we showed that BMP10 phosphorylates several PKA substrates (Figure 32B). However, this result displayed limited reproducibility, as differing phosphorylation profiles were observed across different experiments. Nevertheless, as CREB has been described to be a downstream substrate for PKA, we tested whether its phosphorylation is PKA-dependent using a potent PKA inhibitor, H89. We showed that pre-treatment of HUVECs with H89 attenuated BMP9 and BMP10-induced CREB phosphorylation, suggesting that PKA is important for CREB phosphorylation (Figure 32C). Kinetic analysis revealed that BMP10 induces phosphorylation of CREB starting from 15 mins, peaking at 30 mins and decreasing back to basal levels after 60 mins (Figure

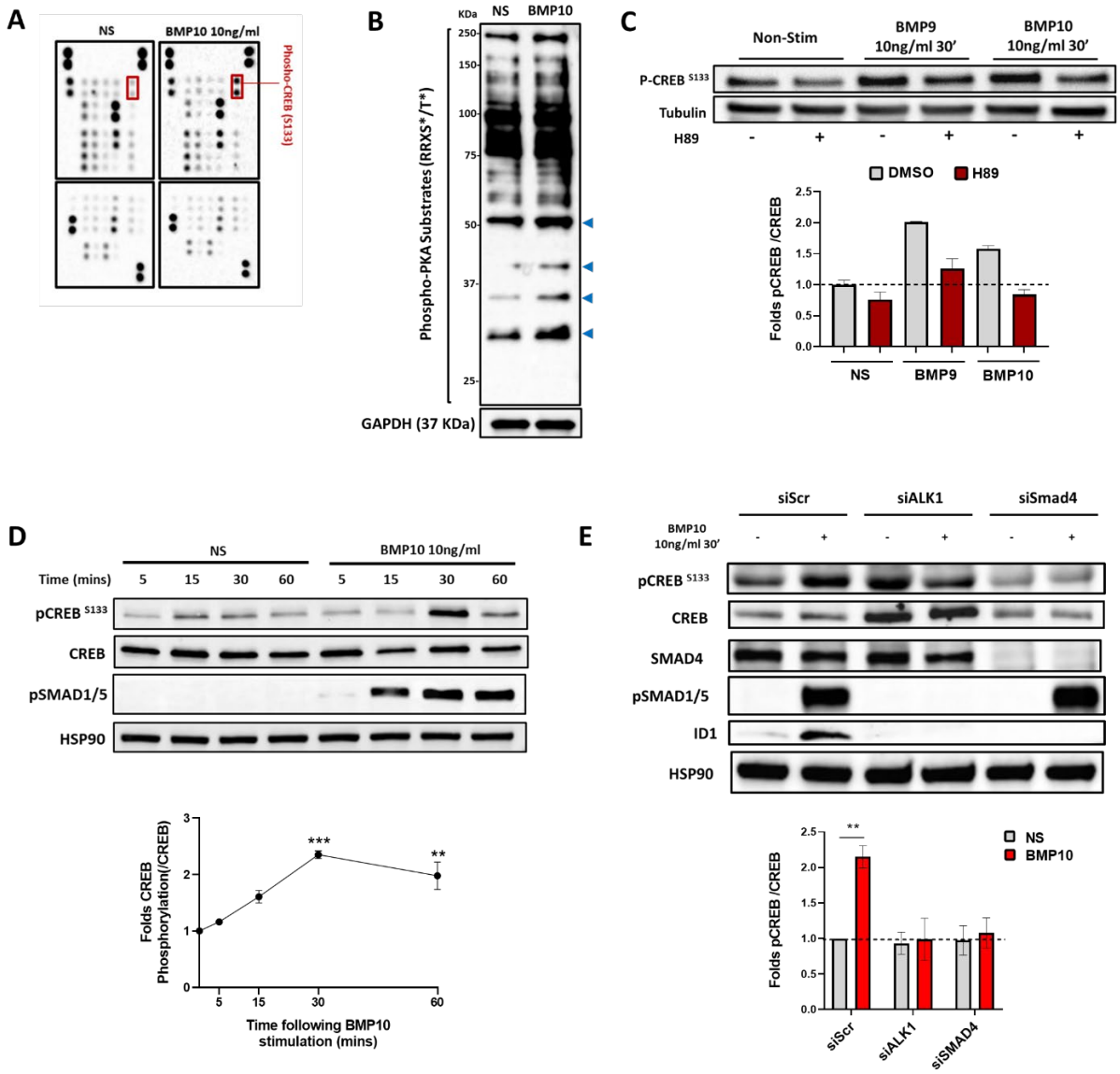

Figure 32. BMP10 induces activation of PKA/CREB pathway in HUVECs

(A) *HUVECs were stimulated with 10 ng/mL BMP10 for 30 min. Cell extracts were subjected to Proteome Profiler Human Phospho-Kinase Array Kit (ARY003C) for the determination of the relative phosphorylation levels of 37 key human protein kinases/substartes 37 human kinases. Highlighted hit represents CREB-S133.* ***(B)*** *Cells were stimulated as in described in A, and lysates were analyzed by WB using Phospho-PKA Substrate (RRXS*/T*) and GAPDH as a loading control.* ***(C)*** *HUVECs were pretreated with PKA inhibitor H89 (10 µM) or left untreated (vehicle) for 30 min. Cells were then stimulated with 10 ng/mL BMP9 or BMP10 for 30 min. WB analsysis was then performed using pCREB-S133 antibody, and quantification of phosphorylation for CREB-S133 reflects the normalized signal for the phosphorylated CREB to total CREB content, presented as mean fold change (Stimulated-vs-NS) ± SEM of n=3 independent experiments.* ***(D)*** *Cells were stimulated with 10ng/mL BMP10 or vehicle for the indicated time points. Cell extracts were subjected to WB analysis using the indicated antibodies. Quantification of phosphorylation for CREB was normalized to total CREB content. Data are presented as fold change of each sample ± SEM normalized to NS at each time point. Blots are representative of n=3 independent experiments. **P < 0.01; ***P < 0.001 (2-way ANOVA followed by Sidak's multiple comparisons post-test).* ***(E)*** *HUVECs were treated either with scrambled siRNA (siScr), siALK1 or siSMAD4 and then stimulated with 10ng/mL BMP10 for 30 min. Cell extracts were analyzed by WB using the indicated antibodies and quantification of CREB phosphorylation was normalized to total protein content. Data are presented as mean folds (BMP10-vs-NS) ± SEM of n=5 independent experiments. Statistical analyses was performed using using two-way ANOVA followed by Sidak's multiple comparisons post-test. **P < 0.01.*

32D). I also tried to better understand the mechanism of PKA/CREB activation by BMP10. Using siRNA against ALK1 and SMAD4, we demonstrated that CREB phosphorylation was dependent on both ALK1 and SMAD4 (Figure 32E). However, we noticed that ALK1 silencing

resulted in increased expression of total CREB, justifying the reason of higher basal phosphorylation in siALK1 group (Figure 32E).

As explained in section 2.4.2.5, the activation of PKA by TGFβ has been shown to occur in a cAMP-independent SMAD-dependent manner [282]. As I demonstrated that SMAD4 plays a role in BMP10-induced CREB phosphorylation, I wanted to better understand whether its role is transcriptional (similar to our findings for P38 MAPK activation) or if it involves activation of PKA by displacing the regulatory subunits, as shown for TGFβ [282]. For this, we conducted experiments using the transcriptional inhibitor Actinomycin D. However, these experiments gave us inconsistent results, making it hard to draw a clear answer (data not shown). Given that CREB phosphorylation can occur not only by PKA but also by other kinases including MK2 and MSK2 [622–625], downstream of P38, we aimed to see if P38 signaling also plays a role in CREB phosphorylation using the P38 inhibitor SB203580. Surprisingly, the inhibition of P38 also resulted in strong reduction in BMP10-induced CREB phosphorylation (data not shown). Therefore, our results show that inhibition of both PKA and P38 signaling strongly attenuated BMP10-induced CREB phosphorylation. This adds another level of complexity to the mechanism, and poses two hypotheses: (1) the inhibitors used might lack specificity, affecting multiple pathways, which has been already mentioned in literature for H89 at least [626, 627] and (2) there could be a collaborative phosphorylation mechanism involving both P38 and PKA in BMP10-induced CREB phosphorylation. Accordingly, several studies showed that PKA activation has shown to play a subsequent role in the activation of P38 signaling, and that both can lead to CREB phosphorylation [622, 628–631]. For instance, Pomerance et al showed that stimulation with 8-bromo-cAMP (cAMP analog), forskolin and thyroid-stimulating hormone, which are potent activators for PKA signaling, promoted phosphorylation of P38 and CREB, and this was inhibited using H89 but not SB203580 [628].

Taken together, our results suggests that CREB is likely phosphorylated by BMP9 and BMP10, and this appears to be at least dependent on SMAD4. However, the exact mechanism behind this phosphorylation regarding upstream kinases and need of a transcriptional step remains unclear. Furthermore, compiling the results from various experiments conducted on CREB, we noticed that there were several times where CREB phosphorylation could not be achieved by BMP10, even when applying same experimental conditions (lysis buffer, cell passage, other parameters). Thus, due to the considerable variability observed in our data and the challenges encountered to understand the reasons behind that, this led us to exclude CREB phosphorylation from the first paper, as it was not yet sufficiently clear and could complicate the interpretation of other findings. However, it remains very interesting to better understand BMP9/10-CREB pathway in ECs, especially considering that CREB and PKA have shown to play important roles in the endothelium [632–637].

Chapter 6. Project 2: BMP9/BMP10/ALK1 Pathway: Towards New Immunomodulatory Mechanism in Vascular Diseases

6.1 Context and Main Objective of the Project

Blood vessels and lymphatic vessels serve as the principal transit routes for immune cells, facilitating their passage to peripheral tissues and immune storage locations under both physiological and pathological conditions. In this context, ECs, which line the inner surface of these vessels, play a crucial role in regulating immune cell trafficking, activation, and function [638]. Inflammation is suspected to trigger or aggravate pathogenesis of HHT and PAH. Perivascular inflammation is frequently observed in PAH patients, which is suspected to contribute to the progression of the disease [639]. Moreover, early electron microscopy analysis of skin telangiectasia from HHT patients revealed the presence of leukocytes, suggesting an inflammatory component of these lesions. However, it remains unclear whether inflammation is a cause or a consequence of these lesions [640, 641]. As explained in section 3.5.1.4, we observed strong vascular defects and inflammation in several of our transgenic mouse models lacking BMP9 or BMP9 and BMP10 [373, 376]. Very interestingly, our phosphoproteomic analysis highlighted that BMP9 and BMP10 phosphorylate gp130, also known as CD130, which is a co-receptor for all IL-6 family cytokines, which play crucial roles in inflammation [642]. These cytokines transmit signals mainly through the JAK/STAT pathway, but also AKT and ERK pathways [642]. Importantly, phosphorylation of gp130 by BMP9 and BMP10 occurred at S^{782}, an important site previoulsy described to regulate surface expression of this receptor [264]. Taken together, we hypotheiszed that BMP9 and BMP10 might play a role in regulating JAK/STAT signaling. Thus, the main objective of this project is to explore the potential immunomodulatory role of BMP9/BMP10/ALK1 signaling and regulation of JAK/STAT signaling.

6.2 Choice of Methodologies

IL-6 family of cytokines encompasses several members including IL-6 it self, in addition to IL-11, IL-31, LIF, CNTF, CT-1 and OSM [256]. Among these, IL-6 is the major pro-inflammatory cytokine within this family [643]. As such, we selected IL-6 to study the potential crosstalk between BMP9/BMP10 and IL-6/JAK/STAT pathway. *In-vitro*, HUVECs were pre-stimulated with BMP9 or BMP10, followed by stimulation with IL-6. We assessed STAT3 phosphorylation (using WB and immunofluorescence) and expression of IL-6 target genes by qPCR. Then, we intended to decipher the molecular mechanisms to explain the crosstalk between the two pathways using inhibitors and siRNA. We recently started using whole tissues and ECs isolated

from transgenic mice with defective Bmp9/Bmp10/Alk1 signaling to confirm the immunomodulatory role of this pathway in preclinical mouse models.

6.3 Results (Manuscript 2 Draft)

Below, I will present the preliminary data obtained from this project and the associated materials and methods, which are provided in the form of draft article, but whose experiments (mainly *in-vivo* part) are still underway. *In-vitro* experiments from this project were initiated by me during the last 6 months of my 3rd year. In the 4th year, the project was then pursued by an M2 intern, Mohamad Skayni, who was under the supervision of my co-supervisor Claire Bouvard (*in-vivo* part) and myself (*in-vitro* part).

Immunomodulatory Role of BMP9 and BMP10 via The Attenuation of IL-6/JAK/STAT Signalling In Endothelial Cells.

Al Tarrass M.[1], Skayni M.[1], Belmudes L.[2], Koca D.[1], Liu H.[1], Azemard V.[1], Castan A.[1] , Battail C.[1,2], Couté Y.[2], Bailly S.[1]* and Bouvard C.[1]*

[1] *Biosanté unit U1292, Grenoble Alpes University, CEA, F-38000 Grenoble, France;*

[2]*BGE UA13, Grenoble Alpes University, CEA, F-38000 Grenoble, France*

*Co-last authors

Corresponding author Email: Claire.bouvard@cea.fr

Abstract

Endothelial cells constitute the inner lining of blood vessels and are known to regulate immune cell trafficking activation and function. BMP9 and BMP10 are two circulating proteins that activate ALK1 receptor, present in endothelial cells. Mutations in this signaling pathway are associated with two rare vascular diseases, pulmonary arterial hypertension (PAH) and hereditary hemmorhagic telangiectasia (HHT). Inflammation is thought to aggravate these diseases, however, the mechanisms and the roles of the BMP9/BMP10/ALK1 pathway in this context are unclear. *In vitro*, using Human Umbilical Endothelial Cells, we show for the first time that BMP9 or BMP10 induces the expression of SOCS3, which negatively regulates IL-6-induced STAT3 phosphorylation. This mechanism is ALK1- and SMAD4-dependent. *In vivo*, we have previously observed inflammation in several knockout mouse models lacking B*mp9* and/or *Bmp10*. Here, we further confirm this inflammatory phenotype and we have started to investigate whether this immunomodulatory mechanism involving SOCS3 and JAK/STAT pathway also plays a role *in vivo*. This might lead to new therapeutic opportunites for PAH and HHT patients.

Introduction

Blood vessels and lymphatic vessels are the major transit ways for immune cells, granting access to all peripheral tissues and immune storage sites in lymphoid organs. Endothelial cells (ECs) regulate immune cell trafficking, activation and function [1]. Deciphering the mechanisms driving the immunomodulatory functions of ECs could have an impact on a wide range of diseases in which immune and vascular cells are involved, such as vascular diseases that may be aggravated or triggered by inflammation, but also liver fibrosis, cancer and infectious diseases.

In 2007, our team identified BMP9 and BMP10 as the functional activators of ALK1 receptor, which is highly expressed by ECs [2], [3]. BMP9 and BMP10 circulate in the blood and activate a complex of receptors composed of type I (ALK1), type II (BMPRII, ACTRIIA, ACTRIIB) and type III (endoglin) receptors [4]. Mutations in this pathway are associated with two rare vascular diseases, HHT

(hereditary hemorrhagic Telangiectasia) [5] and PAH (pulmonary arterial hypertension) [6]. HHT is characterized by frequent nosebleed, arteriovenous malformations (AVMs), especially in the liver, lungs and brain, and skin or mucous telangiectasias [7], [8]. PAH is characterized by an elevated blood pressure in the pulmonary arteries, leading to right heart failure and death [9], [10]. The molecular mechanisms involved in the physiopathology of these diseases are poorly understood and no curative therapy exists yet. Inflammation is suspected to trigger or aggravate these diseases [11]–[14].

Early electron microscopy analysis of skin telangiectasia from HHT patients revealed the presence of leukocytes, suggesting an inflammatory component of these lesions [11], [12]. Although there is no proof yet, inflammation is suspected to be a trigger driving AVM formation in HHT [15]. De novo AVMs in adult *Acvrl1* knockout (KO) mice have shown to require a second hit, which can either be angiogenesis or wound healing, however the potential contribution of inflammation in these mice is unknown [16]. Signs of abnormal angiogenesis have been observed in trachea of *Acvrl1*+/- mice infected with bacteria [17]. Interestingly, HHT patients present immunological abnormalities and a risk for severe and atypical infection, affecting up to 15% of the patients [18]. Endothelial endoglin is increased by inflammation [19] and plays a role in leukocyte adhesion and extravasation [20]. Endoglin is also expressed by activated monocytes, suggesting that patients with Endoglin mutations could have a decreased innate immune response. Interestingly, it has been recently proven that ALK1 is also expressed on Kupffer cells [21], which are liver resident macrophages, and thus could also play a role in liver inflammation via non-endothelial cells. In spite of all these data that caught our attention, the role of the immune system in HHT remains understudied.

An expanding body of knowledge indicates that failure to resolve inflammation and altered immune processes underlie the development of PAH [14]. Concerning the role of BMP9, a study using ECs from PAH patients showed that BMP9 exacerbates IL-6 induced inflammation [22], which can seem in contradiction with another study showing that *Bmpr2*+/- rats are predisposed to inflammation-induced PAH [23], [24]. Overall, the immunomodulatory role of this pathway could depend on the EC subtype considered and to the pathological context, thus requiring more investigation to clarify this.

Since 2007, our efforts have been mainly focused on understanding the role of the BMP9/BMP10/ALK1 pathway in angiogenesis and cardiovascular homeostasis, in physiological and pathological contexts [25]–[27]. We recently obtained results indicating a potential immunomodulatory role of BMP9/BMP10/ALK1 pathway. Indeed, we observed inflammation in several of our transgenic mouse models lacking *Bmp9* or *Bmp9* and Bmp10 [25], [26]. Deletion of *Bmp9* in the 129/Ola genetic background leads to spontaneous perivascular liver fibrosis and a strong inflammation in the liver [26], the kidney and the lungs. C57BL/6 mice lacking both *Bmp9* and *Bmp10* present lung inflammation, and RNAseq analysis revealed an upregulation of the transcription of several inflammatory cytokines and adhesion molecules [25]. However we do not know whether this inflammation is a consequence of the vascular defects observed in these mice, or if BMP9 and BMP10 play a more direct role.

Using a phosphoproteomic analysis (manuscript in preparation), we found that BMP9 and BMP10 could phosphorylate gp130, also called CD130, which is a co-receptor of IL-6 family of cytokines. IL-6 binds IL-6 receptor (IL-6-R) (either membrane bound IL-6-R for classical signaling or soluble IL-6-R for trans signaling) and gp130 [28], [29]. Consequently, this activates JAK/STAT3 signaling pathway and phosphorylated STAT3 will translocate into the nucleus to induce the transcription of target genes, regulating several functions related to angiogenesis and immune cell recruitment [30]–[32]. This prompted us to further investigate a potential cross-talk between BMP9/BMP10/ALK1 and IL-

6/JAK/STAT pathways, while also performing further analyses of the inflammatory phenotype of our transgenic mice models with impaired BMP9/10/ALK1 signaling.

In the present manuscript (work in progress), we show for the first time that BMP9 and BMP10 can attenuate IL-6-induced JAK/STAT signaling in human ECs. *In vitro*, we showed that BMP10 attenuates IL-6 induced STAT3 activation and transcriptional regulation via SMAD-dependent induction of SOCS3 (suppressor of cytokine signaling 3). Moreover, we have started to decipher whether this mechanisms can be confirmed in mouse models.

Results

BMP10 regulates phosphorylation and surface expression of the IL-6 family co-receptor gp130-S^{782} in HUVECs

We have previously performed a phosphoprotemic analysis in response to BMP9 and BMP10 stimulation for 30 min in human endothelial umbilical veins (HUVECs), which identified a total of 289 phosphoproteins differentially regulated by both ligands (manuscript 1). We identified and validated the SMAD pathway, but also indirect activation of the P38 pathway involved in phosphorylation of HSP27 and Eps15. Moreover, this analysis also revealed an inhibitory role of BMP10 on HUVEC cell cycle (manuscript 1). Very interestingly, our phosphoproteomic analysis also showed that BMP9 or BMP10 induced the phosphorylation of gp130-S^{782} (Fig. 1A and Fig. S1A). Gp130, also known as CD130, is a co-receptor for all IL-6 family cytokines, which play crucial roles in inflammation [33]. This phosphorylation event has been associated with a decrease in the surface expression of gp130 in response to several pro-inflammatory cytokines such as TNFα and IL1β, leading to a decreased signaling by IL-6 [34], [35]. Therefore, we investigated whether BMP10 could impact gp130 surface expression using flow cytometry. We found that BMP10 stimulation resulted in a modest reduction of approximately 10-12% in gp130 surface levels compared to non-stimulated cells (NS cells) (Fig. 1B). However, this decrease was not as strong as the one oberserved in response to TNFα (around 40% reduction compared to NS) (Fig. 1B).

BMP10 Attenuates IL-6-induced STAT3-Y^{705} Phosphorylation in HUVECs

Given that gp130 serves as a key receptor in the IL-6/JAK STAT3 signaling cascade, we next tested whether BMP10 would affect this pathway. To this end, HUVECs were pre-stimulated with TNFα or BMP10 for 30 min, followed by stimulation with IL-6 for 15 min, and STAT3-Y^{705} phosphorylation was determined by western blotting analysis of whole cell lysates. As expected, IL-6 induced a robust increase in STAT3-Y^{705} phosphorylation, while BMP10 or TNFα addition alone did not induce this phosphorylation (Fig. 1C). However, pre-stimulation with BMP10 strongly attenuated IL-6-induced STAT3-Y^{705} phosphorylation (Fig. 1C). Similar results were obtained with BMP9, which also induced gp130-S^{782} phosphorylation in our phosphoproteomic analysis (Fig. S1B). As previously shown [35], TNFα reduced STAT3-Y^{705} phosphorylation, but this reduction was less pronounced than that by BMP10 (16% versus 53%, respectively) (Fig. 1C). Interestingly, we also showed that BMP10 pre-stimulation attenuates STAT3-Y^{705} induced by Leukemia inhibitory factor (LIF), another IL-6 family member (Fig. S1C). Since IL-6-induced STAT3-Y^{705} phosphorylation is followed by the dimerization and translocation of STAT3 proteins into the nucleus [36], we next investigated the effect of BMP10 on the translocation of STAT3 from the cytoplasm to the nucleus upon IL-6 treatment. Exposing HUVECs to IL-6 for 15 minutes resulted in a clear nuclear accumulation of STAT3, and pre-stimulation with BMP10 for 30 minutes prior to IL-6 stimulation markedly attenuated this translocation (Fig. 1D).

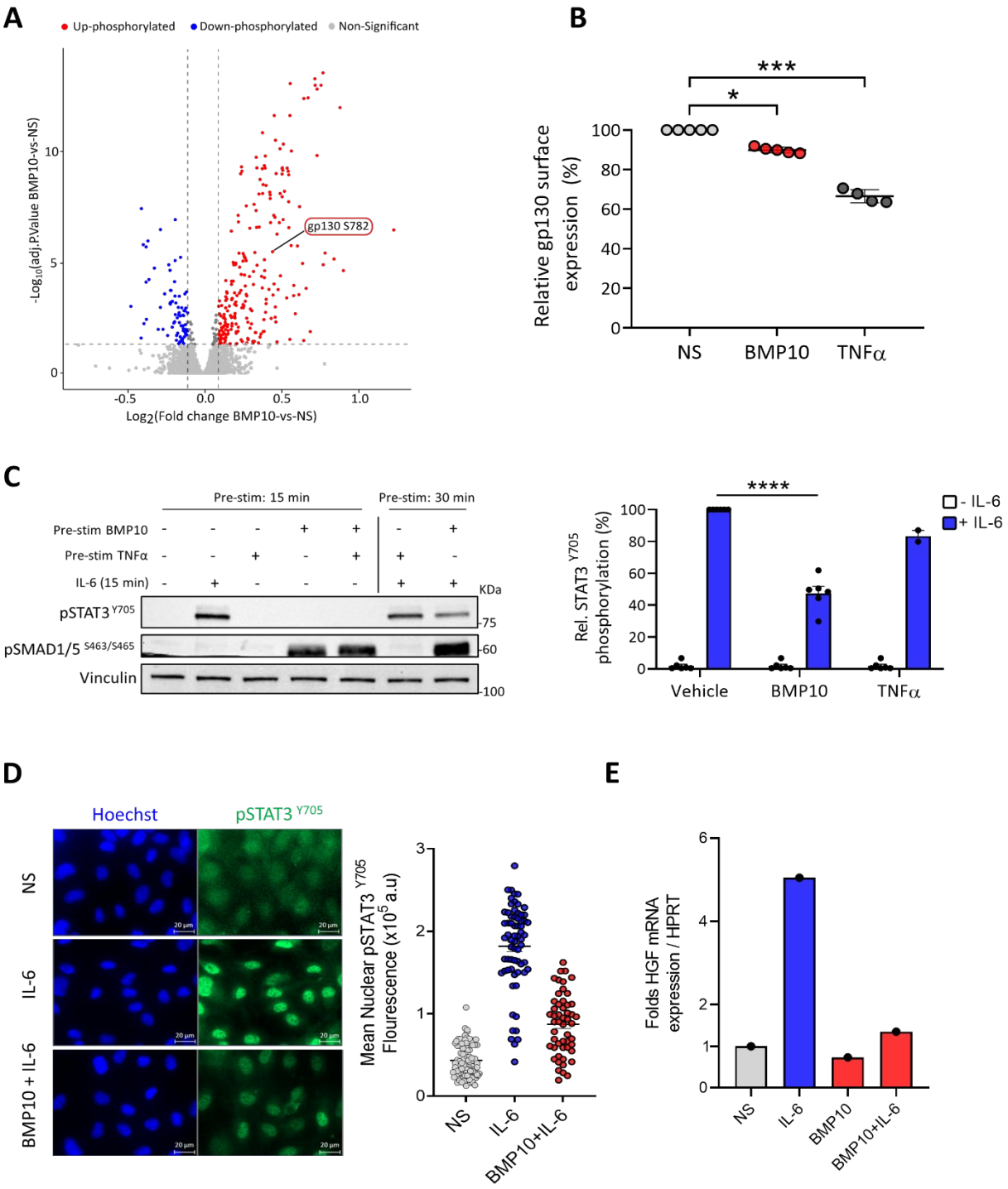

Fig. 1. BMP10 negatively regulates IL-6 pathway in HUVECs (**A**) Volcano plot taken from manuscript 1 representing the log2 fold change in the abundance of phosphopeptides plotted against the $-\log_{10}$ adj. *P*.value, showing differentially phosphorylated sites which are down-regulated (blue) or up-regulated (red) in response to BMP10 stimulation, while highlighting gp130-S^{782}. (**B**) HUVECs were stimulated with 10ng/mL BMP10 or TNFα for 30 min. Cell surface- expression of gp130 was analysed by flow cytometry. (**C**) Cells were stimulated with IL-6 (100 ng/mL), BMP10 (10ng/mL) or TNFα (10ng/mL) for 15 minutes. For pre-stimulations, BMP10 or TNFα were added 30 minutes prior to the addition of IL-6. Cell extracts were subjected to western blotting (WB) analysis using the indicated antibodies. Relative STAT3 phosphorylation (pSTAT3/Vinculin) is expressed as mean + SEM (n=2-6, normalised to IL-6 condition). (**D**) Cells were pre-stimulated or not with BMP10 (10ng/mL) for 30 min, followed by stimulation with IL-6 (100ng/mL) for 15 min. Cells were fixed in 4% PFA and permeabilised in 0.1% Triton X-100. Nuclei were counterstained with Hoechst, and cellular distribution of STAT3 was monitored with an anti-pSTAT3-Y^{705}. Mean nuclear pSTAT3 is expressed ± SD from n=50-70 cells analyzed from 2 fields/condition of 1 experiment. (**E**) Cells were stimulated or not with BMP10 (10ng/mL) or IL-6 (100ng/mL) for 2h. For pre-stimulation, BMP10 was added 30 min prior to the addition of IL-6. RT-qPCR analysis was then performed to determine mRNA expression of HGF, which was normalized to HPRT mRNA level using 2-ΔΔCt method and presented as fold induction (Stimulated-vs-NS) from n=1 experiment.

Next, we investigated whether this attenuation of STAT3 activation by BMP10 was accompanied by a transcriptional downregulation of IL-6 target genes. One such gene is the hepatocyte growth factor (HGF), which has been demonstrated as a strong target induced by IL-6 in ECs [37]. Using RT-qPCR analysis, we observed that IL-6 indeed strongly induced HGF mRNA expression in HUVECs, and this response was significantly attenuated when cells were pre-stimulated with BMP10 (Fig. 1E).

Together, these data clearly support that BMP10 stimulation reduces IL-6/STAT3 signaling in HUVECs. However, due to the observed differences in the regulation of gp130 and STAT3-Y^{705} phosphorylation between BMP10 and TNFα, it seems that gp130 is not the sole factor driving BMP10 down-regulation of IL-6/STAT3 signaling. Therefore, we decided to perform more in-depth analysis to gain further insights about the mechanism driving the regulation of STAT3 phosphorylation by BMP10.

BMP10/ALK1 Signaling Negatively Regulate IL-6-Induced STAT3 Activation via De Novo Protein Synthesis

In endothelial cells, BMP10 mainly signals through its high affinity receptor ALK1 to mediate the activation of downstream signaling and functional outputs. To test the role of ALK1 in the BMP10 negative regulation of JAK/STAT3 signaling activated by IL-6, we used two approaches. (1) We found that the BMP type I receptor inhibitor LDN193189 blocked the BMP10 the inhibition of IL-6-induced STAT3-Y^{705} phosphorylation (Fig. 2A). (2) As this inhibitor is not specific to the ALK1 receptor, we next used an ALK1-targeting siRNA and showed that the BMP10 inhibition of IL-6-induced STAT3-Y^{705} phosphorylation is ALK1-dependent (Fig. 2B).

Previous studies have demonstrated that IL-6/STAT3 signaling pathway can be attenuated in ECs through STAT3 dephosphorylation via the activation of protein tyrosine phosphatases (PTPs), including SHP2, in response to various stimuli such as forskolin (FSK) [38]. Pre-stimulation of HUVECs with either BMP10 or FSK resulted in the attenuation of IL-6-induced STAT3-Y^{705} phosphorylation. However, while the inhibitory mechanism by FSK on STAT3 phosphorylation is tyrosine phosphatase-dependent, as demonstrated by its expected sensitivity to pan PTPs inhibitor Na_3VO_4 , it was not the case of BMP10 (Fig. 2C). This indicates that BMP10 attenuates IL-6-induced STAT3-Y^{705} phosphorylation independently of Tyrosine phosphatase activity.

We next tested whether this inhibition required a transcriptional step and/or de novo protein synthesis. For this, HUVECs were pre-treated with actinomycin D (transcription inhibitor) or cycloheximide (translation inhibitor) before being pre-stimulated with BMP10 for 30 min, followed by IL-6 stimulation for 15 min. Interestingly, despite the relatively rapid onset of BMP10-induced inhibition of IL-6-induced STAT3-Y^{705} phosphorylation within 30 minutes, the results show that this regulatory mechanism relies on both mRNA and protein synthesis (Fig. 2D). The efficacy of both inhibitors was confirmed through their effective inhibition of BMP10-induced ID1 gene expression without affecting SMAD1/5 phosphorylation.

BMP10 Negatively Regulates IL-6-Induced STAT3-Y^{705} phosphorylation via SOCS3 induction in HUVECs

One way to down-regulate IL-6 JAK/STAT3 signaling is through the involvement of SOCS3 [39], which is often induced directly by this pathway, forming a classical negative-feedback loop. Interestingly, in-

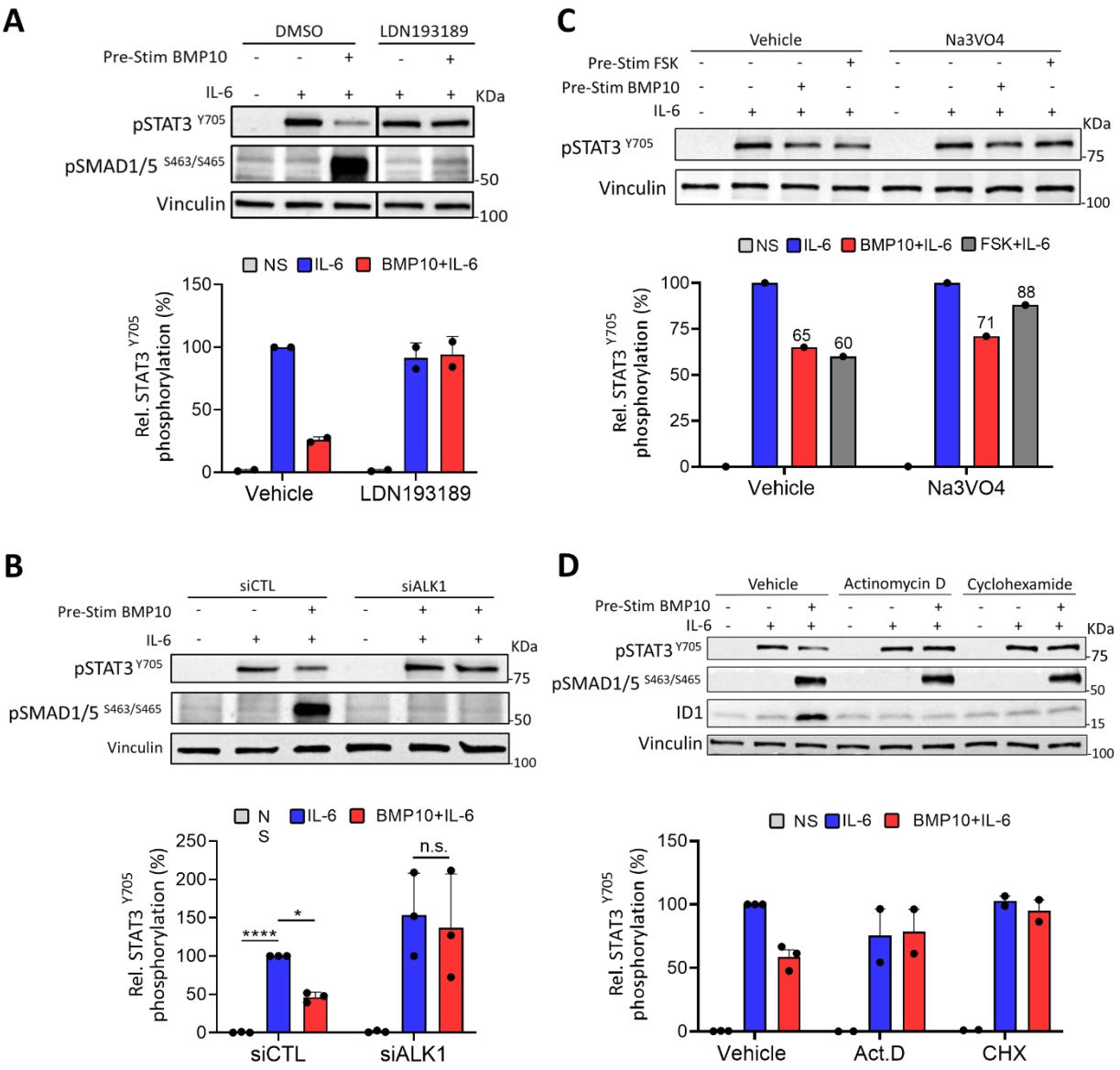

Fig. 2. Attenuation of IL-6-induced STAT3 phosphorylation by BMP10 depends on ALK1 activation, transcription and protein synthesis. (**A, C and D**) HUVECs were pretreated with selective ALK1/2/3/6 inhibitor LDN193189 (5 µM), Na3VO4 (50µM) (C), Actinomycin D (5µg/mL) or Cyclohexamide (10µM) (D), or left untreated (vehicle) for 30 min. Subsequently, cells were pre-stimulated or not with BMP10 (10ng/mL) (A and C) or Forskolin (FSK, 10µM) (C) for 30 min, followed by stimulation with IL-6 (100ng/mL) for 15 min. Cell extracts were subjected to WB analysis using the indicated antibodies. Relative STAT3 phosphorylation (pSTAT3/Vinculin) is expressed as mean + SEM (n=1 (C) and n=2 (A and D) independent experiments, normalised to IL-6 vehicle conditions). (**B**) HUVECs were treated either with scrambled siRNA (siCTL) or siRNA against ALK1 (siALK1) for 48h and then stimulated with the indicated ligands as described in panel A. Cell extracts were analyzed by WB using the indicated antibodies and relative STAT3 phosphorylation (pSTAT3/Vinculin) is expressed as mean + SEM (n=3 independent experiments, normalised to IL-6 siCTL condition). For all panels, *P < 0.05; ***P < 0.001; n.s. non-significant using two-way ANOVA followed by Sidak's multiple comparisons post-test.

silico analysis of the promoter region of SOCS3 using transcription factor (TF)-target gene database revealed the presence of several SMAD binding elements (Fig. 3A). This led us to hypothesize that BMP10 might act as a regulator of SOCS3 expression, considering that BMP10-induced attenuation of IL-6 STAT3 signaling requires de novo protein synthesis (Fig. 2D). To validate this hypothesis, HUVECs were stimulated with BMP10 for varying durations ranging from 30 minutes to 18 hours, and the expression of *SOCS3* mRNA was assessed using RT-qPCR. The results demonstrated that BMP10 rapidly

induced the expression of *SOCS3* mRNA, peaking within 30 min, and then declining to basal levels after 2-4 hours (Fig. 3B). *SOCS3* mRNA induction was also shown in BMP9 (Fig. S2). Stimulating HUVECs with different concentrations of BMP10 revealed a dose-response effect for SOCS3 induction at the protein level, starting to be detectable from 0.1 ng/mL and reaching a plateau at 1 ng/mL, which correlated with the expected dose response for SMAD1/5 phosphorylation and ID1 induction (Fig. 3C). Kinetic assessment of SOCS3 protein expression in response to BMP10 shows that it started within 30 min, peaked at 1 h, and remained quite high after 4 hours (Fig. 3D). Notably, this temporal regulation of SOCS3 expression by BMP10 correlated with the inhibitory effect of BMP10 on IL-6-induced STAT3-YY^{705} phosphorylation (observed within 30 min). To further validate these results, we investigated the involvement of both SMAD4 and SOCS3 in this regulatory mechanism by using pre-designed siRNA against these two genes. As expected, silencing *SMAD4* led to a significant decrease in SMAD4 protein expression, without affecting SMAD1/5 phosphorylation (Fig. 3E). Both the induction of SOCS3 and the inhibitory effect of BMP10 on IL-6 induced STAT3 phosphorylation were lost upon *SMAD4* silencing (Fig. 3E). Very interestingly, silencing SOCS3 blocked the inhibitory effect of BMP10 on IL-6 induced STAT3 phosphorylation (Fig. 3E). Taken together, these results demonstrate that BMP10 exerts its inhibitory effect on IL-6 JAK/STAT3 signaling through SMAD4-dependent expression of SOCS3.

Bmp9/Bmp10 DKO present an increase in inflammatory cytokines in the plasma and an increased STAT3-Y^{705} Phosphorylation in the lungs

In accordance with our data, we have previously demonstrated that *Bmp9/Bmp10* double knockout mice present increased lung inflammation and expression of genes implicated in inflammatory responses, suggesting an immunomodulatory role of BMP9 and BMP10 [25]. To better understand the inflammatory phenotype of these mice, we analyzed the circulatory levels of several cytokines from the plasma of WT and *Bmp9/Bmp10*-DKO mice using a mouse proteome profiler cytokine array. Accross both male and female cohorts (2 mice/condition), 33 cytokines displayed upregulation in either the male or female DKO compared to WT mice, while 6 cytokines showed downregulation (Fig. 4 A, B). Remarkebly, we found that both male and female cohorts from DKO mice exhibited elevated levels of several cytokines associated with inflammatory responses including CCL21, PAI-1, MMP9, and pentraxin 3 (Fig. 4A, B, C). We next investigated the STAT3-Y^{705} phosphorylation levels from whole lung extracts and found significant increase in STAT3-Y^{705} phosphorylation in *Bmp9/Bmp10*-DKO mice compared to WT mice (Fig. 4D).

A

Motif	Source	Strand	Start	Stop	P.Value	Match Sequence	Overlap with Footprints
V SMAD4 Q6 MOO733	TRANSFAC	-	76352670	76352684	6.00E-06	CTAAGGCAGCCACCT	15
V SMAD3 03 MO2794	TRANSFAC	+	76353629	76353645	1.00E-05	CTTAGCCAGACATAGTC	17
V SMAD1 01 M01590	TRANSFAC	+	76360666	76360677	5.00E-06	GAAGACAAAGGA	12

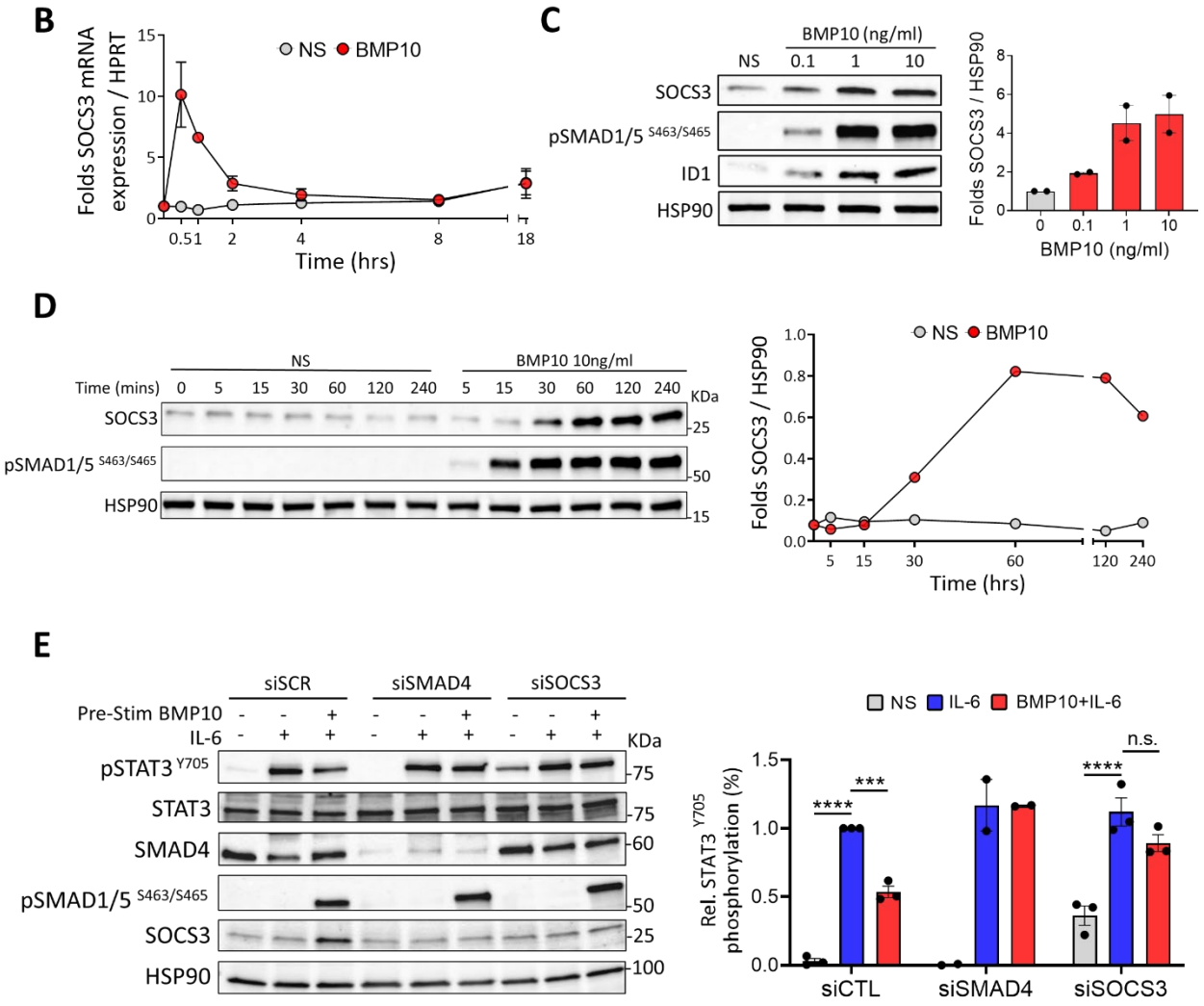

Fig. 3. Attenuation of IL-6-induced STAT3 phosphorylation by BMP10 depends on SOCS3 expression. (**A**) SMAD1/3/4 binding sites and number of overlap with footprints within SOCS3 promoter extracted from TFBS database. (**B**) HUVECs were stimulated with BMP10 or not (NS) for the indicated time points, and SOCS3 mRNA expression was then assessed by RT-qPCR. The level of SOCS3 expression was normalized to HPRT and represented as fold induction of each NS and BMP10 stimulated sample relative NS 0 min ± SEM (n=2 independent experiments). (**C and D**) HUVECs were stimulated with varying doses of BMP10 (0.1-10ng/mL) (C) or with 10ng/mL dose for the indicated time points (D), or were left non-stimulated (NS). Protein extracts were analyzed by WB analysis using the indicated antibodies. For panel C, SOCS3 expression was normalized to HSP90 (loading control) and represented as fold induction by BMP10 relative NS + SEM (n=2 independent experiments). For panel D, SOCS3 expression was normalized to HSP90 and represented as fold induction of each NS and BMP10 stimulated sample relative NS 0 min (n=1 experiment). (**E**) Cells were treated either with scrambled siRNA (siCTL) or siRNA against ALK1 (siALK1) or SOCS3 (siSOCS3) for 48h. Subsequently, cells were pre-stimulated or not with BMP10 (10ng/mL) for 30 min, followed by stimulation with IL-6 (100ng/mL) for 15 min. Cell extracts were subjected to WB analysis using the indicated antibodies. Relative STAT3 phosphorylation (pSTAT3/HSP90) is expressed as mean + SEM (n=2-3 independent experiments, normalised to IL-6 siCTL condition). ***P < 0.001; ****P < 0.0001; n.s. non-significant using two-way ANOVA followed by Tukey's multiple comparisons post-test.

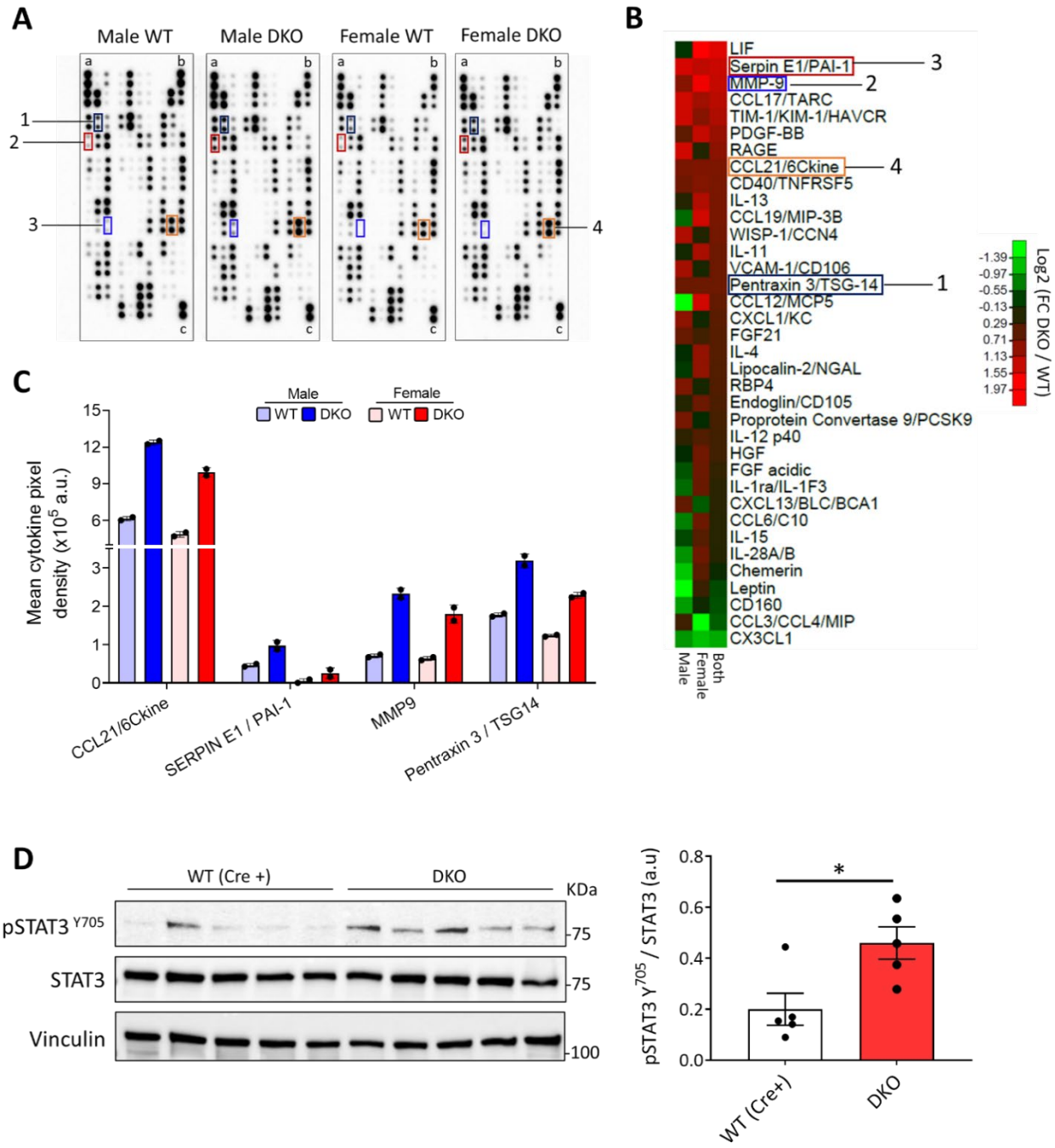

Fig. 4. Mice lacking BMP9 and BMP10 present differential amounts of cytokines in plasma compared to WT littermates, and increased STAT3 phosphoryation in lungs. (**A**) Cytokine array blots of 111 cytokines assessed from the plasma of a cohort of two mice/condition. Each spot represents 1 cytokine, with duplicates aligned vertically. Highlighted cytokines are those which were clearly different between DKO and WT mice in both males and females. 1: Pentraxrin-3/TSG-14; 2: MMP9; 3: Serpin E1/PAI-1; 4:CCL21/6Ckine; a,b,c: Reference spots. (**B**) Heat map representing the relative abundance of 33 cytokines which were significantly regulated between DKO and WT at least in one sex. Pixel densitity of each cytokine was calculated between the corresponding duplicates on the array for each condition, and represented as log2 fold change (FC) in the abundance from DKO compared to WT. "Both" represents the average log2FC (DKO/WT) calculated from both males and females. 1-4 represent cytokines marked in A. (**C**) The detection level of the four marked cytokines in A. Data are presented in the format of mean pixel density of each cytokine calculated between the corresponding duplicates on the array for each condition. a. u., arbitrary unit. (**D**) Lungs were harvested from the euthanized DKO and WT (Cre +) mice, from which protein extracts were prepared and analyzed by WB for pSTAT3 Y^{705} phosphorylation, total STAT3 and Vinculin (loading control). STAT3 phosphorylation (pSTAT3/STAT3) from each condition is expressed as mean ± SEM (n=5 mice/condition). *P < 0.05 using Mann–Whitney test.

Discussion

In this study, we identified a very interesting role of BMP9/BMP10 signaling in attenuating IL-6/JAK STAT3 pathway, with the mechanism detailed for BMP10, but is likely the same for BMP9. The study originated from my recent phosphoproteomic data, which highlighted gp130-S^{782} phosphorylation by BMP9 and BMP10, a site which has been previously described to negatively regulate gp130 surface expression [35]. Unfortunately, I was not able to validate this phosphorylation by WB analysis (data not shown). However, using flow cytometry, I showed that BMP10 induced a modest decrease in gp130 surface levels, but we thought that this decrease would not be sufficient to explain the attenuation in STAT3 phosphorylation. Nevertheless, by testing other mechanisms that play a role in attenuating JAK/STAT3 signaling, we proposed the following scenario. BMP10/ALK1 leads to the phosphorylation of SMAD1/5 and subsequent formation of an active SMAD1/5/SMAD4 complex. This complex then translocates into the nucleus to and induces the expression of SOCS3, which attenuates IL-6/JAK STAT3 pathway (Fig. 5). Thus, it remains unclear whether gp130 is involved in this regulation, but our findings clearly indicate a strong dependence on SOCS3 for the underlying mechanism. Previous studies in non-ECs have shown that TGF-β can regulate SOCS3 expression, however the outcomes of this regulation were context-dependent. For instance, TGF-β stimulation attenuated IL-6-induced SOCS3 expression in Th17-cells [40]. More recently, Dees et al showed that TGF-β induced the expression of DNA methyltransferase 3A (DNMT3A) and DNMT1 in fibroblasts in a SMAD-dependent manner to silence the expression of SOCS3 by promoter hypermethylation [41]. On the other hand, TGF-β induced the expression of SOCS3 in B lymphocytes, macrophages and osteoclasts [42]–[44]. To the best of our knowledge, our data are the first demonstration of the regulation of SOCS3 in response to BMPs. We also showed that BMP10 attenuated IL-6 induced expression of HGF, an important gene implicated in several biological processes including migration, morphogenesis, apoptosis, proliferation and tissue repair [45], [46]. Our results highlight an interesting negative regulation of JAK/STAT signaling pathway induced by the IL-6 inflammatory cytokine, suggesting an immunomodulatory role of BMP10 signaling in ECs. We have focused mainly on IL-6, due to its well characterized roles in inflammation and immune responses, however other cytokines can activate the JAK/STAT pathway, and can be regulated by SOCS3. For instance, We showed that BMP10 attenuated STAT3 phosphorylation induced by LIF, another cytokine of the IL-6 family (Fig. S1C). While SOCS3 is well characterized to inhibit STAT3 activation, it has been also shown to regulate other receptors and cytokines from other families (such as granulocyte-colony stimulation factor, insulin, and leptin) that do not activate STAT3 signaling [47], suggesting a potential role of BMP10 signaling on other cytokine families.

In the last few months of this work, we have tried to assess the immunomodulatory role of BMP9/10 signaling in preclinical mouse models available from our lab. Our group has generated several knockout mouse models lacking B*mp9*, *Bmp10* or *Alk1* to study this signaling pathway in the context of vascular diseases, mainly focusing on HHT. These include (1) constitutively deleted *Bmp9* from 129 Ola background (129Ola *Bmp9*-/-) (2) constitutive *Bmp9*/tamoxifen-inducible *Bmp10* double KOs from C57BL/6 background (*Bmp9/10* DKO) and (3) EC-specific tamoxifen-inducible *Alk1* KOs (Cdh5-CreERT2+/- *Acvrl1* flox/flox). Deletion of *Bmp9* in the 129/Ola genetic background leads to spontaneous perivascular liver fibrosis and a strong inflammation in the liver [48], but also in the kidneys and the lungs (work under review). On the other hand, *Bmp9* and *Bmp10* DKO mice in C57BL/6

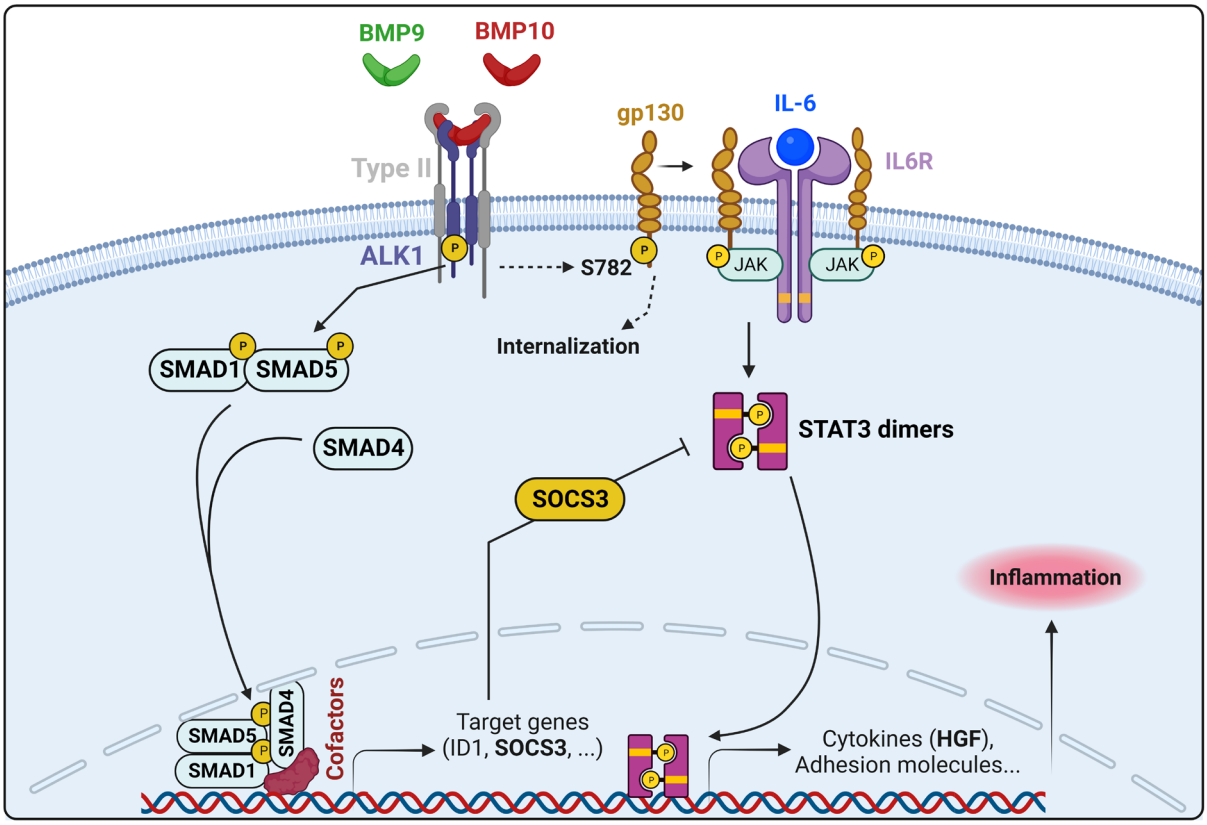

Fig. 5. Working model for the inhibition of IL-6/JAK/STAT3 Signaling BMP9/10/ALK1 via SOCS3. BMP9 and BMP10 signal through their high affinity type-I receptor ALK1, which triggers the phosphorylation of SMAD1/5. Phosphorylated SMAD1/5 forms an active complex with SMAD4, which then translocates into the nucleus to regulate the expression of downstream target genes, including ID1 and SOCS3. Subsequently, SOCS3 suppresses IL-6 JAK/STAT3 through attenuating STAT3 phosphorylation and subsequent regulation of the IL-6 target gene HGF, suggesting an immunomodulatory role of BMP9/BMP10/ALK1 signaling via inhibition of IL-6/JAK/STAT pathway.

background present vascular abnormalities which leads to high cardiac output and heart failure [25]. In addition, these mice present inflammation, and RNAseq analysis revealed an upregulation of cytokines and adhesion molecules associated with inflammatory responses [25]. Performing a cytokine array on the plasma of these mice indicated that *Bmp9/Bmp10* DKO show an increase in several cytokines associated with inflammation. We observed an upregulation in the level of several cytokines that are responsible for immune-EC interaction such as well as cytokines that are considered as biomarkers of chronic inflammation. For instance, CCL21 was shown to be secreted during inflammation by lymphatic endothelial cells and can play a role in dendritic cell recruitment [49]. CCL23 plays pro-inflammatory roles and can be produced by immune cells to upregulate pro-inflammatory cytokines such as CCL2 which is involved in monocyte chemotaxis [50]. Pentraxin 3 is considered as a biomarker of cardiovascular inflammation [51]. Serpin E1 (PAI-1) is an acute phase protein that is highly elevated during inflammation, acute tissue damage, and sepsis [52]. MMP9 plays an essential role in local proteolysis of the extracellular matrix and in leukocyte migration [53]. These preliminary data suggests that *Bmp9/10* DKO mice exhibit an upregulation of leukocyte chemoattractant factors and markers of chronic inflammation and angiogenesis.

Interestingly, we also showed that pSTAT3-Y^{705}/STAT3 levels seems to be higher in the lungs of *Bmp9/Bmp10*-DKO mice in comparison to WT (Fig. 4D), further supporting our *in vitro* data. We have also started to test our working hypothesis in isolated endothelial cells, by interrogating existing datasets. Recent single cell RNA-seq (scRNA-seq) data from our group also shows that deletion of

endothelial *Alk1* is associated with an increase in the percentage of immune cells in lungs and liver, and upregulation of inflammation/immune system pathways in several subsets of ECs (unpublished data). Very interestingly, we found that SOCS3 mRNA expression is downregulated in liver sinusoidal ECs from 129Ola *Bmp9-/-* mice (bulk RNAseq) (work under review) and in a subset of lung endothelial cells in *Alk1* KO mice (scRNA-seq, unpublished). We have also started to isolate ECs from various models, aiming to evaluate STAT3 phosphorylation, along with the expression of SOCS3 and IL-6/JAK/STAT target genes. Preliminary data for assessment of CCL2, a potent inflammatory cytokine and IL-6 target, reveal a trend of elevated *CCL2* mRNA expression in both mouse lung ECs from C57BL/6 mice and liver sinusoidal ECs (LSEC) from the 129 Ola background (Fig. S3). Moreover, we could also see a trend for decreased *SOCS3* mRNA expression from LSEC (Fig. S3). Overall, inflammation is observed in several of our transgenic mouse models, with preliminary data suggesting an immunomodulatory role of BMP9/10/ALK1 signaling *in vivo*, which might be linked to modulation of JAK/STAT3 signaling. Interestingly, several studies have suggested a role of IL-6 signaling in the context of PAH. The group of C. Guignabert demonstrated that smooth muscle cells from PAH patients present increased IL-6/STAT3 signaling through ectopic upregulation of both IL-6 receptor (IL-6R) and gp130 [24]. Interestingly, the authors showed that treatment with IL-6R-specific antagonist reverses experimental pulmonary hypertension in two rat models, suggesting promising therapeutic strategies for future clinical studies in PAH. More recently, Szulcek et al showed that an elevated IL-6 mRNA and protein expression levels in PAH HMVECs and PAH patient sera compared to CTLs [22]. Furthermore, they demonstrated that IL-6 exacerbated the EndMT phenotypic switch in PAH HMVECs, while blocking IL-6 using a neutralizing IL-6 antibody effectively prevented BMP9-induced EndMT in PAH HMVECs. However, the role of BMP9 in protecting or aggravating PAH pathogenesis remains unclear. This can be illustrated through contradictory results showing that removing or blocking BMP9 through genetic or pharmacological means offers protection against experimental PH in rodents, due to vadilation [54], while administration of BMP9 reverses experimental PH in rats [55]. The effects of BMP9 on inflammation may in part explain these apparently contradictory results. Other studies have demonstrated that lung tissues and SMCs from PAH patients present higher pSTAT3 levels in comparison to control groups [56], [57]. Several groups have proposed to block IL-6/IL-6R/gp130/ STAT3 signaling in PAH [58]. On the other hand, to the best of my knowledge, the role of IL-6 and STAT3 signaling in HHT has not been previously addressed. However, inflammation is thought to trigger or aggravate the disease, where IL-6 and STAT3 have been shown to play a role in proliferation and angiogenesis, mainly in cancer [59], [60]. These mechanisms could also be relevant in the context of HHT, where patients also present immunological abnormalities (leukopenia) [18]. One hypothesis could be an increased recruitment of immune cells by endothelial cells, due to an impaired regulation of JAK/STAT signaling. Several drugs targeting IL-6/JAK/STAT pathway are commonly used for their anti-inflammatory properties in diseases such as rheumatoid arthritis, atopic dermatitis or ulcerative colitis (tocilizumab, baricitinib, tofacitinib). Therefore, these drugs could be repurposed for HHT. Interstingly, in addition to EC, ALK1 is also expressed by Kupffer cells [21], which are liver-resident macrophages. We plan to assess whether BMP9 and BMP10 can also attenuate JAK/STAT signaling in these cells. This could be relevant for HHT, as the liver is one of the main organs affected by this disease.

Overall, we describe an immunomodulatory role for BMP9/BMP10/ALK1 pathway, and we describe a new crosstalk between two major signaling pathways. These findings can help us to better understand the pathogenesis of PAH and HHT, and pave the way for new therapeutic opportunities for these rare diseases.

Materials and Methods

Cell Culture

Human umbilical vein endothelial cells (HUVECs) were purchased from Lonza and cultured in endothelial basal medium-2 (EBM-2) supplemented with EGM-2MV SingleQuot additives (fetal bovine serum (FBS), hEGF, hydrocortisone, VEGF, hFGF-B, R3-IGF-1, ascorbic acid, GA-1000, and heparin; Lonza). Cells were incubated at 37 ℃ in a humidified atmosphere containing 5% CO_2.

Reagents

Recombinant human BMP9 and BMP10 were purchased from R&D systems (Catalog # 3209-BP and 3956-BP, respectively). Recombinant human IL-6, TNFα and LIF were purchased from Peprotech (200-06 and 300-01A, and 300-05 respectively). LDN193189, actinomycin D and cycloheximide were purchased from Sigma (Catalog # 1062368-24-4, 50-76-0 and 66-81-9, respectively).

Western Blotting

Following stimulations, cells were washed twice with ice-cold phosphate-buffered saline (PBS) and lysed in Radioimmunoprecipitation assay buffer (RIPA) supplemented with protease inhibitor cocktail (P8340) and phosphatase inhibitor cocktails 2 (P5726) and 3 (P0044) purchased from Sigma. Lysates were then clarified by centrifugation at 21,000g for 10 min at 4°C, and supernates containing proteins were collected into new eppendorf tubes. Protein concentrations were determined using a micro-BCA assay kit (Thermo Scientific), and lysates were then stabilized with Laemmli buffer and boiled at 95°C for 5 mins. Equal protein quantities (10-20µg) were then resolved by SDS-polyacrylamide gel electrophoresis (SDS-PAGE) on 4–20% Precast Protein Gels (Bio-rad) and transferred onto a nitrocellulose membrane using Mini Trans-Blot system (Bio-rad). Membranes were blocked with instant block buffer (Sigma) and subsequently probed with primary antibodies. Supplementary table 1 provides information about all the primary antibodies used. Membranes were incubated with enhanced chemiluminescence substrates (ECL; Bio-rad) or SuperSignal™ West Femto Maximum Sensitivity Substrate (Thermo Scientific™ Catalog number: 34094) and images were developed using ChemiDoc™ Imaging System (Bio-Rad). Chemiluminescent signal intensity was quantified with the Image lab software V6.1 (Bio-Rad). All measurements were performed within the linear range and were normalized to the non-phosphorylated total protein or loading control (STAT3, HSP90, or Vinculin).

Immunofluorescence

HUVECs were seeded at confluency in glass Lab-Tek Chamber Slides (Thermo Fisher Scientific). Cells were then starved and stimulated or not with BMP10 and/or IL-6 as described in the previous section. After stimulation, cells were fixed with 4% paraformaldehyde, permeabilized with 0.1% Triton X100 in PBS and incubated overnight with anti-pSTAT3-Y^{705} antibody (1/200 dilution) at 4°C. For detection, the cells were subsequently incubated with alexa 488 donkey anti-rabbit IgG (AB2340620, Jackson ImmunoResearch) for 1h at room temperature. Nuclei were counterstained with Hoechst 33342 (Sigma-Aldrich) and images were acquired using Apotome fluorescent microscope (ZEN). Analysis was performed using Fiji software by segmentation of nuclei and analysis of nuclear pSTAT3 signal.

Cytokine Array Analysis of Mice Plasma

Blood was collected from *Bmp9/Bmp10*-DKO mice by cardiac puncture and placed in K2-EDTA coated tubes. After centrifugation (10 minutes, 5000 rpm), plasma was collected and stored at -80°C until analysis. We collected plasma samples of 4 WT (2 males and 2 females) and 4 DKO (2 males and 2 females) mice. Samples from same sex and genotype were pooled and subsequently analyzed using Proteome ProfilerTM Mouse XL Cytokine Array Kit (R&D Systems, ARY028, USA) according to manufacturer's instructions. The spots were visualized using the chemi-reagent supplied with the kit and images were developed using ChemiDoc™ Imaging System (Bio-Rad). Chemiluminescent signal intensity was quantified with the Image lab software V6.1 (Bio-Rad). For data analsysis, average signal of each cytokine was calculated, and a fold change (FC) threshold was set to determine upregulated ($FC_{DKO/WT} \geq 1.6$; $Log2FC_{DKO/WT} \geq 0.7$) or downregulated ($FC_{DKO/WT} \leq 0.6$; $log2FC_{DKO/WT} \leq -0.7$). Only cytokines that were up or downregulated in at least one condition are represented in Fig. 4B.

RNA extraction and RT-qPCR

Total RNA was extracted using the NucleoSpin RNA kit (Macherey-Nagel) following the manufacturer's instructions. 500ng of RNA was then reverse-transcribed into cDNA using the iScript cDNA Synthesis Kit (Bio-Rad). Reverse transcription quantitative PCR (RT-qPCR) was then performed using SsoAdvanced Universal SYBR Green Supermix (Bio-Rad) in a CFX96 Real-Time System (Bio-Rad). Data analysis was conducted utilizing the CFX Manager Software V3.1 (Bio-rad), then gene expression levels were calculated utilizing Livak's $2^{-\Delta\Delta Ct}$ method using *HPRT* as housekeeping gene, and results were presented as fold change relative to control non stimulated samples. All primer sequences used for RT-qPCR were pre-designed using primer blast tool and purchased from sigma. Supplementary table 2 summarizes all the genes assessed by RT-qPCR with their respective primer mixes.

RNA interference

HUVECs were transfected with either a scrambled Silencer Negative Control #1 siRNA (siCTL; AM4611, Ambion), pre-designed siRNA (Thermofisher) directed against human *ACVRL1* (encoding ALK1, ; siALK1assay IDs987), *SMAD4* (siSMAD4; assay ID s8405) or human *SOCS3* (siSOCS3; assay ID s17191) at a final concentration of 10nM in 1ml final volume of Opti-MEM (Gibco) using 2.5µL/well Lipofectamine RNAiMAX Transfection Reagent (Invitrogen). 48h post-transfection, cells were serum starved in EBM2 for 6h and were then stimulated or not with 10ng/mL BMP10 for 30 min.

Assesement of Surface gp130 Expression by Flow Cytometry

HUVECs were seeded at confluency in 6-well plates. Cells were starved for 3h in serum free additive free EBM-2, after which they were stimulated or not for 30 min with 10ng/mL of BMP10 or TNFα. Cells were detached using trypsin/EDTA solution (CC-5012; Lonza) diluted at 0.000714%, resuspended in 2% BSA in PBS, and incubated with Alexa 648-conjuagted anti-human CD130 (BD Pharmingen|564151) or mouse IgG2 k Alexa 647 isotype control antibody (BD Pharmingen|557715) for 20 min on ice. Cells were washed twice with 2% BSA/PBS, resuspended in PSB, and 10 000 cells were analysed on FACS Calibr (BD Biosciences) using FCS Express Flow Cytometry Software.

Animal Experimentation

All animal experiments were approved by the institutional guidelines for the use of experimental animals. *Bmp9/Bmp10* double knockout (DKO) mice from C57BL/6 background and *Bmp9* KO mice from 129/Ola background were obtained as previously described by our group [25], [26]. For *Bmp9/Bmp10*-DKO mice, Cre+ mice were used as WT controls, to control for potential Cre toxicity.

For mouse lung protein extracts, lungs were harvested from the euthanized mice and placed in RIPA lysis buffer (supplemented with protease and phosphatase inhibitors) with 1.4 mm ceramic beads. Tissue lysis was achieved by vigorous agitation and vortexing of the tubes using Precellys 24 machine (2x15s 5000 rpm). Samples were incubated on ice for 30 min, and clarified protein lysates were analyzed by SDS-PAGE as described in WB analysis section.

For mouse lung endothelial cell isolation, lungs were minced and digested with collagenase/dispase, incubated with anti CD31 antibody (BD Pharmingen, catalog # 553370) coupled with Sheep anti-Rat IgG magnetic beads (Invitrogen #110.35). Magnetic cell sorting was performed and cells were lyzed in RA1 buffer containing beta mercaptoethanol.

Liver sinusoidal endothelial cell isolation was performed as previously described [26].

Tables

Supplementary Table 1. Primary Antibodies. List of primary antibodies used for WB, IF and Flow cytometry.

Antibody	Supplier|Reference	Dilution	Incubation conditions
pSMAD1/5-S$^{463/465}$	Cell Signaling|9516	1/1000 (WB)	O.N at 4°C
ID1	Santa Cruz|sc-133104	1/500 (WB)	O.N at 4°C
SOCS3	Abcam|ab280884	1/1000 (WB)	O.N at 4°C
HSP90	Cell Signaling|4877	1/1000 (WB)	1h RT
SMAD4	Cell Signaling|9515	1/1000 (WB)	O.N at 4°C
GAPDH	Abcam|ab181602	1/5000 (WB)	1h RT
Vinculin	Cell Signaling|9515	1/1000 (WB)	1h RT
pSTAT3-Y^{705}	Cell Signaling|9145	1/1000 (WB) 1/100 (IF)	O.N at 4°C
STAT3	Cell Signaling|30835	1/1000 (WB)	O.N at 4°C
CD130 Alexa 647	BD Pharmingen|564151	1/40 (FACS)	20 min at 4°C

Supplementary Table 2. RT-qPCR primers. List of forward and reverse primers used for quantitative RT-qPCR designed using Primer-Blast on GenBank sequences. All listed primer pairs are separated by at least one intron on the corresponding genomic DNA or span an exon-exon junction. h, human; m, mouse

Target Gene	GenBank sequence accession number	Forward (5'-3')	Reverse (5'-3')
hSOCS3	NM_003955.5	AGCAGCGATGGAATTACCTGGAAC	TCCAGCCCAATACCTGACACAGAA
hHGF	NM_001289458.1	TCCATGATACCACACGAACACA	GTAGCGTACCTCTGGATTGCT
mSocs3	NM_007707.3	GGGAGCCCCTTTGTAGACTT	CATCCCGGGGAGCTAGT
mCcl2	NM_011333.3	CTGCATCTGCCCTAAGGTCT	AGTGCTTGAGGTGGTTGTGG

References

[1] J. Amersfoort, G. Eelen, and P. Carmeliet, "Immunomodulation by endothelial cells — partnering up with the immune system?," *Nat Rev Immunol*, vol. 22, no. 9, Art. no. 9, Sep. 2022, doi: 10.1038/s41577-022-00694-4.

[2] L. David, C. Mallet, S. Mazerbourg, J.-J. Feige, and S. Bailly, "Identification of BMP9 and BMP10 as functional activators of the orphan activin receptor-like kinase 1 (ALK1) in endothelial cells," *Blood*, vol. 109, no. 5, pp. 1953–1961, Mar. 2007, doi: 10.1182/blood-2006-07-034124.

[3] M. Scharpfenecker *et al.*, "BMP-9 signals via ALK1 and inhibits bFGF-induced endothelial cell proliferation and VEGF-stimulated angiogenesis," *J Cell Sci*, vol. 120, no. Pt 6, pp. 964–972, Mar. 2007, doi: 10.1242/jcs.002949.

[4] B. L. Roman and A. P. Hinck, "ALK1 signaling in development and disease: new paradigms," *Cell Mol Life Sci*, vol. 74, no. 24, pp. 4539–4560, Dec. 2017, doi: 10.1007/s00018-017-2636-4.

[5] E. Tillet and S. Bailly, "Emerging roles of BMP9 and BMP10 in hereditary hemorrhagic telangiectasia," *Front Genet*, vol. 5, p. 456, 2014, doi: 10.3389/fgene.2014.00456.

[6] International PPH Consortium *et al.*, "Heterozygous germline mutations in BMPR2, encoding a TGF-beta receptor, cause familial primary pulmonary hypertension," *Nat Genet*, vol. 26, no. 1, pp. 81–84, Sep. 2000, doi: 10.1038/79226.

[7] M. E. Faughnan *et al.*, "Second International Guidelines for the Diagnosis and Management of Hereditary Hemorrhagic Telangiectasia," *Ann Intern Med*, vol. 173, no. 12, pp. 989–1001, Dec. 2020, doi: 10.7326/M20-1443.

[8] G. A. Mosquera-Klinger, K. Gálvez-Cárdenas, A. M. Valencia, G. A. Mosquera-Klinger, K. Gálvez-Cárdenas, and A. M. Valencia, "Diagnosis and treatment of patients with hereditary hemorrhagic telangiectasia (Rendu-Osler-Weber syndrome) at a university hospital in Colombia," *Revista colombiana de Gastroenterología*, vol. 34, no. 2, pp. 152–158, Jun. 2019, doi: 10.22516/25007440.280.

[9] Y.-C. Lai, K. C. Potoka, H. C. Champion, A. L. Mora, and M. T. Gladwin, "Pulmonary Arterial Hypertension," *Circulation Research*, vol. 115, no. 1, pp. 115–130, Jun. 2014, doi: 10.1161/CIRCRESAHA.115.301146.

[10] B. Lechartier, N. Berrebeh, A. Huertas, M. Humbert, C. Guignabert, and L. Tu, "Phenotypic Diversity of Vascular Smooth Muscle Cells in Pulmonary Arterial Hypertension: Implications for Therapy," *Chest*, vol. 161, no. 1, pp. 219–231, Jan. 2022, doi: 10.1016/j.chest.2021.08.040.

[11] I. M. Braverman, A. Keh, and B. S. Jacobson, “Ultrastructure and three-dimensional organization of the telangiectases of hereditary hemorrhagic telangiectasia,” *J Invest Dermatol*, vol. 95, no. 4, pp. 422–427, Oct. 1990, doi: 10.1111/1523-1747.ep12555569.
[12] A. E. Guttmacher, D. A. Marchuk, and R. I. White, “Hereditary Hemorrhagic Telangiectasia,” *N Engl J Med*, vol. 333, no. 14, pp. 918–924, Oct. 1995, doi: 10.1056/NEJM199510053331407.
[13] M. Humbert *et al.*, “Pathology and pathobiology of pulmonary hypertension: state of the art and research perspectives,” *Eur Respir J*, vol. 53, no. 1, p. 1801887, Jan. 2019, doi: 10.1183/13993003.01887-2018.
[14] M. Rabinovitch, C. Guignabert, M. Humbert, and M. R. Nicolls, “Inflammation and immunity in the pathogenesis of pulmonary arterial hypertension,” *Circ Res*, vol. 115, no. 1, pp. 165–175, Jun. 2014, doi: 10.1161/CIRCRESAHA.113.301141.
[15] H. M. Arthur and B. L. Roman, “An update on preclinical models of hereditary haemorrhagic telangiectasia: Insights into disease mechanisms,” *Front Med (Lausanne)*, vol. 9, p. 973964, Sep. 2022, doi: 10.3389/fmed.2022.973964.
[16] S. O. Park *et al.*, “Real-time imaging of de novo arteriovenous malformation in a mouse model of hereditary hemorrhagic telangiectasia,” *J Clin Invest*, vol. 119, no. 11, pp. 3487–3496, Nov. 2009, doi: 10.1172/JCI39482.
[17] J. H. Thalgott *et al.*, “Decreased Expression of Vascular Endothelial Growth Factor Receptor 1 Contributes to the Pathogenesis of Hereditary Hemorrhagic Telangiectasia Type 2,” *Circulation*, vol. 138, no. 23, pp. 2698–2712, Dec. 2018, doi: 10.1161/CIRCULATIONAHA.117.033062.
[18] A. Guilhem, P. Portalès, S. Dupuis-Girod, S. Rivière, and T. Vincent, “Altered expressions of CXCR4 and CD26 on T-helper lymphocytes in hereditary hemorrhagic telangiectasia,” *Orphanet J Rare Dis*, vol. 16, no. 1, p. 511, Dec. 2021, doi: 10.1186/s13023-021-02139-y.
[19] E. Torsney, R. Charlton, D. Parums, M. Collis, and H. M. Arthur, “Inducible expression of human endoglin during inflammation and wound healing in vivo,” *Inflamm Res*, vol. 51, no. 9, pp. 464–470, Sep. 2002, doi: 10.1007/pl00012413.
[20] E. Rossi *et al.*, “Endothelial endoglin is involved in inflammation: role in leukocyte adhesion and transmigration,” *Blood*, vol. 121, no. 2, pp. 403–415, Jan. 2013, doi: 10.1182/blood-2012-06-435347.
[21] D. Zhao *et al.*, “ALK1 signaling is required for the homeostasis of Kupffer cells and prevention of bacterial infection,” *J Clin Invest*, vol. 132, no. 3, Feb. 2022, doi: 10.1172/JCI150489.
[22] R. Szulcek *et al.*, “Exacerbated inflammatory signaling underlies aberrant response to BMP9 in pulmonary arterial hypertension lung endothelial cells,” *Angiogenesis*, vol. 23, no. 4, p. 699, 2020, doi: 10.1007/s10456-020-09741-x.
[23] W. Tian *et al.*, “Phenotypically Silent Bone Morphogenetic Protein Receptor 2 Mutations Predispose Rats to Inflammation-Induced Pulmonary Arterial Hypertension by Enhancing the Risk for Neointimal Transformation,” *Circulation*, vol. 140, no. 17, pp. 1409–1425, Oct. 2019, doi: 10.1161/CIRCULATIONAHA.119.040629.
[24] Y. Tamura *et al.*, “Ectopic upregulation of membrane-bound IL6R drives vascular remodeling in pulmonary arterial hypertension,” *Journal of Clinical Investigation*, vol. 128, no. 5, pp. 1956–1970, May 2018, doi: 10.1172/JCI96462.
[25] C. Bouvard *et al.*, “Different cardiovascular and pulmonary phenotypes for single- and double-knock-out mice deficient in BMP9 and BMP10,” *Cardiovasc Res*, vol. 118, no. 7, pp. 1805–1820, Jun. 2022, doi: 10.1093/cvr/cvab187.
[26] A. Desroches-Castan *et al.*, “Bone Morphogenetic Protein 9 Is a Paracrine Factor Controlling Liver Sinusoidal Endothelial Cell Fenestration and Protecting Against Hepatic Fibrosis,” *Hepatology*, vol. 70, no. 4, pp. 1392–1408, Oct. 2019, doi: 10.1002/hep.30655.
[27] N. Ricard *et al.*, “BMP9 and BMP10 are critical for postnatal retinal vascular remodeling,” *Blood*, vol. 119, no. 25, pp. 6162–6171, Jun. 2012, doi: 10.1182/blood-2012-01-407593.
[28] S. Rose-John, “IL-6 trans-signaling via the soluble IL-6 receptor: importance for the pro-inflammatory activities of IL-6,” *Int J Biol Sci*, vol. 8, no. 9, pp. 1237–1247, 2012, doi: 10.7150/ijbs.4989.

[29] F. Schaper and S. Rose-John, “Interleukin-6: Biology, signaling and strategies of blockade,” *Cytokine Growth Factor Rev*, vol. 26, no. 5, pp. 475–487, Oct. 2015, doi: 10.1016/j.cytogfr.2015.07.004.
[30] T. C. Barnes, M. E. Anderson, and R. J. Moots, “The Many Faces of Interleukin-6: The Role of IL-6 in Inflammation, Vasculopathy, and Fibrosis in Systemic Sclerosis,” *International Journal of Rheumatology*, vol. 2011, p. e721608, Sep. 2011, doi: 10.1155/2011/721608.
[31] X. Hu, J. Li, M. Fu, X. Zhao, and W. Wang, “The JAK/STAT signaling pathway: from bench to clinic,” *Sig Transduct Target Ther*, vol. 6, no. 1, pp. 1–33, Nov. 2021, doi: 10.1038/s41392-021-00791-1.
[32] G. Kaplanski, V. Marin, F. Montero-Julian, A. Mantovani, and C. Farnarier, “IL-6: a regulator of the transition from neutrophil to monocyte recruitment during inflammation,” *Trends in Immunology*, vol. 24, no. 1, pp. 25–29, Jan. 2003, doi: 10.1016/S1471-4906(02)00013-3.
[33] S. A. Jones and B. J. Jenkins, “Recent insights into targeting the IL-6 cytokine family in inflammatory diseases and cancer,” *Nat Rev Immunol*, vol. 18, no. 12, pp. 773–789, Dec. 2018, doi: 10.1038/s41577-018-0066-7.
[34] R. M. Gibson, W. P. Schiemann, L. B. Prichard, J. M. Reno, L. H. Ericsson, and N. M. Nathanson, “Phosphorylation of human gp130 at Ser-782 adjacent to the Di-leucine internalization motif. Effects on expression and signaling,” *J Biol Chem*, vol. 275, no. 29, pp. 22574–22582, Jul. 2000, doi: 10.1074/jbc.M907658199.
[35] S. Radtke *et al.*, “Cross-regulation of cytokine signalling: Pro-inflammatory cytokines restrict IL-6 signalling through receptor internalisation and degradation,” *Journal of cell science*, vol. 123, pp. 947–59, Mar. 2010, doi: 10.1242/jcs.065326.
[36] P. C. Heinrich, I. Behrmann, S. Haan, H. M. Hermanns, G. Müller-Newen, and F. Schaper, “Principles of interleukin (IL)-6-type cytokine signalling and its regulation,” *Biochem J*, vol. 374, no. Pt 1, pp. 1–20, Aug. 2003, doi: 10.1042/BJ20030407.
[37] M. Lindkvist, M. M. Zegeye, M. Grenegård, and L. U. Ljungberg, “Pleiotropic, Unique and Shared Responses Elicited by IL-6 Family Cytokines in Human Vascular Endothelial Cells,” *Int J Mol Sci*, vol. 23, no. 3, p. 1448, Jan. 2022, doi: 10.3390/ijms23031448.
[38] P. K. Chatterjee, Y. Al-Abed, B. Sherry, and C. N. Metz, “Cholinergic agonists regulate JAK2/STAT3 signaling to suppress endothelial cell activation,” *Am J Physiol Cell Physiol*, vol. 297, no. 5, pp. C1294–C1306, Nov. 2009, doi: 10.1152/ajpcell.00160.2009.
[39] A. Yoshimura, M. Ito, S. Mise-Omata, and M. Ando, “SOCS: negative regulators of cytokine signaling for immune tolerance,” *International Immunology*, vol. 33, no. 12, pp. 711–716, Dec. 2021, doi: 10.1093/intimm/dxab055.
[40] H. Qin *et al.*, “TGF-β Promotes Th17 Cell Development through Inhibition of SOCS31,” *The Journal of Immunology*, vol. 183, no. 1, pp. 97–105, Jul. 2009, doi: 10.4049/jimmunol.0801986.
[41] C. Dees *et al.*, “TGF-β-induced epigenetic deregulation of SOCS3 facilitates STAT3 signaling to promote fibrosis,” *J Clin Invest*, vol. 130, no. 5, pp. 2347–2363, May 2020, doi: 10.1172/JCI122462.
[42] J. Roes, B. K. Choi, and B. B. Cazac, “Redirection of B cell responsiveness by transforming growth factor β receptor,” *Proceedings of the National Academy of Sciences*, vol. 100, no. 12, pp. 7241–7246, Jun. 2003, doi: 10.1073/pnas.0731875100.
[43] A. C. Lovibond, S. J. Haque, T. J. Chambers, and S. W. Fox, “TGF-beta-induced SOCS3 expression augments TNF-alpha-induced osteoclast formation,” *Biochem Biophys Res Commun*, vol. 309, no. 4, pp. 762–767, Oct. 2003, doi: 10.1016/j.bbrc.2003.08.068.
[44] X. Liu, Y. Zhang, Y. Yu, X. Yang, and X. Cao, “SOCS3 promotes TLR4 response in macrophages by feedback inhibiting TGF-β1/Smad3 signaling,” *Molecular Immunology*, vol. 45, no. 5, pp. 1405–1413, Mar. 2008, doi: 10.1016/j.molimm.2007.08.018.
[45] S. Gallo, V. Sala, S. Gatti, and T. Crepaldi, “HGF/Met Axis in Heart Function and Cardioprotection,” *Biomedicines*, vol. 2, no. 4, Art. no. 4, Dec. 2014, doi: 10.3390/biomedicines2040247.
[46] J. Fu *et al.*, “HGF/c-MET pathway in cancer: from molecular characterization to clinical evidence,” *Oncogene*, vol. 40, no. 28, Art. no. 28, Jul. 2021, doi: 10.1038/s41388-021-01863-w.

[47] M. Rottenberg and B. Carow, “SOCS3, a Major Regulator of Infection and Inflammation,” *Frontiers in Immunology*, vol. 5, 2014, Accessed: Aug. 26, 2023. [Online]. Available: https://www.frontiersin.org/articles/10.3389/fimmu.2014.00058
[48] A. Desroches-Castan *et al.*, “Differential Consequences of Bmp9 Deletion on Sinusoidal Endothelial Cell Differentiation and Liver Fibrosis in 129/Ola and C57BL/6 Mice,” *Cells*, vol. 8, no. 9, p. 1079, Sep. 2019, doi: 10.3390/cells8091079.
[49] L. A. Johnson and D. G. Jackson, “Inflammation-induced secretion of CCL21 in lymphatic endothelium is a key regulator of integrin-mediated dendritic cell transmigration,” *International Immunology*, vol. 22, no. 10, pp. 839–849, Oct. 2010, doi: 10.1093/intimm/dxq435.
[50] A. Bonaventura and F. Montecucco, “CCL23 is a promising biomarker of injury in patients with ischaemic stroke,” *Journal of Internal Medicine*, vol. 283, no. 5, pp. 476–478, 2018, doi: 10.1111/joim.12742.
[51] K. Inoue, T. Kodama, and H. Daida, “Pentraxin 3: A Novel Biomarker for Inflammatory Cardiovascular Disease,” *Int J Vasc Med*, vol. 2012, p. 657025, 2012, doi: 10.1155/2012/657025.
[52] G. B. Morrow, C. S. Whyte, and N. J. Mutch, “A Serpin With a Finger in Many PAIs: PAI-1’s Central Function in Thromboinflammation and Cardiovascular Disease,” *Frontiers in Cardiovascular Medicine*, vol. 8, 2021, Accessed: Jun. 09, 2023. [Online]. Available: https://www.frontiersin.org/articles/10.3389/fcvm.2021.653655
[53] Y. Gong, E. Hart, A. Shchurin, and J. Hoover-Plow, “Inflammatory macrophage migration requires MMP-9 activation by plasminogen in mice,” *J Clin Invest*, vol. 118, no. 9, pp. 3012–3024, Sep. 2008, doi: 10.1172/JCI32750.
[54] L. Tu *et al.*, “Selective BMP-9 Inhibition Partially Protects Against Experimental Pulmonary Hypertension,” *Circ Res*, vol. 124, no. 6, pp. 846–855, Mar. 2019, doi: 10.1161/CIRCRESAHA.118.313356.
[55] L. Long *et al.*, “Selective enhancement of endothelial BMPR-II with BMP9 reverses pulmonary arterial hypertension,” *Nat Med*, vol. 21, no. 7, pp. 777–785, Jul. 2015, doi: 10.1038/nm.3877.
[56] M. Bisserier *et al.*, “Combination Therapy with STAT3 Inhibitor Enhances SERCA2a-Induced BMPR2 Expression and Inhibits Pulmonary Arterial Hypertension,” *International Journal of Molecular Sciences*, vol. 22, no. 17, p. 9105, Jan. 2021, doi: 10.3390/ijms22179105.
[57] R. Paulin *et al.*, “Signal Transducers and Activators of Transcription-3/Pim1 Axis Plays a Critical Role in the Pathogenesis of Human Pulmonary Arterial Hypertension,” *Circulation*, vol. 123, no. 11, pp. 1205–1215, Mar. 2011, doi: 10.1161/CIRCULATIONAHA.110.963314.
[58] S. S. Pullamsetti, W. Seeger, and R. Savai, “Classical IL-6 signaling: a promising therapeutic target for pulmonary arterial hypertension,” *J Clin Invest*, vol. 128, no. 5, pp. 1720–1723, doi: 10.1172/JCI120415.
[59] Z. Chen and Z. C. Han, “STAT3: a critical transcription activator in angiogenesis,” *Med Res Rev*, vol. 28, no. 2, pp. 185–200, Mar. 2008, doi: 10.1002/med.20101.
[60] K. Middleton, J. Jones, Z. Lwin, and J. I. G. Coward, “Interleukin-6: An angiogenic target in solid tumours,” *Critical Reviews in Oncology/Hematology*, vol. 89, no. 1, pp. 129–139, Jan. 2014, doi: 10.1016/j.critrevonc.2013.08.004.

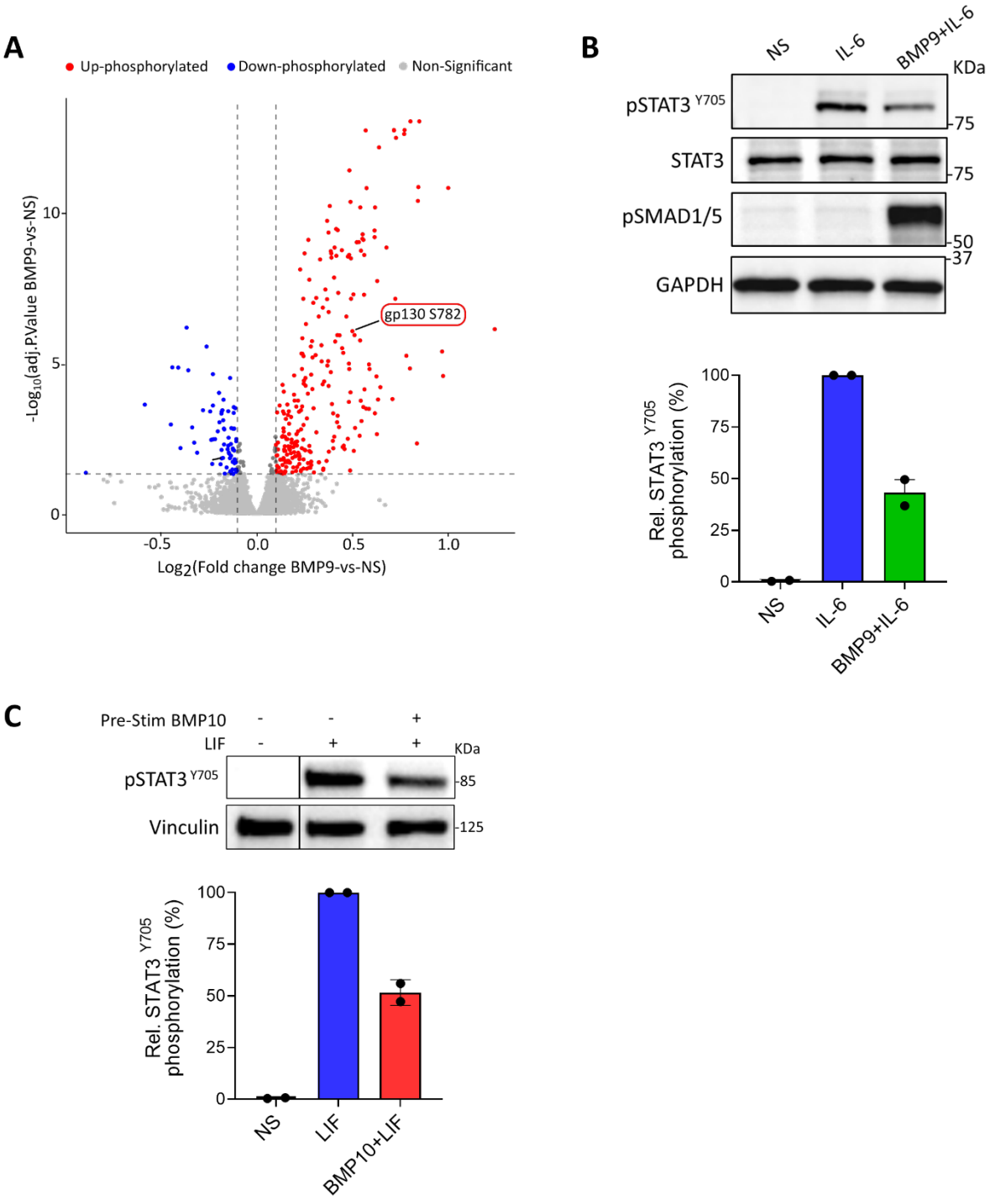

Fig. S1. BMP9 and BMP10 negatively regulate IL-6- and LIF-induced STAT3 pathway in HUVECs, respectively (**A**) Volcano plot taken from manuscript 1 representing the log2 fold change in the abundance of phosphopeptides plotted against the $-\log_{10}$ adj. *P*.value, showing differentially phosphorylated sites which are down-regulated (blue) or up-regulated (red) in response to BMP9 stimulation, while highlighting gp130-S^{782}. (**B**) Cells were pre-stimulated or not with BMP9 (10ng/mL) for 30 min, followed by stimulation with IL-6 (100ng/mL) for 15 min. Cell extracts were subjected to WB analysis using the indicated antibodies. Relative STAT3 phosphorylation (pSTAT3/STAT3) is expressed as mean + SEM (n=2 independent experiments, normalised to IL-6 vehicle condition). (**C**) Cells were pre-stimulated or not with BMP10 (10ng/mL) for 30 min, followed by stimulation with LIF (50ng/mL) for 15 min. Cell extracts were subjected to WB analysis using the indicated antibodies. Relative STAT3 phosphorylation (pSTAT3/Vinculin) is expressed as mean + SEM (n=2 independent experiments, normalised to LIF vehicle condition).

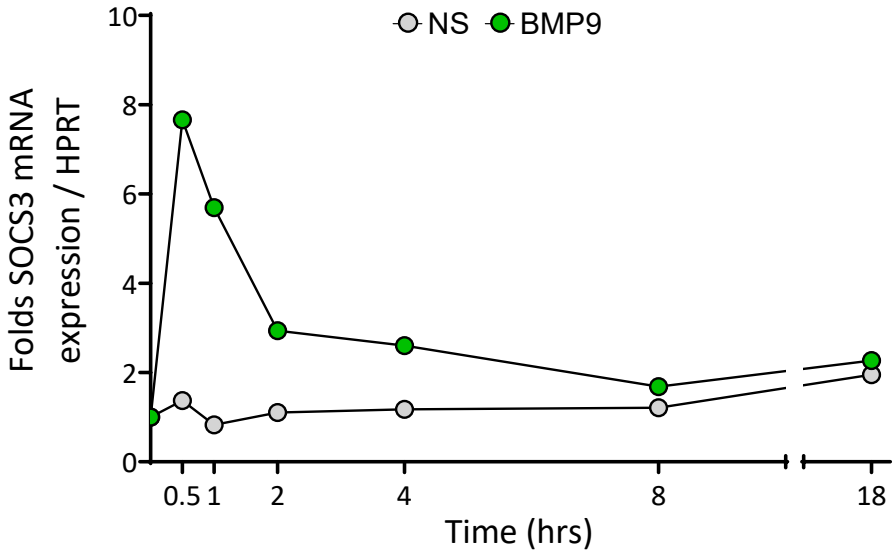

Fig. S2. BMP9 increases SOCS3 expression. HUVECs were stimulated with BMP9 or not (NS) for the indicated time points, and SOCS3 mRNA expression was then assessed by RT-qPCR. The level of SOCS3 expression was normalized to HPRT and represented as fold induction of each NS and BMP10 stimulated sample relative NS 0 min (n=1 experiment).

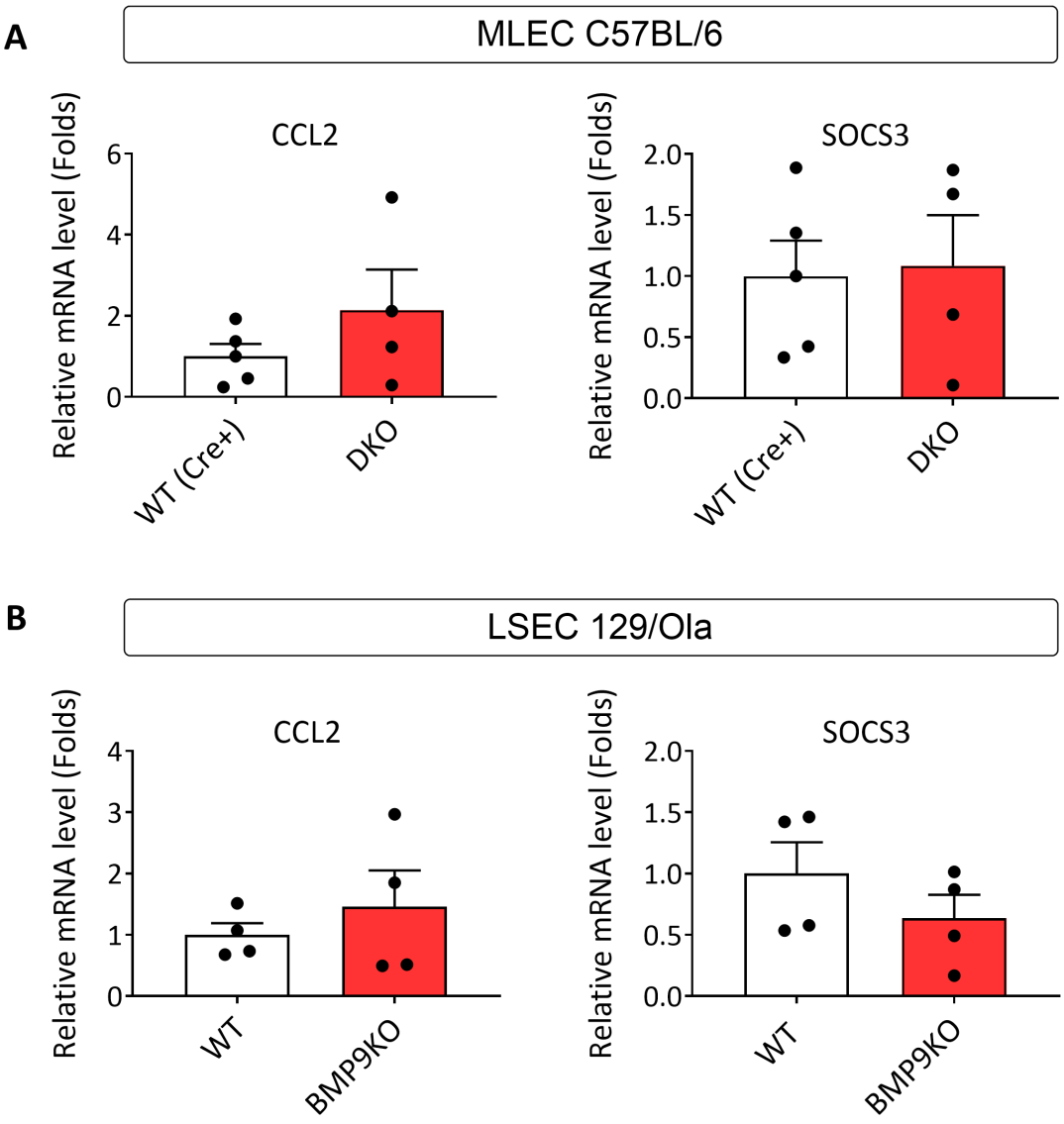

Fig. S3. Assessment of CCL2 and SOCS3 mRNA level in mouse lung EC and liver sinusoidal EC from
(**A**) Mouse lung endothelial cells (MLEC) were isolated from lungs of C57BL/6 DKO (lacking both BMP9 and BMP10) and WT mice as described in the materials and methods section. RT-qPCR analysis was then performed to determine mRNA expression levels of Ccl2 and Socs3, which was normalized to Rpl13 house keeping gene using 2-ΔΔCt method, and presented as fold induction (DKO-vs-WT) ± SEM (n=5 WT and n=4 DKO). (**B**) Liver sinusoidal endothelial cells (LSEC) were isolated from Ola BMP9-/- and WT mice as previously described [28]. RT-qPCR analysis was then performed to determine mRNA expression levels of Ccl2 and Socs3 as described in A, and data presented as fold induction (Bmp9KO-vs-WT) ± SEM (n=4 WT and n=4 Bmp9KO).

6.4 Further Discussion/Other Preliminary data

6.4.1 Classic vs Trans IL-6 Signaling

IL-6 exerts its effects on target cells by binding with its membrane-bound receptor (IL-6R), leading to the recruitment of the ubiquitously expressed signal-transducing gp130 receptor. This mechanism is known as IL-6 classic signaling, which mainly occurs in cells expressing the membrane-bound IL-6R including hepatocytes, macrophages, neutrophils, and certain subsets of T cells [644]. However, these cells can also release soluble IL-6 receptor molecules (sIL-6R) into the bloodstream, primarily through processes like extracellular shedding or alternative splicing [645–647]. Consequently, IL-6 can bind to sIL-6R, promoting intracellular signaling via gp130 in cells lacking the membrane-bound IL-6R, a signaling mode known as IL-6 trans-signaling [648, 649]. For instance, ECs exhibit minimal expression of IL-6R compared to other cell types, and several studies have demonstrated that IL-6 alone induces only modest and sometimes no response without the addition of IL-6R [650–654]. These findings were further confirmed under our experimental conditions, where we showed that using low concentrations of IL-6 (10ng/mL) is not enough to activate STAT3 signaling, and that higher concentrations (50-100ng/mL) were needed. Notably, in addition to STAT3, IL-6 trans-signaling has shown to activate AKT and ERK pathways in ECs [652, 654]. Very recent work by Song et al demonstrated a computational model, which was validated experimentally, and that could be used for predicting the activation of STAT3, AKT and ERK in response to IL-6 classic and/or trans-signaling in ECs (work under review) [655]. The authors demonstrated that IL-6 trans-signaling results in a stronger downstream signaling and plays a dominant role in the overall effects from IL-6, which have been also shown by other groups [650–654, 656, 657]. IL-6 trans-signaling and therapeutic strategies targeting this pathway has been very recently reviewed by John et al [658]. In general, classic IL-6 signaling plays roles in homeostasis and acute inflammatory functions, whilst trans-signaling is more associated with inflammation and tissue damage in various pathological conditions, including chronic inflammatory diseases.

6.4.2 BMP10 Regulates Signal transduction of other IL-6 family cytokines

Gp130 family of cytokines, also called IL-6 family, includes several inflammatory cytokines. These include IL-6 itself, in addition to IL-11, IL-31, LIF, CNTF, CT-1, and OSM [256]. It has been shown that HUVECs are responsive to the majority of these cytokines, and that OSM, in addition to the STAT3 pathway, can activate other signaling pathways such PI3K/AKT and ERK MAPK signaling [653]. I have already performed an experiment showing that BMP10 affects not only IL-6 but also other cytokines of this family including OSM and LIF. STAT3 pathway was activated by OSM, LIF and IL-6, whereas activation of AKT and ERK pathways was only clearly observed with OSM (Fig), consistent with previously published data [653]. Surprisingly, pre-stimulation with BMP10 attenuated OSM-induced AKT and ERK, but not STAT3. Notably,

attenuation of AKT and ERK were more pronounced at lower OSM concentrations. Moreover, BMP10 attenuated both LIF and IL-6-induced STAT3 activation, but the attenuation of LIF response was stronger when lower LIF concentrations were used. These results allowed us to draw out three main conclusions: (1) different IL-6 family members induce different downstream signaling (STAT3, AKT and ERK), (2) the potency of the signals obtained clearly depends on the concentration of the cytokines and (3) importantly, at very high concentrations of OSM and LIF, BMP10 exhibited limited efficacy in attenuating their downstream signaling. Thus, it would be important to determine the optimal concentrations that should be used in order to better understand the regulation of other IL-6 family cytokines by BMP10 in ECs.

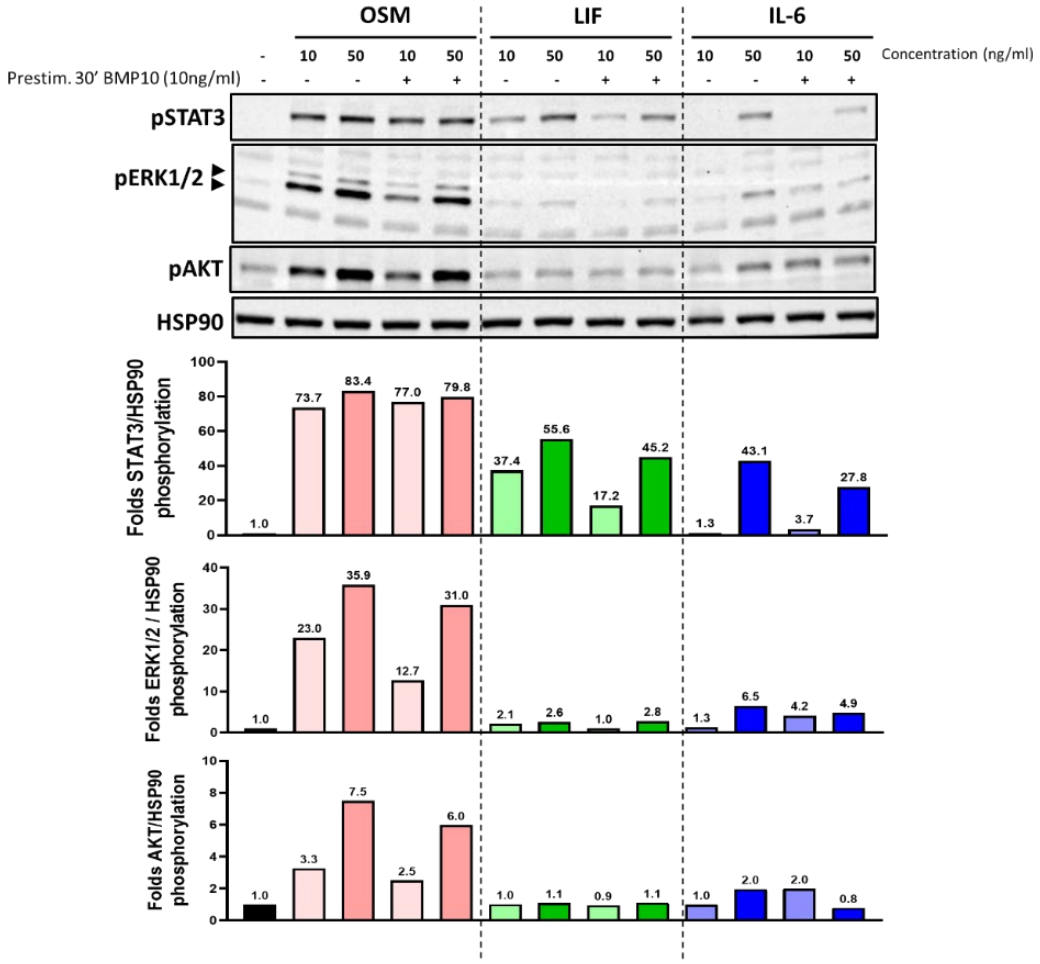

Figure 33. BMP10 regulation of OSM, LIF, and IL-6 Signaling in HUVECs.

HUVECs were pre-stimulated or not with BMP10 (10ng/mLfor 30 min, followed by stimulation with 10 or 50 ng/mL OSM, LIF or IL-6, OSM, or for 15 min. Cell extracts were subjected to WB analysis using the indicated antibodies. Phosphorylation of STAT3, AKT and ERK was calculated using pProtein/HSP90 ratio and is expressed as fold induction relative to non stimulated stimulated cells. This experiment is n=1.

Chapter 7. General Discussion

In this section, I will talk about few technical points used in this study and discuss the general findings of my thesis work.

7.1 Choice of HUVECs as an EC model

Since their isolation in 1973, HUVECs constituted the most commonly used primary non-immortalized EC model system for studying vascular biology *in-vitro* in both normal and pathological conditions [14, 15]. HUVECs possess the advantage of being more readily accessible compared to other types of ECs. They express crucial endothelial markers and pivotal signaling molecules linked to vascular physiology. Furthermore, HUVECs have exhibited responsiveness to various physiological and pathological stimuli, including angiogenic factors, high glucose, inflammatory cytokines, and shear stress [659]. Hence, these cells enable the study of how ECs respond to diverse stimuli or treatments to understand their impact on endothelial functions such as migration, proliferation, and tube formation. At the time of writing this manuscript, PubMed displayed over 21,000 search outcomes related to "HUVEC", displaying a significantly higher utilization in comparison to other EC types such as "HMVEC","HAEC","ECFC", etc. However, it is important to note HUVECs are cells originating from atypical veins (which carry oxygenated blood), and thus represent a very exceptional EC type. Moreover, ECs exhibit significant heterogeneity, which refers to variations in their characteristics, functions, and molecular profiles across different vascular beds and physiological conditions [660]. As such, for obtaining relevant data interpretation, considering EC heterogeneity is of crucial importance when designing and conducting certain experimental setups. In my project, my aim is to examine how BMP9 and BMP10 influence the global phosphoproteome in ECs. For this, we selected HUVECs due to their widespread use, accessibility, and ease of culture. After identifying regulated pathways in HUVECs, it will be interesting to verify their regulation in other EC models available in our lab, including ECFCs and HMVECs.

7.2 Choice of ligand

To date, BMP9 and BMP10 stands as the only identified ligands for ALK1 [305]. Although both ligands shares high sequence similarity within their growth factor domain, they exhibit different binding affinities to the type-II receptors [343] and display both redundant and specific roles *in-vivo* [47]. Notably, microarray experiments revealed that pd-BMP9 and pd-BMP10 induced highly similar transcriptional regulation, suggesting that they act as functionally equivalent ALK1 ligands *in-vitro* on endothelial cells [325], which was further supported by recent unpublished RNA-seq analysis performed in our lab using BMP9 and BMP10-stimulated ECFCs and HMVECs (Al Tabosh et al., under revision). Nevertheless, to the best of my knowledge, there are no published studies that evaluate the phosphoproteomic responses induced by these ligands in any cell type. Therefore, at the beginning of my PhD

project, we aimed to address the global phosphoproteomic responses of HUVECs to both BMP9 and BMP10 individually, rather than prioritizing one over the other. However, after obtaining and analyzing the phosphopoteomic results, we found that both ligands displayed very highly similar phosphoproteomic profiles under our experiment conditions (Chapter 5, Fig. 2C). Since BMP10 is much less studied in comparison to BMP9, we proceeded to do all subsequent validation and functional assays using BMP10 as the chosen ligand, and anytime we checked, we found that BMP9 led to a similar response as that of BMP10.

7.3 Stimulation duration

Phosphoproteomic events generally occur more rapidly in response to extracellular stimuli compared to transcriptomic responses. Therefore, our objective was to select a time point that captures relatively rapid and direct responses, with limited changes in the total proteome. However, selecting this time point was a challenge, as there is limited knowledge regarding non canonical pathways and downstream phosphoproteomic dynamics, apart from the canonical SMAD pathway, associated with these BMP9 and BMP10. Moreover, while we would capture certain phosphoproteomic responses at a chosen time point, it's highly likely that we might miss others. An ideal approach in this case would be to conduct kinetic phosphoproteomic profiling, examining responses across various time points post ligand stimulation. However, considering our desire to use TMT-16 plex labeling approach (described in Chapter 4) with five biological replicates per group (non-stimulated, BMP9-stimulated and BMP10-stimulated groups), a single time point selection necessitated the use 15 out of the 16 available labels. Consequently, conducting a kinetic study would have required a complex experimental design and high cost. As a result, we decided to focus on a single time point. Under our experimental conditions, BMP9/BMP10-induced SMAD1/5 phosphorylation started as early as 5 minutes and attained a plateau after around 30 minutes (Chapter 5, Fig. 4A). Thus, we considered that selecting the 30-minute time point would coincide with a significant activation of BMP9 and BMP10 signaling in ECs. To gain a deeper overview of the dynamic regulation of these phosphorylation events, identified targets were further validated through kinetic western blot analysis (Chapter 5, Fig. 4A). Interestingly, this kinetic analysis, spanning 5 minutes to 4 hours, revealed that the activation of P38 MAPK and the phosphorylation of Eps15 and HSP27 by BMP10 became evident only after 30 mins. However, we demonstrated that, even using a relatively short time-frame of 30 minutes, it was sufficient to trigger the phosphorylation of these non-canonical targets through a transcription-dependent mechanism (will be further discussed in section 7.7).

7.4 BMP dose

In this work, the concentration of BMP9 or BMP10 used is 10ng/mL, which is considered relatively high in comparison to EC_{50} of these ligands (~ 50pg/mL) in HMVEC-l [305]. However, we hypothesized that, while low concentrations such as 1ng/mL are enough to induce a strong phosphorylation of SMAD1/5 [306], higher concentrations might be required to activate other

non-canonical pathways. For instance, BMP9-induced pSMAD2 in ECs was only detectable at BMP9 concentrations ≥ 1ng/mL [112, 349]. Moreover, the 10ng/mL dose is considered physiologically relevant, as it falls within the normal 2 to 12ng/mL range of circulating active BMP9 that was determined by our group using human sera and plasma samples [348]. Importantly, we have later conducted experiments to establish the dose-response activation of the identified targets in our study. Our results showed that, as low as 0.1 ng/mL, BMP10 was enough to induce a modest response, and this response was indeed significantly higher at concentrations ≥ 1ng/mL (Chapter 5, Fig. S3).

7.5 Choice of the Lysis buffer and MS-phosphoprotemic Approach

At the beginning of this project, we were first optimizing the conditions to be used for our MS analysis by testing 4 different lysis buffers. After several experiments performed, we selected Urea lysis buffer which was the most compatible with the MS experimental workflow to be used. In the first year, we performed two independents label-free quantififcation (LFQ) MS phosphoproteomic analyses using BMP10 (first year) and BMP9 (beginning of the 2nd year). From both analyses, we obtained between 2000-3000 identified and quantified phosphosites, out of which we got 89 which differentially phosphorylated by BMP10 vs 81 by BMP9. Moreover, we didn't not obtain phosphorylation of SMADs in both analyses, which is a positive control to validate our approach. Among the obtained differentially phosphorylated sites, only four had phosphospecific antibodies, and we were able to validate only one phosphosite, NIPA ^{S354} (nuclear interacting partner of anaplastic lymphoma kinase), which has been associated in the regulation of G2/M phase of the cell cycle in non-ECs [661, 662]. After several experiments conducted, we were not able to find a clear story/function of this site in ECs (data not shown). Given the surprising low overlap obtained between BMP9 and BMP10 differentially phosphorylated sites (likely because the two experiments and MS analysis were performed independently), in addition our limited findings from these analyses, we decided at the end of the 2nd year to perform TMT labeling approach using both BMP9 and BMP10. The aims were: (1) have a deeper coverage of the phosphoproteome, (2) perform analysis using both BMP9 and BMP10 from the same experiment, and (3) multiplexing to reduce technical variability originating from the experimental workflow. This analysis allowed us to identify and quantify 12779 phosphosites, with 418 differentially regulated sites by BMP9 and/or BMP10, among which we identified phosphorylation of SMAD1, thus validating our approach.

7.6 Experimental approaches for data validation

Validation of phosphoproteomic data has been a real challenge throughout this project, which is always the case in such type of analysis (section 4.3). Among all the DPS obtained, only very few (8/419) had commercially available antibodies that we could buy, and 7/419 sites had home-made raised antibodies (Table 3). Hence, our options for data validation were very limited. This is in contrast to other high-throughput analysis like RNAseq analysis, where designing primers for validating differentially regulated genes is often achievable. I have tried

to validate several interesting targets selected from the phosphoproteomic study, using different experimental approaches using phospho-specific antibodies (if applicable), IP followed by pan pSer WB analysis, proximity ligation assay (PLA), *in-vitro* kinase assays and Phos-tag gels [663] (Table 3). We did not manage to obtain a quantifiable signal with 2 out of 7 commercially available antibodies (Table 3), even when used with a positive control (data not shown). Nevertheless, our MS analysis seem to be reliable as, among the tested antibodies, we were able to validate 3/5 sites with commercial antibodies and 2/3 with home-made antibodies. Moreover, it is important to note that even if the antibody works, the sensitivity of the MS is known to be higher compared to WB analysis [664]. This suggests that many proteins might be truly phosphorylated, but their detection requires higher sensitive technologies such as MS analysis.

Table 3. List of experimental approaches for validating few selected TMT Phosphoproteomic Hits

Protein	Phosphoproteomic Result (BMP9/10_vs_NS)	Phospho-Antibody	Classical WB	IP ---> WB pSer or site-specific Ab	PLA (pSer + Protein qntibody)	Phosphotag gels
SMAD1	S462/463/465	+				
P38	Y182	+				
Eps15	S796	§				
HSP27	S15	+				
	S82	+				
	S83	+				
MSK2	S682	-				
	T687	+				
Gp130	S782	+				
NELF-E	S115	-				
ERG	S276	-				
	S215	#				
GIGYF1/2	S157 (GIGYF1) = S160 (GIGYF2)	-				
	S638 (GIGYF1)	-				
BRF1/2	S54 (BRF1/2)	*				
	S334 (BRF1) = S334 (BRF2)	*				
HES1	S12	-				
AHNAK	S5782	+				
ATR	S435	PMID 8094871				
	S437	PMID 24950377				
MORC2	S739	PMID 25888627				
	S743	-				

⁺ Commercially avaialble; ⁻ Not available; §, #, * Commercially unavailable but kindly provided by Hiroaki Sakurai, Peter Hollenhorst and Nadia Cherradi, respectively.

Phosphosites: **S** = Serine, **T** = Threonine, **Y** = Tyrosine; **Red** = increased DPS, **Blue** = decreased DPS

Green box = Validation, **red box** = no signal/ Experiment didn't work, **orange box** = Antibody didn't work even with positive control, **grey box** = Not tested

7.7 Activation of Direct and Indirect pathways by BMP9/10 signaling in ECs

One of the major findings of this work is the capability of BMP9 and BMP10 to activate both direct and indirect pathways in ECs. The direct canonical pathway involves the rapid phosphorylation of SMAD1/5, starting as early as 5 minutes, and reaching a plateau within 30 minutes, essential for inducing direct BMP target genes like *ID1* and *SMAD6*. In addition to these latter, I have identified two other genes which are rapidly induced by BMP9 and BMP10: GADD45β and SOCS3. These transcriptional processes were responsible for mediating BMP10 regulation of P38 MAPK and STAT signaling in ECs.

GADD45β mediated non-canonical P38 pathway activation by BMP10. Importantly, we showed that blocking P38 had no impact on SMAD1/5 phosphorylation and downstream direct target gene induction of *ID1* and *SMAD6*, but significantly attenuated *SELE*, *PTGS2*, and *HAS2* expression by BMP10. Thus, these results define two sets of BMP10 target genes: SMAD dependent and SMAD- and P38-codependent genes. On the other hand, SOCS3 induction by BMP10 led to the inhibition of IL-6 JAK/STAT3 signaling in ECs.

It is interesting to mention that another transcriptional step has already been described in response to BMP9 in ECs. It has been shown that BMP9 and BMP10 induced rapid (within 1 h) expression of SGK1 (Serum/glucocorticoid-regulated kinase 1) mRNA in HUAEC [390]. Subsequent findings by another group demonstrated that SGK1 synthesis by BMP9 mediates the activation of the mTORC1/p70S6K/S6 axis, starting at 2h post BMP9 stimulation, which induced protein synthesis in ECs [391]. In our study, we have identified differential phosphorylation P70S6K-S^{447} by both BMP9 and BMP10, however we were not able to validate neither SGK1 induction nor P70S6K-S^{447} phosphorylation under our experimental conditions (data not shown). However, it has been shown that defective BMP9/BMP10 signaling in HHT leads to over-activation of the PI3K-AKT pathway though increased phosphorylation of AKT, NDRG1 and S6 (downstream target of P70S6K) in cutaneous telangiectasia biopsies from HHT2 patients and vascular lesions in HHT mouse models [385–387] so it will be important in the future to further study this pathway.

Chapter 8. Perspectives

8.1 Further *in-vitro* characterization of new identified pathways induced by BMP9/BMP10 and their potential roles in ECs

8.1.1 Regulation of New identified Pathways by other BMPs and in other cell types

After highlighting the activation of P38 MAPK signaling and attenuation of IL-6/JAK STAT3 by BMP10, and probably by BMP9, and showing that both pathways rely on SMAD signaling and transcriptional events, it would be interesting to test whether these pathways and their associated mechanisms are also regulated by other BMPs (e.g. BMP2, BMP4, BMP6, etc...). This can be tested in different EC types (HAECs, HMVECs, ECFCs) or even in non-ECs which can respond to BMP9 and BMP10 such as Kupffer cells [330] , C2C12 [665], and embryonic stem cells [666]. This latter would help to highlight the cell-context dependency of the activated pathways by BMP9 and BMP10 in ECs vs non-ECs (direct vs indirect pathways and dependency on SMAD-signaling).

8.1.2 The role of P38 signaling in BMP10-induced Transcriptional Responses in ECs

BMP10 induces the activation of the canonical SMAD signaling (direct pathway), which induces rapid expression of several direct target genes, including GADD45β. This, in turn, leads to the activation of P38 signaling (indirect pathway). Importantly, we showed that activation of P38 plays an important role in the expression of some BMP10 target genes (*SELE*, HAS2, and *PTGS2*). These results suggest that transcriptional responses by BMP10 in ECs are at least partially mediated through activation of the P38 pathway. Therefore, to investigate which BMP10 target genes are P38-dependent, a potential approach would be to perform RNA-sequencing on cells where P38 signaling is disrupted using siRNA or P38 inhibitors. First, it would be important to determine the lowest effective dose of the siRNA or the inhibitor that can block P38 signaling with minimal off-target effects. Then, cells can be pre-treated with the selected dose of siP38 or P38 inhibitor, followed by BMP10 stimulation. This analysis would highlight gene clusters which are regulated by BMP10 in a P38-depdenent manner. These genes can then be validated by qpCR and WB analysis, followed by confirming their roles In ECs using appropriate functional approaches.

8.1.3 Assessing the roles of BMP10-induced phosphorylation of Eps15-S^{796} and HSP27-S$^{78/82}$

8.1.3.1 Eps15

Eps15, and its homolog Eps15R, are endocytic adaptors that play important roles in endocytosis [579, 580]. Interestingly, two previous studies highlighted that Eps15R interacts

with BMPRII [127] and SMAD1 [584], with this latter potentiating SMAD signaling in animal caps. Given the high similarity in the sequence and functional domains of Eps15 and Eps15R [581], this suggests that Eps15 may also play a role in the context of BMP10 signaling and endocytosis of its receptors. To this end, several experiments can be performed, which are briefly explained below.

a. First, we can check if Eps15 and ALK1 or the type-II receptor BMPR2 interact with each other. This can be first performed using overexpression of HA-tagged ALK1 or BMPR2 (available in our lab) and Eps15-GFP-His (Plasmid#170860 in addgene) in HEK293 EBNA (to achieve high transfection efficiency), followed by co-immunoprecipitation experiments. This can be checked in the presence or absence of BMP10 stimulation.

b- Given that endocytosis plays an important role in the context of TGFβ/BMP signaling (section 2.4.1.3), and that Eps15 plays important roles in endocytosis [579, 580], it would be interesting to see if Eps15 play roles in the context of BMP10 receptor endocytosis and/or SMAD signaling In ECs. To do so, we can decrease the expression of Eps15 using siRNA, and then check endocytosis of different receptors involved in BMP10 signaling, as previously studied for other BMP receptors [127]. Moreover, by WB analysis, we can also check the effect of Eps15 silencing on the BMP10-induced pSMAD1/5 response.

c- As mentioned previously, S796 is located between Grb2-/AP2 - binding domains and the C-terminal UIM domain, suggesting a role in clathrin-mediated endocytosis [573]. In case of interesting findings obtained in the above suggested experimental approaches, it would be interesting to investigate whether Eps15-S^{796} phosphorylation is implicated or not in these functions. This can be through generation of phospho-dead (S796A) and phosphomimetic (S796D) mutants, and assessing their impact on the suggested potential roles mentioned earlier.

8.1.3.2 HSP27

As previously explained, phosphorylation of HSP27 mainly at S15/78/82 has been linked to many biological processes [590–592], making it hard to easily understand the role of this phosphorylation by BMP10 in ECs. Actin dynamics/cytoskeletal organization represent one of the major functions of pHSP27 and has been excellently described before [590–592]. In ECs, HSP27 phosphorylation regulates actin-organization which is implicated in the regulation of EC migration, tubulogenesis, and EC barrier integrity/permeability [590, 593, 594, 596, 667–670]. Among these studies, Rada et al demonstrated the relationship between temporal phosphorylation of HSP27, its oligomerization, and regulation of EC permeability [596]. Therefore, using Native SDS-page, we can study the effect of BMP10-induced phosphorylation on HSP27 oligomerization as recently performed by Rada et al [596]. Moreover, since HSP27 phosphorylation affects its localization [671–673], we can check whether BMP10-stimulation affects HSP27 localization in ECs, through assessment of total and phosphorylated HSP27 levels by WB in different cellular compartments following cellular fractionation. Interestingly, depletion of HSP27 by siRNA enhanced endothelial cell barrier permeability and slowed recovery after thrombin stimulation. Therefore, it could be that slow-onset of HSP27

phosphorylation by BMP10 after 30min-1h may play a role in the regulation of EC barrier integrity. Such hypothesis could be tested by pre-stimulating ECs with BMP10 followed by treatment with a permeability inducer such as thrombin, with or without depletion of HSP27, and monitoring their effects on the impedance using iCELLigence system available at our lab, which would reflect the effects on EC permeability.

Nevertheless, the role of HSP27 phosphorylation might be also linked to other roles, including regulation of cell proliferation [597], which is also regulated by BMP10 but with limited understanding to the full downstream mechanism. Interestingly, overexpression of WT HSP27 or phosphomemtic HSP27 (S15D, S78D and S82D) strongly attenuated proliferation of human microvascular endothelial cell line HMEC-1. Thus, flow cytometry analysis can be performed for studying proliferation in response to BMP10 in WT vs HSP27 depleted cells or cells treated with MK2 inhibitor that might give an overview of other potential roles of MK2/HSP27 axis in BMP10-regulated EC functions.

8.1.4 Effect of BMP10 on IL-6-induced gene expression and functions in ECs

We have already showed that BMP10 attenuates expression of IL-6 induced expression of HGF. However, this experiment has been performed once, and out of the 9 genes tested, only HGF showed clear induction by IL-6 and attenuation by BMP10. However, as discussed in section 6.4.1, the reason behind this is likely the need of IL-6 + IL-6R trans-signaling for inducing such genes in ECs [650–654].

- First, we should test IL-6 + IL-6-R trans-signaling in HUVECs (check pSTAT3, pAKT, and pERK). Different doses of IL-6 and/or IL-6R could be tested to determine the optimal conditions required to observe good induction of few aforementioned genes under our experimental conditions, and most importantly verify whether BMP10 attenuates pSTAT3 (and possible pAKT and pERK) from trans-signaling in a similar manner compared to that observed from classical IL-6 signaling.
- Next, HUVECs can be stimulated with IL-6 + IL-6-R with or without pre-stimulation with BMP10 for a single or different time points (e.g., 2h, 8h and 24h), followed by assessment of few IL-6 target genes expression by qPCR. If interesting results were obtained, we could also perform RNA-seq analysis to have a broad overview on the genes regulated by IL-6 in ECs, and see how these are affected by BMP10.
- Study functional outputs associated with IL-6/JAK/STAT3 signaling such as EC barrier function (icelligenece system available at our lab) [674] or EC adhesion to immune cells [675], or other functions that could be derived from the RNAseq-data analysis.

8.1.5 Effect of BMP10 on other IL-6 Family cytokines

I have shown that BMP10 regulates signaling of not only IL-6 but also other family members from the IL-6 family (section 6.4.2). We tested OSM and LIF, but we could also test others such as IL-11, IL-31, and CT-1. However, it would be important to perform a dose response for these cytokines (especially OSM) and determine minimal doses needed to activate downstream signaling (STAT3, AKT and ERK), in order not to use saturating concentrations. Then, this concentration can be tested +/- BMP10 pre-stimulation for assessing the attenuation of signaling downstream of these cytokines. It could be also interesting to verify whether BMP10 attenuation to OSM and LIF signaling that was shown in Figure 33 is also dependent on SOCS3 using siSOCS3, as demonstrated for IL-6 in Chapter 6.

8.2 Investigate the potential roles of newly identified pathways induced by BMP9/BMP10/ALK1 signaling in vascular diseases such as HHT and PAH

8.2.1 Assess the regulation of these pathways in ECs and tissues isolated from HHT and PAH patients

Concerning HHT patients, we closely collaborate with two clinicians, Dr. Alexandre Guilhem (HHT clinician) and Dr. Sophie Dupuis-Girod (head of the French reference center on HHT and member of our team), who follow 1000-1500 HHT patients in the HHT reference center in Lyon. This collaboration has provided our team with access to human material from HHT patients, which allowed a recently graduated PhD colleague during the past 3 years to isolate ECFCs and HUVECs from several HHT patients. In addition, we also have access to frozen peripheral blood mononuclear cells (PBMCs), plasma and skin telangiectasia biopsies from HHT patients. As for PAH, we had access to HMVECs isolated from the lungs of the only 2 PAH patients in France with ALK1 mutations receiving lung transplantation. These cells were generously provided by our collaborator Dr. Christophe Guignabert from National Reference Center for PAH in Paris, France (UMR999). Having access to these cellular models provides us with the possibility to study newly regulated pathways by BMP10 in HHT and PAH derived ECs, and compare them to WT cells. Below, I will suggest few experimental approaches that can be performed on HHT and PAH samples.

8.2.1.1 P38 Signaling

- Study BMP10-mediated regulation of GADD45β mRNA expression as well as the phosphorylation of P38, HSP27 and Eps15 in HHT and PAH derived cells in comparison to the control cells.
- Test downstream regulation of genes that are P38 dependent including *SELE*, *PTGS2*, *HAS2*, or other genes.

- Recent data from the team showed that the transcriptional regulation of *LFNG*, a gene implicated in Notch signaling, is impaired in ALK1 mutated ECFCs from HHT patients and more prominently in HMVECs from PAH patients. Thus, it could be interesting to test if LFNG expression is dependent on P38 signaling in these cells using P38 inhibitor.

8.2.1.2 Potential inflammatory Role of IL-6 JAK/STAT3 Signaling

- For PAH patient cells, we showed that these cells responded similarly to WT cells after BMP10 stimulation, as demonstrated through increase in pSMAD1/5 and attenuation of IL-6-induced STAT3 phosphorylation. This was further confirmed by showing that control and PAH patient cells both exhibited similar regulation patterns for SOCS3 by BMP10. However, we showed that PAH cells have higher basal pSTAT3 levels and response to IL-6. Thus, it could be possible that these cells might exhibit increased transcriptional and functional responses downstream of IL-6 signaling. This can be checked by assessing gene expression (qPCR, WB, ELISA), EC barrier function (icelligenece system available at our lab) [674], EC adhesion to immune cells [675] or other fonctions which are regulated by IL-6 signaling.

- Using HHT patient ECs (ECFCs and HUVECs) in culture and biopsies, we can determine the basal levels of pSTAT3 and SOCS3 and compare them with healthy donors. Moreover, we could study the response of HHT patient ECs to an inflammatory challenge triggered by IL-6 treatment, with or without pre-stimulation with BMP10. This would by checking SOCS3 and pSTAT3 (WB), expression of IL-6 target genes (WB qPCR, ELISA). Then, as explained for PAH patient cells, functional outputs associated with IL-6/JAK/STAT3 signaling such as EC barrier function or EC adhesion to immune cells could be tested.

8.2.3 Investigate the potential immunomodulatory role of BMP9/BMP10-ALK1 signaling *in-vivo*

Inflammation is observed in several of our transgenic mouse models, with preliminary data suggesting an immunomodulatory role of BMP9/10/ALK1 signaling *in-vivo*, which might be linked to modulation of JAK/STAT3 signaling. Thus, these mice models could be used to better understand the immunomodulatory role of BMP9/BMP10-ALK1 signaling, in order to suggest new therapeutic approaches in the role of this pathway in vascular diseases, particularly HHT and PAH. Interesting, preliminary findings from our *in-vivo* experiments highlight potential increased activation of JAK/STAT3 pathway, which could play a role in the observed inflammatory phenotype observed in these mice. Further experiments are required to verify this hypothesis:

- We can assess how mice lacking Bmp9, Bmp10 or Alk1 would react to an inflammatory challenge with LPS or with bacteria in comparison with WT mice. For this, we can use Evans blue assay to assess permeability, quantify immune cells (e.g., neutrophils and

macrophages) in the lungs by immunohistochemistry, and measure elastase in the plasma to assess acute lung injury. Thus, severity of such immune challenges will be compared between WT and KO mice, and pSTAT/STAT3 levels from tissues or isolated ECs can be also analyzed.

- Test inhibitors of the JAK/STAT pathway to rescue or reduce the severity of the phenotype in our preclinical models. For instance, we can treat adult double knockout mice lacking BMP9 and BMP10 (and their control littermates) with a JAK/STAT inhibitor (tofacitinib for example) [676] or block IL-6 signaling through the use of IL-6 neutralizing antibodies. Then, we can assess the severity of the phenotypes associated with these mice compared to vehicle treated group. This would be through the analysis of vascular networks, immune cell infiltration, size of the heart, lung inflammation, blood pressure, all of which are well characterized assays performed in our team.

References

1. Pugsley MK, Tabrizchi R (2000) The vascular system. An overview of structure and function. J Pharmacol Toxicol Methods 44:333–340. https://doi.org/10.1016/s1056-8719(00)00125-8

2. Jouda H, Larrea Murillo L, Wang T (2022) Current Progress in Vascular Engineering and Its Clinical Applications. Cells 11:493. https://doi.org/10.3390/cells11030493

3. Sun H-J, Wu Z-Y, Nie X-W, Bian J-S (2020) Role of Endothelial Dysfunction in Cardiovascular Diseases: The Link Between Inflammation and Hydrogen Sulfide. Frontiers in Pharmacology 10:

4. Wang Z, Zhang W, Xie C, Wen F, Ma C, Lin N, Thian ES, Wang X (2019) Geometric anisotropy on biomaterials surface for vascular scaffold design: engineering and biological advances. J Phys Mater 2:032003. https://doi.org/10.1088/2515-7639/ab1c68

5. Oliver G, Kipnis J, Randolph GJ, Harvey NL (2020) The Lymphatic Vasculature in the 21st Century: Novel Functional Roles in Homeostasis and Disease. Cell 182:270–296. https://doi.org/10.1016/j.cell.2020.06.039

6. Ricard N, Bailly S, Guignabert C, Simons M (2021) The quiescent endothelium: signalling pathways regulating organ-specific endothelial normalcy. Nat Rev Cardiol 18:565–580. https://doi.org/10.1038/s41569-021-00517-4

7. Liu Z, Wang Y, Huang Y, Kim BYS, Shan H, Wu D, Jiang W (2019) Tumor Vasculatures: A New Target for Cancer Immunotherapy. Trends in Pharmacological Sciences 40:613–623. https://doi.org/10.1016/j.tips.2019.07.001

8. Ribatti D, Vacca A, Nico B, Roncali L, Dammacco F (2001) Postnatal vasculogenesis. Mech Dev 100:157–163. https://doi.org/10.1016/s0925-4773(00)00522-0

9. Risau W, Flamme I (1995) Vasculogenesis. Annu Rev Cell Dev Biol 11:73–91. https://doi.org/10.1146/annurev.cb.11.110195.000445

10. Negri S, Faris P, Rosti V, Antognazza MR, Lodola F, Moccia F (2020) Endothelial TRPV1 as an Emerging Molecular Target to Promote Therapeutic Angiogenesis. Cells 9:1341. https://doi.org/10.3390/cells9061341

11. Pardanaud L, Dieterlen-Lièvre F (1999) Manipulation of the angiopoietic/hemangiopoietic commitment in the avian embryo. Development 126:617–627. https://doi.org/10.1242/dev.126.4.617

12. Carmeliet P (2000) Mechanisms of angiogenesis and arteriogenesis. Nat Med 6:389–395. https://doi.org/10.1038/74651

13. Burton GJ, Fowden AL (2015) The placenta: a multifaceted, transient organ. Philos Trans R Soc Lond B Biol Sci 370:20140066. https://doi.org/10.1098/rstb.2014.0066

14. Lau S, Gossen M, Lendlein A, Jung F (2021) Venous and Arterial Endothelial Cells from Human Umbilical Cords: Potential Cell Sources for Cardiovascular Research. Int J Mol Sci 22:978. https://doi.org/10.3390/ijms22020978

15. Jaffe EA, Nachman RL, Becker CG, Minick CR (1973) Culture of human endothelial cells derived from umbilical veins. Identification by morphologic and immunologic criteria. J Clin Invest 52:2745–2756. https://doi.org/10.1172/JCI107470

16. Alitalo K, Tammela T, Petrova TV (2005) Lymphangiogenesis in development and human disease. Nature 438:946–953. https://doi.org/10.1038/nature04480

17. Cueni LN, Detmar M (2008) The lymphatic system in health and disease. Lymphat Res Biol 6:109–122. https://doi.org/10.1089/lrb.2008.1008

18. Koch S, Claesson-Welsh L (2012) Signal transduction by vascular endothelial growth factor receptors. Cold Spring Harb Perspect Med 2:a006502. https://doi.org/10.1101/cshperspect.a006502

19. Fukuhara S, Sako K, Noda K, Nagao K, Miura K, Mochizuki N (2009) Tie2 is tied at the cell-cell contacts and to extracellular matrix by Angiopoietin-1. Exp Mol Med 41:133–139. https://doi.org/10.3858/emm.2009.41.3.016

20. Cao R, Björndahl MA, Religa P, Clasper S, Garvin S, Galter D, Meister B, Ikomi F, Tritsaris K, Dissing S, Ohhashi T, Jackson DG, Cao Y (2004) PDGF-BB induces intratumoral lymphangiogenesis and promotes lymphatic metastasis. Cancer Cell 6:333–345. https://doi.org/10.1016/j.ccr.2004.08.034

21. Wu E, Palmer N, Tian Z, Moseman AP, Galdzicki M, Wang X, Berger B, Zhang H, Kohane IS (2008) Comprehensive dissection of PDGF-PDGFR signaling pathways in PDGFR genetically defined cells. PLoS One 3:e3794. https://doi.org/10.1371/journal.pone.0003794

22. Akwii RG, Sajib MS, Zahra FT, Tullar P, Zabet-Moghaddam M, Zheng Y, Silvio Gutkind J, Doci CL, Mikelis CM (2022) Angiopoietin-2-induced lymphatic endothelial cell migration drives lymphangiogenesis via the β1 integrin-RhoA-formin axis. Angiogenesis 25:373–396. https://doi.org/10.1007/s10456-022-09831-y

23. David L, Feige J-J, Bailly S (2009) Emerging role of bone morphogenetic proteins in angiogenesis. Cytokine Growth Factor Rev 20:203–212. https://doi.org/10.1016/j.cytogfr.2009.05.001

24. Herbert SP, Stainier DYR (2011) Molecular control of endothelial cell behaviour during blood vessel morphogenesis. Nat Rev Mol Cell Biol 12:551–564. https://doi.org/10.1038/nrm3176

25. Liu Z-L, Chen H-H, Zheng L-L, Sun L-P, Shi L (2023) Angiogenic signaling pathways and anti-angiogenic therapy for cancer. Sig Transduct Target Ther 8:1–39. https://doi.org/10.1038/s41392-023-01460-1

26. Shibuya M (2011) Vascular Endothelial Growth Factor (VEGF) and Its Receptor (VEGFR) Signaling in Angiogenesis. Genes Cancer 2:1097–1105. https://doi.org/10.1177/1947601911423031

27. Sawano A, Takahashi T, Yamaguchi S, Aonuma M, Shibuya M (1996) Flt-1 but not KDR/Flk-1 tyrosine kinase is a receptor for placenta growth factor, which is related to vascular endothelial growth factor. Cell Growth Differ 7:213–221

28. Cross MJ, Dixelius J, Matsumoto T, Claesson-Welsh L (2003) VEGF-receptor signal transduction. Trends in Biochemical Sciences 28:488–494. https://doi.org/10.1016/S0968-0004(03)00193-2

29. Fukumura D, Gohongi T, Kadambi A, Izumi Y, Ang J, Yun CO, Buerk DG, Huang PL, Jain RK (2001) Predominant role of endothelial nitric oxide synthase in vascular endothelial growth factor-induced angiogenesis and vascular permeability. Proc Natl Acad Sci U S A 98:2604–2609. https://doi.org/10.1073/pnas.041359198

30. Cardone MH, Roy N, Stennicke HR, Salvesen GS, Franke TF, Stanbridge E, Frisch S, Reed JC (1998) Regulation of cell death protease caspase-9 by phosphorylation. Science 282:1318–1321. https://doi.org/10.1126/science.282.5392.1318

31. Wallez Y, Cand F, Cruzalegui F, Wernstedt C, Souchelnytskyi S, Vilgrain I, Huber P (2007) Src kinase phosphorylates vascular endothelial-cadherin in response to vascular endothelial growth factor: identification of tyrosine 685 as the unique target site. Oncogene 26:1067–1077. https://doi.org/10.1038/sj.onc.1209855

32. Chen XL, Nam J-O, Jean C, Lawson C, Walsh CT, Goka E, Lim S-T, Tomar A, Tancioni I, Uryu S, Guan J-L, Acevedo LM, Weis SM, Cheresh DA, Schlaepfer DD (2012) VEGF-induced vascular permeability is mediated by FAK. Dev Cell 22:146–157. https://doi.org/10.1016/j.devcel.2011.11.002

33. Corre I, Paris F, Huot J (2017) The p38 pathway, a major pleiotropic cascade that transduces stress and metastatic signals in endothelial cells. Oncotarget 8:55684–55714. https://doi.org/10.18632/oncotarget.18264

34. Heldin CH, Westermark B (1999) Mechanism of action and in vivo role of platelet-derived growth factor. Physiol Rev 79:1283–1316. https://doi.org/10.1152/physrev.1999.79.4.1283

35. Papadopoulos N, Lennartsson J (2018) The PDGF/PDGFR pathway as a drug target. Molecular Aspects of Medicine 62:75–88. https://doi.org/10.1016/j.mam.2017.11.007

36. Kohler N, Lipton A (1974) Platelets as a source of fibroblast growth-promoting activity. Exp Cell Res 87:297–301. https://doi.org/10.1016/0014-4827(74)90484-4

37. Hellström M, Kalén M, Lindahl P, Abramsson A, Betsholtz C (1999) Role of PDGF-B and PDGFR-beta in recruitment of vascular smooth muscle cells and pericytes during embryonic blood vessel formation in the mouse. Development 126:3047–3055. https://doi.org/10.1242/dev.126.14.3047

38. Eklund L, Olsen BR (2006) Tie receptors and their angiopoietin ligands are context-dependent regulators of vascular remodeling. Experimental Cell Research 312:630–641. https://doi.org/10.1016/j.yexcr.2005.09.002

39. Kim I, Kim HG, So JN, Kim JH, Kwak HJ, Koh GY (2000) Angiopoietin-1 regulates endothelial cell survival through the phosphatidylinositol 3'-Kinase/Akt signal transduction pathway. Circ Res 86:24–29. https://doi.org/10.1161/01.res.86.1.24

40. Gamble JR, Drew J, Trezise L, Underwood A, Parsons M, Kasminkas L, Rudge J, Yancopoulos G, Vadas MA (2000) Angiopoietin-1 is an antipermeability and anti-inflammatory agent in vitro and targets cell junctions. Circ Res 87:603–607. https://doi.org/10.1161/01.res.87.7.603

41. Kim I, Moon SO, Park SK, Chae SW, Koh GY (2001) Angiopoietin-1 reduces VEGF-stimulated leukocyte adhesion to endothelial cells by reducing ICAM-1, VCAM-1, and E-selectin expression. Circ Res 89:477–479. https://doi.org/10.1161/hh1801.097034

42. Maisonpierre PC, Suri C, Jones PF, Bartunkova S, Wiegand SJ, Radziejewski C, Compton D, McClain J, Aldrich TH, Papadopoulos N, Daly TJ, Davis S, Sato TN, Yancopoulos GD (1997) Angiopoietin-2, a natural antagonist for Tie2 that disrupts in vivo angiogenesis. Science 277:55–60. https://doi.org/10.1126/science.277.5322.55

43. Scharpfenecker M, Fiedler U, Reiss Y, Augustin HG (2005) The Tie-2 ligand angiopoietin-2 destabilizes quiescent endothelium through an internal autocrine loop mechanism. J Cell Sci 118:771–780. https://doi.org/10.1242/jcs.01653

44. Fernández-Chacón M, García-González I, Mühleder S, Benedito R (2021) Role of Notch in endothelial biology. Angiogenesis 24:237–250. https://doi.org/10.1007/s10456-021-09793-7

45. Andersson ER, Lendahl U (2014) Therapeutic modulation of Notch signalling--are we there yet? Nat Rev Drug Discov 13:357–378. https://doi.org/10.1038/nrd4252

46. Roberts AB, Sporn MB (1989) Regulation of endothelial cell growth, architecture, and matrix synthesis by TGF-beta. Am Rev Respir Dis 140:1126–1128. https://doi.org/10.1164/ajrccm/140.4.1126

47. Desroches-Castan A, Tillet E, Bouvard C, Bailly S (2022) BMP9 and BMP10: Two close vascular quiescence partners that stand out. Developmental Dynamics 251:158–177. https://doi.org/10.1002/dvdy.395

48. Gerhardt H, Golding M, Fruttiger M, Ruhrberg C, Lundkvist A, Abramsson A, Jeltsch M, Mitchell C, Alitalo K, Shima D, Betsholtz C (2003) VEGF guides angiogenic sprouting utilizing endothelial tip cell filopodia. J Cell Biol 161:1163–1177. https://doi.org/10.1083/jcb.200302047

49. Blanco R, Gerhardt H (2013) VEGF and Notch in tip and stalk cell selection. Cold Spring Harb Perspect Med 3:a006569. https://doi.org/10.1101/cshperspect.a006569

50. Oh H, Takagi H, Suzuma K, Otani A, Matsumura M, Honda Y (1999) Hypoxia and vascular endothelial growth factor selectively up-regulate angiopoietin-2 in bovine microvascular endothelial cells. J Biol Chem 274:15732–15739. https://doi.org/10.1074/jbc.274.22.15732

51. Hellström M, Phng L-K, Hofmann JJ, Wallgard E, Coultas L, Lindblom P, Alva J, Nilsson A-K, Karlsson L, Gaiano N, Yoon K, Rossant J, Iruela-Arispe ML, Kalén M, Gerhardt H, Betsholtz C (2007) Dll4 signalling through Notch1 regulates formation of tip cells during angiogenesis. Nature 445:776–780. https://doi.org/10.1038/nature05571

52. Lobov IB, Renard RA, Papadopoulos N, Gale NW, Thurston G, Yancopoulos GD, Wiegand SJ (2007) Delta-like ligand 4 (Dll4) is induced by VEGF as a negative regulator of angiogenic sprouting. Proc Natl Acad Sci U S A 104:3219–3224. https://doi.org/10.1073/pnas.0611206104

53. Patan S, Alvarez MJ, Schittny JC, Burri PH (1992) Intussusceptive microvascular growth: a common alternative to capillary sprouting. Arch Histol Cytol 55 Suppl:65–75. https://doi.org/10.1679/aohc.55.suppl_65

54. Mentzer SJ, Konerding MA (2014) Intussusceptive angiogenesis: expansion and remodeling of microvascular networks. Angiogenesis 17:499–509. https://doi.org/10.1007/s10456-014-9428-3

55. Burri PH, Hlushchuk R, Djonov V (2004) Intussusceptive angiogenesis: its emergence, its characteristics, and its significance. Dev Dyn 231:474–488. https://doi.org/10.1002/dvdy.20184

56. de Larco JE, Todaro GJ (1978) Growth factors from murine sarcoma virus-transformed cells. Proc Natl Acad Sci U S A 75:4001–4005

57. Moses HL, Branum EL, Proper JA, Robinson RA (1981) Transforming growth factor production by chemically transformed cells. Cancer Res 41:2842–2848

58. Roberts AB, Anzano MA, Lamb LC, Smith JM, Sporn MB (1981) New class of transforming growth factors potentiated by epidermal growth factor: isolation from non-neoplastic tissues. Proc Natl Acad Sci U S A 78:5339–5343. https://doi.org/10.1073/pnas.78.9.5339

59. Moses HL, Roberts AB, Derynck R (2016) The Discovery and Early Days of TGF-β: A Historical Perspective. Cold Spring Harb Perspect Biol 8:a021865. https://doi.org/10.1101/cshperspect.a021865

60. Hinck AP (2012) Structural studies of the TGF-βs and their receptors - insights into evolution of the TGF-β superfamily. FEBS Lett 586:1860–1870. https://doi.org/10.1016/j.febslet.2012.05.028

61. Morikawa M, Derynck R, Miyazono K (2016) TGF-β and the TGF-β Family: Context-Dependent Roles in Cell and Tissue Physiology. Cold Spring Harb Perspect Biol 8:a021873. https://doi.org/10.1101/cshperspect.a021873

62. David CJ, Massagué J (2018) Contextual determinants of TGFβ action in development, immunity and cancer. Nat Rev Mol Cell Biol 19:419–435. https://doi.org/10.1038/s41580-018-0007-0

63. Hinck AP, Mueller TD, Springer TA (2016) Structural Biology and Evolution of the TGF-β Family. Cold Spring Harb Perspect Biol 8:a022103. https://doi.org/10.1101/cshperspect.a022103

64. Derynck R, Budi EH (2019) Specificity, versatility, and control of TGF-β family signaling. Sci Signal 12:eaav5183. https://doi.org/10.1126/scisignal.aav5183

65. Gray AM, Mason AJ (1990) Requirement for activin A and transforming growth factor--beta 1 pro-regions in homodimer assembly. Science 247:1328–1330. https://doi.org/10.1126/science.2315700

66. Thies RS, Chen T, Davies MV, Tomkinson KN, Pearson AA, Shakey QA, Wolfman NM (2001) GDF-8 propeptide binds to GDF-8 and antagonizes biological activity by inhibiting GDF-8 receptor binding. Growth Factors 18:251–259. https://doi.org/10.3109/08977190109029114

67. Ge G, Hopkins DR, Ho W-B, Greenspan DS (2005) GDF11 forms a bone morphogenetic protein 1-activated latent complex that can modulate nerve growth factor-induced differentiation of PC12 cells. Mol Cell Biol 25:5846–5858. https://doi.org/10.1128/MCB.25.14.5846-5858.2005

68. Sopory S, Nelsen SM, Degnin C, Wong C, Christian JL (2006) Regulation of bone morphogenetic protein-4 activity by sequence elements within the prodomain. J Biol Chem 281:34021–34031. https://doi.org/10.1074/jbc.M605330200

69. Jones WK, Richmond EA, White K, Sasak H, Kusmik W, Smart J, Oppermann H, Rueger DC, Tucker RF (1994) Osteogenic protein-1 (OP-1) expression and processing in Chinese hamster ovary cells: isolation of a soluble complex containing the mature and pro-domains of OP-1. Growth Factors 11:215–225. https://doi.org/10.3109/08977199409046919

70. Brown MA, Zhao Q, Baker KA, Naik C, Chen C, Pukac L, Singh M, Tsareva T, Parice Y, Mahoney A, Roschke V, Sanyal I, Choe S (2005) Crystal structure of BMP-9 and functional interactions with pro-region and receptors. J Biol Chem 280:25111–25118. https://doi.org/10.1074/jbc.M503328200

71. Li Y, Fan W, Link F, Wang S, Dooley S (2022) Transforming growth factor β latency: A mechanism of cytokine storage and signalling regulation in liver homeostasis and disease. JHEP Reports 4:100397. https://doi.org/10.1016/j.jhepr.2021.100397

72. Goebel EJ, Hart KN, McCoy JC, Thompson TB (2019) Structural biology of the TGFβ family. Exp Biol Med (Maywood) 244:1530–1546. https://doi.org/10.1177/1535370219880894

73. Shi M, Zhu J, Wang R, Chen X, Mi L, Walz T, Springer TA (2011) Latent TGF-β structure and activation. Nature 474:343–349. https://doi.org/10.1038/nature10152

74. Mi L-Z, Brown CT, Gao Y, Tian Y, Le VQ, Walz T, Springer TA (2015) Structure of bone morphogenetic protein 9 procomplex. Proc Natl Acad Sci U S A 112:3710–3715. https://doi.org/10.1073/pnas.1501303112

75. Scheufler C, Sebald W, Hülsmeyer M (1999) Crystal structure of human bone morphogenetic protein-2 at 2.7 A resolution. J Mol Biol 287:103–115. https://doi.org/10.1006/jmbi.1999.2590

76. Dong X, Hudson NE, Lu C, Springer TA (2014) Structural determinants of integrin β-subunit specificity for latent TGF-β. Nat Struct Mol Biol 21:1091–1096. https://doi.org/10.1038/nsmb.2905

77. Robertson IB, Rifkin DB (2016) Regulation of the Bioavailability of TGF-β and TGF-β-Related Proteins. Cold Spring Harb Perspect Biol 8:a021907. https://doi.org/10.1101/cshperspect.a021907

78. Roberts AB, Anzano MA, Wakefield LM, Roche NS, Stern DF, Sporn MB (1985) Type beta transforming growth factor: a bifunctional regulator of cellular growth. Proc Natl Acad Sci U S A 82:119–123. https://doi.org/10.1073/pnas.82.1.119

79. Urist MR, Huo YK, Brownell AG, Hohl WM, Buyske J, Lietze A, Tempst P, Hunkapiller M, DeLange RJ (1984) Purification of bovine bone morphogenetic protein by hydroxyapatite chromatography. Proc Natl Acad Sci U S A 81:371–375. https://doi.org/10.1073/pnas.81.2.371

80. Urist MR, Strates BS (1971) Bone morphogenetic protein. J Dent Res 50:1392–1406. https://doi.org/10.1177/00220345710500060601

81. Obradovic Wagner D, Sieber C, Bhushan R, Börgermann JH, Graf D, Knaus P (2010) BMPs: From Bone to Body Morphogenetic Proteins. Science Signaling 3:mr1–mr1. https://doi.org/10.1126/scisignal.3107mr1

82. Johnson AN, Newfeld SJ (2002) The TGF-beta family: signaling pathways, developmental roles, and tumor suppressor activities. ScientificWorldJournal 2:892–925. https://doi.org/10.1100/tsw.2002.178

83. Wrana JL, Tran H, Attisano L, Arora K, Childs SR, Massagué J, O'Connor MB (1994) Two distinct transmembrane serine/threonine kinases from Drosophila melanogaster form an activin receptor complex. Mol Cell Biol 14:944–950. https://doi.org/10.1128/mcb.14.2.944-950.1994

84. Wrana JL, Massagué J (1995) GS domain mutations that constitutively activate T beta R-I, the downstream signaling component in the TGF-beta receptor complex. EMBO J 14:2199–2208. https://doi.org/10.1002/j.1460-2075.1995.tb07214.x

85. Mathews LS, Vale WW (1991) Expression cloning of an activin receptor, a predicted transmembrane serine kinase. Cell 65:973–982. https://doi.org/10.1016/0092-8674(91)90549-e

86. Wrana JL, Attisano L, Cárcamo J, Zentella A, Doody J, Laiho M, Wang XF, Massagué J (1992) TGF beta signals through a heteromeric protein kinase receptor complex. Cell 71:1003–1014. https://doi.org/10.1016/0092-8674(92)90395-s

87. Cárcamo J, Weis FM, Ventura F, Wieser R, Wrana JL, Attisano L, Massagué J (1994) Type I receptors specify growth-inhibitory and transcriptional responses to transforming growth factor beta and activin. Mol Cell Biol 14:3810–3821. https://doi.org/10.1128/mcb.14.6.3810-3821.1994

88. Feng XH, Derynck R (1997) A kinase subdomain of transforming growth factor-beta (TGF-beta) type I receptor determines the TGF-beta intracellular signaling specificity. EMBO J 16:3912–3923. https://doi.org/10.1093/emboj/16.13.3912

89. Kim SK, Henen MA, Hinck AP (2019) Structural biology of betaglycan and endoglin, membrane-bound co-receptors of the TGF-beta family. Exp Biol Med (Maywood) 244:1547–1558. https://doi.org/10.1177/1535370219881160

90. Kim SK, Whitley MJ, Krzysiak TC, Hinck CS, Taylor AB, Zwieb C, Byeon C-H, Zhou X, Mendoza V, López-Casillas F, Furey W, Hinck AP (2019) Structural adaptation in its orphan domain engenders betaglycan with an alternate mode of growth factor binding relative to endoglin. Structure 27:1427-1442.e4. https://doi.org/10.1016/j.str.2019.06.010

91. Henis YI, Moustakas A, Lin HY, Lodish HF (1994) The types II and III transforming growth factor-beta receptors form homo-oligomers. J Cell Biol 126:139–154. https://doi.org/10.1083/jcb.126.1.139

92. Gilboa L, Wells RG, Lodish HF, Henis YI (1998) Oligomeric structure of type I and type II transforming growth factor beta receptors: homodimers form in the ER and persist at the plasma membrane. J Cell Biol 140:767–777. https://doi.org/10.1083/jcb.140.4.767

93. Gilboa L, Nohe A, Geissendörfer T, Sebald W, Henis YI, Knaus P (2000) Bone morphogenetic protein receptor complexes on the surface of live cells: a new oligomerization mode for serine/threonine kinase receptors. Mol Biol Cell 11:1023–1035. https://doi.org/10.1091/mbc.11.3.1023

94. Wells RG, Gilboa L, Sun Y, Liu X, Henis YI, Lodish HF (1999) Transforming growth factor-beta induces formation of a dithiothreitol-resistant type I/Type II receptor complex in live cells. J Biol Chem 274:5716–5722. https://doi.org/10.1074/jbc.274.9.5716

95. Huse M, Chen YG, Massagué J, Kuriyan J (1999) Crystal structure of the cytoplasmic domain of the type I TGF beta receptor in complex with FKBP12. Cell 96:425–436. https://doi.org/10.1016/s0092-8674(00)80555-3

96. Ehrlich M, Gutman O, Knaus P, Henis YI (2012) Oligomeric interactions of TGF-β and BMP receptors. FEBS Lett 586:1885–1896. https://doi.org/10.1016/j.febslet.2012.01.040

97. Massagué J, Seoane J, Wotton D (2005) Smad transcription factors. Genes Dev 19:2783–2810. https://doi.org/10.1101/gad.1350705

98. Attisano L, Lee-Hoeflich ST (2001) The Smads. Genome Biol 2:REVIEWS3010. https://doi.org/10.1186/gb-2001-2-8-reviews3010

99. Wrighton KH, Lin X, Feng X-H (2009) Phospho-control of TGF-β superfamily signaling. Cell Res 19:8–20. https://doi.org/10.1038/cr.2008.327

100. Hayashi H, Abdollah S, Qiu Y, Cai J, Xu Y-Y, Grinnell BW, Richardson MA, Topper JN, Gimbrone MA, Wrana JL, Falb D (1997) The MAD-Related Protein Smad7 Associates with the TGFβ Receptor and Functions as an Antagonist of TGFβ Signaling. Cell 89:1165–1173. https://doi.org/10.1016/S0092-8674(00)80303-7

101. Nakao A, Afrakhte M, Morn A, Nakayama T, Christian JL, Heuchel R, Itoh S, Kawabata M, Heldin N-E, Heldin C-H, Dijke P ten (1997) Identification of Smad7, a TGFβ-inducible antagonist of TGF-β signalling. Nature 389:631–635. https://doi.org/10.1038/39369

102. Hata A, Lagna G, Massagué J, Hemmati-Brivanlou A (1998) Smad6 inhibits BMP/Smad1 signaling by specifically competing with the Smad4 tumor suppressor. Genes Dev 12:186–197

103. Pierreux CE, Nicolás FJ, Hill CS (2000) Transforming growth factor beta-independent shuttling of Smad4 between the cytoplasm and nucleus. Mol Cell Biol 20:9041–9054. https://doi.org/10.1128/MCB.20.23.9041-9054.2000

104. Xu L, Kang Y, Cöl S, Massagué J (2002) Smad2 nucleocytoplasmic shuttling by nucleoporins CAN/Nup214 and Nup153 feeds TGFbeta signaling complexes in the cytoplasm and nucleus. Mol Cell 10:271–282. https://doi.org/10.1016/s1097-2765(02)00586-5

105. Wrana JL, Attisano L, Wieser R, Ventura F, Massagué J (1994) Mechanism of activation of the TGF-beta receptor. Nature 370:341–347. https://doi.org/10.1038/370341a0

106. Huse M, Muir TW, Xu L, Chen YG, Kuriyan J, Massagué J (2001) The TGF beta receptor activation process: an inhibitor- to substrate-binding switch. Mol Cell 8:671–682. https://doi.org/10.1016/s1097-2765(01)00332-x

107. Lo RS, Chen YG, Shi Y, Pavletich NP, Massagué J (1998) The L3 loop: a structural motif determining specific interactions between SMAD proteins and TGF-beta receptors. EMBO J 17:996–1005. https://doi.org/10.1093/emboj/17.4.996

108. Hata A, Chen Y-G (2016) TGF-β Signaling from Receptors to Smads. Cold Spring Harb Perspect Biol 8:a022061. https://doi.org/10.1101/cshperspect.a022061

109. Liu IM, Schilling SH, Knouse KA, Choy L, Derynck R, Wang X-F (2009) TGFbeta-stimulated Smad1/5 phosphorylation requires the ALK5 L45 loop and mediates the pro-migratory TGFbeta switch. EMBO J 28:88–98. https://doi.org/10.1038/emboj.2008.266

110. Daly AC, Randall RA, Hill CS (2008) Transforming growth factor beta-induced Smad1/5 phosphorylation in epithelial cells is mediated by novel receptor complexes and is essential for anchorage-independent growth. Mol Cell Biol 28:6889–6902. https://doi.org/10.1128/MCB.01192-08

111. Wang Y, Ho CC, Bang E, Rejon CA, Libasci V, Pertchenko P, Hébert TE, Bernard DJ (2014) Bone Morphogenetic Protein 2 Stimulates Noncanonical SMAD2/3 Signaling via the BMP Type 1A Receptor in Gonadotrope-Like Cells: Implications for FSH Synthesis. Endocrinology 155:1970–1981. https://doi.org/10.1210/en.2013-1741

112. Upton PD, Davies RJ, Trembath RC, Morrell NW (2009) Bone Morphogenetic Protein (BMP) and Activin Type II Receptors Balance BMP9 Signals Mediated by Activin Receptor-like Kinase-1 in Human Pulmonary Artery Endothelial Cells. J Biol Chem 284:15794–15804. https://doi.org/10.1074/jbc.M109.002881

113. Chacko BM, Qin BY, Tiwari A, Shi G, Lam S, Hayward LJ, De Caestecker M, Lin K (2004) Structural basis of heteromeric smad protein assembly in TGF-beta signaling. Mol Cell 15:813–823. https://doi.org/10.1016/j.molcel.2004.07.016

114. Heldin C-H, Moustakas A (2016) Signaling Receptors for TGF-β Family Members. Cold Spring Harb Perspect Biol 8:a022053. https://doi.org/10.1101/cshperspect.a022053

115. Hill CS (2016) Transcriptional Control by the SMADs. Cold Spring Harb Perspect Biol 8:a022079. https://doi.org/10.1101/cshperspect.a022079

116. Di Guglielmo GM, Le Roy C, Goodfellow AF, Wrana JL (2003) Distinct endocytic pathways regulate TGF-beta receptor signalling and turnover. Nat Cell Biol 5:410–421. https://doi.org/10.1038/ncb975

117. Razani B, Zhang XL, Bitzer M, von Gersdorff G, Böttinger EP, Lisanti MP (2001) Caveolin-1 regulates transforming growth factor (TGF)-beta/SMAD signaling through an interaction with the TGF-beta type I receptor. J Biol Chem 276:6727–6738. https://doi.org/10.1074/jbc.M008340200

118. Ehrlich M (2016) Endocytosis and trafficking of BMP receptors: Regulatory mechanisms for fine-tuning the signaling response in different cellular contexts. Cytokine Growth Factor Rev 27:35–42. https://doi.org/10.1016/j.cytogfr.2015.12.008

119. Le Roy C, Wrana JL (2005) Clathrin- and non-clathrin-mediated endocytic regulation of cell signalling. Nat Rev Mol Cell Biol 6:112–126. https://doi.org/10.1038/nrm1571

120. Penheiter SG, Mitchell H, Garamszegi N, Edens M, Doré JJE, Leof EB (2002) Internalization-dependent and -independent requirements for transforming growth factor beta receptor signaling via the Smad pathway. Mol Cell Biol 22:4750–4759. https://doi.org/10.1128/MCB.22.13.4750-4759.2002

121. Tzavlaki K, Moustakas A (2020) TGF-β Signaling. Biomolecules 10:487. https://doi.org/10.3390/biom10030487

122. Penheiter SG, Singh RD, Repellin CE, Wilkes MC, Edens M, Howe PH, Pagano RE, Leof EB (2010) Type II transforming growth factor-beta receptor recycling is dependent upon the clathrin adaptor protein Dab2. Mol Biol Cell 21:4009–4019. https://doi.org/10.1091/mbc.E09-12-1019

123. Lin H-K, Bergmann S, Pandolfi PP (2004) Cytoplasmic PML function in TGF-β signalling. Nature 431:205–211. https://doi.org/10.1038/nature02783

124. Tsukazaki T, Chiang TA, Davison AF, Attisano L, Wrana JL (1998) SARA, a FYVE domain protein that recruits Smad2 to the TGFbeta receptor. Cell 95:779–791. https://doi.org/10.1016/s0092-8674(00)81701-8

125. Shi W, Chang C, Nie S, Xie S, Wan M, Cao X (2007) Endofin acts as a Smad anchor for receptor activation in BMP signaling. J Cell Sci 120:1216–1224. https://doi.org/10.1242/jcs.03400

126. Nohe A, Keating E, Underhill TM, Knaus P, Petersen NO (2005) Dynamics and interaction of caveolin-1 isoforms with BMP-receptors. J Cell Sci 118:643–650. https://doi.org/10.1242/jcs.01402

127. Hartung A, Bitton-Worms K, Rechtman MM, Wenzel V, Boergermann JH, Hassel S, Henis YI, Knaus P (2006) Different routes of bone morphogenic protein (BMP) receptor endocytosis influence BMP signaling. Mol Cell Biol 26:7791–7805. https://doi.org/10.1128/MCB.00022-06

128. Zhou Z, Xie J, Lee D, Liu Y, Jung J, Zhou L, Xiong S, Mei L, Xiong W-C (2010) Neogenin regulation of BMP-induced canonical Smad signaling and endochondral bone formation. Dev Cell 19:90–102. https://doi.org/10.1016/j.devcel.2010.06.016

129. Massagué J (2012) TGFβ signalling in context. Nat Rev Mol Cell Biol 13:616–630. https://doi.org/10.1038/nrm3434

130. Zawel L, Dai JL, Buckhaults P, Zhou S, Kinzler KW, Vogelstein B, Kern SE (1998) Human Smad3 and Smad4 are sequence-specific transcription activators. Mol Cell 1:611–617. https://doi.org/10.1016/s1097-2765(00)80061-1

131. Shi Y, Wang YF, Jayaraman L, Yang H, Massagué J, Pavletich NP (1998) Crystal structure of a Smad MH1 domain bound to DNA: insights on DNA binding in TGF-beta signaling. Cell 94:585–594. https://doi.org/10.1016/s0092-8674(00)81600-1

132. Ross S, Hill CS (2008) How the Smads regulate transcription. Int J Biochem Cell Biol 40:383–408. https://doi.org/10.1016/j.biocel.2007.09.006

133. Feng X-H, Derynck R (2005) Specificity and versatility in tgf-beta signaling through Smads. Annu Rev Cell Dev Biol 21:659–693. https://doi.org/10.1146/annurev.cellbio.21.022404.142018

134. Morikawa M, Koinuma D, Tsutsumi S, Vasilaki E, Kanki Y, Heldin C-H, Aburatani H, Miyazono K (2011) ChIP-seq reveals cell type-specific binding patterns of BMP-specific Smads and a novel binding motif. Nucleic Acids Res 39:8712–8727. https://doi.org/10.1093/nar/gkr572

135. Inman GJ, Nicolás FJ, Hill CS (2002) Nucleocytoplasmic shuttling of Smads 2, 3, and 4 permits sensing of TGF-beta receptor activity. Mol Cell 10:283–294. https://doi.org/10.1016/s1097-2765(02)00585-3

136. Shi W, Sun C, He B, Xiong W, Shi X, Yao D, Cao X (2004) GADD34-PP1c recruited by Smad7 dephosphorylates TGFbeta type I receptor. J Cell Biol 164:291–300. https://doi.org/10.1083/jcb.200307151

137. Bennett D, Alphey L (2002) PP1 binds Sara and negatively regulates Dpp signaling in Drosophila melanogaster. Nat Genet 31:419–423. https://doi.org/10.1038/ng938

138. Suzuki C, Murakami G, Fukuchi M, Shimanuki T, Shikauchi Y, Imamura T, Miyazono K (2002) Smurf1 regulates the inhibitory activity of Smad7 by targeting Smad7 to the plasma membrane. J Biol Chem 277:39919–39925. https://doi.org/10.1074/jbc.M201901200

139. Murakami G, Watabe T, Takaoka K, Miyazono K, Imamura T (2003) Cooperative Inhibition of Bone Morphogenetic Protein Signaling by Smurf1 and Inhibitory Smads. Mol Biol Cell 14:2809–2817. https://doi.org/10.1091/mbc.E02-07-0441

140. Valdimarsdottir G, Goumans M-J, Itoh F, Itoh S, Heldin C-H, Dijke P ten (2006) Smad7 and protein phosphatase 1α are critical determinants in the duration of TGF-β/ALK1 signaling in endothelial cells. BMC Cell Biology 7:16. https://doi.org/10.1186/1471-2121-7-16

141. Liu C, Xu P, Lamouille S, Xu J, Derynck R (2009) TACE-mediated ectodomain shedding of the type I TGF-beta receptor downregulates TGF-beta signaling. Mol Cell 35:26–36. https://doi.org/10.1016/j.molcel.2009.06.018

142. Gumienny TL, Padgett RW (2002) The other side of TGF-β superfamily signal regulation: thinking outside the cell. Trends in Endocrinology & Metabolism 13:295–299. https://doi.org/10.1016/S1043-2760(02)00615-X

143. Thompson TB, Lerch TF, Cook RW, Woodruff TK, Jardetzky TS (2005) The Structure of the Follistatin:Activin Complex Reveals Antagonism of Both Type I and Type II Receptor Binding. Developmental Cell 9:535–543. https://doi.org/10.1016/j.devcel.2005.09.008

144. Zhang W, Ge Y, Cheng Q, Zhang Q, Fang L, Zheng J (2018) Decorin is a pivotal effector in the extracellular matrix and tumour microenvironment. Oncotarget 9:5480–5491. https://doi.org/10.18632/oncotarget.23869

145. Lin X, Duan X, Liang Y-Y, Su Y, Wrighton KH, Long J, Hu M, Davis CM, Wang J, Brunicardi FC, Shi Y, Chen Y-G, Meng A, Feng X-H (2006) PPM1A functions as a Smad phosphatase to terminate TGFbeta signaling. Cell 125:915–928. https://doi.org/10.1016/j.cell.2006.03.044

146. Duan X, Liang Y-Y, Feng X-H, Lin X (2006) Protein serine/threonine phosphatase PPM1A dephosphorylates Smad1 in the bone morphogenetic protein signaling pathway. J Biol Chem 281:36526–36532. https://doi.org/10.1074/jbc.M605169200

147. Chen HB, Shen J, Ip YT, Xu L (2006) Identification of phosphatases for Smad in the BMP/DPP pathway. Genes Dev 20:648–653. https://doi.org/10.1101/gad.1384706

148. Sapkota G, Knockaert M, Alarcón C, Montalvo E, Brivanlou AH, Massagué J (2006) Dephosphorylation of the Linker Regions of Smad1 and Smad2/3 by Small C-terminal Domain Phosphatases Has Distinct Outcomes for Bone Morphogenetic Protein and Transforming Growth Factor-β Pathways*. Journal of Biological Chemistry 281:40412–40419. https://doi.org/10.1074/jbc.M610172200

149. Yu J, Pan L, Qin X, Chen H, Xu Y, Chen Y, Tang H (2010) MTMR4 attenuates transforming growth factor beta (TGFbeta) signaling by dephosphorylating R-Smads in endosomes. J Biol Chem 285:8454–8462. https://doi.org/10.1074/jbc.M109.075036

150. Lönn P, Morén A, Raja E, Dahl M, Moustakas A (2009) Regulating the stability of TGFβ receptors and Smads. Cell Res 19:21–35. https://doi.org/10.1038/cr.2008.308

151. Alarcón C, Zaromytidou A-I, Xi Q, Gao S, Yu J, Fujisawa S, Barlas A, Miller AN, Manova-Todorova K, Macias MJ, Sapkota G, Pan D, Massagué J (2009) CDK8/9 drive Smad transcriptional action, turnover and YAP interactions in BMP and TGFβ pathways. Cell 139:757–769. https://doi.org/10.1016/j.cell.2009.09.035

152. Guo X, Ramirez A, Waddell DS, Li Z, Liu X, Wang X-F (2008) Axin and GSK3-β control Smad3 protein stability and modulate TGF-β signaling. Genes Dev 22:106–120. https://doi.org/10.1101/gad.1590908

153. Sapkota G, Alarcón C, Spagnoli FM, Brivanlou AH, Massagué J (2007) Balancing BMP Signaling through Integrated Inputs into the Smad1 Linker. Molecular Cell 25:441–454. https://doi.org/10.1016/j.molcel.2007.01.006

154. Miyazawa K, Miyazono K (2017) Regulation of TGF-β Family Signaling by Inhibitory Smads. Cold Spring Harb Perspect Biol 9:a022095. https://doi.org/10.1101/cshperspect.a022095

155. Imamura T, Takase M, Nishihara A, Oeda E, Hanai J, Kawabata M, Miyazono K (1997) Smad6 inhibits signalling by the TGF-beta superfamily. Nature 389:622–626. https://doi.org/10.1038/39355

156. Hayashi H, Abdollah S, Qiu Y, Cai J, Xu YY, Grinnell BW, Richardson MA, Topper JN, Gimbrone MA, Wrana JL, Falb D (1997) The MAD-related protein Smad7 associates with the TGFbeta receptor and functions as an antagonist of TGFbeta signaling. Cell 89:1165–1173. https://doi.org/10.1016/s0092-8674(00)80303-7

157. Nakao A, Afrakhte M, Morén A, Nakayama T, Christian JL, Heuchel R, Itoh S, Kawabata M, Heldin NE, Heldin CH, ten Dijke P (1997) Identification of Smad7, a TGFbeta-inducible antagonist of TGF-beta signalling. Nature 389:631–635. https://doi.org/10.1038/39369

158. Ishida W, Hamamoto T, Kusanagi K, Yagi K, Kawabata M, Takehara K, Sampath TK, Kato M, Miyazono K (2000) Smad6 is a Smad1/5-induced smad inhibitor. Characterization of bone morphogenetic protein-responsive element in the mouse Smad6 promoter. J Biol Chem 275:6075–6079. https://doi.org/10.1074/jbc.275.9.6075

159. Zhang S, Fei T, Zhang L, Zhang R, Chen F, Ning Y, Han Y, Feng X-H, Meng A, Chen Y-G (2007) Smad7 antagonizes transforming growth factor beta signaling in the nucleus by interfering with functional Smad-DNA complex formation. Mol Cell Biol 27:4488–4499. https://doi.org/10.1128/MCB.01636-06

160. Yan X, Pan J, Xiong W, Cheng M, Sun Y, Zhang S, Chen Y (2014) Yin Yang 1 (YY1) synergizes with Smad7 to inhibit TGF-β signaling in the nucleus. Sci China Life Sci 57:128–136. https://doi.org/10.1007/s11427-013-4581-2

161. Bai S, Cao X (2002) A nuclear antagonistic mechanism of inhibitory Smads in transforming growth factor-beta signaling. J Biol Chem 277:4176–4182. https://doi.org/10.1074/jbc.M105105200

162. Moustakas A, Heldin C-H (2005) Non-Smad TGF-beta signals. J Cell Sci 118:3573–3584. https://doi.org/10.1242/jcs.02554

163. Zhang YE (2017) Non-Smad Signaling Pathways of the TGF-β Family. Cold Spring Harb Perspect Biol 9:a022129. https://doi.org/10.1101/cshperspect.a022129

164. Morrison DK (2012) MAP Kinase Pathways. Cold Spring Harb Perspect Biol 4:a011254. https://doi.org/10.1101/cshperspect.a011254

165. Kim EK, Choi E-J (2015) Compromised MAPK signaling in human diseases: an update. Arch Toxicol 89:867–882. https://doi.org/10.1007/s00204-015-1472-2

166. Bhowmick NA, Zent R, Ghiassi M, McDonnell M, Moses HL (2001) Integrin β1 Signaling Is Necessary for Transforming Growth Factor-β Activation of p38MAPK and Epithelial Plasticity*. Journal of Biological Chemistry 276:46707–46713. https://doi.org/10.1074/jbc.M106176200

167. Yu L, Hébert MC, Zhang YE (2002) TGF-β receptor-activated p38 MAP kinase mediates Smad-independent TGF-β responses. The EMBO Journal 21:3749–3759. https://doi.org/10.1093/emboj/cdf366

168. Hanafusa H, Ninomiya-Tsuji J, Masuyama N, Nishita M, Fujisawa J, Shibuya H, Matsumoto K, Nishida E (1999) Involvement of the p38 mitogen-activated protein kinase pathway in transforming growth factor-beta-induced gene expression. J Biol Chem 274:27161–27167. https://doi.org/10.1074/jbc.274.38.27161

169. Sano Y, Harada J, Tashiro S, Gotoh-Mandeville R, Maekawa T, Ishii S (1999) ATF-2 is a common nuclear target of Smad and TAK1 pathways in transforming growth factor-beta signaling. J Biol Chem 274:8949–8957. https://doi.org/10.1074/jbc.274.13.8949

170. Engel ME, McDonnell MA, Law BK, Moses HL (1999) Interdependent SMAD and JNK signaling in transforming growth factor-beta-mediated transcription. J Biol Chem 274:37413–37420. https://doi.org/10.1074/jbc.274.52.37413

171. Hocevar BA, Brown TL, Howe PH (1999) TGF-β induces fibronectin synthesis through a c-Jun N-terminal kinase-dependent, Smad4-independent pathway. The EMBO Journal 18:1345–1356. https://doi.org/10.1093/emboj/18.5.1345

172. Itoh S, Thorikay M, Kowanetz M, Moustakas A, Itoh F, Heldin C-H, ten Dijke P (2003) Elucidation of Smad Requirement in Transforming Growth Factor-β Type I Receptor-induced Responses*. Journal of Biological Chemistry 278:3751–3761. https://doi.org/10.1074/jbc.M208258200

173. Mita H, Tsutsui J, Takekawa M, Witten EA, Saito H (2002) Regulation of MTK1/MEKK4 Kinase Activity by Its N-Terminal Autoinhibitory Domain and GADD45 Binding. Mol Cell Biol 22:4544–4555. https://doi.org/10.1128/MCB.22.13.4544-4555.2002

174. Takekawa M, Tatebayashi K, Itoh F, Adachi M, Imai K, Saito H (2002) Smad-dependent GADD45β expression mediates delayed activation of p38 MAP kinase by TGF-β. The EMBO Journal 21:6473–6482. https://doi.org/10.1093/emboj/cdf643

175. Ungefroren H, Groth S, Ruhnke M, Kalthoff H, Fändrich F (2005) Transforming growth factor-beta (TGF-beta) type I receptor/ALK5-dependent activation of the GADD45beta gene mediates the induction of biglycan expression by TGF-beta. J Biol Chem 280:2644–2652. https://doi.org/10.1074/jbc.M411925200

176. Ungefroren H, Lenschow W, Chen W-B, Faendrich F, Kalthoff H (2003) Regulation of biglycan gene expression by transforming growth factor-beta requires MKK6-p38 mitogen-activated protein Kinase signaling downstream of Smad signaling. J Biol Chem 278:11041–11049. https://doi.org/10.1074/jbc.M300035200

177. Yamaguchi K, Shirakabe K, Shibuya H, Irie K, Oishi I, Ueno N, Taniguchi T, Nishida E, Matsumoto K (1995) Identification of a member of the MAPKKK family as a potential mediator of TGF-beta signal transduction. Science 270:2008–2011. https://doi.org/10.1126/science.270.5244.2008

178. Sakurai H, Suzuki S, Kawasaki N, Nakano H, Okazaki T, Chino A, Doi T, Saiki I (2003) Tumor Necrosis Factor-α-induced IKK Phosphorylation of NF-κB p65 on Serine 536 Is Mediated through the TRAF2, TRAF5, and TAK1 Signaling Pathway*. Journal of Biological Chemistry 278:36916–36923. https://doi.org/10.1074/jbc.M301598200

179. Ninomiya-Tsuji J, Kishimoto K, Hiyama A, Inoue J, Cao Z, Matsumoto K (1999) The kinase TAK1 can activate the NIK-IκB as well as the MAP kinase cascade in the IL-1 signalling pathway. Nature 398:252–256. https://doi.org/10.1038/18465

180. Shirakabe K, Yamaguchi K, Shibuya H, Irie K, Matsuda S, Moriguchi T, Gotoh Y, Matsumoto K, Nishida E (1997) TAK1 mediates the ceramide signaling to stress-activated protein kinase/c-Jun N-terminal kinase. J Biol Chem 272:8141–8144. https://doi.org/10.1074/jbc.272.13.8141

181. Shim J-H, Xiao C, Paschal AE, Bailey ST, Rao P, Hayden MS, Lee K-Y, Bussey C, Steckel M, Tanaka N, Yamada G, Akira S, Matsumoto K, Ghosh S (2005) TAK1, but not TAB1 or TAB2, plays an essential role in multiple signaling pathways in vivo. Genes Dev 19:2668–2681. https://doi.org/10.1101/gad.1360605

182. Mukhopadhyay H, Lee NY (2020) Multifaceted Roles of TAK1 Signaling in Cancer. Oncogene 39:1402–1413. https://doi.org/10.1038/s41388-019-1088-8

183. Jadrich JL, O'Connor MB, Coucouvanis E (2006) The TGF beta activated kinase TAK1 regulates vascular development in vivo. Development 133:1529–1541. https://doi.org/10.1242/dev.02333

184. Sorrentino A, Thakur N, Grimsby S, Marcusson A, von Bulow V, Schuster N, Zhang S, Heldin C-H, Landström M (2008) The type I TGF-beta receptor engages TRAF6 to activate TAK1 in a receptor kinase-independent manner. Nat Cell Biol 10:1199–1207. https://doi.org/10.1038/ncb1780

185. Yamashita M, Fatyol K, Jin C, Wang X, Liu Z, Zhang YE (2008) TRAF6 mediates Smad-independent activation of JNK and p38 by TGF-beta. Mol Cell 31:918–924. https://doi.org/10.1016/j.molcel.2008.09.002

186. Wang C, Deng L, Hong M, Akkaraju GR, Inoue J, Chen ZJ (2001) TAK1 is a ubiquitin-dependent kinase of MKK and IKK. Nature 412:346–351. https://doi.org/10.1038/35085597

187. Mu Y, Sundar R, Thakur N, Ekman M, Gudey SK, Yakymovych M, Hermansson A, Dimitriou H, Bengoechea-Alonso MT, Ericsson J, Heldin C-H, Landström M (2011) TRAF6 ubiquitinates TGFβ type I receptor to promote its cleavage and nuclear translocation in cancer. Nat Commun 2:330. https://doi.org/10.1038/ncomms1332

188. Gudey SK, Sundar R, Mu Y, Wallenius A, Zang G, Bergh A, Heldin C-H, Landström M (2014) TRAF6 Stimulates the Tumor-Promoting Effects of TGFβ Type I Receptor Through Polyubiquitination and Activation of Presenilin 1. Science Signaling 7:ra2–ra2. https://doi.org/10.1126/scisignal.2004207

189. Zhang L, Zhou F, García de Vinuesa A, de Kruijf EM, Mesker WE, Hui L, Drabsch Y, Li Y, Bauer A, Rousseau A, Sheppard K-A, Mickanin C, Kuppen PJK, Lu CX, Ten Dijke P (2013) TRAF4 promotes TGF-β receptor signaling and drives breast cancer metastasis. Mol Cell 51:559–572. https://doi.org/10.1016/j.molcel.2013.07.014

190. Liu Q, Busby JC, Molkentin JD (2009) Interaction between TAK1–TAB1–TAB2 and RCAN1–calcineurin defines a signalling nodal control point. Nat Cell Biol 11:154–161. https://doi.org/10.1038/ncb1823

191. Brown JD, DiChiara MR, Anderson KR, Gimbrone MA, Topper JN (1999) MEKK-1, a component of the stress (stress-activated protein kinase/c-Jun N-terminal kinase) pathway, can selectively activate Smad2-mediated transcriptional activation in endothelial cells. J Biol Chem 274:8797–8805. https://doi.org/10.1074/jbc.274.13.8797

192. Kim K-Y, Kim B-C, Xu Z, Kim S-J (2004) Mixed lineage kinase 3 (MLK3)-activated p38 MAP kinase mediates transforming growth factor-beta-induced apoptosis in hepatoma cells. J Biol Chem 279:29478–29484. https://doi.org/10.1074/jbc.M313947200

193. Sapkota GP (2013) The TGFβ-induced phosphorylation and activation of p38 mitogen-activated protein kinase is mediated by MAP3K4 and MAP3K10 but not TAK1. Open Biol 3:130067. https://doi.org/10.1098/rsob.130067

194. Zhang L, Wang W, Hayashi Y, Jester JV, Birk DE, Gao M, Liu C-Y, Kao WW-Y, Karin M, Xia Y (2003) A role for MEK kinase 1 in TGF-beta/activin-induced epithelium movement and embryonic eyelid closure. EMBO J 22:4443–4454. https://doi.org/10.1093/emboj/cdg440

195. Tu H, Costa M (2020) XIAP's Profile in Human Cancer. Biomolecules 10:1493. https://doi.org/10.3390/biom10111493

196. Reffey SB, Wurthner JU, Parks WT, Roberts AB, Duckett CS (2001) X-linked Inhibitor of Apoptosis Protein Functions as a Cofactor in Transforming Growth Factor-β Signaling*. Journal of Biological Chemistry 276:26542–26549. https://doi.org/10.1074/jbc.M100331200

197. Yamaguchi K, Nagai S, Ninomiya-Tsuji J, Nishita M, Tamai K, Irie K, Ueno N, Nishida E, Shibuya H, Matsumoto K (1999) XIAP, a cellular member of the inhibitor of apoptosis protein family, links the receptors to TAB1-TAK1 in the BMP signaling pathway. EMBO J 18:179–187. https://doi.org/10.1093/emboj/18.1.179

198. Jing Y, Ren Y, Witzel HR, Dobreva G (2021) A BMP4-p38 MAPK signaling axis controls ISL1 protein stability and activity during cardiogenesis. Stem Cell Reports 16:1894–1905. https://doi.org/10.1016/j.stemcr.2021.06.017

199. Kimura N, Matsuo R, Shibuya H, Nakashima K, Taga T (2000) BMP2-induced apoptosis is mediated by activation of the TAK1-p38 kinase pathway that is negatively regulated by Smad6. J Biol Chem 275:17647–17652. https://doi.org/10.1074/jbc.M908622199

200. Guicheux J, Lemonnier J, Ghayor C, Suzuki A, Palmer G, Caverzasio J (2003) Activation of p38 mitogen-activated protein kinase and c-Jun-NH2-terminal kinase by BMP-2 and their implication in the stimulation of osteoblastic cell differentiation. J Bone Miner Res 18:2060–2068. https://doi.org/10.1359/jbmr.2003.18.11.2060

201. Benn A, Hiepen C, Osterland M, Schütte C, Zwijsen A, Knaus P (2017) Role of bone morphogenetic proteins in sprouting angiogenesis: differential BMP receptor-dependent signaling pathways balance stalk vs. tip cell competence. FASEB J 31:4720–4733. https://doi.org/10.1096/fj.201700193RR

202. Liu X, Zhao Y, Peng S, Zhang S, Wang M, Chen Y, Zhang S, Yang Y, Sun C (2016) BMP7 retards peripheral myelination by activating p38 MAPK in Schwann cells. Sci Rep 6:31049. https://doi.org/10.1038/srep31049

203. Rouse J, Cohen P, Trigon S, Morange M, Alonso-Llamazares A, Zamanillo D, Hunt T, Nebreda AR (1994) A novel kinase cascade triggered by stress and heat shock that stimulates MAPKAP kinase-2 and phosphorylation of the small heat shock proteins. Cell 78:1027–1037. https://doi.org/10.1016/0092-8674(94)90277-1

204. Stokoe D, Engel K, Campbell DG, Cohen P, Gaestel M (1992) Identification of MAPKAP kinase 2 as a major enzyme responsible for the phosphorylation of the small mammalian heat shock proteins. FEBS Lett 313:307–313. https://doi.org/10.1016/0014-5793(92)81216-9

205. Xu L, Chen S, Bergan RC (2006) MAPKAPK2 and HSP27 are downstream effectors of p38 MAP kinase-mediated matrix metalloproteinase type 2 activation and cell invasion in human prostate cancer. Oncogene 25:2987–2998. https://doi.org/10.1038/sj.onc.1209337

206. Kondo Y, Higa-Nakamine S, Maeda N, Toku S, Kakinohana M, Sugahara K, Kukita I, Yamamoto H (2016) Stimulation of Cell Migration by Flagellin Through the p38 MAP Kinase Pathway in Cultured Intestinal Epithelial Cells. Journal of Cellular Biochemistry 117:247–258. https://doi.org/10.1002/jcb.25272

207. Verma A, Deb DK, Sassano A, Uddin S, Varga J, Wickrema A, Platanias LC (2002) Activation of the p38 mitogen-activated protein kinase mediates the suppressive effects of type I interferons and transforming growth factor-beta on normal hematopoiesis. J Biol Chem 277:7726–7735. https://doi.org/10.1074/jbc.M106640200

208. Abécassis L, Rogier E, Vazquez A, Atfi A, Bourgeade M-F (2004) Evidence for a role of MSK1 in transforming growth factor-beta-mediated responses through p38alpha and Smad signaling pathways. J Biol Chem 279:30474–30479. https://doi.org/10.1074/jbc.M403294200

209. Shibuya H, Iwata H, Masuyama N, Gotoh Y, Yamaguchi K, Irie K, Matsumoto K, Nishida E, Ueno N (1998) Role of TAK1 and TAB1 in BMP signaling in early Xenopus development. EMBO J 17:1019–1028. https://doi.org/10.1093/emboj/17.4.1019

210. Edlund S, Bu S, Schuster N, Aspenström P, Heuchel R, Heldin N-E, ten Dijke P, Heldin C-H, Landström M (2003) Transforming growth factor-beta1 (TGF-beta)-induced apoptosis of prostate cancer cells involves Smad7-dependent activation of p38 by TGF-beta-activated kinase 1 and mitogen-activated protein kinase kinase 3. Mol Biol Cell 14:529–544. https://doi.org/10.1091/mbc.02-03-0037

211. Bakin AV, Rinehart C, Tomlinson AK, Arteaga CL (2002) p38 mitogen-activated protein kinase is required for TGFbeta-mediated fibroblastic transdifferentiation and cell migration. J Cell Sci 115:3193–3206. https://doi.org/10.1242/jcs.115.15.3193

212. Yoo J, Ghiassi M, Jirmanova L, Balliet AG, Hoffman B, Fornace AJ, Liebermann DA, Bottinger EP, Roberts AB (2003) Transforming growth factor-beta-induced apoptosis is mediated by Smad-dependent expression of GADD45b through p38 activation. J Biol Chem 278:43001–43007. https://doi.org/10.1074/jbc.M307869200

213. Medici D, Potenta S, Kalluri R (2011) Transforming growth factor-β2 promotes Snail-mediated endothelial-mesenchymal transition through convergence of Smad-dependent and Smad-independent signalling. Biochem J 437:515–520. https://doi.org/10.1042/BJ20101500

214. Lawler S, Feng XH, Chen RH, Maruoka EM, Turck CW, Griswold-Prenner I, Derynck R (1997) The type II transforming growth factor-beta receptor autophosphorylates not only on serine and threonine but also on tyrosine residues. J Biol Chem 272:14850–14859. https://doi.org/10.1074/jbc.272.23.14850

215. Lee MK, Pardoux C, Hall MC, Lee PS, Warburton D, Qing J, Smith SM, Derynck R (2007) TGF-β activates Erk MAP kinase signalling through direct phosphorylation of ShcA. EMBO J 26:3957–3967. https://doi.org/10.1038/sj.emboj.7601818

216. Nakerakanti S, Trojanowska M (2012) The Role of TGF-β Receptors in Fibrosis. Open Rheumatol J 6:156–162. https://doi.org/10.2174/1874312901206010156

217. Galliher AJ, Schiemann WP (2007) Src Phosphorylates Tyr284 in TGF-β Type II Receptor and Regulates TGF-β Stimulation of p38 MAPK during Breast Cancer Cell Proliferation and Invasion. Cancer Research 67:3752–3758. https://doi.org/10.1158/0008-5472.CAN-06-3851

218. Yakymovych I, Yakymovych M, Hamidi A, Landström M, Heldin C-H (2022) The type II TGF-β receptor phosphorylates Tyr182 in the type I receptor to activate downstream Src signaling. Sci Signal 15:eabp9521. https://doi.org/10.1126/scisignal.abp9521

219. Gallea S, Lallemand F, Atfi A, Rawadi G, Ramez V, Spinella-Jaegle S, Kawai S, Faucheu C, Huet L, Baron R, Roman-Roman S (2001) Activation of mitogen-activated protein kinase cascades is involved in regulation of bone morphogenetic protein-2-induced osteoblast differentiation in pluripotent C2C12 cells. Bone 28:491–498. https://doi.org/10.1016/s8756-3282(01)00415-x

220. Lai C-F, Cheng S-L (2002) Signal transductions induced by bone morphogenetic protein-2 and transforming growth factor-beta in normal human osteoblastic cells. J Biol Chem 277:15514–15522. https://doi.org/10.1074/jbc.M200794200

221. Zhou Q, Heinke J, Vargas A, Winnik S, Krauss T, Bode C, Patterson C, Moser M (2007) ERK signaling is a central regulator for BMP-4 dependent capillary sprouting. Cardiovasc Res 76:390–399. https://doi.org/10.1016/j.cardiores.2007.08.003

222. Simeone DM, Zhang L, Graziano K, Nicke B, Pham T, Schaefer C, Logsdon CD (2001) Smad4 mediates activation of mitogen-activated protein kinases by TGF-beta in pancreatic acinar cells. Am J Physiol Cell Physiol 281:C311-319. https://doi.org/10.1152/ajpcell.2001.281.1.C311

223. Xie L, Law BK, Chytil AM, Brown KA, Aakre ME, Moses HL (2004) Activation of the Erk pathway is required for TGF-beta1-induced EMT in vitro. Neoplasia 6:603–610. https://doi.org/10.1593/neo.04241

224. Zavadil J, Bitzer M, Liang D, Yang YC, Massimi A, Kneitz S, Piek E, Bottinger EP (2001) Genetic programs of epithelial cell plasticity directed by transforming growth factor-beta. Proc Natl Acad Sci U S A 98:6686–6691. https://doi.org/10.1073/pnas.111614398

225. Lim M, Chuong C-M, Roy-Burman P (2011) PI3K, Erk signaling in BMP7-induced epithelial-mesenchymal transition (EMT) of PC-3 prostate cancer cells in 2- and 3-dimensional cultures. Horm Cancer 2:298–309. https://doi.org/10.1007/s12672-011-0084-4

226. Carnero A, Blanco-Aparicio C, Renner O, Link W, Leal JFM (2008) The PTEN/PI3K/AKT signalling pathway in cancer, therapeutic implications. Curr Cancer Drug Targets 8:187–198. https://doi.org/10.2174/156800908784293659

227. Fruman DA, Rommel C (2014) PI3K and cancer: lessons, challenges and opportunities. Nat Rev Drug Discov 13:140–156. https://doi.org/10.1038/nrd4204

228. Bakin AV, Tomlinson AK, Bhowmick NA, Moses HL, Arteaga CL (2000) Phosphatidylinositol 3-Kinase Function Is Required for Transforming Growth Factor β-mediated Epithelial to Mesenchymal Transition and Cell Migration*. Journal of Biological Chemistry 275:36803–36810. https://doi.org/10.1074/jbc.M005912200

229. Viñals F, Pouysségur J (2001) Transforming Growth Factor β1 (TGF-β1) Promotes Endothelial Cell Survival during In Vitro Angiogenesis via an Autocrine Mechanism Implicating TGF-α Signaling. Mol Cell Biol 21:7218–7230. https://doi.org/10.1128/MCB.21.21.7218-7230.2001

230. Gamell C, Osses N, Bartrons R, Rückle T, Camps M, Rosa JL, Ventura F (2008) BMP2 induction of actin cytoskeleton reorganization and cell migration requires PI3-kinase and Cdc42 activity. Journal of Cell Science 121:3960–3970. https://doi.org/10.1242/jcs.031286

231. Boergermann JH, Kopf J, Yu PB, Knaus P (2010) Dorsomorphin and LDN-193189 inhibit BMP-mediated Smad, p38 and Akt signalling in C2C12 cells. Int J Biochem Cell Biol 42:1802–1807. https://doi.org/10.1016/j.biocel.2010.07.018

232. Yi JY, Shin I, Arteaga CL (2005) Type I transforming growth factor beta receptor binds to and activates phosphatidylinositol 3-kinase. J Biol Chem 280:10870–10876. https://doi.org/10.1074/jbc.M413223200

233. Lamouille S, Derynck R (2007) Cell size and invasion in TGF-beta-induced epithelial to mesenchymal transition is regulated by activation of the mTOR pathway. J Cell Biol 178:437–451. https://doi.org/10.1083/jcb.200611146

234. Yang W-L, Wang J, Chan C-H, Lee S-W, Campos AD, Lamothe B, Hur L, Grabiner BC, Lin X, Darnay BG, Lin H-K (2009) The E3 ligase TRAF6 regulates Akt ubiquitination and activation. Science 325:1134–1138. https://doi.org/10.1126/science.1175065

235. Xia H, Ooi LLPJ, Hui KM (2013) MicroRNA-216a/217-induced epithelial-mesenchymal transition targets PTEN and SMAD7 to promote drug resistance and recurrence of liver cancer. Hepatology 58:629–641. https://doi.org/10.1002/hep.26369

236. Tan E-J, Olsson A-K, Moustakas A (2014) Reprogramming during epithelial to mesenchymal transition under the control of TGFβ. Cell Adh Migr 9:233–246. https://doi.org/10.4161/19336918.2014.983794

237. Zhou BP, Deng J, Xia W, Xu J, Li YM, Gunduz M, Hung M-C (2004) Dual regulation of Snail by GSK-3beta-mediated phosphorylation in control of epithelial-mesenchymal transition. Nat Cell Biol 6:931–940. https://doi.org/10.1038/ncb1173

238. Julien S, Puig I, Caretti E, Bonaventure J, Nelles L, van Roy F, Dargemont C, de Herreros AG, Bellacosa A, Larue L (2007) Activation of NF-kappaB by Akt upregulates Snail expression and induces epithelium mesenchyme transition. Oncogene 26:7445–7456. https://doi.org/10.1038/sj.onc.1210546

239. Gomis RR, Alarcón C, He W, Wang Q, Seoane J, Lash A, Massagué J (2006) A FoxO-Smad synexpression group in human keratinocytes. Proc Natl Acad Sci U S A 103:12747–12752. https://doi.org/10.1073/pnas.0605333103

240. Seoane J, Le H-V, Shen L, Anderson SA, Massagué J (2004) Integration of Smad and forkhead pathways in the control of neuroepithelial and glioblastoma cell proliferation. Cell 117:211–223. https://doi.org/10.1016/s0092-8674(04)00298-3

241. Lamouille S, Connolly E, Smyth JW, Akhurst RJ, Derynck R (2012) TGF-β-induced activation of mTOR complex 2 drives epithelial-mesenchymal transition and cell invasion. J Cell Sci 125:1259–1273. https://doi.org/10.1242/jcs.095299

242. Jaffe AB, Hall A (2005) Rho GTPases: biochemistry and biology. Annu Rev Cell Dev Biol 21:247–269. https://doi.org/10.1146/annurev.cellbio.21.020604.150721

243. Bhowmick NA, Ghiassi M, Bakin A, Aakre M, Lundquist CA, Engel ME, Arteaga CL, Moses HL (2001) Transforming growth factor-beta1 mediates epithelial to mesenchymal transdifferentiation through a RhoA-dependent mechanism. Mol Biol Cell 12:27–36. https://doi.org/10.1091/mbc.12.1.27

244. Edlund S, Landström M, Heldin C-H, Aspenström P (2002) Transforming growth factor-beta-induced mobilization of actin cytoskeleton requires signaling by small GTPases Cdc42 and RhoA. Mol Biol Cell 13:902–914. https://doi.org/10.1091/mbc.01-08-0398

245. Wang Y-K, Yu X, Cohen DM, Wozniak MA, Yang MT, Gao L, Eyckmans J, Chen CS (2012) Bone morphogenetic protein-2-induced signaling and osteogenesis is regulated by cell shape, RhoA/ROCK, and cytoskeletal tension. Stem Cells Dev 21:1176–1186. https://doi.org/10.1089/scd.2011.0293

246. Voorneveld PW, Kodach LL, Jacobs RJ, Liv N, Zonnevylle AC, Hoogenboom JP, Biemond I, Verspaget HW, Hommes DW, de Rooij K, van Noesel CJM, Morreau H, van Wezel T, Offerhaus GJA, van den Brink GR, Peppelenbosch MP, Ten Dijke P, Hardwick JCH (2014) Loss of SMAD4 alters BMP signaling to promote colorectal cancer cell metastasis via activation of Rho and ROCK. Gastroenterology 147:196-208.e13. https://doi.org/10.1053/j.gastro.2014.03.052

247. Shen X, Li J, Hu PP, Waddell D, Zhang J, Wang XF (2001) The activity of guanine exchange factor NET1 is essential for transforming growth factor-beta-mediated stress fiber formation. J Biol Chem 276:15362–15368. https://doi.org/10.1074/jbc.M009534200

248. Papadimitriou E, Vasilaki E, Vorvis C, Iliopoulos D, Moustakas A, Kardassis D, Stournaras C (2012) Differential regulation of the two RhoA-specific GEF isoforms Net1/Net1A by TGF-β and miR-24: role in epithelial-to-mesenchymal transition. Oncogene 31:2862–2875. https://doi.org/10.1038/onc.2011.457

249. Lee J, Moon H-J, Lee J-M, Joo C-K (2010) Smad3 Regulates Rho Signaling via NET1 in the Transforming Growth Factor-β-induced Epithelial-Mesenchymal Transition of Human Retinal Pigment Epithelial Cells *. Journal of Biological Chemistry 285:26618–26627. https://doi.org/10.1074/jbc.M109.073155

250. Ozdamar B, Bose R, Barrios-Rodiles M, Wang H-R, Zhang Y, Wrana JL (2005) Regulation of the polarity protein Par6 by TGFbeta receptors controls epithelial cell plasticity. Science 307:1603–1609. https://doi.org/10.1126/science.1105718

251. Mu Y, Zang G, Engström U, Busch C, Landström M (2015) TGFβ-induced phosphorylation of Par6 promotes migration and invasion in prostate cancer cells. Br J Cancer 112:1223–1231. https://doi.org/10.1038/bjc.2015.71

252. Gunaratne A, Thai BL, Di Guglielmo GM (2013) Atypical Protein Kinase C Phosphorylates Par6 and Facilitates Transforming Growth Factor β-Induced Epithelial-to-Mesenchymal Transition. Mol Cell Biol 33:874–886. https://doi.org/10.1128/MCB.00837-12

253. Wilkes MC, Murphy SJ, Garamszegi N, Leof EB (2003) Cell-type-specific activation of PAK2 by transforming growth factor beta independent of Smad2 and Smad3. Mol Cell Biol 23:8878–8889. https://doi.org/10.1128/MCB.23.23.8878-8889.2003

254. Foletta VC, Lim MA, Soosairajah J, Kelly AP, Stanley EG, Shannon M, He W, Das S, Massague J, Bernard O (2003) Direct signaling by the BMP type II receptor via the cytoskeletal regulator LIMK1. J Cell Biol 162:1089–1098. https://doi.org/10.1083/jcb.200212060

255. Lee-Hoeflich ST, Causing CG, Podkowa M, Zhao X, Wrana JL, Attisano L (2004) Activation of LIMK1 by binding to the BMP receptor, BMPRII, regulates BMP-dependent dendritogenesis. EMBO J 23:4792–4801. https://doi.org/10.1038/sj.emboj.7600418

256. Hu X, Li J, Fu M, Zhao X, Wang W (2021) The JAK/STAT signaling pathway: from bench to clinic. Sig Transduct Target Ther 6:1–33. https://doi.org/10.1038/s41392-021-00791-1

257. Boulanger MJ, Chow D, Brevnova EE, Garcia KC (2003) Hexameric structure and assembly of the interleukin-6/IL-6 alpha-receptor/gp130 complex. Science 300:2101–2104. https://doi.org/10.1126/science.1083901

258. Skiniotis G, Boulanger MJ, Garcia KC, Walz T (2005) Signaling conformations of the tall cytokine receptor gp130 when in complex with IL-6 and IL-6 receptor. Nat Struct Mol Biol 12:545–551. https://doi.org/10.1038/nsmb941

259. Durham GA, Williams JJL, Nasim MT, Palmer TM (2019) Targeting SOCS Proteins to Control JAK-STAT Signalling in Disease. Trends Pharmacol Sci 40:298–308. https://doi.org/10.1016/j.tips.2019.03.001

260. Eulenfeld R, Dittrich A, Khouri C, Müller PJ, Mütze B, Wolf A, Schaper F (2012) Interleukin-6 signalling: more than Jaks and STATs. Eur J Cell Biol 91:486–495. https://doi.org/10.1016/j.ejcb.2011.09.010

261. Trengove MC, Ward AC (2013) SOCS proteins in development and disease. Am J Clin Exp Immunol 2:1–29

262. Yoshimura A, Ito M, Mise-Omata S, Ando M (2021) SOCS: negative regulators of cytokine signaling for immune tolerance. International Immunology 33:711–716. https://doi.org/10.1093/intimm/dxab055

263. Yin Y, Liu W, Dai Y (2015) SOCS3 and its role in associated diseases. Human Immunology 76:775–780. https://doi.org/10.1016/j.humimm.2015.09.037

264. Radtke S, Wüller S, Yang X, Lippok B, Mütze B, Mais C, Leur H, Bode J, Gaestel M, Heinrich P, Behrmann I, Schaper F, Hermanns H (2010) Cross-regulation of cytokine signalling: Pro-inflammatory cytokines restrict IL-6 signalling through receptor internalisation and degradation. Journal of cell science 123:947–59. https://doi.org/10.1242/jcs.065326

265. Zha Z, Bucher F, Nejatfard A, Zheng T, Zhang H, Yea K, Lerner RA (2017) Interferon-γ is a master checkpoint regulator of cytokine-induced differentiation. Proceedings of the National Academy of Sciences 114:E6867–E6874. https://doi.org/10.1073/pnas.1706915114

266. Dees C, Tomcik M, Palumbo-Zerr K, Distler A, Beyer C, Lang V, Horn A, Zerr P, Zwerina J, Gelse K, Distler O, Schett G, Distler JHW (2012) JAK-2 as a novel mediator of the profibrotic effects of transforming growth factor β in systemic sclerosis. Arthritis Rheum 64:3006–3015. https://doi.org/10.1002/art.34500

267. Liu Y, Liu H, Meyer C, Li J, Nadalin S, Königsrainer A, Weng H, Dooley S, Ten Dijke P (2013) Transforming growth factor-β (TGF-β)-mediated connective tissue growth factor (CTGF) expression in hepatic stellate cells requires Stat3 signaling activation. J Biol Chem 288:30708–30719. https://doi.org/10.1074/jbc.M113.478685

268. Xiang G, Ying K, Jiang P, Jia M, Sun Y, Li S, Wu X, Hao S (2022) Growth differentiation factor 11 induces skeletal muscle atrophy via a STAT3-dependent mechanism in pulmonary arterial hypertension. Skelet Muscle 12:10. https://doi.org/10.1186/s13395-022-00292-x

269. Qu X, Liu Y, Cao D, Chen J, Liu Z, Ji H, Chen Y, Zhang W, Zhu P, Xiao D, Li X, Shou W, Chen H (2019) BMP10 preserves cardiac function through its dual activation of SMAD-mediated and STAT3-mediated pathways. J Biol Chem 294:19877–19888. https://doi.org/10.1074/jbc.RA119.010943

270. Bright JJ, Sriram S (1998) TGF-beta inhibits IL-12-induced activation of Jak-STAT pathway in T lymphocytes. J Immunol 161:1772–1777

271. Wierenga ATJ, Schuringa JJ, Eggen BJL, Kruijer W, Vellenga E (2002) Downregulation of IL-6-induced STAT3 tyrosine phosphorylation by TGF-beta1 is mediated by caspase-dependent and -independent processes. Leukemia 16:675–682. https://doi.org/10.1038/sj.leu.2402425

272. Hjertner O, Hjorth-Hansen H, Börset M, Seidel C, Waage A, Sundan A (2001) Bone morphogenetic protein-4 inhibits proliferation and induces apoptosis of multiple myeloma cells. Blood 97:516–522. https://doi.org/10.1182/blood.v97.2.516

273. Kawamura C, Kizaki M, Yamato K, Uchida H, Fukuchi Y, Hattori Y, Koseki T, Nishihara T, Ikeda Y (2000) Bone morphogenetic protein-2 induces apoptosis in human myeloma cells with modulation of STAT3. Blood 96:2005–2011

274. Cocolakis E, Dai M, Drevet L, Ho J, Haines E, Ali S, Lebrun J-J (2008) Smad signaling antagonizes STAT5-mediated gene transcription and mammary epithelial cell differentiation. J Biol Chem 283:1293–1307. https://doi.org/10.1074/jbc.M707492200

275. Qin H, Wang L, Feng T, Elson CO, Niyongere SA, Lee SJ, Reynolds SL, Weaver CT, Roarty K, Serra R, Benveniste EN, Cong Y (2009) TGF-β Promotes Th17 Cell Development through Inhibition of SOCS31. The Journal of Immunology 183:97–105. https://doi.org/10.4049/jimmunol.0801986

276. Dees C, Pötter S, Zhang Y, Bergmann C, Zhou X, Luber M, Wohlfahrt T, Karouzakis E, Ramming A, Gelse K, Yoshimura A, Jaenisch R, Distler O, Schett G, Distler JH (2020) TGF-β-induced epigenetic deregulation of SOCS3 facilitates STAT3 signaling to promote fibrosis. J Clin Invest 130:2347–2363. https://doi.org/10.1172/JCI122462

277. Roes J, Choi BK, Cazac BB (2003) Redirection of B cell responsiveness by transforming growth factor β receptor. Proceedings of the National Academy of Sciences 100:7241–7246. https://doi.org/10.1073/pnas.0731875100

278. Lovibond AC, Haque SJ, Chambers TJ, Fox SW (2003) TGF-beta-induced SOCS3 expression augments TNF-alpha-induced osteoclast formation. Biochem Biophys Res Commun 309:762–767. https://doi.org/10.1016/j.bbrc.2003.08.068

279. Liu X, Zhang Y, Yu Y, Yang X, Cao X (2008) SOCS3 promotes TLR4 response in macrophages by feedback inhibiting TGF-β1/Smad3 signaling. Molecular Immunology 45:1405–1413. https://doi.org/10.1016/j.molimm.2007.08.018

280. Taskén K, Aandahl EM (2004) Localized effects of cAMP mediated by distinct routes of protein kinase A. Physiol Rev 84:137–167. https://doi.org/10.1152/physrev.00021.2003

281. Wang L, Zhu Y, Sharma K (1998) Transforming growth factor-beta1 stimulates protein kinase A in mesangial cells. J Biol Chem 273:8522–8527. https://doi.org/10.1074/jbc.273.14.8522

282. Zhang L, Duan CJ, Binkley C, Li G, Uhler MD, Logsdon CD, Simeone DM (2004) A transforming growth factor beta-induced Smad3/Smad4 complex directly activates protein kinase A. Mol Cell Biol 24:2169–2180. https://doi.org/10.1128/MCB.24.5.2169-2180.2004

283. Kaiser J, Maibach M, Piovesana E, Salpeter I, Escher N, Ormen Y, Schwab ME (2020) TGFβ1 Induces Axonal Outgrowth via ALK5/PKA/SMURF1-Mediated Degradation of RhoA and Stabilization of PAR6. eNeuro 7:ENEURO.0104-20.2020. https://doi.org/10.1523/ENEURO.0104-20.2020

284. Yang H, Li G, Wu J-J, Wang L, Uhler M, Simeone DM (2013) Protein Kinase A Modulates Transforming Growth Factor-β Signaling through a Direct Interaction with Smad4 Protein. J Biol Chem 288:8737–8749. https://doi.org/10.1074/jbc.M113.455675

285. Yang H, Lee CJ, Zhang L, Sans MD, Simeone DM (2008) Regulation of transforming growth factor β-induced responses by protein kinase A in pancreatic acinar cells. Am J Physiol Gastrointest Liver Physiol 295:G170–G178. https://doi.org/10.1152/ajpgi.00492.2007

286. Gangopahyay A, Oran M, Bauer EM, Wertz JW, Comhair SA, Erzurum SC, Bauer PM (2011) Bone morphogenetic protein receptor II is a novel mediator of endothelial nitric-oxide synthase activation. J Biol Chem 286:33134–33140. https://doi.org/10.1074/jbc.M111.274100

287. Liu H, Margiotta JF, Howard MJ (2005) BMP4 supports noradrenergic differentiation by a PKA-dependent mechanism. Developmental Biology 286:521–536. https://doi.org/10.1016/j.ydbio.2005.08.022

288. Ohta Y, Nakagawa K, Imai Y, Katagiri T, Koike T, Takaoka K (2008) Cyclic AMP enhances Smad-mediated BMP signaling through PKA-CREB pathway. J Bone Miner Metab 26:478–484. https://doi.org/10.1007/s00774-008-0850-8

289. Luo K (2017) Signaling Cross Talk between TGF-β/Smad and Other Signaling Pathways. Cold Spring Harb Perspect Biol 9:a022137. https://doi.org/10.1101/cshperspect.a022137

290. Dowdy SC, Mariani A, Janknecht R (2003) HER2/Neu- and TAK1-mediated Up-regulation of the Transforming Growth Factor β Inhibitor Smad7 via the ETS Protein ER81*. Journal of Biological Chemistry 278:44377–44384. https://doi.org/10.1074/jbc.M307202200

291. Hoffmann A, Preobrazhenska O, Wodarczyk C, Medler Y, Winkel A, Shahab S, Huylebroeck D, Gross G, Verschueren K (2005) Transforming Growth Factor-β-activated Kinase-1 (TAK1), a MAP3K, Interacts with Smad Proteins and Interferes with Osteogenesis in Murine Mesenchymal Progenitors*. Journal of Biological Chemistry 280:27271–27283. https://doi.org/10.1074/jbc.M503368200

292. Yanagisawa M, Nakashima K, Takeda K, Ochiai W, Takizawa T, Ueno M, Takizawa M, Shibuya H, Taga T (2001) Inhibition of BMP2-induced, TAK1 kinase-mediated neurite outgrowth by Smad6 and Smad7. Genes to Cells 6:1091–1099. https://doi.org/10.1046/j.1365-2443.2001.00483.x

293. Jung SM, Lee J-H, Park J, Oh YS, Lee SK, Park JS, Lee YS, Kim JH, Lee JY, Bae Y-S, Koo S-H, Kim S-J, Park SH (2013) Smad6 inhibits non-canonical TGF-β1 signalling by recruiting the deubiquitinase A20 to TRAF6. Nat Commun 4:2562. https://doi.org/10.1038/ncomms3562

294. Mazars A, Lallemand F, Prunier C, Marais J, Ferrand N, Pessah M, Cherqui G, Atfi A (2001) Evidence for a role of the JNK cascade in Smad7-mediated apoptosis. J Biol Chem 276:36797–36803. https://doi.org/10.1074/jbc.M101672200

295. Kretzschmar M, Doody J, Massagué J (1997) Opposing BMP and EGF signalling pathways converge on the TGF-beta family mediator Smad1. Nature 389:618–622. https://doi.org/10.1038/39348

296. Matsuura I, Wang G, He D, Liu F (2005) Identification and characterization of ERK MAP kinase phosphorylation sites in Smad3. Biochemistry 44:12546–12553. https://doi.org/10.1021/bi050560g

297. Li Z, Fei T, Zhang J, Zhu G, Wang L, Lu D, Chi X, Teng Y, Hou N, Yang X, Zhang H, Han J-DJ, Chen Y-G (2012) BMP4 Signaling Acts via dual-specificity phosphatase 9 to control ERK activity in mouse embryonic stem cells. Cell Stem Cell 10:171–182. https://doi.org/10.1016/j.stem.2011.12.016

298. Zhang L, Zhou F, Drabsch Y, Gao R, Snaar-Jagalska BE, Mickanin C, Huang H, Sheppard K-A, Porter JA, Lu CX, ten Dijke P (2012) USP4 is regulated by AKT phosphorylation and directly deubiquitylates TGF-β type I receptor. Nat Cell Biol 14:717–726. https://doi.org/10.1038/ncb2522

299. Runyan CE, Schnaper HW, Poncelet A-C (2004) The phosphatidylinositol 3-kinase/Akt pathway enhances Smad3-stimulated mesangial cell collagen I expression in response to transforming growth factor-beta1. J Biol Chem 279:2632–2639. https://doi.org/10.1074/jbc.M310412200

300. Fuentealba LC, Eivers E, Ikeda A, Hurtado C, Kuroda H, Pera EM, De Robertis EM (2007) Integrating Patterning Signals: Wnt/GSK3 Regulates the Duration of the BMP/Smad1 Signal. Cell 131:980–993. https://doi.org/10.1016/j.cell.2007.09.027

301. Aragón E, Goerner N, Zaromytidou A-I, Xi Q, Escobedo A, Massagué J, Macias MJ (2011) A Smad action turnover switch operated by WW domain readers of a phosphoserine code. Genes Dev 25:1275–1288. https://doi.org/10.1101/gad.2060811

302. Wang G, Yu Y, Sun C, Liu T, Liang T, Zhan L, Lin X, Feng X-H (2016) STAT3 selectively interacts with Smad3 to antagonize TGF-β signaling. Oncogene 35:4388–4398. https://doi.org/10.1038/onc.2015.446

303. Nakashima K, Yanagisawa M, Arakawa H, Kimura N, Hisatsune T, Kawabata M, Miyazono K, Taga T (1999) Synergistic signaling in fetal brain by STAT3-Smad1 complex bridged by p300. Science 284:479–482. https://doi.org/10.1126/science.284.5413.479

304. Ulloa L, Doody J, Massagué J (1999) Inhibition of transforming growth factor-beta/SMAD signalling by the interferon-gamma/STAT pathway. Nature 397:710–713. https://doi.org/10.1038/17826

305. David L, Mallet C, Mazerbourg S, Feige J-J, Bailly S (2007) Identification of BMP9 and BMP10 as functional activators of the orphan activin receptor-like kinase 1 (ALK1) in endothelial cells. Blood 109:1953–1961. https://doi.org/10.1182/blood-2006-07-034124

306. Scharpfenecker M, van Dinther M, Liu Z, van Bezooijen RL, Zhao Q, Pukac L, Löwik CWGM, ten Dijke P (2007) BMP-9 signals via ALK1 and inhibits bFGF-induced endothelial cell proliferation and VEGF-stimulated angiogenesis. J Cell Sci 120:964–972. https://doi.org/10.1242/jcs.002949

307. Tillet E, Bailly S (2015) Emerging roles of BMP9 and BMP10 in hereditary hemorrhagic telangiectasia. Frontiers in Genetics 5:

308. Susan-Resiga D, Essalmani R, Hamelin J, Asselin M-C, Benjannet S, Chamberland A, Day R, Szumska D, Constam D, Bhattacharya S, Prat A, Seidah NG (2011) Furin is the major processing enzyme of the cardiac-specific growth factor bone morphogenetic protein 10. J Biol Chem 286:22785–22794. https://doi.org/10.1074/jbc.M111.233577

309. Bidart M, Ricard N, Levet S, Samson M, Mallet C, David L, Subileau M, Tillet E, Feige J-J, Bailly S (2012) BMP9 is produced by hepatocytes and circulates mainly in an active mature form complexed to its prodomain. Cell Mol Life Sci 69:313–324. https://doi.org/10.1007/s00018-011-0751-1

310. Jiang H, Salmon RM, Upton PD, Wei Z, Lawera A, Davenport AP, Morrell NW, Li W (2016) The Prodomain-bound Form of Bone Morphogenetic Protein 10 Is Biologically Active on Endothelial Cells*. Journal of Biological Chemistry 291:2954–2966. https://doi.org/10.1074/jbc.M115.683292

311. Sengle G, Ono RN, Sasaki T, Sakai LY (2011) Prodomains of Transforming Growth Factor β (TGFβ) Superfamily Members Specify Different Functions: EXTRACELLULAR MATRIX INTERACTIONS AND GROWTH FACTOR BIOAVAILABILITY*. Journal of Biological Chemistry 286:5087–5099. https://doi.org/10.1074/jbc.M110.188615

312. Choi H, Kim B-G, Kim YH, Lee S-J, Lee YJ, Oh SP (2023) BMP10 functions independently from BMP9 for the development of a proper arteriovenous network. Angiogenesis 26:167–186. https://doi.org/10.1007/s10456-022-09859-0

313. Nakano N, Hori H, Abe M, Shibata H, Arimura T, Sasaoka T, Sawabe M, Chida K, Arai T, Nakahara K, Kubo T, Sugimoto K, Katsuya T, Ogihara T, Doi Y, Izumi T, Kimura A (2007) Interaction of BMP10 with Tcap may modulate the course of hypertensive cardiac hypertrophy. Am J Physiol Heart Circ Physiol 293:H3396-3403. https://doi.org/10.1152/ajpheart.00311.2007

314. Tillet E, Ouarné M, Desroches-Castan A, Mallet C, Subileau M, Didier R, Lioutsko A, Belthier G, Feige J-J, Bailly S (2018) A heterodimer formed by bone morphogenetic protein 9 (BMP9) and BMP10 provides most BMP biological activity in plasma. J Biol Chem 293:10963–10974. https://doi.org/10.1074/jbc.RA118.002968

315. Liu W, Deng Z, Zeng Z, Fan J, Feng Y, Wang X, Cao D, Zhang B, Yang L, Liu B, Pakvasa M, Wagstaff W, Wu X, Luo H, Zhang J, Zhang M, He F, Mao Y, Ding H, Zhang Y, Niu C, Haydon RC, Luu HH, Wolf JM, Lee MJ, Huang W, He T-C, Zou Y (2020) Highly expressed BMP9/GDF2 in postnatal mouse liver and lungs may account for its pleiotropic effects on stem cell differentiation, angiogenesis, tumor growth and metabolism. Genes Dis 7:235–244. https://doi.org/10.1016/j.gendis.2019.08.003

316. López-Coviella I, Berse B, Krauss R, Thies RS, Blusztajn JK (2000) Induction and maintenance of the neuronal cholinergic phenotype in the central nervous system by BMP-9. Science 289:313–316. https://doi.org/10.1126/science.289.5477.313

317. Mottershead DG, Sugimura S, Al-Musawi SL, Li J-J, Richani D, White MA, Martin GA, Trotta AP, Ritter LJ, Shi J, Mueller TD, Harrison CA, Gilchrist RB (2015) Cumulin, an Oocyte-secreted Heterodimer of the Transforming Growth Factor-β Family, Is a Potent Activator of Granulosa Cells and Improves Oocyte Quality. J Biol Chem 290:24007–24020. https://doi.org/10.1074/jbc.M115.671487

318. Suzuki A, Kaneko E, Maeda J, Ueno N (1997) Mesoderm induction by BMP-4 and -7 heterodimers. Biochem Biophys Res Commun 232:153–156. https://doi.org/10.1006/bbrc.1997.6219

319. Little SC, Mullins MC (2009) Bone morphogenetic protein heterodimers assemble heteromeric type I receptor complexes to pattern the dorsoventral axis. Nat Cell Biol 11:637–643. https://doi.org/10.1038/ncb1870

320. Sengle G, Charbonneau NL, Ono RN, Sasaki T, Alvarez J, Keene DR, Bächinger HP, Sakai LY (2008) Targeting of bone morphogenetic protein growth factor complexes to fibrillin. J Biol Chem 283:13874–13888. https://doi.org/10.1074/jbc.M707820200

321. Luyten FP, Cunningham NS, Ma S, Muthukumaran N, Hammonds RG, Nevins WB, Woods WI, Reddi AH (1989) Purification and partial amino acid sequence of osteogenin, a protein initiating bone differentiation. J Biol Chem 264:13377–13380

322. Wang Y, Hong S, Li M, Zhang J, Bi Y, He Y, Liu X, Nan G, Su Y, Zhu G, Li R, Zhang W, Wang J, Zhang H, Kong Y, Shui W, Wu N, He Y, Chen X, Luu HH, Haydon RC, Shi LL, He T-C, Qin J (2013) Noggin resistance contributes to the potent osteogenic capability of BMP9 in mesenchymal stem cells. J Orthop Res 31:1796–1803. https://doi.org/10.1002/jor.22427

323. Yao Y, Jumabay M, Ly A, Radparvar M, Wang AH, Abdmaulen R, Boström KI (2012) Crossveinless 2 regulates bone morphogenetic protein 9 in human and mouse vascular endothelium. Blood 119:5037–5047. https://doi.org/10.1182/blood-2011-10-385906

324. Jumabay M, Zhumabai J, Mansurov N, Niklason KC, Guihard PJ, Cubberly MR, Fogelman AM, Iruela-Arispe L, Yao Y, Saparov A, Boström KI (2018) Combined effects of bone morphogenetic protein 10 and crossveinless-2 on cardiomyocyte differentiation in mouse adipocyte-derived stem cells. J Cell Physiol 233:1812–1822. https://doi.org/10.1002/jcp.25983

325. Salmon RM, Guo J, Wood JH, Tong Z, Beech JS, Lawera A, Yu M, Grainger DJ, Reckless J, Morrell NW, Li W (2020) Molecular basis of ALK1-mediated signalling by BMP9/BMP10 and their prodomain-bound forms. Nat Commun 11:1621. https://doi.org/10.1038/s41467-020-15425-3

326. Panchenko MP, Williams MC, Brody JS, Yu Q (1996) Type I receptor serine-threonine kinase preferentially expressed in pulmonary blood vessels. Am J Physiol 270:L547-558. https://doi.org/10.1152/ajplung.1996.270.4.L547

327. Johnson DW, Berg JN, Baldwin MA, Gallione CJ, Marondel I, Yoon SJ, Stenzel TT, Speer M, Pericak-Vance MA, Diamond A, Guttmacher AE, Jackson CE, Attisano L, Kucherlapati R, Porteous ME, Marchuk DA (1996) Mutations in the activin

receptor-like kinase 1 gene in hereditary haemorrhagic telangiectasia type 2. Nat Genet 13:189–195. https://doi.org/10.1038/ng0696-189

328. Seki T, Yun J, Oh SP (2003) Arterial Endothelium-Specific Activin Receptor-Like Kinase 1 Expression Suggests Its Role in Arterialization and Vascular Remodeling. Circulation Research 93:682–689. https://doi.org/10.1161/01.RES.0000095246.40391.3B

329. Corti P, Young S, Chen C-Y, Patrick MJ, Rochon ER, Pekkan K, Roman BL (2011) Interaction between alk1 and blood flow in the development of arteriovenous malformations. Development 138:1573–1582. https://doi.org/10.1242/dev.060467

330. Zhao D, Yang F, Wang Y, Li S, Li Y, Hou F, Yang W, Liu D, Tao Y, Li Q, Wang J, He F, Tang L (2022) ALK1 signaling is required for the homeostasis of Kupffer cells and prevention of bacterial infection. J Clin Invest 132:e150489. https://doi.org/10.1172/JCI150489

331. Jonker L, Arthur HM (2002) Endoglin expression in early development is associated with vasculogenesis and angiogenesis. Mechanisms of Development 110:193–196. https://doi.org/10.1016/S0925-4773(01)00562-7

332. Galaris G, Montagne K, Thalgott JH, Goujon GJPE, van den Driesche S, Martin S, Mager H-JJ, Mummery CL, Rabelink TJ, Lebrin F (2021) Thresholds of Endoglin Expression in Endothelial Cells Explains Vascular Etiology in Hereditary Hemorrhagic Telangiectasia Type 1. Int J Mol Sci 22:8948. https://doi.org/10.3390/ijms22168948

333. Schoonderwoerd MJA, Goumans M-JTH, Hawinkels LJAC (2020) Endoglin: Beyond the Endothelium. Biomolecules 10:289. https://doi.org/10.3390/biom10020289

334. Roman BL, Hinck AP (2017) ALK1 signaling in development and disease: new paradigms. Cell Mol Life Sci 74:4539–4560. https://doi.org/10.1007/s00018-017-2636-4

335. Lux A, Attisano L, Marchuk DA (1999) Assignment of transforming growth factor beta1 and beta3 and a third new ligand to the type I receptor ALK-1. J Biol Chem 274:9984–9992. https://doi.org/10.1074/jbc.274.15.9984

336. Seki T, Hong K-H, Oh SP (2006) Nonoverlapping expression patterns of ALK1 and ALK5 reveal distinct roles of each receptor in vascular development. Lab Invest 86:116–129. https://doi.org/10.1038/labinvest.3700376

337. Park SO, Lee YJ, Seki T, Hong K-H, Fliess N, Jiang Z, Park A, Wu X, Kaartinen V, Roman BL, Oh SP (2008) ALK5- and TGFBR2-independent role of ALK1 in the pathogenesis of hereditary hemorrhagic telangiectasia type 2. Blood 111:633–642. https://doi.org/10.1182/blood-2007-08-107359

338. Saito T, Bokhove M, Croci R, Zamora-Caballero S, Han L, Letarte M, de Sanctis D, Jovine L (2017) Structural Basis of the Human Endoglin-BMP9 Interaction: Insights into BMP Signaling and HHT1. Cell Rep 19:1917–1928. https://doi.org/10.1016/j.celrep.2017.05.011

339. Barbara NP, Wrana JL, Letarte M (1999) Endoglin is an accessory protein that interacts with the signaling receptor complex of multiple members of the transforming growth factor-beta superfamily. J Biol Chem 274:584–594. https://doi.org/10.1074/jbc.274.2.584

340. Cheifetz S, Bellón T, Calés C, Vera S, Bernabeu C, Massagué J, Letarte M (1992) Endoglin is a component of the transforming growth factor-beta receptor system in human endothelial cells. J Biol Chem 267:19027–19030

341. Nickel J, Ten Dijke P, Mueller TD (2018) TGF-β family co-receptor function and signaling. Acta Biochim Biophys Sin (Shanghai) 50:12–36. https://doi.org/10.1093/abbs/gmx126

342. Lawera A, Tong Z, Thorikay M, Redgrave RE, Cai J, van Dinther M, Morrell NW, Afink GB, Charnock-Jones DS, Arthur HM, Ten Dijke P, Li W (2019) Role of soluble endoglin in BMP9 signaling. Proc Natl Acad Sci U S A 116:17800–17808. https://doi.org/10.1073/pnas.1816661116

343. Townson SA, Martinez-Hackert E, Greppi C, Lowden P, Sako D, Liu J, Ucran JA, Liharska K, Underwood KW, Seehra J, Kumar R, Grinberg AV (2012) Specificity and structure of a high affinity activin receptor-like kinase 1 (ALK1) signaling complex. J Biol Chem 287:27313–27325. https://doi.org/10.1074/jbc.M112.377960

344. Hwan Kim Y, Vu P-N, Choe S-W, Jeon C-J, Arthur HM, Vary CPH, Lee YJ, Oh SP (2020) Overexpression of Activin Receptor-Like Kinase 1 in Endothelial Cells Suppresses Development of Arteriovenous Malformations in Mouse

Models of Hereditary Hemorrhagic Telangiectasia. Circ Res 127:1122–1137. https://doi.org/10.1161/CIRCRESAHA.119.316267

345. Miyazono K, Kamiya Y, Morikawa M (2010) Bone morphogenetic protein receptors and signal transduction. The Journal of Biochemistry 147:35–51. https://doi.org/10.1093/jb/mvp148

346. Theilmann AL, Hawke LG, Hilton LR, Whitford MKM, Cole DV, Mackeil JL, Dunham-Snary KJ, Mewburn J, James PD, Maurice DH, Archer SL, Ormiston ML (2020) Endothelial BMPR2 Loss Drives a Proliferative Response to BMP (Bone Morphogenetic Protein) 9 via Prolonged Canonical Signaling. Arterioscler Thromb Vasc Biol 40:2605–2618. https://doi.org/10.1161/ATVBAHA.119.313357

347. Tao B, Kraehling JR, Ghaffari S, Ramirez CM, Lee S, Fowler JW, Lee WL, Fernandez-Hernando C, Eichmann A, Sessa WC (2020) BMP-9 and LDL crosstalk regulates ALK-1 endocytosis and LDL transcytosis in endothelial cells. J Biol Chem 295:18179–18188. https://doi.org/10.1074/jbc.RA120.015680

348. David L, Mallet C, Keramidas M, Lamandé N, Gasc J-M, Dupuis-Girod S, Plauchu H, Feige J-J, Bailly S (2008) Bone morphogenetic protein-9 is a circulating vascular quiescence factor. Circ Res 102:914–922. https://doi.org/10.1161/CIRCRESAHA.107.165530

349. Star GP, Giovinazzo M, Langleben D (2010) Bone morphogenic protein-9 stimulates endothelin-1 release from human pulmonary microvascular endothelial cells: a potential mechanism for elevated ET-1 levels in pulmonary arterial hypertension. Microvasc Res 80:349–354. https://doi.org/10.1016/j.mvr.2010.05.010

350. Baeyens N, Nicoli S, Coon BG, Ross TD, Van den Dries K, Han J, Lauridsen HM, Mejean CO, Eichmann A, Thomas J-L, Humphrey JD, Schwartz MA (2015) Vascular remodeling is governed by a VEGFR3-dependent fluid shear stress set point. eLife 4:e04645. https://doi.org/10.7554/eLife.04645

351. Baeyens N, Larrivée B, Ola R, Hayward-Piatkowskyi B, Dubrac A, Huang B, Ross TD, Coon BG, Min E, Tsarfati M, Tong H, Eichmann A, Schwartz MA (2016) Defective fluid shear stress mechanotransduction mediates hereditary hemorrhagic telangiectasia. Journal of Cell Biology 214:807–816. https://doi.org/10.1083/jcb.201603106

352. Vion A-C, Alt S, Klaus-Bergmann A, Szymborska A, Zheng T, Perovic T, Hammoutene A, Oliveira MB, Bartels-Klein E, Hollfinger I, Rautou P-E, Bernabeu MO, Gerhardt H (2018) Primary cilia sensitize endothelial cells to BMP and prevent excessive vascular regression. Journal of Cell Biology 217:1651–1665. https://doi.org/10.1083/jcb.201706151

353. Peacock HM, Tabibian A, Criem N, Caolo V, Hamard L, Deryckere A, Haefliger J-A, Kwak BR, Zwijsen A, Jones EAV (2020) Impaired SMAD1/5 Mechanotransduction and Cx37 (Connexin37) Expression Enable Pathological Vessel Enlargement and Shunting. Arteriosclerosis, Thrombosis, and Vascular Biology 40:e87–e104. https://doi.org/10.1161/ATVBAHA.119.313122

354. Mendez P-L, Obendorf L, Jatzlau J, Burdzinski W, Reichenbach M, Nageswaran V, Haghikia A, Stangl V, Hiepen C, Knaus P (2022) Atheroprone fluid shear stress-regulated ALK1-Endoglin-SMAD signaling originates from early endosomes. BMC Biol 20:210. https://doi.org/10.1186/s12915-022-01396-y

355. Goumans M-J, Zwijsen A, Ten Dijke P, Bailly S (2018) Bone Morphogenetic Proteins in Vascular Homeostasis and Disease. Cold Spring Harb Perspect Biol 10:a031989. https://doi.org/10.1101/cshperspect.a031989

356. Lamouille S, Mallet C, Feige J-J, Bailly S (2002) Activin receptor-like kinase 1 is implicated in the maturation phase of angiogenesis. Blood 100:4495–4501. https://doi.org/10.1182/blood.V100.13.4495

357. David L, Mallet C, Vailhé B, Lamouille S, Feige J-J, Bailly S (2007) Activin receptor-like kinase 1 inhibits human microvascular endothelial cell migration: potential roles for JNK and ERK. J Cell Physiol 213:484–489. https://doi.org/10.1002/jcp.21126

358. Ota T, Fujii M, Sugizaki T, Ishii M, Miyazawa K, Aburatani H, Miyazono K (2002) Targets of transcriptional regulation by two distinct type I receptors for transforming growth factor-beta in human umbilical vein endothelial cells. J Cell Physiol 193:299–318. https://doi.org/10.1002/jcp.10170

359. Rostama B, Turner JE, Seavey GT, Norton CR, Gridley T, Vary CPH, Liaw L (2015) DLL4/Notch1 and BMP9 interdependent signaling induces human endothelial cell quiescence via P27KIP1 and thrombospondin-1. Arterioscler Thromb Vasc Biol 35:2626–2637. https://doi.org/10.1161/ATVBAHA.115.306541

360. Park JES, Shao D, Upton PD, Desouza P, Adcock IM, Davies RJ, Morrell NW, Griffiths MJD, Wort SJ (2012) BMP-9 induced endothelial cell tubule formation and inhibition of migration involves Smad1 driven endothelin-1 production. PLoS One 7:e30075. https://doi.org/10.1371/journal.pone.0030075

361. Goumans M-J, Valdimarsdottir G, Itoh S, Rosendahl A, Sideras P, ten Dijke P (2002) Balancing the activation state of the endothelium via two distinct TGF-beta type I receptors. EMBO J 21:1743–1753. https://doi.org/10.1093/emboj/21.7.1743

362. Krebs LT, Starling C, Chervonsky AV, Gridley T (2010) Notch1 activation in mice causes arteriovenous malformations phenocopied by ephrinB2 and EphB4 mutants. Genesis 48:146–150. https://doi.org/10.1002/dvg.20599

363. Kohli V, Schumacher JA, Desai SP, Rehn K, Sumanas S (2013) Arterial and venous progenitors of the major axial vessels originate at distinct locations. Dev Cell 25:196–206. https://doi.org/10.1016/j.devcel.2013.03.017

364. Suzuki Y, Ohga N, Morishita Y, Hida K, Miyazono K, Watabe T (2010) BMP-9 induces proliferation of multiple types of endothelial cells in vitro and in vivo. Journal of Cell Science 123:1684–1692. https://doi.org/10.1242/jcs.061556

365. Mitchell D, Pobre EG, Mulivor AW, Grinberg AV, Castonguay R, Monnell TE, Solban N, Ucran JA, Pearsall RS, Underwood KW, Seehra J, Kumar R (2010) ALK1-Fc Inhibits Multiple Mediators of Angiogenesis and Suppresses Tumor Growth. Molecular Cancer Therapeutics 9:379–388. https://doi.org/10.1158/1535-7163.MCT-09-0650

366. Long L, Ormiston ML, Yang X, Southwood M, Gräf S, Machado RD, Mueller M, Kinzel B, Yung LM, Wilkinson JM, Moore SD, Drake KM, Aldred MA, Yu P, Upton PD, Morrell NW (2015) Selective enhancement of endothelial BMPR-II with BMP9 reverses pulmonary arterial hypertension. Nat Med 21:777–785. https://doi.org/10.1038/nm.3877

367. Li W, Long L, Yang X, Tong Z, Southwood M, King R, Caruso P, Upton PD, Yang P, Bocobo GA, Nikolic I, Higuera A, Salmon RM, Jiang H, Lodge KM, Hoenderdos K, Baron RM, Yu PB, Condliffe AM, Summers C, Nourshargh S, Chilvers ER, Morrell NW Circulating BMP9 Protects the Pulmonary Endothelium during Inflammation-induced Lung Injury in Mice. Am J Respir Crit Care Med 203:1419–1430. https://doi.org/10.1164/rccm.202005-1761OC

368. Upton PD, Park JES, De Souza PM, Davies RJ, Griffiths MJD, Wort SJ, Morrell NW (2020) Endothelial protective factors BMP9 and BMP10 inhibit CCL2 release by human vascular endothelial cells. J Cell Sci 133:jcs239715. https://doi.org/10.1242/jcs.239715

369. Akla N, Viallard C, Popovic N, Lora Gil C, Sapieha P, Larrivée B (2018) BMP9 (Bone Morphogenetic Protein-9)/Alk1 (Activin-Like Kinase Receptor Type I) Signaling Prevents Hyperglycemia-Induced Vascular Permeability. Arterioscler Thromb Vasc Biol 38:1821–1836. https://doi.org/10.1161/ATVBAHA.118.310733

370. Arthur HM, Roman BL (2022) An update on preclinical models of hereditary haemorrhagic telangiectasia: Insights into disease mechanisms. Front Med (Lausanne) 9:973964. https://doi.org/10.3389/fmed.2022.973964

371. Ricard N, Ciais D, Levet S, Subileau M, Mallet C, Zimmers TA, Lee S-J, Bidart M, Feige J-J, Bailly S (2012) BMP9 and BMP10 are critical for postnatal retinal vascular remodeling. Blood 119:6162–6171. https://doi.org/10.1182/blood-2012-01-407593

372. Chen H, Brady Ridgway J, Sai T, Lai J, Warming S, Chen H, Roose-Girma M, Zhang G, Shou W, Yan M (2013) Context-dependent signaling defines roles of BMP9 and BMP10 in embryonic and postnatal development. Proc Natl Acad Sci U S A 110:11887–11892. https://doi.org/10.1073/pnas.1306074110

373. Bouvard C, Tu L, Rossi M, Desroches-Castan A, Berrebeh N, Helfer E, Roelants C, Liu H, Ouarné M, Chaumontel N, Mallet C, Battail C, Bikfalvi A, Humbert M, Savale L, Daubon T, Perret P, Tillet E, Guignabert C, Bailly S (2022) Different cardiovascular and pulmonary phenotypes for single- and double-knock-out mice deficient in BMP9 and BMP10. Cardiovasc Res 118:1805–1820. https://doi.org/10.1093/cvr/cvab187

374. Levet S, Ciais D, Merdzhanova G, Mallet C, Zimmers TA, Lee S-J, Navarro FP, Texier I, Feige J-J, Bailly S, Vittet D (2013) Bone morphogenetic protein 9 (BMP9) controls lymphatic vessel maturation and valve formation. Blood 122:598–607. https://doi.org/10.1182/blood-2012-12-472142

375. Yoshimatsu Y, Lee YG, Akatsu Y, Taguchi L, Suzuki HI, Cunha SI, Maruyama K, Suzuki Y, Yamazaki T, Katsura A, Oh SP, Zimmers TA, Lee S-J, Pietras K, Koh GY, Miyazono K, Watabe T (2013) Bone morphogenetic protein-9 inhibits lymphatic vessel formation via activin receptor-like kinase 1 during development and cancer progression. Proc Natl Acad Sci U S A 110:18940–18945. https://doi.org/10.1073/pnas.1310479110

376. Desroches-Castan A, Tillet E, Ricard N, Ouarné M, Mallet C, Belmudes L, Couté Y, Boillot O, Scoazec J-Y, Bailly S, Feige J-J (2019) Bone Morphogenetic Protein 9 Is a Paracrine Factor Controlling Liver Sinusoidal Endothelial Cell Fenestration and Protecting Against Hepatic Fibrosis. Hepatology 70:1392–1408. https://doi.org/10.1002/hep.30655

377. Chen H, Shi S, Acosta L, Li W, Lu J, Bao S, Chen Z, Yang Z, Schneider MD, Chien KR, Conway SJ, Yoder MC, Haneline LS, Franco D, Shou W (2004) BMP10 is essential for maintaining cardiac growth during murine cardiogenesis. Development 131:2219–2231. https://doi.org/10.1242/dev.01094

378. Larrivée B, Prahst C, Gordon E, del Toro R, Mathivet T, Duarte A, Simons M, Eichmann A (2012) ALK1 signaling inhibits angiogenesis by cooperating with the Notch pathway. Dev Cell 22:489–500. https://doi.org/10.1016/j.devcel.2012.02.005

379. Ruiz S, Zhao H, Chandakkar P, Chatterjee PK, Papoin J, Blanc L, Metz CN, Campagne F, Marambaud P (2016) A mouse model of hereditary hemorrhagic telangiectasia generated by transmammary-delivered immunoblocking of BMP9 and BMP10. Sci Rep 6:37366. https://doi.org/10.1038/srep37366

380. Levet S, Ouarné M, Ciais D, Coutton C, Subileau M, Mallet C, Ricard N, Bidart M, Debillon T, Faravelli F, Rooryck C, Feige J-J, Tillet E, Bailly S (2015) BMP9 and BMP10 are necessary for proper closure of the ductus arteriosus. Proc Natl Acad Sci U S A 112:E3207-3215. https://doi.org/10.1073/pnas.1508386112

381. Graupera M, Potente M (2013) Regulation of angiogenesis by PI3K signaling networks. Exp Cell Res 319:1348–1355. https://doi.org/10.1016/j.yexcr.2013.02.021

382. Kobialka P, Graupera M (2019) Revisiting PI3-kinase signalling in angiogenesis. Vasc Biol 1:H125–H134. https://doi.org/10.1530/VB-19-0025

383. Dimmeler S, Assmus B, Hermann C, Haendeler J, Zeiher AM (1998) Fluid shear stress stimulates phosphorylation of Akt in human endothelial cells: involvement in suppression of apoptosis. Circ Res 83:334–341. https://doi.org/10.1161/01.res.83.3.334

384. Gomes AM, Pinto TS, da Costa Fernandes CJ, da Silva RA, Zambuzzi WF (2020) Wortmannin targeting phosphatidylinositol 3-kinase suppresses angiogenic factors in shear-stressed endothelial cells. Journal of Cellular Physiology 235:5256–5269. https://doi.org/10.1002/jcp.29412

385. Alsina-Sanchís E, García-Ibáñez Y, Figueiredo AM, Riera-Domingo C, Figueras A, Matias-Guiu X, Casanovas O, Botella LM, Pujana MA, Riera-Mestre A, Graupera M, Viñals F (2018) ALK1 Loss Results in Vascular Hyperplasia in Mice and Humans Through PI3K Activation. Arteriosclerosis, Thrombosis, and Vascular Biology 38:1216–1229. https://doi.org/10.1161/ATVBAHA.118.310760

386. Ola R, Dubrac A, Han J, Zhang F, Fang JS, Larrivée B, Lee M, Urarte AA, Kraehling JR, Genet G, Hirschi KK, Sessa WC, Canals FV, Graupera M, Yan M, Young LH, Oh PS, Eichmann A (2016) PI3 kinase inhibition improves vascular malformations in mouse models of hereditary haemorrhagic telangiectasia. Nat Commun 7:13650. https://doi.org/10.1038/ncomms13650

387. Ola R, Künzel SH, Zhang F, Genet G, Chakraborty R, Pibouin-Fragner L, Martin K, Sessa W, Dubrac A, Eichmann A (2018) SMAD4 Prevents Flow Induced Arteriovenous Malformations by Inhibiting Casein Kinase 2. Circulation 138:2379–2394. https://doi.org/10.1161/CIRCULATIONAHA.118.033842

388. Carracedo A, Pandolfi PP (2008) The PTEN–PI3K pathway: of feedbacks and cross-talks. Oncogene 27:5527–5541. https://doi.org/10.1038/onc.2008.247

389. Torres J, Pulido R (2001) The tumor suppressor PTEN is phosphorylated by the protein kinase CK2 at its C terminus. Implications for PTEN stability to proteasome-mediated degradation. J Biol Chem 276:993–998. https://doi.org/10.1074/jbc.M009134200

390. Araki M, Hisamitsu T, Kinugasa-Katayama Y, Tanaka T, Harada Y, Nakao S, Hanada S, Ishii S, Fujita M, Kawamura T, Saito Y, Nishiyama K, Watanabe Y, Nakagawa O (2018) Serum/glucocorticoid-regulated kinase 1 as a novel transcriptional target of bone morphogenetic protein-ALK1 receptor signaling in vascular endothelial cells. Angiogenesis 21:415–423. https://doi.org/10.1007/s10456-018-9605-x

391. Medina-Jover F, Gendrau-Sanclemente N, Viñals F (2020) SGK1 is a signalling hub that controls protein synthesis and proliferation in endothelial cells. FEBS Letters 594:3200–3215. https://doi.org/10.1002/1873-3468.13901

392. BelAiba RS, Djordjevic T, Bonello S, Artunc F, Lang F, Hess J, Görlach A (2006) The serum- and glucocorticoid-inducible kinase Sgk-1 is involved in pulmonary vascular remodeling: role in redox-sensitive regulation of tissue factor by thrombin. Circ Res 98:828–836. https://doi.org/10.1161/01.RES.0000210539.54861.27

393. Catela C, Kratsios P, Hede M, Lang F, Rosenthal N (2010) Serum and glucocorticoid-inducible kinase 1 (SGK1) is necessary for vascular remodeling during angiogenesis. Dev Dyn 239:2149–2160. https://doi.org/10.1002/dvdy.22345

394. Di Cristofano A (2017) SGK1: The Dark Side of PI3K Signaling. Curr Top Dev Biol 123:49–71. https://doi.org/10.1016/bs.ctdb.2016.11.006

395. Castel P, Ellis H, Bago R, Toska E, Razavi P, Carmona FJ, Kannan S, Verma CS, Dickler M, Chandarlapaty S, Brogi E, Alessi DR, Baselga J, Scaltriti M (2016) PDK1-SGK1 Signaling Sustains AKT-Independent mTORC1 Activation and Confers Resistance to PI3Kα Inhibition. Cancer Cell 30:229–242. https://doi.org/10.1016/j.ccell.2016.06.004

396. Toska E, Castel P, Chhangawala S, Arruabarrena-Aristorena A, Chan C, Hristidis VC, Cocco E, Sallaku M, Xu G, Park J, Minuesa G, Shifman SG, Socci ND, Koche R, Leslie CS, Scaltriti M, Baselga J (2019) PI3K Inhibition Activates SGK1 via a Feedback Loop to Promote Chromatin-Based Regulation of ER-Dependent Gene Expression. Cell Rep 27:294-306.e5. https://doi.org/10.1016/j.celrep.2019.02.111

397. Medina-Jover F, Riera-Mestre A, Viñals F (2022) Rethinking growth factors: the case of BMP9 during vessel maturation. Vasc Biol 4:R1–R14. https://doi.org/10.1530/VB-21-0019

398. Pintucci G, Moscatelli D, Saponara F, Biernacki PR, Baumann FG, Bizekis C, Galloway AC, Basilico C, Mignatti P (2002) Lack of ERK activation and cell migration in FGF-2-deficient endothelial cells. The FASEB Journal 16:598–600. https://doi.org/10.1096/fj.01-0815fje

399. Srinivasan R, Zabuawala T, Huang H, Zhang J, Gulati P, Fernandez S, Karlo JC, Landreth GE, Leone G, Ostrowski MC (2009) Erk1 and Erk2 Regulate Endothelial Cell Proliferation and Migration during Mouse Embryonic Angiogenesis. PLoS One 4:e8283. https://doi.org/10.1371/journal.pone.0008283

400. Ricard N, Scott RP, Booth CJ, Velazquez H, Cilfone NA, Baylon JL, Gulcher JR, Quaggin SE, Chittenden TW, Simons M (2019) Endothelial ERK1/2 signaling maintains integrity of the quiescent endothelium. J Exp Med 216:1874–1890. https://doi.org/10.1084/jem.20182151

401. Williams CK, Li J-L, Murga M, Harris AL, Tosato G (2006) Up-regulation of the Notch ligand Delta-like 4 inhibits VEGF-induced endothelial cell function. Blood 107:931–939. https://doi.org/10.1182/blood-2005-03-1000

402. Fish JE, Wythe JD (2015) The molecular regulation of arteriovenous specification and maintenance. Developmental Dynamics 244:391–409. https://doi.org/10.1002/dvdy.24252

403. Akil A, Gutiérrez-García AK, Guenter R, Rose JB, Beck AW, Chen H, Ren B (2021) Notch Signaling in Vascular Endothelial Cells, Angiogenesis, and Tumor Progression: An Update and Prospective. Frontiers in Cell and Developmental Biology 9:

404. Swaminathan B, Youn S-W, Naiche LA, Du J, Villa SR, Metz JB, Feng H, Zhang C, Kopan R, Sims PA, Kitajewski JK (2022) Endothelial Notch signaling directly regulates the small GTPase RND1 to facilitate Notch suppression of endothelial migration. Sci Rep 12:1655. https://doi.org/10.1038/s41598-022-05666-1

405. Moya IM, Umans L, Maas E, Pereira PNG, Beets K, Francis A, Sents W, Robertson EJ, Mummery CL, Huylebroeck D, Zwijsen A (2012) Stalk Cell Phenotype Depends on Integration of Notch and Smad1/5 Signaling Cascades. Developmental Cell 22:501–514. https://doi.org/10.1016/j.devcel.2012.01.007

406. Mostafa S, Pakvasa M, Coalson E, Zhu A, Alverdy A, Castillo H, Fan J, Li A, Feng Y, Wu D, Bishop E, Du S, Spezia M, Li A, Hagag O, Deng A, Liu W, Li M, Ho SS, Athiviraham A, Lee MJ, Wolf JM, Ameer GA, Luu HH, Haydon RC, Strelzow J, Hynes K, He T-C, Reid RR (2019) The wonders of BMP9: From mesenchymal stem cell differentiation, angiogenesis, neurogenesis, tumorigenesis, and metabolism to regenerative medicine. Genes Dis 6:201–223. https://doi.org/10.1016/j.gendis.2019.07.003

407. Eiraku N, Chiba N, Nakamura T, Amir MS, Seong C-H, Ohnishi T, Kusuyama J, Noguchi K, Matsuguchi T (2019) BMP9 directly induces rapid GSK3-β phosphorylation in a Wnt-independent manner through class I PI3K-Akt axis in osteoblasts. FASEB J 33:12124–12134. https://doi.org/10.1096/fj.201900733RR

408. Amir MS, Chiba N, Seong CH, Kusuyama J, Eiraku N, Ohnishi T, Nakamura N, Matsuguchi T (2022) HIF-1α plays an essential role in BMP9-mediated osteoblast differentiation through the induction of a glycolytic enzyme, PDK1. J Cell Physiol 237:2183–2197. https://doi.org/10.1002/jcp.30752

409. García-Álvaro M, Addante A, Roncero C, Fernández M, Fabregat I, Sánchez A, Herrera B (2015) BMP9-Induced Survival Effect in Liver Tumor Cells Requires p38MAPK Activation. International Journal of Molecular Sciences 16:20431–20448. https://doi.org/10.3390/ijms160920431

410. Addante A, Roncero C, Lazcanoiturburu N, Méndez R, Almalé L, García-Álvaro M, ten Dijke P, Fabregat I, Herrera B, Sánchez A (2020) A Signaling Crosstalk between BMP9 and HGF/c-Met Regulates Mouse Adult Liver Progenitor Cell Survival. Cells 9:752. https://doi.org/10.3390/cells9030752

411. Lichtner B, Knaus P, Lehrach H, Adjaye J (2013) BMP10 as a potent inducer of trophoblast differentiation in human embryonic and induced pluripotent stem cells. Biomaterials 34:9789–9802. https://doi.org/10.1016/j.biomaterials.2013.08.084

412. McAllister KA, Grogg KM, Johnson DW, Gallione CJ, Baldwin MA, Jackson CE, Helmbold EA, Markel DS, McKinnon WC, Murrell J (1994) Endoglin, a TGF-beta binding protein of endothelial cells, is the gene for hereditary haemorrhagic telangiectasia type 1. Nat Genet 8:345–351. https://doi.org/10.1038/ng1294-345

413. International PPH Consortium, Lane KB, Machado RD, Pauciulo MW, Thomson JR, Phillips JA, Loyd JE, Nichols WC, Trembath RC (2000) Heterozygous germline mutations in BMPR2, encoding a TGF-beta receptor, cause familial primary pulmonary hypertension. Nat Genet 26:81–84. https://doi.org/10.1038/79226

414. Robert F, Desroches-Castan A, Bailly S, Dupuis-Girod S, Feige J-J (2020) Future treatments for hereditary hemorrhagic telangiectasia. Orphanet J Rare Dis 15:4. https://doi.org/10.1186/s13023-019-1281-4

415. Faughnan ME, Granton JT, Young LH (2009) The pulmonary vascular complications of hereditary haemorrhagic telangiectasia. European Respiratory Journal 33:1186–1194. https://doi.org/10.1183/09031936.00061308

416. Folz BJ, Zoll B, Alfke H, Toussaint A, Maier RF, Werner JA (2006) Manifestations of hereditary hemorrhagic telangiectasia in children and adolescents. Eur Arch Otorhinolaryngol 263:53–61. https://doi.org/10.1007/s00405-005-0956-8

417. Letteboer TGW, Mager H-J, Snijder RJ, Lindhout D, Ploos van Amstel H-K, Zanen P, Westermann KJJ (2008) Genotype-phenotype relationship for localization and age distribution of telangiectases in hereditary hemorrhagic telangiectasia. Am J Med Genet A 146A:2733–2739. https://doi.org/10.1002/ajmg.a.32243

418. Mosquera-Klinger GA, Gálvez-Cárdenas K, Valencia AM, Mosquera-Klinger GA, Gálvez-Cárdenas K, Valencia AM (2019) Diagnosis and treatment of patients with hereditary hemorrhagic telangiectasia (Rendu-Osler-Weber syndrome) at a university hospital in Colombia. Revista colombiana de Gastroenterología 34:152–158. https://doi.org/10.22516/25007440.280

419. Santos MA (2017) Hereditary Hemorrhagic Telangiectasia (Osler-Weber-Rendu syndrome). J Gen Intern Med 32:218–219. https://doi.org/10.1007/s11606-016-3870-4

420. AAssar OS, Friedman CM, White RI (1991) The natural history of epistaxis in hereditary hemorrhagic telangiectasia. Laryngoscope 101:977–980. https://doi.org/10.1288/00005537-199109000-00008

421. Jan W, Tameez Ud Din A, Chaudhary FMD, Tameez-ud-din A, Nawaz F Hereditary Hemorrhagic Telangiectasia: A Rare Cause of Anemia. Cureus 11:e5349. https://doi.org/10.7759/cureus.5349

422. Faughnan ME, Mager JJ, Hetts SW, Palda VA, Lang-Robertson K, Buscarini E, Deslandres E, Kasthuri RS, Lausman A, Poetker D, Ratjen F, Chesnutt MS, Clancy M, Whitehead KJ, Al-Samkari H, Chakinala M, Conrad M, Cortes D, Crocione C, Darling J, de Gussem E, Derksen C, Dupuis-Girod S, Foy P, Geisthoff U, Gossage JR, Hammill A, Heimdal K, Henderson K, Iyer VN, Kjeldsen AD, Komiyama M, Korenblatt K, McDonald J, McMahon J, McWilliams J, Meek ME, Mei-Zahav M, Olitsky S, Palmer S, Pantalone R, Piccirillo JF, Plahn B, Porteous MEM, Post MC, Radovanovic I, Rochon PJ, Rodriguez-Lopez J, Sabba C, Serra M, Shovlin C, Sprecher D, White AJ, Winship I, Zarrabeitia R (2020) Second International Guidelines for the Diagnosis and Management of Hereditary Hemorrhagic Telangiectasia. Ann Intern Med 173:989–1001. https://doi.org/10.7326/M20-1443

423. Gallione CJ, Repetto GM, Legius E, Rustgi AK, Schelley SL, Tejpar S, Mitchell G, Drouin E, Westermann CJJ, Marchuk DA (2004) A combined syndrome of juvenile polyposis and hereditary haemorrhagic telangiectasia associated with mutations in MADH4 (SMAD4). Lancet 363:852–859. https://doi.org/10.1016/S0140-6736(04)15732-2

424. Wooderchak-Donahue WL, McDonald J, O'Fallon B, Upton PD, Li W, Roman BL, Young S, Plant P, Fülöp GT, Langa C, Morrell NW, Botella LM, Bernabeu C, Stevenson DA, Runo JR, Bayrak-Toydemir P (2013) BMP9 mutations cause a vascular-anomaly syndrome with phenotypic overlap with hereditary hemorrhagic telangiectasia. Am J Hum Genet 93:530–537. https://doi.org/10.1016/j.ajhg.2013.07.004

425. Balachandar S, Graves TJ, Shimonty A, Kerr K, Kilner J, Xiao S, Slade R, Sroya M, Alikian M, Curetean E, Thomas E, McConnell VPM, McKee S, Boardman-Pretty F, Devereau A, Fowler TA, Caulfield MJ, Alton EW, Ferguson T, Redhead J, McKnight AJ, Thomas GA, Genomics England Research Consortium, Aldred MA, Shovlin CL (2022) Identification and validation of a novel pathogenic variant in GDF2 (BMP9) responsible for hereditary hemorrhagic telangiectasia and pulmonary arteriovenous malformations. Am J Med Genet A 188:959–964. https://doi.org/10.1002/ajmg.a.62584

426. Hernandez F, Huether R, Carter L, Johnston T, Thompson J, Gossage JR, Chao E, Elliott AM (2015) Mutations in RASA1 and GDF2 identified in patients with clinical features of hereditary hemorrhagic telangiectasia. Hum Genome Var 2:15040. https://doi.org/10.1038/hgv.2015.40

427. Faughnan ME, Palda VA, Garcia-Tsao G, Geisthoff UW, McDonald J, Proctor DD, Spears J, Brown DH, Buscarini E, Chesnutt MS, Cottin V, Ganguly A, Gossage JR, Guttmacher AE, Hyland RH, Kennedy SJ, Korzenik J, Mager JJ, Ozanne AP, Piccirillo JF, Picus D, Plauchu H, Porteous MEM, Pyeritz RE, Ross DA, Sabba C, Swanson K, Terry P, Wallace MC, Westermann CJJ, White RI, Young LH, Zarrabeitia R, HHT Foundation International - Guidelines Working Group (2011) International guidelines for the diagnosis and management of hereditary haemorrhagic telangiectasia. J Med Genet 48:73–87. https://doi.org/10.1136/jmg.2009.069013

428. Kritharis A, Al-Samkari H, Kuter DJ (2018) Hereditary hemorrhagic telangiectasia: diagnosis and management from the hematologist's perspective. Haematologica 103:1433–1443. https://doi.org/10.3324/haematol.2018.193003

429. Bernabeu C, Bayrak-Toydemir P, McDonald J, Letarte M (2020) Potential Second-Hits in Hereditary Hemorrhagic Telangiectasia. J Clin Med 9:3571. https://doi.org/10.3390/jcm9113571

430. Albiñana V, Cuesta AM, Rojas-P I de, Gallardo-Vara E, Recio-Poveda L, Bernabéu C, Botella LM (2020) Review of Pharmacological Strategies with Repurposed Drugs for Hereditary Hemorrhagic Telangiectasia Related Bleeding. J Clin Med 9:1766. https://doi.org/10.3390/jcm9061766

431. Gaillard S, Dupuis-Girod S, Boutitie F, Rivière S, Morinière S, Hatron P-Y, Manfredi G, Kaminsky P, Capitaine A-L, Roy P, Gueyffier F, Plauchu H, ATERO Study Group (2014) Tranexamic acid for epistaxis in hereditary hemorrhagic telangiectasia patients: a European cross-over controlled trial in a rare disease. J Thromb Haemost 12:1494–1502. https://doi.org/10.1111/jth.12654

432. Geisthoff UW, Seyfert UT, Kübler M, Bieg B, Plinkert PK, König J (2014) Treatment of epistaxis in hereditary hemorrhagic telangiectasia with tranexamic acid - a double-blind placebo-controlled cross-over phase IIIB study. Thromb Res 134:565–571. https://doi.org/10.1016/j.thromres.2014.06.012

433. Sautter NB, Smith TL (2016) Treatment of Hereditary Hemorrhagic Telangiectasia-Related Epistaxis. Otolaryngol Clin North Am 49:639–654. https://doi.org/10.1016/j.otc.2016.02.010

434. Ruiz-Llorente L, Gallardo-Vara E, Rossi E, Smadja DM, Botella LM, Bernabeu C (2017) Endoglin and alk1 as therapeutic targets for hereditary hemorrhagic telangiectasia. Expert Opin Ther Targets 21:933–947. https://doi.org/10.1080/14728222.2017.1365839

435. Dupuis-Girod S, Bailly S, Plauchu H (2010) Hereditary hemorrhagic telangiectasia: from molecular biology to patient care. J Thromb Haemost 8:1447–1456. https://doi.org/10.1111/j.1538-7836.2010.03860.x

436. Brinkerhoff BT, Poetker DM, Choong NW (2011) Long-term therapy with bevacizumab in hereditary hemorrhagic telangiectasia. N Engl J Med 364:688–689. https://doi.org/10.1056/NEJMc1012774

437. Bose P, Holter JL, Selby GB (2009) Bevacizumab in hereditary hemorrhagic telangiectasia. N Engl J Med 360:2143–2144. https://doi.org/10.1056/NEJMc0901421

438. Flieger D, Hainke S, Fischbach W (2006) Dramatic improvement in hereditary hemorrhagic telangiectasia after treatment with the vascular endothelial growth factor (VEGF) antagonist bevacizumab. Ann Hematol 85:631–632. https://doi.org/10.1007/s00277-006-0147-8

439. Crist AM, Zhou X, Garai J, Lee AR, Thoele J, Ullmer C, Klein C, Zabaleta J, Meadows SM (2019) Angiopoietin-2 Inhibition Rescues Arteriovenous Malformation in a Smad4 Hereditary Hemorrhagic Telangiectasia Mouse Model. Circulation 139:2049–2063. https://doi.org/10.1161/CIRCULATIONAHA.118.036952

440. Jin Y, Muhl L, Burmakin M, Wang Y, Duchez A-C, Betsholtz C, Arthur HM, Jakobsson L (2017) Endoglin prevents vascular malformation by regulating flow-induced cell migration and specification through VEGFR2 signalling. Nat Cell Biol 19:639–652. https://doi.org/10.1038/ncb3534

441. Ruiz S, Chandakkar P, Zhao H, Papoin J, Chatterjee PK, Christen E, Metz CN, Blanc L, Campagne F, Marambaud P (2017) Tacrolimus rescues the signaling and gene expression signature of endothelial ALK1 loss-of-function and improves HHT vascular pathology. Hum Mol Genet 26:4786–4798. https://doi.org/10.1093/hmg/ddx358

442. Ruiz S, Zhao H, Chandakkar P, Papoin J, Choi H, Nomura-Kitabayashi A, Patel R, Gillen M, Diao L, Chatterjee PK, He M, Al-Abed Y, Wang P, Metz CN, Oh SP, Blanc L, Campagne F, Marambaud P (2020) Correcting Smad1/5/8, mTOR, and VEGFR2 treats pathology in hereditary hemorrhagic telangiectasia models. J Clin Invest 130:942–957. https://doi.org/10.1172/JCI127425

443. Park H, Furtado J, Poulet M, Chung M, Yun S, Lee S, Sessa WC, Franco CA, Schwartz MA, Eichmann A (2021) Defective Flow-Migration Coupling Causes Arteriovenous Malformations in Hereditary Hemorrhagic Telangiectasia. Circulation 144:805–822. https://doi.org/10.1161/CIRCULATIONAHA.120.053047

444. Han C, Choe S-W, Kim YH, Acharya AP, Keselowsky BG, Sorg BS, Lee Y-J, Oh SP (2014) VEGF neutralization can prevent and normalize arteriovenous malformations in an animal model for hereditary hemorrhagic telangiectasia 2. Angiogenesis 17:823–830. https://doi.org/10.1007/s10456-014-9436-3

445. Castel P, Carmona FJ, Grego-Bessa J, Berger MF, Viale A, Anderson KV, Bague S, Scaltriti M, Antonescu CR, Baselga E, Baselga J (2016) Somatic PIK3CA mutations as a driver of sporadic venous malformations. Sci Transl Med 8:332ra42. https://doi.org/10.1126/scitranslmed.aaf1164

446. Spiekerkoetter E, Tian X, Cai J, Hopper RK, Sudheendra D, Li CG, El-Bizri N, Sawada H, Haghighat R, Chan R, Haghighat L, de Jesus Perez V, Wang L, Reddy S, Zhao M, Bernstein D, Solow-Cordero DE, Beachy PA, Wandless TJ, Ten Dijke P, Rabinovitch M (2013) FK506 activates BMPR2, rescues endothelial dysfunction, and reverses pulmonary hypertension. J Clin Invest 123:3600–3613. https://doi.org/10.1172/JCI65592

447. Zhu W, Shen F, Mao L, Zhan L, Kang S, Sun Z, Nelson J, Zhang R, Zou D, McDougall CM, Lawton MT, Vu TH, Wu Z, Scaria A, Colosi P, Forsayeth J, Su H (2017) Soluble FLT1 Gene Therapy Alleviates Brain Arteriovenous Malformation Severity. Stroke 48:1420–1423. https://doi.org/10.1161/STROKEAHA.116.015713

448. Bernabeu C (2023) Therapeutic Targeting of the Ang2/Tie Pathway in Endothelial Cells as a Potential Treatment of Hereditary Hemorrhagic Telangiectasia. Arteriosclerosis, Thrombosis, and Vascular Biology 43:1404–1408. https://doi.org/10.1161/ATVBAHA.123.319631

449. Zhou X, Pucel JC, Nomura-Kitabayashi A, Chandakkar P, Guidroz AP, Jhangiani NL, Bao D, Fan J, Arthur HM, Ullmer C, Klein C, Marambaud P, Meadows SM (2023) ANG2 Blockade Diminishes Proangiogenic Cerebrovascular Defects Associated With Models of Hereditary Hemorrhagic Telangiectasia. Arteriosclerosis, Thrombosis, and Vascular Biology 43:1384–1403. https://doi.org/10.1161/ATVBAHA.123.319385

450. Ardelean DS, Jerkic M, Yin M, Peter M, Ngan B, Kerbel RS, Foster FS, Letarte M (2014) Endoglin and activin receptor-like kinase 1 heterozygous mice have a distinct pulmonary and hepatic angiogenic profile and response to anti-VEGF treatment. Angiogenesis 17:129–146. https://doi.org/10.1007/s10456-013-9383-4

451. Banerjee K, Lin Y, Gahn J, Cordero J, Gupta P, Mohamed I, Graupera M, Dobreva G, Schwartz MA, Ola R (2023) SMAD4 maintains the fluid shear stress set point to protect against arterial-venous malformations. J Clin Invest e168352. https://doi.org/10.1172/JCI168352

452. Zhu W, Chen W, Zou D, Wang L, Bao C, Zhan L, Saw D, Wang S, Winkler E, Li Z, Zhang M, Shen F, Shaligram S, Lawton M, Su H (2018) Thalidomide Reduces Hemorrhage of Brain Arteriovenous Malformations in a Mouse Model. Stroke 49:1232–1240. https://doi.org/10.1161/STROKEAHA.117.020356

453. Al-Samkari H, Eng W (2022) A precision medicine approach to hereditary hemorrhagic telangiectasia and complex vascular anomalies. J Thromb Haemost 20:1077–1088. https://doi.org/10.1111/jth.15715

454. Kim YH, Kim M-J, Choe S, Sprecher D, Lee YJ, Oh SP (2017) Selective effects of oral anti-angiogenic tyrosine kinase inhibitors on an animal model of hereditary hemorrhagic telangiectasia. J Thromb Haemost 15:1095–1102. https://doi.org/10.1111/jth.13683

455. Faughnan ME, Gossage JR, Chakinala MM, Oh SP, Kasthuri R, Hughes CCW, McWilliams JP, Parambil JG, Vozoris N, Donaldson J, Paul G, Berry P, Sprecher DL (2019) Pazopanib may reduce bleeding in hereditary hemorrhagic telangiectasia. Angiogenesis 22:145–155. https://doi.org/10.1007/s10456-018-9646-1

456. Parambil JG, Gossage JR, McCrae KR, Woodard TD, Menon KVN, Timmerman KL, Pederson DP, Sprecher DL, Al-Samkari H (2022) Pazopanib for severe bleeding and transfusion-dependent anemia in hereditary hemorrhagic telangiectasia. Angiogenesis 25:87–97. https://doi.org/10.1007/s10456-021-09807-4

457. McWilliams JP, Majumdar S, Kim GH, Lee J, Seals K, Tangchaiburana S, Gilbert S, Duckwiler GR (2022) North American Study for the Treatment of Recurrent Epistaxis with Doxycycline: The NOSTRIL trial. J Thromb Haemost 20:1115–1125. https://doi.org/10.1111/jth.15662

458. Thompson KP, Sykes J, Chandakkar P, Marambaud P, Vozoris NT, Marchuk DA, Faughnan ME (2022) Randomized, double-blind, placebo-controlled, crossover trial of oral doxycycline for epistaxis in hereditary hemorrhagic telangiectasia. Orphanet J Rare Dis 17:405. https://doi.org/10.1186/s13023-022-02539-8

459. Invernizzi R, Quaglia F, Klersy C, Pagella F, Ornati F, Chu F, Matti E, Spinozzi G, Plumitallo S, Grignani P, Olivieri C, Bastia R, Bellistri F, Danesino C, Benazzo M, Balduini CL (2015) Efficacy and safety of thalidomide for the treatment of severe recurrent epistaxis in hereditary haemorrhagic telangiectasia: results of a non-randomised, single-centre, phase 2 study. Lancet Haematol 2:e465-473. https://doi.org/10.1016/S2352-3026(15)00195-7

460. Baysal M, Ümit EG, Kırkızlar HO, Özdöver AC, Demir AM (2019) Thalidomide for the Management of Bleeding Episodes in Patients with Hereditary Hemorrhagic Telangiectasia: Effects on Epistaxis Severity Score and Quality of Life. Turk J Haematol 36:43–47. https://doi.org/10.4274/tjh.galenos.2018.2018.0190

461. Riera-Mestre A, Cerdà P, Iriarte A, Graupera M, Viñals F (2022) Translational medicine in hereditary hemorrhagic telangiectasia. European Journal of Internal Medicine 95:32–37. https://doi.org/10.1016/j.ejim.2021.09.003

462. Hessels J, Kroon S, Boerman S, Nelissen RC, Grutters JC, Snijder RJ, Lebrin F, Post MC, Mummery CL, Mager J-J (2022) Efficacy and Safety of Tacrolimus as Treatment for Bleeding Caused by Hereditary Hemorrhagic Telangiectasia: An Open-Label, Pilot Study. J Clin Med 11:5280. https://doi.org/10.3390/jcm11185280

463. Dupuis-Girod S, Fargeton A-E, Grobost V, Rivière S, Beaudoin M, Decullier E, Bernard L, Bréant V, Colombet B, Philouze P, Bailly S, Faure F, Hermann R (2020) Efficacy and Safety of a 0.1% Tacrolimus Nasal Ointment as a Treatment for Epistaxis in Hereditary Hemorrhagic Telangiectasia: A Double-Blind, Randomized, Placebo-Controlled, Multicenter Trial. J Clin Med 9:1262. https://doi.org/10.3390/jcm9051262

464. Andorfer KEC, Seebauer CT, Koller M, Zeman F, Berneburg M, Fischer R, Vielsmeier V, Bohr C, Kühnel TS (2022) TIMolol nasal spray as a treatment for epistaxis in hereditary hemorrhagic telangiectasia (HHT) - Study protocol of the prospective, randomized, double-blind, controlled cross-over TIM-HHT trial. Clin Hemorheol Microcirc 80:307–315. https://doi.org/10.3233/CH-211253

465. Mei-Zahav M, Gendler Y, Bruckheimer E, Prais D, Birk E, Watad M, Goldschmidt N, Soudry E (2020) Topical Propranolol Improves Epistaxis Control in Hereditary Hemorrhagic Telangiectasia (HHT): A Randomized Double-Blind Placebo-Controlled Trial. J Clin Med 9:3130. https://doi.org/10.3390/jcm9103130

466. Iriarte A, Ochoa-Callejero L, García-Sanmartín J, Cerdà P, Garrido P, Narro-Íñiguez J, Mora-Luján Jm, Jucglà A, Sánchez-Corral M, Cruellas F, Gamundi E, Ribas J, Castellote J, Viñals F, Martínez A, Riera-Mestre A (2021) Adrenomedullin as a potential biomarker involved in patients with hereditary hemorrhagic telangiectasia. European Journal of Internal Medicine 88:89–95. https://doi.org/10.1016/j.ejim.2021.03.039

467. Geven C, Bergmann A, Kox M, Pickkers P (2018) Vascular Effects of Adrenomedullin and the Anti-Adrenomedullin Antibody Adrecizumab in Sepsis. Shock 50:132. https://doi.org/10.1097/SHK.0000000000001103

468. Guignabert C, Bailly S, Humbert M (2017) Restoring BMPRII functions in pulmonary arterial hypertension: opportunities, challenges and limitations. Expert Opin Ther Targets 21:181–190. https://doi.org/10.1080/14728222.2017.1275567

469. Simonneau G, Montani D, Celermajer DS, Denton CP, Gatzoulis MA, Krowka M, Williams PG, Souza R (2019) Haemodynamic definitions and updated clinical classification of pulmonary hypertension. Eur Respir J 53:1801913. https://doi.org/10.1183/13993003.01913-2018

470. Hoeper MM, Simon R Gibbs J (2014) The changing landscape of pulmonary arterial hypertension and implications for patient care. Eur Respir Rev 23:450–457. https://doi.org/10.1183/09059180.00007814

471. Aldred MA, Morrell NW, Guignabert C (2022) New Mutations and Pathogenesis of Pulmonary Hypertension: Progress and Puzzles in Disease Pathogenesis. Circ Res 130:1365–1381. https://doi.org/10.1161/CIRCRESAHA.122.320084

472. Eyries M, Montani D, Nadaud S, Girerd B, Levy M, Bourdin A, Trésorier R, Chaouat A, Cottin V, Sanfiorenzo C, Prevot G, Reynaud-Gaubert M, Dromer C, Houeijeh A, Nguyen K, Coulet F, Bonnet D, Humbert M, Soubrier F (2019) Widening the landscape of heritable pulmonary hypertension mutations in paediatric and adult cases. European Respiratory Journal 53:. https://doi.org/10.1183/13993003.01371-2018

473. Humbert M, Guignabert C, Bonnet S, Dorfmüller P, Klinger JR, Nicolls MR, Olschewski AJ, Pullamsetti SS, Schermuly RT, Stenmark KR, Rabinovitch M (2019) Pathology and pathobiology of pulmonary hypertension: state of the art and research perspectives. Eur Respir J 53:1801887. https://doi.org/10.1183/13993003.01887-2018

474. Lai Y-C, Potoka KC, Champion HC, Mora AL, Gladwin MT (2014) Pulmonary Arterial Hypertension. Circulation Research 115:115–130. https://doi.org/10.1161/CIRCRESAHA.115.301146

475. Lechartier B, Berrebeh N, Huertas A, Humbert M, Guignabert C, Tu L (2022) Phenotypic Diversity of Vascular Smooth Muscle Cells in Pulmonary Arterial Hypertension: Implications for Therapy. Chest 161:219–231. https://doi.org/10.1016/j.chest.2021.08.040

476. Humbert M, Lau EMT, Montani D, Jaïs X, Sitbon O, Simonneau G (2014) Advances in Therapeutic Interventions for Patients With Pulmonary Arterial Hypertension. Circulation 130:2189–2208. https://doi.org/10.1161/CIRCULATIONAHA.114.006974

477. Chester AH, Yacoub MH (2014) The role of endothelin-1 in pulmonary arterial hypertension. Glob Cardiol Sci Pract 2014:62–78. https://doi.org/10.5339/gcsp.2014.29

478. Giaid A, Yanagisawa M, Langleben D, Michel RP, Levy R, Shennib H, Kimura S, Masaki T, Duguid WP, Stewart DJ (1993) Expression of endothelin-1 in the lungs of patients with pulmonary hypertension. N Engl J Med 328:1732–1739. https://doi.org/10.1056/NEJM199306173282402

479. Stewart DJ, Levy RD, Cernacek P, Langleben D (1991) Increased plasma endothelin-1 in pulmonary hypertension: marker or mediator of disease? Ann Intern Med 114:464–469. https://doi.org/10.7326/0003-4819-114-6-464

480. Davie N, Haleen SJ, Upton PD, Polak JM, Yacoub MH, Morrell NW, Wharton J (2002) ET(A) and ET(B) receptors modulate the proliferation of human pulmonary artery smooth muscle cells. Am J Respir Crit Care Med 165:398–405. https://doi.org/10.1164/ajrccm.165.3.2104059

481. Tuder RM, Cool CD, Geraci MW, Wang J, Abman SH, Wright L, Badesch D, Voelkel NF (1999) Prostacyclin synthase expression is decreased in lungs from patients with severe pulmonary hypertension. Am J Respir Crit Care Med 159:1925–1932. https://doi.org/10.1164/ajrccm.159.6.9804054

482. Hoshikawa Y, Voelkel NF, Gesell TL, Moore MD, Morris KG, Alger LA, Narumiya S, Geraci MW (2001) Prostacyclin receptor-dependent modulation of pulmonary vascular remodeling. Am J Respir Crit Care Med 164:314–318. https://doi.org/10.1164/ajrccm.164.2.2010150

483. Kaufmann P, Okubo K, Bruderer S, Mant T, Yamada T, Dingemanse J, Mukai H (2015) Pharmacokinetics and Tolerability of the Novel Oral Prostacyclin IP Receptor Agonist Selexipag. Am J Cardiovasc Drugs 15:195–203. https://doi.org/10.1007/s40256-015-0117-4

484. Chen M, Lai Y, Chen R, Lu J, Zhang Y, Liu H, Wang D, Zhong Y, Zheng Z, Hong C (2022) Efficacy and safety of selexipag, an oral prostacyclin receptor agonist for the treatment of pulmonary hypertension: A meta-analysis. Pulm Pharmacol Ther 72:102100. https://doi.org/10.1016/j.pupt.2021.102100

485. Yung L-M, Yang P, Joshi S, Augur ZM, Kim SSJ, Bocobo GA, Dinter T, Troncone L, Chen P-S, McNeil ME, Southwood M, Poli de Frias S, Knopf J, Rosas IO, Sako D, Pearsall RS, Quisel JD, Li G, Kumar R, Yu PB (2020) ACTRIIA-Fc rebalances activin/GDF versus BMP signaling in pulmonary hypertension. Sci Transl Med 12:eaaz5660. https://doi.org/10.1126/scitranslmed.aaz5660

486. Humbert M, McLaughlin V, Gibbs JSR, Gomberg-Maitland M, Hoeper MM, Preston IR, Souza R, Waxman A, Escribano Subias P, Feldman J, Meyer G, Montani D, Olsson KM, Manimaran S, Barnes J, Linde PG, de Oliveira Pena J, Badesch DB, PULSAR Trial Investigators (2021) Sotatercept for the Treatment of Pulmonary Arterial Hypertension. N Engl J Med 384:1204–1215. https://doi.org/10.1056/NEJMoa2024277

487. Hoeper MM, Badesch DB, Ghofrani HA, Gibbs JSR, Gomberg-Maitland M, McLaughlin VV, Preston IR, Souza R, Waxman AB, Grünig E, Kopeć G, Meyer G, Olsson KM, Rosenkranz S, Xu Y, Miller B, Fowler M, Butler J, Koglin J, de Oliveira Pena J, Humbert M, STELLAR Trial Investigators (2023) Phase 3 Trial of Sotatercept for Treatment of Pulmonary Arterial Hypertension. N Engl J Med 388:1478–1490. https://doi.org/10.1056/NEJMoa2213558

488. Humbert M, McLaughlin V, Gibbs JSR, Gomberg-Maitland M, Hoeper MM, Preston IR, Souza R, Waxman AB, Ghofrani H-A, Escribano Subias P, Feldman J, Meyer G, Montani D, Olsson KM, Manimaran S, de Oliveira Pena J, Badesch DB (2023) Sotatercept for the treatment of pulmonary arterial hypertension: PULSAR open-label extension. Eur Respir J 61:2201347. https://doi.org/10.1183/13993003.01347-2022

489. Ramazi S, Zahiri J (2021) Post-translational modifications in proteins: resources, tools and prediction methods. Database 2021:baab012. https://doi.org/10.1093/database/baab012

490. Ubersax JA, Ferrell Jr JE (2007) Mechanisms of specificity in protein phosphorylation. Nat Rev Mol Cell Biol 8:530–541. https://doi.org/10.1038/nrm2203

491. Ardito F, Giuliani M, Perrone D, Troiano G, Muzio LL (2017) The crucial role of protein phosphorylation in cell signaling and its use as targeted therapy (Review). Int J Mol Med 40:271–280. https://doi.org/10.3892/ijmm.2017.3036

492. Smoly I, Shemesh N, Ziv-Ukelson M, Ben-Zvi A, Yeger-Lotem E (2017) An Asymmetrically Balanced Organization of Kinases versus Phosphatases across Eukaryotes Determines Their Distinct Impacts. PLOS Computational Biology 13:e1005221. https://doi.org/10.1371/journal.pcbi.1005221

493. Manning G, Whyte DB, Martinez R, Hunter T, Sudarsanam S (2002) The protein kinase complement of the human genome. Science 298:1912–1934. https://doi.org/10.1126/science.1075762

494. Sharma K, D'Souza RCJ, Tyanova S, Schaab C, Wiśniewski JR, Cox J, Mann M (2014) Ultradeep human phosphoproteome reveals a distinct regulatory nature of Tyr and Ser/Thr-based signaling. Cell Rep 8:1583–1594. https://doi.org/10.1016/j.celrep.2014.07.036

495. Olsen JV, Blagoev B, Gnad F, Macek B, Kumar C, Mortensen P, Mann M (2006) Global, in vivo, and site-specific phosphorylation dynamics in signaling networks. Cell 127:635–648. https://doi.org/10.1016/j.cell.2006.09.026

496. Walther TC, Mann M (2010) Mass spectrometry-based proteomics in cell biology. J Cell Biol 190:491–500. https://doi.org/10.1083/jcb.201004052

497. Goshe MB (2006) Characterizing phosphoproteins and phosphoproteomes using mass spectrometry. Briefings in Functional Genomics 4:363–376. https://doi.org/10.1093/bfgp/eli007

498. Riley NM, Coon JJ (2016) Phosphoproteomics in the Age of Rapid and Deep Proteome Profiling. Anal Chem 88:74–94. https://doi.org/10.1021/acs.analchem.5b04123

499. Müller T, Winter D (2017) Systematic Evaluation of Protein Reduction and Alkylation Reveals Massive Unspecific Side Effects by Iodine-containing Reagents. Mol Cell Proteomics 16:1173–1187. https://doi.org/10.1074/mcp.M116.064048

500. Manea M, Mezo G, Hudecz F, Przybylski M (2007) Mass spectrometric identification of the trypsin cleavage pathway in lysyl-proline containing oligotuftsin peptides. J Pept Sci 13:227–236. https://doi.org/10.1002/psc.836

501. Swaney DL, Wenger CD, Coon JJ (2010) Value of using multiple proteases for large-scale mass spectrometry-based proteomics. J Proteome Res 9:1323–1329. https://doi.org/10.1021/pr900863u

502. Bahl JMC, Jensen SS, Larsen MR, Heegaard NHH (2008) Characterization of the Human Cerebrospinal Fluid Phosphoproteome by Titanium Dioxide Affinity Chromatography and Mass Spectrometry. Anal Chem 80:6308–6316. https://doi.org/10.1021/ac800835y

503. Solari FA, Dell'Aica M, Sickmann A, Zahedi RP (2015) Why phosphoproteomics is still a challenge. Mol BioSyst 11:1487–1493. https://doi.org/10.1039/C5MB00024F

504. Fíla J, Honys D (2012) Enrichment techniques employed in phosphoproteomics. Amino Acids 43:1025–1047. https://doi.org/10.1007/s00726-011-1111-z

505. Thingholm TE, Larsen MR (2009) The use of titanium dioxide micro-columns to selectively isolate phosphopeptides from proteolytic digests. Methods Mol Biol 527:57–66, xi. https://doi.org/10.1007/978-1-60327-834-8_5

506. Yang C, Zhong X, Li L (2014) Recent advances in enrichment and separation strategies for mass spectrometry-based phosphoproteomics. Electrophoresis 35:3418–3429. https://doi.org/10.1002/elps.201400017

507. Engholm-Keller K, Larsen MR (2013) Technologies and challenges in large-scale phosphoproteomics. PROTEOMICS 13:910–931. https://doi.org/10.1002/pmic.201200484

508. Karas Michael, Hillenkamp Franz (1988) Laser desorption ionization of proteins with molecular masses exceeding 10,000 daltons. Anal Chem 60:2299–2301. https://doi.org/10.1021/ac00171a028

509. Fenn JB, Mann M, Meng CK, Wong SF, Whitehouse CM (1989) Electrospray ionization for mass spectrometry of large biomolecules. Science 246:64–71. https://doi.org/10.1126/science.2675315

510. Goodwin RJA, Pennington SR, Pitt AR (2008) Protein and peptides in pictures: imaging with MALDI mass spectrometry. Proteomics 8:3785–3800. https://doi.org/10.1002/pmic.200800320

511. Li C, Chu S, Tan S, Yin X, Jiang Y, Dai X, Gong X, Fang X, Tian D (2021) Towards Higher Sensitivity of Mass Spectrometry: A Perspective From the Mass Analyzers. Front Chem 9:813359. https://doi.org/10.3389/fchem.2021.813359

512. Hu A, Noble WS, Wolf-Yadlin A (2016) Technical advances in proteomics: new developments in data-independent acquisition. F1000Research

513. Salek M, Lehmann WD (2003) Neutral loss of amino acid residues from protonated peptides in collision-induced dissociation generates N- or C-terminal sequence ladders. J Mass Spectrom 38:1143–1149. https://doi.org/10.1002/jms.531

514. Tholey A, Reed J, Lehmann WD (1999) Electrospray tandem mass spectrometric studies of phosphopeptides and phosphopeptide analogues. J Mass Spectrom 34:117–123. https://doi.org/10.1002/(SICI)1096-9888(199902)34:2<117::AID-JMS769>3.0.CO;2-V

515. Elias JE, Gygi SP (2007) Target-decoy search strategy for increased confidence in large-scale protein identifications by mass spectrometry. Nat Methods 4:207–214. https://doi.org/10.1038/nmeth1019

516. Couté Y, Bruley C, Burger T (2020) Beyond Target-Decoy Competition: Stable Validation of Peptide and Protein Identifications in Mass Spectrometry-Based Discovery Proteomics. Anal Chem 92:14898–14906. https://doi.org/10.1021/acs.analchem.0c00328

517. Mermelekas G, Vlahou A, Zoidakis J (2015) SRM/MRM targeted proteomics as a tool for biomarker validation and absolute quantification in human urine. Expert Rev Mol Diagn 15:1441–1454. https://doi.org/10.1586/14737159.2015.1093937

518. Thompson A, Schäfer J, Kuhn K, Kienle S, Schwarz J, Schmidt G, Neumann T, Hamon C (2003) Tandem Mass Tags: A Novel Quantification Strategy for Comparative Analysis of Complex Protein Mixtures by MS/MS. Anal Chem 75:1895–1904. https://doi.org/10.1021/ac0262560

519. Rauniyar N, Yates JR (2014) Isobaric labeling-based relative quantification in shotgun proteomics. J Proteome Res 13:5293–5309. https://doi.org/10.1021/pr500880b

520. Ong S-E, Blagoev B, Kratchmarova I, Kristensen DB, Steen H, Pandey A, Mann M (2002) Stable Isotope Labeling by Amino Acids in Cell Culture, SILAC, as a Simple and Accurate Approach to Expression Proteomics *. Molecular & Cellular Proteomics 1:376–386. https://doi.org/10.1074/mcp.M200025-MCP200

521. Bantscheff M, Schirle M, Sweetman G, Rick J, Kuster B (2007) Quantitative mass spectrometry in proteomics: a critical review. Anal Bioanal Chem 389:1017–1031. https://doi.org/10.1007/s00216-007-1486-6

522. Jia S, Wang R, Wu K, Jiang H, Du Z (2019) Elucidation of the Mechanism of Action for Metal Based Anticancer Drugs by Mass Spectrometry-Based Quantitative Proteomics. Molecules 24:581. https://doi.org/10.3390/molecules24030581

523. Stasyk T, Huber LA (2012) Mapping in vivo signal transduction defects by phosphoproteomics. Trends in Molecular Medicine 18:43–51. https://doi.org/10.1016/j.molmed.2011.11.001

524. Boersema PJ, Raijmakers R, Lemeer S, Mohammed S, Heck AJR (2009) Multiplex peptide stable isotope dimethyl labeling for quantitative proteomics. Nat Protoc 4:484–494. https://doi.org/10.1038/nprot.2009.21

525. Engholm-Keller K, Birck P, Størling J, Pociot F, Mandrup-Poulsen T, Larsen MR (2012) TiSH--a robust and sensitive global phosphoproteomics strategy employing a combination of TiO2, SIMAC, and HILIC. J Proteomics 75:5749–5761. https://doi.org/10.1016/j.jprot.2012.08.007

526. Michalski A, Cox J, Mann M (2011) More than 100,000 detectable peptide species elute in single shotgun proteomics runs but the majority is inaccessible to data-dependent LC-MS/MS. J Proteome Res 10:1785–1793. https://doi.org/10.1021/pr101060v

527. Thiede B, Lamer S, Mattow J, Siejak F, Dimmler C, Rudel T, Jungblut PR (2000) Analysis of missed cleavage sites, tryptophan oxidation and N-terminal pyroglutamylation after in-gel tryptic digestion. Rapid Communications in Mass Spectrometry 14:496–502. https://doi.org/10.1002/(SICI)1097-0231(20000331)14:6<496::AID-RCM899>3.0.CO;2-1

528. Winter D, Kugelstadt D, Seidler J, Kappes B, Lehmann WD (2009) Protein phosphorylation influences proteolytic cleavage and kinase substrate properties exemplified by analysis of in vitro phosphorylated Plasmodium falciparum glideosome-associated protein 45 by nano-ultra performance liquid chromatography-tandem mass spectrometry. Anal Biochem 393:41–47. https://doi.org/10.1016/j.ab.2009.06.022

529. Schlosser A, Vanselow JT, Kramer A (2005) Mapping of phosphorylation sites by a multi-protease approach with specific phosphopeptide enrichment and NanoLC-MS/MS analysis. Anal Chem 77:5243–5250. https://doi.org/10.1021/ac050232m

530. Mirzaei H, Regnier F (2006) Enhancing Electrospray Ionization Efficiency of Peptides by Derivatization. Anal Chem 78:4175–4183. https://doi.org/10.1021/ac0602266

531. Brancia FL, Oliver SG, Gaskell SJ (2000) Improved matrix-assisted laser desorption/ionization mass spectrometric analysis of tryptic hydrolysates of proteins following guanidination of lysine-containing peptides. Rapid Communications in Mass Spectrometry 14:2070–2073. https://doi.org/10.1002/1097-0231(20001115)14:21<2070::AID-RCM133>3.0.CO;2-G

532. Wind M, Edler M, Jakubowski N, Linscheid M, Wesch H, Lehmann WD (2001) Analysis of protein phosphorylation by capillary liquid chromatography coupled to element mass spectrometry with 31P detection and to electrospray mass spectrometry. Anal Chem 73:29–35. https://doi.org/10.1021/ac0009595

533. Barrett DA, Brown VA, Watson RC, Davies MC, Shaw PN, Ritchie HJ, Ross P (2001) Effects of acid treatment on the trace metal content of chromatographic silica: bulk analysis, surface analysis and chromatographic performance of bonded phases. J Chromatogr A 905:69–83. https://doi.org/10.1016/s0021-9673(00)01000-1

534. Winter D, Seidler J, Ziv Y, Shiloh Y, Lehmann WD (2009) Citrate boosts the performance of phosphopeptide analysis by UPLC-ESI-MS/MS. J Proteome Res 8:418–424. https://doi.org/10.1021/pr800304n

535. Kim J, Camp DG, Smith RD (2004) Improved detection of multi-phosphorylated peptides in the presence of phosphoric acid in liquid chromatography/mass spectrometry. J Mass Spectrom 39:208–215. https://doi.org/10.1002/jms.593

536. van der Mijn JC, Labots M, Piersma SR, Pham TV, Knol JC, Broxterman HJ, Verheul HM, Jiménez CR (2015) Evaluation of different phospho-tyrosine antibodies for label-free phosphoproteomics. J Proteomics 127:259–263. https://doi.org/10.1016/j.jprot.2015.04.006

537. Budamgunta H, Maes E, Willems H, Menschaert G, Schildermans K, Kumar AA, Boonen K, Baggerman G (2019) Multiple solvent elution, a method to counter the effects of coelution and ion suppression in LC-MS analysis in bottom up proteomics. J Chromatogr B Analyt Technol Biomed Life Sci 1124:256–264. https://doi.org/10.1016/j.jchromb.2019.06.017

538. Ham BM, Yang F, Jayachandran H, Jaitly N, Monroe ME, Gritsenko MA, Livesay EA, Zhao R, Purvine SO, Orton D, Adkins J, Camp DG, Rossie S, Smith RD (2008) The Influence of Sample Preparation and Replicate Analyses on HeLa Cell Phosphoproteome Coverage. J Proteome Res 7:2215–2221. https://doi.org/10.1021/pr700575m

539. Boersema PJ, Mohammed S, Heck AJR (2009) Phosphopeptide fragmentation and analysis by mass spectrometry. Journal of Mass Spectrometry 44:861–878. https://doi.org/10.1002/jms.1599

540. Potel CM, Lemeer S, Heck AJR (2019) Phosphopeptide Fragmentation and Site Localization by Mass Spectrometry: An Update. Anal Chem 91:126–141. https://doi.org/10.1021/acs.analchem.8b04746

541. Pedreira-García WM, Pérez-Morales J, Chardón-Colón C, Cabán-Rivera J, Santiago-Cardona P (2021) Immunoblot validation of phospho-specific antibodies using lung cancer cell lines. Methods Mol Biol 2279:75–90. https://doi.org/10.1007/978-1-0716-1278-1_7

542. Mann A, Keen AC, Mark H, Dasgupta P, Javitch JA, Canals M, Schulz S, Robert Lane J (2021) New phosphosite-specific antibodies to unravel the role of GRK phosphorylation in dopamine D2 receptor regulation and signaling. Sci Rep 11:8288. https://doi.org/10.1038/s41598-021-87417-2

543. Jovanovic JN (2006) Phosphorylation Site-Specific Antibodies as Research Tools in Studies of Native GABAA Receptors. In: Kittler JT, Moss SJ (eds) The Dynamic Synapse: Molecular Methods in Ionotropic Receptor Biology. CRC Press/Taylor & Francis, Boca Raton (FL)

544. Reverberi R, Reverberi L (2007) Factors affecting the antigen-antibody reaction. Blood Transfus 5:227–240. https://doi.org/10.2450/2007.0047-07

545. Acharya P, Quinlan A, Neumeister V (2017) The ABCs of finding a good antibody: How to find a good antibody, validate it, and publish meaningful data. F1000Res 6:851. https://doi.org/10.12688/f1000research.11774.1

546. Ning T, Ning C, Li S, Mo C, Liu Z, Wang H (2022) Integrative proteomics and phosphoproteomics profiling on osteogenic differentiation of periodontal ligament stem cell. PROTEOMICS 22:2200067. https://doi.org/10.1002/pmic.202200067

547. Willger SD, Liu Z, Olarte RA, Adamo ME, Stajich JE, Myers LC, Kettenbach AN, Hogan DA (2015) Analysis of the Candida albicans Phosphoproteome. Eukaryot Cell 14:474–485. https://doi.org/10.1128/EC.00011-15

548. Zahid S, Oellerich M, Asif AR, Ahmed N (2012) Phosphoproteome profiling of substantia nigra and cortex regions of Alzheimer's disease patients. Journal of Neurochemistry 121:954–963. https://doi.org/10.1111/j.1471-4159.2012.07737.x

549. Kwon Y, Lee S, Park N, Ju S, Shin S, Yoo S, Lee H, Lee C (2022) Phosphoproteome Profiling Using an Isobaric Carrier without the Need for Phosphoenrichment. Anal Chem 94:4192–4200. https://doi.org/10.1021/acs.analchem.1c04188

550. Krug K, Mertins P, Zhang B, Hornbeck P, Raju R, Ahmad R, Szucs M, Mundt F, Forestier D, Jane-Valbuena J, Keshishian H, Gillette MA, Tamayo P, Mesirov JP, Jaffe JD, Carr StevenA, Mani DR (2019) A Curated Resource for Phosphosite-specific Signature Analysis*[S]. Molecular & Cellular Proteomics 18:576–593. https://doi.org/10.1074/mcp.TIR118.000943

551. Engholm-Keller K, Waardenberg AJ, Müller JA, Wark JR, Fernando RN, Arthur JW, Robinson PJ, Dietrich D, Schoch S, Graham ME (2019) The temporal profile of activity-dependent presynaptic phospho-signalling reveals long-lasting patterns of poststimulus regulation. PLoS Biol 17:e3000170. https://doi.org/10.1371/journal.pbio.3000170

552. Savage SR, Zhang B (2020) Using phosphoproteomics data to understand cellular signaling: a comprehensive guide to bioinformatics resources. Clinical Proteomics 17:27. https://doi.org/10.1186/s12014-020-09290-x

553. Stasyk T, Dubrovska A, Lomnytska M, Yakymovych I, Wernstedt C, Heldin C-H, Hellman U, Souchelnytskyi S (2005) Phosphoproteome profiling of transforming growth factor (TGF)-beta signaling: abrogation of TGFbeta1-dependent phosphorylation of transcription factor-II-I (TFII-I) enhances cooperation of TFII-I and Smad3 in transcription. Mol Biol Cell 16:4765–4780. https://doi.org/10.1091/mbc.e05-03-0257

554. Zakharchenko O, Cojoc M, Dubrovska A, Souchelnytskyi S (2013) A role of TGFß1 dependent 14-3-3σ phosphorylation at Ser69 and Ser74 in the regulation of gene transcription, stemness and radioresistance. PLoS One 8:e65163. https://doi.org/10.1371/journal.pone.0065163

555. Zhao Y, Zhang J, Sun H, Brasier AR (2021) Crosstalk of the IκB Kinase with Spliced X-Box Binding Protein 1 Couples Inflammation with Glucose Metabolic Reprogramming in Epithelial-Mesenchymal Transition. J Proteome Res 20:3475–3488. https://doi.org/10.1021/acs.jproteome.1c00093

556. Prado DS, Cattley RT, Shipman CW, Happe C, Lee M, Boggess WC, MacDonald ML, Hawse WF (2021) Synergistic and additive interactions between receptor signaling networks drive the regulatory T cell versus T helper 17 cell fate choice. J Biol Chem 297:101330. https://doi.org/10.1016/j.jbc.2021.101330

557. Okayama A, Miyagi Y, Oshita F, Ito H, Nakayama H, Nishi M, Kurata Y, Kimura Y, Ryo A, Hirano H (2015) Identification of Tyrosine-Phosphorylated Proteins Upregulated during Epithelial-Mesenchymal Transition Induced with TGF-β. J Proteome Res 14:4127–4136. https://doi.org/10.1021/acs.jproteome.5b00082

558. Kim B-G, Lee J-H, Ahn J-M, Park SK, Cho J-H, Hwang D, Yoo J-S, Yates JR, Ryoo H-M, Cho J-Y (2009) "Two-stage double-technique hybrid (TSDTH)" identification strategy for the analysis of BMP2-induced transdifferentiation of premyoblast C2C12 cells to osteoblast. J Proteome Res 8:4441–4454. https://doi.org/10.1021/pr900231a

559. Van Hoof D, Muñoz J, Braam SR, Pinkse MWH, Linding R, Heck AJR, Mummery CL, Krijgsveld J (2009) Phosphorylation dynamics during early differentiation of human embryonic stem cells. Cell Stem Cell 5:214–226. https://doi.org/10.1016/j.stem.2009.05.021

560. Chen Y-X, Li Y, Wang W-M, Zhang W, Chen X-N, Xie Y-Y, Lu J, Huang Q-H, Chen N (2010) Phosphoproteomic study of human tubular epithelial cell in response to transforming growth factor-beta-1-induced epithelial-to-mesenchymal transition. Am J Nephrol 31:24–35. https://doi.org/10.1159/000253865

561. Ali NA, Molloy MP (2011) Quantitative phosphoproteomics of transforming growth factor-β signaling in colon cancer cells. Proteomics 11:3390–3401. https://doi.org/10.1002/pmic.201100036

562. Muñoz J, Heck AJR (2011) Quantitative proteome and phosphoproteome analysis of human pluripotent stem cells. Methods Mol Biol 767:297–312. https://doi.org/10.1007/978-1-61779-201-4_22

563. Ferrão PM, de Oliveira FL, Degrave WM, Araujo-Jorge TC, Mendonça-Lima L, Waghabi MC (2012) A phosphoproteomic approach towards the understanding of the role of TGF-β in Trypanosoma cruzi biology. PLoS One 7:e38736. https://doi.org/10.1371/journal.pone.0038736

564. Ahn J, Yoon Y, Yeu Y, Lee H, Park S (2013) Impact of TGF-b on breast cancer from a quantitative proteomic analysis. Comput Biol Med 43:2096–2102. https://doi.org/10.1016/j.compbiomed.2013.09.022

565. D'Souza RCJ, Knittle AM, Nagaraj N, van Dinther M, Choudhary C, ten Dijke P, Mann M, Sharma K (2014) Time-resolved dissection of early phosphoproteome and ensuing proteome changes in response to TGF-β. Sci Signal 7:rs5. https://doi.org/10.1126/scisignal.2004856

566. Mönnich M, Borgeskov L, Breslin L, Jakobsen L, Rogowski M, Doganli C, Schrøder JM, Mogensen JB, Blinkenkjær L, Harder LM, Lundberg E, Geimer S, Christensen ST, Andersen JS, Larsen LA, Pedersen LB (2018) CEP128 Localizes to the Subdistal Appendages of the Mother Centriole and Regulates TGF-β/BMP Signaling at the Primary Cilium. Cell Rep 22:2584–2592. https://doi.org/10.1016/j.celrep.2018.02.043

567. Lu C, Sidoli S, Kulej K, Ross K, Wu CH, Garcia BA (2019) Coordination between TGF-β cellular signaling and epigenetic regulation during epithelial to mesenchymal transition. Epigenetics Chromatin 12:11. https://doi.org/10.1186/s13072-019-0256-y

568. Papadopoulos A, Chalmantzi V, Mikhaylichenko O, Hyvönen M, Stellas D, Kanhere A, Heath J, Cunningham DL, Fotsis T, Murphy C (2020) Combined transcriptomic and phosphoproteomic analysis of BMP4 signaling in human embryonic stem cells. Stem Cell Res 50:102133. https://doi.org/10.1016/j.scr.2020.102133

569. Zhong X, Lietz CB, Shi X, Buchberger AR, Frost DC, Li L (2020) Highly multiplexed quantitative proteomic and phosphoproteomic analyses in vascular smooth muscle cell dedifferentiation. Anal Chim Acta 1127:163–173. https://doi.org/10.1016/j.aca.2020.06.054

570. Hornbeck PV, Kornhauser JM, Tkachev S, Zhang B, Skrzypek E, Murray B, Latham V, Sullivan M (2012) PhosphoSitePlus: a comprehensive resource for investigating the structure and function of experimentally determined post-translational modifications in man and mouse. Nucleic Acids Res 40:D261–D270. https://doi.org/10.1093/nar/gkr1122

571. Souchelnytskyi S, ten Dijke P, Miyazono K, Heldin CH (1996) Phosphorylation of Ser165 in TGF-beta type I receptor modulates TGF-beta1-induced cellular responses. EMBO J 15:6231–6240

572. Saitoh M, Nishitoh H, Amagasa T, Miyazono K, Takagi M, Ichijo H (1996) Identification of important regions in the cytoplasmic juxtamembrane domain of type I receptor that separate signaling pathways of transforming growth factor-beta. J Biol Chem 271:2769–2775. https://doi.org/10.1074/jbc.271.5.2769

573. Zhou Y, Tanaka T, Sugiyama N, Yokoyama S, Kawasaki Y, Sakuma T, Ishihama Y, Saiki I, Sakurai H (2014) p38-Mediated phosphorylation of Eps15 endocytic adaptor protein. FEBS Lett 588:131–137. https://doi.org/10.1016/j.febslet.2013.11.020

574. Tsuchimochi K, Otero M, Dragomir CL, Plumb DA, Zerbini LF, Libermann TA, Marcu KB, Komiya S, Ijiri K, Goldring MB (2010) GADD45beta enhances Col10a1 transcription via the MTK1/MKK3/6/p38 axis and activation of C/EBPbeta-TAD4 in terminally differentiating chondrocytes. J Biol Chem 285:8395–8407. https://doi.org/10.1074/jbc.M109.038638

575. Takekawa M, Saito H (1998) A Family of Stress-Inducible GADD45-like Proteins Mediate Activation of the Stress-Responsive MTK1/MEKK4 MAPKKK. Cell 95:521–530. https://doi.org/10.1016/S0092-8674(00)81619-0

576. Miyake Z, Takekawa M, Ge Q, Saito H (2007) Activation of MTK1/MEKK4 by GADD45 through Induced N-C Dissociation and Dimerization-Mediated trans Autophosphorylation of the MTK1 Kinase Domain. Molecular and Cellular Biology 27:2765. https://doi.org/10.1128/MCB.01435-06

577. Bullard SA, Seo S, Schilling B, Dyle MC, Dierdorff JM, Ebert SM, DeLau AD, Gibson BW, Adams CM (2016) Gadd45a Protein Promotes Skeletal Muscle Atrophy by Forming a Complex with the Protein Kinase MEKK4♦. J Biol Chem 291:17496–17509. https://doi.org/10.1074/jbc.M116.740308

578. van der Heide LP, van Dinther M, Moustakas A, ten Dijke P (2011) TGFbeta activates mitogen- and stress-activated protein kinase-1 (MSK1) to attenuate cell death. J Biol Chem 286:5003–5011. https://doi.org/10.1074/jbc.M110.167379

579. van Bergen en Henegouwen PM (2009) Eps15: a multifunctional adaptor protein regulating intracellular trafficking. Cell Commun Signal 7:24. https://doi.org/10.1186/1478-811X-7-24

580. Enshoji M, Miyano Y, Yoshida N, Nagano M, Watanabe M, Kunihiro M, Siekhaus DE, Toshima JY, Toshima J (2022) Eps15/Pan1p is a master regulator of the late stages of the endocytic pathway. Journal of Cell Biology 221:e202112138. https://doi.org/10.1083/jcb.202112138

581. Milesi C, Alberici P, Pozzi B, Oldani A, Beznoussenko GV, Raimondi A, Soppo BE, Amodio S, Caldieri G, Malabarba MG, Bertalot G, Confalonieri S, Parazzoli D, Mironov AA, Tacchetti C, Di Fiore PP, Sigismund S, Offenhäuser N (2019) Redundant and nonredundant organismal functions of EPS15 and EPS15L1. Life Sci Alliance 2:e201800273. https://doi.org/10.26508/lsa.201800273

582. Iannolo G, Salcini AE, Gaidarov I, Goodman OB, Baulida J, Carpenter G, Pelicci PG, Di Fiore PP, Keen JH (1997) Mapping of the molecular determinants involved in the interaction between eps15 and AP-2. Cancer Res 57:240–245

583. Parachoniak CA, Park M (2009) Distinct recruitment of Eps15 via Its coiled-coil domain is required for efficient down-regulation of the met receptor tyrosine kinase. J Biol Chem 284:8382–8394. https://doi.org/10.1074/jbc.M807607200

584. Callery EM, Park CY, Xu X, Zhu H, Smith JC, Thomsen GH (2012) Eps15R is required for bone morphogenetic protein signalling and differentially compartmentalizes with Smad proteins. Open Biol 2:120060. https://doi.org/10.1098/rsob.120060

585. Rogalla T, Ehrnsperger M, Preville X, Kotlyarov A, Lutsch G, Ducasse C, Paul C, Wieske M, Arrigo AP, Buchner J, Gaestel M (1999) Regulation of Hsp27 oligomerization, chaperone function, and protective activity against oxidative stress/tumor necrosis factor alpha by phosphorylation. J Biol Chem 274:18947–18956. https://doi.org/10.1074/jbc.274.27.18947

586. Pichon S, Bryckaert M, Berrou E (2004) Control of actin dynamics by p38 MAP kinase - Hsp27 distribution in the lamellipodium of smooth muscle cells. J Cell Sci 117:2569–2577. https://doi.org/10.1242/jcs.01110

587. Zheng C, Lin Z, Zhao ZJ, Yang Y, Niu H, Shen X (2006) MAPK-activated Protein Kinase-2 (MK2)-mediated Formation and Phosphorylation-regulated Dissociation of the Signal Complex Consisting of p38, MK2, Akt, and Hsp27 *. Journal of Biological Chemistry 281:37215–37226. https://doi.org/10.1074/jbc.M603622200

588. Stokoe D, Campbell DG, Nakielny S, Hidaka H, Leevers SJ, Marshall C, Cohen P (1992) MAPKAP kinase-2; a novel protein kinase activated by mitogen-activated protein kinase. EMBO J 11:3985–3994

589. Salinthone S, Tyagi M, Gerthoffer WT (2008) Small heat shock proteins in smooth muscle. Pharmacol Ther 119:44–54. https://doi.org/10.1016/j.pharmthera.2008.04.005

590. Kostenko S, Moens U (2009) Heat shock protein 27 phosphorylation: kinases, phosphatases, functions and pathology. Cell Mol Life Sci 66:3289–3307. https://doi.org/10.1007/s00018-009-0086-3

591. Arrigo A-P (2017) Mammalian HspB1 (Hsp27) is a molecular sensor linked to the physiology and environment of the cell. Cell Stress and Chaperones 22:517–529. https://doi.org/10.1007/s12192-017-0765-1

592. Choi S-K, Kam H, Kim K-Y, Park SI, Lee Y-S (2019) Targeting Heat Shock Protein 27 in Cancer: A Druggable Target for Cancer Treatment? Cancers (Basel) 11:1195. https://doi.org/10.3390/cancers11081195

593. Hirano S, Rees RS, Yancy SL, Welsh MJ, Remick DG, Yamada T, Hata J, Gilmont RR (2004) Endothelial barrier dysfunction caused by LPS correlates with phosphorylation of HSP27in vivo. Cell Biol Toxicol 20:1–14. https://doi.org/10.1023/B:CBTO.0000021019.50889.aa

594. Chang E, Heo K-S, Woo C-H, Lee H, Le N-T, Thomas TN, Fujiwara K, Abe J (2011) MK2 SUMOylation regulates actin filament remodeling and subsequent migration in endothelial cells by inhibiting MK2 kinase and HSP27 phosphorylation. Blood 117:2527–2537. https://doi.org/10.1182/blood-2010-08-302281

595. Shi Y, Jiang X, Zhang L, Pu H, Hu X, Zhang W, Cai W, Gao Y, Leak RK, Keep RF, Bennett MVL, Chen J (2017) Endothelium-targeted overexpression of heat shock protein 27 ameliorates blood-brain barrier disruption after ischemic brain injury. Proc Natl Acad Sci U S A 114:E1243–E1252. https://doi.org/10.1073/pnas.1621174114

596. Rada CC, Mejia-Pena H, Grimsey NJ, Canto Cordova I, Olson J, Wozniak JM, Gonzalez DJ, Nizet V, Trejo J (2021) Heat shock protein 27 activity is linked to endothelial barrier recovery after proinflammatory GPCR-induced disruption. Sci Signal 14:eabc1044. https://doi.org/10.1126/scisignal.abc1044

597. Trott D, McManus CA, Martin JL, Brennan B, Dunn MJ, Rose ML (2009) Effect of phosphorylated hsp27 on proliferation of human endothelial and smooth muscle cells. PROTEOMICS 9:3383–3394. https://doi.org/10.1002/pmic.200800961

598. Nahomi RB, Palmer A, Green KM, Fort PE, Nagaraj RH (2014) Pro-inflammatory cytokines downregulate Hsp27 and cause apoptosis of human retinal capillary endothelial cells. Biochimica et Biophysica Acta (BBA) - Molecular Basis of Disease 1842:164–174. https://doi.org/10.1016/j.bbadis.2013.11.011

599. Selvaraj N, Kedage V, Hollenhorst PC (2015) Comparison of MAPK specificity across the ETS transcription factor family identifies a high-affinity ERK interaction required for ERG function in prostate cells. Cell Commun Signal 13:12. https://doi.org/10.1186/s12964-015-0089-7

600. Kedage V, Strittmatter BG, Dausinas PB, Hollenhorst PC (2017) Phosphorylation of the oncogenic transcription factor ERG in prostate cells dissociates polycomb repressive complex 2, allowing target gene activation. J Biol Chem 292:17225–17235. https://doi.org/10.1074/jbc.M117.796458

601. Strittmatter BG, Jerde TJ, Hollenhorst PC (2021) Ras/ERK and PI3K/AKT signaling differentially regulate oncogenic ERG mediated transcription in prostate cells. PLoS Genet 17:e1009708. https://doi.org/10.1371/journal.pgen.1009708

602. Greulich BM, Plotnik JP, Jerde TJ, Hollenhorst PC (2021) Toll-like receptor 4 signaling activates ERG function in prostate cancer and provides a therapeutic target. NAR Cancer 3:zcaa046. https://doi.org/10.1093/narcan/zcaa046

603. Shah AV, Birdsey GM, Randi AM (2016) Regulation of endothelial homeostasis, vascular development and angiogenesis by the transcription factor ERG. Vascul Pharmacol 86:3–13. https://doi.org/10.1016/j.vph.2016.05.003

604. Fish JE, Cantu Gutierrez M, Dang LT, Khyzha N, Chen Z, Veitch S, Cheng HS, Khor M, Antounians L, Njock M-S, Boudreau E, Herman AM, Rhyner AM, Ruiz OE, Eisenhoffer GT, Medina-Rivera A, Wilson MD, Wythe JD (2017) Dynamic regulation of VEGF-inducible genes by an ERK/ERG/p300 transcriptional network. Development 144:2428–2444. https://doi.org/10.1242/dev.146050

605. Shah AV, Birdsey GM, Peghaire C, Pitulescu ME, Dufton NP, Yang Y, Weinberg I, Osuna Almagro L, Payne L, Mason JC, Gerhardt H, Adams RH, Randi AM (2017) The endothelial transcription factor ERG mediates Angiopoietin-1-dependent control of Notch signalling and vascular stability. Nat Commun 8:16002. https://doi.org/10.1038/ncomms16002

606. Dufton NP, Peghaire CR, Osuna-Almagro L, Raimondi C, Kalna V, Chauhan A, Webb G, Yang Y, Birdsey GM, Lalor P, Mason JC, Adams DH, Randi AM (2017) Dynamic regulation of canonical TGFβ signalling by endothelial transcription factor ERG protects from liver fibrogenesis. Nat Commun 8:895. https://doi.org/10.1038/s41467-017-01169-0

607. Soni S, Anand P, Padwad YS (2019) MAPKAPK2: the master regulator of RNA-binding proteins modulates transcript stability and tumor progression. Journal of Experimental & Clinical Cancer Research 38:121. https://doi.org/10.1186/s13046-019-1115-1

608. Winzen R, Kracht M, Ritter B, Wilhelm A, Chen CY, Shyu AB, Müller M, Gaestel M, Resch K, Holtmann H (1999) The p38 MAP kinase pathway signals for cytokine-induced mRNA stabilization via MAP kinase-activated protein kinase 2 and an AU-rich region-targeted mechanism. EMBO J 18:4969–4980. https://doi.org/10.1093/emboj/18.18.4969

609. Pereira B, Billaud M, Almeida R (2017) RNA-Binding Proteins in Cancer: Old Players and New Actors. Trends Cancer 3:506–528. https://doi.org/10.1016/j.trecan.2017.05.003

610. Maitra S, Chou C-F, Luber CA, Lee K-Y, Mann M, Chen C-Y (2008) The AU-rich element mRNA decay-promoting activity of BRF1 is regulated by mitogen-activated protein kinase-activated protein kinase 2. RNA 14:950–959. https://doi.org/10.1261/rna.983708

611. Duan T-L, He G-J, Hu L-D, Yan Y-B (2019) The Intrinsically Disordered C-Terminal Domain Triggers Nucleolar Localization and Function Switch of PARN in Response to DNA Damage. Cells 8:836. https://doi.org/10.3390/cells8080836

612. Manke IA, Nguyen A, Lim D, Stewart MQ, Elia AEH, Yaffe MB (2005) MAPKAP kinase-2 is a cell cycle checkpoint kinase that regulates the G2/M transition and S phase progression in response to UV irradiation. Mol Cell 17:37–48. https://doi.org/10.1016/j.molcel.2004.11.021

613. Yaffe MB, Rittinger K, Volinia S, Caron PR, Aitken A, Leffers H, Gamblin SJ, Smerdon SJ, Cantley LC (1997) The structural basis for 14-3-3:phosphopeptide binding specificity. Cell 91:961–971. https://doi.org/10.1016/s0092-8674(00)80487-0

614. Borisova ME, Voigt A, Tollenaere MAX, Sahu SK, Juretschke T, Kreim N, Mailand N, Choudhary C, Bekker-Jensen S, Akutsu M, Wagner SA, Beli P (2018) p38-MK2 signaling axis regulates RNA metabolism after UV-light-induced DNA damage. Nat Commun 9:1017. https://doi.org/10.1038/s41467-018-03417-3

615. Tollenaere MAX, Villumsen BH, Blasius M, Nielsen JC, Wagner SA, Bartek J, Beli P, Mailand N, Bekker-Jensen S (2015) p38- and MK2-dependent signalling promotes stress-induced centriolar satellite remodelling via 14-3-3-dependent sequestration of CEP131/AZI1. Nat Commun 6:10075. https://doi.org/10.1038/ncomms10075

616. Nordgaard C, Tollenaere MAX, Val AMD, Bekker-Jensen DB, Blasius M, Olsen JV, Bekker-Jensen S (2021) Regulation of the Golgi Apparatus by p38 and JNK Kinases during Cellular Stress Responses. Int J Mol Sci 22:9595. https://doi.org/10.3390/ijms22179595

617. Fu R, Olsen MT, Webb K, Bennett EJ, Lykke-Andersen J (2016) Recruitment of the 4EHP-GYF2 cap-binding complex to tetraproline motifs of tristetraprolin promotes repression and degradation of mRNAs with AU-rich elements. RNA 22:373–382. https://doi.org/10.1261/rna.054833.115

618. Tollenaere MAX, Tiedje C, Rasmussen S, Nielsen JC, Vind AC, Blasius M, Batth TS, Mailand N, Olsen JV, Gaestel M, Bekker-Jensen S (2019) GIGYF1/2-Driven Cooperation between ZNF598 and TTP in Posttranscriptional Regulation of Inflammatory Signaling. Cell Rep 26:3511-3521.e4. https://doi.org/10.1016/j.celrep.2019.03.006

619. Luo Y, Na Z, Slavoff SA (2018) P-Bodies: Composition, Properties, and Functions. Biochemistry 57:2424–2431. https://doi.org/10.1021/acs.biochem.7b01162

620. Renaud CCN, Bidère N (2021) Function of Centriolar Satellites and Regulation by Post-Translational Modifications. Frontiers in Cell and Developmental Biology 9:

621. Grierson PM, Dodhiawala PB, Cheng Y, Chen TH-P, Khawar IA, Wei Q, Zhang D, Li L, Herndon J, Monahan JB, Ruzinova MB, Lim K-H (2021) The MK2/Hsp27 axis is a major survival mechanism for pancreatic ductal adenocarcinoma under genotoxic stress. Sci Transl Med 13:eabb5445. https://doi.org/10.1126/scitranslmed.abb5445

622. Delghandi MP, Johannessen M, Moens U (2005) The cAMP signalling pathway activates CREB through PKA, p38 and MSK1 in NIH 3T3 cells. Cellular Signalling 17:1343–1351. https://doi.org/10.1016/j.cellsig.2005.02.003

623. Tan Y, Rouse J, Zhang A, Cariati S, Cohen P, Comb MJ (1996) FGF and stress regulate CREB and ATF-1 via a pathway involving p38 MAP kinase and MAPKAP kinase-2. EMBO J 15:4629–4642

624. Zhang H, Kong Q, Wang J, Jiang Y, Hua H (2020) Complex roles of cAMP–PKA–CREB signaling in cancer. Experimental Hematology & Oncology 9:32. https://doi.org/10.1186/s40164-020-00191-1

625. Wiggin GR, Soloaga A, Foster JM, Murray-Tait V, Cohen P, Arthur JSC (2002) MSK1 and MSK2 are required for the mitogen- and stress-induced phosphorylation of CREB and ATF1 in fibroblasts. Mol Cell Biol 22:2871–2881. https://doi.org/10.1128/MCB.22.8.2871-2881.2002

626. Limbutara K, Kelleher A, Yang C-R, Raghuram V, Knepper MA (2019) Phosphorylation Changes in Response to Kinase Inhibitor H89 in PKA-Null Cells. Sci Rep 9:2814. https://doi.org/10.1038/s41598-019-39116-2

627. Lochner A, Moolman JA (2006) The Many Faces of H89: A Review. Cardiovascular Drug Reviews 24:261–274. https://doi.org/10.1111/j.1527-3466.2006.00261.x

628. Pomerance M, Abdullah H-B, Kamerji S, Corrèze C, Blondeau J-P (2000) Thyroid-stimulating Hormone and Cyclic AMP Activate p38 Mitogen-activated Protein Kinase Cascade: INVOLVEMENT OF PROTEIN KINASE A, Rac1, AND REACTIVE OXYGEN SPECIES *. Journal of Biological Chemistry 275:40539–40546. https://doi.org/10.1074/jbc.M002097200

629. Schulte G, Fredholm BB (2003) The Gs-coupled adenosine A2b receptor recruits divergent pathways to regulate ERK1/2 and p38☆. Experimental Cell Research 290:168–176. https://doi.org/10.1016/S0014-4827(03)00324-0

630. Hossain M, Imran KM, Rahman MS, Yoon D, Marimuthu V, Kim Y-S (2020) Sinapic acid induces the expression of thermogenic signature genes and lipolysis through activation of PKA/CREB signaling in brown adipocytes. BMB Rep 53:142–147. https://doi.org/10.5483/BMBRep.2020.53.3.093

631. Zhu G, Liu Y, Zhi Y, Jin Y, Li J, Shi W, Liu Y, Han Y, Yu S, Jiang J, Zhao X (2019) PKA- and Ca2+-dependent p38 MAPK/CREB activation protects against manganese-mediated neuronal apoptosis. Toxicology Letters 309:10–19. https://doi.org/10.1016/j.toxlet.2019.04.004

632. Kanki H, Sasaki T, Matsumura S, Kawano T, Todo K, Okazaki S, Nishiyama K, Takemori H, Mochizuki H (2020) CREB Coactivator CRTC2 Plays a Crucial Role in Endothelial Function. J Neurosci 40:9533–9546. https://doi.org/10.1523/JNEUROSCI.0407-20.2020

633. Niwano K, Arai M, Koitabashi N, Hara S, Watanabe A, Sekiguchi K, Tanaka T, Iso T, Kurabayashi M (2006) Competitive Binding of CREB and ATF2 to cAMP/ATF Responsive Element Regulates eNOS Gene Expression in Endothelial Cells. Arteriosclerosis, Thrombosis, and Vascular Biology 26:1036–1042. https://doi.org/10.1161/01.ATV.0000215179.76144.39

634. Yamamizu K, Matsunaga T, Katayama S, Kataoka H, Takayama N, Eto K, Nishikawa S-I, Yamashita JK (2012) PKA/CREB Signaling Triggers Initiation of Endothelial and Hematopoietic Cell Differentiation via Etv2 Induction. STEM CELLS 30:687–696. https://doi.org/10.1002/stem.1041

635. Zhao X, Nedvetsky P, Stanchi F, Vion A-C, Popp O, Zühlke K, Dittmar G, Klussmann E, Gerhardt H (2019) Endothelial PKA activity regulates angiogenesis by limiting autophagy through phosphorylation of ATG16L1. Elife 8:e46380. https://doi.org/10.7554/eLife.46380

636. Nedvetsky PI, Zhao X, Mathivet T, Aspalter IM, Stanchi F, Metzger RJ, Mostov KE, Gerhardt H (2016) cAMP-dependent protein kinase A (PKA) regulates angiogenesis by modulating tip cell behavior in a Notch-independent manner. Development 143:3582–3590. https://doi.org/10.1242/dev.134767

637. Bakre MM, Zhu Y, Yin H, Burton DW, Terkeltaub R, Deftos LJ, Varner JA (2002) Parathyroid hormone-related peptide is a naturally occurring, protein kinase A-dependent angiogenesis inhibitor. Nat Med 8:995–1003. https://doi.org/10.1038/nm753

638. Amersfoort J, Eelen G, Carmeliet P (2022) Immunomodulation by endothelial cells - partnering up with the immune system? Nat Rev Immunol 22:576–588. https://doi.org/10.1038/s41577-022-00694-4

639. Rabinovitch M, Guignabert C, Humbert M, Nicolls MR (2014) Inflammation and immunity in the pathogenesis of pulmonary arterial hypertension. Circ Res 115:165–175. https://doi.org/10.1161/CIRCRESAHA.113.301141

640. Guttmacher AE, Marchuk DA, White RI (1995) Hereditary hemorrhagic telangiectasia. N Engl J Med 333:918–924. https://doi.org/10.1056/NEJM199510053331407

641. Braverman IM, Keh A, Jacobson BS (1990) Ultrastructure and three-dimensional organization of the telangiectases of hereditary hemorrhagic telangiectasia. J Invest Dermatol 95:422–427. https://doi.org/10.1111/1523-1747.ep12555569

642. Jones SA, Jenkins BJ (2018) Recent insights into targeting the IL-6 cytokine family in inflammatory diseases and cancer. Nat Rev Immunol 18:773–789. https://doi.org/10.1038/s41577-018-0066-7

643. Baran P, Hansen S, Waetzig GH, Akbarzadeh M, Lamertz L, Huber HJ, Ahmadian MR, Moll JM, Scheller J (2018) The balance of interleukin (IL)-6, IL-6·soluble IL-6 receptor (sIL-6R), and IL-6·sIL-6R·sgp130 complexes allows simultaneous classic and trans-signaling. J Biol Chem 293:6762–6775. https://doi.org/10.1074/jbc.RA117.001163

644. Schaper F, Rose-John S (2015) Interleukin-6: Biology, signaling and strategies of blockade. Cytokine Growth Factor Rev 26:475–487. https://doi.org/10.1016/j.cytogfr.2015.07.004

645. Wolf J, Rose-John S, Garbers C (2014) Interleukin-6 and its receptors: a highly regulated and dynamic system. Cytokine 70:11–20. https://doi.org/10.1016/j.cyto.2014.05.024

646. Schumacher N, Meyer D, Mauermann A, von der Heyde J, Wolf J, Schwarz J, Knittler K, Murphy G, Michalek M, Garbers C, Bartsch JW, Guo S, Schacher B, Eickholz P, Chalaris A, Rose-John S, Rabe B (2015) Shedding of Endogenous Interleukin-6 Receptor (IL-6R) Is Governed by A Disintegrin and Metalloproteinase (ADAM) Proteases while a Full-length IL-6R Isoform Localizes to Circulating Microvesicles. J Biol Chem 290:26059–26071. https://doi.org/10.1074/jbc.M115.649509

647. Riethmueller S, Somasundaram P, Ehlers JC, Hung C-W, Flynn CM, Lokau J, Agthe M, Düsterhöft S, Zhu Y, Grötzinger J, Lorenzen I, Koudelka T, Yamamoto K, Pickhinke U, Wichert R, Becker-Pauly C, Rädisch M, Albrecht A, Hessefort M, Stahnke D, Unverzagt C, Rose-John S, Tholey A, Garbers C (2017) Proteolytic Origin of the Soluble Human IL-6R In Vivo and a Decisive Role of N-Glycosylation. PLOS Biology 15:e2000080. https://doi.org/10.1371/journal.pbio.2000080

648. Rose-John S (2012) IL-6 trans-signaling via the soluble IL-6 receptor: importance for the pro-inflammatory activities of IL-6. Int J Biol Sci 8:1237–1247. https://doi.org/10.7150/ijbs.4989

649. Jones SA, Rose-John S (2002) The role of soluble receptors in cytokine biology: the agonistic properties of the sIL-6R/IL-6 complex. Biochim Biophys Acta 1592:251–263. https://doi.org/10.1016/s0167-4889(02)00319-1

650. Romano M, Sironi M, Toniatti C, Polentarutti N, Fruscella P, Ghezzi P, Faggioni R, Luini W, van Hinsbergh V, Sozzani S, Bussolino F, Poli V, Ciliberto G, Mantovani A (1997) Role of IL-6 and Its Soluble Receptor in Induction of Chemokines and Leukocyte Recruitment. Immunity 6:315–325. https://doi.org/10.1016/S1074-7613(00)80334-9

651. Lo C-W, Chen M-W, Hsiao M, Wang S, Chen C-A, Hsiao S-M, Chang J-S, Lai T-C, Rose-John S, Kuo M-L, Wei L-H (2011) IL-6 Trans-Signaling in Formation and Progression of Malignant Ascites in Ovarian Cancer. Cancer Research 71:424–434. https://doi.org/10.1158/0008-5472.CAN-10-1496

652. Zegeye MM, Lindkvist M, Fälker K, Kumawat AK, Paramel G, Grenegård M, Sirsjö A, Ljungberg LU (2018) Activation of the JAK/STAT3 and PI3K/AKT pathways are crucial for IL-6 trans-signaling-mediated pro-inflammatory response in human vascular endothelial cells. Cell Communication and Signaling 16:55. https://doi.org/10.1186/s12964-018-0268-4

653. Lindkvist M, Zegeye MM, Grenegård M, Ljungberg LU (2022) Pleiotropic, Unique and Shared Responses Elicited by IL-6 Family Cytokines in Human Vascular Endothelial Cells. Int J Mol Sci 23:1448. https://doi.org/10.3390/ijms23031448

654. Montgomery A, Tam F, Gursche C, Cheneval C, Besler K, Enns W, Manku S, Rey K, Hanson PJ, Rose-John S, McManus BM, Choy JC (2021) Overlapping and distinct biological effects of IL-6 classic and trans-signaling in vascular endothelial cells. American Journal of Physiology-Cell Physiology 320:C554–C565. https://doi.org/10.1152/ajpcell.00323.2020

655. Song M, Wang Y, Annex BH, Popel AS (2023) Experiment-based Computational Model Predicts that IL-6 Trans-Signaling Plays a Dominant Role in IL-6 mediated signaling in Endothelial Cells. bioRxiv 2023.02.03.526721. https://doi.org/10.1101/2023.02.03.526721

656. Alsaffar H, Martino N, Garrett JP, Adam AP (2018) Interleukin-6 promotes a sustained loss of endothelial barrier function via Janus kinase-mediated STAT3 phosphorylation and de novo protein synthesis. Am J Physiol Cell Physiol 314:C589–C602. https://doi.org/10.1152/ajpcell.00235.2017

657. Zegeye MM, Andersson B, Sirsjö A, Ljungberg LU (2020) IL-6 trans-Signaling Impairs Sprouting Angiogenesis by Inhibiting Migration, Proliferation and Tube Formation of Human Endothelial Cells. Cells 9:1414. https://doi.org/10.3390/cells9061414

658. Rose-John S, Jenkins BJ, Garbers C, Moll JM, Scheller J (2023) Targeting IL-6 trans-signalling: past, present and future prospects. Nat Rev Immunol 1–16. https://doi.org/10.1038/s41577-023-00856-y

659. Cao Y, Gong Y, Liu L, Zhou Y, Fang X, Zhang C, Li Y, Li J (2017) The use of human umbilical vein endothelial cells (HUVECs) as an in vitro model to assess the toxicity of nanoparticles to endothelium: a review. Journal of Applied Toxicology 37:1359–1369. https://doi.org/10.1002/jat.3470

660. Gifre-Renom L, Daems M, Luttun A, Jones EAV (2022) Organ-Specific Endothelial Cell Differentiation and Impact of Microenvironmental Cues on Endothelial Heterogeneity. International Journal of Molecular Sciences 23:1477. https://doi.org/10.3390/ijms23031477

661. Bassermann F, von Klitzing C, Münch S, Bai R-Y, Kawaguchi H, Morris SW, Peschel C, Duyster J (2005) NIPA defines an SCF-type mammalian E3 ligase that regulates mitotic entry. Cell 122:45–57. https://doi.org/10.1016/j.cell.2005.04.034

662. Illert AL, Zech M, Moll C, Albers C, Kreutmair S, Peschel C, Bassermann F, Duyster J (2012) Extracellular signal-regulated kinase 2 (ERK2) mediates phosphorylation and inactivation of nuclear interaction partner of anaplastic lymphoma kinase (NIPA) at G2/M. J Biol Chem 287:37997–38005. https://doi.org/10.1074/jbc.M112.373464

663. O'Donoghue L, Smolenski A (2022) Analysis of protein phosphorylation using Phos-tag gels. Journal of Proteomics 259:104558. https://doi.org/10.1016/j.jprot.2022.104558

664. Yu L-R, Veenstra TD (2021) Characterization of Phosphorylated Proteins Using Mass Spectrometry. Curr Protein Pept Sci 22:148–157. https://doi.org/10.2174/1389203721999201123200439

665. Dang TTH, Yun JW (2021) BMP10 positively regulates myogenic differentiation in C2C12 myoblasts via the Smad 1/5/8 signaling pathway. Mol Cell Biochem 476:2085–2097. https://doi.org/10.1007/s11010-021-04064-x

666. Knöfler M, Haider S, Saleh L, Pollheimer J, Gamage TKJB, James J (2019) Human placenta and trophoblast development: key molecular mechanisms and model systems. Cell Mol Life Sci 76:3479–3496. https://doi.org/10.1007/s00018-019-03104-6

667. Evans IM, Britton G, Zachary IC (2008) Vascular endothelial growth factor induces heat shock protein (HSP) 27 serine 82 phosphorylation and endothelial tubulogenesis via protein kinase D and independent of p38 kinase. Cellular Signalling 20:1375–1384. https://doi.org/10.1016/j.cellsig.2008.03.002

668. Sawada J, Li F, Komatsu M (2016) R-Ras Inhibits VEGF-Induced p38MAPK Activation and HSP27 Phosphorylation in Endothelial Cells. Journal of Vascular Research 52:347–359. https://doi.org/10.1159/000444526

669. Rousseau S, Houle F, Landry J, Huot J (1997) p38 MAP kinase activation by vascular endothelial growth factor mediates actin reorganization and cell migration in human endothelial cells. Oncogene 15:2169–2177. https://doi.org/10.1038/sj.onc.1201380

670. Piotrowicz RS, Hickey E, Levin EG (1998) Heat shock protein 27 kDa expression and phosphorylation regulates endothelial cell migration. FASEB j 12:1481–1490. https://doi.org/10.1096/fasebj.12.14.1481

671. Geum D, Son GH, Kim K (2002) Phosphorylation-dependent cellular localization and thermoprotective role of heat shock protein 25 in hippocampal progenitor cells. J Biol Chem 277:19913–19921. https://doi.org/10.1074/jbc.M104396200

672. Bryantsev AL, Kurchashova SY, Golyshev SA, Polyakov VY, Wunderink HF, Kanon B, Budagova KR, Kabakov AE, Kampinga HH (2007) Regulation of stress-induced intracellular sorting and chaperone function of Hsp27 (HspB1) in mammalian cells. Biochem J 407:407–417. https://doi.org/10.1042/BJ20070195

673. Guo K, Gan L, Zhang S, Cui FJ, Cun W, Li Y, Kang NX, Gao MD, Liu KY (2012) Translocation of HSP27 into liver cancer cell nucleus may be associated with phosphorylation and O-GlcNAc glycosylation. Oncol Rep 28:494–500. https://doi.org/10.3892/or.2012.1844

674. Yang J, Sun H, Zhang J, Hu M, Wang J, Wu G, Wang G (2015) Regulation of β-Adrenergic Receptor Trafficking and Lung Microvascular Endothelial Cell Permeability by Rab5 GTPase. Int J Biol Sci 11:868–878. https://doi.org/10.7150/ijbs.12045

675. Xu K, Saaoud F, Yu S, Drummer C, Shao Y, Sun Y, Lu Y, Sun J, Yu J, Jiang X, Wang H, Yang X (2022) Monocyte Adhesion Assays for Detecting Endothelial Cell Activation in Vascular Inflammation and Atherosclerosis. Methods Mol Biol 2419:169–182. https://doi.org/10.1007/978-1-0716-1924-7_10

676. Palmroth M, Kuuliala K, Peltomaa R, Virtanen A, Kuuliala A, Kurttila A, Kinnunen A, Leirisalo-Repo M, Silvennoinen O, Isomäki P (2021) Tofacitinib Suppresses Several JAK-STAT Pathways in Rheumatoid Arthritis In Vivo and Baseline Signaling Profile Associates With Treatment Response. Front Immunol 12:738481. https://doi.org/10.3389/fimmu.2021.738481

Annex 1: Impact of heterozygous ALK1 mutations on the transcriptomic response to BMP9 and BMP10 in endothelial cells from Hereditary Hemorrhagic Telangiectasia and Pulmonary Arterial Hypertension donors

I have collaborated as a co-author on a study performed in our lab by Al Tabosh et al titled "Impact of heterozygous ALK1 mutations on the transcriptomic response to BMP9 and BMP10 in endothelial cells from Hereditary Hemorrhagic Telangiectasia and Pulmonary Arterial Hypertension donors". The research paper of this study is provided in the following pages and is currently under revision.

Impact of heterozygous ALK1 mutations on the transcriptomic response to BMP9 and BMP10 in endothelial cells from Hereditary Hemorrhagic Telangiectasia and Pulmonary Arterial Hypertension donors

Al Tabosh T.[1], Liu H.[1], Koca D.[1], M Al Tarrass[1], Tu L.[2,3], Giraud S.[4], Delagrange L. [4,5], Beaudoin M.[4,5], Rivière S.[6], Grobost V.[7], Rondeau-Lutz M.[8], Dupuis O.[9,10], Ricard N.[1], Tillet E[1], Machillot P[1], Salomon A.[1], Picart C.[1], Battail C.[1], Dupuis-Girod S.[1,4,5], Guignabert C.[2,3], Desroches-Castan A.[1*], and Bailly S.[1*^]

[1]Biosanté unit U1292, Grenoble Alpes University, INSERM, CEA, F-38000 Grenoble, France; [2]Université Paris-Saclay, Faculté de Médecine, Pulmonary Hypertension: Pathophysiology and Novel Therapies, 94276 Le Kremlin-Bicêtre, France; [3]INSERM UMR_S 999 «Pulmonary Hypertension: Pathophysiology and Novel Therapies», Hôpital Marie Lannelongue, 92350 Le Plessis-Robinson, France; [4]Genetics Department, Femme-Mère-Enfants Hospital, Hospices Civils de Lyon, F-69677 Bron, France; [5]National Reference Center for HHT, F-69677 Bron, France; [6]Internal Medicine Department, CHU of Montpellier, St Eloi Hospital and Center of Clinical Investigation, INSERM, CIC 1411, F-34295 Montpellier CEDEX 7, France; [7]Internal Medicine Department, CHU Estaing, 63100 Clermont-Ferrand, France; [8]Internal Medicine Department, University Hospital of Strasbourg, 67091 Strasbourg CEDEX, France; [9]Obstetrics & Gynecology Department, Hospices Civils de Lyon, Lyon-Sud Hospital, Pierre-Bénite, France; [10]Faculty of Medicine, Lyon University, Lyon, France.

*Co-last-authors

^Corresponding author: sabine.bailly@cea.fr

Total word count : 11 539

Author's ORCID
Desroches-Castan A: 0000-0002-3301-9504
Liu H: 0000-0003-3830-3421
Koca D: 0000-0003-4838-3090
Salomon A : 0000-0003-4425-6860
Al Tabosh T: 0009-0006-7577-2904
Al Tarrass M: 0009-0003-9337-9100
Tu L: 0000-0003-2336-5099
Rondeau-Lutz M: 0000-0001-7977-1411
Machillot P: 0000-0002-5640-929X
Picart C : 0000-0003-0130-1000
Dupuis-Girod S: 0000-0002-8834-5526
Guignabert C: 0000-0002-8545-4452
Tillet E: 0000-0002-0076-8007
Ricard N: 0000-0002-7572-173X
Battail C: 0000-0001-6849-7824

Bailly S: 0000-0003-1043-7030

Disclosures

The authors have no conflict of interest to disclose. Material preparation, data collection and analysis were performed by Al Tabosh A., Al Tarrass M., Tu L., Machillot P., Salomon A., Tillet E., Ricard N. Samples were collected by Giraud S., Delagrange L., Beaudoin M., Rivière S., Grobost V., Rondeau-Lutz M., Dupuis O., Dupuis-Girod S. Bioinformatic analyses were performed by Koca D., Liu H. and Battail C. Guignabert C. and Picart C. participated for important intellectual content of the study. Desroches-Castan A., and Bailly S. participated in the redaction of the manuscript which was approved by all authors.

Acknowledments

The authors are indebted to Véronique Collin-Faure for her help in cytometry experiment and analysis. We thank the patients, their families and the nurses who were involved in this trial. This work was funded by the National Institute for Health and Medical Research (INSERM), the University of Grenoble-Alpes, by the CEA (commissariat à l'énergie atomique et aux énergies alternatives DRF/IRIG/DS), the Fondation pour la Recherche Médicale (EQU202003010188), the Association Maladie de Rendu-Osler (AMRO/HHT France), the association FAVA-multi, the H2020-msca-ITN-2018 (V.A. Cure-84316) and the French National Agency for research (ANR) grant no. ANR-17-CE14-0006 (Be9inPH). This project received funding from GRAL, a programme from the Chemistry Biology Health (CBH) Graduate School of University Grenoble Alpes (ANR-17-EURE-0003).

Abstract

Heterozygous ALK1 (Activin receptor-Like Kinase 1) mutations are associated with the development of two vascular diseases: hereditary hemorrhagic telangiectasia (HHT) and more rarely pulmonary arterial hypertension (PAH). Here, we aimed to understand the impact of ALK1 mutations on BMP9 and BMP10 transcriptomic responses in endothelial cells.

RNA-sequencing was performed on Endothelial colony-forming cells (ECFCs) and human microvascular endothelial cells (HMVECs) carrying heterozygous loss-of-function ALK1 mutations compared to control counterparts following stimulation with BMP9 or BMP10.

In control ECFCs, BMP9 and BMP10 stimulations induced similar transcriptomic responses with around 800 differentially expressed protein-coding genes (DEGs). Comparison of the transcriptome between control and ALK1-mutated ECFCs revealed very similar profiles, both at the baseline and upon stimulation. Consistently, control and ALK1-mutated ECFCs displayed a similar Smad1/5 response, which could not be explained by a compensation in cell-surface ALK1 level. Conversely, PAH HMVECs carrying heterozygous ALK1 mutations revealed strong transcriptional dysregulations compared to controls with >1200 DEGs at the baseline. Because our study involved two variables, ALK1 genotype and BMP stimulation, we performed a two-factor differential expression analysis and identified few genes, including the NOTCH signaling regulator LFNG (Lunatic Fringe), whose expression was also confirmed in other ALK1-mutated endothelial cell models.

In conclusion, ALK1 heterozygosity does not impact the activation of the canonical Smad pathway by BMP9/10, nor causes overt transcriptional dysregulations. This suggests that the haploinsufficiency model of HHT and PAH pathogenesis might need to be reconsidered, unless pathogenesis is sufficiently driven by the few identified dysregulated genes like LFNG.

Key words: ALK1; BMP; HHT; PAH; RNA-seq, LFNG

Nonstandard Abbreviations and Acronyms:

ALK1 Activin receptor like kinase 1
BMP Bone morphogenetic protein
PAH pulmonary arterial hypertension
HHT Hereditary hemorrhagic telangiectasia
mPAP Mean pulmonary arterial pressure
PVR pulmonary vascular resistance
ECFCs endothelial colony-forming cells
HMVECs human microvascular endothelial cells

Introduction

Hereditary hemorrhagic telangiectasia (HHT [MIM: 187300, 600376, 175050]), also known as Osler–Weber–Rendu syndrome, is a rare genetic vascular disease characterized by the development of multiple focal vascular malformations (VMs), including muco-cutaneous telangiectases responsible for recurrent, spontaneous epistaxis and visceral arteriovenous malformations[1]. HHT is an autosomal-dominant disease presenting complete penetrance over the age of 50, but with highly variable expressivity. It is mostly caused by mutations in *ENG* (MIM: 131195) and *ACVRL1* (MIM: 601284), which account for 85% of cases, and more rarely in *SMAD4 (*MIM: 600993) accounting for less than 2%[2, 3]. Additionally, mutations in *GDF2 (*MIM: 615506)*,* were reported in few individuals presenting HHT-like symptoms[4]. The protein products of all 4 genes are components of the BMP/TGFß signaling pathway. *ACVRL1* encodes for the type 1 receptor ALK1, *ENG* for the co-receptor endoglin, *SMAD4* for a transcription factor downstream of the receptors and *GDF2* for BMP9, a high affinity ligand for this receptor complex[5]. The current signaling model is that BMP9 or BMP10 binds the co-receptor endoglin, which facilitates their binding to the signaling compex composed of the type I receptor ALK1 and a type 2 receptor that can either be BMPR2, ActR2B or ActR2A. Upon ligand binding, the type 2 receptor phosphorylates the type 1 receptor which subsequently phosphorylates the transcription factors Smad1, Smad5 and Smad8, allowing their interactaction with Smad4. The formed Smad complex then translocates to the nucleus where it binds to DNA together with other transcription factors in order to regulate the expression of many genes[6]. The receptor ALK1 and its co-receptor endoglin are mostly expressed on endothelial cells, supporting a key role for these receptors in vascular physiology[7]. It has been demonstrated that the BMP9/BMP10-ALK1-endoglin signaling pathway promotes

vascular quiescence[8]. The current working model is that mutations within this signaling pathway would lead to an increase in angiogenesis. Thus, anti-angiogenic drugs, mainly blocking VEGF signaling pathway, have been proposed as a therapeutic option for HHT patients and tend to improve symptoms (bleedings and high cardiac output secondary to liver AVMs) but do not cure the disease[9, 10].

HHT causal mutations result in the loss of function (LOF) of the gene product[11, 12] and are inherited through an autosomal-dominant manner. Therefore, HHT has long been speculated to be caused by haploinsufficiency of the mutated *ENG* or *ACVRL1* gene product, with previous reports pointing at a reduction in endoglin and ALK1 expression in HHT1 and HHT2 patient-derived cells, respectively[13]. However, haploinsufficiency does not explain why vascular lesions in HHT patients occur focally in specific vascular beds[14], despite the systemic presence of the pathogenic germline mutation in all blood vessels.

In recent years, mutations in the same signaling pathway have been identified in rare cases of pulmonary arterial hypertension (PAH)[15]. PAH is defined as a resting mean pulmonary artery pressure (mPAP) > 20 mmHg with a pulmonary artery wedge pressure (≤ 15 mmHg) and elevated pulmonary vascular resistance (PVR) of >2 Wood units)[16, 17]. PAH can develop sporadically, be associated with risk factors such as drug or toxins or other diseases (i.e., connective tissue disease, HIV infection, portal hypertension, congenital heart disease, or schistosomiasis), or inherited. Altough germline mutations in *BMPR2* gene are major predisposing factors for idiopathic (15-40%) and heritable (60-80%) PAH, less common or rare mutations in other genes encoding key members of the Smad1/5/8 signaling including in *ALK1, GDF2(BMP9)* and *BMP10* have been identified, underlining the critical role of this signaling pathway in PAH[15].

ALK1 mutations are responsible for nearly half HHT cases and a minority of PAH patients, and the same *ALK1* mutations can predispose to the two vascular disorders[18–20]. Despite our understanding of the genetics and of downstream pathways involved in HHT and PAH, the molecular mechanisms that initiate HHT-related VMs and PAH are poorly understood[21]. Here, we aimed to understand the impact of *ALK1* mutations on the downstream BMP9/BMP10-ALK1 signaling pathway by studying the transcriptome of heterozygote *ALK1*-mutated primary endothelial cells to better understand the underlying molecular mechanisms and to propose new therapeutic approaches for these two diseases. To address this question, we used two different endothelial models carrying heterozygous LOF *ALK1* mutations: (1) endothelial colony-forming cells (ECFCs) that were isolated from the cord blood of HHT newborns and (2) human microvascular endothelial cells (HMVECs) isolated from explanted lungs of PAH patients.

We first used ECFCs, which allowed us to address the sole role of heterozygous *ALK1* mutations in cells not yet exposed to a sick microenvironment. These circulating cells, possessing vasoregenerative potential[22], are a particularly interesting model as they could be the cells responsible for endothelial cell turnover in the liver leading to new malformations. Indeed, it has been shown that some HHT patients who had received liver transplantations

developed new HHT hepatic lesions several years later, leading to a second liver transplantation[23]. We also had access to *ALK1*-mutated microvascular endothelial cells from the explanted lungs of two PAH patients, which is a very rare event as *ALK1* mutations occur in only around 6% of patients with PAH, which affects 15-50 individuals per million[15]. The limited availability of *ALK1*-mutated HMVECs prompted us to additionally include HMVECs from 3 PAH patients with more frequent heterozygous mutations in the type 2 BMP9/10 receptor BMPR2*,* for validation of target genes by RT-qPCR. In order to validate some of the results, we also used human umbilical vacular endothelial cells (HUVECs) derived from the umbilical cords of HHT newborns.

We performed RNA-sequencing on each type of cells compared to control counterparts, unstimulated or following an overnight stimulation with BMP9 or BMP10. Together, our data support that *ALK1* heterozygosity does not impact the activation of the canonical Smad pathway by BMP9/10, nor cause overt transcriptional dysregulations in ECFCs. However, using two-factor differential expression analysis, in order to take into account the two variables (*ALK1* mutation and stimulation), we were able to highlight from HMVECs' RNA-seq analyses few genes exhibiting impaired regulation by BMP9/BMP10 in mutated cells. These included *LFNG,* encoding the NOTCH signaling modulator lunatic fringe, which was also found differentially regulated in *ALK1*-mutated ECFCs and HUVECs and might thus be important in the pathogenesis of HHT and PAH.

Results

Isolation and characterization of ECFCs carrying ALK1 mutations

Control (CTL-H) and *ALK1*-mutated ECFCs (MUT-H) from newborns who have inherited heterozygous *ALK1* mutations from an HHT parent were clonally isolated from cord blood following the recommendations of the Vascular Biology Standardization Subcommittee[24]. Isolated ECFCs (3 CTL-H and 2 MUT-H, Table 1) displayed the classical endothelial cobblestone-like morphology (Suppl Figure 1A) and were VE-cadherin (CD144) positive (Suppl Figure 1B and C). These cells were also positive for the endothelial cell markers CD31 and CD146 and negative for the hematopoietic cell-specific surface antigen CD45 (Suppl Figure 1, D-F), confirming their endothelial identity. The functional activity of the two ALK1 mutants (MUT-H1; non sense mutation p.Trp141X and MUT-H2; missense mutation p.His280Asp, Table 1) was tested using the BMP response element (BRE) luciferase reporter assay (Figure 1A), as previously described by our group[12]. Our data indicate that these two *ALK1* pathogenic variants are not able to respond to a BMP9 stimulation (100 pg/mL, Figure 1A) supporting that they are both LOF mutations.

RNA-seq analysis in CTL ECFCs in response to BMP9 or BMP10 stimulation

In order to decipher the impact of *ALK1*-mutations on gene regulation in response to BMP9 and BMP10, RNA-sequencing was performed on ECFCs from 3 CTLs (CTL-H1, -H2 and -H3) and 2 *ALK1* mutated ECFCs (MUT-H1 and H2, Table 1) that were either nonstimulated (NS) or stimulated for 18h with BMP9 or BMP10 (10 ng/mL). The experiment was repeated three

times, after which RNA extraction for all samples was performed, followed by quality control, library preparation and RNA sequencing. Principal component analysis (PCA) showed that we could discriminate stimulated (BMP9 or BMP10, blue and red shapes, respectively) from NS conditions (grey shape) in all ECFCs and that we could not discriminate CTL ECFCs from *ALK1*-mutated ECFCs (Figure 1B).

We first analyzed the BMP9 and BMP10 response versus (*vs)* NS condition in CTL ECFCs. Differential gene expression analysis using an absolute log_2 fold change threshold of 1 (lLFC(BMP response/NS condition)l≥1) and a p-adjusted value ≤0.05 (Benjamini-Hochberg procedure) (Supplementary information SI1) identified respectively 828 and 787 differentially expressed genes (DEGs) coding for proteins upon BMP9 or BMP10 stimulation (Table 2). These DEGs were nearly equally distributed between up and down-regulated genes (Table 2). Interestingly, BMP9 and BMP10 induced a highly similar transcriptomic response evidenced by the high Pearson correlation coefficient = 0.993 when plotting the LFCs of the DEGs obtained in response to BMP9 *vs* those obtained in response to BMP10 (Figure 1C) and the high number of shared DEGs regulated by both ligands 81.4% (Suppl Figure 2A). This similarity was also reflected in the volcano plots of BMP9- and BMP10-stimulated *vs* NS ECFCs, which highlighted the same top dysregulated genes, in terms of LFC or p-adjusted value (Figure 1D and E). Among these top DEGs, we detected many genes known to be regulated by BMP9 and BMP10 in other ECs (*SMAD6, SMAD7, SMAD9, ID1, ID2, ENG, HEY2*, *BMPER*, *TMEM100*, *APLN*) (Figure 1D and E). We also identified new DEGs with very similar regulation patterns between BMP9 and BMP10, including *STAT4*, *SLC40A1*, *SLC9A9*, *CLEC1B*, *CLEC3B*, *BMP4*, *KAT7*, *MPP4*, *HDDC2*, *CREB3L1*, *DRC1*, *GCHFR,* and *LEFTY2* (Figure 1D and E). In accordance with the high similarity between BMP9 and BMP10 response, no DEGs could be identified when directly comparing BMP9 to BMP10-stimulated CTL ECFCs (Table 2). Additionally, gene set enrichment analysis (GSEA) using hallmark gene sets from MsigDB was performed independently on total genes (whether DEGs or not) regulated by BMP9 or BMP10 in CTL ECFCs (Supplementary information SI2). The top 20 enriched genesets identified were very similar between BMP9 and BMP10 (Figure 1F). As expected, TGFß signaling was positively enriched by BMP9 and BMP10 stimulation but we could also identify epithelial mesenchymal transition, protein secretion and several signaling pathways (IL6-JAK-STAT3, KRAS and MTORC1) as positively enriched terms (Figure 1F). On the other hand, many hallmarks related to cell cycle were negatively enriched (MYC-targets, mitotic spindle, G2M checkpoint and E2F targets, Figure 1F), supporting the reported role of BMP9 and BMP10 in maintaining vascular quiescence[8, 25]. Together, these results demonstrate that under these stimulatory conditions, BMP9 and BMP10 induce a very similar transcriptomic response in CTL ECFCs.

ALK1 heterozygosity in ECFCs does not impair the global transcriptomic response to BMP9 or BMP10

To uncover the effect of heterozygous *ALK1* mutations on gene regulation, we analyzed the basal transcriptome of MUT versus CTL ECFCs, before any stimulation, and in response to BMP9 or BMP10. In accordance with the PCA which could not differentiate CTL from MUT

ECFCs (Figure 1B), only 28 DEGs were identified between NS CTL and MUT ECFCs (Table 2). Similarly, following a BMP9 or BMP10 stimulation, only 19 and 30 DEGs were significantly differentially expressed between the two ECFC groups (Table 2).

Upon analyzing the transcriptomic response of MUT ECFCs to BMP9 or BMP10, 604 and 564 DEGs were identified, respectively (Table 2). As in CTL ECFCs, BMP9 and BMP10 induced a similar response in *ALK1*-mutated cells, with 77.2% DEGs commonly regulated by both ligands (Suppl Figure 2B) and a highly similar global regulation pattern (Pearson correlation coefficient = 0.989, Sup Figure 2C).

We next compared the log fold changes of each list of target genes in stimulated CTL *vs* stimulated *ALK1*-mutated ECFCs and found that most regulated genes demonstrated the same regulation patterns in the two cell groups upon BMP9 or BMP10 stimulation (Pearson correlation coefficient= 0.958 and 0.962 respectively, Figure 2A and B). Consistently, we could identify in *ALK1*-mutated ECFCs the same top protein-coding genes regulated by BMP9 or BMP10 as in CTL ECFCs (*SMAD6, SMAD7, SMAD9, ID1, ID2, ENG, HEY2, BMPER, TMEM100, STAT4, APLN, SLC40A1, SLC9A9, CLEC1B, CLEC3B, BMP4, KAT7, MPP4, HDDC2, CREB3L1, DRC1, GCHFR, LEFTY2;* Figure 2C and D). Altogether, these data unexpectedly show that CTL and *ALK1*-mutated ECFCs display highly similar transcriptomic profiles following BMP9 or BMP10 stimulation.

ALK1 heterozygosity in ECFCs does not impair p-Smad1/5 response to BMP9

To understand this surprising result, we next investigated the status of Smad1/5 phosphorylation induced by BMP9 on a higher number of LOF *ALK1*-mutated ECFCs (n=6, Table 1, Fig1A and Suppl Figure 3). We focused on BMP9 regulation as BMP9 and BMP10 showed a similar transcriptomic response (Figure 1C). MUT ECFCs stimulated with BMP9 (10 ng/mL) for one hour displayed similar levels of nuclear p-Smad1/5 immunofluorescence intensities to stimulated CTLs (Figure 3A and B). To validate this result, we performed a BRE luciferase reporter assay in CTL (n=2) and MUT (n=4) ECFCs (Table 1) stimulated with increasing doses of BMP9 (0.2-10 ng/mL) for 18 hours. Both CTL and MUT ECFCs exhibited a clear dose-dependent response to BMP9 (Figure 3C); yet, no significant differences were observed between the 2 groups (Figure 3C), which displayed identical half maximal effective concentrations (EC_{50}: 517 pg/mL for CTL *vs* 514 pg/mL for MUT ECFCs; inset Figure 3C). We also quantified the mRNA levels of *ID1,* a target gene known to be strongly induced by BMP9, and found no difference between CTL (n=4) and MUT (n=4) ECFCs (Table 1, Figure 3D). To examine whether the similar Smad1/5 activation in MUT *vs* CTL ECFCs was due to a compensation in ALK1 protein levels in *ALK1*-mutated ECFCs, we assessed the levels of membranous ALK1 by flow cytometry analysis in five different MUT ECFCs (Table 1, Suppl Figure 3) in comparison to 3 CTL ECFCs. We found that *ALK1*-mutated ECFCs carrying a missense mutation had a slightly lower level of membranous ALK1 level than CTL ECFCs, and those carrying an *ALK1* nonsense mutation displayed a 50% reduction in the level of cell surface ALK1 (Figure 3E and F). Thus the similar Smad signalling response in CTL and *ALK1*-mutated ECFCs cannot be attributed to a compensatory level of ALK1. Altogether, these

results support that *ALK1*-mutated ECFCs maintain intact activation of the canonical Smad1/5 signaling pathway in response to BMP9.

PAH patient-derived lung endothelial cells carrying ALK1 mutations display different transcriptomic profiles compared to CTLs at the basal state

Having not detected any differences in the transcriptomic nor in the early Smad1/5 response to BMP9 or BMP10 in newborn-derived *ALK1*-mutated ECFCs, we investigated the transcriptomic response in HMVECs carrying *ALK1*-mutations derived from transplanted sick lungs of PAH patients (MUT-P1 and -P2, Table 3). The two *ALK1* mutations were missense mutations mapping to the kinase domain of ALK1 and were both confirmed as LOF mutations using the BRE luciferase assay (Figure 4A).

To delineate the transcriptomic signature of these cells, RNA-sequencing was performed, using the same experimental conditions described for ECFCs, i.e. using 3 CTLs and 2 *ALK1*-mutated HMVECs from PAH patients (MUT-P1 and -P2, Table 3) that were either stimulated overnight with BMP9 or BMP10 (10 ng/mL) or were left unstimulated (NS). Hierarchical clustering discriminated four clusters: (1) NS and stimulated MUT-P2 samples, (2) NS and stimulated MUT-P1 samples, (3) NS CTLs and (4) BMP9 and BMP10-stimulated CTL samples (from left to right, Suppl Figure 4). This clustering showed that, unlike MUT-H ECFCs, the transcriptomes of MUT-P HMVECs were clearly different from those of CTLs. Interestingly, MUT-P HMVECs from each patient separated into two different clusters (Suppl Figure 4), highlighting variability between the two patients, which might be related to different disease stage or different treatments. The differential expression analysis (lLFCl≥1 and p-adjusted value ≤0.05, Benjamini-Hochberg correction) (Supplementary information SI3) comparing NS *ALK1*-mutated and CTL HMVECs identified 1261 protein coding DEGs (Table 2), with both down-regulated (58%) and up-regulated (42%) genes. GSEA using hallmark gene sets in NS CTL *vs* *ALK1*-mutated HMVECs (Supplementary information SI4) revealed a positive enrichment of several gene sets involved in cell cycle (E2F targets, G2M checkpoint, MYC-targets and mitotic spindle) and a negative enrichment in genes related to various signaling pathways (KRAS signaling, WNT-beta-catenin signaling and TNFα signaling; Figure 4B). Together, these data show that *ALK1*-mutated HMVECs derived from diseased lungs have a severely altered basal transcriptome compared to CTL HMVECs.

BMP9 and BMP10 induce cell type-specific transcriptomic reponses

We then analyzed the BMP9 and BMP10 transcriptomic response in CTL HMVECs. Differential expression analysis identified 704 and 481 DEGs in BMP9- and BMP10-stimulated CTL HMVECs, respectively (Table 2). Although the number of DEGs was lower in BMP10 stimulated cells, the gene regulation patterns in BMP9- *vs* BMP10-stimulated CTL HMVECs were highly correlated (Pearson correlation coefficient =0.844), further supporting, as for ECFCs (Fig 1C), that BMP9 and BMP10 induce a very similar transcriptomic response *in vitro*. This similarity was also reflected in the volcano plots of BMP9- and BMP10-stimulated *vs* NS cells, which highlighted similar top deregulated genes, in terms of LFC or p-adjusted value (Figure 4C and

D). Interestingly, by comparing BMP9/10-regulated genes in CTL HMVECs to those in CTL ECFCs, with the limitation that these data come from two independent RNA-sequencing, only a quarter of the DEGS was shared between ECFCs and HMVECs (27% for BMP9 and 26% for BMP10; Suppl Figure 5A and B). *ID1*, *SMAD6*, *SMAD7*, *ENG*, *KAT7, CLEC1B*, *CLEC3B*, and *APLN* were identified as top targets in both ECFCs (Figure 1 D and E) and HMVECs (highlighted in blue in Figure 4C and 4D). On the other hand, some top target genes were specific to HMVECs (LOX and NOG) (highlighted by an asterix in Figure 4C and D).

ALK1-mutated HMVECs display slightly different transcriptomic responses to BMP9 and BMP10 compared to CTL HMVECs

We next analyzed the BMP9 or BMP10 response in *ALK1*-mutated *vs* CTL HMVECs. BMP9 and BMP10 stimulation resulted in the regulation of 295 and 206 DEGs, respectively (Table 2). This corresponds to around 60% less DEGs compared to stimulated CTLs. This decrease in the number of DEGs suggests that *ALK1*-mutated HMVECs might possess a reduced capacity to respond to BMP9 or BMP10. When comparing the log fold changes of each list of dysregulated genes in stimulated CTL *vs* patient HMVECs, we obtained fairly high Pearson correlation coefficients (0.728 for BMP9 and 0.855 for BMP10; Figure 4E and F). However, these correlations were lower than the ones obtained in ECFCs (Figure 2A and B), suggesting that the BMP9 and BMP10 responses in *ALK1*-mutated HMVECs might be more affected than in *ALK1*-mutated ECFCs.

Since we are simultaneously analyzing two variables (genotype and stimulation) and because there was a clear difference between CTL and MUT HMVECs at the basal level (Table 2), we performed a two-factor analysis as previously described[26] (See Materials and Methods section) considering the two factors: genotype and BMP9 or BMP10 treatment (Benjamini–Hochberg adjusted for multiple comparisons padj<0.05) (Supplementary information SI5). We found 44 protein-coding interaction term genes differentially regulated by BMP9 in CTL versus *ALK1*-mutated HMVECs and 15 in response to BMP10, which were all shared with BMP9 stimulation (marked by an asterix, Suppl Figure 6). We selected 25 genes out of these 44 (highlighted in blue in Suppl Figure 6) for validation by RT-qPCR on independent BMP9 stimulations. Selection criteria were (1) to show clear visible differences in regulation between CTLs and MUTs in response to BMP9 and BMP10 and (2) have minimal interindividual heterogeneity between members of each group (CTL or MUT group; data not shown). The regulation of 24 out of the 25 selected genes (the exception being *CEBPD)*, were confirmed by RT-qPCR (data not shown), validating the robustness of the two-factor analysis.

LFNG (lunatic fringe) shows impaired regulation by BMP9 in ALK1-mutated HMVECs, ECFCs and HUVECs

Among the 24 genes validated, we focused on 6 of them (*LFNG*, *JAG2*, *TNFRSF1B*, *SLC6A6*, *SOX13* and *CEBPG)* for two main reasons. First, these genes showed the highest differences in regulation between CTL and MUT HMVECs. Second, they were also identified as DEGs in response to BMP9 and BMP10 in CTL ECFCs with the same sense of regulation, making them

good candidates to compare the effect of *ALK1* mutation on gene regulation by BMP9 across the different models of endothelial cells. We tested their regulation by RT-qPCR in CTL and *ALK1*-mutated HMVECs and ECFCs. Among these 6 genes, only *LFNG* mRNA expression was found to be significantly differentially regulated between CTL and *ALK1*-mutated cells in both HMVECs (n=2) and ECFCs (n=4) (Figure 5A, 5B and Suppl Fig 7A, 7B). As we were limited by the number of *ALK1*-mutated HMVECs available and in order to test whether mutations in the same pathway would respond similarly, we tested 3 *BMPR2*-mutated HMVECs derived from transplanted lungs of PAH patients (Table 3). As shown on figure 5A, *LFNG* mRNA upregulation by BMP9 was strongly reduced in HMVECs derived from PAH patients carrying either *ALK1* or *BMPR2* mutation compared to CTLs (FC =10.3 in CTLs *vs* 2.7 and 2.6 in *ALK1*- (n=2) and *BMPR2*- (n=3) mutated cells respectively, Figure 5A). RT-qPCR analysis performed in CTL ECFCs, showed that *LFNG* mRNA expression was also significantly upregulated by BMP9 (FC=5.1, Figure 5B), altough not as strongly as in CTL HMVECs (FC=10.3, Figure 5A), and that this increase was significantly reduced in *ALK1*-mutated ECFCs (FC=3.1, n=4, Figure 5B). The results obtained by RT-qPCR in HMVECs validate the two-factor analysis generated from the RNA-seq data in HMVECs, as illustrated in the count-plot representation (Figure 5C), which shows that *LFNG* mRNA expression was significantly induced in response to BMP9 or BMP10 in CTLs (mean fold change (FC)=14 and 10 in response to BMP9 and BMP10, respectively), but only weakly induced in *ALK1*-mutated cells. The RNA-seq analysis performed in CTL ECFCs also identified *LFNG* as DEG, but the two factor analysis did not identify any differentialy regulated genes between BMP-stimulated CTLs and *ALK1*-mutated ECFCs. The BMP9 regulations of *JAG2*, *TNFRSF1B*, *SLC6A6*, *SOX13* and *CEBPG* mRNA expression were all confirmed by RT-qPCR in CTL HMVECs and, consistent with the two-factor analysis, their induction was repressed in *ALK1*- and *BMPR2*-mutated HMVECs, except for SLC6A6 that followed the same reduction trend but that did not reach statistical significance (Suppl Fig 7A). The BMP9 regulation of these genes was confirmed in CTL ECFCs, however their regulation in *ALK1*-mutated cells showed either similar or slightly weaker regulation by BMP9 compared to CTLs (Suppl Fig 7B). Together, these results support the hypothesis that *LFNG* transcriptional regulation by BMP9 could be affected by ALK1 heterozygosity but did not allow to conclude on the other interaction term genes studied.

To further test this hypothesis, we studied the BMP9 response in human umbilical vein endothelial cells (HUVECs), another type of endothelial cells that can be isolated from newborns. RT-qPCR for *LFNG*, *JAG2*, *TNFRSF1B*, *SLC6A6*, *SOX13* and *CEBPG* were performed on 3 CTLs and 3 LOF *ALK1*-mutated HUVECs (CTL-H' and MUT-H') stimulated or not with BMP9 for 18hr. These genes were all induced in response to BMP9 in CTL HUVECs, although SOX13 stimulation did not reach significance (Figure 5D and Suppl Fig 7C). As for HMVECs and ECFCs (Figure 5A and B), we found a significant decrease in the level of induction of *LFNG* mRNA expression by BMP9 in *ALK1*-mutated HUVECs compared to CTLs (FC= 4.9 in CTL-H' and 2.6 in MUT-H'; Figure 5D). The BMP9 regulation of *JAG2*, *TNFRSF1B* and *SLC6A6* mRNA expressions were also found to be significantly reduced in *ALK1*-mutated *vs* CTL HUVECs (Suppl Figure 7C).

To further validate these results, we next set-up an experiment using an siRNA approach, where we could decrease ALK1 expression to the half, in order to mimic ALK1 heterozygosity. We found that reducing *ALK1* mRNA levels in CTL HMVECs by 50 or 90% (inset in Figure 5E), dose-dependently suppressed *LFNG* induction by BMP9 (Figure 5E).
Together, these data show that *ALK1* heterozygosity could impair the BMP9 regulation of *LFNG* mRNA expression and possibly other genes, depending on the endothelial cellular model.

Discussion
To our knowledge, this is the first study assessing the BMP9 and BMP10 transcriptomic responses in endothelial cells carrying heterozygous *ALK1* mutations. In this work, we performed RNA-seq analyses on two types of primary *ALK1*-mutated cells: (1) ECFCs derived from HHT newborns, whereby ECFCs are not yet exposed to a sick environment and (2) HMVECs derived from severely ill explanted lungs of end-stage PAH patients. This work uncovered several important findings, including the fact that ALK1 heterozygosity does not impair Smad1/5 activation nor strongly affect the transcriptomic response to BMP9 nor BMP10 stimulation. Consequently, our data challenge the current model of haploinsufficiency, that needs to be reconsidered since a LOF mutation in a single *ALK1* allele does not strongly affect the transcriptomic response.
The first interesting point from this work is the comparison between BMP9 and BMP10 transcriptomic responses in endothelial cells. BMP9 and BMP10 have been identified as two high affinity ligands for ALK1 with very similar affinities. BMP9, but not BMP10, can also bind the type 1 receptor ALK2, yet with a much lower affinity than ALK1[27]. In addition, different affinities for the type 2 receptors to BMP9 *vs* BMP10 have been described. Here, we show that BMP9 and BMP10, despite the reported differences in receptor binding affinities, induced highly similar transcriptomic responses in both ECFCs and HMVECs. This is in accordance with recent work that compared transcriptomic regulation by precursor forms of BMP9 and BMP10 in pulmonary arterial endothelial cells using lower BMP doses[28]. Nonetheless, these *in vitro* findings do not rule out specific *in vivo* roles that can arise from differences in spatiotemporal expression patterns, as recently described[29].
Another interesting point was the use of two different endothelial cell types (ECFCs and HMVECs) for studying BMP9 and BMP10 transcriptomic responses. With the limitation that these two RNA-seq analyses were performed independently, it is interesting to note that the transcriptomic profiles of ECFCs and HMVECs in response to BMP9 or BMP10 stimulation were not largely overlapping, with only 26-27% of genes commonly regulated in both cell types, still Pearson correlations between BMP9 or BMP10 stimulated ECFCs and HMVECs, were 0.71 and 0.75, respectively, supporting that it is more a question of thresholds than a differential pattern of gene regulation. These differences demonstrate that, despite being cultured *in vitro*, these cells retain organotypic specificities. This specificity could be due to predetermined BMP Smad binding sites in specific endothelial subtypes as already described[30]. Among the cell type-specific targets, we identified *LOX* as a strongly

downregulated target in response to BMP9 or BMP10 in HMVECs but not in ECFCs. Interestingly, *LOX*, which codes for a lysyl oxidase that is implicated in crosslinking of extracellular matrix components, was found to be elevated in the proliferating pulmonary endothelium of PAH patients[31]. We also detected *NOG*, encoding the strong BMP antagonist noggin[32, 33] as a target upregulated in HMVECs by BMP9/10, but not in ECFCs.

This work also shows the similarity in the BMP9 or BMP10 response between CTL and *ALK1*-mutated ECFCs, both at the transcriptomic level and at the Smad1/5 activation level. This result is rather surprising, as it demonstrates, for the first time, that losing one functional *ALK1* allele does not considerably affect the downstream Smad signaling response. The intact activation of the pathway in mutated ECFCs was neither due to the high dose of BMP9 and BMP10 used, as similar results were obtained using low doses of BMP9 in the BRE luciferase assay on CTL and MUT ECFCs (Figure 3C), nor due to a compensation in ALK1 expression, as decreased levels of membranous ALK1 were detected in the heterozygote ECFCs (Figure 3F). Our findings thus support the hypothesis that 50% of functional membranous ALK1 is sufficient for driving normal canonical signal transduction. Our data would support the hypothesis that dimeric ALK1 signaling complexes composed of one functional ALK1 receptor and one non-funtional ALK1 receptor could be functionally active, but this point needs to be further demonstrated. This hypothesis is consistent with a previous study reporting the sole need of one functional type 1 receptor within the ACVR1/BMPR1 (in this case, an ACVR1 kinase active and a BMPR1 kinase inactive) to phosphorylate Smad1/5 in response to BMP2/7 heterodimers[34].

More importantly, the nearly identical transcriptomic responses to BMP9 or BMP10 between CTL and *ALK1*-mutated ECFCs suggest that haploinsufficiency might not be sufficient for the development of HHT. This result is in accordance with the recent identification of a bi-allelic loss of *ALK1* or *ENG* in at least 50% of tested cutaneous telangiectasia samples isolated from HHT patients[35], supporting the hypothesis that a second « knudsonian » somatic hit in the other allele is necessary to drive HHT pathogenesis. This notion is not novel to the vascular anomalies field, as it was already shown for venous, glomuvenous and cerebral cavernous malformations[36, 37]. These somatic mutations could explain why some lesions develop only focally in HHT patients, and how related patients, carrying the same mutation, can develop different manifestations of the disease. However, this hypothesis has not yet been validated neither in liver or lung AVMs nor in diffuse lesions.

In contrast to *ALK1*-mutated ECFCs isolated from a non-sick environment, *ALK1*-mutated HMVECs isolated from the lungs of endstage PAH patients revealed strong dysregulations in gene expression compared to controls, already in non-stimulated cells (1261 DEGs, Table 2). This might not be surprising, as these cells not only harbored heterozygous *ALK1* mutations, but have also been exposed to a pathogenic, likely inflammatory environment as is usually described for lungs of PAH patients[38] and as evidenced by the enrichment in proliferation and inflammation-related gene sets in the mutated cells by our GSEA (Figure 4B). Due to these large transcriptomic differences already at the basal level, it was difficult to pinpoint which genes are differently regulated by BMP9 and BMP10 in the presence of an *ALK1* mutation,

regardless of their initial differences at the basal level. Hence, using a two-factor analysis, which takes into account the two variables (genotype and BMP stimulation), we validated six of them by RT-qPCR in both *ALK1*- and *BMPR2*-mutated HMVECs (*LFNG*, *JAG2*, *TNFRSF1B*, *SLC6A6*, *SOX13* and *CEBPG*, Figure 5A and Suppl Figure 7A). Among them, one retained our attention, *LFNG,* as it was found to be significantly dysregulated in the three *ALK1*-mutated endothelial cell types (HMVECs, ECFCs and HUVECs), when assessed by RT-qPCR. However, its dysregulation in *ALK1*-mutated ECFCs or HUVECs was not as drastic as in *ALK1*- or *BMPR2*-mutated HMVECs. Intriguingly, the BMP9 regulation of *LFNG* was impaired in *ALK1*-mutated ECFCs, despite their normal Smad1/5 activation. One possible explanation for that, as proposed by Morikawa et al[30], is that different Smad1/5 binding sites have different affinities for Smad1/5 complex, with some high affinity sites, such as that of *ID1*, and other low affinity ones, such as those of *JAG1* and *HEY1*, thus requiring higher or more sustained levels of Smad1/5 activation or the involvement of other DNA binding protein partners for their regulation[30]. In that same study, *LFNG*'s promoter was shown by chromatin immunoprecipitation-sequencing to be bound by Smad1/5 in response to BMP9 stimulation in HUVECs[30]. *LFNG* could be one of these genes with low Smad1/5 binding affinity and/or needing other Smad binding partners, making it more sensitive to ALK1 heterozygosity. *ALK1*-mutated HUVECs, but not *ALK1*-mutated ECFCs, additionally displayed significant dysregulations in *JAG2, TNFRSF1B* and *SLC6A6* mRNA expression*,* suggesting that HUVECs might be more sensitive to *ALK1* LOF than ECFCs. This could be due to the fact that HUVECs are derived from a vessel environment in contrast to ECFCs, which are circulating cells.

Interestingly, *LFNG* and *JAG2* are two components of the Notch signaling pathway, which is a master regulator of tip/stalk cell differentiation and arterial specification[39]. Furthermore, multiple Notch-defective mouse models were reported to develop AVMs[40–43], which represent a major pathological feature of HHT. In addition, BMP and Notch pathways synergistically upregulate several shared transcription factors such as Hey1, Hey2 and Hes1[44, 45]. Here, we report a new intersection point between BMP and Notch axes, through BMP9/10-mediated regulation of *LFNG*. *LFNG* codes for lunatic fringe, a glycosyl transferase that post-translationally modifies Notch1, leading to inhibition of its activation by Jagged ligands while enhancing its activation by Delta-like ligands (Dll)[46–48]. It is noteworthy that reduced activation of Dll4-mediated Notch signaling results in excessive sprouting[49] during the activation phase of angiogenesis and promotes cell cycle reentry during the maturation phase[50]. Knowing that *Alk1*-depleted HHT mouse models display hypersprouting and increased vascular density in their developing retinas[51], it is plausible that suppressed upregulation of *LFNG* by BMP9 in the presence of *ALK1*-mutations might be contributing to this phenotype by mitigating Dll4 activation.

This work provides, to our knowledge, the first *in vitro* line of evidence that *ALK1* heterozygosity on its own does not drastically impair the response of endothelial cells to BMP9 nor BMP10, neither at an early step of signal transduction (phosphorylation of Smad1/5), nor downstream at the transcriptomic level, supporting that one functional receptor could be enough for canonical signaling. We also show that the two high affinity

ALK1 ligands, BMP9 and BMP10, induce highly similar transcriptomic changes *in vitro*, pointing to an overlapping function in this context. Interestingly, through deeper investigations, we could identify at least one gene, i.e. *LFNG*, whose regulation by BMP9 was weakly impaired in newborn heterozygous *ALK1*-mutated endothelial cells, but more intensely suppressed in *ALK1* or *BMPR2*-mutated HMVECs from PAH patients. Altogether, our findings suggest that heterozygous *ALK1* mutations could be priming events awaiting further triggers for driving lesion development. This requires further validation by studying the effects of angiogenic or inflammatory triggers or shear stress[52] on BMP9/10-ALK1 signaling in heterozygous *ALK1*-mutated endothelial cells, all of which were beyond the scope of this work. In parallel, future studies investigating the role of *LFNG,* and more largely the Notch signaling pathway, are needed to establish their implication in driving early HHT pathogenesis.

References

1. Shovlin CL (2010) Hereditary haemorrhagic telangiectasia: Pathophysiology, diagnosis and treatment. Blood Rev 24:203–219. https://doi.org/10.1016/j.blre.2010.07.001

2. Gallione CJ, Repetto GM, Legius E, et al (2004) A combined syndrome of juvenile polyposis and hereditary haemorrhagic telangiectasia associated with mutations in MADH4 (SMAD4). The Lancet 363:852–859. https://doi.org/10.1016/S0140-6736(04)15732-2

3. Lesca G, Burnichon N, Raux G, et al (2006) Distribution ofENG andACVRL1 (ALK1) mutations in French HHT patients. Hum Mutat 27:598–598. https://doi.org/10.1002/humu.9421

4. Wooderchak-Donahue WL, McDonald J, O'Fallon B, et al (2013) BMP9 mutations cause a vascular-anomaly syndrome with phenotypic overlap with hereditary hemorrhagic telangiectasia. Am J Hum Genet 93:530–537. https://doi.org/10.1016/j.ajhg.2013.07.004

5. David L, Mallet C, Mazerbourg S, et al (2007) Identification of BMP9 and BMP10 as functional activators of the orphan activin receptor-like kinase 1 (ALK1) in endothelial cells. Blood 109:1953–1961. https://doi.org/10.1182/blood-2006-07-034124

6. Shi Y, Massagué J (2003) Mechanisms of TGF-β Signaling from Cell Membrane to the Nucleus. Cell 113:685–700. https://doi.org/10.1016/S0092-8674(03)00432-X

7. David L, Feige J-J, Bailly S (2009) Emerging role of bone morphogenetic proteins in angiogenesis. Cytokine Growth Factor Rev 20:203–212. https://doi.org/10.1016/j.cytogfr.2009.05.001

8. David L, Mallet C, Keramidas M, et al (2008) Bone Morphogenetic Protein-9 Is a Circulating Vascular Quiescence Factor. Circ Res 102:914–922. https://doi.org/10.1161/CIRCRESAHA.107.165530

9. Robert F, Desroches-Castan A, Bailly S, et al (2020) Future treatments for hereditary hemorrhagic telangiectasia. Orphanet J Rare Dis 15:4. https://doi.org/10.1186/s13023-019-1281-4

10. Dupuis-Girod S, Shovlin CL, Kjeldsen AD, et al (2022) European Reference Network for Rare Vascular Diseases (VASCERN): When and how to use intravenous bevacizumab in Hereditary Haemorrhagic Telangiectasia (HHT)? Eur J Med Genet 65:104575. https://doi.org/10.1016/j.ejmg.2022.104575

11. Mallet C, Lamribet K, Giraud S, et al (2015) Functional analysis of endoglin mutations from hereditary hemorrhagic telangiectasia type 1 patients reveals different mechanisms for endoglin loss of function. Hum Mol Genet 24:1142–1154. https://doi.org/10.1093/hmg/ddu531

12. Ricard N, Bidart M, Mallet C, et al (2010) Functional analysis of the BMP9 response of ALK1 mutants from HHT2 patients: a diagnostic tool for novel ACVRL1 mutations. Blood 116:1604–1612. https://doi.org/10.1182/blood-2010-03-276881

13. Pece-Barbara N, Cymerman U, Vera S, et al (1999) Expression Analysis of Four Endoglin Missense Mutations Suggests That Haploinsufficiency Is the Predominant Mechanism for Hereditary Hemorrhagic Telangiectasia Type 1. Hum Mol Genet 8:2171–2181. https://doi.org/10.1093/hmg/8.12.2171

14. Shovlin CL, Guttmacher AE, Buscarini E, et al (2000) Diagnostic criteria for hereditary hemorrhagic telangiectasia (Rendu-Osler-Weber syndrome). Am J Med Genet 91:66–67. https://doi.org/10.1002/(sici)1096-8628(20000306)91:1<66::aid-ajmg12>3.0.co;2-p

15. Aldred MA, Morrell NW, Guignabert C (2022) New Mutations and Pathogenesis of Pulmonary Hypertension: Progress and Puzzles in Disease Pathogenesis. Circ Res 130:1365–1381. https://doi.org/10.1161/CIRCRESAHA.122.320084

16. Simonneau G, Montani D, Celermajer DS, et al (2019) Haemodynamic definitions and updated clinical classification of pulmonary hypertension. Eur Respir J 53:1801913. https://doi.org/10.1183/13993003.01913-2018

17. Humbert M, Kovacs G, Hoeper MM, et al (2022) 2022 ESC/ERS Guidelines for the diagnosis and treatment of pulmonary hypertension. Eur Heart J 43:3618–3731. https://doi.org/10.1093/eurheartj/ehac237

18. Walsh LJ, Collins C, Ibrahim H, et al (2022) Pulmonary arterial hypertension in hereditary hemorrhagic telangiectasia associated with ACVRL1 mutation: a case report. J Med Case Reports 16:99. https://doi.org/10.1186/s13256-022-03296-9

19. Yokokawa T, Sugimoto K, Kimishima Y, et al (2020) Pulmonary Hypertension and Hereditary Hemorrhagic Telangiectasia Related to an *ACVRL1* Mutation. Intern Med 59:221–227. https://doi.org/10.2169/internalmedicine.3625-19

20. Girerd B, Montani D, Coulet F, et al (2010) Clinical Outcomes of Pulmonary Arterial Hypertension in Patients Carrying an *ACVRL1* (*ALK1*) Mutation. Am J Respir Crit Care Med 181:851–861. https://doi.org/10.1164/rccm.200908-1284OC

21. Roman BL, Hinck AP (2017) ALK1 signaling in development and disease: new paradigms. Cell Mol Life Sci CMLS 74:4539–4560. https://doi.org/10.1007/s00018-017-2636-4

22. Paschalaki KE, Randi AM (2018) Recent Advances in Endothelial Colony Forming Cells Toward Their Use in Clinical Translation. Front Med 5:295. https://doi.org/10.3389/fmed.2018.00295

23. Dumortier J, Dupuis-Girod S, Valette P-J, et al (2019) Recurrence of Hereditary Hemorrhagic Telangiectasia After Liver Transplantation: Clinical Implications and Physiopathological Insights. 69:9

24. Smadja DM, Melero-Martin JM, Eikenboom J, et al (2019) Standardization of methods to quantify and culture endothelial colony-forming cells derived from peripheral blood: Position

paper from the International Society on Thrombosis and Haemostasis SSC. J Thromb Haemost 17:1190–1194. https://doi.org/10.1111/jth.14462

25. Ricard N, Ciais D, Levet S, et al (2012) BMP9 and BMP10 are critical for postnatal retinal vascular remodeling. Blood 119:6162–6171. https://doi.org/10.1182/blood-2012-01-407593

26. Panov J, Simchi L, Feuermann Y, Kaphzan H (2020) Bioinformatics Analyses of the Transcriptome Reveal Ube3a-Dependent Effects on Mitochondrial-Related Pathways. Int J Mol Sci 21:4156. https://doi.org/10.3390/ijms21114156

27. Scharpfenecker M, van Dinther M, Liu Z, et al (2007) BMP-9 signals via ALK1 and inhibits bFGF-induced endothelial cell proliferation and VEGF-stimulated angiogenesis. J Cell Sci 120:964–972. https://doi.org/10.1242/jcs.002949

28. Salmon RM, Guo J, Wood JH, et al (2020) Molecular basis of ALK1-mediated signalling by BMP9/BMP10 and their prodomain-bound forms. Nat Commun 11:1621. https://doi.org/10.1038/s41467-020-15425-3

29. Desroches-Castan A, Tillet E, Bouvard C, Bailly S (2022) BMP9 and BMP10 : Two close vascular quiescence partners that stand out. Dev Dyn 251:158–177. https://doi.org/10.1002/dvdy.395

30. Morikawa M, Koinuma D, Tsutsumi S, et al (2011) ChIP-seq reveals cell type-specific binding patterns of BMP-specific Smads and a novel binding motif. Nucleic Acids Res 39:8712–8727. https://doi.org/10.1093/nar/gkr572

31. Vadasz Z, Balbir Gurman A, Meroni P, et al (2019) Lysyl oxidase—a possible role in systemic sclerosis–associated pulmonary hypertension: a multicentre study. Rheumatology 58:1547–1555. https://doi.org/10.1093/rheumatology/kez035

32. Zimmerman LB, De Jesús-Escobar JM, Harland RM (1996) The Spemann Organizer Signal noggin Binds and Inactivates Bone Morphogenetic Protein 4. Cell 86:599–606. https://doi.org/10.1016/S0092-8674(00)80133-6

33. Gazzerro E, Gangji V, Canalis E (1998) Bone morphogenetic proteins induce the expression of noggin, which limits their activity in cultured rat osteoblasts. J Clin Invest 102:2106–2114. https://doi.org/10.1172/JCI3459

34. Tajer B, Dutko JA, Little SC, Mullins MC (2021) BMP heterodimers signal via distinct type I receptor class functions. Proc Natl Acad Sci 118:e2017952118. https://doi.org/10.1073/pnas.2017952118

35. Snellings DA, Gallione CJ, Clark DS, et al (2019) Somatic Mutations in Vascular Malformations of Hereditary Hemorrhagic Telangiectasia Result in Bi-allelic Loss of ENG or ACVRL1. Am J Hum Genet 105:894–906. https://doi.org/10.1016/j.ajhg.2019.09.010

36. Brouillard P, Vikkula M (2007) Genetic causes of vascular malformations. Hum Mol Genet 16:R140–R149. https://doi.org/10.1093/hmg/ddm211

37. Snellings DA, Girard R, Lightle R, et al (2022) Developmental venous anomalies are a genetic primer for cerebral cavernous malformations. Nat Cardiovasc Res 1:246–252. https://doi.org/10.1038/s44161-022-00035-7

38. Rabinovitch M, Guignabert C, Humbert M, Nicolls MR (2014) Inflammation and Immunity in the Pathogenesis of Pulmonary Arterial Hypertension. Circ Res 115:165–175. https://doi.org/10.1161/CIRCRESAHA.113.301141

39. Fernández-Chacón M, García-González I, Mühleder S, Benedito R (2021) Role of Notch in endothelial biology. Angiogenesis 24:237–250. https://doi.org/10.1007/s10456-021-09793-7

40. Carlson TR, Yan Y, Wu X, et al (2005) Endothelial expression of constitutively active *Notch4* elicits reversible arteriovenous malformations in adult mice. Proc Natl Acad Sci 102:9884–9889. https://doi.org/10.1073/pnas.0504391102

41. Krebs LT, Starling C, Chervonsky AV, Gridley T (2010) *Notch1* activation in mice causes arteriovenous malformations phenocopied by ephrinB2 and EphB4 mutants. genesis NA-NA. https://doi.org/10.1002/dvg.20599

42. Krebs LT, Shutter JR, Tanigaki K, et al (2004) Haploinsufficient lethality and formation of arteriovenous malformations in Notch pathway mutants. Genes Dev 18:2469–2473. https://doi.org/10.1101/gad.1239204

43. Murphy PA, Kim TN, Lu G, et al (2012) *Notch4* Normalization Reduces Blood Vessel Size in Arteriovenous Malformations. Sci Transl Med 4:. https://doi.org/10.1126/scitranslmed.3002670

44. Larrivée B, Prahst C, Gordon E, et al (2012) ALK1 Signaling Inhibits Angiogenesis by Cooperating with the Notch Pathway. Dev Cell 22:489–500. https://doi.org/10.1016/j.devcel.2012.02.005

45. Moya IM, Umans L, Maas E, et al (2012) Stalk Cell Phenotype Depends on Integration of Notch and Smad1/5 Signaling Cascades. Dev Cell 22:501–514. https://doi.org/10.1016/j.devcel.2012.01.007

46. Kakuda S, Haltiwanger RS (2017) Deciphering the Fringe-Mediated Notch Code: Identification of Activating and Inhibiting Sites Allowing Discrimination between Ligands. Dev Cell 40:193–201. https://doi.org/10.1016/j.devcel.2016.12.013

47. LeBon L, Lee TV, Sprinzak D, et al (2014) Fringe proteins modulate Notch-ligand cis and trans interactions to specify signaling states. eLife 3:e02950. https://doi.org/10.7554/eLife.02950

48. Brückner K, Perez L, Clausen H, Cohen S (2000) Glycosyltransferase activity of Fringe modulates Notch–Delta interactions. Nature 406:411–415. https://doi.org/10.1038/35019075

49. Benedito R, Roca C, Sörensen I, et al (2009) The Notch Ligands Dll4 and Jagged1 Have Opposing Effects on Angiogenesis. Cell 137:1124–1135. https://doi.org/10.1016/j.cell.2009.03.025

50. Ehling M, Adams S, Benedito R, Adams RH (2013) Notch controls retinal blood vessel maturation and quiescence. Development 140:3051–3061. https://doi.org/10.1242/dev.093351

51. Tual-Chalot S, Mahmoud M, Allinson KR, et al (2014) Endothelial Depletion of Acvrl1 in Mice Leads to Arteriovenous Malformations Associated with Reduced Endoglin Expression. PLoS ONE 9:e98646. https://doi.org/10.1371/journal.pone.0098646

52. Baeyens N (2018) Fluid shear stress sensing in vascular homeostasis and remodeling: Towards the development of innovative pharmacological approaches to treat vascular dysfunction. Biochem Pharmacol 158:185–191. https://doi.org/10.1016/j.bcp.2018.10.023

Materials and Methods

Trial design

The study was approved by the local research ethics committee (Hospice civils de Lyon, CPP 2021-A01792-39) and by the French Medical Products Agency (ANSM). Written informed consent was obtained from all patients in accordance with national regulations. The trial was conducted in accordance with the principles of the Declaration of Helsinki[1] and Good Clinical Practice guidelines. This trial was registered with the ClinicalTrials.gov Identifier #NCT05632484. (https://clinicaltrials.gov/ct2/show/NCT05632484?cond=HHT&map_cntry=FR&draw=3&rank=12).

Primary endothelial cell isolation

Human umbilical cord blood (UCB) samples (35–110 mL) were collected in heparin-coated syringes from 6 newborns carrying HHT-linked *ALK1* mutations and 3 healthy subjects (Table 1). Isolation of endothelial colony-forming cells (ECFCs) was performed as recommended by the Vascular Biology Standardization Subcommittee[2]. UCB samples were diluted at a 1:3 ratio in RPMI 1640 medium (Gibco) supplemented with 2% fetal bovine serum (FBS; Biosera). Then, mononuclear cell (MNC) fractions were isolated through density gradient centrifugation using 1.077 g/ml Pancoll solution (Pan Biotech) followed by successive washing steps. Finally, MNC were plated in 10µg/mL fibronectin-coated 24-well tissue culture plates in microvascular endothelial cell growth medium-2 (EGM-2 MV; Lonza) with 10% FBS at a density of 5×10^6 cells/cm^2. Cells were incubated in 5% CO_2 at 37°C and the medium was changed daily during the first 7 days and every other day thereafter. Following the first passage, the serum composition was reduced to 5%. ECFCs were used up to 45 days after cord blood processing.

In parallel, human umbilical vein endothelial cells (HUVECs) were isolated, as previously described[3], from the umbilical vein of a number of newborns from which ECFCs were isolated (Table 1).

Human microvascular endothelial cells (HMVECs) were isolated from the explanted lungs of PAH patients during lung transplantation as previously described[4, 5] (Table 3).

Cell culture

ECFCs, HMVECs and HUVECs were maintained in EGM-2 MV medium (Lonza). For RNA-sequencing and RT-qPCR, cells were washed twice with phosphate buffered saline (PBS) and were incubated for 18h in EBM-2 (Endothelial Basal Medium, Lonza) with or without 10ng/ml recombinant human BMP9 (3209-BP, R&D Systems) or recombinant human BMP10 (2926-BP; R&D Systems). Murine NIH-3T3 fibroblasts were maintained in high glucose, sodium pyruvate and GlutaMAX-supplemented Dulbecco's modified Eagle medium (DMEM; Gibco) with 10% FBS (Biosera) and 1% Pen/Strep (Gibco).

Immunofluorescence

For VE-cadherin staining, ECFCs were seeded at confluency in glass Lab-Tek Chamber Slides (Thermo Fisher Scientific), fixed the next day with 4% paraformaldehyde, permeabilized with 0.1% Triton X100 in PBS, saturated with 1% bovine serum albumin (BSA; Sigma-Aldrich) in PBS and incubated at 4°C for 1h with anti-VE-cadherin (1:100; #2158; Cell Signaling Technology). For detection, the cells were subsequently incubated with alexa fluor 488 donkey anti-rabbit IgG (AB_2340620, Jackson ImmunoResearch) for 30min at room temperature. Nuclei were counterstained with Hoechst 33342 (Sigma-Aldrich) and images were acquired using Axio Imager 2 (ZEISS) and analyzed on ZEN Microscopy Software.

Phospho-Smad1/5 (p-Smad1/5) immunostaining in ECFCs was performed as previously described[6]. 20,000 cells/well were seeded in 96-well black cell culture microplate (Greiner Bio-One 655090) for 24h.Then, cells were starved for 2hr in EBM-2 and stimulated for 1hr with 10ng/mL recombinant human BMP9 (R&D Systems). Cells were then fixed with 4% paraformaldehyde, permeabilized with 0.2% Triton X100 in PBS, saturated with 3% BSA in PBS and incubated overnight at 4°C with anti-p-Smad1/5 (1:800; #9516; Cell Signaling Technology). The cells were subsequently incubated with alexa fluor 488 donkey anti-rabbit IgG (AB_2340620, Jackson ImmunoResearch) and nuclei were counterstained with Hoechst 33342. Images were acquired using IN Cell Analyzer 2500HS widefield fluorescence microscope using a 20X objective. At least 16 different fields were imaged/well and 3 independent experiments were performed with 2 technical replicates each. To allow comparison between wells, the exposure time was kept constant across all wells. The acquired images were then analyzed using InCarta software (General Electrics Healthcare, USA).

Flow cytometry

Cells were seeded 25000 cells/cm^2 and allowed to grow for 48 hours. Cells were detached using trypsin/EDTA solution (CC-5012; Lonza) diluted at 0.000714%, resuspended in 2% BSA in PBS at 1x10^7 cells/mL and incubated with one of the following antibodies: fluorescein isothiocyanate (FITC)–conjugated mouse anti-human CD31 (clone WM59; 557508; BD Pharmingen), FITC-conjugated mouse anti-human CD45 (clone HI30; 560976; BD Pharmingen), phycoerythrin (PE)-conjugated mouse anti-human CD144 (clone 55-7H1; 560410; BD Pharmingen), PE mouse anti-human CD146 (clone P1H12; 550315; BD Pharmingen), unconjugated goat anti-human ALK1 antibody (AF370; R&D Systems) followed by alexa fluor 488 donkey anti-goat IgG (AB_2340430, Jackson ImmunoResearch) or an isotype control antibody. Ten to twenty thousand cells were analyzed on the BD FACSMelody sorter (BD Biosciences) using FCS Express Flow Cytometry Software.

Site-directed mutagenesis

Plasmids encoding the ALK1 mutations understudied were generated by polymerase chain reaction through site-directed mutagenesis of a pcDNA3-1(+) plasmid encoding WT N-terminal HA-tagged ALK1 using the QuikChange Lightning kit (Agilent) following the manufacturer's instructions. All mutated plasmids were verified by full sequencing (Eurofins). Primer sequences used for mutagenesis are listed in Suppl Table 1.

Luciferase reporter assay

NIH-3T3 cells in white 96-well culture plates (Greiner) were transfected in Opti-MEM (Invitrogen) using lipofectamine 2000 (Invitrogen) with 75ng pGL3(BRE)2-luc, 30ng pRL-TKluc and 5ng of plasmids encoding either HA-tagged WT or mutant ALK1 as previously described[7]. Five hours post transfection, cells were stimulated with or without recombinant human BMP9 (100 pg/mL) for 18 hours. For direct luciferase activity measurements in primary ECFCs, the cells were transfected in Opti-MEM using lipofectamine 3000 (Invitrogen) with 40ng pGL3(BRE)2-luc and 60ng pRL-TKluc. Three hours post transfection, ECFCs were stimulated with or without recombinant BMP9 in increasing concentrations (0.2 ng/mL–10 ng/mL) for 6 hours. Firefly and renilla luciferase activities were sequentially measured with twinlite Firefly and Renilla Luciferase Reporter Gene Assay System (Perkin Elmer) using the SPARK multimode microplate reader (Tecan) and final luciferase activities were reported as firefly luciferase activities normalized to renilla luciferase activities.

RNA sequencing and bioinformatic analysis

Cells from each donor were seeded in 3 culture vessels and were stimulated or not overnight with 10ng/ml of BMP9 or BMP10. Stimulations were repeated two or three times for each donor, generating technical replicates. After an overnight stimulation, the cells were trypsinized, spun and frozen as dry pellets at -80°C prior sending to Genewiz (https://www.genewiz.com) for RNA extraction, quality control, library preparation and RNA-sequencing. Mapped reads and sample metadata were imported into R software (version 4.0.3[8]), and loaded in DESeq2 R package (version 1.30.1[9]). Replicates were collapsed using the "collapseReplicates" function from the DESeq2 package. In order to reduce noise, genes that had less than 150 counts across all samples were filtered out. Differential gene expression analysis was performed using the DESeq2 package, and the Wald test was used to determine the significance of $\log_2$ fold change. Pairwise comparisons between conditions, as well as intercept terms for two-factor analysis, were retrieved using the "results" function from the DESeq2 package. Regularized log transformed data was used to perform Principle Component Analysis (PCA) and to plot expression heatmaps and countplots. Heatmaps were generated using the "ComplexHeatmap" (version 2.6.2[10], R package, and hierarchical clustering was based on Euclidian distance and Complete linkage. Gene set enrichment analysis (GSEA)[11] was performed using the "clusterProfiler" R package (version 3.18.1[12]). The ordering vector for GSEA was based on the stat value of the Wald test. Gene set on which GSEA was based was "Hallmark pathways", obtained from Broad Institutes MsigDB (version 7.5.1[13]). All p-values were adjusted for multiple testing using the Benjamini-Hochberg procedure, to obtain a false discovery rate (FDR). Only protein-coding DEGs are shown in volcano and scatter plots.

RNA extraction and RT-qPCR

Cells were lysed and RNA was extracted using the NucleoSpin RNA kit (Macherey-Nagel) according to the manufacturer's instructions. 1µg RNA was reverse-transcribed using iScript cDNA Synthesis Kit (Bio-Rad) in a T100 thermal cycler (Bio-rad), and quantitative PCR was performed on 1/10 diluted cDNA samples using SsoAdvanced Universal SYBR Green Supermix (Bio-Rad) in a CFX96 Real-Time System, (Bio-Rad). Data analysis was performed with CFX Manager Software V3.1 (Bio-Rad) and relative expression levels were calculated using the delta Ct (ΔCt) method with *HPRT* serving as the housekeeping gene. Alternatively, fold changes in expression levels were calculated using the Livak's ΔΔCt method. Primer sequences used for RT-qPCR are listed in Suppl Table2.

RNA interference

CTL HMVECs (250,000 cells/well in 6-well plates) were transfected using Lipofectamine RNAiMAX Transfection Reagent (2.5µL/well, Invitrogen) with either Silencer Negative Control #1 siRNA (AM4611, Ambion) at a final concentration of 1nM or Silencer Select pre-designed siRNA directed against human ALK1 (siALK1, 4392420, siRNA ID s987, Ambion) at a final concentration of 0.0035nM or 1nM, to induce different degrees of ALK1 silencing. Lipofectamine and siRNA mixes were incubated at room temperature for 20mins followed by cell transfection in Opti-MEM (11058021, Gibco). Five hours later, an equivalent volume to Opti-MEM of EGM-2MV medium with 10% FBS was added per well to obtain 5% final composition. Forty-eight hours post-transfection, cells were stimulated or not with BMP9 10ng/mL for 18hrs to study *LFNG* regulation by BMP9 as a function of ALK1 level.

Supplementary References

1. World Medical Association (2013) World Medical Association Declaration of Helsinki: ethical principles for medical research involving human subjects. JAMA 310:2191–2194. https://doi.org/10.1001/jama.2013.281053

2. Smadja DM, Melero-Martin JM, Eikenboom J, et al (2019) Standardization of methods to quantify and culture endothelial colony-forming cells derived from peripheral blood: Position paper from the International Society on Thrombosis and Haemostasis SSC. J Thromb Haemost 17:1190–1194. https://doi.org/10.1111/jth.14462

3. Garnier-Raveaud S, Usson Y, Cand F, et al (2001) Identification of membrane calcium channels essential for cytoplasmic and nuclear calcium elevations induced by vascular endothelial growth factor in human endothelial cells. Growth Factors Chur Switz 19:35–48. https://doi.org/10.3109/08977190109001074

4. Tu L, Dewachter L, Gore B, et al (2011) Autocrine Fibroblast Growth Factor-2 Signaling Contributes to Altered Endothelial Phenotype in Pulmonary Hypertension. Am J Respir Cell Mol Biol 45:311–322. https://doi.org/10.1165/rcmb.2010-0317OC

5. Bordenave J, Tu L, Berrebeh N, et al (2020) Lineage Tracing Reveals the Dynamic Contribution of Pericytes to the Blood Vessel Remodeling in Pulmonary Hypertension. Arterioscler Thromb Vasc Biol 40:766–782. https://doi.org/10.1161/ATVBAHA.119.313715

6. Sales A, Khodr V, Machillot P, et al (2022) Differential bioactivity of four BMP-family members as function of biomaterial stiffness. Biomaterials 281:121363. https://doi.org/10.1016/j.biomaterials.2022.121363

7. Ricard N, Bidart M, Mallet C, et al (2010) Functional analysis of the BMP9 response of ALK1 mutants from HHT2 patients: a diagnostic tool for novel ACVRL1 mutations. Blood 116:1604–1612. https://doi.org/10.1182/blood-2010-03-276881

8. R Core Team (2022) R: A Language and Environment for Statistical Computing. R Foundation for Statistical Computing, Vienna, Austria

9. Love MI, Huber W, Anders S (2014) Moderated estimation of fold change and dispersion for RNA-seq data with DESeq2. Genome Biol 15:550. https://doi.org/10.1186/s13059-014-0550-8

10. Gu Z (2022) Complex Heatmap Visualization. iMeta. https://doi.org/10.1002/imt2.43

11. Subramanian A, Tamayo P, Mootha VK, et al (2005) Gene set enrichment analysis: A knowledge-based approach for interpreting genome-wide expression profiles. Proc Natl Acad Sci 102:15545–15550. https://doi.org/10.1073/pnas.0506580102

12. Yu G, Wang L-G, Han Y, He Q-Y (2012) clusterProfiler: an R package for comparing biological themes among gene clusters. OMICS J Integr Biol 16:284–287. https://doi.org/10.1089/omi.2011.0118

13. Liberzon A, Subramanian A, Pinchback R, et al (2011) Molecular signatures database (MSigDB) 3.0. Bioinformatics 27:1739–1740. https://doi.org/10.1093/bioinformatics/btr260

Figure Legends

Fig 1 BMP9 and BMP10 induce a similar transcriptomic response in control ECFCs

a Relative BRE (BMP Response Element) luciferase activity measured in NIH-3T3 cells overexpressing either WT or mutant *ALK1* plasmids identified in *ALK1*-mutated ECFCs (p.Trp141X, MUT-H1) and (p.His280Asp, MUT-H2) used in the ECFC RNA-seq analysis. BRE firefly luciferase activities were normalized to renilla luciferase activity. Data shown are mean ± SEM from 3 independent experiments. **b-f** 3 CTL (CTL-H1, CTL-H2 and CTL-H3) and 2 *ALK1*-mutated ECFCs (MUT-H1 and MUT-H2) were stimulated or not with BMP9 or BMP10 (10 ng/mL) for 18 hours. The experiment was repeated three times after which bulk RNA-seq analysis was performed. **b** Principal component analysis (PCA) showing clustering of RNA-seq samples by treatment (BMP9 or BMP10 stimulation *vs* NS) in CTL and MUT ECFCs. Each dot represents the mean of 3 experiments for 1 sample. **c** Scatter plot comparing $\log_2$ fold change (LFC) values of protein coding DEGs regulated in CTL ECFCs by BMP9 *vs* those regulated by BMP10 both compared to NS. Pearson correlation is reported. **d-e** Volcano plot representations showing global changes in gene expression in CTL ECFCs after BMP9 **(d)** or BMP10 **(e)** stimulation. DEGs with high LFC and high statistical significance are annotated. **f** Gene-set enrichment analysis (GSEA) performed using hallmark gene sets. The bar plot represents the top significant gene set categories enriched in CTL ECFCs upon BMP10 or BMP9-stimulation ordered using normalized enrichment scores (NES).

Fig 2 ALK1 heterozygosity in ECFCs does not impair the global transcriptomic response to BMP9 or BMP10

a-d 3 CTL (CTL-H1, CTL-H2 and CTL-H3) and 2 *ALK1*-mutated ECFCs (MUT-H1 and MUT-H2) were stimulated or not with BMP9 or BMP10 (10 ng/mL) for 18 hours. The experiment was repeated three times after which bulk RNA-seq analysis was performed. **a-b** Scatter plots comparing $\log_2$ fold change (LFCs) values of protein coding DEGs regulated by BMP9 **(a)** or BMP10 **(b)** in CTL ECFCs *vs* MUT ECFCs. Pearson correlation is reported. **c-d** Volcano plots representations showing global changes in gene expression in *ALK1*-mutated ECFCs after BMP9 **(c)** or BMP10 **(d)** stimulation *vs* NS. DEGs with high LFC and high statistical significance are annotated.

Fig 3 ALK1 heterozygosity in ECFCs does not impair the p-Smad1/5 response to BMP9

a-b 3 CTL and 6 MUT ECFCs (MUT-H1-H6) were stimulated with BMP9 (10ng/mL) for 1hr then fixed and immunostained for phospho-Smad1/5 (p-Smad1/5). Cells were stimulated in duplicates and at least 16 different fields were imaged in each well. **a** Representative p-Smad1/5 immunostainings in 1 CTL and 1 MUT ECFC in the absence or presence of BMP9 for 1hr. The nuclei were counterstained using Hoechst 33342. **b** p-Smad1/5 fluorescence was quantified in the nuclei using IN Carta Image Analysis Software. Data presented are mean relative fluorescent intensity (RFU) ± SEM of 3 independent experiments. **c** 2 CTL and 4 MUT (MUT-H1-H4) ECFCs were transiently transfected with pGL3(BRE)2-luc and pRL-TK-luc. Cells were then either non-treated or stimulated with increasing concentrations of BMP9 (0.2, 0.5, 1, 10ng/mL) for 6 hours. Firefly luciferase activities were normalized to renilla luciferase activities. Data shown are mean ± SD from 1 representative experiment of 4, and each point corresponds to one donor. The inset represents the calculated BMP9 EC_{50} for CTL and MUT ECFCs. **d** RT-qPCR quantification of I*D1* mRNA expression normalized to HPRT level in 4 CTL and 4 MUT (MUT-H1-H4) ECFCs following an 18h stimulation with 10ng/ml BMP9**.** Data are mean ± SEM of 3 independent stimulations presented as ΔΔCt compared to CTL NS. **e** Flow cytometric analysis

comparing cell-surface ALK1 levels in 3 CTL *vs* 5 MUT ECFCs either carrying an *ACVRL1* missense mutations (MUT-H2, MUT-H4 and MUT-H6) or a nonsense mutations (MUT-H1 and MUT-H3). Isotypic control is illustrated in grey. One representative flow cytometry histogram of 3 is shown. **F,** Quantification of the ALK1 cell-surface expression by flow cytometry (in percentage of in MUT ECFCs with missense or nonsense mutations compared to CTL ECFCs). Data are means ± SEM of 3 independent experiments. Two-way Anova followed by Sidak's multiple comparisons tests were used for statistical analysis of panels B-D, except for the inset of figure C where Mann-Whitney test was used. Kruskal–Wallis test followed by Dunn's multiple comparison's test was used for F. For all panels, ns: non-significant, *P<0.05, **P<0.01, ***P<0.001 and ****P<0.0001.

Fig 4 ALK1-mutated HMVECs display substantially different transcriptomic profiles compared to controls

a Relative BRE (BMP Response Element) luciferase activity measured in NIH-3T3 cells overexpressing either WT or mutant *ALK1* plasmids identified in *ALK1*-mutated HMVECs (p.Gly319Arg, MUT-P1) and (p.Arg484Trp, MUT-P2) that are included in the HMVEC RNA-seq analysis. BRE luciferase activities were normalized to renilla luciferase activities. Data shown are mean ± SEM from of 3 independent experiments. **b-f** 3 CTL and 2 *ALK1*-mutated (MUT-P1 and MUT-P2) HMVECs were stimulated or not with BMP9 or BMP10 (10 ng/mL) for 18 hours. The experiment was repeated three times after which bulk RNA-seq analysis was performed. **b** GSEA performed using hallmark gene sets. The bar plot represents the top significant gene set categories enriched in non-stimulated MUT HMVECs compared to unstimulated CTL HMVECs. Each bar represents a hallmark gene set and bars are ordered from top to bottom by decreasing order of enrichment score (NES). **c-d** Volcano plot representations showing global changes in gene expression in CTL HMVECs after BMP9 **(c)** or BMP10 **(d)** stimulation. DEGs with high LFC and high statistical significance are annotated. DEGs annotated in blue correspond to DEGs identified in CTL ECFCs (Fig-1D-E). **e-f** Scatter plots comparing $\log_2$ fold change (LFCs) of DEGs regulated by BMP9 **(e)** or BMP10 **(f)** in CTL HMVECs *vs* MUT HMVECs. Pearson correlation is reported.

Fig 5 Regulation of LFNG mRNA expression by BMP9 in CTL and ALK1-mutated HMVECs, ECFCs and HUVECs

a-b RT-qPCR quantification of the mRNA expression level of *LFNG* in 3 CTL, 2 *ALK1*-mutated (MUT-P1 and -P2) and 3 *BMPR2*-mutated HMVECs (MUT-P3-P5) **(a)**, 3 CTL and 4 *ALK1*-mutated ECFCs (MUT-H1-H4) **(b)**. *LFNG* mRNA expression level is normalized to *HPRT* mRNA expression and presented as ΔΔCt compared to mean CTL NS. Data shown are mean ± SEM of at least 3 independent stimulations. **c** Count plot representation showing the regularized log transformed counts of *LFNG* mRNA in CTL-P and *ALK1*-MUT-P HMVECs in unstimulated (NS) and BMP9 or BMP10 stimulated cells. **d** RT-qPCR quantification of the mRNA expression level of *LFNG* in 3 CTL and 3 *ALK1*-mutated (MUT-H3-H5) HUVECs. *LFNG* mRNA expression level is normalized to *HPRT* mRNA expression and presented as ΔΔCt compared to mean CTL NS. Data shown are mean ± SEM of at least 3 independent stimulations. A, B, D, Two-way Anova followed by Sidak's multiple comparisons test were used for statistical analysis of panels. ns: non-significant, **P<0.01 and ****P<0.0001 *vs* NS and $^{\#\#}$P<0.01 and $^{\#\#\#\#}$P<0.0001 *vs* CTL. **e** 2 CTL HMVECs were treated either with scrambled siRNA (siScr) or 2 different concentrations of siRNA against *ACVRL1* (siALK1) to generate a gradient of ALK1 expression and then stimulated with 10ng/mL BMP9 for 18hr. *LFNG* mRNA expression normalized to *HPRT* mRNA level is presented as $2^{-\Delta Ct}$. Data shown are mean ± SD of 2 CTL HMVECs. Inset represents *ACVRL1* mRNA expression presented as ΔΔCt compared to scrambled siRNA-transfected cells.

Table 1 List of ALK1-mutated ECFCs and HUVECs isolated from HHT donors

List of *ALK1*-mutated ECFCs and HUVECs that were isolated from newborns indicating the carried mutation (DNA and protein), the type of mutation, the mutated ALK1 domain and the assays in which they were used. RNA-seq: RNA-sequencing, RT-qPCR: reverse transcription quantitative polymerase chain reaction, p-Smad1/5 IF: phospho-Smad1/5 immunofluorescence, BLA: (BRE) BMP Responsive Element Luciferase Assay, FC: flow cytometry.

Table 2 Number of protein-coding DEGs identified by differential expression analysis in CTL and ALK1-mutated ECFCs and HMVECs

3 CTL ECFCs and 2 *ALK1*-mutated ECFCs (MUT-H1-H2) or 3 CTL HMVECs and 2 *ALK1*-mutated HMVECs (MUT-P1-P2) were stimulated or not with BMP9 or BMP10 (10 ng/mL) for 18 hours. The experiment was repeated three times to generate technical replicates, after which bulk RNA-seq analysis was performed using DESeq2 package with an absolute $\log_2$ fold change threshold of 1 ($|\text{Log}_2\text{FC}| \geq 1$) and a p-adjusted value ≤0.05 (Benjamini-Hochberg procedure). Data show protein coding DEGS analyzed by NS: non-stimulated, B9: BMP9-stimulated, B10: BMP10-stimulated

Table 3 PAH patient characteristics

List of *ALK1*- and *BMPR2*-mutated HMVECs that were isolated from explanted lungs of PAH patients, indicating the carried mutation, the type of mutation and the mutated or deleted *ALK1* or *BMPR2* domain, in addition to some characteristics and treatments of the patient. PAPm: mean pulmonary arterial pressure, NYHA: New York Heart Association.

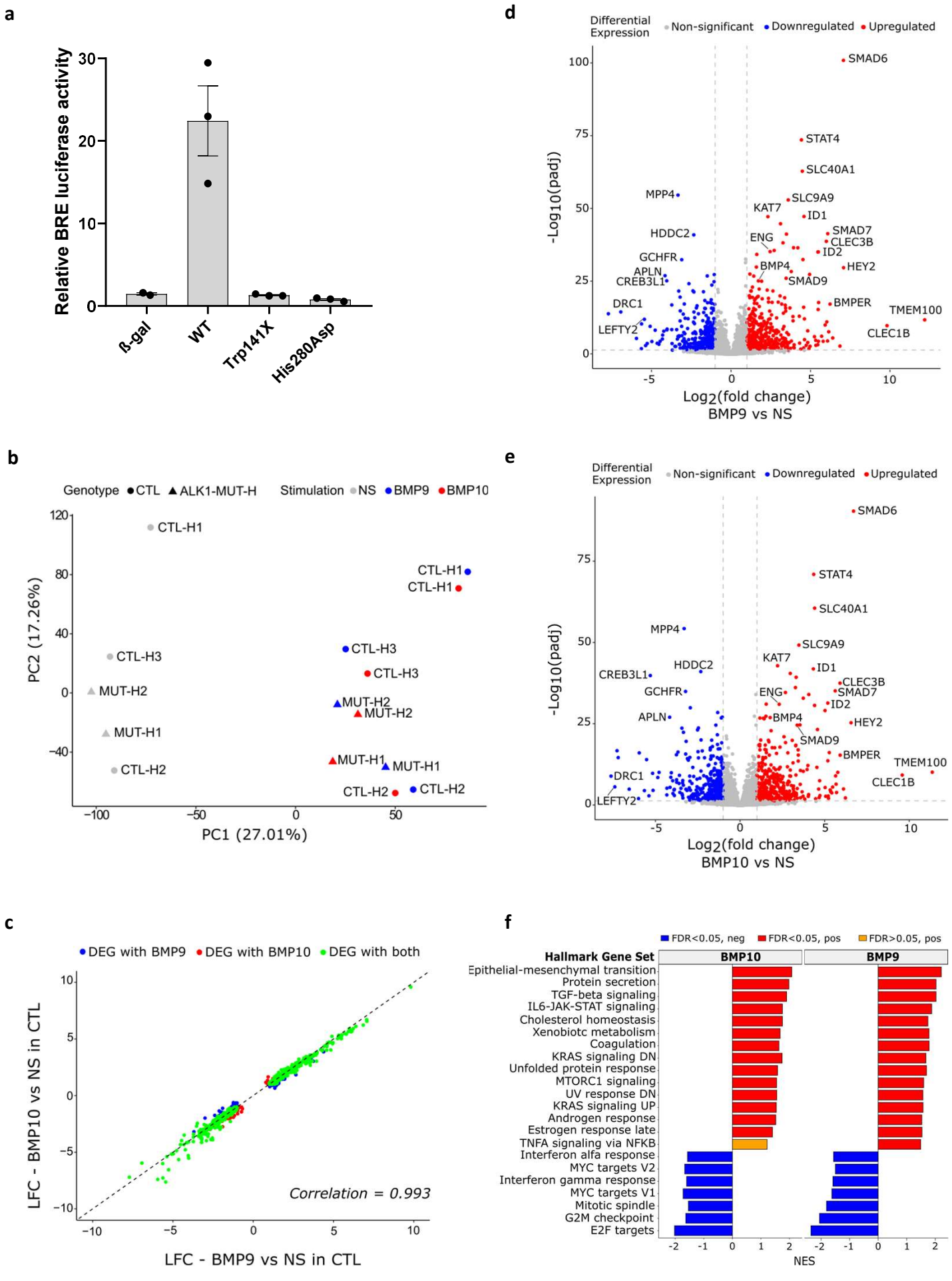

Fig 1 BMP9 and BMP10 induce a similar transcriptomic response in control ECFCs.

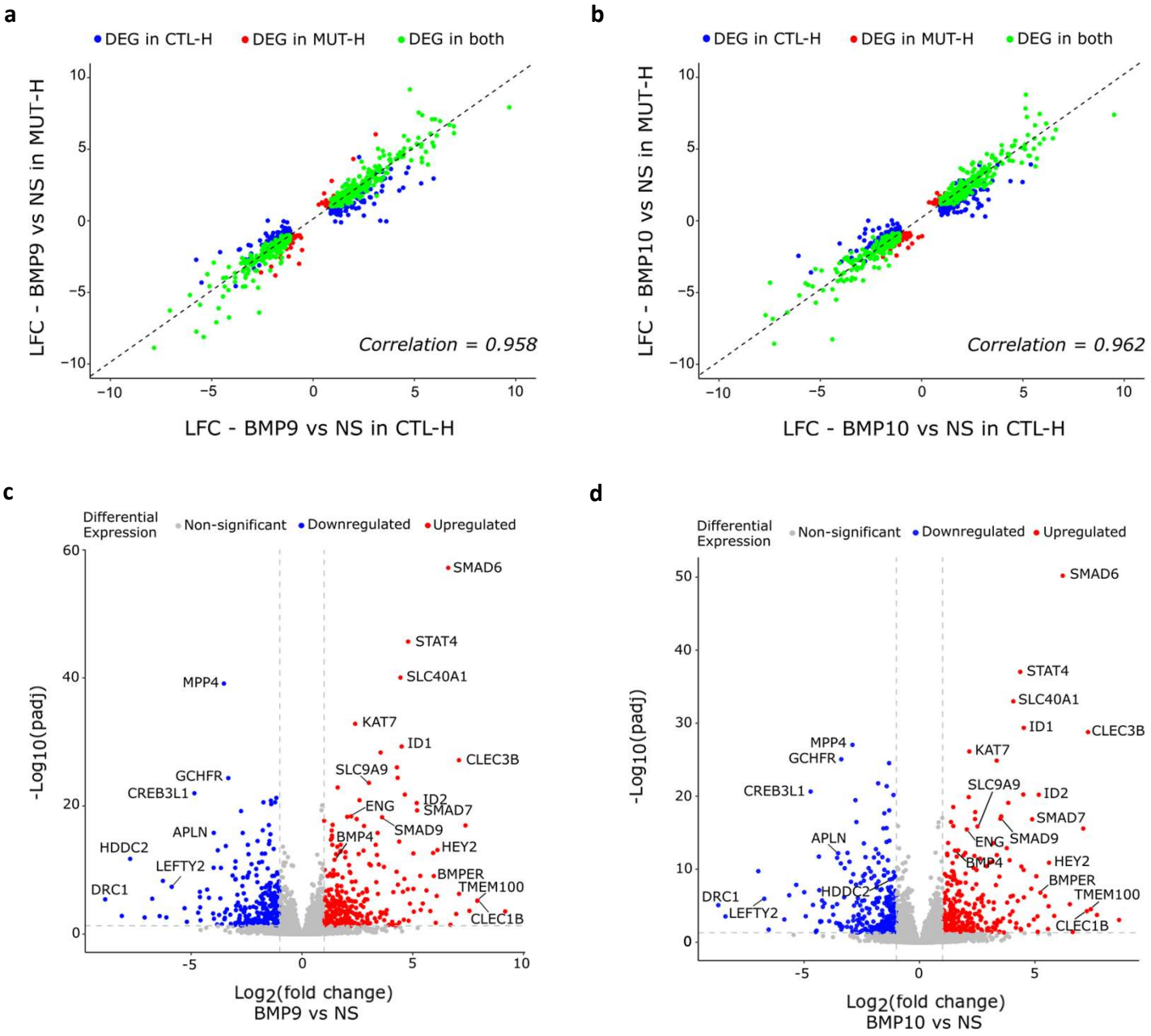

Fig 2 *ALK1* heterozygosity in ECFCs does not impair the global transcriptomic response to BMP9 or BMP10

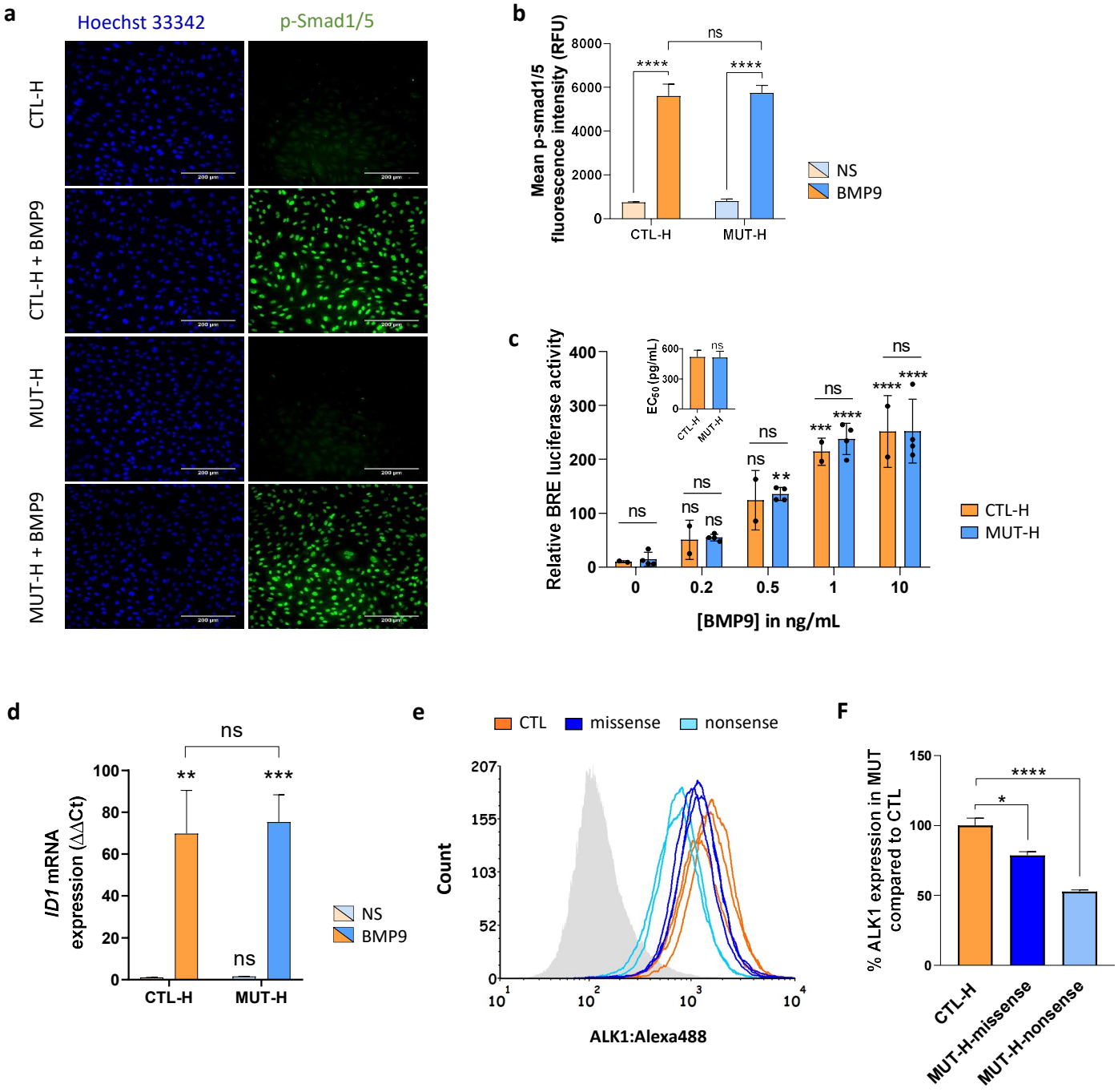

Fig 3 *ALK1* heterozygosity in ECFCs does not impair the p-Smad1/5 response to BMP9

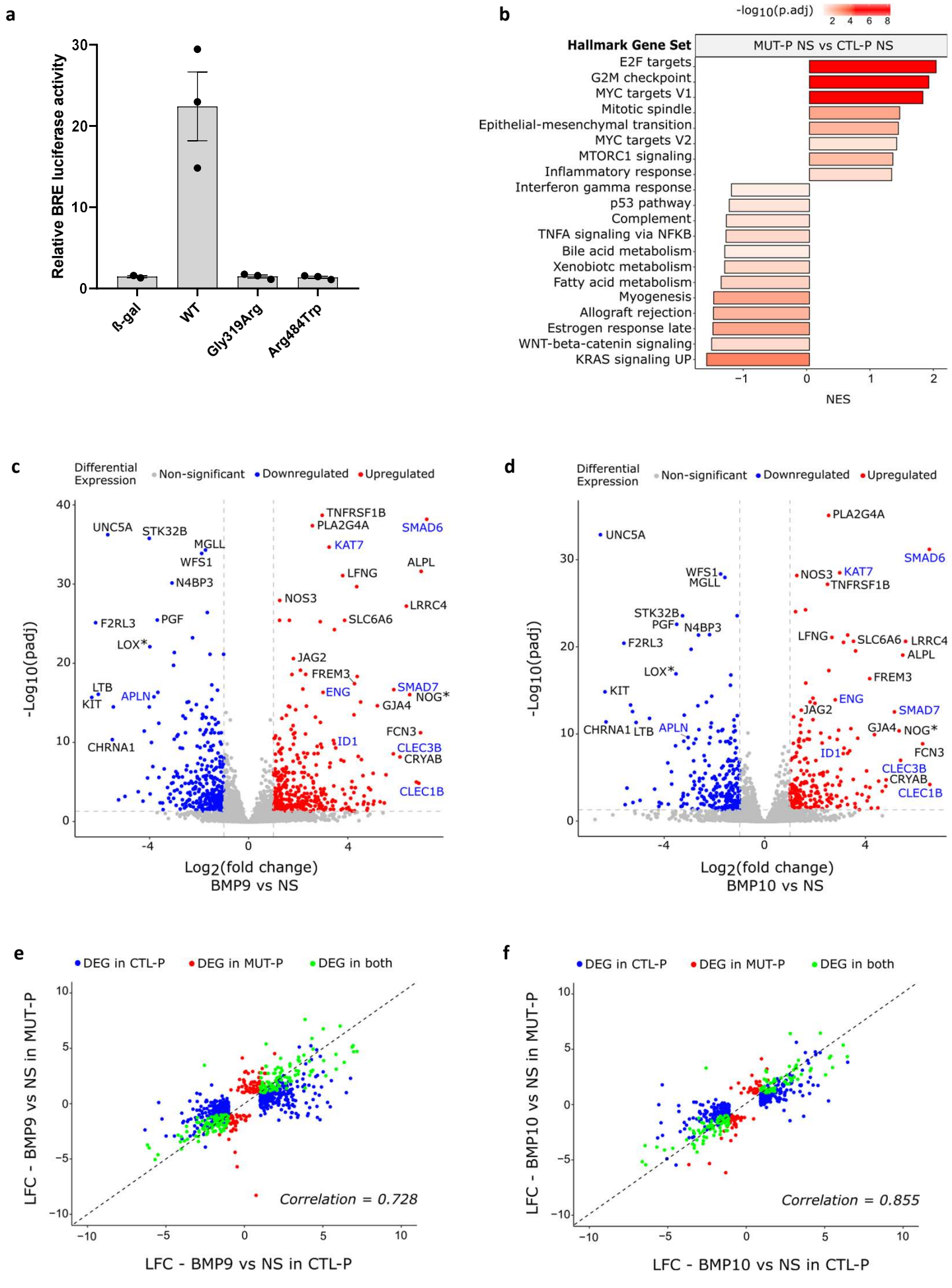

Fig 4 *ALK1*-mutated HMVECs display substantially different transcriptomic profiles compared to controls

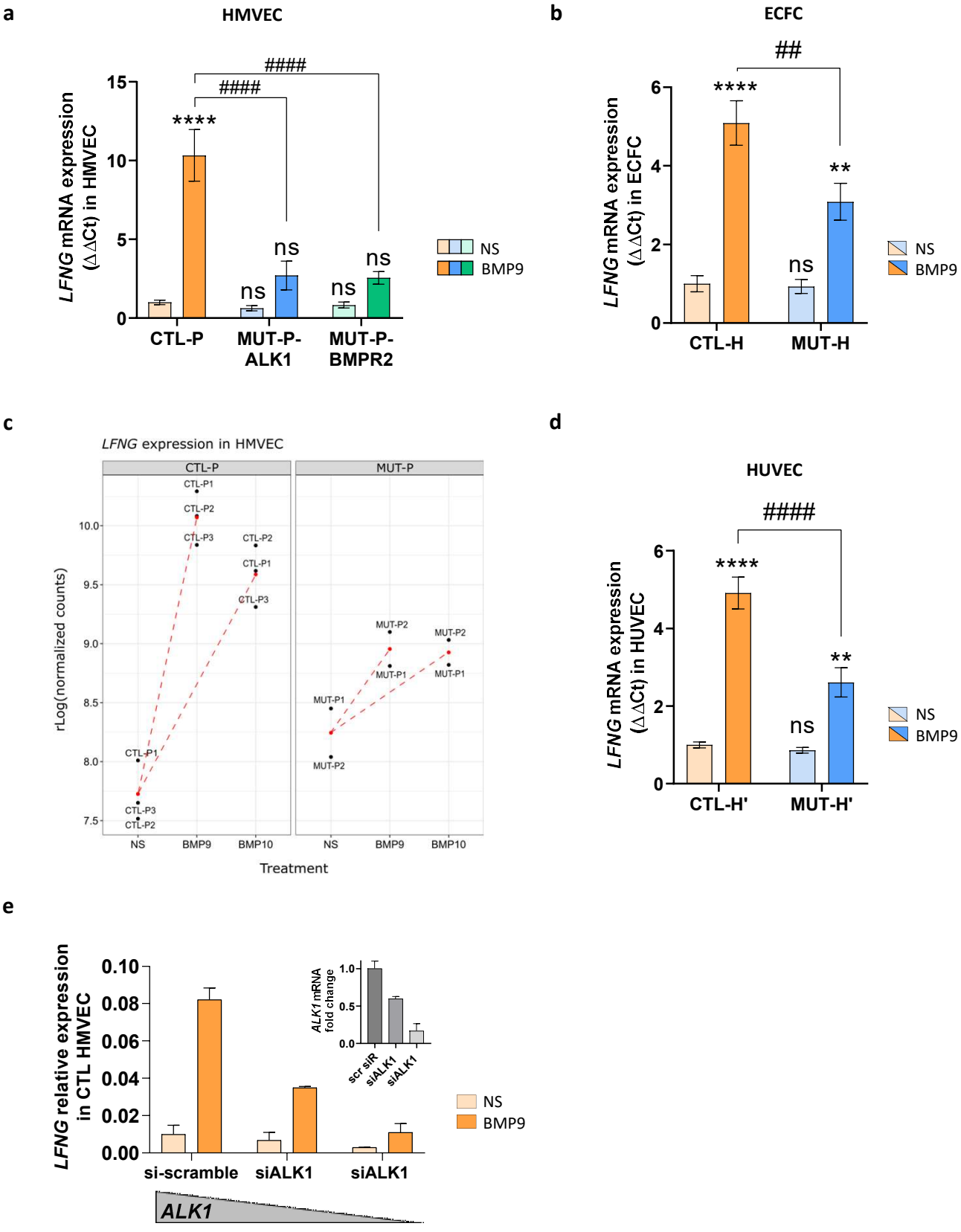

Fig 5 Regulation of *LFNG* mRNA expression by BMP9 in in CTL and *ALK1*-mutated HMVECs, ECFCs and HUVECs.

Table 1 List of *ALK1*-mutated ECFCs and HUVECs isolated from HHT donors

ID	ALK1 mutation		Type of mutation	Domain	Cells isolated	Assays
MUT-H1	c.423G>A	p.Trp141X	Nonsense	Transmembrane	ECFC	RNA-seq, RT-qPCR, p-Smad1/5 IF, BLA, FC
MUT-H2	c.838C>G	p.His280Asp	Missense	Kinase	ECFC	RNA-seq, RT-qPCR, p-Smad1/5 IF, BLA, FC
MUT-H3	c.190C>T	p.Gln64X	Nonsense	Extracellular	ECFC/HUVEC	RT-qPCR (ECFC and HUVEC), p-Smad1/5 IF, BLA, FC
MUT-H4	c.1231C>T	p.Arg411Trp	Missense	Kinase	ECFC/HUVEC	RT-qPCR (ECFC and HUVEC), p-Smad1/5 IF, BLA, FC
MUT-H5	c.1112dup	p.Thr372HisfsX20	Frameshift	Kinase	ECFC/HUVEC	RT-qPCR (ECFC and HUVEC), FC
MUT-H6	c.1413C>G	p.Cys471Trp	Missense	Kinase	ECFC/HUVEC	BLA, FC

Table 2 Number of protein-coding DEGs identified by differential expression analysis in CTL and *ALK1*-mutated ECFCs and HMVECs

	ECFCs			HMVECs		
Comparison	**Total DEGs**	**Upregulated**	**Downregulated**	**Total DEGs**	**Upregulated**	**Downregulated**
CTL NS vs B9	828	456	372	704	366	338
CTL NS vs B10	787	418	369	481	225	256
CTL B9 vs B10	0	0	0	2	0	2
MUT NS vs B9	604	310	294	295	158	137
MUT NS vs B10	564	278	286	206	90	116
MUT B9 vs B10	0	0	0	0	0	0
CTL NS vs MUT NS	28	11	17	1261	528	733
CTL B9 vs MUT B9	19	6	13	1262	502	760
CTL B10 vs MUT B10	30	7	23	1164	503	661

Table 3 PAH patient characteristics

ID	Affected gene	mutation		Type of mutation	Domain	Age	Gender	PAPm (mmHg)	NYHA Functional class	Therapies
MUT-P1	*ACVRL1*	c.955G>C	p.Gly319Arg	Missense	Kinase	14	Female	90	IV	bosentan, sildenafil, treprostinil
MUT-P2	*ACVRL1*	c.1450C>T	p.Arg484Trp	Missense	Kinase	19	Female	100	II	bosentan, sildenafil, epoprostenol
MUT-P3	*BMPR2*	del exon 11-13		Large deletion	kinase + cytoplasmic tail	37	Female	74	IV	bosentan, sildenafil, treprostinil
MUT-P4	*BMPR2*	c.314+3A>T		Splice site	Extracellular	14	Female		II	bosentan
MUT-P5	*BMPR2*	c.901T>C	p.Ser301Pro	Missense	kinase	26	Female	99	IV	none, transplanted immediately upon diagnosis

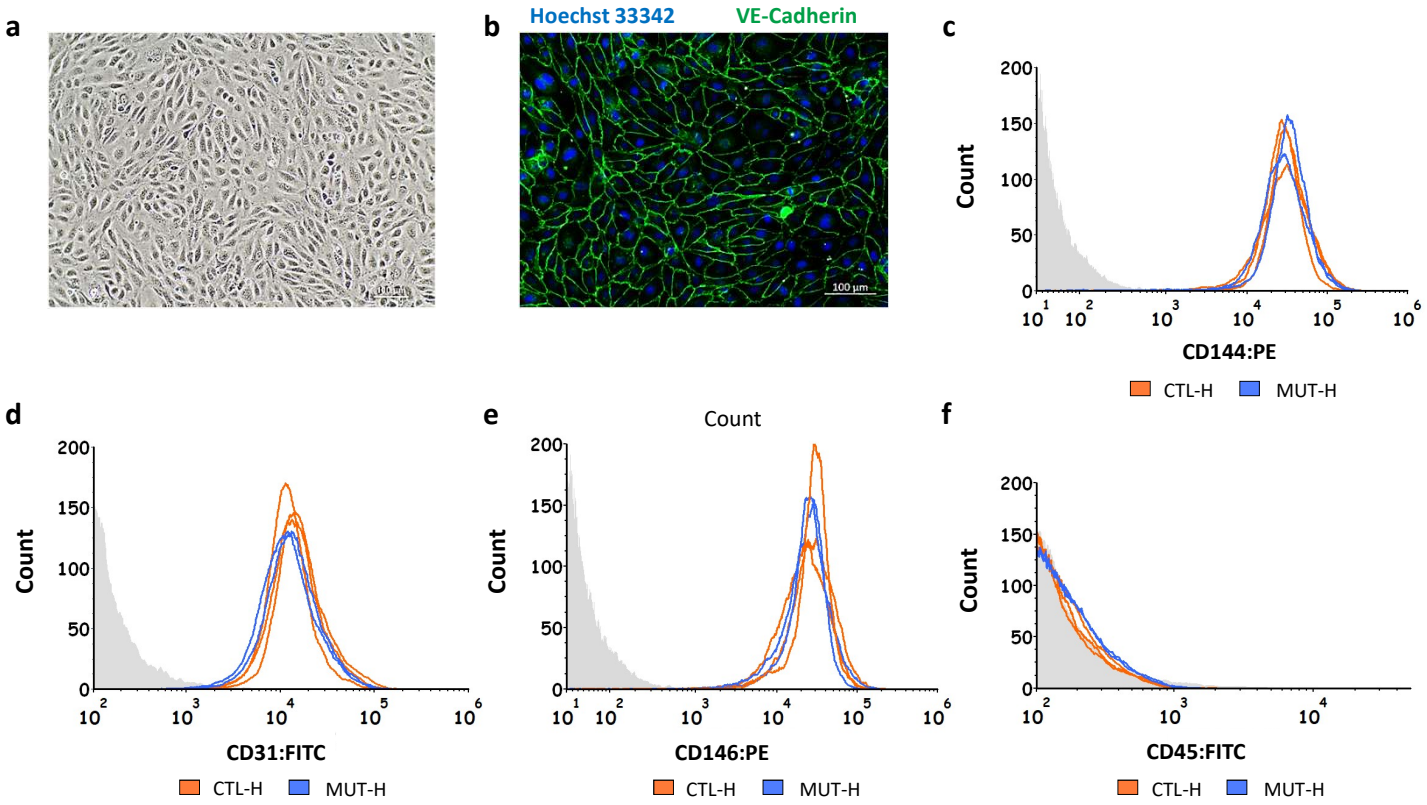

Suppl Fig 1 Characterization of isolated ECFCs from CTL and *ALK1*-mutated donors

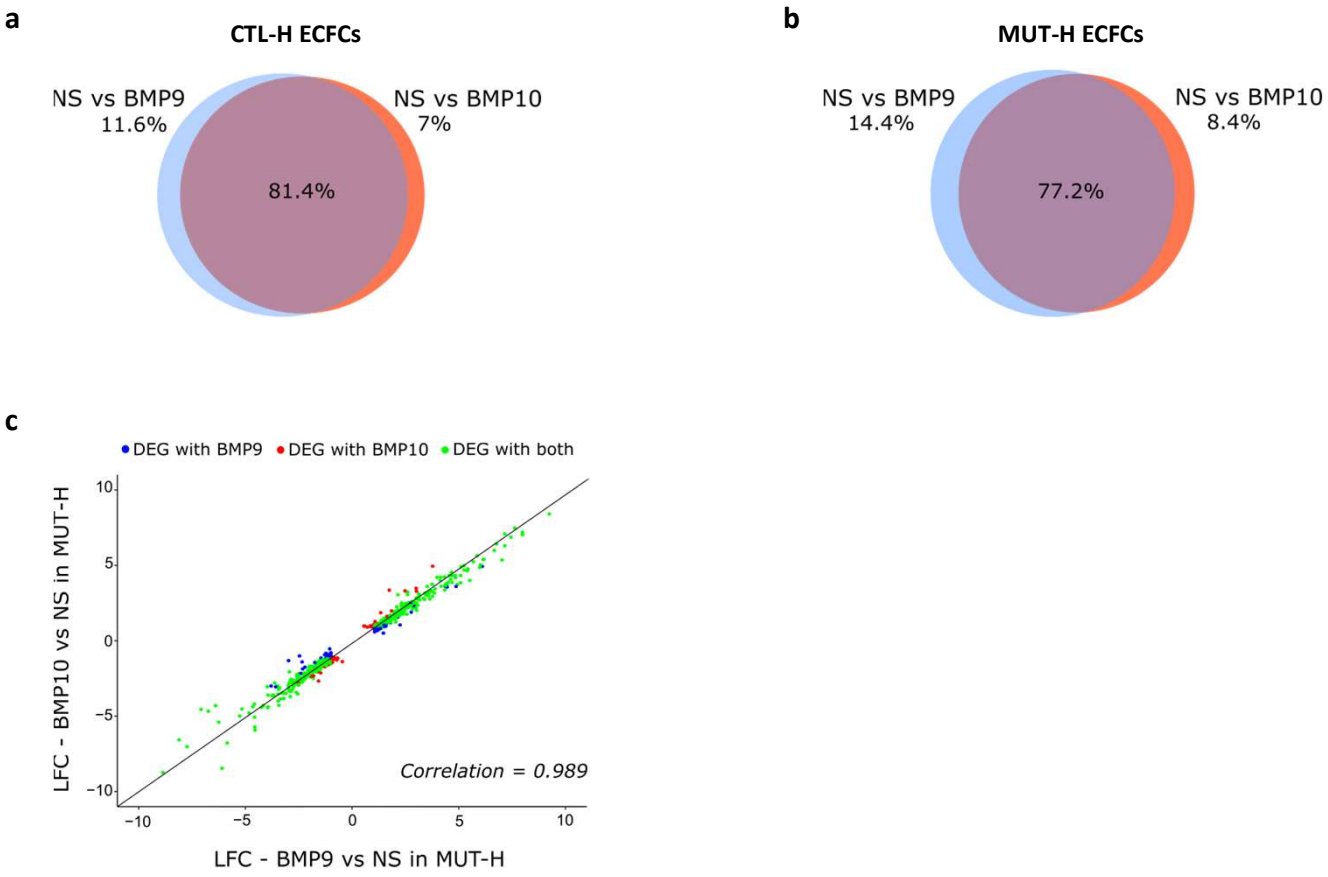

Suppl Fig 2 BMP9 and BMP10 induce a similar transcriptomic response in CTL and *ALK1*-mutated ECFCs

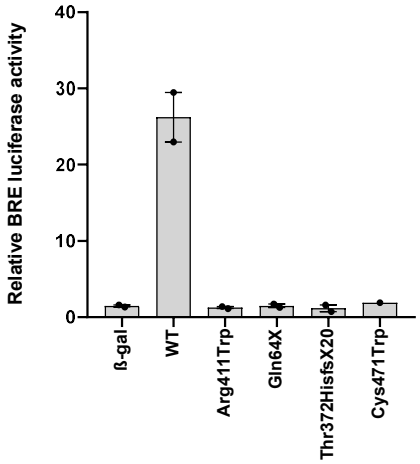

Suppl Fig 3 BRE luciferase activity of *ALK1* mutations identified in ECFCs and HUVECs

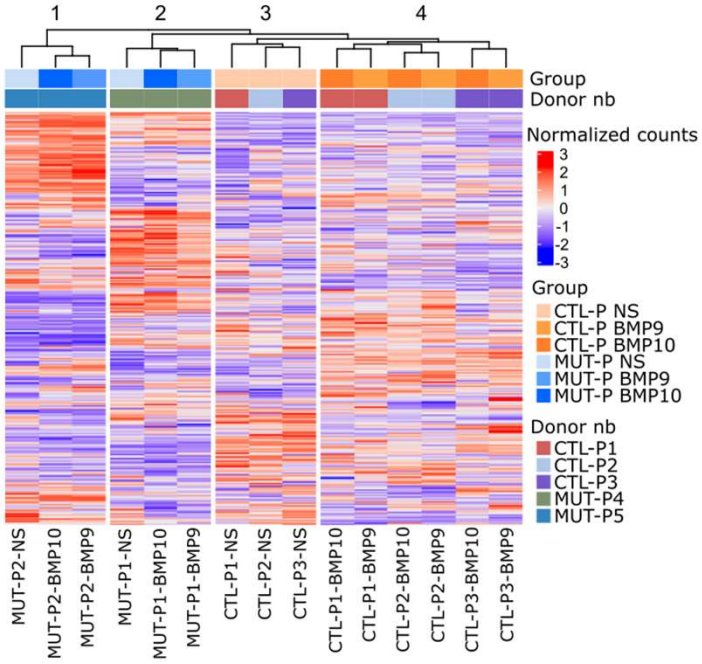

Suppl Fig 4 Hierarchical clustering of HMVECs transcriptomic data

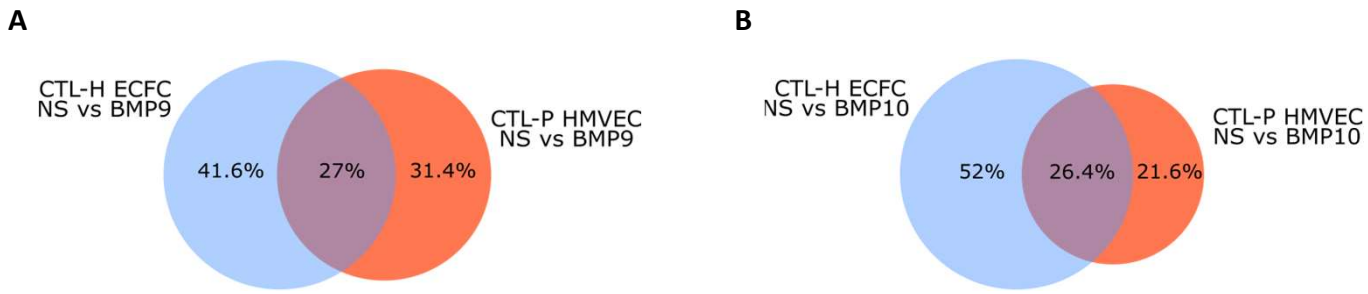

Suppl Fig 5 BMP9 and BMP10 induce specific transcriptomic changes in CTL ECFCs versus CTL HMVECs

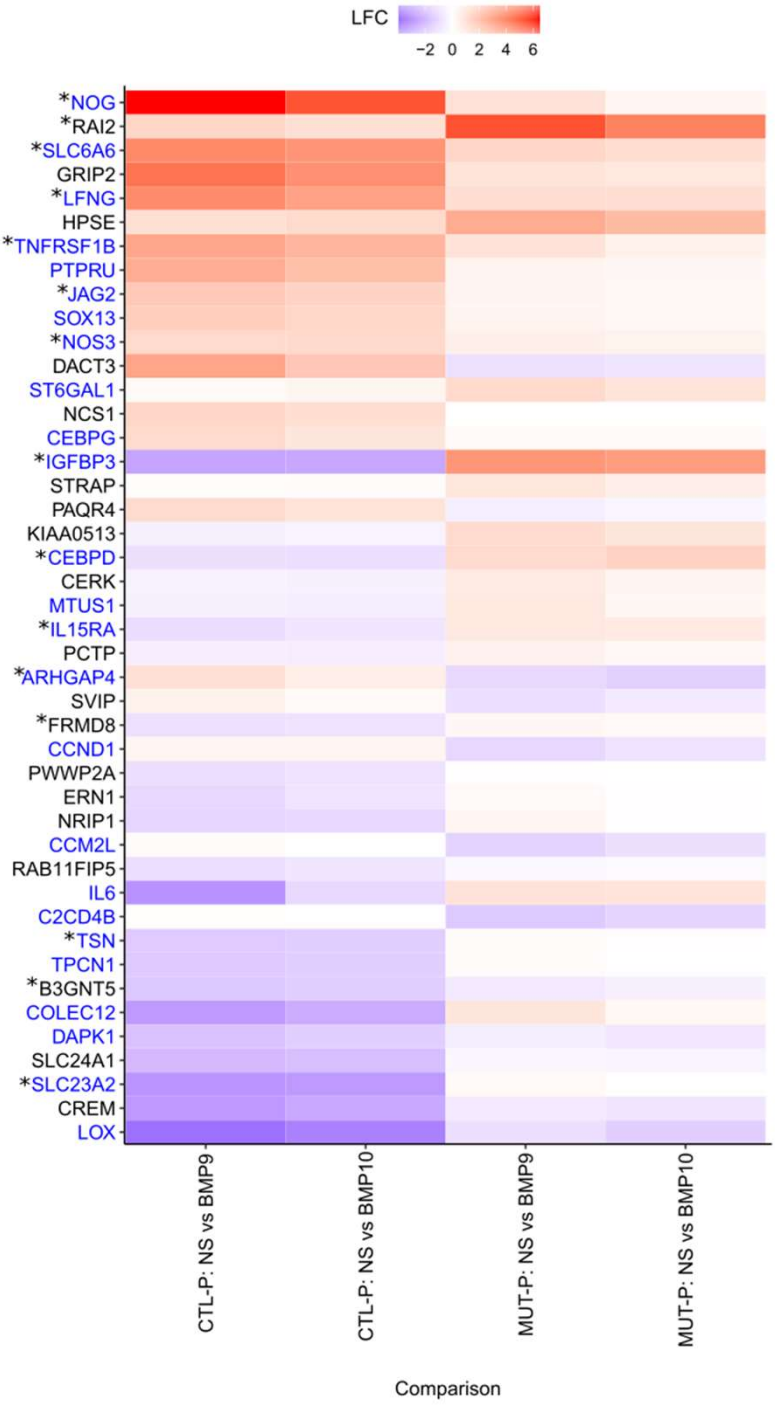

Suppl Fig 6 Regulation patterns of hits identified by the two-factor analysis in *ALK1*-mutated HMVECs

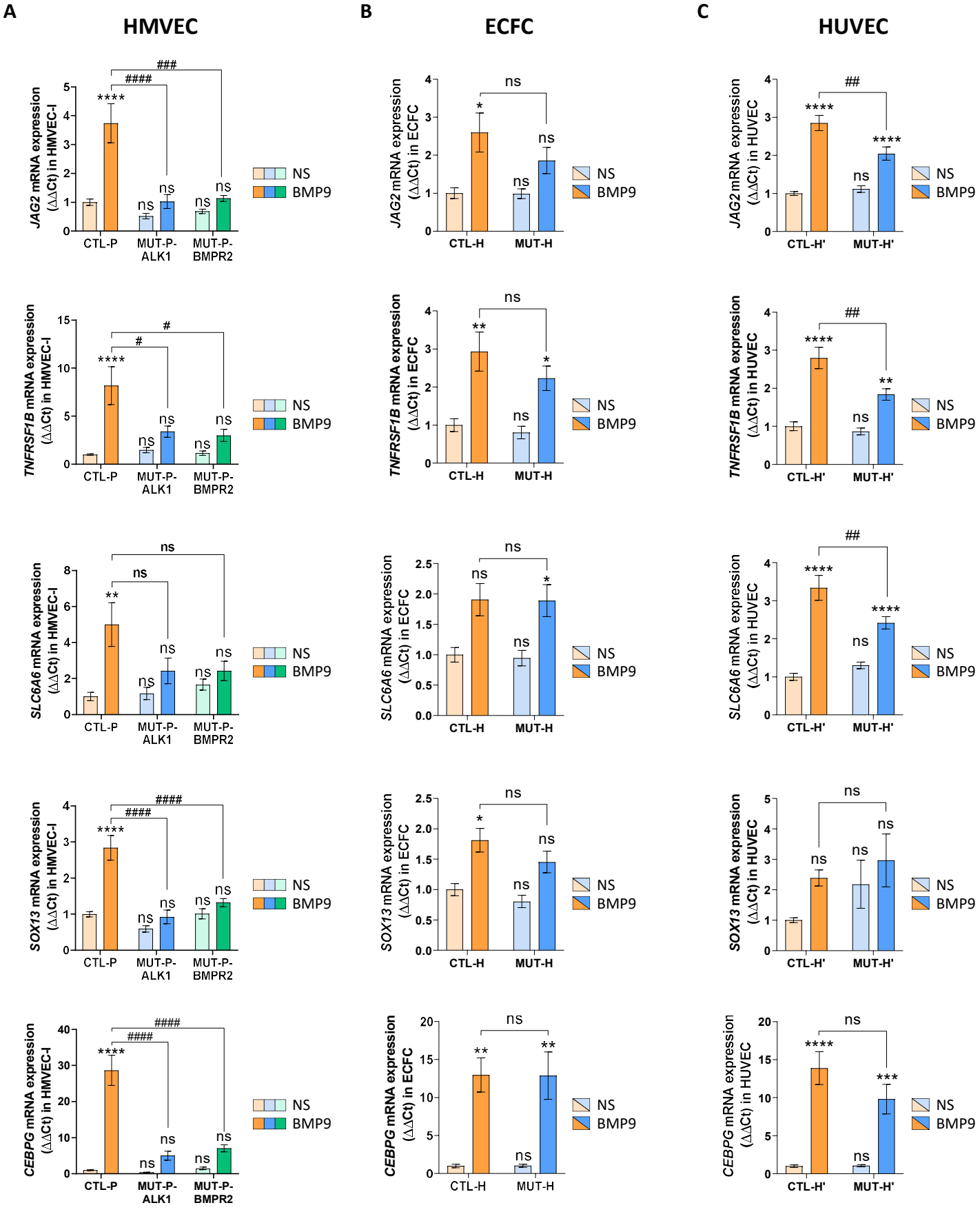

Suppl Fig 7 RT-qPCR validation of selected two-factor interaction genes in CTL and *ALK1*-mutated HMVECs, ECFCs and HUVEC.

Annex 2: Hereditary hemorrhagic telangiectasia : from signaling insights to therapeutic advances

In the 4th year of PhD, I have collaborated as a co-first author in a review titled “From signaling insights to HHT treatments”. This review presents up-to-date knowledge around mutations in BMP9-BMP10/ENG/ALK1/SMAD4 signaling pathway in endothelial cells and its crosstalk with pro-angiogenic pathways, which allowed the repurposing of new drugs for HHT treatment. The review is provided in the following pages and is currently under revision.

Hereditary hemorrhagic telangiectasia : from signaling insights to therapeutic advances

Al Tabosh T.[1¥], Al Tarrass M.[1¥], Tourvieilhe L.[2¥], Guilhem A.[2, 3], *Dupuis-Girod S.[1,2*], and Bailly S.[1*^]*

[1]Biosanté unit U1292, Grenoble Alpes University, INSERM, CEA, F-38000 Grenoble, France; [2]Hospices Civils de Lyon, National HHT Reference Center and Genetics Department, Femme-Mère-Enfants Hospital, F-69677 Bron, France; [3] TAI-IT Autoimmunité unit RIGHT-UMR1098, Burgundy University, INSERM, EFS-BFC, 25020 BESANCON, France

¥ Co-first authors

*Co-last-authors

^Corresponding author: sabine.bailly@cea.fr

The authors have declared that no conflict of interest exists."

Abstract

Hereditary Hemorrhagic Telangiectasia (HHT) is an inherited vascular disorder with highly variable expressivity, affecting up to 1 in 5000 individuals. This disease is characterized by small arteriovenous malformations (AVMs) in muco-cutaneous areas (telangiectases) and larger visceral AVMs in the lungs, liver and brain. HHT is caused by loss-of-function mutations in the BMP9-BMP10/ENG/ALK1/SMAD4 endothelial-specific signaling pathway. This review presents up-to-date insights on this mutated signaling pathway and its crosstalk with pro-angiogenic pathways, in particular the VEGF pathway, that allowed the repurposing of new drugs for HHT treatment. However, despite the substantial benefits of these new treatments in terms of alleviating symptom severity, this not-so-uncommon bleeding disorder still currently lacks any FDA- or EMA-approved therapies.

Main text

1) Genetic basis of HHT

HHT or Rendu-Osler syndrome is a hereditary disease that is transmitted in an autosomal dominant manner and is caused by loss-of-function (LOF) mutations in certain components of the predominantly endothelial BMP9/10-ALK1-ENG signaling pathway, that is an important mediator of vascular quiescence (1). Specifically, mutations in *ENG* (chromosomal locus 9q34.11, encoding the co-receptor endoglin) and *ACVRL1* (chromosomal locus 12q13.13, encoding the type I receptor ALK1) are nearly equally responsible for the majority of HHT

cases and give rise to the two major forms of the disease, HHT1 (OMIM 187300) and HHT2 (OMIM 600376), respectively (2–4). Collectively, by mid-2023, over 600 different pathogenic mutations in *ENG* and *ACVRL1,* spanning the entire coding sequences of both genes were documented in the previous HHT mutation database (http://www.arup.utah.edu/database/hht/). While reported *ENG* mutations were mostly non-sense or frameshift mutations leading to premature termination codons, a higher prevalence of missense mutations was observed for *ACVRL1*. In addition to *ENG* and *ACVRL1,* less than 2% of HHT patients were found to carry mutations in the *SMAD4* gene (chromosomal locus 18q21.2), resulting in a combined syndrome of HHT and juvenile polyposis (JP-HHT; OMIM 175050) (4, 5). Based on the *SMAD4* mutation repository developed by Wooderchak et al, at least 26 different mutations in *SMAD4* were described in patients with the combined JP-HHT syndrome, most of which are missense mutations and deletions mainly concentrated at the MH2 domain of SMAD4 (6).

Together, mutations in *ENG*, *ACVRL1* and *SMAD4* are responsible for more than 90% of HHT cases, leaving a minority of clinically diagnosed individuals with an unknown genetic basis. In some cases, this can be attributed to limitations of current sequencing technologies in detecting certain variants in the previously identified loci or to the exclusion of testing non-coding regions (7); however, additional chromosomal loci could also be implicated in HHT development. As such, mutations in *GDF2* (chromosomal locus 10q11.22, encoding BMP9) were described in few cases displaying an HHT-like syndrome (8–12). This rare form of HHT was annotated as HHT5 (OMIM #615506). In addition, mutations in *RASA1*, which are commonly associated with hereditary capillary malformations with or without AVMs (13, 14) have been reported in few patients presenting HHT symptoms (15–17). More recently, *EPHB4* LOF variants were reported in a few individuals exhibiting atypical HHT symptoms and HHT-like hepatic abnormalities (18). Furthermore, one study described an overrepresentation of rare mutations in *DROSHA*, a key enzyme involved in miRNA processing, among clinically diagnosed HHT patients who did not carry any mutations in the typical HHT-associated genes (19). Interestingly, this study also demonstrated that zebrafish and mice with endothelial-specific Drosha deficiency developed vascular defects resembling those observed in HHT patients (19). Moreover, at least three pulmonary arterial hypertension patients carrying a mutation in *BMPR2* (chromosomal locus 2q33.1-q33.2, encoding the type II TGF-β family receptor BMPRII) were found to exhibit HHT symptoms (20–22), suggesting a potential, rare involvement of this gene in HHT.

2) Clinical manifestations of HHT

AVMs are the hallmark of HHT. According to the international classification of vascular anomalies, AVMs are characterized by malformed arteries, veins and capillaries with direct arteriovenous communications resulting in arteriovenous shunting (23) (Figure 1). The stepwise development of AVMs in the context of HHT has been histologically documented in cutaneous biopsies by Braverman et al. in 1990 (24). The process was found to commence with focal dilatations of the postcapillary venules that progressively encompass the normal capillaries, finally establishing a direct connection with dilated arterioles. Interestingly, the process seemed to involve an immune arm, as perivascular lymphocytic infiltrates were

evident at the site of the AVM. It is noteworthy that all clinical signs of HHT result from AVMs, which can be present at variable scales.

At the microvascular level, HHT AVMs appear as mucocutaneous telangiectases, after which the disease is named. HHT-associated telangiectases typically appear as minute-sized round red spots that are flat or slightly elevated and fade under pressure. They concern specific body areas, the palmar faces of finger pads and hands, the lips, the tongue, the nasal cavity and the gastrointestinal (GI) tract (25, 26) (Figure 1). On the nasal mucosa, telangiectases are responsible for the spontaneous and recurrent epistaxis leading to iron-deficient anemia in about 50% of the patients (27). Similarly, GI telangiectases, which can affect any part of the tract, occasionally result in occult bleeding.

At the macrovascular level, larger AVMs mainly affect the lungs, the central nervous system and the liver (Figure 1). Consequently, they can result in life-threatening complications. For instance, pulmonary AVMs can cause chronic hypoxemia, ischemic strokes, cerebral abscesses and hemoptysis (28). On the other hand, hepatic AVMs can lead to high-output cardiac failure, biliary ischemia and portal hypertension (29). Cerebral AVMs are generally asymptomatic but can rarely provoke hemorrhagic stroke or epilepsy.

Cohort studies have revealed the deleterious effect of aging on epistaxis, skin telangiectases and liver AVMs, while pulmonary and cerebral AVMs were shown to appear early in life (30). Although HHT1 and HHT2 patients are clinically undistinguishable, *ACVRL1* mutations are associated with higher rates of liver AVMs and digestive telangiectases, while *ENG* mutations are more predominantly linked to pulmonary and cerebral AVMs (31). Interestingly, hepatic relapse of the vascular lesions has been described in some HHT patients receiving liver transplants (32).

In addition to the well documented HHT symptoms, i.e. epistaxis, telangiectases and AVMs, HHT patients exhibit a heightened infectious risk in soft tissues, bones and joints involving *Staphylococcus aureus*, as well as cerebral infections involving bacteria from the oro-digestive flora (33). HHT is also associated with immunological abnormalities, mainly characterized by a T-helper lymphopenia, although without any clear correlation with the aforementioned infectious risks (34).

3) The second-hit hypothesis

The LOF nature of HHT causal mutations and the autosomal dominant inheritance of the disease led to the longstanding belief that HHT is caused by haploinsufficiency of the mutated gene product. This was corroborated with several reports demonstrating a reduction in endoglin levels in HHT1-derived cells (35–37) and in ALK1 levels in some HHT2-derived cells compared to control counterparts (36–38). In line with these studies, mice heterozygous for

mutations in *Eng* or *Acvrl1* ($Eng^{+/-}$ or $Alk1^{+/-}$) display reduced expression levels of the affected gene and develop some HHT-like lesions at the adult stage, albeit with a low penetrance, including telangiectases, nosebleeds and dilated vessels with reduced vascular smooth muscle cell (VSMC) coverage (39–41).

However, the haploinsufficiency model does not explain why HHT vascular lesions develop focally in characteristic vascular beds, despite the presence of the germline HHT causal mutation in all endothelial cells (ECs) of the body (42). This model also fails to elucidate the differences in disease expressivity that are observed even between related patients carrying the same mutation (43). These disparities put forth the second-hit hypothesis in HHT, which is becoming more and more accepted by the HHT scientific community (44). This hypothesis implies that the germline mutation (first-hit) predisposes the endothelium to vascular defects that strictly develop in the presence of additional, local factors (second-hit) that could be either environmental or genetic. Along these lines, several preclinical studies have demonstrated the role of pro-angiogenic and pro-inflammatory triggers in driving HHT pathogenesis (45). For instance, $Eng^{+/-}$ or $Alk1^{+/-}$ mice at the age of 8-10 weeks, which typically do not exhibit any vascular defects until several months later, acquired cerebrovascular dysplasia upon local administration of viral vectors encoding vascular endothelial growth factor (VEGF) into their brains, as opposed to normal angiogenesis in wild type (WT) mice receiving the same treatment (46, 47). In addition, unlike WT mice, inducible *Eng* or *Alk1* knockout mice readily and consistently developed visceral arteriovenous malformations (AVMs) in their brains only upon local VEGF overexpression (48–51) as well as dermal AVMs strictly after wounding or upon local VEGF or lipopolysaccharide (LPS) treatment (52–55). Interestingly, blocking VEGF in inducible $Alk1^{-/-}$ mice partially reversed or blocked the development of AVMs induced by VEGF, LPS or wounding (50, 54), in line with the well-documented effectiveness of the humanized anti-VEGF antibody bevacizumab in alleviating HHT symptoms (Table 1) (56, 57). In addition to angiogenic and inflammatory stimuli, several other environmental triggers have been proposed as potential second-hits in HHT, including mechanical stress and sun exposure. A study on 103 HHT patients revealed a higher number of telangiectases on the dominant hand and on the lower lip, which are expected to be more frequently exposed to mechanical stimuli, than the other hand and the upper lip (58). The number of telangiectases on the lips was also found to be positively correlated with sunlight exposure (58).

Another study supporting the two-hit hypothesis in HHT patients was released in 2019, but this time involving a genetic second-hit (59). Using next-generation sequencing, Snellings et al detected low-frequency somatic mutations, mostly in trans configuration, leading to biallelic loss of *ENG* or *ACVRL1* in cutaneous telangiectases on the hands of some HHT patients (59). Consequently, HHT vascular malformations were proposed to develop when specific endothelial clones acquire somatic mutations leading to loss of heterozygosity (59). This is a well-known pathogenic mechanism in cancer, known as the Knudsonian two-hit mechanism (60), which was also shown in some heritable vascular anomalies, including venous, glomuvenous and cerebral cavernous malformations (61, 62). It remains to be validated whether this hypothesis holds true for HHT-related AVMs. As sunlight comprises mutagenic ultraviolet radiation, it is plausible that dermal telangiectases might develop on the hands due to somatic mutations triggered by prolonged exposure to sunlight. This hypothesis might explain the late-onset development of some AVMs (skin, Liver) (63), as somatic mutations

accumulate with time, but cannot explain the ones that appear early in life (cerebral and pulmonary AVMs) (63, 64). Therefore, the second-hit hypothesis could indeed be responsible for some HHT-related vascular defects but might not represent a universal pathogenic mechanism in HHT.

4) Signaling pathways involved in HHT

a. BMP9/10-ALK1 pathway

Endoglin and ALK1 are two transmembrane receptors mainly expressed on ECs, explaining why mutations in this pathway result in vascular abnormalities. BMP9 and BMP10 are the high affinity ligands of the receptors ALK1 and endoglin (65, 66). Endoglin is a co-receptor for BMP9 and BMP10 and serves as a reservoir of these ligands on the surface of ECs (67), enhancing ligand-induced responses (65). In line with endoglin's role as an upstream co-receptor of the ALK1 pathway, it was shown that AVMs induced by endothelial loss of *Eng* could be corrected by overexpression of ALK1, while endoglin overexpression could not compensate for the loss of *Alk1* (68). BMP9 or BMP10 recruit a heterocomplex of two type II receptors (BMPRII or ActRIIA, which are the main type II receptors expressed on ECs) and two type I receptors (ALK1) (1, 69). Upon BMP9 or BMP10 binding, the serine/threonine kinase type II receptor phosphorylates the serine/threonine kinase type I receptor ALK1, leading to its activation. Subsequently, activated ALK1 phosphorylates the transcription factors SMAD1/5, allowing their binding to SMAD4, which is a common downstream signaling mediator shared with the TGFβ pathway (Figure 2). The trimeric SMAD complex then migrates to the nucleus, where it interacts with other transcription factors to regulate the transcription of many target genes (1, 69). In addition, few studies show that BMP9 and BMP10 can activate non-canonical BMP signaling pathways, including P38, ERK, Wingless (Wnt) and NOTCH signaling (70). It is widely accepted that BMP9 and BMP10 lead to vascular maturation and quiescence (71). The current working model suggests that BMP9/10-ENG-ALK1-SMAD4 signaling maintains vascular homeostasis via attenuation of pro-angiogenic pathways, and in particular the VEGF signaling pathway. However, the mechanisms underlying this attenuation are still not fully characterized.

The immunosuppressor tacrolimus (FK506) has been identified in two independent screens as a potent activator of SMAD1/5 signaling using a reporter assay based on the Id1 promoter (72, 73). However, the mechanism by which tacrolimus activates this pathway is not clearly understood. Tacrolimus is a macrolide with immunomodulatory and anti-angiogenic properties commonly used in patients who had undergone organ transplantation (74). It inhibits the phosphatase calcineurin, which dephosphorylates the nuclear factor of activated T cells (NFAT) proteins (Figure 3) (75, 76). Activation of calcineurin has also been shown to be downstream of VEGF (77) (figure 2). Interestingly, we have previously shown that BMP9 regulates the calcineurin-NFAT pathway in lymphatic differentiation (78). Tacrolimus can also activate BMP signaling pathway by blocking FKBP12 (Figure 3) (79), which is known to bind

and suppress ALK1 activation (73). In ECs, it was shown that tacrolimus activated SMAD1/5 signaling and inhibited AKT and P38 phosphorylation induced by VEGF (72). The same group showed that Tacrolimus injection in BMP9/BMP10-immunodepleted postnatal retinas prevented hypervascularization (Table 2). However, the molecular mechanisms involved in this protective effect of tacrolimus are not yet fully elucidated.

b. VEGF-VEGFR2 pathway

VEGF-A, herein referred to as VEGF, is one of the most potent and extensively studied angiogenic factors. VEGF signaling occurs through its binding to the receptor tyrosine kinase VEGFR2, which activates several downstream pathways (Figure 2). These include the ERK1/2 pathway, the PI3K-AKT-mTOR pathway, the SRC and small GTPases pathways, and others that are poorly understood, including the P38 MAPK (77, 80) (Figure 2). The PI3K-AKT-mTOR pathway is negatively regulated by the phosphatase and tensin homolog (PTEN) that is active when unphosphorylated. VEGF-A, VEGF-B and PlGF can also bind VEGFR1 with higher affinity than VEGFR2, but the former exhibits low kinase activity, making VEGFR1 a decoy receptor (23). VEGF signaling is thus modulated by the different relative expression levels of VEGFR2 versus VEGFR1 in ECs.

The beneficial effect of blocking VEGF signaling in HHT patients dates back to 2006, when an HHT patient suffering from a malignant mesothelioma unexpectedly showed amelioration of HHT symptoms following anti-angiogenic cancer treatment with an anti-VEGF-A monoclonal antibody (bevacizumab) (81). The following year, BMP9 and BMP10 were identified as two high affinity ligands for the receptors ALK1 and endoglin (65, 66). It was shown that these two ligands inhibited angiogenesis *in vitro* (EC proliferation and migration) and in *ex vivo* models (66, 82). Few years later, the first clinical trial using bevacizumab showed very positive results on 25 patients suffering from HHT (Table 1) (83). Since then, preclinical HHT models have been developed in order to test different therapeutic approaches. The main model used is the murine retina, a two dimensional-like vascular structure that forms via angiogenesis during early postnatal days. It has been shown that the loss of *Alk1, Eng, Smad4* or *Bmp9/Bmp10* led to spontaneous AVMS in the retina (45) .However, it is noteworthy that these models do not recapitulate AVMs observed in HHT patients, which are found in the skin, lungs, liver and brain. Nevertheless, using these models, it was shown that blocking VEGF signaling reduced the development of vascular malformations (50, 54). These mouse models supported that AVM formation involved aberrant EC responses, including enhanced proliferation, impaired flow-migration coupling and abnormal cellular behavior in response to angiogenic signals like VEGF (45).

To date, there is a limited understanding of how BMP9 or BMP10 mitigate VEGF signaling. It has been found that BMP9 induces the expression of VEGFR1, thus restricting downstream VEGF signaling (84) (Figure 2). Conversely, the loss of ALK1 expression in ECs using siRNA promoted an elevation of several key pro-angiogenic regulators (*DLL4*, *ANGPT2* (encoding

angiopoietin 2) and *KDR* (encoding VEGFR2) (72). Accordingly, it was shown that *Alk1*$^{+/-}$ mice presented a reduced level of VEGFR1 expression, and that VEGFR1 levels were reduced in skin biopsies from HHT2 patients (85).

Concerning the molecular mechanisms involved downstream of the VEGF signaling pathway, studies in mice have shown that the loss of *Alk1* or *Smad4* activated the PI3K/AKT pathway (86–88). Similar results were obtained *in vitro* in human umbilical vein ECs (HUVECs) using siRNA against ALK1 (86, 88). Inversely, BMP9 treatment for 2 hours in HUVECs was found to increase PTEN expression and activity leading to a decrease in AKT activity (Figure 2) (87, 88). Activated AKT subsequently activates the mTORC1 complex, which in turn activates the signaling cascade P70S6K/S6 (Figure 2). Interestingly, this pathway has been found activated in skin telangiectases from HHT patients (87, 89). In HUVECs, BMP9 was also found to induce the expression of SGK1 kinase, which can also activate the mTORC1/P70S6K/S6 pathway (90). In this work, it was proposed that activation of this pathway would play a role in regulating protein synthesis. Additionally, BMP9 was also shown to inhibit ERK activation, although the specific mechanism behind this inhibition remains unclear (Figure 2). In parallel, BMP9 and BMP10 have been shown to inhibit endothelial cell proliferation, but the underlying mechanism is not yet clearly characterized. One study showed that BMP9-induced inhibition of EC proliferation was SMAD1/5-dependent and required the expression of the CDK4/6 inhibitor P27^{KIP} (91). On the contrary, *Smad4* loss enhanced flow-mediated KLF4-TIE2-PI3K/AKT signaling, leading to cell cycle progression, which was inhibited using CDK4/6 inhibitors (92). Accordingly, the CDK4/6 inhibitors, Palbociclib and ribociclib, inhibited the formation of retinal AVMs and the knockdown of CDK6 prevented the development of retinal AVMs (Table 2) (92, 93).

c. Angiopoietin-Tie2 pathway

Genetic HHT mouse models have also shown an increase in Angiopoietin 2 (Ang2) levels (94, 95). The angiopoietin-Tie2 pathway is critical for maintaining vessel stability by regulating, as for VEGF, the PI3K/AKT pathway (Figure 2). Ang1, produced by mural cells, activates the receptor tyrosine kinase TIE2 to maintain VSMC coverage. An increase in TIE2 antagonist Ang2 produced by ECs inhibits Ang1-mediated TIE2 activation, leading to destabilization of VSMC-EC interaction and a decrease in vascular quiescence (80, 96). Accordingly, it has been recently shown that blocking Ang2 (LC10 monoclonal antibody) can prevent or reduce AVMs and other associated HHT-abnormalities in mice (94, 95) (Figure 2). However, in contradiction to these mouse models, Ang2 circulating levels in HHT patients tend to be reduced compared to healthy individuals (97, 98). Thus, although Ang2 seems to be a new promising therapeutic target, further work is needed before pursuing to clinical trials (99).

5) Preclinical data, clinical trials and perspectives in HHT

Since 2009, anti-angiogenic drugs developed in oncology have been increasingly used in drug repurposing strategies in patients with HHT (100, 101). Today, numerous preclinical (50, 54, 72, 85, 86, 88, 92–95, 102–110) and clinical studies (57, 83, 102, 111–133) targeting angiogenesis in the scope of HHT have been carried out and are summarized in Tables 1 and 2. Drugs used in the aforementioned studies and their distinct sites of action are depicted in Figure 3.

Today, with our current knowledge of the pathophysiological mechanisms of HHT owing to preclinical models and therapeutic trials, the main therapeutic lines of action to be considered include: first, avoiding angiogenic and inflammatory stimuli by all means, in line with the second hit hypothesis. Whenever possible, "mechanical" prevention, such as sun protection, application of nasal ointments and avoidance of nasal cauterization during childhood, is recommended to reduce the development of cutaneous and mucosal telangiectases. In addition, it is essential to prevent and treat anemia and iron deficiency, whose repercussions are probably not limited to hematology alone, but also include the risk of infection and stroke (42, 134).

Another important point is moving towards personalized medicine for each patient. While studies across 14 years that involved more than 400 patients ensured the safety of bevacizumab, they demonstrated that the response varied depending on its elimination rate (57, 83). Indeed, pharmacokinetic studies highlighted a correlation between a progressive decrease in response to the drug and low plasma bevacizumab concentration. Thus, as in cancer, there is a concentration threshhold for efficacy. So taking into account the metabolisms of different patients and adapting the dosage accordingly would allow to maintain its efficacy and optimize the risk-benefit balance. It is therefore essential to monitor bevacizumab levels during maintenance therapy in order to maintain bioactive levels within the therapeutic window, especially if efficacy appears to be declining (118).

Another aspect that should be considered more carefully is tailoring treatment to disease severity in order to limit drug toxicity. To reduce systemic adverse effects, anti-angiogenic treatments applied locally have been studied. For example, tacrolimus ointment 0.1% twice daily is promising (135) and could be a good option for patients with moderate epistaxis, although this awaits further confirmation by larger studies. Moreover, the use of tacrolimus in HHT patients in the future could be questionable as few HHT patients under this regiment after liver transplantation developed new hepatic vascular lesions and needed a second transplantation (32). Other anti-angiogenic drugs with local use are more debated. Two randomized trials showed that intranasal bevacizumab was not effective (136, 137). This result was confirmed in a systematic review (138) conducted on thirteen studies. Some studies evaluated submucosal administration associated with electrocautery (139), which is not recommended, and/or cyanoacrylate glue (140), whereas others cautiously excluded this confounding factor (141, 142). In addition, non-selective beta-adrenergic receptor blockers

with anti-angiogenic properties reducing VEGF and MMP-9 tissue expression have been studied (143). For instance, four randomized studies using topical timolol in the form of a nasal spray or gel for epistaxis and an ophtalmic solution for cutaneous telangiectasia reported discordant results in cohorts ranging from 6 to 58 patients (144–147). This is consistent with a systematic review from 2022 (148) on topical beta-blockers suggesting that propranolol is more promising than timolol. Topical propranolol was reported to increase hemoglobin levels (149, 150), but its use warrants monitoring for bradycardia occurrence, even when administered locally.

6) Future challenges in HHT

Although great progress has been made in the treatment of HHT patients, there are still some remaining challenges. Perhaps the greatest challenge is determining whether large AVMs observed in HHT patients would respond to anti-angiogenic therapies. Indeed, several antiangiogenic drugs, particularly those administered orally, including tyrosine kinase inhibitors, AKT inhibitors, pomalidomide and mTOR inhibitors are currently being tested on visceral AVMs, but no regression of visceral AVMs has been observed so far. Only skin or mucosal telangiectases have been found to be reduced in few cases (123, 126). In the Metafore study (83), cardiac index and hepatic blood flow were decreased after bevacizumab treatment, but large liver AVMs on CT scan were unchanged, and despite a marked improvement in digestive bleeding, the number of GI telangiectases was not reduced (83). Although some preclinical studies reported that anti-angiogenic treatments, such as PI3K inhibitors, could revert established AVMs in preclinical models (88), these AVMs were only seen in neonatal retinas of mice. Similarly, it was shown that in zebrafish *Eng* mutants, the HHT-like phenotype was abrogated by inhibiting VEGF signaling with drugs targeting VEGFR2, but only strictly in embryos (110). In both models, the treatment was effective during active angiogenesis (embryonic or postnatal stages), which is not the case after remodeling of vascular structure in large AVMs. Thus there is a real need for testing the efficacy of drugs in preclinical models on large AVMs or AVMs at adult stages. Accordingly, recent preclinical HHT models that better mimic HHT symptoms have been developed in adult mice and zebrafish (54, 104, 105, 110).

Another challenge is to identify the best target to inhibit angiogenesis in HHT patients. VEGF signaling is complex and drives numerous downstream pathways, so adverse complications can be caused by inhibiting the VEGF pathway as a whole (151). Thus, one could imagine that targeting specific downstream pathways of VEGF could reduce these complications. A recent study addressed this point by using an adult endoglin mutant zebrafish model that developed several HHT symptoms (110). They found that inhibiting mTORC1 (using rapamycin, also known as sirolimus) or MEK pathways prevented vascular abnormalities (Table 2), whereas inhibiting P38 or nitric oxide synthase pathways had no effect. Combined subtherapeutic

mTORC1 and MEK inhibitors demonstrated synergistic effects in treating HHT. However, it remains unclear at this stage whether it will be more beneficial in the future to only target particular downstream targets of VEGF (PI3K, MEK), which are activated by many signaling pathways or to target a specific pro-angiogenic growth factor, such as VEGF.

In the present review, we focused on therapeutic approaches that aim to block activated signaling pathways due to LOF of the BMP9/10-ALK1 signaling pathway, but another possibility would be to increase the deficient signaling pathway (more ligands, more receptors, activation of the downstream signaling pathway). However, the validity of such a therapeutic option fundementally relies on whether HHT vascular lesions are driven by haploinsufficiency or biallelic loss of the affected gene.

Summary and conclusions

Ever since the discovery that HHT is due to mutations in a single signaling pathway nearly thirty years ago, considerable progress has been made in treating HHT symptoms by blocking the VEGF angiogenic pathway. However, the molecular mechanism underlying the interaction between BMP9/BMP10 and VEGF signaling is still not fully elucidated. In addition, as described in this review, several points remain to be better characterized, such as the development of AVMs, preclinical adult models for AVMs, biomarkers for personalized anti-angiogenic treatments, the choice of therapeutic target (growth factors such as VEGF or more focused downstream signaling (TKI, AKT, MTORC1, MEK)), the possibility and efficacy of localized treatment and the benefit of preventative anti-angiogenic treatments. Larger scale and real-life data are particularly difficult to obtain since these treatments are used off-label due to a lack of better options. This is partly due to the general abstention of pharmaceutical industries from repurposing drugs in rare diseases. In the meantime, anti-angiogenic drugs hold a promising potential in HHT and represent avenues worth investigating before taking on the future challenges associated with gene therapy.

Acknowledgments

The team is supported by the National Institute for Health and Medical Research (INSERM), the University of Grenoble-Alpes, the CEA (commissariat à l'énergie atomique et aux énergies alternatives DRF/IRIG/DS), the Hospices Civils de Lyon (HCL), the Fondation pour la Recherche Médicale (EQU202003010188), the Association Maladie de Rendu-Osler (AMRO/HHT France), the association FAVA-multi, the H2020-msca-ITN-2018 (V.A. Cure-84316), the French National Agency for research (ANR) grant no. ANR-20-CE14-0002 (SMAD4pathy) and GRAL, a program from the Chemistry Biology Health (CBH) Graduate School of University Grenoble Alpes (ANR-17-EURE-0003).

Table 1 : Therapeutic strategies targeting the VEGF pathway

Therapeutic group	Evidence in pre-clinical models			Evidence in HHT patients			
	Drug used	References	Key findings	Drug used	References and study type	n	Key findings
Anti-VEGF-A monoclonal antibodies	**bevacizumab**	Walker EJ, 2012[50]	VEGF blockade reduces vascular density in a brain AVM-induced mouse model (*Alk1*-KO+VEGF)	**bevacizumab**	Dupuis-Girod S, 2012[83] *Prospective phase 2 open label*	25	Decrease in cardiac ouput and reduction of the duration and number of episodes of epistaxis
					Chavan A, 2013[111] *Prospective case series*	3	Reduction in epistaxis frequency, quantity and duration of bleeding per episode; normalization of cardiac output
					Thompson A, 2014[112] *Prospective open label*	6	Low bevacizumab doses improve epistaxis severity and frequency
					Guilhem A, 2017[113] *Retrospective*	46	Improvement of 74% of the cohort
					Chavan A, 2017[114] *Prospective*	21	Clinical improvement (pain, dyspnea, fatigability and general performance) w/o significant toxicity in 18 patients
	G6-31 antibody	Han C, 2014[54]	Reduces wound-induced skin AVMs and hemorrhages in *Alk1*-KO adult mice		Iyer V, 2018[115] *Retrospective*	34	Reduction in epistaxis severity score and RBC transfusion requirements
					Al-Samkari H, 2020[116] *Survey-based*	291	Bevacizumab reported to be effective in reducing bleeding symptoms and improving hematologic parameters
		Ardelean D, 2014[103]	Normalizes the lung peripheral microvessel density and attenuates the secondary right ventricular hypertrophy in *Eng+/-* and *Alk1+/-* mice		Vazquez C, 2020[117] *Retrospective*	20	Reduction in RBC transfusion requirements, increase in hemoglobin levels
					Al-Samkari H, 2021[57] *Retrospective*	238	Reduction in RBC transfusion requirements and in IV iron supplementation, increase in hemoglobin levels
					Dupuis-Girod S 2023[118] *Prospective randomized trial*	24	Reduction in RBC transfusion requirements and in IV iron supplementation, increase in hemoglobin levels
					Ongoing trial (TRUST) *NCT04404881*	33 est.	
					Singular case reports	28	
Extracellular receptor trap for VEGF-A, VEGF-B and PlGF				**aflibercept**	Villanueva B, 2023[119]	1	Reduction in RBC transfusion requirements, increase in hemoglobin levels
Anti-VEGFR2 antibody	**D5B1**	Thalgott JH, 2018[85]	Reduces telangiectases in trachea of *Alk1*-KO mice infected with *M pulmonis*				
	DC101	Tual-Chalot S, 2020[104]	Reduces pelvic AVMs and HOHF in adult in *Eng*-ieKO mice				

AVM : arteriovenous malformation; RBC: red blood cell; PlGF:Placenta Growth factor; VEGF: Vascular endothelial growth factor;w/o: without; IV: intrevenous

Table 2 :Therapeutic strategies targeting intracellular pathways

Therapeutic group	Evidence in pre-clinical models			Evidence in HHT patients			
	Drug used	References	Key findings	Drug used	References and study type	n	Key findings
TKI	**sorafenib, pazopanib, erlotinib, sunitinib**	Kim YH, 2017[105]	Sorafenib and pazopanib analog improve while erlotinib worsenes anemia and gastro-intestinal bleeding, no effect on wound-induced skin AVMs in adult *Alk1*-ieKO mice	**pazopanib**	Parambil JG, 2018[120]	1	Normalization of iron levels, increase in hemoglobin levels
					Faughnan M, 2019[121] *Prospective open label*	7	Improvement in hemoglobin levels and/or epistaxis in all treated patients
					Parambil JG, 2022[122] *Retrospective*	13	RBC transfusion independence within 12 months of treatment, increase in hemoglobin levels
	SU5416	Jin Y, 2017[106]	Reduces retinal AVMs in *Eng*-ieKO		Moon JY, 2022[123]	1	Improvement in cutaneous HHT
	nintedanib	Ruiz S, 2020[107]	Prevents and reverses retinal AVMs in BMP9/10ib		Ongoing trial (Paz)	70	*NCT03850964*
				nintedanib	Kovacs-Sipos E, 2017[124]	1	Decrease in frequency and curation of epistaxis
					Ongoing trial (EPICURE)	60	*NCT03954782*
					Ongoing trial (EPISTOP)	48 .	*NCT04976036*
PI3K and AKT inhibitors	**wortmannin**	Ola R, 2016[88] Ola R 2018[86]	Prevents and reverses the formation of retinal AVMs in *Alk1*-ieKO, BMP9/10ib and *Smad4*-ieKO mice	**BKM120 (buparlisib)**	Geisthoff, 2014[125]	1	Decrease in the frequency of epistaxis, which stopped after 6 weeks
	pictilisib	Ola R, 2016[88]	Reduces retinal AVMs in *Alk1*-ieKO	**VAD044**	Ongoing trial	80	*NCT05406362*
mTOR inhibitor	**sirolimus**	Ruiz S, 2020[107]	Prevents and reverses retinal AVMs in BMP9/10ib	**sirolimus**	Skaro A, 2006[126]	1	Regression of telangectases
					Ongoing trial	10	NCT05269849
Calcineurin inhibitor/ FKBP12 competitor	**tacrolimus (FK506)**	Ruiz S, 2017[72]	Reduces retinal AVMs in BMP9/10ib mice	**tacrolimus**	Sommer N, 2019[133] *Case report*	1	Decrease in frequency and curation of epistaxis
					Pruijsen J, 2021[127]	1	Decrease in gastro-intestinal bleeding, RBC transfusion
					Hessels J, 2023[128] *Prospective open label*	25	Reduction in RBC transfusion requirements, increase in hemoglobin levels
IMIDs	**thalidomide**	Lebrin F, 2010[102]	Inhibits angiogenesis by increasing mural cell coverage of the vasculature of Eng+/- mice	**thalidomide**	Lebrin F, 2010[102] *Case series*	7	Reduction in RBC transfusion requirements, increase in hemoglobin levels
					Invernizzi, 2015[129] *Prospective open label*	31	Reduction in RBC transfusion, increase in hemoglobin levels, decrease of all epistaxis parameters
		Peng H, 2015[108]	Reverses telangiectases, controls nosebleeds and leads to vascular remodeling in the zebrafish model		Fang J, 2017[130] *Prospective open label*	7	Reduction in ESS scores
	thalidomide, lenalidomide	Zhu W, 2018[109]	Inhibit brain AVM development and improve vascular integrity of existing brain AVM in adult *Alk1*-ieKO mice		Baysal M, 2019[131] *Retrospective*	6	Reduction in ESS scores, increase in hemoglobin levels
				pomalidomide	Samour M, 2016[132] *Phase I*	6	Reduction in ESS scores, increase in hemoglobin, reduction in iron infusions
					Ongoing trial	145	*NCT03910244*
Anti-Ang2 antibody	**LC10**	Crist A, 2019[95]	Prevents and reverses retinal AVM in *Smad4*-ieKO mice				
		Zhou X, 2023[94]	Limits and prevents brain AVM and blood vessel enlargment in *Eng-*, *Alk1*- and *Smad4*-KO mice				
CDK4/6 inhibitors	**palbociclib, ribociclib**	Dinakaran S, 2023[93]	CDK4/6 inhibition decreases the formation of retinal AVMs and brain vascular defects in BMP9/10ib mice				
	palbociclib	Banerjee K, 2023[92]	CDK4/6 inhibition decreases the formation of retinal AVMs in *Smad4*-ieKO mice				
Drug combination	**TKI and mTOR inhibitor**	Ruiz S, 2020[107]	Nintedanib and sirolimus prevent and reverse retinal AVMs				
	MEK and mTOR inhibitors	Snodgrass R, 2023[110]	Subtherapeutic MEK inhibitor and sirolimus normalise enlarged vessels in *Eng*^{mu130} zebrafish embryos				

AVM : arteriovenous malformation; ESS : epistaxis severity score; IMIDs : immunomodulatory imide drugs ; RBC: red blood cell; TKI : Tyrosine-kinase inhibitor; ANG2 : Angiopoietin 2; FKBP12: 12-kDa FK506-binding protein

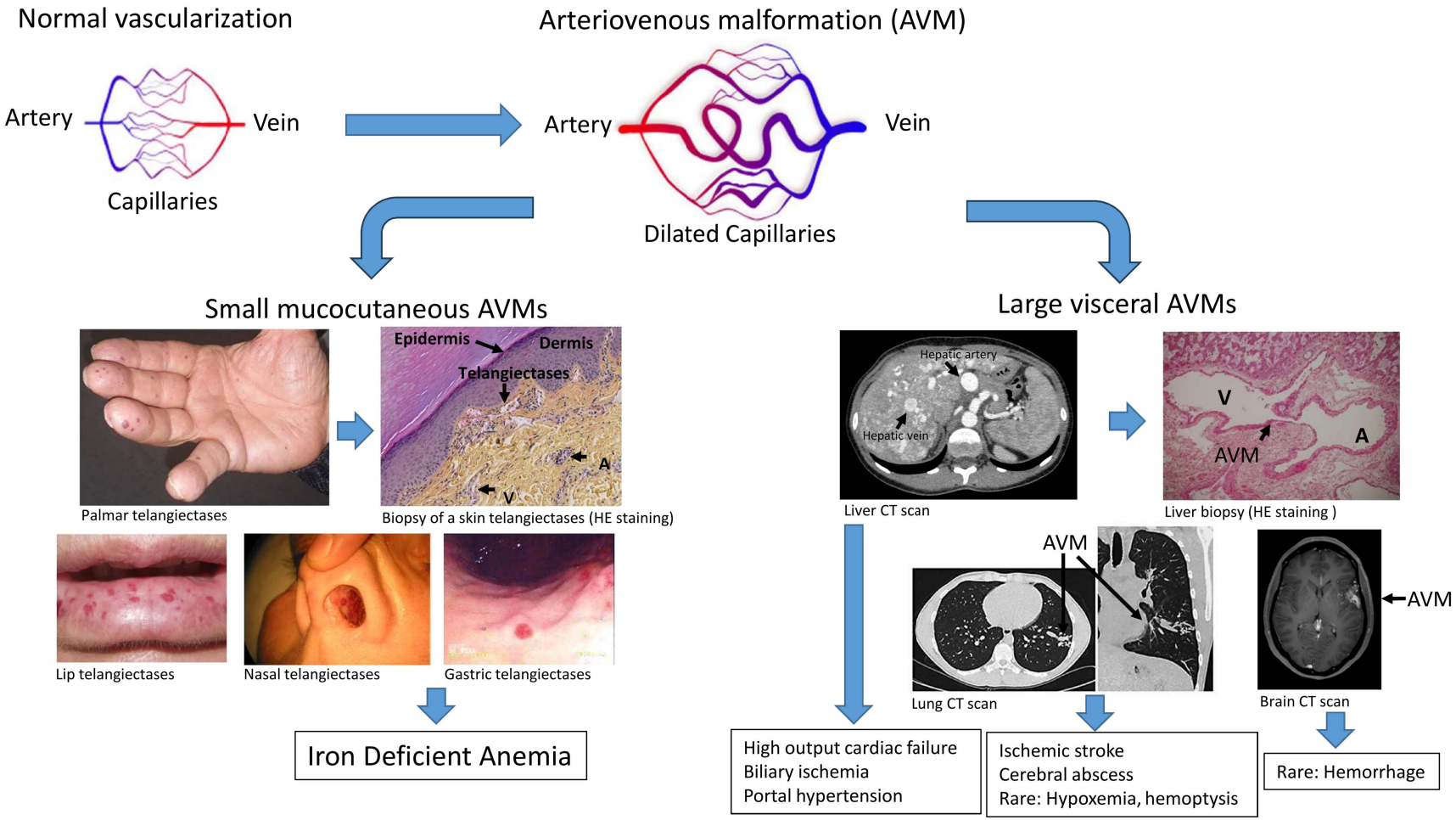

Figure 1: Arteriovenous malformations (AVMs): The hallmark of HHT and its clinical consequences.

In HHT, AVMs begin by focal dilations of the postcapillary venules (V) that progressively encompass the normal capillaries (C) and establish a direct connection with dilated arterioles (A), leading to arteriovenous malformation (AVM), muscularization of large vessel and dilations of capillary beds often surrounded by inflammatory cells. At the microvascular level, AVMs appear as telangiectases on specific muco-cutaneous areas (finger pads, lips, tongue, nasal and digestive mucosa). They are responsible of the spontaneous and recurrent epistaxis/bleeding leading to iron-deficient anemia. At the macrovascular level, large AVMs mainly affect the liver leading to high output cardiac failure, biliary ischemia and portal hypertension; the lung AVMs can provoke ischemic stroke and cerebral abscess and more rarely hypoxemia and Hemoptysis. Central nervous system AVMs is rarely complicated by hemorrhage. Liver section is a courtesy of Pr JY Scoazec (Institut Gustave Roussy, University Paris-Saclay, France). Skin and liver sections were stained hematoxylin and eosin (HE).

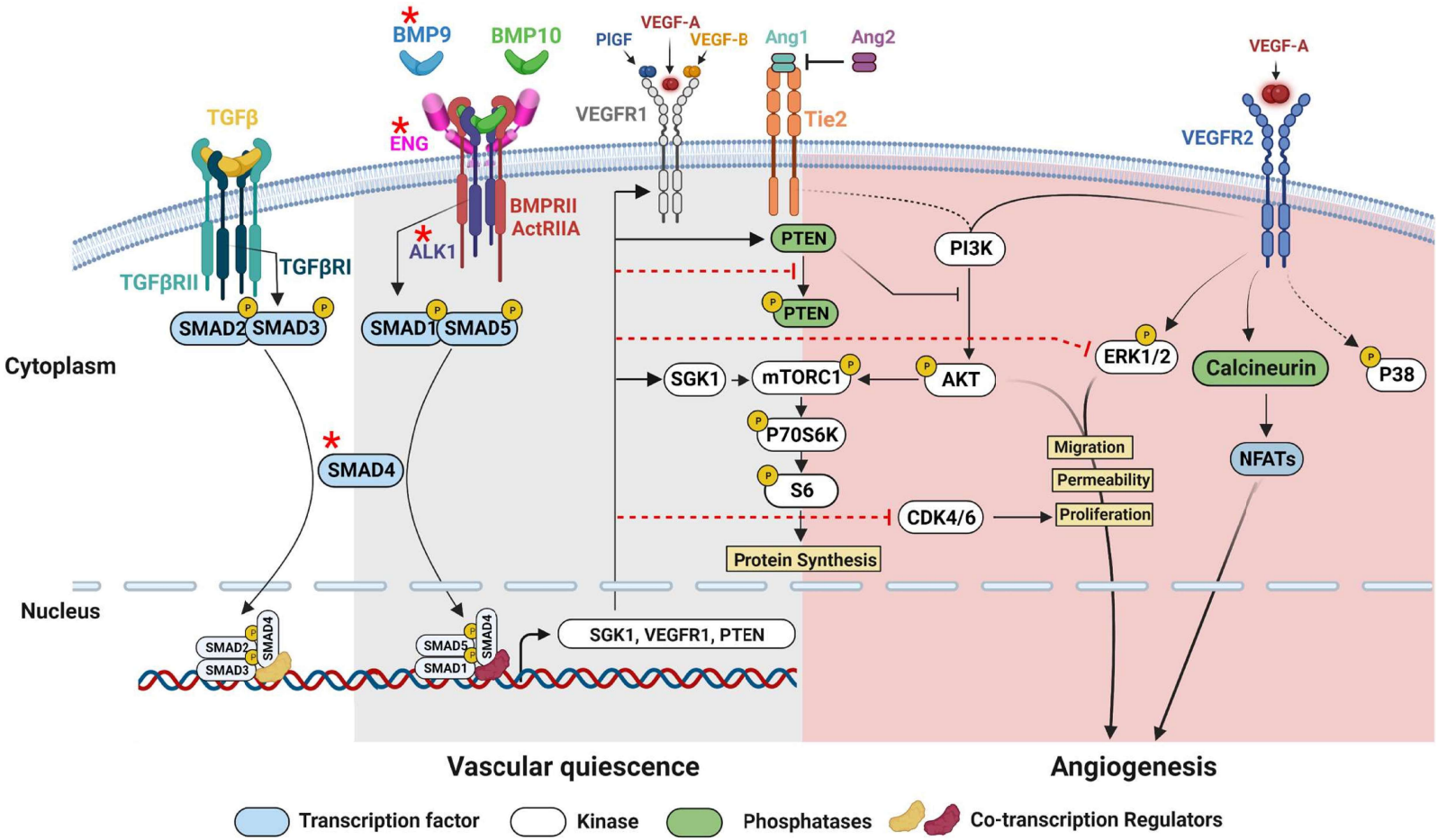

Figure 2: BMP9/10-ENG-ALK1-SMAD4 signaling pathway maintains vascular quiescence by repressing angiogenic pathways.

HHT is due to loss of function mutations (shown with an asterix) in *ENG*, *ALK1*, *SMAD4* and more rarely *BMP9* which are all in the same signaling pathway. BMP9 or BMP10 recruit a signaling heterocomplex composed of two type II receptors (BMPRII or ActRIIA), two type I receptors (ALK1) and the co-receptor endoglin. Upon BMP binding, the type II receptor phosphorylates ALK1 which subsequently phosphorylates the transcription factors SMAD1/5 which binds SMAD4, which is shared with the TGFβ pathway, to regulate, in association with other transcription factors, transcriptional regulation of many genes. BMP9 and BMP10 maintains vascular quiescence (grey) via repression of angiogenesis pathways (pink). VEGF-A binds to VEGFR2, which activates the ERK1/2 and P38 MAPK pathways and the PI3K-AKT-mTORC1 pathway which in turn activates the signaling cascade P70S6K/S6. VEGF can also activate the calcineurin phosphatase, which activates, via dephosphorylation, the transcription factor family NFATs. The PI3K-AKT-mTOR pathway is negatively regulated by the phosphatase (PTEN) that is active when unphosphorylated. VEGF-A can also bind to VEGFR1, but this will not generate signal. Two other members of the VEGF family, VEGF-B and PlGF, also bind to VEGFR1. BMP9 induces the expression of VEGFR1 thus inhibiting VEGF signaling. It also induces PTEN expression and phosphorylation which inhibit AKT activity as well as the expression of SGK1 kinase, which can activate the mTORC1/P70S6K/S6 pathway. BMP9 inhibits ERK activation through an uncharacterized mechanism. Angiopoietin 1 (Ang1) activates TIE2 receptor to maintain vascular quiescence and this pathway can be antagonized by Ang2.

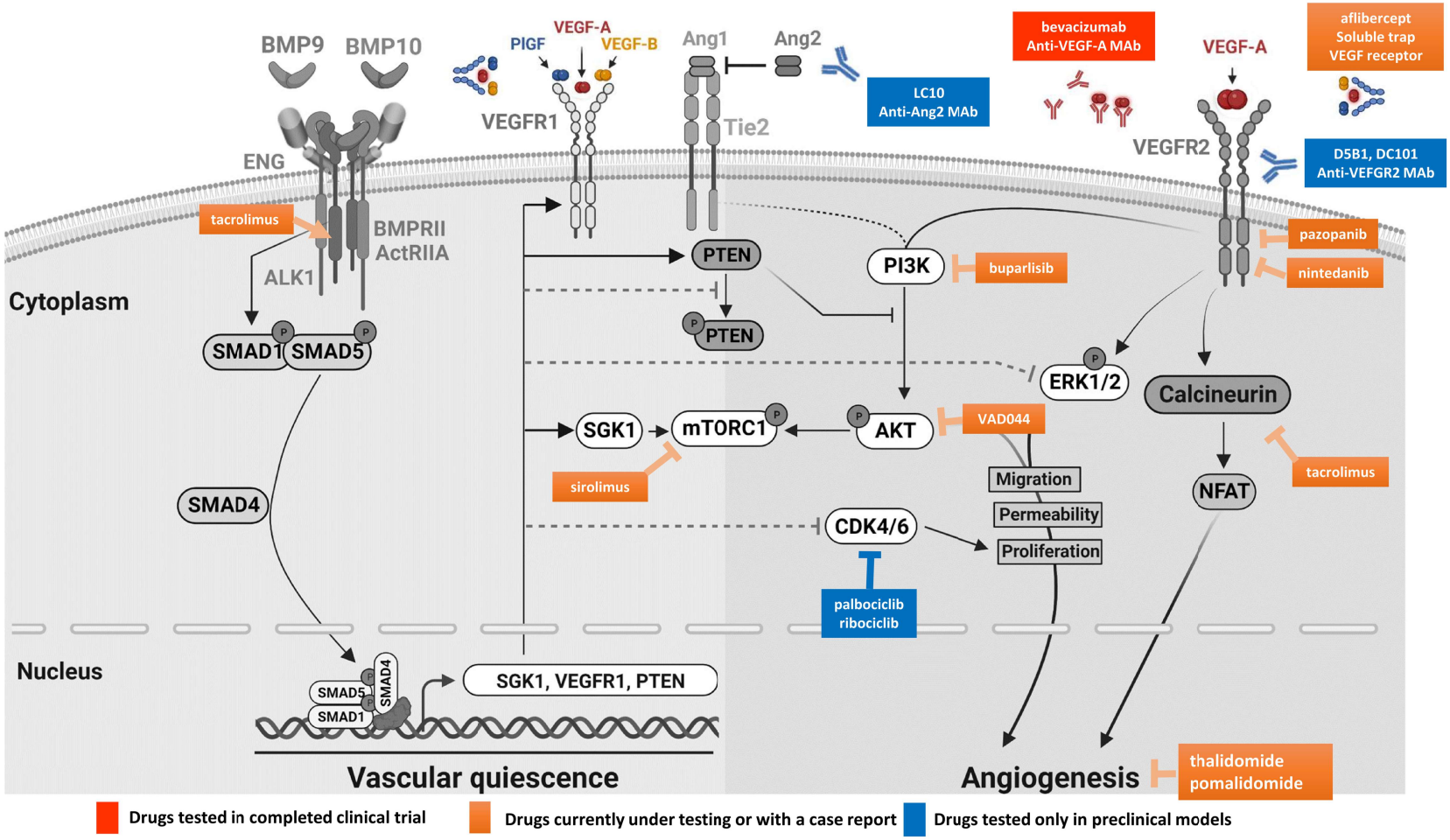

Figure 3: Therapeutic targets of anti-angiogenic drugs tested in preclinical models and in HHT patients

Drugs tested in completed clinical trials (red), drugs currently under testing or with a case report (orange) and drugs tested only in preclinical models (blue). For further details go to Tables 1 and 2. Drugs have been developed to block VEGF-A signaling using neutralizing anti-VEGF-A monoclonal antibodies (bevacizumab), or soluble trap/decoy receptor that binds VEGF-A, VEGF-B and PlGF (aflibercept), or neutralizing anti-VEGFR2 antibodies (D5B1 and DC101). Drugs developed to block intracellular signaling such as tyrosine kinase receptors inhibitors that block VEGFR2 activity but also other receptors are alo tested: pazopanib (VEGFR, PDGFR, c-KIT and FGFR) and nintedanib (VEGFR, PDGFR, and FGFR). Drugs have also been developed to block PI3K and AKT (VAD044) but also mTORC1 (sirolimus), calcineurin and FKBP12 (tacrolimus). Immunomodulatory imide drugs (IMIDS) such as thalidomide and pomalidomide have been tested in HHT patients. Other drugs have been tested so far only in preclinical models such as the neutralizing anti-Ang2 monoclonal antibodies (LC10) and inhibitors of CDK4/6 (palbociclib and ribociclib).

References

1. Desroches-Castan A, et al. BMP9 and BMP10: Two close vascular quiescence partners that stand out. *Developmental dynamics : an official publication of the American Association of Anatomists*. 2022;251(1).

2. McAllister KA, et al. Endoglin, a TGF-P binding protein of endothelial cells, is the gene for hereditary haemorrhagic telangiectasia type. 1994;8:7.

3. Johnson DW, et al. Mutations in the activin receptor–like kinase 1 gene in hereditary haemorrhagic telangiectasia type 2. *Nat Genet*. 1996;13(2):189–195.

4. McDonald J, et al. Curaçao diagnostic criteria for hereditary hemorrhagic telangiectasia is highly predictive of a pathogenic variant in ENG or ACVRL1 (HHT1 and HHT2). *Genetics in Medicine*. 2020;22(7):1201–1205.

5. Gallione CJ, et al. SMAD4 mutations found in unselected HHT patients. *Journal of Medical Genetics*. 2006;43(10):793–797.

6. Wooderchak WL, et al. Repository of SMAD4 Mutations: Reference for Genotype/ Phenotype Correlation. *J Data Mining in Genom Proteomics*. 2010;01(01).

7. Wooderchak-Donahue WL, et al. Genome sequencing reveals a deep intronic splicing *ACVRL1* mutation hotspot in Hereditary Haemorrhagic Telangiectasia. *J Med Genet*. 2018;55(12):824–830.

8. Wooderchak-Donahue WL, et al. BMP9 Mutations Cause a Vascular-Anomaly Syndrome with Phenotypic Overlap with Hereditary Hemorrhagic Telangiectasia. *The American Journal of Human Genetics*. 2013;93(3):530–537.

9. Balachandar S, et al. Identification and validation of a novel pathogenic variant in *GDF2* (BMP9) responsible for hereditary hemorrhagic telangiectasia and pulmonary arteriovenous malformations. *American J of Med Genetics Pt A*. 2022;188(3):959–964.

10. Liu J, et al. Homozygous *GDF2* -Related Hereditary Hemorrhagic Telangiectasia in a Chinese Family. *Pediatrics*. 2020;146(2):e20191970.

11. Hodgson J, et al. Homozygous *GDF2* nonsense mutations result in a loss of circulating BMP9 and BMP10 and are associated with either PAH or an “HHT-like” syndrome in children. *Molec Gen & Gen Med*. 2021;9(12).

12. Farhan A, et al. Clinical manifestations of patients with *GDF2* mutations associated with hereditary hemorrhagic telangiectasia type 5. *American J of Med Genetics Pt A*. 2022;188(1):199–209.

13. Revencu N, et al. RASA1 mutations and associated phenotypes in 68 families with capillary malformation-arteriovenous malformation. *Hum Mutat*. 2013;34(12):1632–1641.

14. Orme CM, et al. Capillary malformation--arteriovenous malformation syndrome: review of the literature, proposed diagnostic criteria, and recommendations for management. *Pediatr Dermatol*. 2013;30(4):409–415.

15. El Hajjam M, et al. RASA1 phenotype overlaps with hereditary haemorrhagic telangiectasia: two case reports. *J Med Genet*. 2021;58(9):645–647.

16. Hernandez F, et al. Mutations in RASA1 and GDF2 identified in patients with clinical features of hereditary hemorrhagic telangiectasia. *Hum Genome Var*. 2015;2:15040.

17. Wooderchak-Donahue WL, et al. Expanding the clinical and molecular findings in RASA1 capillary malformation-arteriovenous malformation. *Eur J Hum Genet*. 2018;26(10):1521–1536.

18. Guilhem A, et al. Seven cases of hereditary haemorrhagic telangiectasia-like hepatic vascular abnormalities associated with *EPHB4* pathogenic variants. *J Med Genet*. 2023;jmg-2022-109107.

19. Jiang X, et al. Inactivating mutations in Drosha mediate vascular abnormalities similar to hereditary hemorrhagic telangiectasia. *Sci Signal*. 2018;11(513):eaan6831.

20. Rigelsky CM, et al. BMPR2 mutation in a patient with pulmonary arterial hypertension and suspected hereditary hemorrhagic telangiectasia. *Am J Med Genet A*. 2008;146A(19):2551–2556.

21. Ye F, et al. A novel BMPR2 mutation in a patient with heritable pulmonary arterial hypertension and suspected hereditary hemorrhagic telangiectasia: A case report. *Medicine (Baltimore)*. 2020;99(31):e21342.

22. Scarpato BM, et al. The Shunt of It. *Chest*. 2023;163(5):e201–e205.

23. Wassef M, et al. Vascular Anomalies Classification: Recommendations From the International Society for the Study of Vascular Anomalies. *Pediatrics*. 2015;136(1):e203-214.

24. Braverman IM, Keh A, Jacobson BS. Ultrastructure and three-dimensional organization of the telangiectases of hereditary hemorrhagic telangiectasia. *J Invest Dermatol*. 1990;95(4):422–427.

25. McDonald J, et al. Frequency of epistaxis and telangiectasia in patients with hereditary hemorrhagic telangiectasia (HHT) in comparison with the general population: Curaçao diagnostic criteria revisited. *Genet Med*. 2023;25(8):100865.

26. Hyldahl SJ, et al. Skin and mucosal telangiectatic lesions in hereditary hemorrhagic telangiectasia patients. *Int J Dermatol*. 2022;61(12):1497–1505.

27. Kasthuri RS, et al. Prevalence and predictors of anemia in hereditary hemorrhagic telangiectasia. *Am J Hematol*. [published online ahead of print: June 22, 2017].

28. Dupuis-Girod S, Cottin V, Shovlin CL. The Lung in Hereditary Hemorrhagic Telangiectasia. *Respiration*. 2017;94(4):315–330.

29. Buscarini E, et al. Liver involvement in hereditary hemorrhagic telangiectasia. *Abdom Radiol (NY)*. 2018;43(8):1920–1930.

30. Plauchu H, et al. Age-related clinical profile of hereditary hemorrhagic telangiectasia in an epidemiologically recruited population. *Am J Med Genet*. 1989;32(3):291–297.

31. Lesca G, et al. Genotype-phenotype correlations in hereditary hemorrhagic telangiectasia: data from the French-Italian HHT network. *Genet Med*. 2007;9(1):14–22.

32. Dumortier J, et al. Recurrence of Hereditary Hemorrhagic Telangiectasia After Liver Transplantation: Clinical Implications and Physiopathological Insights. *Hepatology*. 2019;69(5):2232–2240.

33. Dupuis-Girod S, et al. Hemorrhagic hereditary telangiectasia (Rendu-Osler disease) and infectious diseases: an underestimated association. *Clin Infect Dis*. 2007;44(6):841–845.

34. Guilhem A, et al. Immunological abnormalities associated with hereditary haemorrhagic telangiectasia. *J Intern Med*. 2013;274(4):351–362.

35. Cymerman U, et al. Identification of Hereditary Hemorrhagic Telangiectasia Type 1 in Newborns by Protein Expression and Mutation Analysis of Endoglin. *Pediatr Res*. 2000;47(1):24–24.

36. Fernandezl A, et al. Blood outgrowth endothelial cells from Hereditary Haemorrhagic Telangiectasia patients reveal abnormalities compatible with vascular lesions. *Cardiovascular Research*. 2005;68(2):235–248.

37. Fernandez-L A, et al. Mutation study of Spanish patients with hereditary hemorrhagic telangiectasia and expression analysis of Endoglin and ALK1. *Hum Mutat*. 2006;27(3):295–295.

38. Abdalla SA. Analysis of ALK-1 and endoglin in newborns from families with hereditary hemorrhagic telangiectasia type 2. *Human Molecular Genetics*. 2000;9(8):1227–1237.

39. Bourdeau A, Dumont DJ, Letarte M. A murine model of hereditary hemorrhagic telangiectasia. *J Clin Invest*. 1999;104(10):1343–1351.

40. Srinivasan S. A mouse model for hereditary hemorrhagic telangiectasia (HHT) type 2. *Human Molecular Genetics*. 2003;12(5):473–482.

41. Arthur HM, et al. Endoglin, an Ancillary TGFβ Receptor, Is Required for Extraembryonic Angiogenesis and Plays a Key Role in Heart Development. *Developmental Biology*. 2000;217(1):42–53.

42. Faughnan ME, et al. Second International Guidelines for the Diagnosis and Management of Hereditary Hemorrhagic Telangiectasia. *Ann Intern Med*. 2020;173(12):989–1001.

43. Kritharis A, Al-Samkari H, Kuter DJ. Hereditary hemorrhagic telangiectasia: diagnosis and management from the hematologist's perspective. *Haematologica*. 2018;103(9):1433–1443.

44. Bernabeu C, et al. Potential Second-Hits in Hereditary Hemorrhagic Telangiectasia. *J Clin Med*. 2020;9(11):3571.

45. Arthur HM, Roman BL. An update on preclinical models of hereditary haemorrhagic telangiectasia: Insights into disease mechanisms. *Front Med*. 2022;9:973964.

46. Xu B, et al. Vascular Endothelial Growth Factor Induces Abnormal Microvasculature in the Endoglin Heterozygous Mouse Brain. *J Cereb Blood Flow Metab*. 2004;24(2):237–244.

47. Hao Q, et al. VEGF Induces More Severe Cerebrovascular Dysplasia in Eng+/− than in Alk1+/− Mice. *Transl Stroke Res*. 2010;1(3):197–201.

48. Choi E-J, et al. Novel Brain Arteriovenous Malformation Mouse Models for Type 1 Hereditary Hemorrhagic Telangiectasia. *PLoS ONE*. 2014;9(2):e88511.

49. Choi E-J, et al. Minimal Homozygous Endothelial Deletion of Eng with VEGF Stimulation Is Sufficient to Cause Cerebrovascular Dysplasia in the Adult Mouse. *Cerebrovasc Dis*. 2012;33(6):540–547.

50. Walker EJ, et al. Bevacizumab Attenuates VEGF-Induced Angiogenesis and Vascular Malformations in the Adult Mouse Brain. *Stroke*. 2012;43(7):1925–1930.

51. Walker EJ, et al. Arteriovenous malformation in the adult mouse brain resembling the human disease. *Ann Neurol*. 2011;69(6):954–962.

52. Park SO, et al. Real-time imaging of de novo arteriovenous malformation in a mouse model of hereditary hemorrhagic telangiectasia. *J Clin Invest*. 2009;JCI39482.

53. Garrido-Martin EM, et al. Common and Distinctive Pathogenetic Features of Arteriovenous Malformations in Hereditary Hemorrhagic Telangiectasia 1 and Hereditary Hemorrhagic Telangiectasia 2 Animal Models—Brief Report. *ATVB*. 2014;34(10):2232–2236.

54. Han C, et al. VEGF neutralization can prevent and normalize arteriovenous malformations in an animal model for hereditary hemorrhagic telangiectasia 2. *Angiogenesis*. 2014;17(4):823–830.

55. Mahmoud M, et al. Pathogenesis of Arteriovenous Malformations in the Absence of Endoglin. *Circulation Research*. 2010;106(8):1425–1433.

56. Dupuis-Girod S, et al. European Reference Network for Rare Vascular Diseases (VASCERN): When and how to use intravenous bevacizumab in Hereditary Haemorrhagic Telangiectasia (HHT)? *European Journal of Medical Genetics*. 2022;65(10):104575.

57. Al-Samkari H, et al. An international, multicenter study of intravenous bevacizumab for bleeding in hereditary hemorrhagic telangiectasia: the InHIBIT-Bleed study. *Haematologica*. 2021;106(8):2161–2169.

58. Geisthoff U, et al. Trauma Can Induce Telangiectases in Hereditary Hemorrhagic Telangiectasia. *JCM*. 2020;9(5):1507.

59. Snellings DA, et al. Somatic Mutations in Vascular Malformations of Hereditary Hemorrhagic Telangiectasia Result in Bi-allelic Loss of ENG or ACVRL1. *Am J Hum Genet*. 2019;105(5):894–906.

60. Maris JM, Knudson AG. Revisiting tissue specificity of germline cancer predisposing mutations. *Nat Rev Cancer*. 2015;15(2):65–66.

61. Brouillard P, Vikkula M. Genetic causes of vascular malformations. *Human Molecular Genetics*. 2007;16(R2):R140–R149.

62. Snellings DA, et al. Developmental venous anomalies are a genetic primer for cerebral cavernous malformations. *Nat Cardiovasc Res*. 2022;1(3):246–252.

63. Plauchu H, et al. Age-related clinical profile of hereditary hemorrhagic telangiectasia in an epidemiologically recruited population. *Am J Med Genet*. 1989;32(3):291–297.

64. Brinjikji W, et al. Prevalence and characteristics of brain arteriovenous malformations in hereditary hemorrhagic telangiectasia: a systematic review and meta-analysis. *Journal of Neurosurgery*. 2017;127(2):302–310.

65. David L, et al. Identification of BMP9 and BMP10 as functional activators of the orphan activin receptor-like kinase 1 (ALK1) in endothelial cells. *Blood*. 2007;109(5):1953–1961.

66. Scharpfenecker M, et al. BMP-9 signals via ALK1 and inhibits bFGF-induced endothelial cell proliferation and VEGF-stimulated angiogenesis. *Journal of Cell Science*. 2007;120(6):964–972.

67. Lawera A, et al. Role of soluble endoglin in BMP9 signaling. *Proc Natl Acad Sci USA*. 2019;116(36):17800–17808.

68. Hwan Kim Y, et al. Overexpression of Activin Receptor-Like Kinase 1 in Endothelial Cells Suppresses Development of Arteriovenous Malformations in Mouse Models of Hereditary Hemorrhagic Telangiectasia. *Circ Res*. 2020;127(9):1122–1137.

69. Roman BL, Hinck AP. ALK1 signaling in development and disease: new paradigms. *Cell Mol Life Sci*. 2017;74(24):4539–4560.

70. García de Vinuesa A, et al. BMP signaling in vascular biology and dysfunction. *Cytokine Growth Factor Rev*. 2016;27:65–79.

71. Ricard N, et al. The quiescent endothelium: signalling pathways regulating organ-specific endothelial normalcy. *Nature Reviews Cardiology*. 2021;1–16.

72. Ruiz S, et al. Tacrolimus rescues the signaling and gene expression signature of endothelial ALK1 loss-of-function and improves HHT vascular pathology. *Hum Mol Genet*. 2017;26(24):4786–4798.

73. Spiekerkoetter E, et al. FK506 activates BMPR2, rescues endothelial dysfunction, and reverses pulmonary hypertension. *J Clin Invest*. 2013;123(8):3600–3613.

74. Posadas Salas MA, Srinivas TR. Update on the clinical utility of once-daily tacrolimus in the management of transplantation. *Drug Des Devel Ther*. 2014;8:1183–1194.

75. Horsley V, Pavlath GK. NFAT: ubiquitous regulator of cell differentiation and adaptation. *J Cell Biol*. 2002;156(5):771–774.

76. Tocci MJ, Sigal NH. Recent advances in the mechanism of action of cyclosporine and FK506. *Curr Opin Nephrol Hypertens*. 1992;1(2):236–242.

77. Simons M, Gordon E, Claesson-Welsh L. Mechanisms and regulation of endothelial VEGF receptor signalling. *Nat Rev Mol Cell Biol*. 2016;17(10):611–625.

78. Subileau M, et al. Bone Morphogenetic Protein 9 Regulates Early Lymphatic-Specified Endothelial Cell Expansion during Mouse Embryonic Stem Cell Differentiation. *Stem Cell Reports*. 2019;12(1):98–111.

79. Chen YG, Liu F, Massague J. Mechanism of TGFbeta receptor inhibition by FKBP12. *EMBO J*. 1997;16(13):3866–3876.

80. Graupera M, Potente M. Regulation of angiogenesis by PI3K signaling networks. *Exp Cell Res*. 2013;319(9):1348–1355.

81. Flieger D, Hainke S, Fischbach W. Dramatic improvement in hereditary hemorrhagic telangiectasia after treatment with the vascular endothelial growth factor (VEGF) antagonist bevacizumab. *Ann Hematol*. 2006;85(9):631–632.

82. David L, et al. Bone Morphogenetic Protein-9 Is a Circulating Vascular Quiescence Factor. *Circulation Research*. 2008;102(8):914–922.

83. Dupuis-Girod S, et al. Bevacizumab in Patients With Hereditary Hemorrhagic Telangiectasia and Severe Hepatic Vascular Malformations and High Cardiac Output. *JAMA*. 2012;307(9):948–55.

84. Larrivée B, et al. ALK1 signaling inhibits angiogenesis by cooperating with the Notch pathway. *Dev Cell*. 2012;22(3):489–500.

85. Thalgott JH, et al. Decreased Expression of Vascular Endothelial Growth Factor Receptor 1 Contributes to the Pathogenesis of Hereditary Hemorrhagic Telangiectasia Type 2. *Circulation*. 2018;138(23):2698–2712.

86. Ola R, et al. SMAD4 Prevents Flow Induced Arteriovenous Malformations by Inhibiting Casein Kinase 2. *Circulation*. 2018;138(21):2379–2394.

87. Alsina-Sanchís E, et al. ALK1 Loss Results in Vascular Hyperplasia in Mice and Humans Through PI3K Activation. *Arterioscler Thromb Vasc Biol*. 2018;38(5):1216–1229.

88. Ola R, et al. PI3 kinase inhibition improves vascular malformations in mouse models of hereditary haemorrhagic telangiectasia. *Nat Commun*. 2016;7(1):13650.

89. Iriarte A, et al. PI3K (Phosphatidylinositol 3-Kinase) Activation and Endothelial Cell Proliferation in Patients with Hemorrhagic Hereditary Telangiectasia Type 1. *Cells*. 2019;8(9):971.

90. Medina-Jover F, Gendrau-Sanclemente N, Viñals F. SGK1 is a signalling hub that controls protein synthesis and proliferation in endothelial cells. *FEBS Lett*. 2020;594(19):3200–3215.

91. Rostama B, et al. DLL4/Notch1 and BMP9 interdependent signaling induces human endothelial cell quiescence via P27KIP1 and thrombospondin-1. *Arterioscler Thromb Vasc Biol*. 2015;35(12):2626–2637.

92. Banerjee K, et al. SMAD4 maintains the fluid shear stress set point to protect against arterial-venous malformations. *J Clin Invest*. 2023;e168352.

93. Dinakaran S, et al. CDK6-mediated endothelial cell cycle acceleration drives arteriovenous malformations in hereditary hemorrhagic telangiectasia. *bioRxiv*. 2023;2023.09.15.554413.

94. Zhou X, et al. ANG2 Blockade Diminishes Proangiogenic Cerebrovascular Defects Associated With Models of Hereditary Hemorrhagic Telangiectasia. *Arterioscler Thromb Vasc Biol*. 2023;43(8):1384–1403.

95. Crist AM, et al. Angiopoietin-2 Inhibition Rescues Arteriovenous Malformation in a Smad4 Hereditary Hemorrhagic Telangiectasia Mouse Model. *Circulation*. 2019;139(17):2049–2063.

96. Kim M, et al. Opposing actions of angiopoietin-2 on Tie2 signaling and FOXO1 activation. *J Clin Invest*. 2016;126(9):3511–3525.

97. Ojeda-Fernandez L, et al. Reduced plasma levels of Ang-2 and sEng as novel biomarkers in hereditary hemorrhagic telangiectasia (HHT). *Clin Chim Acta*. 2010;411(7–8):494–499.

98. Fernandez-L A, et al. Gene expression fingerprinting for human hereditary hemorrhagic telangiectasia. *Hum Mol Genet*. 2007;16(13):1515–1533.

99. Bernabeu C. Therapeutic Targeting of the Ang2/Tie Pathway in Endothelial Cells as a Potential Treatment of Hereditary Hemorrhagic Telangiectasia. *Arterioscler Thromb Vasc Biol*. 2023;43(8):1404–1408.

100. Ardelean DS, Letarte M. Anti-angiogenic therapeutic strategies in hereditary hemorrhagic telangiectasia. *Front Genet*. 2015;6:35.

101. Snodgrass RO, Chico TJA, Arthur HM. Hereditary Haemorrhagic Telangiectasia, an Inherited Vascular Disorder in Need of Improved Evidence-Based Pharmaceutical Interventions. *Genes (Basel)*. 2021;12(2):174.

102. Lebrin F, et al. Thalidomide stimulates vessel maturation and reduces epistaxis in individuals with hereditary hemorrhagic telangiectasia. *Nat Med*. 2010;16(4):420–428.

103. Ardelean DS, et al. Endoglin and activin receptor-like kinase 1 heterozygous mice have a distinct pulmonary and hepatic angiogenic profile and response to anti-VEGF treatment. *Angiogenesis*. 2014;17(1):129–146.

104. Tual-Chalot S, et al. Loss of Endothelial Endoglin Promotes High-Output Heart Failure Through Peripheral Arteriovenous Shunting Driven by VEGF Signaling. *Circ Res*. 2020;126(2):243–257.

105. Kim YH, et al. Selective effects of oral antiangiogenic tyrosine kinase inhibitors on an animal model of hereditary hemorrhagic telangiectasia. *J Thromb Haemost*. 2017;15(6):1095–1102.

106. Jin Y, et al. Endoglin prevents vascular malformation by regulating flow-induced cell migration and specification through VEGFR2 signalling. *Nat Cell Biol*. 2017;19(6):639–652.

107. Ruiz S, et al. Correcting Smad1/5/8, mTOR, and VEGFR2 treats pathology in hereditary hemorrhagic telangiectasia models. *J Clin Invest.* 2020;130(2):942–957.

108. Peng H-L, et al. Thalidomide Effects in Patients with Hereditary Hemorrhagic Telangiectasia During Therapeutic Treatment and in Fli-EGFP Transgenic Zebrafish Model. *Chinese Medical Journal*. 2015;128(22):3050.

109. Zhu W, et al. Thalidomide Reduces Hemorrhage of Brain Arteriovenous Malformations in a Mouse Model. *Stroke*. 2018;49(5):1232–1240.

110. Snodgrass RO, et al. Therapeutic targeting of vascular malformation in a zebrafish model of hereditary haemorrhagic telangiectasia. *Dis Model Mech*. 2023;16(4):dmm049567.

111. Chavan A, et al. Systemic therapy with bevacizumab in patients with hereditary hemorrhagic telangiectasia (HHT). *Vasa*. 2013;42(2):106–110.

112. Thompson AB, et al. Very Low Dose Bevacizumab for the Treatment of Epistaxis in Patients with Hereditary Hemorrhagic Telangiectasia. *Allergy Rhinol (Providence)*. 2014;5(2):ar.2014.5.0091.

113. Guilhem A, et al. Intra-venous bevacizumab in hereditary hemorrhagic telangiectasia (HHT): A retrospective study of 46 patients. *PLOS ONE*. 2017;12(11):e0188943.

114. Chavan A, et al. Emerging role of bevacizumab in management of patients with symptomatic hepatic involvement in Hereditary Hemorrhagic Telangiectasia. *American Journal of Hematology*. 2017;92(11):E641–E644.

115. Iyer VN, et al. Intravenous Bevacizumab for Refractory Hereditary Hemorrhagic Telangiectasia–Related Epistaxis and Gastrointestinal Bleeding. *Mayo Clinic Proceedings*. 2018;93(2):155–166.

116. Al-Samkari H, et al. An international survey to evaluate systemic bevacizumab for chronic bleeding in hereditary haemorrhagic telangiectasia. *Haemophilia*. 2020;26(6):1038–1045.

117. Vázquez C, et al. Bevacizumab for treating Hereditary Hemorrhagic Telangiectasia patients with severe hepatic involvement or refractory anemia. *PLOS ONE*. 2020;15(2):e0228486.

118. Dupuis-Girod S, et al. Efficacy and safety of intravenous bevacizumab on severe bleeding associated with hemorrhagic hereditary telangiectasia: A national, randomized multicenter trial. *Journal of Internal Medicine*;n/a(n/a). https://doi.org/10.1111/joim.13714.

119. Villanueva B, et al. Aflibercept for Gastrointestinal Bleeding in Hereditary Hemorrhagic Telangiectasia: A Case Report. *Medicina*. 2023;59(9):1533.

120. Parambil JG, Woodard TD, Koc ON. Pazopanib effective for bevacizumab-unresponsive epistaxis in hereditary hemorrhagic telangiectasia. *The Laryngoscope*. 2018;128(10):2234–2236.

121. Faughnan ME, et al. Pazopanib may reduce bleeding in hereditary hemorrhagic telangiectasia. *Angiogenesis*. 2019;22(1):145–155.

122. Parambil JG, et al. Pazopanib for severe bleeding and transfusion-dependent anemia in hereditary hemorrhagic telangiectasia. *Angiogenesis*. 2022;25(1):87–97.

123. Moon JY, et al. Improvement of Cutaneous Hereditary Hemorrhagic Telangiectasia With Pazopanib—A Multikinase Inhibitor. *JAMA Dermatology*. 2022;158(2):214–216.

124. Kovacs-Sipos E, et al. Nintedanib as a novel treatment option in hereditary haemorrhagic telangiectasia. *Case Reports*. 2017;2017:bcr.

125. Geisthoff UW, Nguyen H-LP, Hess D. Improvement in hereditary hemorrhagic telangiectasia after treatment with the phosphoinositide 3-kinase inhibitor BKM120. *Ann Hematol*. 2014;93(4):703–704.

126. McAlister VC. Regression of Cutaneous and Gastrointestinal Telangiectasia with Sirolimus and Aspirin in a Patient with Hereditary Hemorrhagic Telangiectasia. *Ann Intern Med*. 2006;144(3):226–227.

127. Pruijsen JM, et al. Tacrolimus in Gastrointestinal Bleeding in a Young Boy With Hereditary Hemorrhagic Telangiectasia. *JPGN Reports*. 2021;2(4):e133.

128. Hessels J, et al. Efficacy and Safety of Tacrolimus as Treatment for Bleeding Caused by Hereditary Hemorrhagic Telangiectasia: An Open-Label, Pilot Study. *J Clin Med*. 2022;11(18):5280.

129. Invernizzi R, et al. Efficacy and safety of thalidomide for the treatment of severe recurrent epistaxis in hereditary haemorrhagic telangiectasia: results of a non-randomised, single-centre, phase 2 study. *The Lancet Haematology*. 2015;2(11):e465–e473.

130. Fang J, et al. Thalidomide for Epistaxis in Patients with Hereditary Hemorrhagic Telangiectasia: A Preliminary Study. *Otolaryngology–Head and Neck Surgery*. 2017;157(2):217–221.

131. Baysal M, et al. Thalidomide for the Management of Bleeding Episodes in Patients with Hereditary Hemorrhagic Telangiectasia: Effects on Epistaxis Severity Score and Quality of Life. *Turk J Haematol*. 2019;36(1):43–47.

132. Samour M, et al. Pomalidomide in Hereditary Hemorrhagic Telangiectasia: Interim Results of a Phase I Study. *Blood*. 2016;128(22):210.

133. Sommer N, et al. Treatment with low-dose tacrolimus inhibits bleeding complications in a patient with hereditary hemorrhagic telangiectasia and pulmonary arterial hypertension. *Pulmonary Circulation*. 2019;9(2):2045894018805406.

134. Shovlin CL. Pulmonary Arteriovenous Malformations. *Am J Respir Crit Care Med*. 2014;190(11):1217–1228.

135. Dupuis-Girod S, et al. ELLIPSE Study. *mAbs*. 2014;6(3):793–798.

136. Dupuis-Girod S, et al. Effect of Bevacizumab Nasal Spray on Epistaxis Duration in Hereditary Hemorrhagic Telangectasia: A Randomized Clinical Trial. *JAMA*. 2016;316(9):934–942.

137. Riss D, et al. Intranasal submucosal bevacizumab for epistaxis in hereditary hemorrhagic telangiectasia: a double-blind, randomized, placebo-controlled trial. *Head Neck*. 2015;37(6):783–787.

138. Stokes P, Rimmer J. Intranasal bevacizumab in the treatment of HHT -related epistaxis: a systematic review. *Rhinology*. 2018;56(1):3–10.

139. Khanwalkar AR, et al. Randomized, controlled, double-blinded clinical trial of effect of bevacizumab injection in management of epistaxis in hereditary hemorrhagic telangiectasia patients undergoing surgical cauterization. *Int Forum Allergy Rhinol*. 2022;12(8):1034–1042.

140. Khoueir N, et al. Injection of bevacizumab and cyanoacrylate glue for hereditary hemorrhagic telangiectasia. *Laryngoscope*. 2019;129(10):2210–2215.

141. Dheyauldeen S, et al. Bevacizumab in hereditary hemorrhagic telangiectasia-associated epistaxis: Effectiveness of an injection protocol based on the vascular anatomy of the nose. *The Laryngoscope*. 2012;122(6):1210–1214.

142. Steineger J, et al. Long-term experience with intranasal bevacizumab therapy. *The Laryngoscope*. 2018;128(10):2237–2244.

143. Storch CH, Hoeger PH. Propranolol for infantile haemangiomas: insights into the molecular mechanisms of action. *Br J Dermatol*. 2010;163(2):269–274.

144. Jeon H, Cohen B. Lack of efficacy of topical timolol for cutaneous telangiectasias in patients with hereditary hemorrhagic telangiectasia: Results of a pilot study. *Journal of the American Academy of Dermatology*. 2017;76(5):997–999.

145. Peterson AM, et al. Efficacy of Timolol in a Novel Intranasal Thermosensitive Gel for Hereditary Hemorrhagic Telangiectasia–Associated Epistaxis: A Randomized Clinical Trial. *JAMA Otolaryngology–Head & Neck Surgery*. 2020;146(11):1006–1014.

146. Dupuis-Girod S, et al. Efficacy of TIMOLOL nasal spray as a treatment for epistaxis in hereditary hemorrhagic telangiectasia. A double-blind, randomized, placebo-controlled trial. *Sci Rep*. 2019;9(1):11986.

147. Andorfer KEC, et al. TIMolol Nasal Spray as a Treatment for Epistaxis in Hereditary Hemorrhagic Telangiectasia (TIM-HHT)—A Prospective, Randomized, Double-Blind, Controlled, Cross-Over Trial. *Pharmaceutics*. 2022;14(11):2335.

148. Albarki H, Rimmer J. The Use of Beta-Blockers in Hereditary Hemorrhagic Telangiectasia-Related Epistaxis: A Systematic Review. *Am J Rhinol Allergy*. 2022;36(6):890–896.

149. Mei-Zahav M, et al. Topical propranolol improves epistaxis in patients with hereditary hemorrhagic telangiectasia - a preliminary report. *Journal of Otolaryngology - Head & Neck Surgery*. 2017;46(1):58.

150. Mei-Zahav M, et al. Topical Propranolol Improves Epistaxis Control in Hereditary Hemorrhagic Telangiectasia (HHT): A Randomized Double-Blind Placebo-Controlled Trial. *Journal of Clinical Medicine*. 2020;9(10):3130.

151. Totzeck M, Mincu RI, Rassaf T. Cardiovascular Adverse Events in Patients With Cancer Treated With Bevacizumab: A Meta-Analysis of More Than 20 000 Patients. *J Am Heart Assoc*. 2017;6(8):e006278.

Annex 3: BMP9/10-ALK1-Endoglin Pathway as a Target of Anti-Angiogenic Therapy in Cancer

During my PhD, I have written a book chapter in the form of a minireview with my colleague Tala Al Tabosh, titled “BMP9/10-ALK1-Endoglin Pathway as a Target of Anti-Angiogenic Therapy in Cancer”. This minireview tackled a side of BMP9/BMP10 signaling that is not directly linked to my main PhD project, but is rather interesting. The minireview is provided in the following pages.

Book Chapter

The BMP9/10-ALK1-Endoglin Pathway as a Target of Anti-Angiogenic Therapy in Cancer

Al Tabosh T[#], Al Tarrass M[#] and Bailly S*

Universite Grenoble Alpes, Inserm, CEA, Biology of Cancer and Infection Laboratory, France

[#]These authors contributed equally to this work

***Corresponding Author:** Bailly S, Universite Grenoble Alpes, Inserm, CEA, Biology of Cancer and Infection Laboratory, F-38000 Grenoble, France

Published **November 26, 2021**

How to cite this book chapter: Al Tabosh T, Al Tarrass M, Bailly S. The BMP9/10-ALK1-Endoglin Pathway as a Target of Anti-Angiogenic Therapy in Cancer. In: Hussein Fayyad Kazan, editor. Immunology and Cancer Biology. Hyderabad, India: Vide Leaf. 2021.

Abstract

The growth and dissemination of solid tumors heavily relies on angiogenesis, making it an attractive therapeutic target in cancer. Tumor angiogenesis is orchestrated by a plethora of secreted factors and signaling pathways. The initial inhibition of the VEGF-pathway, despite successful preclinical studies, yielded only modest clinical benefits in patients, promoting the search

for other anti-angiogenic targets. The BMP9/10-ALK1-endoglin pathway is an important regulator of vascular development. This pathway has been investigated by multiple groups as a therapeutic target for tumor angiogenesis inhibition. For that, various pharmacological and genetic means were used to target different components of this pathway. Here, we recapitulate the outcome of most cellular, preclinical and clinical studies targeting BMP9/10-ALK1-endoglin pathway as an attempt to block tumor angiogenesis.

Introduction

Angiogenesis, the formation of new blood vessels from pre-existing ones, is active during physiological development to provide the growing tissues with an adequate supply of oxygen and nutrients while removing metabolic wastes. In adulthood, the vascular tree generally reaches a quiescent state, with few exceptions including wound healing and the female menstrual cycle. This vascular quiescence is tightly regulated by a variety of pro-angiogenic and anti-angiogenic factors that coordinate angiogenic processes in a spatiotemporal manner [1]. Vascular endothelial growth factor (VEGF), basic fibroblastic growth factor (bFGF), angiogenin, thrombospondin (TSP), angiopoietins, and transforming growth factor-β (TGF-β) are all examples of angiogenic factors that control the ON-OFF angiogenic switch [2]. In solid malignancies, dysregulation of the angiogenic switch towards the pro-angiogenic phenotype promotes the development of a highly vascularized niche that supports tumor growth and provides an escape route for metastatic dissemination [3]. Therefore, inhibition of tumor angiogenesis is considered an important therapeutic strategy in cancer treatment [4].

The main goal of anti-angiogenic therapies is to abrogate the formation of new blood vessels within the tumor, in an attempt to deprive cancer cells from oxygen and nutrients, and consequently inhibit tumor growth and progression. Moreover, tumor induced angiogenesis is associated with the formation of aberrant vascular network characterized by acidosis, interstitial hypertension and hypoxia. This abnormal microenvironment

endangers the efficacy and proper delivery of therapeutics to solid tumors [5]. Therefore, the development of anti-angiogenic therapies and combining them with cytotoxic drugs constitutes an important aspect in cancer therapies.

Targeting VEGF signaling has been demonstrated as the prime antiangiogenic target in the clinic for the last two decades. Anti-VEGF therapies, including blocking antibodies against VEGF (bevacizumab), kinase inhibitors (sunitinib, imatinib, sorafenib, axitinib and regorafenib), and decoy receptors, have been included in the first line therapies against advanced and metastatic cancers [6]. Unfortunately, in contrast to the promising results from preclinical studies, the use of this monotherapy has yielded only modest therapeutic benefit in some tumor types, failed in others and was associated with the generation of resistant and more aggressive tumors [7,8]. Hence, alternative and/or complementary therapeutics directed at novel targets of vascular development are urgently needed.

Members of the Transforming growth β (TGF-β) superfamily of signaling molecules have been previously described as important modulators of vasculogenic and angiogenic processes. Among them, BMP9 and BMP10, which bind with high affinity to a signaling complex of receptors composed of activin receptor-like-kinase-1 (ALK1) and endoglin [9] which are mostly expressed on endothelial cells, play an essential role in vascular development [10]. This signaling complex is composed of two type I receptors (ALK1), two type II receptors (BMPRII, ActRIIA or ActRIIB) and the co-receptor endoglin. Both type I and type II receptors possess Serine/Threonine kinase activities. Binding of BMP9/10 to this receptor complex leads to the phosphorylation of ALK1 by the constitutively active type II receptor. Consequently, activated ALK1 phosphorylates transcription factors known as Smads that modulate target gene expression [9,11,12]. Endoglin is a homodimeric cell-surface co-receptor that lacks enzymatic activity and functions as a co-receptor in association with ALK1, enhancing ALK1 signaling [13]. ALK1 and endoglin display highly similar expression patterns, being mostly restricted to endothelial cells. Complete genetic ablation of either ALK1 or endoglin in mice results in

embryonic lethality due to impairment of blood vessel development [14]. In addition, heterozygous loss-of-function mutations in either gene in humans give rise to two closely related forms of the vascular disorder hereditary hemorrhagic telangiectasia (HHT) [15].

Interestingly, an elevated expression level of both ALK1 and endoglin was reported in the angiogenic tumor endothelium [16,17] and the BMP9/10-ALK1-endoglin pathway was proposed to be involved in resistance to anti-VEGF therapy in tumors [18]. In addition, BMP9 is known to regulate the development of lymphatic vessels [19,20], which has implications for metastatic spread of tumor cells through lymphatic vasculature [21]. As a result, the BMP9/10-ALK1-endoglin signaling pathway emerged as an interesting candidate target for anti-angiogenic cancer therapies. Consequently, extensive *in vitro* and *in vivo* studies have been performed in the past two decades to investigate the implication of this pathway in tumor angiogenesis, using multiple cancer models. Most preclinical studies revealed promising anti-angiogenic responses, giving rise to several clinical trials aiming to improve the overall survival of cancer patients. Here, we provide a brief overview of the cellular, preclinical and clinical studies targeting BMP9/10-ALK1-endoglin pathway as an attempt to block tumor angiogenesis.

Targeting ALK1 as an Anti-Angiogenic Therapy in Cancer

Different biological compounds have been designed/identified to interfere with ALK1 signaling including the BMP type-I receptor inhibitors LDN-193189 [22], OD16 and OD29 [23], and the miRNA miR-199b-5p [24], all of which have demonstrated effective inhibition of ALK1 signaling. However, the specificity of designed drugs and crosstalk with other pathways make it difficult to predict the final outcome of such inhibitors. For this reason, targeting ALK1 have been majorly studied in the context of tumor angiogenesis through highly specific designed products such as ALK1-Fc fusion ligand trap (dalantercept/ACE-041) developed by Acceleron Pharma Inc [25], and PF-03446962

(fully human antibody that targets extracellular domain of ALK1) developed by Pfizer [26], both of which have been implicated in independent clinical trials.

Preclinical Studies

ALK1 Ligand Trap

The characterization of the ALK1-Fc fusion protein has demonstrated its ability to specifically trap BMP9 and BMP10, but not any other ligand of the TGF-β family [27]. In vitro studies showed that dalantercept, and its mouse counterpart RAP-041, inhibited BMP9 and BMP10 induced Smad1/5 phosphorylation and downstream signaling (e.g, id1 gene expression), without affecting TGF-β induced Smad2 phosphorylation [27,28]. Moreover, functional assays showed that dalantercept blocks cord formation and endothelial sprouting *in vitro* in human umbilical vein endothelial cells (HUVEC), as well as FGF induced neovascularization and VEGF-induced vessel formation *in vivo* in a chick chorioallantoic membrane (CAM) assay [27]. The anti-tumor effects of ALK-1 Fc were primarily investigated through the application of RAP-041 in rat insulin promoter – SV40 large T antigen (RIP1-Tag2) model of pancreatic neuroendocrine tumorigenesis. Results showed an impaired tumor growth already after 2 weeks [28] and a decrease in the number of hepatic micro metastasis compared to the control cohort after a prolonged 4-week treatment [29]. Similar results have been obtained by blocking metastatic dissemination in the transgenic spontaneous mouse mammary tumor virus (MMTV)-polyoma middle T antigen (PyMT) and the syngeneic transplantable E0771 breast cancer models [30]. Likewise, dalantercept reduced tumor burden in MCF-7 mammary adenocarcinoma orthotopic model [27]. On the other hand, in another study of poorly/non-metastatic melanoma, breast, head and neck cancer, no effect was observed on primary tumor growth at the experimental endpoint following the use of RAP-041 as a monotherapy [31].

ALK1 Antibody

The ALK1 antibody (PF-03446962) directly binds to the extracellular domain of ALK1 (residues 42-56) with a high affinity, but doesn't bind to other closely related ALKs, such as ALK2/3/4/5/or ALK7, thus reducing potential off-target effects. *In vitro* studies demonstrated that PF-03446962 prevented binding of BMP9 to endothelial cells (ECs), inhibited BMP9-induced Smad1 phosphorylation, and BMP responsive element (BRE)-luciferase transcriptional reporter activity [32]. Moreover, the monoclonal antibody efficiently blocked serum-induced Smad1 phosphorylation, migration, endothelial sprouting, as well as tube formation in HUVECs [32,33]. Similarly, a reduction in tumor growth and inhibition of both microvascular and lymphatic vessel density has been reported in MDA-MB-231 human breast cancer xenografts when using PF-03446962 [33].

Although both strategies are directed to block the signaling through ALK1, the modes of action of dalantercept and PF-03446962 are distinct, one blocking the ligands the other blocking the receptor. Both approaches demonstrated that ALK1-targeting induces changes in the vascular network and subsequent alterations in the tumor microenvironment, described through in-depth vasculature characterization using several approaches such as monitoring pericyte coverage, vascular perfusion, as well as sprouting and leakiness of the vessels [30-34], all of which are critical factors that describe what is known by "vascular normalization". In the context of tumor anti-angiogenic therapies, the vascular normalization hypothesis states that antiangiogenic therapy aims to restore the balance between pro- and antiangiogenic factors back towards equilibrium. As a result, vessel structure and function become more normal: vessels are more mature with enhanced perivascular coverage, blood flow is more homogeneous, vessel permeability and hypoxia are reduced, and importantly the delivery of systemically administered anticancer therapies into tumors is more uniform [35]. Nevertheless, contradicting data have been described when assessing the functionality of the tumor-associated vasculature following administration of either RAP-041 or PF-03446962. For instance, PF-03446962

quantitatively disrupted vascular normalization in M24met/R xenograft tumors [33], while ALK1-Fc treatment that increased coverage of tumor endothelial cells by NG2-expressing cells (i.e. pericytes) [31]. Hu-lowe et al [33] displayed that flow rates were only affected in large, functional blood vessels, whereas smaller ones were unaffected. Contradictory to this result, Hawinkels et al [31] described a slight increase in perfusion. These results demonstrate that targeting the same receptor by two different approaches in different tumor models yields different results, and suggests more investigation of the underlying mechanisms following ALK1 activation.

Alk1+/- Mice

Other means of targeting ALK1 signaling as a therapeutic approach in cancer angiogenesis include genetic approaches using heterozygote mice. Cunha et al reported that blunted ALK1 expression using RIP1-Tag2; $Alk1^{+/-}$ mice showed a significant retardation in tumor progression through the angiogenic switch, reduced de novo tumor growth, and impaired angiogenesis in comparison to RIP1-Tag2; $Alk1^{+/+}$ mice, consistent with results of using RAP-041 which has been addressed in this same work [28,29].

Combinatory Treatments

Combinatorial treatments of ALK1-blocking agents with other targeted therapies have also shown promising results in targeting both tumor angiogenesis and progression. For instance, combined use of ALK1-Fc fusion along with chemotherapy (Doxorubicin or Cisplatin) has shown increased cytotoxic effect and impaired tumor growth in melanoma, head and neck cancer, and breast cancer models [31]. Likewise, in experimental breast carcinomas, RAP-041-induced blunted vessel density was further diminished in combined therapy group (RAP-041 + Docetaxel), accompanied by a significant reduction in the metastatic count in the lungs [30]. Moreover, Dual targeting of VEGF and BMP9/10 signals using a newly designed ALK1FLT1-Fc (ALK-Fc fused to VEGFR1-Fc) trap significantly inhibited both angiogenesis and growth of human

BxPC3 pancreatic tumor xenografts [36]. Of note, co-administration of RAP-041 and VEGFR2 neutralizing antibody DC101 showed no additional therapeutic benefit in MMTV-PyMT breast cancer model [30]. Interestingly, tumors described previously as resistant to VEGF inhibitors showed a significant decrease in tumor burden and associated vasculature when exposed to PF-03446962, through a mechanism suggesting disruption of vascular normalization phenotype induced by bevacizumab [33]. It was also shown that combinatorial use of dalantercept with the VEGFR2 tyrosine kinase inhibitor sunitinib leads to tumor stasis in renal cell carcinoma [37].

Clinical Trials

The results obtained from preclinical studies of the two ALK1 targeting agents in different cancer models prompted several clinical trials to assess safety, pharmacokinetics, pharmacodynamics, and anti-tumor efficacy in patients with advanced cancer, either as monotherapy or in combination with other antiangiogenic approaches. Phase I clinical trials in patients with different tumors, including non-small lung cancer carcinoma, hepatocellular carcinoma (HCC), persistent or recurrent ovarian carcinoma and related malignancies, as well as relapsed/refractory multiple myeloma showed that both dalantercept and PF-03446962 were generally well tolerated, gave promising and motivating responses, and had a manageable safety profile distinct from that of anti-VEGF therapy [26,38-40]. None of the patients enrolled in these clinical trials displayed the most severe adverse events (AE) reported following bevacizumab treatment (gastrointestinal perforation, impaired wound healing, and serious bleeding). Commonly observed AE upon dalantercept administration were peripheral oedema, fatigue and anemia, whilst fatigue, nausea and thrombocytopenia (not associated with bleeding) were typical of PF-03446962 infusion [25,26]. Moreover, several patients enrolled in these trials developed telangiectases, which are often observed in HHT patients, demonstrating an on-target effect of blocking ALK1 receptor signaling. Though safe, independent phase II clinical trials utilizing dalantercept as monotherapy in patients with recurrent/persistent endometrial carcinoma, ovarian

carcinoma, and squamous cell carcinoma of the head and neck revealed insufficient single agent activity with limited efficacy that did not reach the intended primary endpoint [41-43]. Similarly, phase II clinical trials assessing the efficacy of PF-03446962 in pre-treated patients with refractory urothelial cancer and advanced malignant pleural mesothelioma demonstrated no or limited activity as single drug [44,45].

Acceleron Pharma Inc has recruited patients to test efficacy of combining dalantercept with sorafenib and axitinib in advanced HCC and renal cell carcinoma (RCC), respectively. Results from the dose-escalation and expansion cohorts evaluating the combination of dalantercept plus axitinib in advanced RCC showed that the combination of these two therapies is well tolerated and associated with a clinical response [46]. However, the phase II trial of this combination in RCC patients showed that the addition of dalantercept to axitinib did not appear to improve treatment-related outcomes in previously treated patients with advanced RCC reporting 1 treatment related death and a lower objective response rate in the combination group (19%) in comparison to placebo plus axitinib (24.6%). Likewise, combinatorial phase Ib study of dalantercept and sorafenib showed no improvement in antitumor activity in patients with HCC [47]. In a similar fashion, Pfizer also tested the combination of PF-03446962 with regorafenib in patients with refractory metastatic colorectal cancer, however the combined therapy was associated with unacceptable toxicity and did not demonstrate notable clinical activity in these patients [48].

Targeting Endoglin as an Anti-Angiogenic Therapy in Cancer

Another proposed anti-tumorigenic target within the ALK1 signaling pathway is endoglin (CD105). Several lines of evidence support the rationale for targeting endoglin as a novel anti-angiogenic therapy in cancer. Endoglin is highly expressed on the tumor-associated vascular and lymphatic endothelium, and its expression holds prognostic significance in certain tumors [17]. In addition, gene expression profiling of circulating endothelial cells (CEC), which are elevated in the blood of

cancer patients and are thought to contribute to tumor angiogenesis, revealed an increase of endoglin expression of CEC-enriched samples from metastatic patients compared to healthy subjects [49]. Moreover, a soluble form of endoglin, which is shed following cleavage of the membrane-bound form by matrix metalloproteinase 14 [50], is detected in the serum of patients with different solid tumors [17]. Last but not least, anti-VEGF was shown to increase endoglin expression on tumor-endothelial cells [51], in line with suggestions implicating the ALK1 signaling pathway in resistance to anti-VEGF therapies.

With that, several groups focused on targeting endoglin to suppress tumor angiogenesis, either by directly blocking endoglin using an antibody raised against it or by sequestering its ligands through an endoglin ligand trap composed of the extracellular region of endoglin fused to an immunoglobulin Fc domain (Eng-Fc).

Preclinical Studies

Endoglin Antibody

In vitro, TRC105, a chimeric antibody that binds human endoglin with high avidity, triggered the apoptosis of HUVECs through antibody-dependent cellular cytotoxity [52]. Preclinically, SN6j, a parental antibody of TRC105, showed promising anti-tumorigenic effects without significant side effects. Antibody treatment reduced microvessel density and angiogenesis in multiple metastatic tumor models and suppressed tumor metastasis, leading to prolonged survival of the tumor-bearing mice [53]. In addition, combination of SN6j with the chemotherapeutic agent cyclophosphamide synergistically enhanced antitumor efficacy [54].

Endoglin Ligand Trap and Genetic Targeting

Endoglin ligand traps also triggered anti-angiogenic responses both *in vitro* and *in vivo*. Exogenous treatment or expression of HUVECs with Eng-Fc efficiently inhibited spontaneous and VEGF-induced sprouting on matrigel and in 3D collagen matrices [50]. *In vivo*, Eng-Fc blocked angiogenesis by

suppressing VEGF-induced vessel formation or sprouting in CAM assay and angioreactors respectively. The ligand trap also successfully decreased tumor burden in a colon-26 adenocarcinoma model [55]. Contrary to these findings, one group exploring the impact of single or dual genetic targeting of ALK1 and endoglin on tumor angiogenesis reported no effect of genetic ablation of one copy of the *Eng* gene on tumor angiogenesis and growth in a mouse model of pancreatic neuroendocrine tumors [56]. On the other hand, reducing Acvrl1 gene dosage in the same model decreased tumor vasculature and delayed tumor growth. Interestingly, dual targeting of Acvrl1 and Eng, through genetic ablation of one copy of each gene, resulted in a synergistic reduction of overall tumor burden, suggesting a beneficial impact of combinatorial targeting of ALK1 and endoglin. The different effects of endoglin targeting on tumor angiogenesis could be explained by the different levels of target inhibition when using antibodies versus genetic ablation of a single *Eng* allele or by inherent differences between disease models rendering some more responsive to therapy than others.

Clinical Trials

The encouraging preclinical results led to some phase I clinical studies assessing TRC105 safety, pharmacokinetics and anti-tumor efficacy in patients with advanced or metastatic solid tumors [57,58]. In these studies, TRC105 resulted in a short-term stable disease in some patients with two showing exceptional ongoing responses after 18 and 48 months. The safety assessment of TRC105 identified well-tolerated adverse events at clinically relevant doses mostly comprising infusion reactions, low-grade headaches and anemia that is probably caused by suppression of endoglin-expressing proerythroblasts. Interestingly, some patients receiving TRC105 developed mucocutaneous telangiectases [58] or epistaxis [57], well known symptoms of the vascular disorder HHT caused by endoglin or ALK1 mutations, demonstrating on-target effect of TRC105. Finally, TRC105 treatment induced a significant induction of VEGF levels in patients of one study, which could be a potential compensatory mechanism for the anti-angiogenic effect of TRC105 [57]. This further encouraged combination therapies

comprising TRC105 and anti-VEGF treatments, which is feasible due to the distinct identified safety profile of TRC105 compared to anti-VEGF therapies.

These studies were followed by a phase II clinical trial assessing the tolerability and efficacy of TRC105 administration on 13 heavily pre-treated patients with urothelial carcinoma. TRC105 was once again well-tolerated, but its anti-tumor activity was not satisfactory with only 2 patients achieving stable disease for 4 months and a median overall survival of 8.3 months [59]. However, in this study TRC105 seemed to have a positive impact on immune subsets, notably regulatory T cells, suggesting potential benefit for combining TRC105 with immunotherapy. In support of that, enhanced therapeutic effects were recently reported when combining TRC105 with PD1 inhibition in four preclinical cancer models [60].

Another phase II study aimed to investigate the efficacy of TRC105 administration in HCC patients that have previously progressed on sorafenib. Evidence of clinical activity was not enough to proceed [61], but combination therapy with sorafenib in HCC was tested in a following phase I trial [61]. The combination of both agents was well-tolerated using the recommended single agent doses and encouraging activity triggered the launch of a phase II study. A few other clinical trials assessed the combination of TRC105 with other VEGF-targeting agents such as bevacizumab [62,63] and axitinib [64]. The combination of TRC105 with bevacizumab was well-tolerated [62]. Despite initial reports showing clinical response, TRC105 addition to bevacizumab failed to improve progression-free survival in patients with refractory metastatic RCC [63]. Following this trial, TRC105's efficacy was assessed with axitinib instead of bevacizumab in metastatic RCC patients. This combination therapy was also well-tolerated and provided encouraging evidence of activity leading to further investigations [64].

Targeting BMP9 and BMP10 as an Anti-Angiogenic Therapy in Cancer

Most preclinical studies addressing the role of the ALK1 signaling pathway in tumor angiogenesis relied on the pharmacological targeting of ALK1 or endoglin, either using neutralizing antibodies or soluble forms of ALK1 or endoglin. However, these approaches globally suppress the signaling pathway without considering potential specific roles of BMP9 versus BMP10 in tumor angiogenesis. By following tumor growth and dissemination in a syngeneic orthotopic mammary cancer model genetically deficient in *Bmp9*, *Bmp10* or both, we showed that deletion of *Bmp9*, but not *Bmp10*, increases tumor vascular density and decreases vessel normalization, leading to enhanced tumor growth and metastasis [65]. In addition, mice deficient in both *Bmp9* and *Bmp10* did not show any added therapeutic benefit compared to *Bmp9*-deficient mice. These results suggest that BMP10 targeting can be omitted, and specific targeting of BMP9 rather than ALK1 or endoglin could be more suitable in this model. Interestingly, this study also highlighted BMP9 as an angiogenic quiescence factor that promotes vessel normalization. In this case, activating the BMP9 pathway rather than blocking it can provide new means for cancer therapy, especially when combined with chemo- or immunotherapies [65]. In line with the role of BMP9 as a vascular quiescence factor, Bmp9 deficiency in a pancreatic neuroendocrine tumor model led to hyperbranching and increased metastases, despite a contradictory decrease in tumor growth [56]. On the other hand, blocking BMP9 through a monoclonal anti-BMP9 antibody showed anti-tumor activity and an increase in the normalization of tumor blood vessels in a model of RCC [66]. All in all, targeting different components, and sometimes even the same element, within a signaling pathway can yield different or opposing outcomes in different models.

Conclusion

The BMP9/10-ALK1-endoglin pathway is an important regulator of vascular development that recently captivated the attention of

the scientific and medical community as a target for inhibiting tumor angiogenesis and growth [67]. Several groups attempted to block different components of this pathway (ALK1, endoglin or BMP9) using distinct pharmacological and genetic means either alone or in combination with chemo- or antiangiogenic therapy. Despite the encouraging reported effects of blocking this pathway on tumor angiogenesis and growth in most preclinical models tested, single agent therapies in patients with different solid malignancies generated only modest effects. In this regard, combinatorial clinical trials integrating BMP9/10-ALK1-endoglin and other pathways targeting agents are still ongoing with the hope of better potential.

Targeting the tumor vasculature to "starve a tumor to death" instead of targeting tumor cells with chemotherapeutic drugs was conceived over four decades ago and has led to the development of antiangiogenic drugs approved in cancer since now two decades. However, antiangiogenic therapies so far have not fulfilled expectations and provide only transitory improvements. More recent work is now proposing the opposite, that is to promote angiogenesis in order to increase influx of chemotherapeutic drugs into tumor cells [68]. It will be interesting in the future to see how the BMP9/10-ALK1-endoglin pathway will fit into this new hypothesis.

References

1. Ricard N, Bailly S, Guignabert C, Simons M. The quiescent endothelium: signalling pathways regulating organ-specific endothelial normalcy. Nat Rev Cardiol. 2021; 18: 565–580.
2. Ribatti D, Nico B, Crivellato E, Roccaro AM, Vacca A. The history of the angiogenic switch concept. Leukemia. 2007; 21: 44–52.
3. Bergers G, Benjamin LE. Tumorigenesis and the angiogenic switch. Nat Rev Cancer. 2003; 3: 401–410.
4. Marmé D. Tumor Angiogenesis: A Key Target for Cancer Therapy. Oncol Res Treat. 2018; 41: 164.
5. Munn LL. Aberrant vascular architecture in tumors and its importance in drug-based therapies. Drug Discov Today. 2003; 8: 396–403.

6. Meadows KL, Hurwitz HI. Anti-VEGF Therapies in the Clinic. Cold Spring Harbor Perspectives in Medicine. 2012; 2: a006577–a006577.
7. Crawford Y, Ferrara N. Tumor and stromal pathways mediating refractoriness/resistance to anti-angiogenic therapies. Trends in Pharmacological Sciences. 2009; 30: 624–630.
8. Kieran MW, Kalluri R, Cho YJ. The VEGF pathway in cancer and disease: responses, resistance, and the path forward. Cold Spring Harb Perspect Med. 2012; 2: a006593.
9. David L, Mallet C, Mazerbourg S, Feige JJ, Bailly S. Identification of BMP9 and BMP10 as functional activators of the orphan activin receptor-like kinase 1 (ALK1) in endothelial cells. Blood. 2007; 109: 1953–1961.
10. Desroches-Castan A, Tillet E, Bouvard C, Bailly S. BMP9 and BMP10 : Two close vascular quiescence partners that stand out. Developmental Dynamics. 2021.
11. Townson SA. Specificity and Structure of a High Affinity Activin Receptor-like Kinase 1 (ALK1) Signaling Complex. Journal of Biological Chemistry. 2012; 287: 27313–27325.
12. Shi Y, Massagué J. Mechanisms of TGF-β Signaling from Cell Membrane to the Nucleus. Cell. 2003; 113: 685–700.
13. Kim SK, Henen MA, Hinck AP. Structural biology of betaglycan and endoglin, membrane-bound co-receptors of the TGF-beta family. Exp Biol Med (Maywood). 2019; 244: 1547–1558.
14. Tual-Chalot S, Oh SP, Arthur HM. Mouse models of hereditary hemorrhagic telangiectasia: recent advances and future challenges. Front. Genet. 2015; 6.
15. Dupuis-Girod S, Bailly S, Plauchu H. Hereditary hemorrhagic telangiectasia: from molecular biology to patient care: Hereditary hemorrhagic telangiectasia. Journal of Thrombosis and Haemostasis. 2010; 8: 1447–1456.
16. Seki T, Yun J, Oh SP. Arterial endothelium-specific activin receptor-like kinase 1 expression suggests its role in arterialization and vascular remodeling. Circ Res. 2003; 93: 682–689.
17. Bernabeu C, Lopez-Novoa JM, Quintanilla M. The emerging role of TGF-β superfamily coreceptors in cancer. Biochimica

et Biophysica Acta (BBA) - Molecular Basis of Disease. 2009; 1792: 954–973.
18. Hu-Lowe DD. Targeting Activin Receptor-Like Kinase 1 Inhibits Angiogenesis and Tumorigenesis through a Mechanism of Action Complementary to Anti-VEGF Therapies. Cancer Res. 2011; 71: 1362–1373.
19. Niessen K, Zhang G, Ridgway JB, Chen H, Yan M. ALK1 signaling regulates early postnatal lymphatic vessel development. Blood. 2010; 115: 1654–1661.
20. Levet S. Bone morphogenetic protein 9 (BMP9) controls lymphatic vessel maturation and valve formation. Blood. 2013; 122: 598–607.
21. Duong T, Koopman P, Francois M. Tumor lymphangiogenesis as a potential therapeutic target. J Oncol. 2012; 2012: 204946.
22. Cuny GD. Structure-activity relationship study of bone morphogenetic protein (BMP) signaling inhibitors. Bioorg Med Chem Lett. 2008; 18: 4388–4392.
23. Ma J. Inhibiting Endothelial Cell Function in Normal and Tumor Angiogenesis Using BMP Type I Receptor Macrocyclic Kinase Inhibitors. Cancers (Basel). 2021; 13: 2951.
24. Lin X. MiR-199b-5p Suppresses Tumor Angiogenesis Mediated by Vascular Endothelial Cells in Breast Cancer by Targeting ALK1. Front Genet. 2019; 10: 1397.
25. Bendell JC. Safety, pharmacokinetics, pharmacodynamics, and antitumor activity of dalantercept, an activin receptor-like kinase-1 ligand trap, in patients with advanced cancer. Clin Cancer Res. 2014; 20: 480–489.
26. Simonelli M. Phase I study of PF-03446962, a fully human monoclonal antibody against activin receptor-like kinase-1, in patients with hepatocellular carcinoma. Ann Oncol. 2016; 27: 1782–1787.
27. Mitchell D. ALK1-Fc inhibits multiple mediators of angiogenesis and suppresses tumor growth. Mol Cancer Ther. 2010; 9: 379–388.
28. Cunha SI. Genetic and pharmacological targeting of activin receptor-like kinase 1 impairs tumor growth and angiogenesis. J Exp Med. 2010; 207: 85–100.

29. Eleftheriou NM. Compound genetically engineered mouse models of cancer reveal dual targeting of ALK1 and endoglin as a synergistic opportunity to impinge on angiogenic TGF-β signaling. Oncotarget. 2016; 7: 84314–84325.
30. Cunha SI. Endothelial ALK1 Is a Therapeutic Target to Block Metastatic Dissemination of Breast Cancer. Cancer Res. 2015; 75: 2445–2456.
31. Hawinkels LJAC. Activin Receptor-like Kinase 1 Ligand Trap Reduces Microvascular Density and Improves Chemotherapy Efficiency to Various Solid Tumors. Clin Cancer Res. 2016; 22: 96–106.
32. van Meeteren LA. Anti-human activin receptor-like kinase 1 (ALK1) antibody attenuates bone morphogenetic protein 9 (BMP9)-induced ALK1 signaling and interferes with endothelial cell sprouting. J Biol Chem. 2012; 287: 18551–18561.
33. Hu-Lowe DD. Targeting activin receptor-like kinase 1 inhibits angiogenesis and tumorigenesis through a mechanism of action complementary to anti-VEGF therapies. Cancer Res. 2011; 71: 1362–1373.
34. Cunha SI, Pietras K. ALK1 as an emerging target for antiangiogenic therapy of cancer. Blood. 2011; 117: 6999–7006.
35. Goel S, Wong AHK, Jain RK. Vascular Normalization as a Therapeutic Strategy for Malignant and Nonmalignant Disease. Cold Spring Harb Perspect Med. 2012; 2: a006486.
36. Akatsu Y. Dual targeting of vascular endothelial growth factor and bone morphogenetic protein-9/10 impairs tumor growth through inhibition of angiogenesis. Cancer Sci. 2017; 108: 151–155.
37. Wang X. Inhibition of ALK1 signaling with dalantercept combined with VEGFR TKI leads to tumor stasis in renal cell carcinoma. Oncotarget. 2016; 7: 41857–41869.
38. Goff LW. A Phase I Study of the Anti-Activin Receptor-Like Kinase 1 (ALK-1) Monoclonal Antibody PF-03446962 in Patients with Advanced Solid Tumors. Clin Cancer Res. 2016; 22: 2146–2154.

39. Doi T. A phase I study of the human anti-activin receptor-like kinase 1 antibody PF-03446962 in Asian patients with advanced solid tumors. Cancer Med. 2016; 5: 1454–1463.
40. Bendell JC. Safety, pharmacokinetics, pharmacodynamics, and antitumor activity of dalantercept, an activin receptor-like kinase-1 ligand trap, in patients with advanced cancer. Clin Cancer Res. 2014; 20: 480–489.
41. Burger RA. Phase II evaluation of dalantercept in the treatment of persistent or recurrent epithelial ovarian cancer: An NRG Oncology/Gynecologic Oncology Group study. Gynecol Oncol. 2018; 150: 466–470.
42. Makker V. Phase II evaluation of dalantercept, a soluble recombinant activin receptor-like kinase 1 (ALK1) receptor fusion protein, for the treatment of recurrent or persistent endometrial cancer: an NRG Oncology/Gynecologic Oncology Group Study 0229N. Gynecol Oncol. 2015; 138: 24–29.
43. Jimeno A. A phase 2 study of dalantercept, an activin receptor-like kinase-1 ligand trap, in patients with recurrent or metastatic squamous cell carcinoma of the head and neck. Cancer. 2016; 122: 3641–3649.
44. Necchi A. PF-03446962, a fully-human monoclonal antibody against transforming growth-factor β (TGFβ) receptor ALK1, in pre-treated patients with urothelial cancer: an open label, single-group, phase 2 trial. Invest New Drugs. 2014; 32: 555–560.
45. Wheatley-Price P. A Phase II Study of PF-03446962 in Patients with Advanced Malignant Pleural Mesothelioma. CCTG Trial IND.207. J Thorac Oncol. 2016; 11: 2018–2021.
46. Voss MH. The DART Study: Results from the Dose-Escalation and Expansion Cohorts Evaluating the Combination of Dalantercept plus Axitinib in Advanced Renal Cell Carcinoma. Clin Cancer Res. 2017; 23: 3557–3565.
47. Abou-Alfa GK. A Phase Ib, Open-Label Study of Dalantercept, an Activin Receptor-Like Kinase 1 Ligand Trap, plus Sorafenib in Advanced Hepatocellular Carcinoma. Oncologist. 2019; 24: 161-e170.
48. Clarke JM. A phase Ib study of the combination regorafenib with PF-03446962 in patients with refractory metastatic

colorectal cancer (REGAL-1 trial). Cancer Chemother Pharmacol. 2019; 84: 909–917.
49. Smirnov DA. Global Gene Expression Profiling of Circulating Endothelial Cells in Patients with Metastatic Carcinomas. Cancer Res. 2006; 66: 2918–2922.
50. Hawinkels LJAC. Matrix Metalloproteinase-14 (MT1-MMP)–Mediated Endoglin Shedding Inhibits Tumor Angiogenesis. Cancer Res. 2010; 70: 4141–4150.
51. Bockhorn M. Differential vascular and transcriptional responses to anti-vascular endothelial growth factor antibody in orthotopic human pancreatic cancer xenografts. Clin Cancer Res. 2003; 9: 4221–4226.
52. Seon BK. Endoglin-targeted cancer therapy. Curr Drug Deliv. 2011; 8: 135–143.
53. Uneda S. Anti-endoglin monoclonal antibodies are effective for suppressing metastasis and the primary tumors by targeting tumor vasculature. Int J Cancer. 2009; 125: 1446–1453.
54. Takahashi N, Haba A, Matsuno F, Seon BK. Antiangiogenic therapy of established tumors in human skin/severe combined immunodeficiency mouse chimeras by anti-endoglin (CD105) monoclonal antibodies, and synergy between anti-endoglin antibody and cyclophosphamide. Cancer Res. 2001; 61: 7846–7854.
55. Castonguay R. Soluble Endoglin Specifically Binds Bone Morphogenetic Proteins 9 and 10 via Its Orphan Domain, Inhibits Blood Vessel Formation, and Suppresses Tumor Growth. Journal of Biological Chemistry. 2011; 286: 30034–30046.
56. Nikolas M Eleftheriou, Jonas Sjölund, Matteo Bocci, Eliane Cortez, Se-Jin Lee. et al. Compound genetically engineered mouse models of cancer reveal dual targeting of ALK1 and endoglin as a synergistic opportunity to impinge on angiogenic TGF-β signaling. Oncotarget. 2016; 7: 84314–84325.
57. Karzai FH. A phase I study of TRC105 anti-endoglin (CD105) antibody in metastatic castration-resistant prostate cancer. BJU Int. 2015; 116: 546–555.

58. Rosen LS. A Phase I First-in-Human Study of TRC105 (Anti-Endoglin Antibody) in Patients with Advanced Cancer. Clinical Cancer Research. 2012; 18: 4820–4829.
59. Apolo AB. A Phase II Clinical Trial of TRC105 (Anti-Endoglin Antibody) in Adults With Advanced/Metastatic Urothelial Carcinoma. Clin Genitourin Cancer. 2017; 15: 77–85.
60. Schoonderwoerd MJA. Targeting Endoglin-Expressing Regulatory T Cells in the Tumor Microenvironment Enhances the Effect of PD1 Checkpoint Inhibitor Immunotherapy. Clin Cancer Res. 2020; 26: 3831–3842.
61. Duffy AG. Phase I and Preliminary Phase II Study of TRC105 in Combination with Sorafenib in Hepatocellular Carcinoma. Clin Cancer Res. 2017; 23: 4633–4641.
62. Gordon MS. An open-label phase Ib dose-escalation study of TRC105 (anti-endoglin antibody) with bevacizumab in patients with advanced cancer. Clin Cancer Res. 2014; 20: 5918–5926.
63. Dorff TB. Bevacizumab alone or in combination with TRC105 for patients with refractory metastatic renal cell cancer. Cancer. 2017; 123: 4566–4573.
64. Toni K Choueiri, M Dror Michaelson, Edwin M Posadas, Guru P Sonpavde, David F McDermott, et al. An Open Label Phase Ib Dose Escalation Study of TRC105 (Anti-Endoglin Antibody) with Axitinib in Patients with Metastatic Renal Cell Carcinoma. Oncologist. 2019; 24: 202–210.
65. Marie Ouarné, Claire Bouvard, Gabriela Boneva, Christine Mallet, Johnny Ribeiro, et al. BMP9, but not BMP10, acts as a quiescence factor on tumor growth, vessel normalization and metastasis in a mouse model of breast cancer. J Exp Clin Cancer Res. 2018; 37: 209.
66. Verena Brand, Christian Lehmann, Christian Umkehrer, Stefan Bissinger, Martina Thier, et al. Impact of selective anti-BMP9 treatment on tumor cells and tumor angiogenesis. Molecular Oncology. 2016; 10: 1603–1620.
67. Sherwood LM, Parris EE, Folkman J. Tumor Angiogenesis: Therapeutic Implications. New England Journal of Medicine. 1971; 285: 1182–1186.
68. Rivera LB, Bergers G. CANCER. Tumor angiogenesis, from foe to friend. Science. 2015; 349: 694–695.